PALLADIUM-CATALYZED ARYL AMINATIONS OF HALO NUCLEOSIDES

PLATINUM-CATALYZED SYNTHESIS OF NEW BENZO[*c*]PHENANTHRENE DERIVATIVES

AND

SYNTHESIS OF A *CIS* RING-OPENED AMINO TRIOL FROM BENZO[*a*]PYRENE SERIES 1 DIOL EPOXIDE

By

PAUL F. THOMSON

A dissertation submitted to the Graduate Faculty in Chemistry in partial fulfillment of the requirements for the degree of Doctor of Philosophy, The City University of New York

2012

Approval page

This manuscript has been read and accepted for the
Graduate Faculty in Chemistry in the satisfaction of the
dissertation requirement for the degree of Doctor of Philosophy.

Dr. Mahesh K. Lakshman

_____ _____

Date Chair of Examining Committee

Dr. Maria Tamargo

_____ _____

Date Executive Officer

Dr. Barbara Zajc

Dr. Shengping Zheng

Supervisory Committee

THE CITY UNIVERSITY OF NEW YORK

Abstract

PALLADIUM-CATALYZED ARYL AMINATIONS OF HALO NUCLEOSIDES

PLATINUM-CATALYZED SYNTHESIS OF NEW BENZO[*c*]PHENANTHRENE DERIVATIVES

AND

SYNTHESIS OF A *CIS* RING-OPENED AMINO TRIOL FROM BENZO[*a*]PYRENE SERIES 1 DIOL EPOXIDE

By

Paul F. Thomson

Adviser: Dr. Mahesh K. Lakshman

Palladium-catalyzed aryl amination has been utilized for synthesis of N^6-aryl adenosines from silyl-protected 6-bromo and 6-chloropurine nucleosides and arylamines. Analysis of conditions revealed that for chloro analogues, 10 mol% palladium acetate/15 mol% Xantphos/Cs_2CO_3 in toluene, at 100 ºC, was effective. For the bromo analogues 5 mol% $Pd(OAc)_2$/7.5 mol% Xantphos was adequate. Generality of method was evaluated using a variety of arylamines. Synthesis of biologically relevant deoxyadenosine and adenosine dimers was then accomplished. This work compares the reactivities of 6-bromo and 6-chloropurine nucleosides in Pd-catalyzed aryl-amination reactions.

Synthesis of novel 5-methylbenzo[*c*]phenanthrene, 4,5-dihydrobenzo[*l*]acephenanthrylene, and benzo[*l*]acephenanthrylene, as well as their putative dihydrodiol and diol epoxide metabolites, has been accomplished. These compounds are needed to understand the influence of substituents remote from the fjord region on molecular distortion, and to assess the metabolism and DNA damage as a function of molecular non-planarity. A new metal-catalyzed chemistry was utilized, and which complements known photochemical cyclization as a means to access such compounds. Briefly, Pd-catalyzed C–C bond formation of bromo benzaldehydes with naphthylboronic acids gave biaryl aldehydes. Corey-Fuchs olefination led to biaryl alkynes, which underwent platinum-catalyzed cyclizations to yield the requisite parent hydrocarbons and precursors to the putative metabolites. The metabolites display a diequatorial arrangement of the hydroxyls and X-ray crystallographic data showed decreases in the overall molecular

distortion upon remote functionalization. Biological evaluation is anticipated to understand the effect of molecular distortion and subsequent cellular events.

Diastereoselective synthesis of (±)-10*β*-amino-7*β*,8*α*,9*β*-trihydroxy-1,2,3-4-tetrahydrobenzo[*a*]pyrene was accomplished from (±)-7*β*,8*α*-dibenzoyloxy-1,2,3-4-tetrahydrobenzo[*a*]pyrene. This is required to synthesize nucleoside adducts produced by a *cis* ring-opening of benzo[*a*]pyrene diol epoxide 1. The dihydrodibenzoate was converted to the diol epoxide and then reacted with lithium chloride and acetic anhydride to give a peracyl *trans* chloro triol with a benzylic chloride. Displacement of chloride by azide, deprotection of acyl groups, and reduction of the azide afforded the requisite amino triol. This compound will be used to synthesize deoxyadenosine and deoxyguanosine adducts (the latter have not been synthesized to date).

Acknowledgements

First and foremost, I would like to extend my most sincere gratitude to my adviser, Dr. Mahesh K. Lakshman. Over the recent and past years on my path to becoming a research scientist, he has offered immense support, constant motivation, invaluable advice, and demonstrated a passion for chemistry that is most inspirational to me. I am indebted to him for helping to cultivate my own deep interest in chemistry, and for his efforts in helping to mold me into a better scientist.

I would also like to extend my deepest gratitude to my wife, Kereecha (Wendy) Thomson for her support, encouragement and faith in me over the years, as well as her patience through the tough times. In the same vein, I would also like to thank my parents, Peter Thomson and Molvena Nelson, my brother Gavin and Aunt Pat for their unwavering support.

There are a number of people to whom I owe a debt of gratitude over the years at City College. Although some names may be inadvertently omitted, I am truly thankful to you. I am most grateful to my committee members for their critique and help with my dissertation. Dr. Barbara Zajc, who like my mentor, has known me a long time and has always been supportive of my chemistry and my well being, and had offered critical advice during the progress of my work. Dr. Shengping Zheng and Dr. Klaus Grohmann for their time and support at such short notice. Former members of my committee, Dr. Alec Greer and Dr. Rajeev Muthyala are also thanked for their time and input. I thank Dr. Mark Biscoe for his helpful advice, input, and spirited discussions from time to time.

My time at City College would not have been possible were it not for the financial aid and access to facilities for my research. In this respect, I would like to extend my deep thanks to Dr. Jerry Guyden and the RCMI staff for their constant support and advice. Dr. Guyden is always encouraging and I am grateful for our talks that helped me to appreciate the opportunities I have been given. Dr. Mark Steinberg, Ms. Sonia Matthews, and Dr. Michael Weiner are respectfully thanked for my continuous support via the MARC/RISE program. Dr. Millicent Roth, Mrs. Nkem Stanley, and Ms. Connie Harper from the CCAPP are thanked for introducing me to the sciences here at City College, as well as their constant support. I am also grateful to the NIH for a Ruth L. Kirstenstein pre-doctoral fellowship. Dr. Padmanava Pradhan is thanked for all his help with the CCNY NMR facilities and helpful discussion on spectral analyses. Dr. Damon Parrish is thanked for X-ray crystallography on my synthetic samples. Dr.

Bill Boggess and Ms. Novia Sevova, and Dr. Cliff Soll are thanked for numerous mass spectrometric anaylses. Dr. Jan Balzarini and Dr. Erik De Clercq are thanked for their work on anti-viral assays of many of my compounds.

I would also like to extend deep thanks to the City College Chemistry Department, namely Prof. Simon Simms, Ms. Denise Addison, Mrs. Jemma Poyer, Mr. Derek Quinlan, Mr. Hugo Schimatz, for their help and assistance. Prof. Gerald Koeppl, Mrs. Diane Adebowale and Ms. Vivian Mason are also thanked for their helpful assistance at the CUNY Graduate Center.

Over the years I have made many friends and collaborated with many on some interesting projects. In this regards I would like to thank Dr. Mark Nuqui, Mr. John Hilmer, Dr. Pallavi Lagisetty, Dr. Suyeal Bae, and Dr. Hari Prasad Kokatla for their friendship, help, and assistance in completing good projects. I would also like to thank the following friends (past and present) who made the time in the laboratories enjoyable and upbeat, Dr. Manish Singh, Mr. Rakesh Kumar, Mr. Hari Kiran Akula, Dr. Arun Ghose, Dr. Ramendra Pratap, Dr. Elise Champeil, Ms. Maggie He, Ms. Shivani Kake, Ms. Maria Del Solar, and Dr. Dickens St. Hilaire.

Finally, I would like to thank my grandfather, Mr. Juan E. Thomson, the man responsible for all that I am today. I am deeply indebted to him for all he has imparted and instilled in me. I will continue to set the example Grandpa, and pass on the great knowledge to your grandson, Brandon.

TABLE OF CONTENTS

LIST OF SCHEMES

CHAPTER 1

CHAPTER 2

CHAPTER 3

CHAPTER 4

LIST OF FIGURES

CHAPTER 1

LIST OF TABLES

CHAPTER 1

Palladium-Catalyzed Aryl Aminations of Halo Nucleosides

Chapter 1

Unified Methodology for Aryl Amination Reactions of 6-Bromo- and 6-Chloropurine Nucleosides with a Palladium-Xantphos Catalytic System

1.1 Introduction

Metal catalyzed reactions for C–C and C–heteroatom bond formation have become an important facet in the area of organic synthesis.[1] These reactions allow facile access to a variety of organic compounds. Of the many metals involved in bond formation (example sodium[2a], copper[2b,c], and nickel[2d]), the use of palladium (Pd) as a catalyst for carbon-nitrogen (C–N) bond formations has been of increased interest over the years, especially in the area of catalyst development.[1] This is because C–N bond-forming reactions (i.e. aminations) are useful for the introduction of amino groups into organic molecules. In this respect, Pd-mediated *aryl aminations* are so "user friendly" that they are steadily becoming a standard in the synthetic repertoire for access to a wide range of products.[1] Currently, a typical aryl amination involves a reaction between an aryl halide or aryl sulfonate and an amine, mediated by a palladium-ligand complex to give the coupled aryl amine (Scheme 1).

Scheme 1. A Typical Aryl Amination Reaction

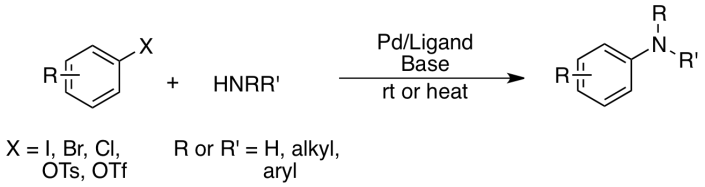

Though the classic methods for metal-catalyzed aryl amination predominately use Pd, there were other methods that existed and led up to its inception. The Fritz Ullmann reaction utilized copper (Cu) as a catalyst for *ipso*-substitution between various electron-deficient aryl bromides and iodides as a route to C–C coupled biaryls (Scheme 2, eq. 1).[2b] Further modification of this coupling reaction by Irma Goldberg allowed for successful aryl amination between aryl bromides and amines mediated by copper (Scheme 2, eq. 2).[2c] These reactions however are not without limitations. The scope was restricted due to harsh reaction conditions (e.g. high temperatures, long reaction times), and the stoichiometric amounts of copper required for successful reactions.[2b,c] Due to this, the potential applicability of metal-catalyzed aryl aminations was limited, and this hindered the utility of the method for many years.[3] To address this issue, a reinvestigation of metal-catalyzed *N*-arylation ensued, which led to the use of Pd in the early 1980s.

Scheme 2. Early Copper-Catalyzed Coupling Reactions

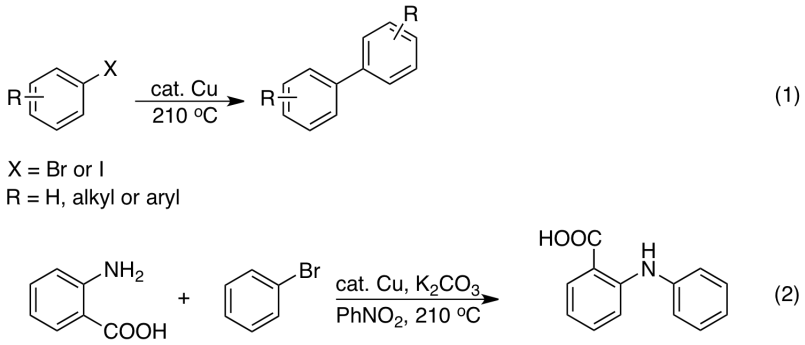

The first example for Pd-catalyzed aryl amination emerged from work by Migita and co-workers.[4] The work, considered a major breakthrough, circumvented the previous problems and allowed a facile means to aryl amines. Using Pd(II)chloride and tri-*ortho*-tolylphosphine [(*o*-tol)$_3$P] as a catalyst, various aryl bromides were coupled with *N*,*N*-diethylaminotributyltin (a *N*-stannyl amide) to give aryl amination products (Scheme 3).[4] Modest to good yields (16-81%) were obtained but there were some limitations to the scope of the reaction. These include use of aryl bromides as the only viable aromatic substrates, the toxicity of *N*-stannyl amides and tin byproducts, as well as the lability of the *N*-stannyl amides.[4]

Scheme 3. Aryl Amination involving Aryl Bromides and Stannyl Amides

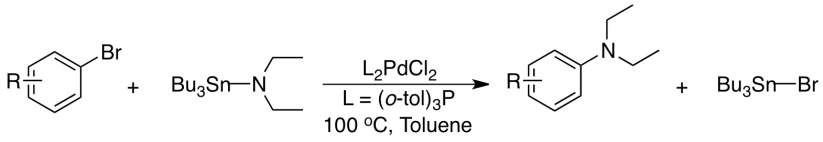

After about a decade, this early work led to the renewed interest and evaluation of Pd-catalyzed C–N bond forming processes. First, Hartwig reported some mechanistic studies on Migita's protocol where findings indicated an oxidative addition, reductive elimination process with Pd(0) complexes and transmetalation from tin as the rate-limiting step.[5] Shortly after, Buchwald reported his findings based on Migita's protocol,[6] and which had some overlap with Hartwig's report. Buchwald's work helped expand the scope of the reaction by generating tin amides in situ while using lowered Pd catalyst loading.[6] Though the reaction was still subject to lability and toxicity issues with tin-based amides, and was restricted to only secondary amines or primary anilines, the reactions showed improved yields of products with various electron-neutral, -rich and -deficient aryl bromides.[6]

Later, the limitations associated with the use of tin-based amides were addressed concurrently in the laboratories of Buchwald[7] and Hartwig.[8] The new protocol now centered on a tin-free aryl amination (Scheme 4).

Scheme 4. Buchwald–Hartwig Tin-Free C–N Bond-Forming Reactions

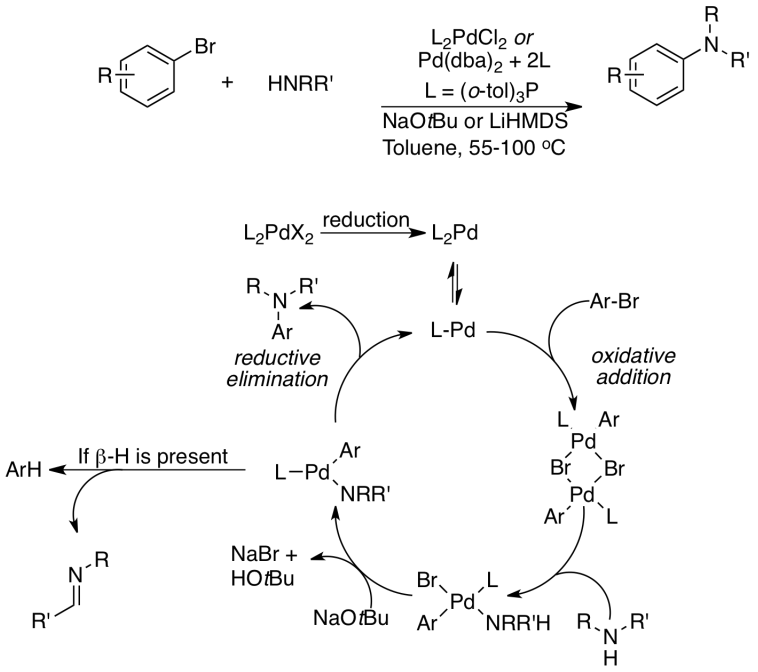

Both reports independently found that tin-based amides can be replaced with free amines through the use of a strong base, for example sodium *tert*-butoxide (NaO*t*Bu) or lithium hexamethyldisilazide (LiHMDS). The catalytic cycle proposed the formation of Pd(0)-ligand complexes in order for oxidative addition to initiate the cycle as the rate-determining step. The base assists in deprotonation of the Pd-amine complex leading to reductive elimination and product formation, while β-hydride elimination resulted in a minor side reaction (Scheme 4).[7,8] This new protocol helped expand the scope of the reaction where primary amines could be coupled with various aryl bromides, and even cyclic secondary amines and alkyl anilines made suitable substrates.[7,8]

Further studies by Buchwald[9] and Hartwig[10] offered improvements to the tin-free method. These included lowered Pd catalyst loading (0.5-1%), and reactions at room temperature. Use of bidentate phosphine ligands, such as (±)-2,2'-bis(diphenylphosphino)-1,1'-binaphthyl [(±)-BINAP] utilized by Buchwald, and 1,1'-bis(diphenylphosphino)ferrocene (DPPF) employed by Hartwig, were proposed to

help suppress β-hydride elimination via chelation to Pd. These ligands prevented open coordination sites at the Pd and helped improve yields (Scheme 5). [9,10]

Scheme 5. Buckwald's and Hartwig's Work on the Use of Bidentate Phosphine Ligands in C–N Bond-Forming Reactions

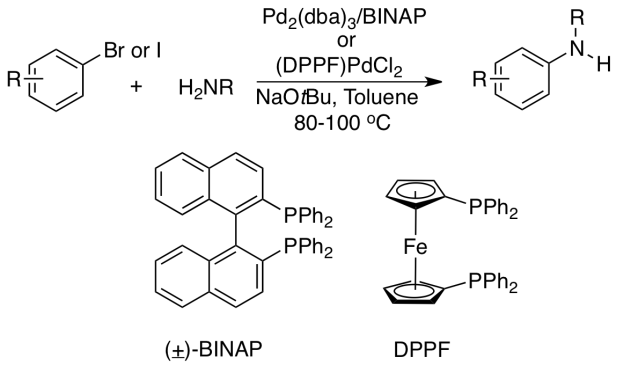

Since then, conditions have been developed that involve milder bases such as Cs_2CO_3 and K_3PO_4,[11] reactions of aryl triflates,[12] and otherwise unreactive aryl chlorides.[13] At present, any Pd-catalyzed C–N bond-forming reaction between aryl halides or phenol sulfonates and 1° or 2° aliphatic amines, anilines, imides, amides, sulfonamides, sulfoximines has now come to be known as the *Buchwald–Hartwig amination reaction*. From a mechanistic standpoint, a collaborative report by Blackmond, Buchwald and Hartwig using Pd/BINAP complexes that helped elucidate the key steps (Scheme 6).[14c]

This work studied the detailed mechanistic basis for aryl aminations catalyzed by Pd-BINAP complexes in reactions of amines with bromobenzenes, using rate measurements and ^{31}P NMR spectroscopy.[14c] The data strongly supported the necessity of a Pd(BINAP) complex in order to initiate the oxidative-addition of bromobenzene. This is contrary to two previous held mechanistic misconceptions where the amine was believed to be coordinated to a Pd(0) complex prior to oxidative addition,[14a] and that a $Pd(BINAP)_2$ complex was involved directly in the catalytic cycle.[14b] The new data confirmed that a Pd(BINAP) complex, formed from $Pd(BINAP)_2$ complex lying off the catalytic cycle, is the major pathway responsible for initiating aryl amination (Scheme 6).[14c] This resulting Pd(BINAP)(Ar)(Br) complex then reacts with the amine and base in order to form an arylpalladium amido-ligand complex that undergoes reductive elimination giving the aryl amine (Scheme 6).[14c] Currently, the generally accepted Pd-catalyzed bond-forming reaction entails the following key steps for aryl amination: (i) oxidative addition

of a Pd-ligand complex to the aryl halide or sulfonate, (ii) arylpalladium amido-complex formation, and (iii) reductive elimination resulting in the aryl aminated product.

Scheme 6. Key Mechanistic Steps in the Pd-Catalyzed C–N Bond-Forming Reaction

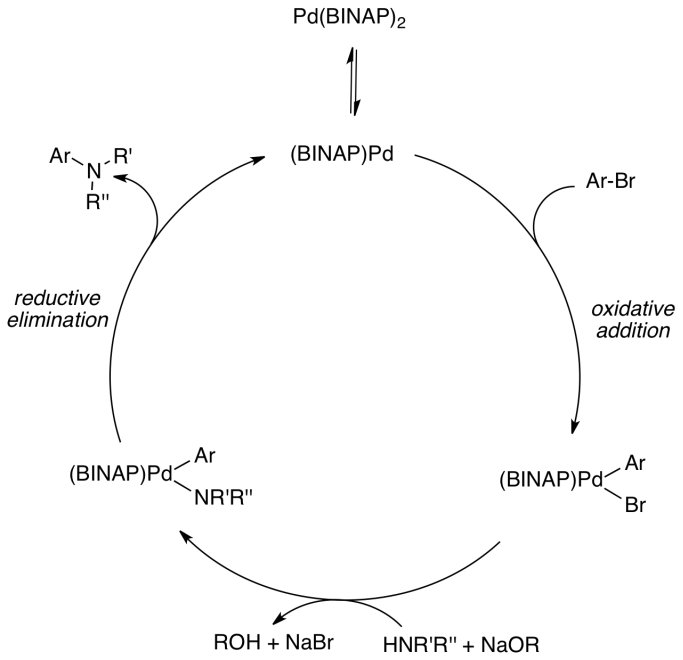

In 1996 Wagaw and Buchwald reported that various bromopyridines could be efficiently aminated with alkyl and aryl amines using tris(dibenzylideneacetone)dipalladium(0) [$Pd_2(dba)_3$], bis(diphenylphosphino)propane (DPPP), and NaO*t*Bu.[15] More importantly, the work showed that bidentate ligands inhibited ligand exchange by the pyridine derivatives from the Pd-ligand complexes, a process that could terminate the catalytic cycle. The methodology was also successful with (±)-BINAP as an effective and generally applicable ligand (Scheme 7).[15]

On the basis of this work, Lakshman and co-workers presented that nucleosides, which have pyridyl motifs, could be aminated using Pd catalysts (Figure 1 and Scheme 8).[16] There were some considerations. Halo nucleosides have multiple nitrogen and oxygen atoms and can be quite labile via deglycosylation.[17] The multiple heteroatoms on nucleosides could hamper the reaction through their potential coordination to the metal. This chemistry is of interest as *aryl* amines had not been carefully evaluated for their reactions with nucleosides, and they do not react as easily as *alkyl* amines via the nucleophilic aromatic substitution (S_NAr) process.[16] Given the scant literature for aryl amination of

nucleosides, development of a metal-catalyzed amination process became important in the realm of nucleoside modification.

Scheme 7. Examples of the Amination of Bromopyridines

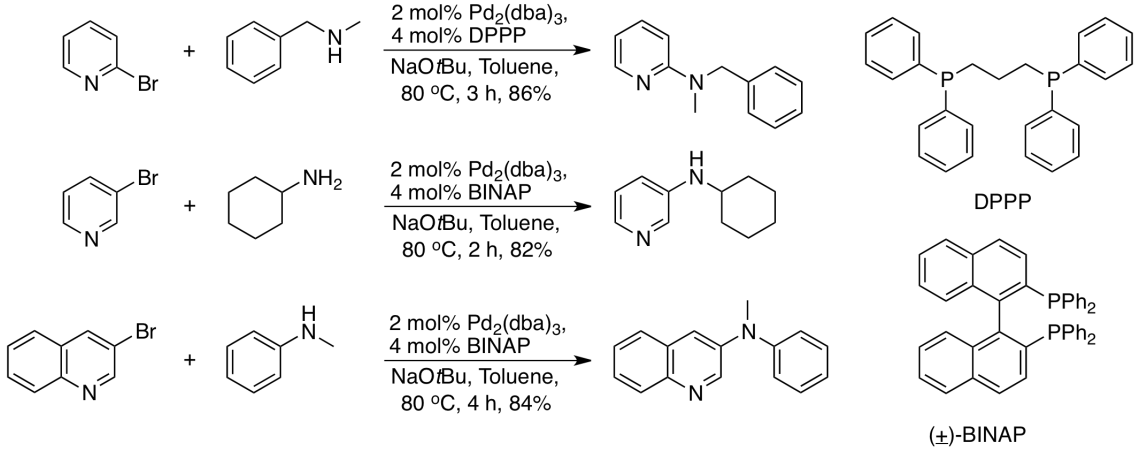

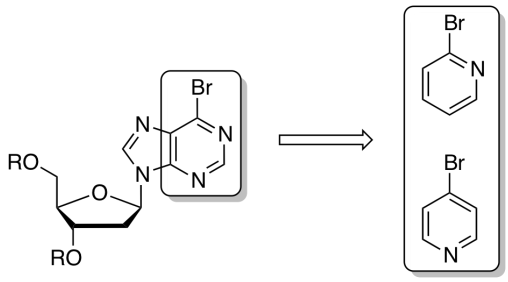

Figure 1. The Embedded Pyridine Structural Motif in 6-Bromo-9-[2-deoxyribofuranosyl]purine.

Scheme 8. Proposal for Aryl Amination Reactions of a Bromo Nucleoside

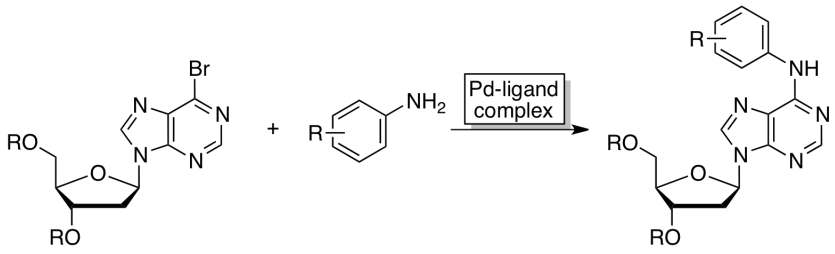

Purine nucleosides modified at the C-6, C-2, or C-8 positions are of structural, biochemical and pharmacological importance (Figure 2).[18] For example, some amino-modified nucleosides are modulators of adenosine receptors, acting as partial agonists, and show less pronounced cardiovascular effects.[19] Some exhibit inhibitory action toward DNA polymerases in cancer cells,[20] others have

demonstrated anti-malarial properties. These examples showcase the value of modified nucleosides as potential therapeutics.[21] Also, nucleoside adducts with metabolites of polycyclic aromatic hydrocarbons and dimeric nucleosides are of structural and biochemical interest since they are implicated in mutagenesis and tumorigenesis.[22] Hence, studies on developing novel approaches to known as well as previously unavailable classes of modified nucleosides become important, and Pd catalysis offers an excellent opportunity.

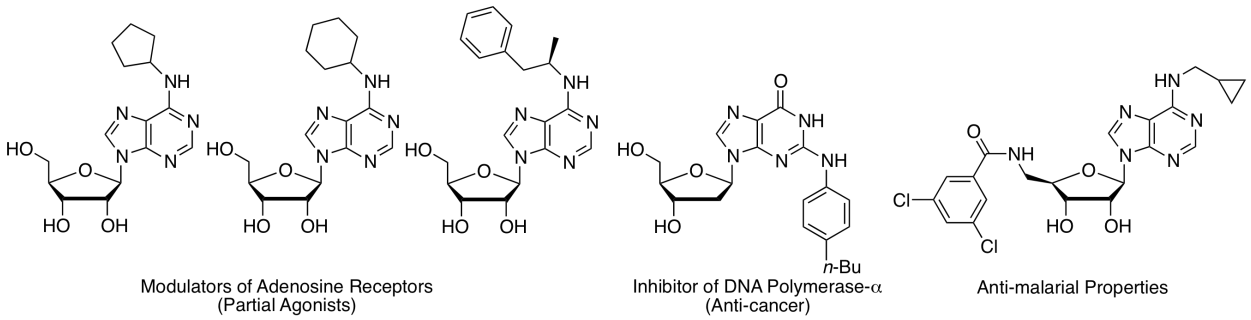

Figure 2. Examples of Amine Functionalized Nucleosides and their Biological Importance.

Research by Lakshman and co-workers, based on the report by Wagaw and Buckwald,[15] led to the first discovery of Pd-catalyzed aryl amination as a way to access N^6-aryl 2'-deoxyadenosine derivatives.[16] The substrate 6-bromo-9-(3',5'-di-*O*-*tert*-butyldimethylsilyl-β-D-*erythro*-pentofuranosyl)purine (**1**), was aminated with aryl amines using $Pd_2(dba)_3$ in conjunction with ligands (±)-BINAP or 2-(dicyclohexylphosphino)-2'-(*N*,*N*-dimethylamino)-1,1'-biphenyl (DavePhos). Mild bases such as Cs_2CO_3 and K_3PO_4 worked better than NaO*t*Bu,[15] and reactions proceeded well in 1,2-dimethoxyethane (DME). The optimal conditions for a general method involved the combination of $Pd_2(dba)_3$, DavePhos, K_3PO_4, in DME at 80 ºC. Reactions with a variety of aryl amines then led to N^6-aryl 2'-deoxyadenosine analogs (Table 1).[16]

Reactions could be conducted with electron-neutral, -deficient and -rich aryl amines. Generally good yields were obtained, although the electron-deficient amines gave lower yields (entries 2 and 3). The work demonstrated that N^6-aryl 2'-deoxyadenosine analogs can be efficiently synthesized via Pd-catalyzed C–N bond-forming chemistry.[16]

Mechanistically, the S_NAr displacement typically observed with alkyl amines was found to not be a contributing factor, as no displacement of the bromide was observed with *p*-toluidine in the *absence of*

the catalyst. Thus, the transformation most likely involved a palladium-mediated oxidative addition, reductive elimination route for C–N bond formation (Scheme 9, below).[16]

Table 1. Reactions of Various Aryl Amines with 6-Bromo-9-(3',5'-di-*O*-*tert*-butyldimethylsilyl-β-D-*erythro*-pentofuranosyl)purine (**1**)[16]

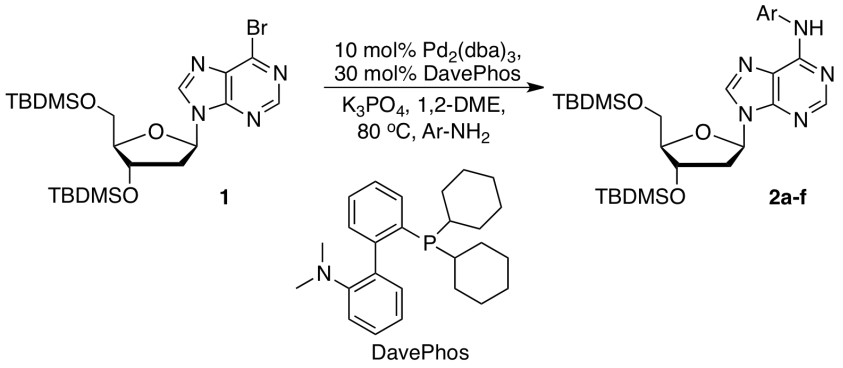

Entry	Aryl Amine	Product, Yield (%)
1	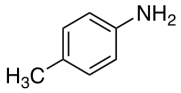	**2a**, 69
2	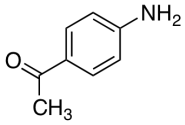	**2b**, 52
3	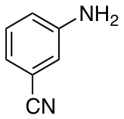	**2c**, 61
4	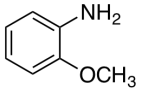	**2d**, 72
5	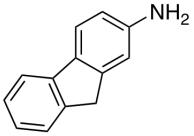	**2e**, 68
6	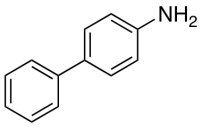	**2f**, 64

Scheme 9. Plausible Mechanistic Pathway Leading to the N^6-Aryl Nucleosides

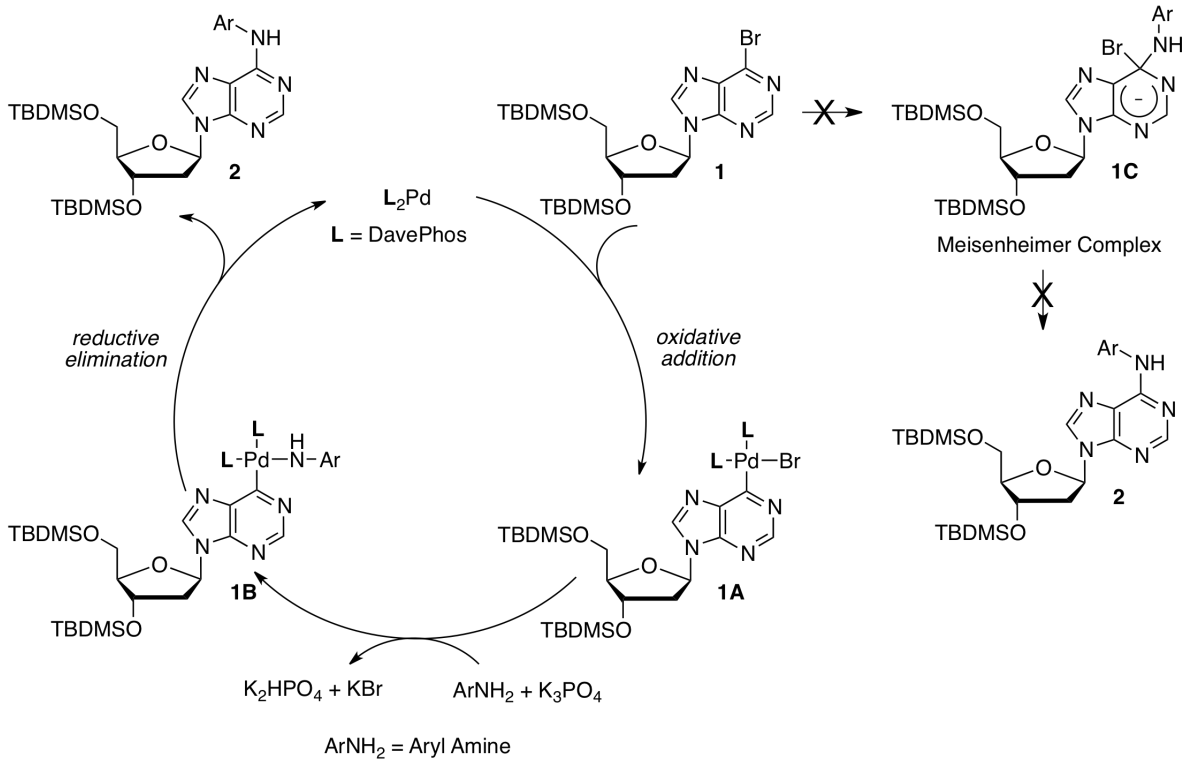

At about the same time, Hopkins and coworkers demonstrated the first use of Pd catalysis for nucleoside modification in the synthesis of a 2'-deoxyguanosine dimer (dG–dG).[23] Nucleoside dimers are typically formed *in vitro* by nitrous acid-mediated diazotization of the exocyclic amino groups of nucleobases, and result in subsequent cross-linking of DNA.[24] Such processes could have a physiological role due to the presence of nitrite in cured meats.[24] Thus, facile methods for the non-biomimetic synthesis of nucleoside dimers are important for biological studies.[24] Utilizing a Pd-catalyzed approach, Hopkins and coworkers developed methodology for other nucleoside dimer syntheses as well. Using $Pd_2(dba)_3$, (*R*)-(+)-BINAP, and NaO*t*Bu in toluene at 80 ºC, the dG–dG dimer was obtained in 40% yield via reaction of 2-bromo-O^6-benzyl-3',5'-di-*O*-(*tert*-butyldimethylsilyl)-2'-deoxyinosine (**3**) with O^6-benzyl-3',5'-di-*O*-(*tert*-butyldimethylsilyl)-2'deoxyinosine (**4**) (Figure 3 and Table 2, entry 1).[23]

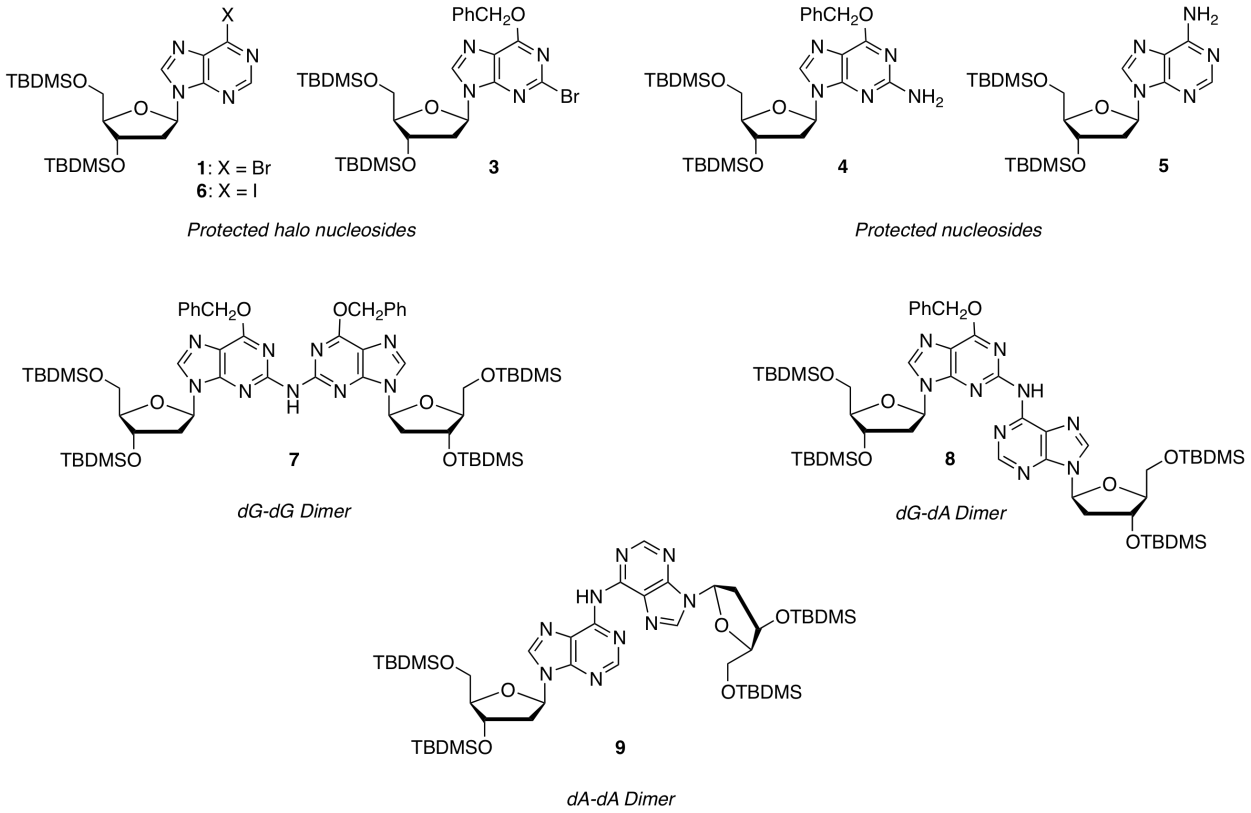

Figure 3. Structures of the Nucleoside Precursors and Dimers obtained from them.

Later, studies by De Riccardis and Johnson improved the yield of the dG–dG dimer to 90% using $Pd(OAc)_2$/(±)-BINAP/Cs_2CO_3 in the reaction of **3** and **4** (Figure 3 and Table 2, entry 2).[25] In that same report, De Riccardis and Johnson evaluated synthesis of the unsymmetrical dG–dA dimer. Use of $Pd(OAc)_2$/(±)-BINAP/Cs_2CO_3 in toluene at 90 ºC gave only 24% of dG–dA dimer when **3** and 3',5'-di-*O*-(*tert*-butyldimethylsilyl)-2'-deoxyadenosine (**5**) was used. However, upon interchanging the halogen and amino group on the reacting nucleosides, that is using bromo nucleoside **1** and O^6-benzyl-2'-deoxyguanosine derivative **4**, the coupled dG–dA dimer was obtained in an improved 60% yield (Table 2, entry 4). Also, the reaction of 6-iodo-9-(3',5'-di-*O*-*tert*-butyldimethylsilyl-β-D-*erythro*-pentofuranosyl)purine (**6**) with **4** under the same conditions also gave the dG–dA dimer, but in a lower 45% yield, along with a minor side product determined to be a dG–dA–dA trimer in 17% yield (structure not shown).[25] Lastly, the same report evaluated the synthesis of the dA–dA dimer.[25] Under the same $Pd(OAc)_2$/(±)-BINAP/Cs_2CO_3 conditions, 2'-deoxyadenosine derivative **5** could be coupled with bromo nucleoside **1** to give the dA–dA dimer in 21% yield, where as coupling with the iodo nucleoside **6** improved the yield to 51% (Table 2,

entries 6 and 7).[25]

Table 2. Results for Dimer Synthesis from the Reported Literature[23,25]

Entry	Partners	Conditions	Dimer, Yield (%)
1	**3** + **4**	$Pd_2(dba)_3$/(R)-(+)-BINAP/NaO*t*Bu	**dG–dG**, 40
2	**3** + **4**	$Pd(OAc)_2$/(±)-BINAP/Cs_2CO_3	**dG–dG**, 90
3	**3** + **5**	$Pd(OAc)_2$/(±)-BINAP/Cs_2CO_3	**dG–dA**, 24
4	**1** + **4**	$Pd(OAc)_2$/(±)-BINAP/Cs_2CO_3	**dG–dA**, 60
5	**6** + **4**	$Pd(OAc)_2$/(±)-BINAP/Cs_2CO_3	**dG–dA**, 45
6	**1** + **5**	$Pd(OAc)_2$/(±)-BINAP/Cs_2CO_3	**dA–dA**, 21
7	**6** + **5**	$Pd(OAc)_2$/(±)-BINAP/Cs_2CO_3	**dA–dA**, 51

Subsequent work from Lakshman's group showed that for C–N bond formation at the C–6 position of adenosine nucleosides, ligands such as 2-(dicyclohexylphosphino)-2'-(*N*,*N*-dimethylamino)-1,1'-biphenyl (DavePhos) and (±)-BINAP, were superior to 2-(dicyclohexylphosphino)-1,1'-biphenyl (cyclohexyl JohnPhos).[26] Hence for successful aryl amination of nucleosides, specific Pd-ligand complexes are necessary for optimal transformations.

Since these initial discoveries, Pd-catalyzed C–N bond-formation has become a standard for nucleoside modification as exemplified by the range of modified nucleosides that can be synthesized (Figure 4).[22,27-32] Additionally, the application of Pd-catalyzed amination in the synthesis of polycyclic aromatic hydrocarbon–nucleoside adducts warrants specific note.[22] Polycyclic aromatic hydrocarbons (PAHs) are pollutants present in air, water and soil that can affect health.[33] Several PAHs possess potent carcinogenic activity and undergo metabolic activation to form diol epoxides. These electrophilic diol epoxides react at the exocyclic amino groups of purine bases in DNA resulting in covalent DNA modification.[33] These DNA lesions can lead to mutations and tumorigenesis.[33,34] Pd-catalysis offers a facile chemical route to PAH-nucleoside adducts for studies aimed at better understanding the structural, functional, and biological factors influenced by nucleoside modification within DNA (Figure 5).[35-37]

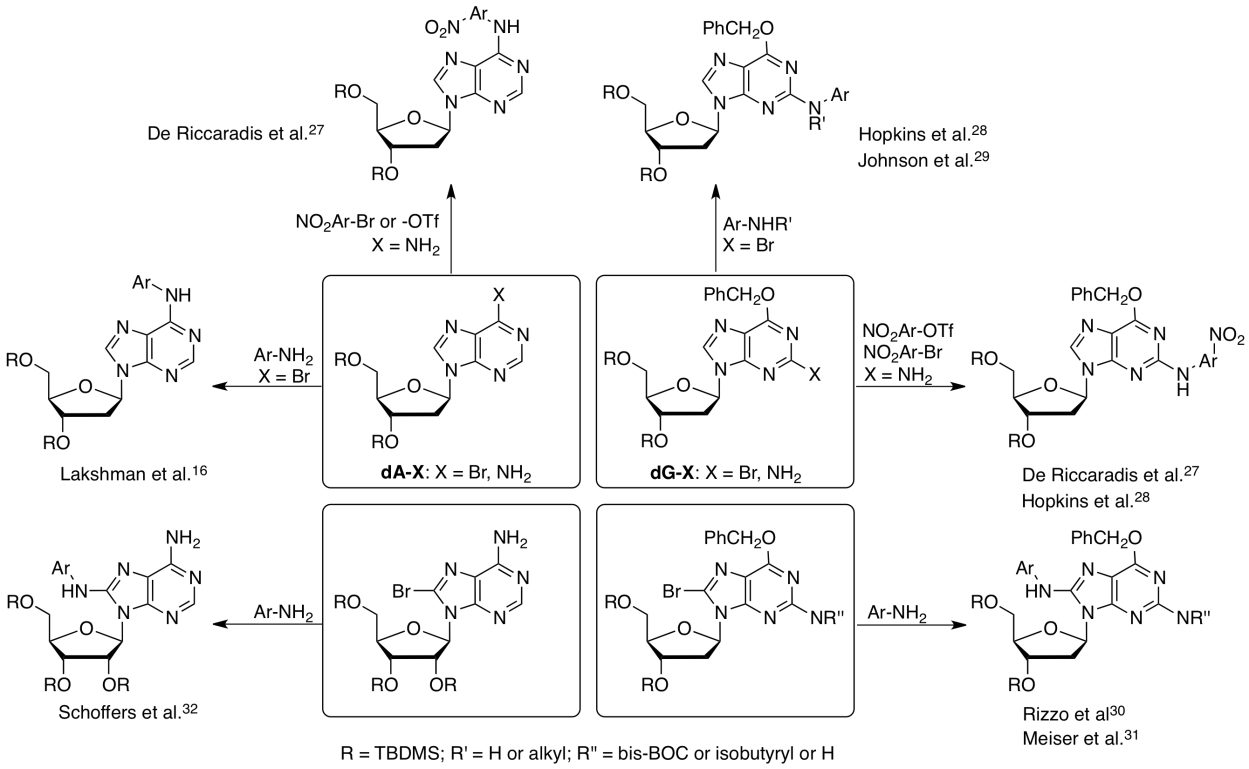

Figure 4. Array of Modified Nucleosides Accessible via Pd Catalysis.

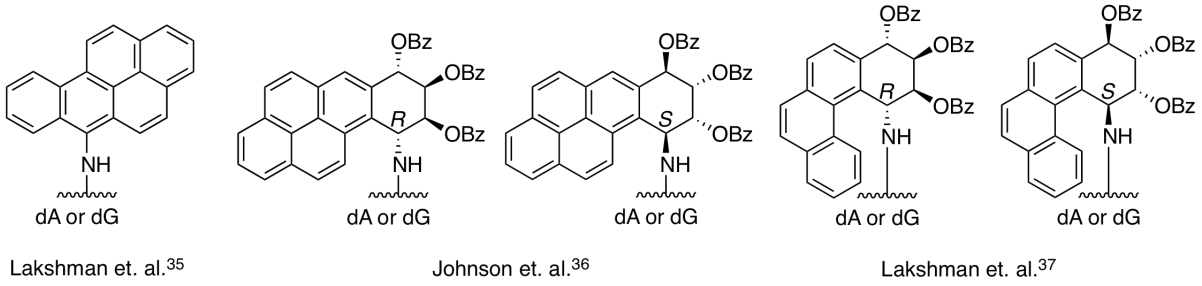

Figure 5. Sampling of PAH-Nucleoside Adducts Readily Available via Pd-catalysis.

In all of the cases mentioned previously, the halo nucleosides used in the Pd-catalyzed aminations were the bromopurine derivatives and iodopurine derivatives to a lesser extent. Much less is known about the utility of chloropurine derivatives for Pd-catalyzed aryl amination reactions. In simple aromatic systems, S_NAr displacements follow the order F > Cl > Br > I.[38] However, among nucleosides, the C-6 bromopurine nucleosides were shown to be more reactive than C-6 chloro analogs, and where the order for S_NAr displacement follows I > Br > Cl > F (discussed later).[38b,39] There are a limited number of examples of Pd-catalyzed amination reactions involving C-6 chloropurine derivatives.

Scheme 10. Examples Where C-6 Chloropurine Nucleosides Were Used in Amination Reactions

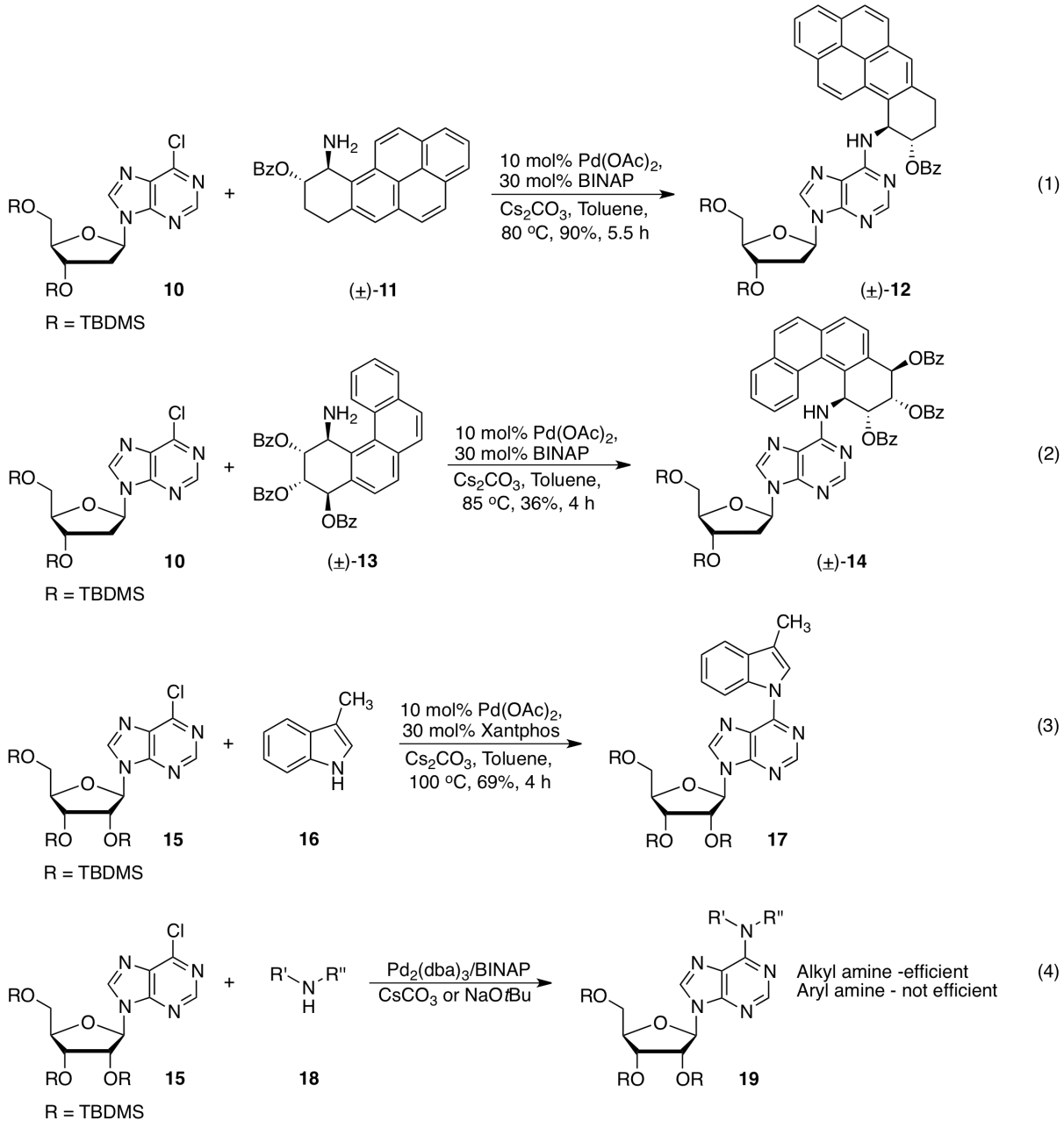

Using a catalytic system comprised of $Pd(OAc)_2$/BINAP/Cs_2CO_3, Lakshman and co-workers investigated the amination of silyl-protected 6-chloro-9-[2-deoxy-3,5-di-*O*-(*tert*-butyldimethylsilyl)-β-D-ribofuranosyl]purine (**10**) with (±)-10-amino-7-benzoyloxy-7,8,9,10-tetrahydrobenzo[*a*]pyrene [(±)-**11**] (Scheme 10, eq. 1),[40] as well as the amino tribenzoates of benzo[*c*]phenanthrene **[**(±)-**13]** (Scheme 10, eq. 2)[37] and amino tribenzoates derived from benzo[*a*]pyrenes (not shown).[37] Lakshman and co-workers have also studied the C–N(sp^2) bond-forming reactions of 6-bromo- and 6-chloropurine nucleosides with

various azoles using a $Pd(OAc)_2$/Xantphos/Cs_2CO_3 catalytic system.[41] For example, 6-chloro-9-[2,3,5-tri-*O*-(*tert*-butyldimethylsilyl)-β-D-ribofuranosyl]purine (**15**) was successfully coupled with 3-methylindole (**16**) to give the C-6-azolyl purine nucleoside **17** (Scheme 10, eq. 3).[41] Lastly, a report by Koomen et al.[42] showed reactions of alkyl amines with **11** using a $Pd_2(dba)_3$/(±)-BINAP catalytic system and either Cs_2CO_3 or *t*BuOK as base. Though the alkyl amines gave good results for amination, comparable reactions with arylamines were not efficient (Scheme 10, eq. 4).[42] In recent years the diversity of Pd-catalyzed transformations involving nucleosides has grown considerably, leading to reviews on the topic.[22,43]

Table 3. Examples of S_NAr Displacement Reactions of Acetyl-protected 6-Bromopurine Nucleosides with Aryl Amines

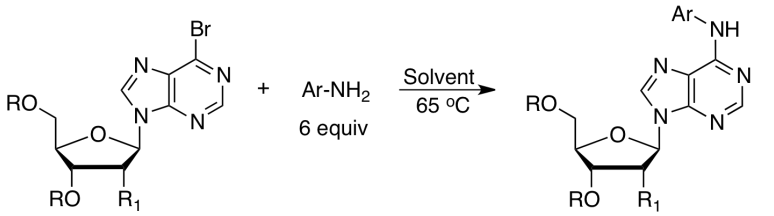

20: R = Ac, R_1 = H
22: R = Ac, R_1 = OAc

21a: R = Ac, R_1 = H
23a,d,i: R = Ac, R_1 = OAc

Entry	Substrate	Aryl Amine	Solvent	Product, Yield (%)
1	**20**	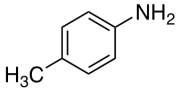	MeOH	**21a**, 91
2	**22**	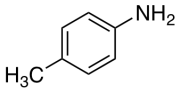	DMF	**23a**, 65
3	**22**	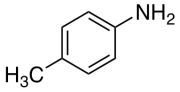	MeOH	**23a**, 85
4	**22**	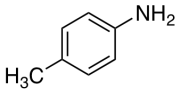	EtOH	**23a**, 82
5	**22**	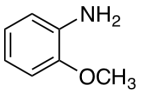	MeOH	**23d**, 91
6	**22**		DMF	**23i**, 92

A complimentary method to Pd-catalyzed amination reactions involving nucleosides is in a report by Véliz and Beal.[39] The work centered on amination reactions via S_NAr displacement of halides at the C–6 position of purine nucleosides by amines (Table 3). 6-Bromo ribo- and 2'-deoxyribonucleosides with

acetyl protecting groups were efficiently reacted with 6 equivalents of aryl amines, generally in polar solvents.[39] The work also showed that *tert*-butyldimethylsilyl (TBDMS) protection was a deterrent to displacement reactions with, *p*-toluidine, *o*-anisidine and imidazole, as opposed to acetyl protected nucleosides that proceeded well with the same aryl amines.[39] Whereas displacement reactions proceeded well with the bromo nucleoside analogs, reactions of the chloro derivatives *did not* proceed under the same conditions.[39] This is contrary to the reactivity trend of S_NAr reactions of simple aromatic systems that follows F > Cl > Br > I.[38]

Since there has been scant literature on the Pd-mediated aryl amination reactions involving 6-chloropurine nucleosides and because S_NAr reactions of chloro nucleosides are ineffective, we decide to conduct this evaluation. In addition, there are no studies comparing on the aryl amination of 6-chloropurine nucleosides to the more utilized 6-bromopurine nucleosides catalyzed by Pd. Hence, given the importance of the nucleoside modification and a gap in the knowledge, we decided to evaluate the utility of 6-chloropurine nucleoside analogs under Pd-catalyzed aryl amination conditions, and to compare the amination results from the 6-chloro- and 6-bromopurine nucleoside derivatives.

1.2 Results and Discussion

The halopurine nucleosides selected for this analysis were the silyl-protected 6-bromo- and 6-chloro-2'-deoxynucleoside derivatives, as well as the silyl- and acetyl-protected 6-bromo- and 6-chloropurine ribonucleosides shown in Figure 6. The principal aim of this study involved assessing the optimal, general conditions for aryl amination reactions of bromo and chloropurine nucleosides, which can provide access to the N^6-aryl purine nucleoside derivatives. A comparison of amination conditions for the chloro and bromo analogs will also prove to be highly important.

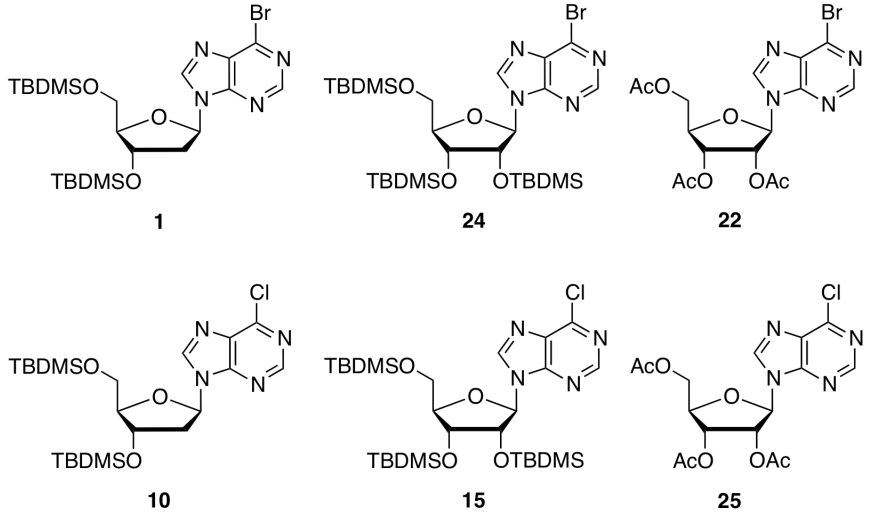

Figure 6. Structures of Nucleoside Substrates Used for the Investigation.

Bromonucleosides **1**, **24**, and **22** were synthesized by a diazotization-bromination protocol reported by Nair,[44] with suitable modifications to provide the required substrates.[39,41] Chloronucleoside **10** was prepared by silylation[45] of 6-chloro-9-(2-deoxy-β-D-ribofuranosyl)purine.[46] Chloropurine ribonucleosides **15** and **25** were prepared by silylation and acetylation of 6-chloro-9-(β-D-ribofuranosyl)purine.[41,47] Acetate-protected **25** can also be prepared by the chlorination of inosine triacetate.[48]

With these precursors, the next step was exploration of suitable catalysts for the aryl amination. Based on the prior literature,[16,22,26,35,37-43,49-55] six ligands (Figure 7) were chosen for investigation. 2-(Dicyclohexylphosphino)-2'-*N*,*N*-(dimethylamino)-1,1'-biphenyl (DavePhos, **L1**), (±)-2,2'-bis(diphenylphosphino)-1,1'-binaphthyl [(±)-BINAP, **L2**], and 4,5-bis(diphenylphosphino)-9,9-dimethylxanthene (Xantphos, **L3**), were chosen based on their previous successful use for nucleoside

modification. In addition to these, 2-(dicyclohexylphosphino)-1,1'-biphenyl (dicyclohexyl JohnPhos, **L4**) and 2-(di-*tert*-butylphosphino)-1,1'-biphenyl (JohnPhos, **L5**) were selected for their similarity to **L1**. The mono-phosphine 4-(diphenylphosphino)-9,9-dimethylxanthene (**L6**) was included for comparison to **L3**. The metal sources chosen were $Pd(OAc)_2$, $Pd_2(dba)_3$, and $Pd(PPh_3)_4$. The bases selected were K_3PO_4 and Cs_2CO_3.

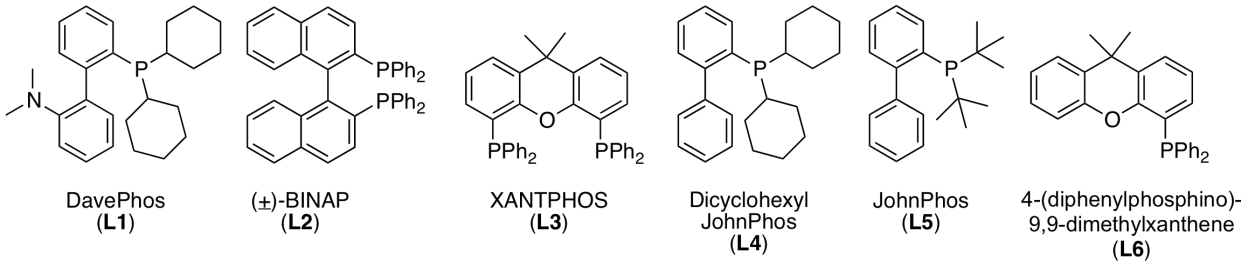

Figure 7. Structures of Ligands Used for the Investigation.

Using the earlier literature on aryl amination of bromopurine 2'-deoxynucleoside **1**,[16,26] additional optimizations were done using *p*-toluidine as the test amine. From the extensive experiments performed, results in Table 4 represent the most significant ones. Our first task was to further tune conditions in entry 1, which had worked reasonably well for **1**.[16] Using 10 mol% $Pd(OAc)_2$/15 mol% **L1** under the same conditions as entry 1, a poor 37% product yield was achieved in 9 h (entry 2). Use of 10 mol% $Pd_2(dba)_3$/30 mol% **L1**/1.5 molar equiv Cs_2CO_3 in toluene at 100 ºC gave about the same product yield (41%) in 4 h (entry 3). These results led to the consideration of other ligands, namely **L2** and **L3**. With 10 mol% $Pd(OAc)_2$/15 mol% **L2**/1.5 molar equiv Cs_2CO_3 in toluene at 100 ºC, a reasonable 64% product yield was achieved within 1 h (entry 4), whereas 10 mol% $Pd(OAc)_2$/15 mol% **L3**/1.5 molar equiv. Cs_2CO_3 gave an excellent 89% yield of product within 1 h (entry 5).

Given this high yield, we then considered reducing the loading of $Pd(OAc)_2$ and **L3** by half. Under identical conditions, but with 5 mol% $Pd(OAc)_2$/7.5 mol% **L3**, again an excellent 90% yield of product was obtained (entry 6). Subsequently, under these "best conditions", **L3** was replaced with the mono-phosphane ligands, **L4** and **L5**. However, lower product yields were obtained in these cases (entries 7 and 8) and longer reaction times were observed.

Table 4. Preliminary Results for Aminations Involving the Halonucleosides and *p*-Toluidine

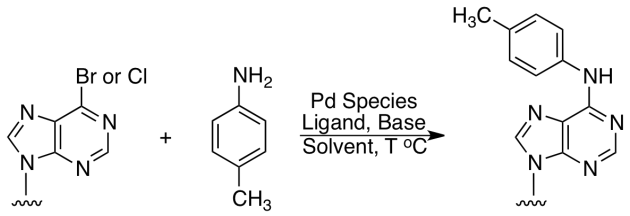

Entry	Substrate	Pd species (mol%)	Ligand (mol%)	Base	Solvent	T °C	Time, h[a]	Yield (%)[b]
			*Reactions of bromo nucleosides **1** and **24** with p-toluidine*					
1	**1**	$Pd_2(dba)_3$ (10)	**L1** (30)	K_3PO_4	DME	80	3	69[c]
2	**1**	$Pd(OAc)_2$ (10)	**L1** (15)	K_3PO_4	DME	80	9	37
3	**1**	$Pd_2(dba)_3$ (10)	**L1** (30)	Cs_2CO_3	PhMe	100	4	41
4	**1**	$Pd(OAc)_2$ (10)	**L2** (15)	Cs_2CO_3	PhMe	100	1	64
5	**1**	$Pd(OAc)_2$ (10)	**L3** (15)	Cs_2CO_3	PhMe	100	1	**89**
6	**1**	$Pd(OAc)_2$ (5)	**L3** (7.5)	Cs_2CO_3	PhMe	100	1	**90**
7	**1**	$Pd(OAc)_2$ (5)	**L4** (7.5)	Cs_2CO_3	PhMe	100	6	70
8	**1**	$Pd(OAc)_2$ (5)	**L5** (7.5)	Cs_2CO_3	PhMe	100	24	56[d]
9	**24**	$Pd(OAc)_2$ (10)	**L2** (15)	Cs_2CO_3	PhMe	100	2	76
10	**24**	$Pd(OAc)_2$ (5)	**L3** (7.5)	Cs_2CO_3	PhMe	100	1	**93**
11	**24**	$Pd(OAc)_2$ (5)	**L6** (7.5)	Cs_2CO_3	PhMe	100	7	66
			*Reactions of chloro nucleosides **10** and **15** with p-toluidine*					
12	**10**	$Pd_2(dba)_3$ (10)	**L1** (30)	K_3PO_4	DME	80	22	49
13	**10**	$Pd_2(dba)_3$ (10)	**L1** (30)	Cs_2CO_3	DME	80	26	52
14	**10**	$Pd_2(dba)_3$, (10)	**L1** (30)	Cs_2CO_3	PhMe	100	1	80
15	**10**	$Pd(OAc)_2$ (10)	**L1** (15)	Cs_2CO_3	PhMe	100	1	59
16	**10**	$Pd(OAc)_2$ (10)	**L2** (15)	Cs_2CO_3	PhMe	100	1	**88**
17	**10**	$Pd(OAc)_2$ (5)	**L2** (7.5)	Cs_2CO_3	PhMe	100	1	67
18	**10**	$Pd(OAc)_2$ (10)	**L3** (15)	Cs_2CO_3	PhMe	100	1	**86**
19	**10**	$Pd(OAc)_2$ (5)	**L3** (7.5)	Cs_2CO_3	PhMe	100	1	**86**
20	**15**	$Pd(OAc)_2$ (10)	**L2** (15)	Cs_2CO_3	PhMe	100	2	**88**
21	**15**	$Pd(OAc)_2$ (5)	**L2** (7.5)	Cs_2CO_3	PhMe	100	2	**88**
22	**15**	$Pd(OAc)_2$ (10)	**L3** (15)	Cs_2CO_3	PhMe	100	1	**92**
23	**15**	$Pd(OAc)_2$ (5)	**L3** (7.5)	Cs_2CO_3	PhMe	100	1	74
24	**15**	$Pd(OAc)_2$ (5)	**L6** (15)	Cs_2CO_3	PhMe	100	5	60
			*Reactions of chloro nucleoside **15** with o-toluidine*					
25	**15**	$Pd(OAc)_2$ (10)	**L2** (15)	Cs_2CO_3	PhMe	100	1	86 (87[e])
26	**15**	$Pd(OAc)_2$ (5)	**L2** (7.5)	Cs_2CO_3	PhMe	100	1	73 (76[e])
27	**15**	$Pd(OAc)_2$ (10)	**L3** (15)	Cs_2CO_3	PhMe	100	1	**92**
			*Reactions of acetate-protected nucleosides **22** and **25** with p-toluidine*					
28	**22**	$Pd(OAc)_2$ (5)	**L3** (7.5)	Cs_2CO_3	PhMe	100	1.5	82
29	**25**	$Pd(OAc)_2$ (10)	**L3** (15)	Cs_2CO_3	PhMe	100	1.5	62
			*Reactions of **1** and **10** with p-toluidine using $Pd(PPh_3)_4$ as catalyst*					
30	**1**	$Pd(PPh_3)_4$ (5)	none	Cs_2CO_3	PhMe	100	4	56
31	**10**	$Pd(PPh_3)_4$ (5)	none	Cs_2CO_3	PhMe	100	5	62

[a] Reactions were conducted as in reference 16 and were monitored by TLC for complete consumption of halonucleoside. [b] Yields are of isolated and purified products. [c] Reported in reference 16. [d] Reaction was incomplete. [e] Reaction time was 2 h.

These results formed the basis for further investigations of the reactions of bromopurine ribonucleoside **24**. As seen from entries 9 and 10 in Table 4, the lower $Pd(OAc)_2$/**L3** catalytic loading

returned excellent yields for the amination of **24**. This demonstrated the efficiency of the 5 mol% $Pd(OAc)_2$/7.5 mol% **L3**/1.5 molar equiv Cs_2CO_3 for the aryl amination of bromonucleoside derivatives. Critically, the presence of two phosphine units in **L3** is necessary for the formation of an effective catalyst because replacing **L3** with the mono-phosphine **L6**, under the same reaction conditions, produced an inferior result (entry 11). Hence, for the bromo nucleosides, the optimal conditions are the lower catalytic loading of 5 mol% $Pd(OAc)_2$/7.5 mol% **L3**.

Optimization of amination conditions for the chloronucleosides followed. With chloropurine 2'-deoxynucleoside **10**, use of 10 mol% $Pd_2(dba)_3$/30 mol% **L1** with 1.5 molar equiv. of K_3PO_4 (entry 12) or Cs_2CO_3 (entry 13) in DME gave modest yields. With Cs_2CO_3 as a base, use of toluene as solvent gave a high product yield of 80%, at 100 ºC (entry 14). Use of 10 mol% $Pd(OAc)_2$ in place of $Pd_2(dba)_3$ lowered the product yield to 59% (entry 15). Next, **L2** was investigated. A catalyst comprised of 10 mol% $Pd(OAc)_2$/15 mol% **L2**/1.5 molar equiv Cs_2CO_3 gave a high 88% yield of product in toluene, at 100 ºC (entry 16). This yield decreased to 67% when the catalytic loading was reduced by half (entry 17). When **L3** was used under these same conditions (entries 18 and 19), both high and low catalytic loading led to an identical product yield of 86%.

Chloropurine ribonucleoside **15**, was then investigated. Use of 10 mol% $Pd(OAc)_2$/15 mol% **L2** gave a high yield of 88% (entry 20), and the same yield was attained when the catalytic loading was decreased by half (entry 21). Change of the ligand to **L3** allowed for some notable differences; 10 mol% $Pd(OAc)_2$/15 mol% **L3** gave an excellent 92% product yield (entry 22). Reduction of the catalyst loading by half however, reduced the product yield to 74% (entry 23). The necessity of having two phosphine units on **L3** was again tested by utilizing the mono-phosphine **L6**. A lower product yield of 60% was obtained (entry 24), again indicating the superiority of ligands with two phosphine units.

These results showed some insightful differences in reactions of **10** and **15**. The higher and lower $Pd(OAc)_2$/**L3** catalytic loading with **10** gave identical results (entries 18 and 19). With $Pd(OAc)_2$/**L2**, marked differences were observed, and the higher catalyst loading worked best (entries 16 and 17). With **15** however, the exact opposite was observed.

In order to obtain further insight, three additional reactions of **15** with the sterically hindered *o*-toluidine were performed. Reactions of *o*-toluidine and **15** with 10 mol% $Pd(OAc)_2$/15 mol% **L2** gave 86%

product yield, while the lower catalytic loading of 5 mol% $Pd(OAc)_2$/7.5 mol% **L2** gave 73%, both in 1 hour. When these reactions were re-run for 2 hr, the yields did not change appreciably (entries 25 and 26). Use of 10 mol% $Pd(OAc)_2$/15 mol% **L3** with *o*-toluidine however gave an excellent 92% product yield (entry 27). This indicated that 10 mol% $Pd(OAc)_2$/15 mol% **L3** catalytic loading works consistently well for reactions with both **10** and **15**.

Overall, the optimal catalytic system for aryl amination reactions of 6-bromo- and 6-chloropurine nucleosides was determined to be $Pd(OAc)_2$/**L3**/Cs_2CO_3 in toluene, at 100 ºC. This catalytic system works well even at a lower loading, giving excellent product yields with the bromopurine nucleosides. In light of these results, we also compared reactions of acetate-protected 6-bromo- and 6-chloropurine nucleosides, **22** and **25**, using the best conditions for reactions of the corresponding silylated derivatives. In both cases, the results with acetate-protected nucleosides (entries 28 and 29) were lower than those for the silyl-protected analogs (entries 10 and 22). It is noteworthy that with either acetate- or silyl-protected nucleoside substrates, no product formation was observed when the $Pd(OAc)_2$/**L3** catalyst was absent. This clearly indicated that reactions *do not* occur via the S_NAr pathway,[39] but rather through the oxidative addition, reductive elimination catalytic cycle involving Pd.[16] In closing the optimizations, the utility of $Pd(PPh_3)_4$ also was evaluated. This Pd(0) catalyst has been used for Suzuki-Miyauri cross-coupling reactions with halonucleosides.[54,56] Reactions of **1** and **10** with *p*-toluidine using 5 mol% $Pd(PPh_3)_4$, 1.5 molar equiv Cs_2CO_3 in toluene at 100 ºC, gave inferior results (entries 30 and 31), compared to those obtained from reactions of **1** and **10** with the lower catalytic loading of **L2** or **L3**. Hence, based on these optimizations, we decided to test the catalytic efficiency of $Pd(OAc)_2$/**L3**/Cs_2CO_3 with aryl amines with different electronic and steric properties.

Results in Table 5 show that both the bromo- and chloropurine nucleosides (**1**, **24** and **10**, **15**) are suitable substrates for aminations involving aryl amines under the optimized Pd-catalyzed conditions. For reactions involving bromopurine nucleosides **1** and **24**, 5 mol% $Pd(OAc)_2$/7.5 mol% **L3**/1.5 molar equiv Cs_2CO_3 with 2 molar equiv amine in toluene, at 100 ºC (Condition **A**) was used. For reactions of chloropurine nucleosides **10** and **15**, 10 mol% $Pd(OAc)_2$/15 mol% **L3**/1.5 molar equiv Cs_2CO_3 with 2 molar equiv amine in toluene, at 100 ºC (Condition **B**) was used.

Table 5. Reactions of Bromo- (**1** and **24**) and Chloropurine (**10** and **15**) Nucleosides with Various Aryl Amines

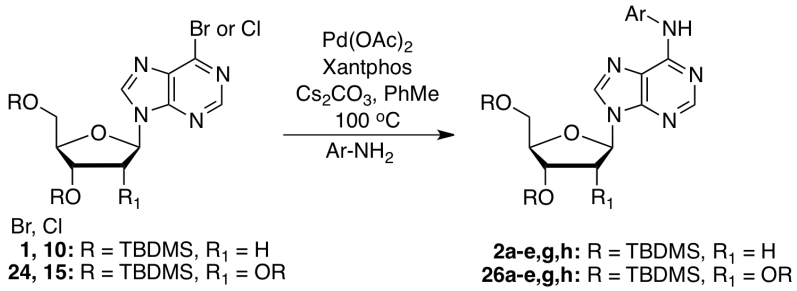

Entry	Amine	Substrate	Conditions,[a] Time[b]	Product: Yield (%)[c]
1	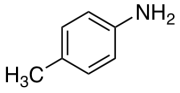	**1**	**A**, 1 h	**2a**: 90
2		**24**	**A**, 1 h	**26a**: 93
3		**10**	**B**, 1 h	**2a**: 86
4		**15**	**B**, 1 h	**26a**: 92
5	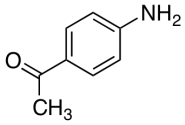	**1**	**A**, 1 h	**2b**: 88
6		**24**	**A**, 1 h	**26b**: 92
7		**10**	**B**, 1 h	**2b**: 92
8		**15**	**B**, 1 h	**26b**: 92
9	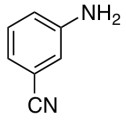	**1**	**A**, 1 h	**2c**: 79
10		**24**	**A**, 1.5 h	**26c**: 87
11		**10**	**B**, 1 h	**2c**: 72
12		**15**	**B**, 1 h	**26c**: 91
13	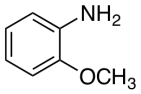	**1**	**A**, 1 h	**2d**: 87
14		**24**	**A**, 1 h	**26d**: 86
15		**10**	**B**, 1 h	**2d**: 87
16		**15**	**B**, 1 h	**26d**: 93
17	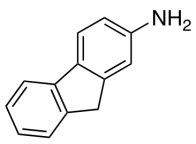	**1**	**A**, 1 h	**2e**: 88
18		**24**	**A**, 1 h	**26e**: 84
19		**10**	**B**, 1 h	**2e**: 92
20		**15**	**B**, 1 h	**26e**: 99

21	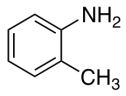	**1**	**A**, 1 h	**2g**: 68
22		**24**	**A**, 1 h	**26g**: 84
23		**10**	**B**, 1 h	**2g**: 78
24		**15**	**B**, 1 h	**26g**: 92
25	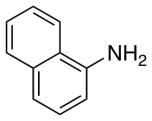	**1**	**A**, 1 h	**2h**: 91
26		**24**	**A**, 1 h	**26h**: 88
27		**10**	**B**, 1 h	**2h**: 95
28		**15**	**B**, 1 h	**26h**: 89

[a] Reactions were performed at a nucleoside concentration of 0.1 M in the reaction solvent. Conditions **A**: 5 mol% $Pd(OAc)_2$/7.5 mol% **L3**/1.5 molar equiv Cs_2CO_3, PhMe, 100 ºC. Conditions **B**: 10 mol% $Pd(OAc)_2$/15 mol% **L3**/1.5 molar equiv Cs_2CO_3, PhMe, 100 ºC. [b] Reactions monitored by TLC for consumption of halonucleoside. [c] Yields are of isolated and purified products.

For **1** and **24**, Condition **A** worked well and gave good to excellent product yields. Although the reaction of *o*-toluidine with **1** gave the lowest yield of 68% (entry 21), the other sterically hindered amine, *o*-anisdine, gave good yields for **1** and **24** (entries 13 and 14). Reactions of **1** and **24** with the electron-deficient *p*-acetyl aniline proceeded with high yields (entries 5 and 6), and reasonably good yields were also obtained with *m*-cyano aniline (entries 9 and 10).

Reactions with chloropurine nucleosides **10** and **15** proceeded well under Condition **B**. Table 5 clearly shows that chloropurine nucleosides are excellent coupling partners in Pd-catalyzed C–N bond forming reactions. Reactions with **10** and **15** resulted in product yields ≥72% with all amines tested.

When comparing these Pd-catalyzed transformations to conventional S_NAr reactions involving 6-halopurine nucleosides, the following observations can be made. With bromopurine nucleoside **24**, Pd-catalyzed reactions gave a comparable product yield (Table 5, entry 2) to the S_NAr displacement reaction with **22** reported in Véliz and Beal (Table 3, entries 2-4).[39] However, the S_NAr displacement required 6 molar equiv of arylamine compared to the 2 molar equiv needed for the Pd-catalyzed reactions. Additionally, Pd-catalyzed reactions involving chloronucleosides gave high yields of various aminated products, whereas chloropurine nucleosides were unreactive under S_NAr reactions.[39]

With reactions of simple aryl amines completed, we focused our attention on more complex structures. We determined whether nucleosides could act as aryl amines in Pd-catalyzed reactions with

halonucleosides, leading to nucleoside dimers. As previously mentioned, nucleoside dimers (Figure 3) are of great interest as they can be formed by nitrous acid-induced DNA cross-linking, a process thought to occur due to the presence of nitrites in cured meats, and these could play a physiological role.[23,24] Pd-catalyzed chemistry has proven to be reasonable in the non-biomimetic synthesis of these nucleoside dimers produced by DNA cross-linking.[24,25]

Among the various dimers produced (Figure 3), the synthesis of dA–dA (**9**) is considered quite challenging. Reactions involving bromopurine nucleoside **1** and protected 2'-deoxyadenosine **5** (Table 2, entry 6), using a Pd/BINAP complex, only gave a low 21% product yield.[25] The use of iodopurine nucleoside **6** (Figure 3) was necessary to obtain a better result (Table 2, entry 7).[25] Hence, on the basis of our results, we reassessed aryl amination reactions of **1** with **5** and also determined the reactivity of chloropurine nucleoside **10** with **5** for synthesis of dimeric nucleosides. In this study we also evaluated reactions leading to the unknown adenosine-adenosine (A–A) dimer **28**. These results are shown in Table 6.

From Table 6, it is clear that 6-bromopurine nucleosides, **1** and **24** are efficient substrates for Pd-catalyzed amination with the amino group of protected 2'-deoxyadenosine and adenosine nucleosides, **5** and **27**. Good yields were observed under Condition **A** (entries 1 and 2) and Condition **B** (entries 3 and 4), and these are the best results to date for the synthesis of these dimers. Chloropurine nucleosides **10** and **15** were just as efficient reactants in these amination reactions, and gave comparable product yields to the bromo analogs (entries 5 and 6). This dispels the previous notion that an iodopurine nucleoside is necessary for Pd-catalyzed synthesis of dA–dA dimers.[25]

Table 6. Results for Reactions Leading to dA–dA and A–A Dimers using $Pd(OAc)_2$/Xantphos/Cs_2CO_3

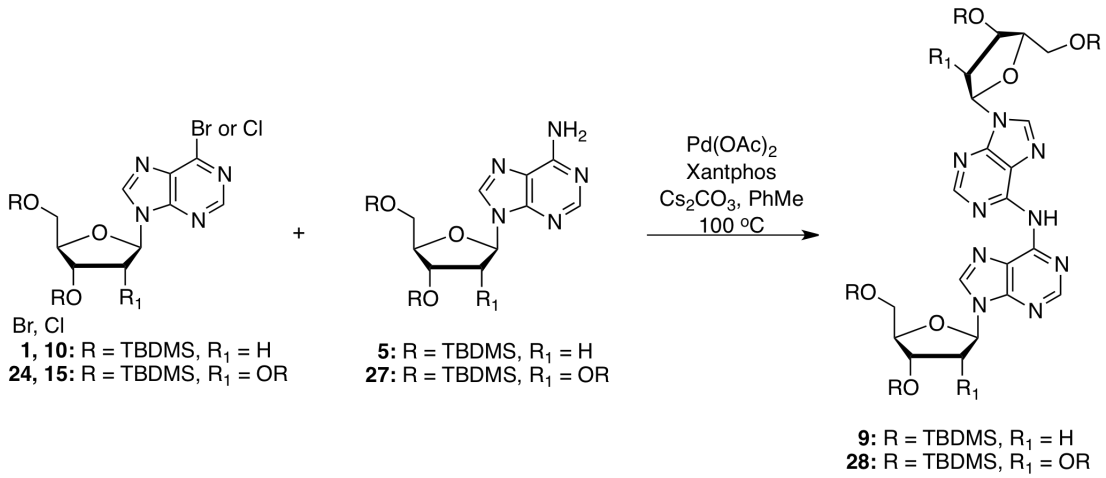

Entry	Partners	Conditions,[a] time[b]	Product: Yield (%)[c]
1	**1** + **5**	**A**, 1 h	**9**: 65
2	**24** + **27**	**A**, 1 h	**28**: 70
3	**1** + **5**	**B**, 1 h	**9**: 79
4	**24** + **27**	**B**, 1 h	**28**: 84
5	**10** + **5**	**B**, 1 h	**9**: 77
6	**15** + **27**	**B**, 1 h	**28**: 81

[a] Reactions were performed at a nucleoside concentration of 0.1 M in reaction solvent. Conditions **A**: 5 mol% $Pd(OAc)_2$/7.5 mol% **L3**/1.5 molar equiv Cs_2CO_3, 2.0 molar equiv amine, PhMe, 100 ºC. Condition **B**: 10 mol% $Pd(OAc)_2$/15 mol% **L3**/1.5 molar equiv Cs_2CO_3, 2.0 molar equiv amine PhMe, 100 ºC. [b] Reactions were monitored by TLC for consumption of halonucleoside. [c] Yields are of isolated and purified products.

Finally, in order to assess the biological properties of this group of modified nucleosides, the products were desilyated using known literature protocols where KF[57] or tris(dimethylamino)sulfonium difluorotrimethylsilicate (TASF)[58] served as sources of fluoride for cleavage of the TBDMS protecting groups (See Table 7 in the Experimental Section). These deprotected nucleosides were then subjected to a variety of antiviral assays.[59] The results indicated that though none expressed a marked activity at subtoxic concentrations, several showed a mild cytostatic and/or cytotoxic activity against several cell lines (CC_{50} or MIC in the 10-100 μg mL^{-1} range). Particularly, the desilylated product from **26h** (Figure 8) showed cytostatic activity against CRFK cells (CC_{50}: 4.32 μM). This compound can be further explored for other antiproliferative activity. Additionally, this may highlight the potential for a new array of modified nucleosides suited for antiviral analysis that would otherwise be unattainable or not readily accessible before the advent of Pd-catalyzed amination.

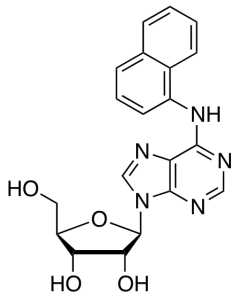

Figure 8. Desilyated Product N^6-(1-Naphthyl)adenosine showed Cytostatic Activity against CRFK Cells.

1.3 Conclusions

In conclusion, for access to a variety of N^6-aryl adenosine derivatives, the use of a Pd-catalyzed C–N bond formation reaction is highly effective. The work herein shows that for 6-bromopurine nucleosides, 5 mol% $Pd(OAc)_2$/7.5 mol% Xantphos with Cs_2CO_3 as base, in toluene, at 100 ºC was effective for reactions with aryl amines. Correspondingly, for 6-chloropurine nucleosides, 10 mol% $Pd(OAc)_2$/15 mol% Xantphos with Cs_2CO_3 in toluene, at 100 ºC was just as effective for the same reactions. While reactions were conducted at a higher catalytic loading with the chloropurine nucleosides, notably the bromopurine nucleoside reactions could be conducted at half the catalytic loading. The method demonstrates generality as electron-rich, electron-deficient, and electron-neutral, sterically hindered and unhindered aryl amines gave good to excellent yields. Silyl-protected nucleoside substrates appeared better compared to acetyl-protected nucleosides.[39] The method is eminently applicable to the efficient synthesis of biologically relevant deoxyadenosine (dA–dA) and the corresponding adenosine (A–A) dimers in higher yields than previously reported.[25] A comparison of the reactions of bromopurine and chloropurine nucleosides showed both to be effective substrates for amination reactions, and this work is the first detailed analysis of aryl aminations of 6-chloropurine nucleosides.

1.4 Experimental Section – Chapter 1

General Comments. Thin layer chromatography was performed on 250 μm glass-back silica plates and column chromatographic purifications were performed on 200-300 mesh silica gel. The Pd catalysts and all ligands (with the exception of 4-(diphenylphosphino)-9,9-dimethylxanthene) were purchased from commercial suppliers. All other reagents were obtained from commercial sources and were used without further purification. 1,4-Dioxane was distilled over $LiAlH_4$ and was freshly distilled over Na prior to use. Toluene was distilled over Na. Nucleoside substrates were prepared as described previously.[39,41,44-48] ^{1}H NMR spectra were recorded at 500 MHz in the solvents indicated (when $CDCl_3$ was used, it was deacidified by percolating the solvent through a bed of solid $NaHCO_3$ and basic alumina). All proton spectra are referenced to the residual solvent resonance. No attempt has been made to ascertain the position of the aryl amino proton (-N<u>H</u>-Ar) in the products. Therefore, this and the aromatic protons are collectively assigned as Ar-H. The sugar protons are numbered 1'-5' beginning at the anomeric carbon and proceeding via the carbon chain to the primary carbinol carbon.

General Method for C–N Bond Formation Under Conditions A. $Pd(OAc)_2$ (5 mol %), Xantphos (7.5 mol %), and Cs_2CO_3 (1.5 molar equiv) were premixed in a small volume of toluene in an oven-dried, screw cap vial equipped with a stirring bar. Bromo nucleoside (1 molar equiv, 0.08 mmol of **1** or **24**), aryl amine (2 molar equiv), and toluene were then added to the vial so that the final reaction mixture was 0.1 M in nucleoside concentration. The vial was flushed with nitrogen gas, sealed with a Teflon-lined cap, and placed in a sand bath that was maintained at 101-102 ^{o}C. The reactions were monitored by TLC. Upon completion, the mixtures were diluted with Et_2O (7 mL) and washed with brine (5 mL). The organic phase was separated, dried over Na_2SO_4, and concentrated. Products were purified by chromatography on a silica gel column using appropriate solvents (listed under individual headings below).

General Method for C–N Bond Formation Under Conditions B. $Pd(OAc)_2$ (10 mol%), Xantphos (15 mol%), and Cs_2CO_3 (1.5 molar equiv) were premixed in a small volume of toluene in an oven-dried, screw cap vial equipped with a stirring bar. Chloro nucleoside (1 molar equiv, 0.08 mmol of **10** or 0.085 mmol of **15**), amine (2 molar equiv), and toluene were then added to the vial so that the final reaction

mixture was 0.1M in nucleoside concentration. The vial was flushed with nitrogen gas, sealed with a Teflon-lined cap, and placed in a sand bath that was maintained at 101-102 ^{o}C. The reactions were monitored by TLC. Upon completion, the mixtures were diluted with Et_2O (7 mL) and washed with brine (5 mL). The organic phase was separated, dried over Na_2SO_4, and concentrated. Products were purified by chromatography on a silica gel column using appropriate solvents (listed under individual headings below).

NMR Data for the N^6-Aryl Adenosine Derivatives

3',5'-Di-*O*-(*tert*-butyldimethylsilyl)-N^6-(4-methylphenyl)-2'-deoxyadenosine (2a)[16]

Chromatography with 5% EtOAc in CH_2Cl_2 yielded **2a** as an orange-yellow oil. R_f (SiO_2/20% acetone in hexanes) = 0.48. ^{1}H NMR (500 MHz, $CDCl_3$): δ 8.50 (s, 1H, Ar-H), 8.17 (s, 1H, Ar-H), 7.65 (d, 2H, Ar-H, *J* = 8.1 Hz), 7.61 (s, 1H, Ar-H), 7.19 (d, 2H, Ar-H, *J* = 8.1 Hz), 6.48 (t, 1H, H-1', *J* = 6.4 Hz), 4.63–4.61 (m, 1H, H-3'), 4.03 (app q, 1H, H-4', J_{app} ~ 3.4 Hz), 3.89 (dd, 1H, H-5', *J* = 4.0, 11.1 Hz), 3.78 (dd, 1H, H-5', *J* = 2.9, 11.1 Hz), 2.66 (app quint, 1H, H-2', J_{app} ~ 6.3 Hz), 2.45 (ddd, 1H, H-2', *J* = 4.1, 5.9, 13.0 Hz) 2.34 (s, 3H, CH_3), 0.93 and 0.92 (2s, 18H, *tert*–Bu), 0.11 and 0.10 (2s, 12H, $SiCH_3$). ^{13}C NMR (125 MHz, $CDCl_3$): δ 152.8, 152.3, 149.1, 139.0, 135.9, 133.3, 129.5, 120.7, 87.9, 84.4, 71.9, 62.8, 41.4, 26.0, 25.8, 20.9, 18.4, 18.0, –4.6, –4.8, –5.4, –5.5.

3',5'-Di-*O*-(*tert*-butyldimethylsilyl)-N^6-(4-acetylphenyl)-2'-deoxyadenosine (2b)[16]

Chromatography with 10% acetone in CH_2Cl_2 yielded **2b** as a yellow-white solid. R_f (SiO_2/20% acetone in hexanes) = 0.29. ^{1}H NMR (500 MHz, $CDCl_3$): δ 8.57 (s, 1H, Ar-H), 8.24 (s, 1H, Ar-H), 8.15 (s, 1H, Ar-H) 7.99–7.94 (m, 4H, Ar-H), 6.48 (t, 1H, H-1', *J* = 6.3 Hz), 4.63–4.60 (m, 1H, H-3'), 4.02 (app q, 1H, H-4', J_{app} ~ 3.4 Hz), 3.89 (dd, 1H, H-5', *J* = 4.0, 11.2 Hz), 3.78 (dd, 1H, H-5', *J* = 2.9, 11.2 Hz), 2.65 (app quint, 1H, H-2', J_{app} ~ 6.2 Hz), 2.57 (s, 3H, $COCH_3$), 2.46 (ddd, 1H, H-2', *J* = 4.0, 6.0, 13.0 Hz), 0.92 and 0.91 (2s, 18H, *tert*–Bu), 0.10 and 0.09 (2s, 12H, $SiCH_3$). ^{13}C NMR (125 MHz, $CDCl_3$): δ 196.8, 152.5, 151.5, 149.4, 143.4, 139.8, 131.8, 129.8, 121.1, 118.9, 88.0, 84.5, 71.8, 62.7, 41.5, 26.3, 26.4 25.9, 25.7, 18.4, 18.0, –4.6, –4.8, –5.4, –5.5.

3',5'-Di-*O*-(*tert*-butyldimethylsilyl)-N^6-(3-cyanophenyl)-2'-deoxyadenosine (2c)[16]

Chromatography with 5% EtOAc in CH_2Cl_2 yielded **2c** as an orange-yellow oil. R_f (SiO_2/20% acetone in hexanes) = 0.33. ^{1}H NMR (500 MHz, $CDCl_3$): δ 8.57 (s, 1H, Ar-H), 8.47 (s, 1H, Ar-H), 8.26 (s, 1H, Ar-H) 8.12 (s, 1H, Ar-H) 7.91 (d, 1H, Ar-H, *J* = 6.9 Hz), 7.45 (t, 1H, Ar-H, *J* = 7.6 Hz), 7.36 (d, 1H, Ar-H, *J* = 7.5 Hz), 6.49 (t, 1H, H-1', *J* = 6.3 Hz), 4.66–4.61 (m, 1H, H-3'), 4.03 (app q, 1H, H-4', J_{app} ~ 3.2 Hz), 3.91 (dd, 1H, H-5', *J* = 4.1, 11.2 Hz), 3.79 (dd, 1H, H-5', *J* = 2.8, 11.2 Hz), 2.65 (app quint, 1H, H-2', J_{app} ~ 6.3 Hz), 2.48 (ddd, 1H, H-2', *J* = 4.8, 6.1, 13.0 Hz), 0.94 and 0.93 (2s, 18H, *tert*–Bu), 0.11 and 0.10 (2s, 12H, $SiCH_3$). ^{13}C NMR (125 MHz, $CDCl_3$): δ 152.5, 151.5, 149.4, 139.8, 129.7, 126.5, 123.8, 122.9, 120.8, 118.8, 113.0, 88.0, 84.6, 71.8, 62.7, 41.5, 25.9, 25.7, 18.4, 18.0, –4.6, –4.8, –5.4, –5.5.

3',5'-Di-*O*-(*tert*-butyldimethylsilyl)-N^6-(2-methylphenyl)-2'-deoxyadenosine (2g)

Chromatography with 5% EtOAc in CH_2Cl_2 yielded **2g** as an orange-yellow oil. R_f (SiO_2/20% acetone in hexanes) = 0.48. ^{1}H NMR (500 MHz, $CDCl_3$): δ 8.46 (s, 1H, Ar-H), 8.16 (s, 1H, Ar-H), 7.93 (dd, 1H, Ar-H, *J* = 2.7, 7.4 Hz), 7.52 (d, 1H, Ar-H, *J* = 9.3 Hz), 7.29–7.25 (m, 2H, Ar-H), 7.12 (t, 1H, Ar-H *J* = 7.4 Hz), 6.47 (t, 1H, H-1', *J* = 6.3 Hz), 4.63–4.61 (m, 1H, H-3'), 4.02 (app q, 1H, H-4', J_{app} ~ 3.2 Hz), 3.88 (dd, 1H, H-5', *J* = 4.2, 11.2 Hz), 3.78 (dd, 1H, H-5', *J* = 3.0, 11.2 Hz), 2.67 (app quint, 1H, H-2', J_{app} ~ 6.1 Hz), 2.45 (ddd, 1H, H-2', *J* = 3.9, 5.9, 12.7 Hz), 2.34 (s, 3H, CH_3), 0.92 and 0.91 (2s, 18H, *tert*–Bu), 0.10 and 0.09 (2s, 12H, $SiCH_3$). ^{13}C NMR (125 MHz, $CDCl_3$): δ 153.0, 152.9, 149.2, 139.1, 136.2, 130.9, 130.7, 126.7, 125.2, 124.0, 120.6, 87.9, 84.4, 71.9, 62.8, 41.2, 26.0, 25.8, 18.4, 18.1, 18.0, –4.6, –4.8, –5.4, –5.5. HRMS (ESI) calculated for $C_{29}H_{48}N_5O_3Si_2$ $[M + H]^+$ 570.3290, found 570.3298.

3',5'-Di-*O*-(*tert*-butyldimethylsilyl)-N^6-(2-methoxyphenyl)-2'-deoxyadenosine (2d)[16]

Chromatography with 5% EtOAc in CH_2Cl_2 yielded **2d** as an orange-yellow oil. R_f (SiO_2/20% acetone in hexanes) = 0.41. ^{1}H NMR (500 MHz, $CDCl_3$): δ 8.77–8.75 (m, 1H, Ar-H), 8.54 (s, 1H, Ar-H), 8.22 (s, 1H, Ar-H), 8.14 (s, 1H, Ar-H), 7.06–7.03 (m, 2H, Ar-H), 6.95–6.93 (m, 1H, Ar-H), 6.48 (t, 1H, H-1', *J* = 6.4 Hz), 4.63 (m, 1H, H-3'), 4.03 (app q, 1H, H-4', J_{app} ~ 3.4 Hz), 3.95 (s, 3H, OCH_3), 3.87 (dd, 1H, H-5', *J* = 4.6, 11.3 Hz), 3.78 (dd, 1H, H-5', *J* = 3.4, 11.3 Hz), 2.70 (app quint, 1H, H-2', J_{app} ~ 5.8 Hz), 2.45 (ddd, 1H, H-2', *J* = 3.7, 6.3, 13.1 Hz), 0.93 and 0.92 (2s, 18H, *tert*–Bu), 0.09 and 0.08 (2s, 12H, $SiCH_3$). ^{13}C NMR (125 MHz, $CDCl_3$): δ 152.7, 152.1, 149.1, 148.5, 139.0, 128.4, 122.8, 121.3, 120.9, 119.9, 110.0, 87.9, 84.4, 72.1, 62.9, 55.7, 41.1, 26.0, 25.8, 18.4, 18.0, –4.7, –4.8, –5.4, –5.5.

3',5'-Di-*O*-(*tert*-butyldimethylsilyl)-N^6-(1-naphthyl)-2'-deoxyadenosine (2h)

Chromatography with 5% EtOAc in CH_2Cl_2 yielded **2h** as an orange-yellow oil. R_f (SiO_2/20% acetone in hexanes) = 0.47. ^{1}H NMR (500 MHz, $CDCl_3$): δ 8.46 (s, 1H, Ar-H), 8.22 (s, 1H, Ar-H), 8.10–8.07 (m, 2H, Ar-H), 8.02 (s, 1H, Ar-H), 7.91 (dd, 1H, Ar-H, *J* = 3.4, 6.3 Hz), 7.75 (d, 1H, Ar-H, *J* = 8.3 Hz), 7.55 (t, 1H, Ar-H, *J* = 7.3 Hz), 7.53–7.50 (m, 2H, Ar-H), 6.50 (t, 1H, H-1', *J* = 6.3 Hz), 4.65-4.62 (m, 1H, H-3'), 4.04 (app q, 1H, H-4', J_{app} ~ 3.4 Hz), 3.90 (dd, 1H, H-5', *J* = 4.4, 11.2 Hz), 3.80 (dd, 1H, H-5', *J* = 2.9, 11.2 Hz), 2.69 (app quint, 1H, H-2', J_{app} ~ 6.8 Hz), 2.47 (ddd, 1H, H-2', *J* = 3.9, 5.9, 12.7 Hz), 0.93 and 0.92 (2s, 18H, *tert*–Bu), 0.11 and 0.10 (2s, 12H, $SiCH_3$). ^{13}C NMR (125 MHz, $CDCl_3$): δ 153.5, 153.0, 149.4, 139.3, 134.4, 133.2, 128.6, 128.3, 126.2, 126.1, 125.8, 121.6, 121.3, 120.9, 88.0, 84.5, 71.9, 62.8, 41.3, 26.0, 25.8, 18.4, 18.0, –4.6, –4.8, –5.3, –5.4. HRMS (ESI) calculated for $C_{32}H_{48}N_5O_3Si_2$ $[M + H]^+$ 606.3290, found 606.3281.

3',5'-Di-*O*-(*tert*-butyldimethylsilyl)-N^6-(2-fluorenyl)-2'-deoxyadenosine (2e)[16]

Chromatography with 5% EtOAc in CH_2Cl_2 yielded **2e** as a yellow foam. R_f (SiO_2/20% acetone in hexanes) = 0.41. ^{1}H NMR (500 MHz, $CDCl_3$): δ 8.56 (s, 1H, Ar-H), 8.21 (s, 1H, Ar-H), 8.18 (s, 1H, Ar-H), 7.89 (s, 1H, Ar-H), 7.77 (d, 1H, Ar-H, *J* = 8.2 Hz), 7.74 (d, 1H, Ar-H, *J* = 7.3 Hz), 7.67 (dd, 1H, Ar-H, *J* = 1.8, 8.2 Hz), 7.54 (d, 1H, Ar-H, *J* = 7.3 Hz), 7.37 (t, 1H, Ar-H, *J* = 7.3 Hz), 7.28–7.26 (m, 1H, Ar-H), 6.50 (t, 1H, H-1', *J* = 6.4 Hz), 4.65–4.62 (m, 1H, H-3'), 4.04 (app q, 1H, H-4', J_{app} ~ 3.7 Hz), 3.95 (s, 2H, CH_2), 3.90 (dd, 1H, H-5', *J* = 4.3, 11.3 Hz), 3.80 (dd, 1H, H-5', *J* = 3.0, 11.3 Hz), 2.67 (app quint, 1H, H-2', J_{app} ~ 6.4 Hz), 2.48 (ddd, 1H, H-2', *J* = 3.7, 6.1, 12.8 Hz), 0.93 and 0.92 (2s, 18H, *tert*–Bu), 0.12 and 0.11 (2s, 12H, $SiCH_3$). ^{13}C NMR (125 MHz, $CDCl_3$): δ 152.8, 152.2, 149.1, 144.4, 143.1, 141.5, 139.1, 137.6, 137.4, 126.7, 126.1, 124.9, 120.2, 119.4, 119.2, 117.2, 87.9, 84.5, 71.9, 62.8, 41.4, 37.1, 26.0, 25.8, 18.4, 18.0, –4.6, –4.9, –5.4, –5.5.

Deoxyadenosine-deoxyadenosine dimer (9)[25]

Chromatography with 5% EtOAc in CH_2Cl_2 yielded **9** as a yellow-white foam. R_f (SiO_2/20% acetone in hexanes) = 0.31. ^{1}H NMR (500 MHz, $CDCl_3$): δ 9.05 (s, 1H, Ar-H), 8.86 (s, 2H, Ar-H), 8.30 (s, 2H, Ar-H), 6.52 (d, 2H, H-1', *J* = 6.4 Hz), 4.64–4.62 (m, 2H, H-3'), 4.04 (d, 2H, H-4', *J* = 3.4 Hz), 3.89 (dd, 2H, H-5', *J* = 4.3, 11.3 Hz), 3.78 (dd, 2H, H-5', *J* = 3.1, 11.3 Hz), 2.69 (quintet, 2H, H-2', *J* = 6.4 Hz), 2.49 (app ddd,

2H, H-2', J_{app} ~ 4.0, 5.8, 13.1 Hz), 0.92 and 0.89 (3s, 36H, *tert*–Bu), 0.11 and 0.10 (2s, 24H, $SiCH_3$). ^{13}C NMR (125 MHz, $CDCl_3$): δ 152.9, 150.6, 149.9, 140.8, 122.7, 88.0, 84.6, 71.9, 62.8, 41.4, 26.0, 25.8, 18.4, 18.0, –4.6, –4.8, –5.4, –5.5. HRMS (ESI) calculated for $C_{44}H_{80}N_9O_6Si_4$ $[M + H]^+$ 942.5303, found 942.5304.

2',3',5'-Tri-*O*-(*tert*-butyldimethylsilyl)-N^6-(4-methylphenyl)adenosine (26a)

Chromatography with 5% EtOAc in hexanes yielded **26a** as a white solid. R_f (SiO_2/20% EtOAc in hexanes) = 0.42. ^1H NMR (500 MHz, $CDCl_3$): δ 8.48 (s, 1H, Ar-H), 8.19 (s, 1H, Ar-H), 7.68 (d, 2H, Ar-H, *J* = 8.3 Hz), 7.71 (s, 1H, Ar-H), 7.18 (d, 2H, Ar-H, *J* = 8.3 Hz), 6.06 (d, 1H, H-1', *J* = 5.4 Hz), 4.70 (t, 1H, H-2', *J* = 4.6 Hz), 4.32 (t, 1H, H-3', *J* = 3.6 Hz), 4.14 (app q, 1H, H-4', J_{app} ~ 3.4 Hz), 4.04 (dd, 1H, H-5', *J* = 3.9, 11.2 Hz), 3.79 (dd, 1H, H-5', *J* = 2.4, 11.2 Hz), 2.35 (s, 3H, CH_3), 0.96, 0.94 and 0.79 (3s, 27H, *tert*–Bu), 0.15, 0.14, 0.11, 0.10, –0.04 and –0.23 (6s, 18H, $SiCH_3$). ^{13}C NMR (125 MHz, $CDCl_3$): δ 152.8, 152.3, 149.4, 139.6, 136.0, 133.2, 129.5, 120.7, 120.5, 88.3, 85.6, 75.8, 72.1, 62.6, 26.1, 25.8, 25.7, 20.8, 18.5, 18.1, 17.8, –4.4, –4.7, –5.1, –5.4. HRMS (ESI) calculated for $C_{35}H_{62}N_5O_4Si_3$ $[M + H]^+$ 700.4104, found 700.4113.

2',3',5'-Tri-*O*-(*tert*-butyldimethylsilyl)-N^6-(4-acetylphenyl)adenosine (26b)

Chromatography with 20% EtOAc in hexanes yielded **26b** as a white solid. R_f (20% EtOAc in hexanes) = 0.12. ^1H NMR (500 MHz, $CDCl_3$): δ 8.58 (s, 1H, Ar-H), 8.27 (s, 1H, Ar-H), 8.01 (s, 1H, Ar-H), 8.00–7.95 (m, 4H, Ar-H), 6.08 (d, 1H, H-1', *J* = 5.4 Hz), 4.67 (t, 1H, H-2', *J* = 4.6 Hz), 4.32 (t, 1H, H-3', *J* = 3.9 Hz), 4.14 (app q, 1H, H-4', J_{app} ~ 3.2 Hz), 4.04 (dd, 1H, H-5', *J* = 3.9, 11.2 Hz), 3.80 (dd, 1H, H-5', *J* = 2.4, 11.2 Hz), 2.58 (s, 3H, CH_3), 0.96, 0.93 and 0.79 (3s, 27H, *tert*–Bu), 0.15, 0.14, 0.10, 0.10, –0.04 and –0.23 (6s, 18H, $SiCH_3$). ^{13}C NMR (125 MHz, $CDCl_3$): 196.8, 152.5, 151.5, 149.8, 143.4, 140.3, 131.7, 129.8, 121.1, 118.8, 88.3, 85.6, 76.0, 71.9, 62.5, 26.3, 25.8, 25.7, 25.6, 18.5, 18.1, 17.8, –4.4, –4.5, –4.7, –5.1, –5.3, –5.4. HRMS (ESI) calculated for $C_{36}H_{61}N_5O_5Si_3Na$ $[M + Na]^+$ 750.3873, found 750.3820.

2',3',5'-Tri-*O*-(*tert*-butyldimethylsilyl)-N^6-(3-cyanophenyl)adenosine (26c)

Chromatography with 10% EtOAc in hexanes yielded **26c** as a white solid. R_f (SiO_2/20% EtOAc in hexanes) = 0.24. ^1H NMR (500 MHz, $CDCl_3$): δ 8.56 (s, 1H, Ar-H), 8.48 (s, 1H, Ar-H), 8.28 (s, 1H, Ar-H), 7.90–7.88 (dd, 1H, Ar-H, *J* = 1.5, 8.3 Hz), 7.85 (s, 1H, Ar-H), 7.45 (t, 1H, Ar-H, *J* = 8.1 Hz), 7.36 (d, 1H,

Ar-H, *J* = 7.3 Hz), 6.08 (d, 1H, H-1', *J* = 4.9 Hz), 4.68 (t, 1H, H-2', *J* = 4.6 Hz), 4.32 (t, 1H, H-3', *J* = 3.9 Hz), 4.15 (app q, 1H, H-4', *J* ~ 3.2 Hz), 4.04 (dd, 1H, H-5', *J* = 3.9, 11.2 Hz), 3.80 (dd, 1H, H-5', *J* = 2.4, 11.2 Hz), 0.97, 0.93 and 0.79 (3s, 27H, *tert*–Bu), 0.15, 0.14, 0.11, 0.10, –0.03 and –0.23 (6s, 18H, $SiCH_3$). ^{13}C NMR (125 MHz, $CDCl_3$): δ 152.5, 151.5, 149.8, 140.4, 139.8, 129.7, 126.4, 123.6, 122.8, 120.9, 118.8, 113.0, 88.4, 85.6, 75.9, 71.9, 62.5, 26.1, 25.8, 25.6, 18.1, 17.8, –4.4, –4.7, –5.1, –5.4. HRMS (ESI) calculated for $C_{35}H_{58}N_6O_4Si_3Na$ $[M + Na]^+$ 733.3720, found 733.3695.

2',3',5'-Tri-*O*-(*tert*-butyldimethylsilyl)-N^6-(2-methylphenyl)adenosine (26g)

Chromatography with 10% EtOAc in hexanes yielded **26g** as a light yellow syrup. R_f (SiO_2/20% EtOAc in hexanes) = 0.43. ^1H NMR (500 MHz, $CDCl_3$): δ 8.45 (s, 1H, Ar-H), 8.18 (s, 1H, Ar-H), 8.02 (d, 1H, Ar-H, *J* = 7.8 Hz), 7.39 (s, 1H, Ar-H), 7.31–7.25 (m, 2H, Ar-H), 7.12 (app t, 1H, Ar-H, J_{app} ~ 7.6 Hz), 6.05 (d, 1H, H-1', *J* = 4.9 Hz), 4.74 (t, 1H, H-2', *J* = 4.6 Hz), 4.34 (t, 1H, H-3', *J* = 3.6 Hz), 4.14 (app q, 1H, H-4', J_{app} ~ 3.4 Hz), 4.04 (dd, 1H, H-5', *J* = 3.9, 11.2 Hz), 3.79 (dd, 1H, H-5', *J* = 2.4, 11.2 Hz), 2.38 (s, 3H, CH_3), 0.96, 0.94 and 0.79 (3s, 27H, *tert*–Bu), 0.14, 0.13, 0.11, 0.10, –0.03 and –0.22 (6s, 18H, $SiCH_3$). ^{13}C NMR (125 MHz, $CDCl_3$): δ 152.9, 152.8, 149.5, 139.7, 136.3, 130.7, 130.4, 126.7, 124.9, 123.5, 120.9, 88.3, 85.6, 75.6, 72.1, 62.6, 26.1, 25.8, 25.7, 18.5, 18.1, 18.0, 17.8, –4.4, –4.7, –5.1, –5.4. HRMS (ESI) calculated for $C_{35}H_{62}N_5O_4Si_3$ $[M + H]^+$ 700.4104, found 700.4094.

2',3',5'-Tri-*O*-(*tert*-butyldimethylsilyl)-N^6-(2-methoxyphenyl)adenosine (26d)

Chromatography with 5% EtOAc in hexanes yielded **26d** as a white solid. R_f (SiO_2/20% EtOAc in hexanes) = 0.38. ^1H NMR (500 MHz, $CDCl_3$): δ 8.81–8.75 (m, 1H, Ar-H), 8.53 (s, 1H, Ar-H), 8.24 (s, 1H, Ar-H), 8.14 (s, 1H, Ar-H), 7.08–7.01 (m, 2H, Ar-H), 6.97–6.92 (m, 1H, Ar-H), 6.05 (d, 1H, H-1', *J* = 5.9 Hz), 4.77 (t, 1H, H-2', *J* = 4.4 Hz), 4.33 (t, 1H, H-3', *J* = 3.2 Hz), 4.14 (app q, 1H, H-4', J_{app} ~ 3.4 Hz), 4.04 (dd, 1H, H-5', *J* = 4.4, 11.2 Hz), 3.95 (s, 3H, OCH_3), 3.79 (dd, 1H, H-5', *J* = 3.4, 11.2 Hz), 0.96, 0.94 and 0.78 (3s, 27H, *tert*–Bu), 0.14, 0.13, 0.12, 0.11, –0.05 and –0.27 (6s, 18H, $SiCH_3$). ^{13}C NMR (125 MHz, $CDCl_3$): δ 152.6, 152.1, 149.5, 148.4, 139.8, 128.5, 122.7, 121.4, 120.9, 119.7, 110.0, 88.2, 85.8, 75.5, 72.3, 62.8, 55.7, 26.1, 25.9, 25.7, 18.1, 17.8, –4.4, –4.6, –5.1, –5.3. HRMS (ESI) calculated for $C_{35}H_{62}N_5O_5Si_3$ $[M + H]^+$ 716.4053, found 716.4059.

2',3',5'-Tri-*O*-(*tert*-butyldimethylsilyl)-N^6-(1-naphthyl)adenosine (26h)

Chromatography with 5% EtOAc in hexanes yielded **26h** as a light brown solid. R_f (SiO_2/20% EtOAc in hexanes) = 0.25. ^{1}H NMR (500 MHz, $CDCl_3$): δ 8.45 (s, 1H, Ar-H), 8.25 (s, 1H, Ar-H), 8.15 (d, 1H, Ar-H, *J* = 7.3 Hz), 8.10–8.05 (m, 1H, Ar-H), 7.95 (s, 1H, Ar-H), 7.92–7.84 (m, 1H, Ar-H), 7.77 (d, 1H, Ar-H, *J* = 8.3 Hz), 7.56 (t, 1H, Ar-H, *J* = 7.8 Hz), 7.54–7.51 (m, 2H, Ar-H), 6.08 (d, 1H, H-1', *J* = 4.9 Hz), 4.75 (dd, 1H, H-2', *J* = 4.9 Hz), 4.35 (dd, 1H, H-3', *J* = 3.9 Hz), 4.16 (app q, 1H, H-4', J_{app} ~ 3.4 Hz), 4.06 (dd, 1H, H-5', *J* = 4.3, 11.2 Hz), 3.83 (dd, 1H, H-5', *J* = 2.9, 11.2 Hz), 0.97, 0.94 and 0.81 (3s, 27H, *tert*–Bu), 0.16, 0.15, 0.12, 0.11, –0.02 and –0.19 (6s, 18H, $SiCH_3$). ^{13}C NMR (125 MHz, $CDCl_3$): δ 153.4, 152.9, 149.7, 139.9, 134.4, 133.2, 128.7, 128.1, 126.2, 126.1, 125.7, 125.6, 121.5, 120.9, 88.4, 85.5, 75.7, 72.0, 62.5, 26.1, 25.8, 25.7, 18.5, 18.1, 17.8, –4.4, –4.7, –5.0, –5.3. HRMS (ESI) calculated for $C_{38}H_{62}N_5O_4Si_3$ $[M + H]^+$ 736.4104, found 736.4113.

2',3',5'-Tri-*O*-(*tert*-butyldimethylsilyl)-N^6-(2-fluorenyl)adenosine (26e)

Chromatography with 5% EtOAc in hexanes yielded **26e** as a yellow foam. R_f (SiO_2/20% EtOAc in hexanes) = 0.50. ^{1}H NMR (500 MHz, $CDCl_3$): ^{1}H NMR (500 MHz, $CDCl_3$): δ 8.55 (s, 1H, Ar-H), 8.22 (s, 1H, Ar-H), 8.20 (s, 1H, Ar-H), 7.92 (s, 1H, Ar-H), 7.77 (d, 1H, Ar-H, *J* = 8.2 Hz), 7.74 (d, 1H, Ar-H, *J* = 7.3 Hz), 7.68 (d, 1H, Ar-H, *J* = 7.9 Hz), 7.54 (d, 1H, Ar-H, *J* = 7.3 Hz), 7.36 (t, 1H, Ar-H, *J* = 7.3 Hz), 7.28 (d, 1H, Ar-H, *J* = 7.3 Hz), 6.08 (d, 1H, H-1', *J* = 5.5 Hz), 4.72 (t, 1H, H-2', *J* = 4.9 Hz), 4.33 (t, 1H, H-3', *J* = 3.7 Hz), 4.15 (app q, 1H, H-4', J_{app} ~ 3.1 Hz), 4.05 (dd, 1H, H-5', *J* = 3.9, 11.3 Hz), 3.95 (s, 2H, CH_2), 3.81 (dd, 1H, H-5', *J* = 2.4, 11.3 Hz), 0.97, 0.94 and 0.80 (3s, 27H, *tert*–Bu), 0.16, 0.15, 0.12, 0.11, –0.03 and –0.22 (6s, 18H, $SiCH_3$). ^{13}C NMR (125 MHz, $CDCl_3$): δ 152.8, 152.2, 149.4, 144.4, 143.1, 141.6, 139.7, 137.7, 137.3, 126.7, 126.1, 124.9, 120.7, 120.2, 119.4, 119.1, 117.0, 88.3, 85.7, 76.0, 72.1, 62.6, 37.1, 26.1, 25.9, 25.7, 19.0, 18.5, 18.1, 17.9, –4.4, –4.7, –5.1, –5.4. HRMS (ESI) calculated for $C_{41}H_{63}N_5O_4Si_3Na$ $[M + Na]^+$ 796.4080, found 796.4077.

2',3',5'-Tri-*O*-acetyl-N^6-(4-methylphenyl)adenosine

Chromatography with 20% acetone in hexanes yielded the title compound as a white foam. R_f (SiO_2/30% acetone in hexanes) = 0.16. ^{1}H NMR (500 MHz, $CDCl_3$): δ 8.50 (s, 1H, Ar-H), 7.98 (s, 1H, Ar-H), 7.71 (s, 1H, Ar-H), 7.63 (d, 2H, Ar-H, *J* = 8.3 Hz), 7.19 (d, 2H, Ar-H, *J* = 8.3 Hz), 6.21 (d, 1H, H-1', *J* = 5.4 Hz),

5.94 (t, 1H, H-2', J = 5.4 Hz), 5.68 (t, 1H, H-3', J = 4.9 Hz), 4.50–4.35 (m, 2H, H-4',5'), 4.38 (dd, 1H, H-5', J = 5.4, 13.2 Hz), 2.35 (s, 3H, CH_3), 2.15 (s, 3H, $OCOCH_3$), 2.14 (s, 3H, $OCOCH_3$), 2.10 (s, 3H, $OCOCH_3$). ^{13}C NMR (125 MHz, $CDCl_3$): δ 170.4, 169.6, 169.4, 153.3, 152.5, 149.2, 138.7, 135.6, 133.6, 129.6, 120.9, 120.6, 86.2, 80.3, 73.2, 70.6, 63.1, 20.9, 20.8, 20.6, 20.4.

Adenosine-adenosine dimer (28)

Chromatography with 15% EtOAc in hexanes yielded **28** as a white solid. R_f (SiO_2/20% EtOAc in hexanes) = 0.38. ^{1}H NMR (500 MHz, $CDCl_3$): δ 9.07 (s, 1H, Ar-H), 8.87 (s, 2H, Ar-H), 8.34 (s, 2H, Ar-H), 6.12 (d, 2H, H-1', J = 5.4 Hz), 4.69 (t, 2H, H-2', J = 4.9 Hz), 4.31 (t, 2H, H-3', J = 3.7 Hz), 4.15 (app q, 2H, H-4', J_{app} ~ 3.2 Hz), 4.04 (dd, 2H, H-5', J = 3.2, 11.2 Hz), 3.81 (dd, 2H, H-5', J = 2.9, 11.2 Hz), 0.96, 0.94 and 0.78 (3s, 54H, *tert*–Bu), 0.14, 0.13, 0.11, –0.05, –0.05 and –0.27 (6s, 36H, $SiCH_3$). ^{13}C NMR (125 MHz, $CDCl_3$): δ 153.0, 150.9, 149.9, 141.3, 122.6, 88.3, 85.8, 76.0, 72.2, 62.7, 26.0, 25.8, 25.6, 18.5, 18.1, 17.8, –4.4, –4.7, –5.1, –5.4. HRMS (ESI) calculated for $C_{56}H_{108}N_9O_8Si_6$ $[M + H]^+$ 1202.6931, found 1202.6944.

Desilylation Procedures

Using KF.

To the TBDMS-protected arylated nucleoside in MeOH was added KF (2 molar equiv/TBDMS group) and the mixture was stirred at 80 °C for 15–24 h. The mixture was evaporated to dryness and the residue was dissolved in a small volume of acetone and passed through a short silica gel plug. The product was obtained by elution with acetone.

Using TAS-F.

A 1.3M solution of TAS-F $[(Me_2N)_3S^+Me_3SiF_2^-]$ was prepared by dissolving TAS-F (*very hygroscopic*) in dry CH_3CN. A solution of the TBDMS-protected arylated nucleoside was dissolved in CH_3CN and was cooled to 0 °C. The TAS-F solution (1.5 molar equiv/TBDMS group) was added at 0 °C. The mixture was stirred at 0 °C for 30 min and then at room temperature for 24 h. The mixture was evaporated to dryness and crude products were purified by chromatography on silica gel.

Table 7. Substrates and Conditions used for the Desilylation Reactions

Entry	Substrates	Desilylation Conditions	Yield[a]
1	**2a**	KF, MeOH, 80 °C, 24 h	91%
2	**2b**	KF, MeOH, 80 °C, 24 h	55%
3	**2c**	KF, MeOH, 80 °C, 24 h	39%
4	**2g**	KF, MeOH, 80 °C, 24 h	96%
5	**2d**	KF, MeOH, 80 °C, 24 h	99%
6	**2h**	KF, MeOH, 80 °C, 24 h	99%
7	**26a**	KF, MeOH, 80 °C, 24 h	54%[b]
8	**26b**	TAS-F, CH_3CN, 24 h	89%[b]
9	**26c**	KF, MeOH, 80 °C, 24 h	62%[b]
10	**26g**	KF, MeOH, 80 °C, 24 h	80%[b]
11	**26d**	KF, MeOH, 80 °C, 24 h	76%[b]
12	**26h**	TAS-F, CH_3CN, 24 h	86%[b]

[a] Yields reported are of isolated and purified products. [b] Performed by Dr. P. Lagisetty.

^{1}H NMR data for the desilylated compounds

N^6-(4-Methylphenyl)-2'-deoxyadenosine

From 43 mg of **2a** the title compound was obtained as a yellow-white solid after chromatography on silica gel using CH_2Cl_2 followed by acetone. R_f (SiO_2/5% MeOH in CH_2Cl_2) = 0.11. ^{1}H NMR (500 MHz, acetone-d_6): δ 8.77 (s, 1H, Ar-H), 8.39 (s, 1H, Ar-H), 8.33 (s, 1H, Ar-H), 7.96 (d, 2H, Ar-H, *J* = 8.0 Hz), 7.21 (d, 2H, Ar-H, *J* = 8.0 Hz), 6.50 (dd, 1H, H-1', *J* = 6.0, 8.6 Hz), 5.39 (dd, 1H, OH, *J* = 3.2, 9.3 Hz), 4.68 (br s, 1H, H-3'), 4.46 (d, 1H, OH, *J* = 3.3 Hz), 4.12 (br d, 1H, H-4', *J* = 1.8 Hz), 3.85–3.82 (m, 1H, H-5'), 3.73 (br t, 1H, H-5', *J* = 9.2 Hz), 2.95 (ddd, 1H, H-2', *J* = 4.9, 8.2, 13.2 Hz), 2.40 (ddd, 1H, H-2', *J* = 1.8, 5.8, 13.2 Hz), 2.35 (s, 3H, CH_3).

N^6-(4-Acetylphenyl)-2'-deoxyadenosine

From 46 mg of **2b** the title compound was obtained as a yellow-white solid after chromatography on silica gel using CH_2Cl_2 followed by acetone. R_f (SiO_2/5% MeOH in CH_2Cl_2) = 0.13. ^{1}H NMR (500 MHz, acetone-d_6): δ 9.21 (s, 1H, Ar-H), 8.52 (s, 1H, Ar-H), 8.42 (s, 1H, Ar-H), 8.30 (d, 2H, Ar-H, *J* = 8.5 Hz), 8.05 (d, 2H, Ar-H, *J* = 8.5 Hz), 6.53 (dd, 1H, H-1', *J* = 5.9, 8.2 Hz), 5.20 (dd, 1H, OH, *J* = 3.4, 8.5 Hz), 4.69 (br s, 1H, H-3'), 4.48 (d, 1H, OH, *J* = 3.3 Hz), 4.13 (br d, 1H, H-4', *J* = 2.2 Hz), 3.85–3.82 (m, 1H, H-5'),

3.75 (br t, 1H, H-5', J = 8.7 Hz), 2.95 (ddd, 1H, H-2', J = 5.8, 8.7, 13.0 Hz), 2.59 (s, 3H, $COCH_3$), 2.43 (ddd, 1H, H-2', J = 1.8, 5.5, 13.0 Hz).

N^6-(3-Cyanophenyl)-2'-deoxyadenosine

From 35 mg of **2c** the title compound was obtained as a white solid after chromatography on silica gel using CH_2Cl_2 followed by acetone. R_f (SiO_2/5% MeOH in CH_2Cl_2) = 0.10. ^{1}H NMR (500 MHz, acetone-d_6): δ 9.22 (s, 1H, Ar-H), 8.70 (s, 1H, Ar-H), 8.52 (s, 1H, Ar-H), 8.42 (s, 1H, Ar-H), 8.38-8.37 (m, 1H, Ar-H), 7.62 (t, 1H, Ar-H, J = 7.7 Hz), 7.50 (d, 1H, Ar-H, J = 7.6 Hz), 6.53 (dd, 1H, H-1', J = 6.0, 8.2 Hz), 5.15 (dd, 1H, OH, J = 3.2, 8.6 Hz), 4.69 (br s, 1H, H-3'), 4.48 (d, 1H, OH, J = 3.1 Hz), 4.13 (br d, 1H, H-4', J = 2.1 Hz), 3.86–3.83 (m, 1H, H-5'), 3.75-3.72 (m, 1H, H-5'), 2.95 (m, 1H, H-2', ddd, 1H, H-2', J = 5.3, 8.1, 13.0 Hz), 2.43 (ddd, 1H, H-2', J = 2.1, 6.6, 13.0 Hz).

N^6-(2-Methylphenyl)-2'-deoxyadenosine

From 43 mg of **2g** the title compound was obtained as a pale yellow oil after chromatography on silica gel using CH_2Cl_2 followed by acetone. R_f (SiO_2/5% MeOH in CH_2Cl_2) = 0.13. ^{1}H NMR (500 MHz, acetone-d_6): δ 8.36 (s, 1H, Ar-H), 8.32 (s, 1H, Ar-H), 8.28 (s, 1H, Ar-H), 7.85 (d, 1H, Ar-H, J = 8.0 Hz), 7.32 (d, 1H, Ar-H, J = 7.5 Hz), 7.27 (t, 1H, Ar-H, J = 7.5 Hz), 7.17 (t, 1H, Ar-H, J = 7.4 Hz), 6.51 (dd, 1H, H-1', J = 5.9, 8.6 Hz), 5.47 (d, 1H, OH, J = 8.2 Hz), 4.68 (s, 1H, H-3'), 4.49 (s, 1H, OH), 4.13 (d, 1H, H-4', J = 1.8 Hz), 3.84 (d, 1H, H-5', J = 12.2 Hz), 3.73 (br t, 1H, H-5', J = 9.5 Hz), 2.95 (ddd, 1H, H-2', J = 5.3, 8.1, 13.4 Hz), 2.40 (ddd, 1H, H-2', J = 2.0, 5.7, 13.2 Hz), 2.38 (s, 3H, CH_3).

N^6-(2-Methoxyphenyl)-2'-deoxyadenosine

From 29 mg of **2d** the title compound was obtained as a yellow oil after chromatography on silica gel using CH_2Cl_2 followed by acetone. R_f (SiO_2/5% MeOH in CH_2Cl_2) = 0.14. ^{1}H NMR (500 MHz, acetone-d_6): δ 8.84 (dt, 1H, Ar-H, J = 2.8, 7.8 Hz), 8.48 (s, 1H, Ar-H), 8.39 (s, 1H, Ar-H), 8.38 (s, 1H, Ar-H), 7.14–7.03 (m, 3H, Ar-H), 6.53 (dd, 1H, H-1', J = 5.8, 8.6 Hz), 5.31 (dd, 1H, OH, J = 3.4, 9.2 Hz), 4.69 (br s, 1H, H-3'), 4.49 (d, 1H, OH, J = 3.5 Hz), 4.13 (br d, 1H, H-4', J = 2.0 Hz), 4.04 (s, 3H, OCH_3), 3.87–3.83 (m, 1H, H-5'), 3.74 (br t, 1H, H-5', J = 9.0 Hz), 2.96 (ddd, 1H, H-2', J = 5.5, 8.6, 13.6 Hz), 2.43 (ddd, 1H, H-2', J = 2.0, 5.8, 13.2 Hz).

N^6-(1-Naphthyl)-2'-deoxyadenosine

From 45 mg of **2h** the title compound was obtained as an orange oil after chromatography on silica gel using CH_2Cl_2 followed by acetone. R_f (SiO_2/5% MeOH in CH_2Cl_2) = 0.12. ^{1}H NMR (500 MHz, acetone-d_6 after exchange with MeOH-d_4): δ 9.02 (s, 1H, Ar-H), 8.36 (s, 1H, Ar-H), 8.23 (d, 1H, Ar-H, *J* = 3.1), 8.13 (d, 1H, Ar-H, *J* = 8.2 Hz), 8.01–7.96 (m, 2H, Ar-H), 7.87 (d, 1H, Ar-H, *J* = 8.2 Hz), 7.60 (t, 1H, Ar-H, *J* = 7.9 Hz), 7.57–7.55 (m, 2H, Ar-H), 6.53 (dd, 1H, H-1', *J* = 5.8, 8.7 Hz), 4.69 (d, 1H, H-3', *J* = 5.3 Hz), 4.14 (br d, 1H, H-4', *J* = 1.9 Hz), 3.85 (dd, 1H, H-5', *J* = 2.5, 12.3 Hz), 3.73 (br d, 1H, H-5', *J* = 12.3 Hz), 2.98 (ddd, 1H, H-2', *J* = 5.5, 8.7, 13.3 Hz), 2.42 (ddd, 1H, H-2'', *J* = 1.8, 5.8, 13.3 Hz).

***N*^{6}-(4-Methylphenyl)adenosine**

From 80 mg of **26a** the title compound was obtained as a white solid after chromatography on silica gel using 15% MeOH in CH_2Cl_2. R_f (SiO_2/10% MeOH in CH_2Cl_2) = 0.42. ^{1}H NMR (500 MHz, acetone-d_6): δ 8.80 (s, 1H, Ar-H), 8.41 (s, 1H, Ar-H), 8.35 (s, 1H, Ar-H), 7.95 (d, 2H, Ar-H, *J* = 7.7 Hz), 7.22 (d, 2H, Ar-H, *J* = 7.7 Hz), 6.0o (d, 1H, H-1', *J* = 6.5 Hz), 5.62 (d, 1H, OH, *J* = 8.5 Hz), 4.95 (t, 1H, H-2', *J* = 5.5 Hz), 4.77 (br, 1H, OH), 4.48 (br, 1H, OH), 4.41 (m, 1H, H-3'), 4.22 (m, 1H, H-4'), 3.86 (d, 1H, H-5', *J* = 12.5 Hz), 3.73 (app t, 1H, H-5', *J* ~ 10.2 Hz), 2.35 (s, 3H, CH_3).

***N*^{6}-(4-Acetylphenyl)adenosine**

From 95 mg of **26b** the title compound was obtained as a white solid after chromatography on silica gel using 15% MeOH in CH_2Cl_2. R_f (SiO_2/10% MeOH in CH_2Cl_2) = 0.18. ^{1}H NMR (500 MHz, DMSO-d_6): δ 10.38 (s, 1H, Ar-H), 8.63 (s, 1H, Ar-H), 8.52 (s, 1H, Ar-H), 8.20 (d, 2H, Ar-H, *J* = 8.5 Hz), 7.95 (d, 2H, Ar-H, *J* = 8.5 Hz), 5.99 (d, 1H, H-1', *J* = 5.9 Hz), 5.51 (d, 1H, OH, *J* = 5.9 Hz), 5.25–5.20 (m, 2H, H-2', OH), 4.64 (m, 1H, H-3'), 4.19 (m, 1H, H-4'), 3.99 (br, 1H, OH), 3.78–3.60 (m, 2H, H-5'), 2.55 (s, 3H, CH_3).

***N*^{6}-(3-Cyanophenyl)adenosine**

From 40 mg of **26c** the title compound was obtained as a white solid after chromatography on silica gel using 15% MeOH in CH_2Cl_2. R_f (SiO_2/10% MeOH in CH_2Cl_2) = 0.37. ^{1}H NMR (500 MHz, acetone-d_6): δ 9.24 (br s, 1H, Ar-H), 8.69 (s, 1H, Ar-H), 8.53 (s, 1H, Ar-H), 8.41 (s, 1H, Ar-H), 8.38 (d, 1H, Ar-H, *J* = 6.9 Hz), 7.62 (t, 1H, Ar-H, *J* = 7.9 Hz), 7.50 (d, 1H, Ar-H, *J* = 7.5 Hz), 6.04 (d, 1H, H-1', *J* = 6.5 Hz), 5.65 (br s, 1H, OH), 5.39 (br s, 1H, OH), 4.92 (t, 1H, H-2', *J* = 5.5 Hz), 4.43 (m, 1H, H–3'), 4.20 (m, 1H, H-4'), 3.93–3.83 (m, 2H, H-5', OH), 3.74 (d, 1H, H-5', *J* = 11.5 Hz).

N^6-(2-Methylphenyl)adenosine

From 78 mg of **26g** the title compound was obtained as a white solid after chromatography on silica gel using 15% MeOH in CH_2Cl_2. R_f (SiO_2/10% MeOH in CH_2Cl_2) = 0.29. ^{1}H NMR (500 MHz, acetone-d_6): δ 8.29 (s, 1H, Ar-H), 8.26 (s, 1H, Ar-H), 7.82 (d, 1H, Ar-H, *J* = 7.5 Hz), 7.29 (d, 1H, Ar-H, *J* = 7.0 Hz), 7.25 (t, 1H, Ar-H, *J* = 7.5 Hz), 7.15 (t, 1H, Ar-H, *J* = 7.5 Hz), 5.98 (d, 1H, H-1', *J* = 6.5 Hz), 5.12 (br, 1H, OH), 4.92 (t, 1H, H-2', *J* = 5.2 Hz), 4.38 (d, 1H, OH, *J* = 3.9 Hz), 4.19 (m, 1H, H-3'), 4.21 (m, 1H, H-4'), 4.16 (br, 1H, OH), 3.85 (d, 1H, H-5', *J* = 11.9 Hz), 3.70 (d, 1H, H-5', *J* = 11.9 Hz), 2.36 (s, 3H, CH_3).

N^6-(2-Methoxyphenyl)adenosine

From 90 mg of **26d** the title compound was obtained in as a white solid after chromatography on silica gel using 15% MeOH in CH_2Cl_2. R_f (SiO_2/10% MeOH in CH_2Cl_2) = 0.35. ^{1}H NMR (500 MHz, acetone-d_6 after exchange with MeOH-d_4): δ 8.84 (dd, 1H, Ar-H, *J* = 1.5, 8.3 Hz), 8.49 (s, 1H, Ar-H), 8.39 (s, 1H, Ar-H), 7.15-7.04 (m, 3H, Ar-H), 6.05 (d, 1H, H-1', *J* = 6.8 Hz), 4.95 (t, 1H, H-2', *J* = 6.0 Hz), 4.43 (br m, 1H, H-3'), 4.22 (m, 1H, H-4'), 4.04 (s, 3H, OCH_3), 3.87 (dd, 1H, H-5', *J* = 2.4, 12.2 Hz), 3.73 (br d, 1H, H-5', *J* = 12.2 Hz).

N^6-(1-Naphthyl)adenosine

From 65 mg of **26h** the title compound was obtained as a white solid after chromatography on silica gel using 15% MeOH in CH_2Cl_2. R_f (SiO_2/10% MeOH in CH_2Cl_2) = 0.29. ^{1}H NMR (500 MHz, acetone-d_6 after exchange with MeOH-d_4): δ 9.03 (s, 1H, Ar-H), 8.34 (br s, 1H, Ar-H), 8.24–8.25 (m, 1H, Ar-H), 8.13 (d, 1H, Ar-H, *J* = 8.3 Hz), 8.02–7.99 (m, 1H, Ar-H), 7.97 (t, 1H, Ar-H, *J* = 8.3 Hz), 7.89 (d, 1H, Ar-H, *J* = 8.3 Hz), 7.61 (t, 1H, Ar-H, *J* = 7.8 Hz), 7.56–7.55 (m, 2H, Ar-H), 6.03 (d, 1H, H-1', *J* = 6.4 Hz), 4.98 (m, 1H, H-2'), 4.42 (m, 1H, H-4'), 3.87 (d, 1H, H-5', *J* = 12.7 Hz), 3.72 (d, 1H, H-5', *J* = 12.7 Hz).

Biological Assays. All anti-viral assays were performed by Jan Balzarini and Erik De Clercq and co-workers, at Rega Institute for Medical Research, Minderbroedersstraat 10, B-3000, Leuven, Belgium. The antiviral assays, other than the anti-HIV assays, were based on inhibition of virus-induced cytopathicity in HEL [herpes simplex virus type 1 (HSV-1) (KOS), HSV-2 (G), vaccinia virus, vesicular stomatitis virus, cytomegalovirus (HCMV) and varicella-zoster virus (VZV)], Vero (parainfluenza-3, reovirus-1, Sindbis virus and Coxsackie B4), HeLa (vesicular stomatitis virus, Coxsackie virus B4, and respiratory syncytial virus), Crandel-Rees feline kidney (CRFK) [feline coronavirus (FIPV) and feline herpesvirus] or MDCK [influenza A (H1N1; H3N2) and influenza B] cell cultures. Confluent cell cultures (or nearly confluent for MDCK cells) in microtiter 96-well plates were inoculated with 100 $CCID_{50}$ of virus (1 $CCID_{50}$ being the virus dose to infect 50% of the cell cultures). After a 1 h virus adsorption period, residual virus was removed, and the cell cultures were incubated in the presence of varying concentrations (100, 20, 4, … µg/mL) of the test compounds. Viral cytopathicity was recorded as soon as it reached completion in the control virus-infected cell cultures that were not treated with the test compounds. The minimal cytotoxic concentration (MCC) of the compounds was defined as the compound concentration that caused a microscopically visible alteration of cell morphology. The CC_{50} was defined as the compound concentration that resulted in a 50% reduction of the MTT-directed (blue) viability staining of the (CRFK) cell cultures. The methodology of the anti-HIV assays was as follows: human MT-4 (~ 3×10^5 cells/cm^3) cells were infected with 100 $CCID_{50}$ of $HIV(III_B)$ or HIV-2(ROD)/mL and seeded in 200-µL wells of a microtiter plate containing appropriate dilutions of the test compounds. After 4 days of incubation at 37 °C, the viability of the cell cultures was determined with the MTT dye staining method.

Results of the Biological Testing

Table 8. Anti-Feline Corona Virus (FIPV) and Anti-Feline Herpes Virus Activity and Cytotoxicity in CRFK Cell Cultures[a]

Compound	CC_{50}[b] (μg/mL)	EC_{50}[c] (μg/mL) Feline Corona Virus (FIPV)	EC_{50}[c] (μg/mL) Feline Herpes Virus
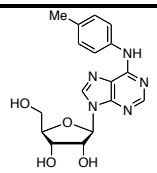	>100	>100	>100
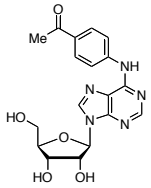	>100	>100	>100
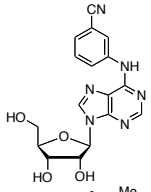	>100	>100	>100
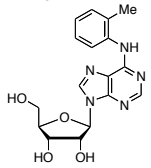	>100	>100	>100
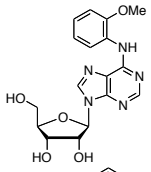	20.6	>20	>20
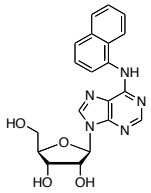	1.7	>0.8	>0.8
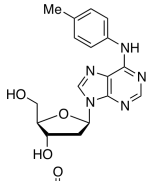	96.6	>20	>20
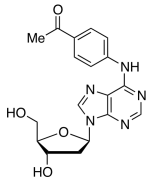	>100	>100	>100

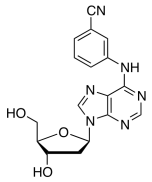	83.2	>20	>20
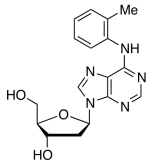	>100	>100	>100
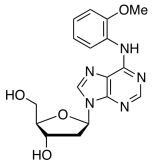	58.9	>20	>20
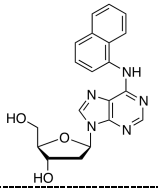	22.5	>20	>20
HHA	>100	1.8	2.4
UDA	>100	11.7	53.1
Ganciclovir	>25	>25	0.99

[a] CRFK cells: Crandell-Rees Feline Kidney cells. [b] 50% Cytotoxic concentration, as determined by measuring the cell viability with the colorimetric formazan-based MTS assay. [c] 50% Effective concentration, or concentration producing 50% inhibition of virus-induced cytopathic effect, as determined by measuring the cell viability with the colorimetric formazan-based MTS assay.

Table 9. Cytotoxicity and Antiviral Activity of Compounds in Human Embryonic (HEL) Cell Cultures

Compound	Minimum cytotoxic concentration[a] (μg/mL)	EC_{50}[b] (μg/mL)				
		Herpes simplex virus-1 (KOS)	Herpes simplex virus-2 (G)	Vaccinia virus	Vesicular stomatitis virus	Herpes simplex virus-1 TK^- KOS ACV^r
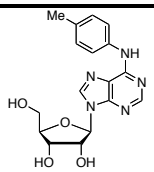	>100	>100	>100	>100	>100	>100
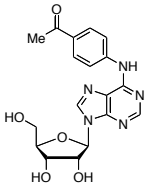	>100	>100	>100	>100	>100	>100
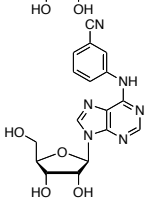	>100	>100	>100	>100	>100	>100

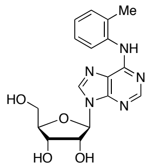	>100	>100	>100	>100	>100	>100
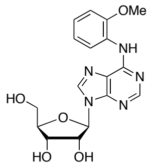	>100	>100	>100	>100	>100	>100
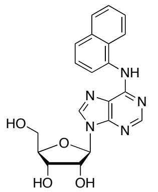	>100	>100	>100	>100	>100	>100
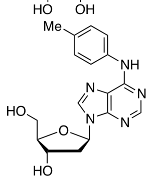	>100	>100	>100	>100	>100	>100
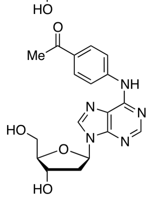	>100	>100	>100	>100	>100	>100
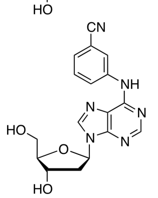	>100	>100	>100	>100	>100	>100
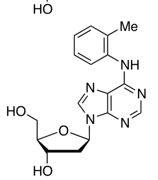	>100	>100	>100	>100	>100	>100
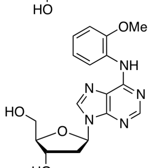	>100	>100	>100	>100	>100	>100
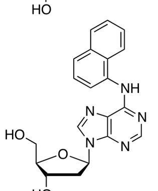	>100	>100	>100	>100	>100	>100
Brivudin	>83	0.016	16	1.9	>83	>83
Ribavirin	>83	46	>83	36	36	>83
Cidofovir	>70	0.28	0.28	>70	>70	1.12
Ganciclovir	>25	0.02	0.025	>25	>25	2.0

[a] Required to cause a microscopically detectable alteration of normal cell morphology. [b] Required to reduce virus-induced cytopathogenicity by 50%.

Table 10. Cytotoxicity and Antiviral Activity of Compounds in HeLa Cell Cultures

Compound	Minimum cytotoxic concentration[a] (µg/mL)	EC_{50}[b] (µg/mL) Vesicular stomatitis virus	Coxsackie virus B4	Respiratory syncytial virus
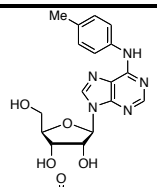	>100	>100	>100	>100
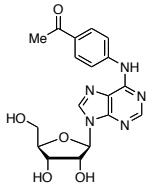	>100	>100	>100	>100
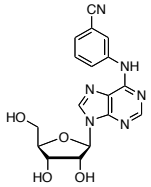	>100	>100	>100	>100
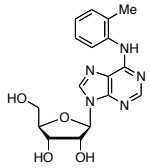	>100	>100	>100	>100
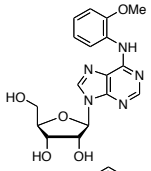	>100	>100	>100	45
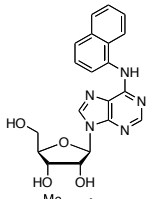	>100	>100	>100	>100
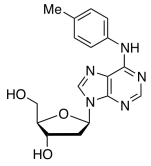	>100	>100	>100	>100

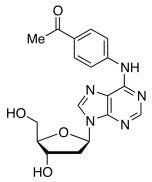	>100	>100	>100	>100
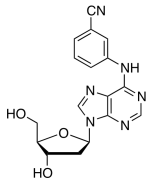	>100	>100	>100	>100
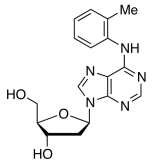	>100	>100	>100	>100
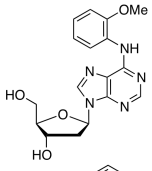	>100	>100	>100	>100
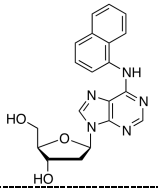	100	>20	>20	>20
DS-5000	>100	>100	45	0.8
(S)-DHPA	>52	>52	>52	>52
Ribavirin	>83	7.2	36	1.5

[a] Required to cause a microscopically detectable alteration of normal cell morphology. [b] Required to reduce virus-induced cytopathogenicity by 50%.

Table 11. Cytotoxicity and Antiviral Activity of Compounds in VERO Cell Cultures

Compound	Minimum cytotoxic concentration[a] (µg/mL)	EC_{50}[b] (µg/mL) Para-influenza -3 virus	Reovirus 1	Sindbis virus	Coxsackie virus B4	Punta Toro virus
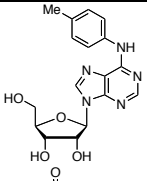	>100	>100	>100	>100	>100	>100
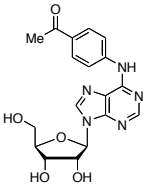	>100	>100	>100	>100	>100	>100

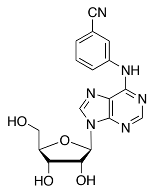	>100	>100	>100	>100	>100	>100
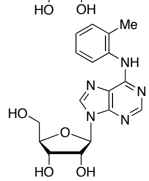	>100	>100	>100	>100	>100	>100
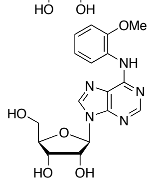	>100	>100	>100	>100	>100	>100
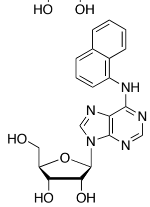	>100	>100	>100	>100	>100	>100
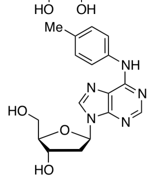	>100	>100	>100	>100	>100	>100
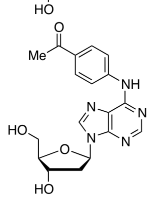	>100	>100	>100	>100	>100	>100
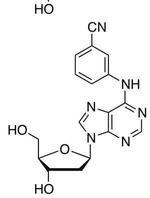	>100	>100	>100	>100	>100	>100
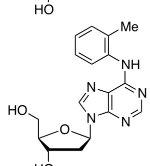	>100	>100	>100	>100	>100	>100
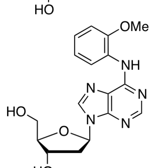	>100	>100	>100	>100	>100	>100
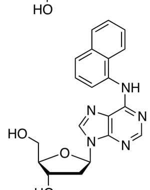	100	>20	>20	>20	>20	>20

DS-5000	>100	>100	>100	4	20	12
(S)-DHPA	>52	>52	>52	>52	>52	>52
Ribavirin	>83	36	>83	>83	>83	36

[a] Required to cause a microscopically detectable alteration of normal cell morphology. [b] Required to reduce virus-induced cytopathogenicity by 50%.

1.5 Appendix

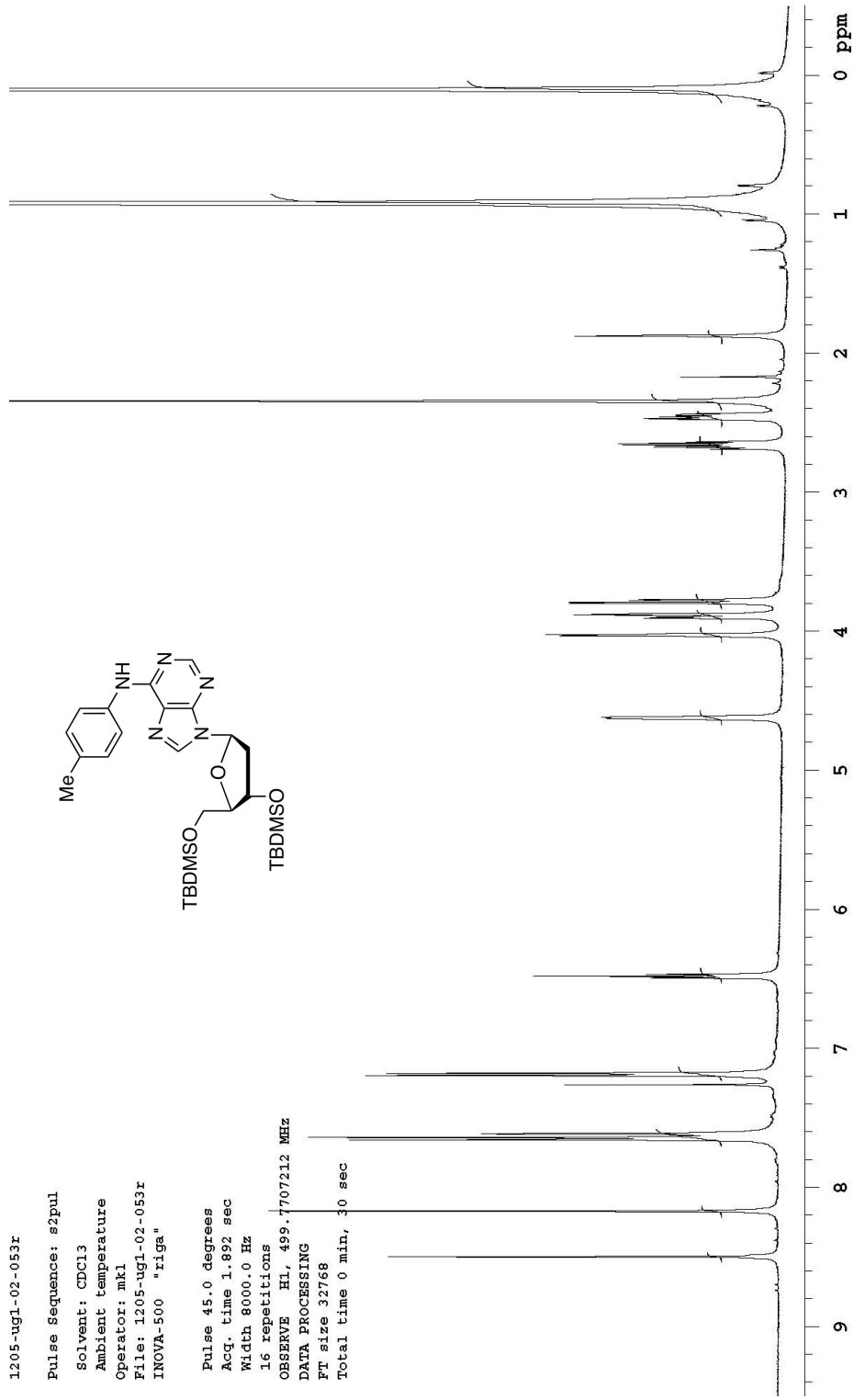
1205-ug1-02-053r
Pulse Sequence: s2pul
Solvent: CDCl3
Ambient temperature
Operator: mkl
File: 1205-ug1-02-053r
INOVA-500 "riga"
Pulse 45.0 degrees
Acq. time 1.892 sec
Width 8000.0 Hz
16 repetitions
OBSERVE H1, 499.7707212 MHz
DATA PROCESSING
FT size 32768
Total time 0 min, 30 sec
NH
N
N
N
N
O
Me
TBDMSO
TBDMSO
9
8
7
6
5
4
3
2
1
0 ppm

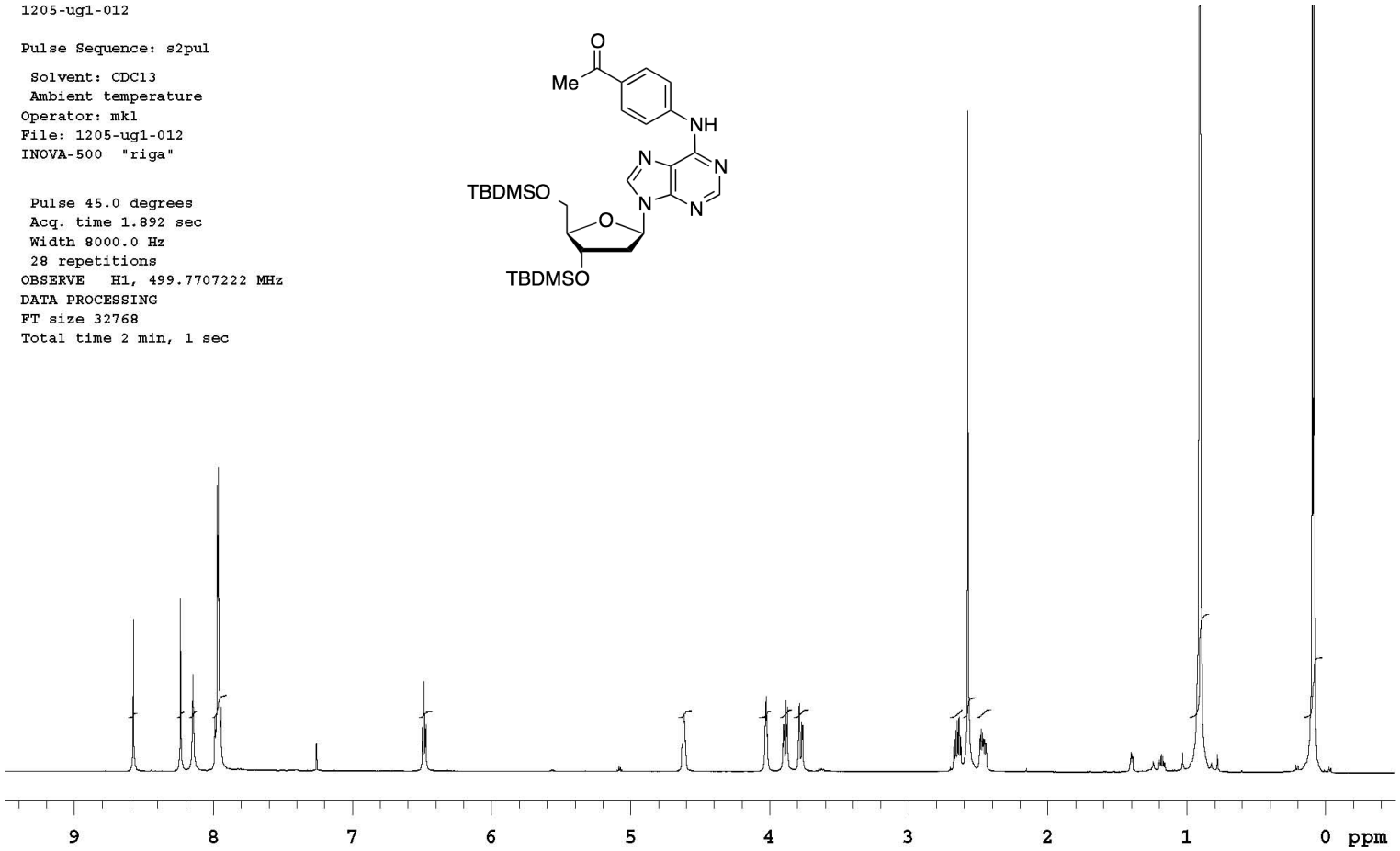
1205-ug1-012
Pulse Sequence: s2pul
Solvent: CDCl3
Ambient temperature
Operator: mkl
File: 1205-ug1-012
INOVA-500 "riga"
Pulse 45.0 degrees
Acq. time 1.892 sec
Width 8000.0 Hz
28 repetitions
OBSERVE H1, 499.7707222 MHz
DATA PROCESSING
FT size 32768
Total time 2 min, 1 sec
O
Me
NH
N
N
N
N
TBDMSO
O
TBDMSO
9
8
7
6
5
4
3
2
1
0 ppm

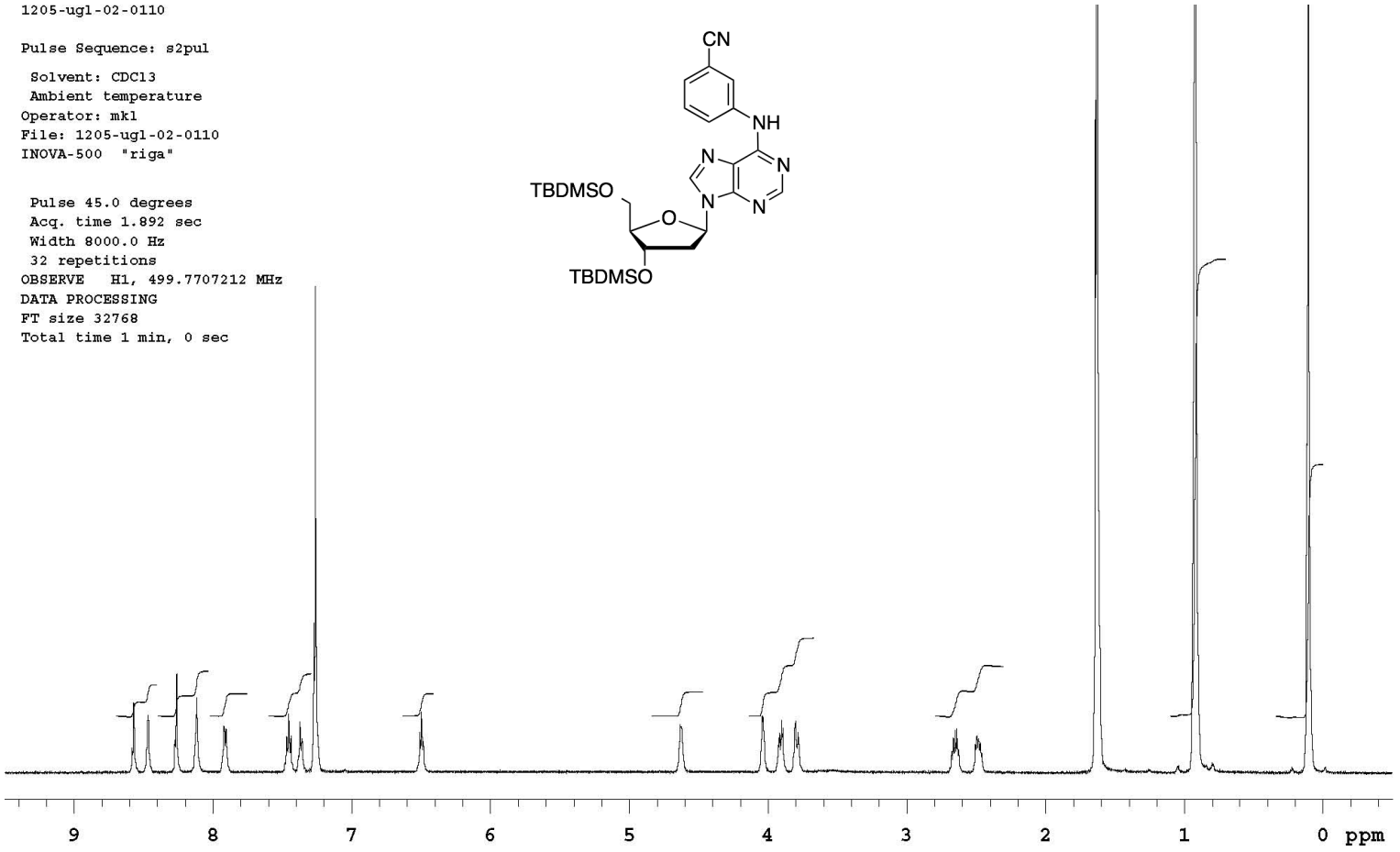
1205-ugl-02-0110
Pulse Sequence: s2pul
Solvent: CDCl3
Ambient temperature
Operator: mkl
File: 1205-ugl-02-0110
INOVA-500 "riga"
Pulse 45.0 degrees
Acq. time 1.892 sec
Width 8000.0 Hz
32 repetitions
OBSERVE H1, 499.7707212 MHz
DATA PROCESSING
FT size 32768
Total time 1 min, 0 sec
CN
NH
N
N
N
N
TBDMSO
O
TBDMSO
9
8
7
6
5
4
3
2
1
0 ppm

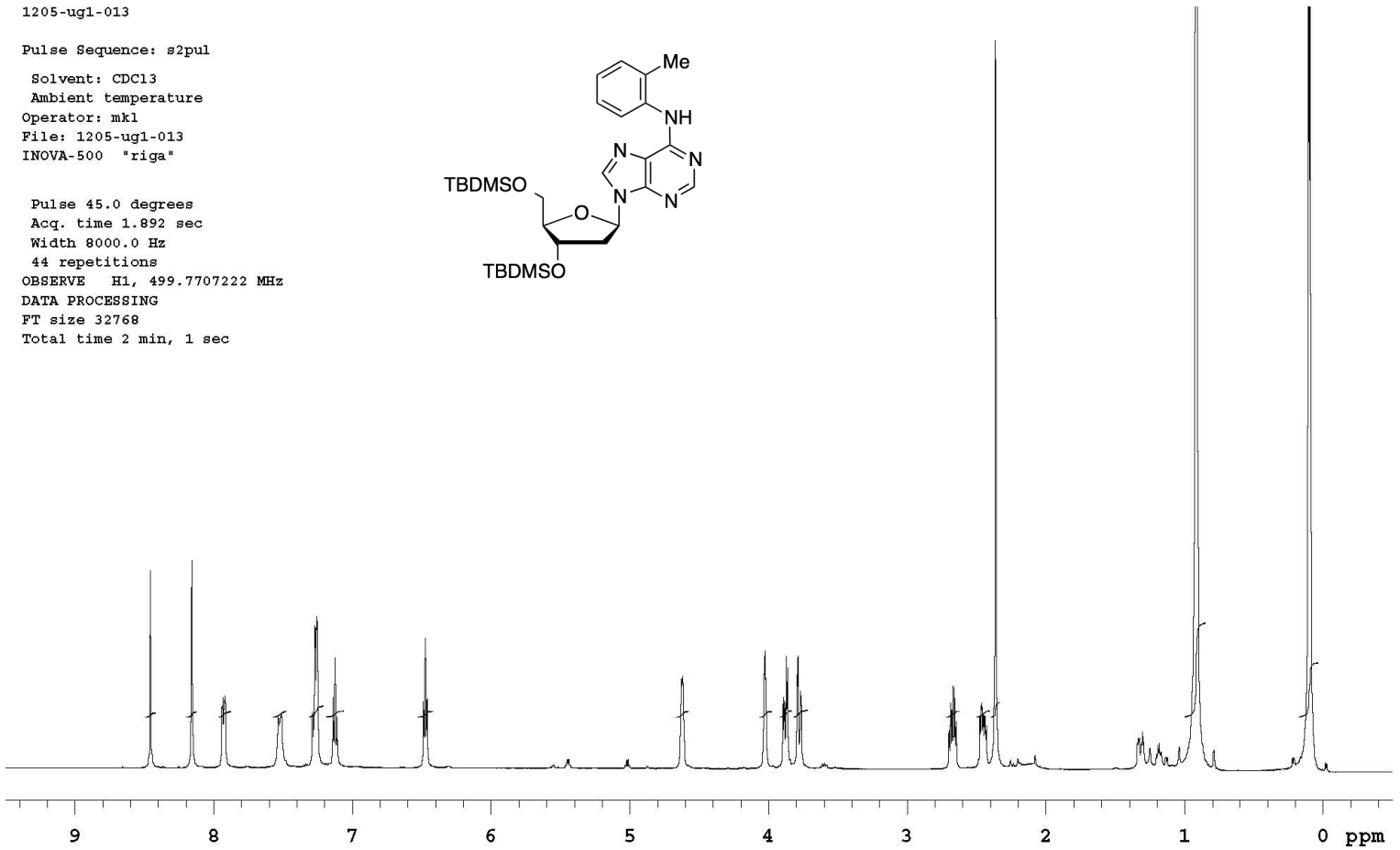
1205-ug1-013
Pulse Sequence: s2pul
Solvent: CDCl3
Ambient temperature
Operator: mkl
File: 1205-ug1-013
INOVA-500 "riga"
Pulse 45.0 degrees
Acq. time 1.892 sec
Width 8000.0 Hz
44 repetitions
OBSERVE H1, 499.7707222 MHz
DATA PROCESSING
FT size 32768
Total time 2 min, 1 sec
Me
NH
N
N
N
N
TBDMSO
O
TBDMSO
9
8
7
6
5
4
3
2
1
0 ppm

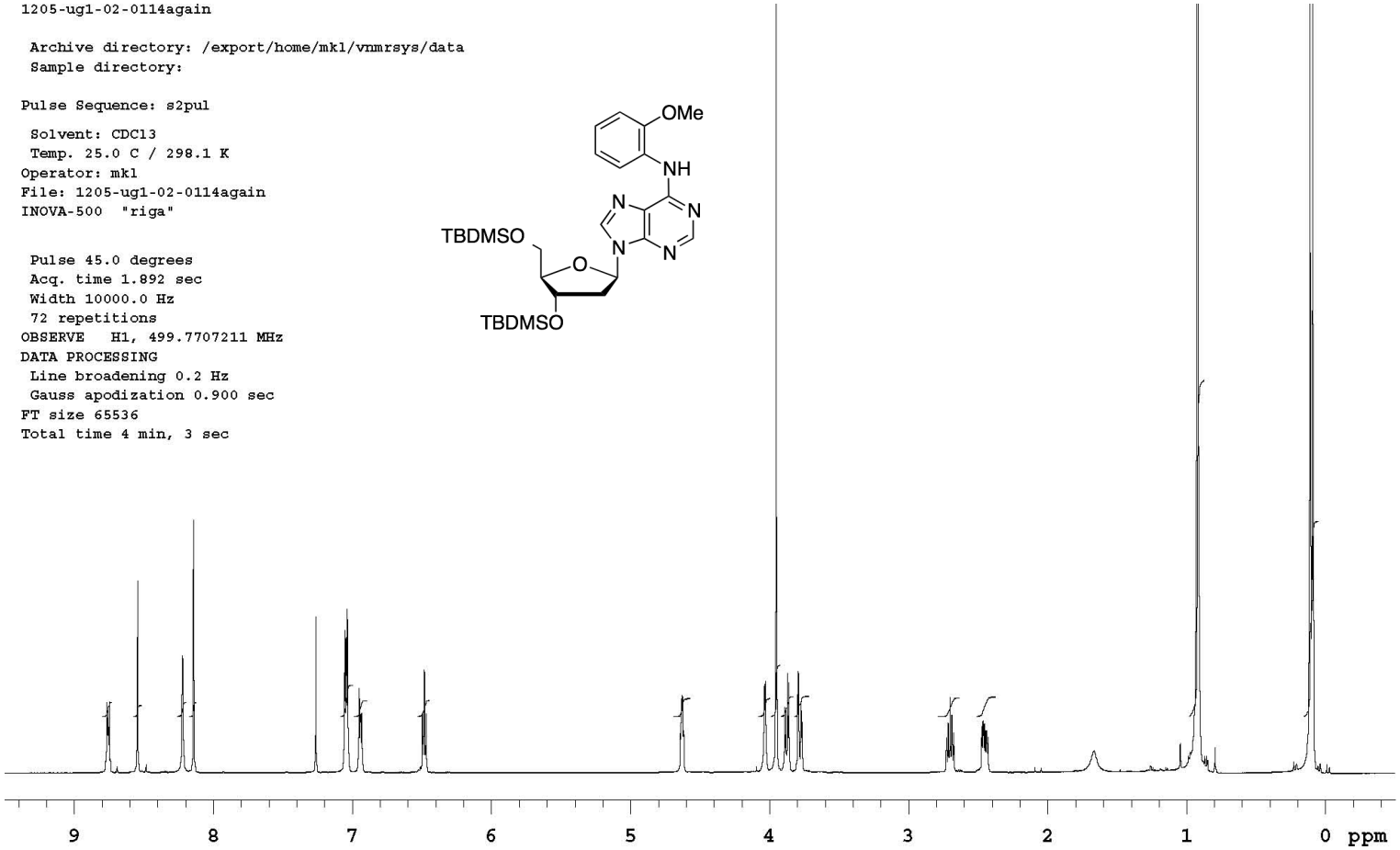
1205-ug1-02-0114again
Archive directory: /export/home/mkl/vnmrsys/data
Sample directory:
Pulse Sequence: s2pul
Solvent: CDCl3
Temp. 25.0 C / 298.1 K
Operator: mkl
File: 1205-ug1-02-0114again
INOVA-500 "riga"
Pulse 45.0 degrees
Acq. time 1.892 sec
Width 10000.0 Hz
72 repetitions
OBSERVE H1, 499.7707211 MHz
DATA PROCESSING
Line broadening 0.2 Hz
Gauss apodization 0.900 sec
FT size 65536
Total time 4 min, 3 sec
OMe
NH
N
N
N
N
TBDMSO
O
TBDMSO
9
8
7
6
5
4
3
2
1
0 ppm

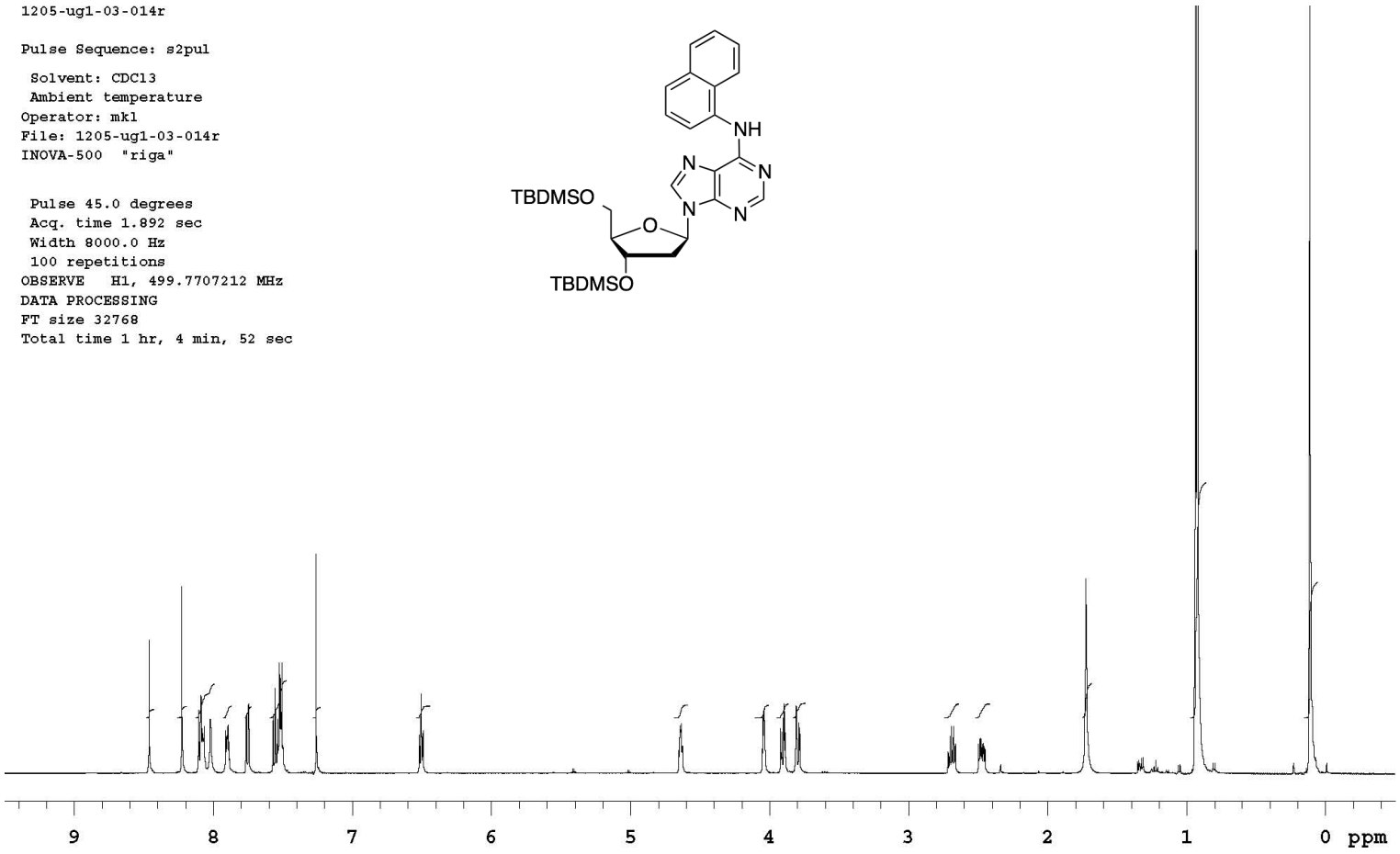
1205-ug1-03-014r
Pulse Sequence: s2pul
Solvent: CDCl3
Ambient temperature
Operator: mkl
File: 1205-ug1-03-014r
INOVA-500 "riga"
Pulse 45.0 degrees
Acq. time 1.892 sec
Width 8000.0 Hz
100 repetitions
OBSERVE H1, 499.7707212 MHz
DATA PROCESSING
FT size 32768
Total time 1 hr, 4 min, 52 sec
NH
N
N
N
N
O
TBDMSO
TBDMSO
9
8
7
6
5
4
3
2
1
0 ppm

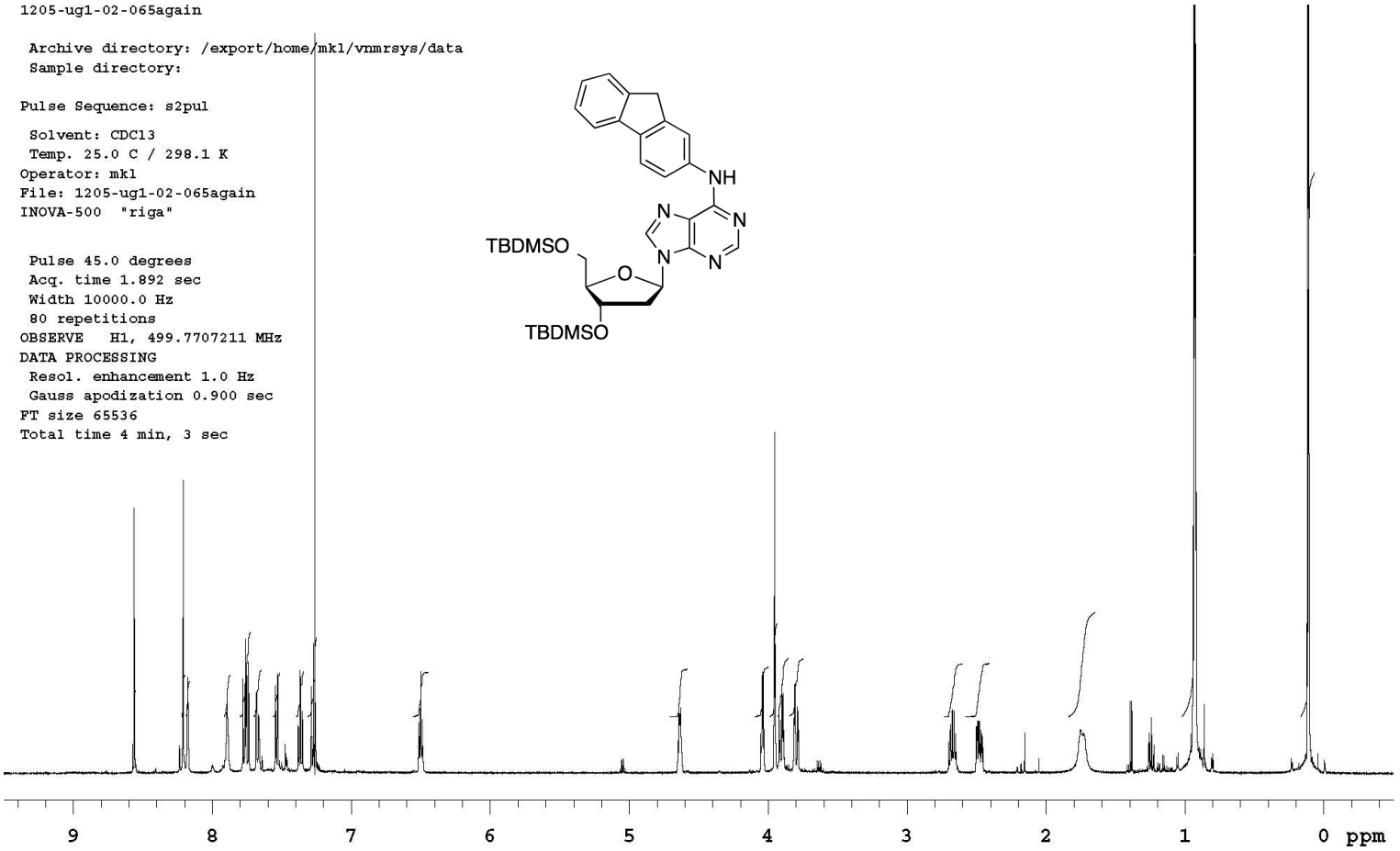
1205-ug1-02-065again
Archive directory: /export/home/mkl/vnmrsys/data
Sample directory:
Pulse Sequence: s2pul
Solvent: CDCl3
Temp. 25.0 C / 298.1 K
Operator: mkl
File: 1205-ug1-02-065again
INOVA-500 "riga"
Pulse 45.0 degrees
Acq. time 1.892 sec
Width 10000.0 Hz
80 repetitions
OBSERVE H1, 499.7707211 MHz
DATA PROCESSING
Resol. enhancement 1.0 Hz
Gauss apodization 0.900 sec
FT size 65536
Total time 4 min, 3 sec
NH
N
N
N
N
O
TBDMSO
TBDMSO
9
8
7
6
5
4
3
2
1
0 ppm

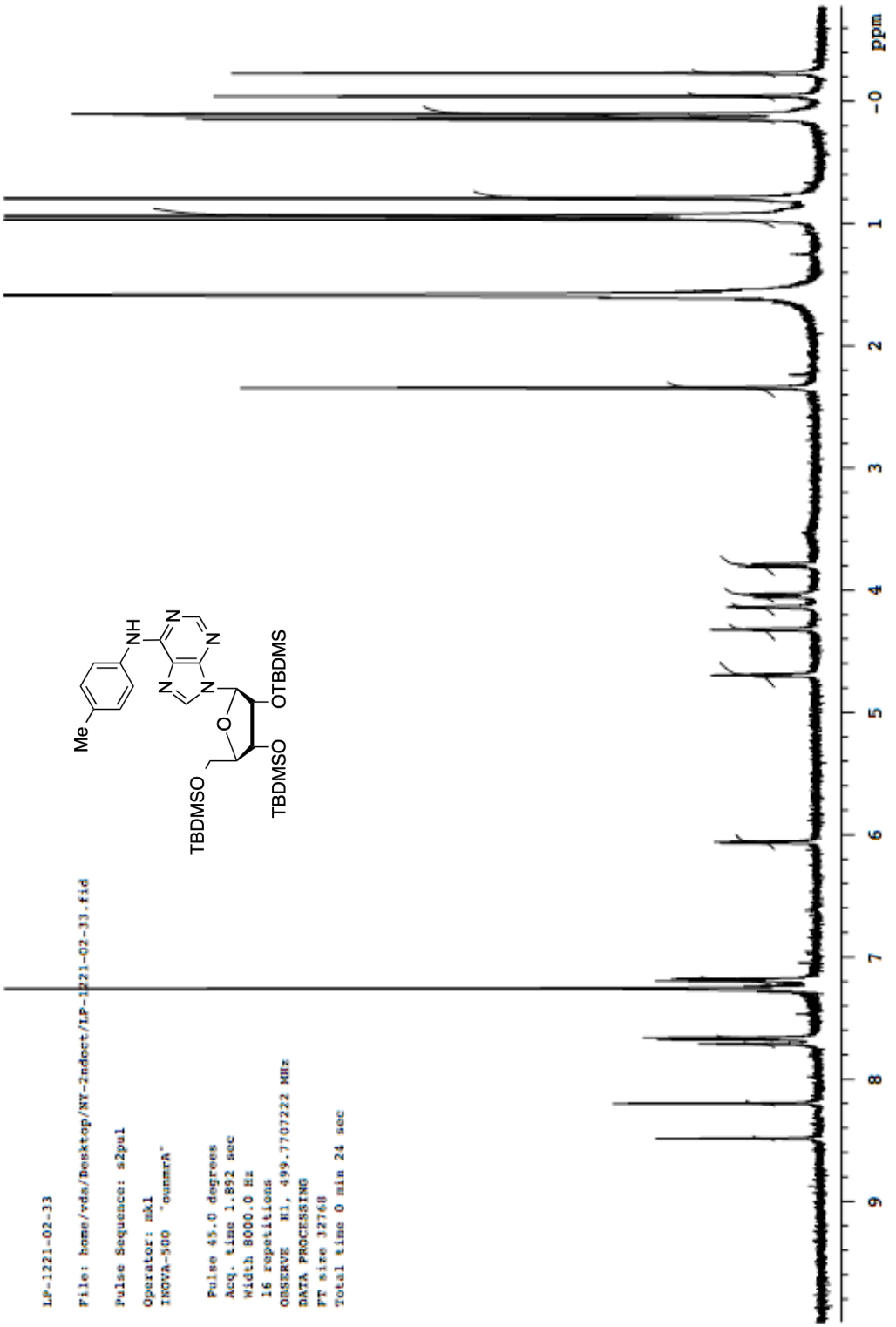
LP-1221-02-33
File: home/vds/Desktop/NY-2ndoct/LP-1221-02-33.fid
Pulse Sequence: s2pul
Operator: mkl
INOVA-500 "ommrA"
Pulse 45.0 degrees
Acq. time 1.892 sec
Width 8000.0 Hz
16 repetitions
OBSERVE H1, 499.7707222 MHz
DATA PROCESSING
FT size 32768
Total time 0 min 24 sec
Me
NH
N
N
N
N
O
TBDMSO
TBDMSO
OTBDMS
9
8
7
6
5
4
3
2
1
-0
ppm

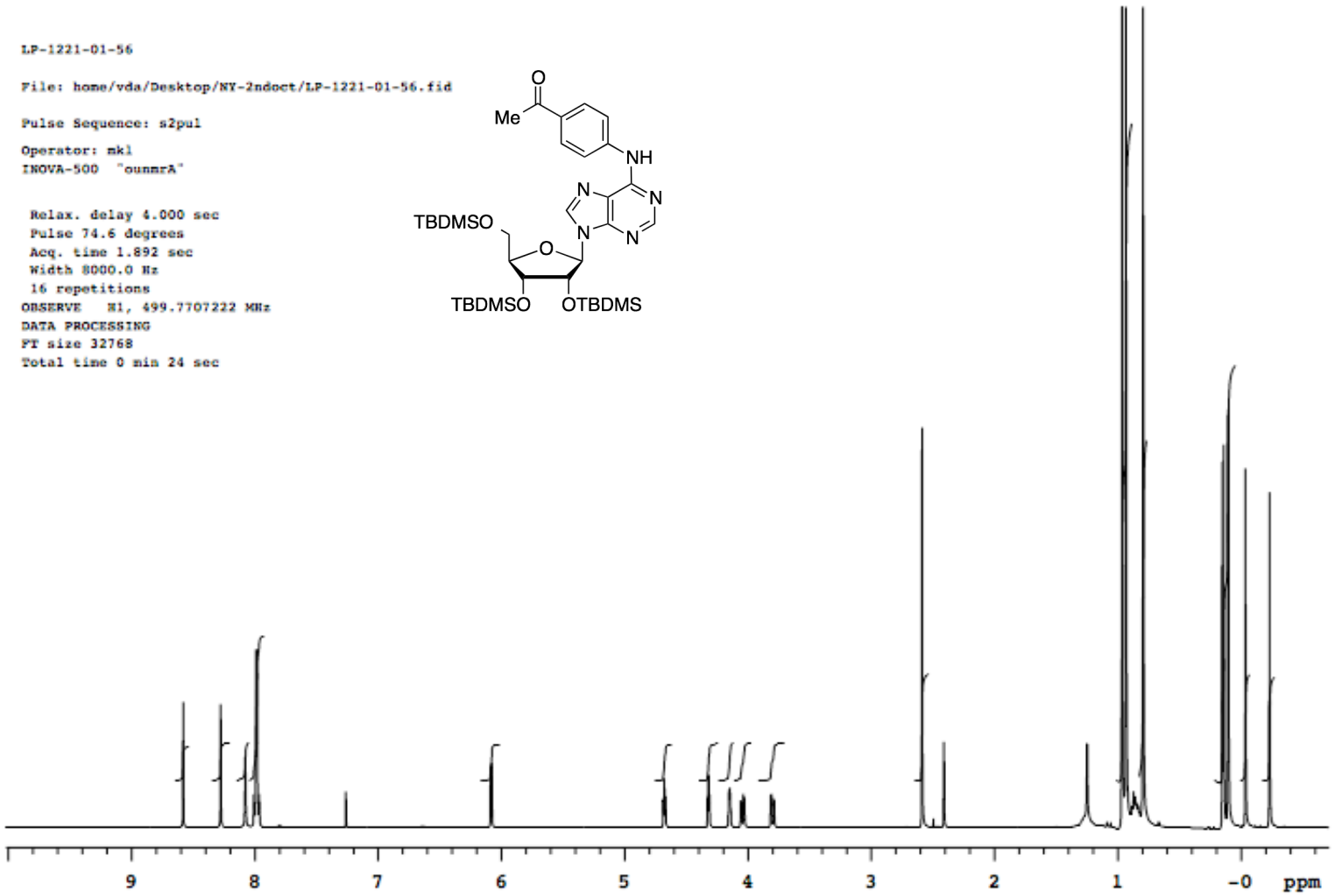
LP-1221-01-56
File: home/vda/Desktop/NY-2ndoct/LP-1221-01-56.fid
Pulse Sequence: s2pul
Operator: mkl
INOVA-500 "ounmrA"
Relax. delay 4.000 sec
Pulse 74.6 degrees
Acq. time 1.892 sec
Width 8000.0 Hz
16 repetitions
OBSERVE H1, 499.7707222 MHz
DATA PROCESSING
FT size 32768
Total time 0 min 24 sec
Me
O
NH
N
N
N
N
TBDMSO
O
TBDMSO
OTBDMS
9
8
7
6
5
4
3
2
1
-0
ppm

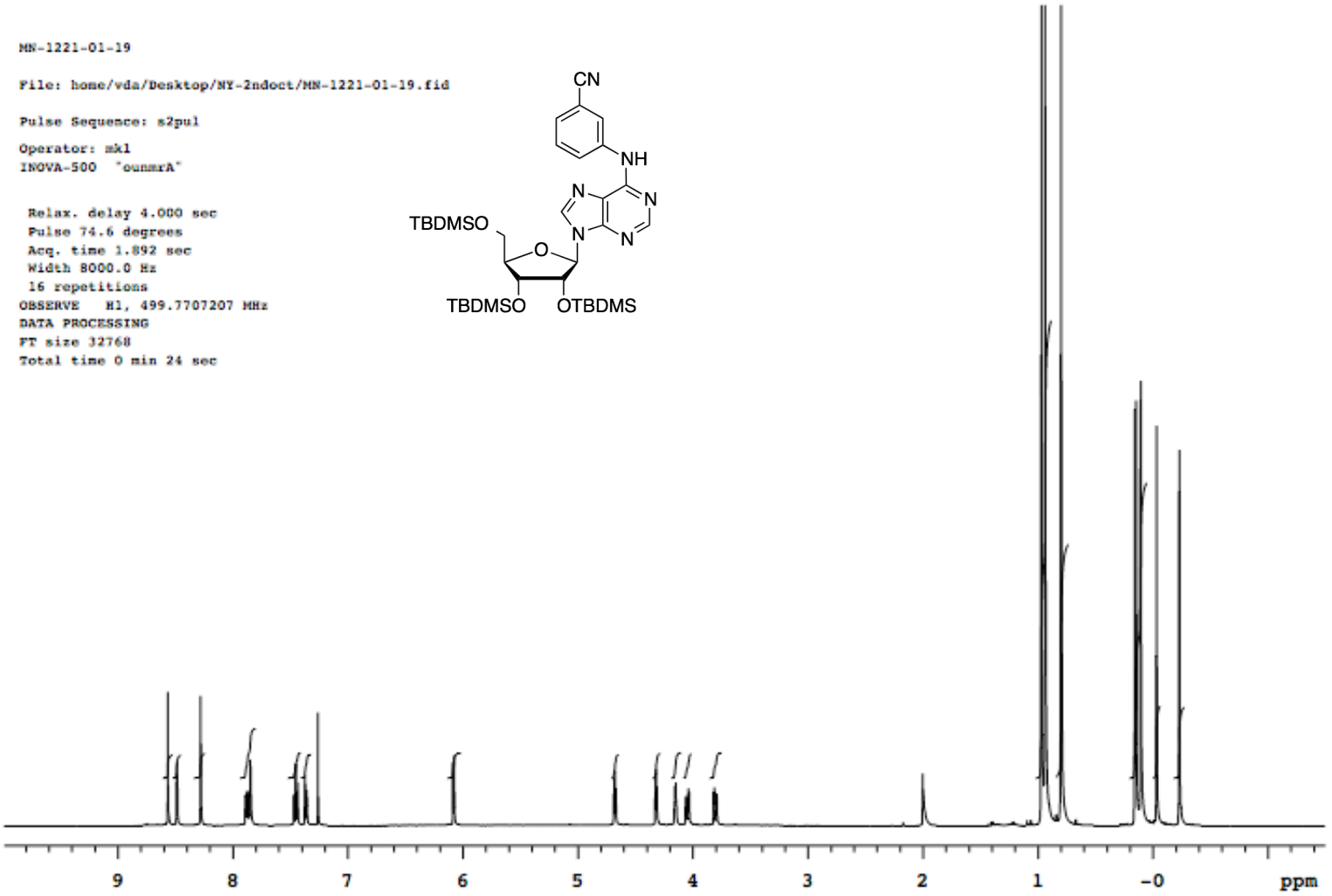
MN-1221-01-19
File: home/vda/Desktop/NY-2ndoct/MN-1221-01-19.fid
Pulse Sequence: s2pul
Operator: mkl
INOVA-500 "ounmrA"
Relax. delay 4.000 sec
Pulse 74.6 degrees
Acq. time 1.892 sec
Width 8000.0 Hz
16 repetitions
OBSERVE H1, 499.7707207 MHz
DATA PROCESSING
FT size 32768
Total time 0 min 24 sec
CN
NH
N
N
N
N
TBDMSO
O
TBDMSO
OTBDMS
9
8
7
6
5
4
3
2
1
-0
ppm

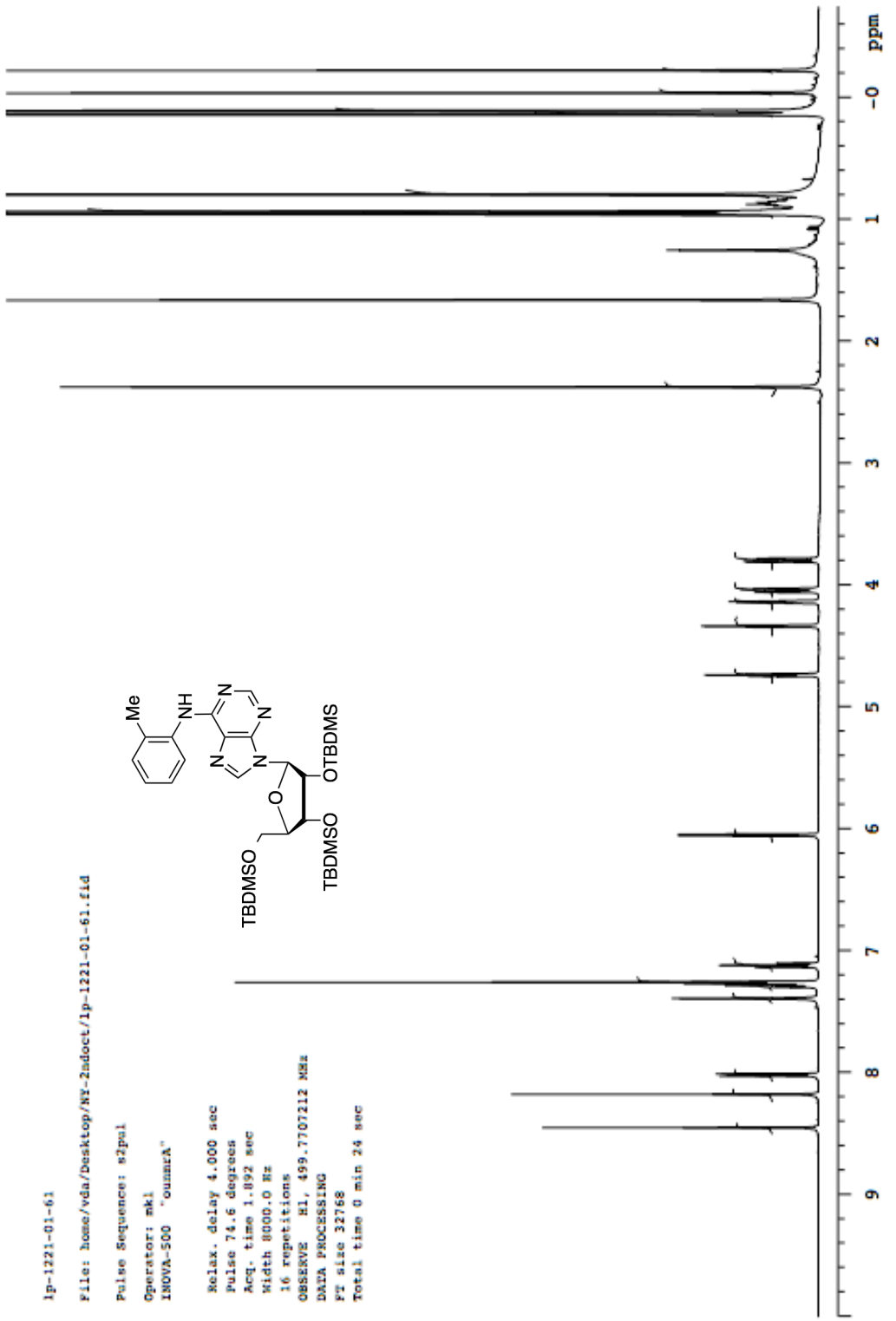
1p-1221-01-61
File: home/vda/Desktop/NY-2adoct/1p-1221-01-61.fid
Pulse Sequence: s2pul
Operator: mkl
INOVA-500 "ouamrA"
Relax. delay 4.000 sec
Pulse 74.6 degrees
Acq. time 1.892 sec
Width 8000.0 Hz
16 repetitions
OBSERVE H1, 499.7707212 MHz
DATA PROCESSING
FT size 32768
Total time 0 min 24 sec
Me
NH
N
N
N
N
O
TBDMSO
TBDMSO
OTBDMS
9
8
7
6
5
4
3
2
1
-0
ppm

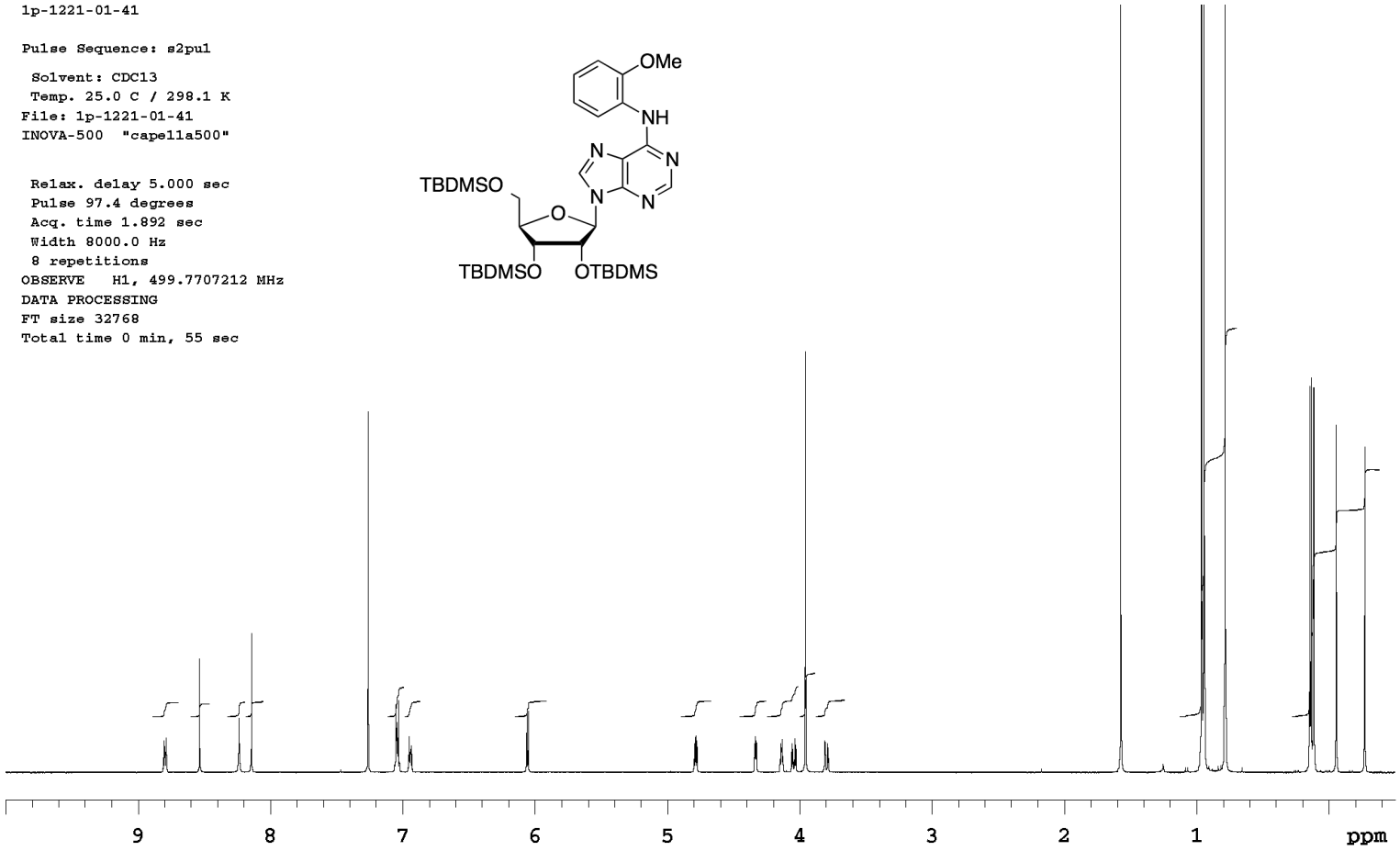
1p-1221-01-41
Pulse Sequence: s2pul
Solvent: CDCl3
Temp. 25.0 C / 298.1 K
File: 1p-1221-01-41
INOVA-500 "capel1a500"
Relax. delay 5.000 sec
Pulse 97.4 degrees
Acq. time 1.892 sec
Width 8000.0 Hz
8 repetitions
OBSERVE H1, 499.7707212 MHz
DATA PROCESSING
FT size 32768
Total time 0 min, 55 sec
OMe
NH
N
N
N
N
TBDMSO
O
TBDMSO
OTBDMS
9
8
7
6
5
4
3
2
1
ppm

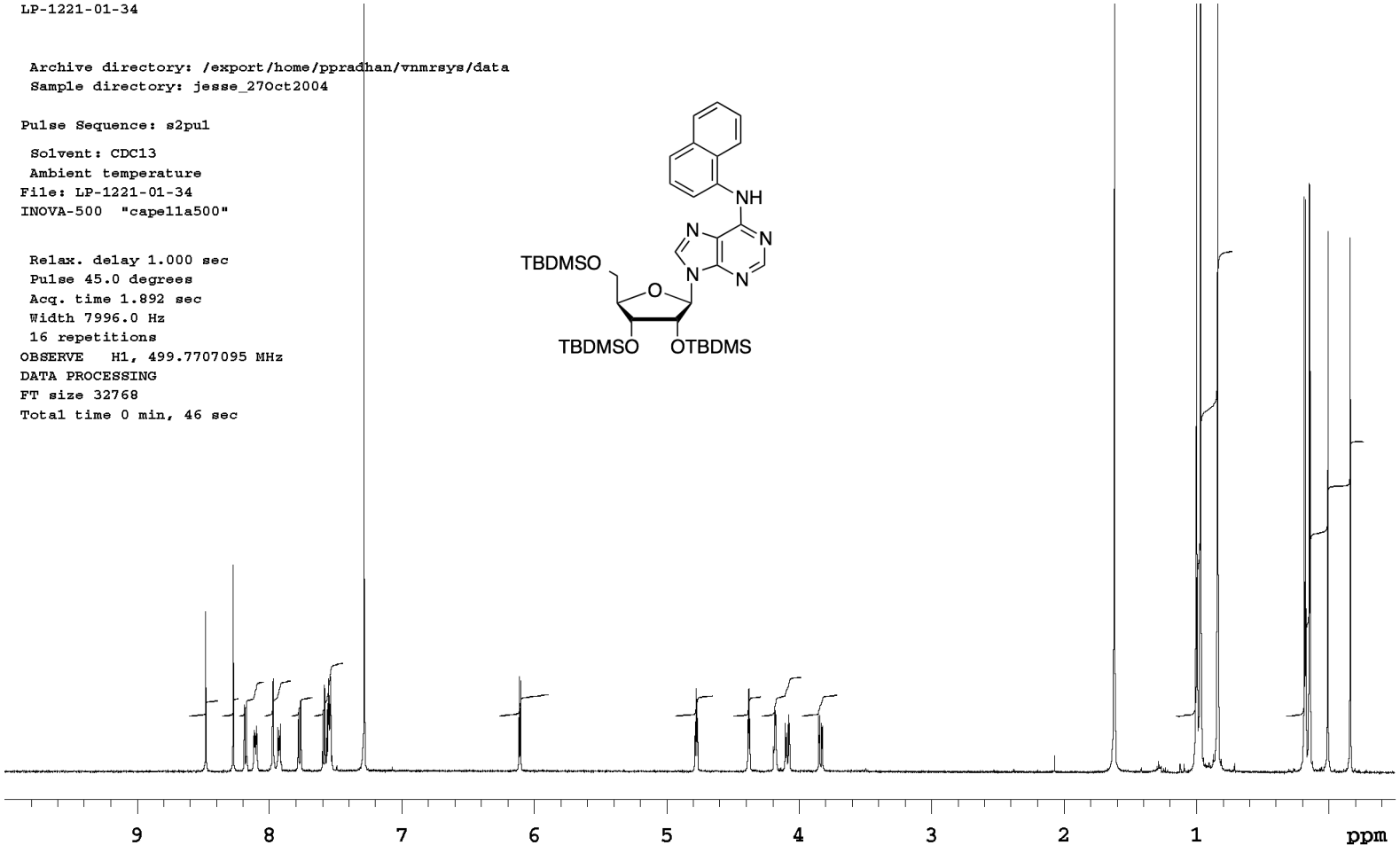
LP-1221-01-34
Archive directory: /export/home/ppradhan/vnmrsys/data
Sample directory: jesse_27Oct2004
Pulse Sequence: s2pul
Solvent: CDC13
Ambient temperature
File: LP-1221-01-34
INOVA-500 "capella500"
Relax. delay 1.000 sec
Pulse 45.0 degrees
Acq. time 1.892 sec
Width 7996.0 Hz
16 repetitions
OBSERVE H1, 499.7707095 MHz
DATA PROCESSING
FT size 32768
Total time 0 min, 46 sec
NH
N
N
N
N
TBDMSO
O
TBDMSO
OTBDMS
9
8
7
6
5
4
3
2
1
ppm

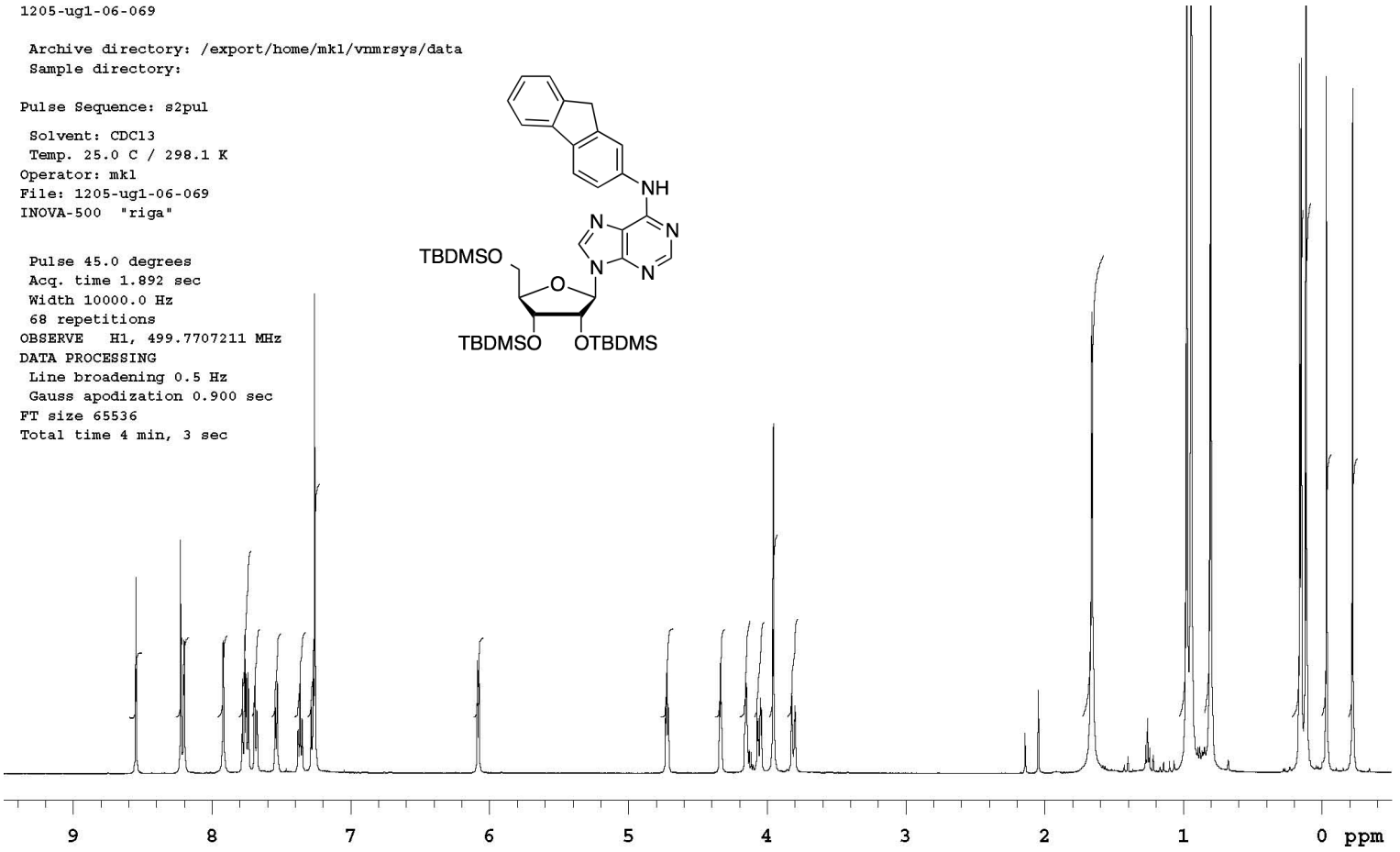
1205-ug1-06-069
Archive directory: /export/home/mkl/vnmrsys/data
Sample directory:
Pulse Sequence: s2pul
Solvent: CDCl3
Temp. 25.0 C / 298.1 K
Operator: mkl
File: 1205-ug1-06-069
INOVA-500 "riga"
Pulse 45.0 degrees
Acq. time 1.892 sec
Width 10000.0 Hz
68 repetitions
OBSERVE H1, 499.7707211 MHz
DATA PROCESSING
Line broadening 0.5 Hz
Gauss apodization 0.900 sec
FT size 65536
Total time 4 min, 3 sec
NH
N
N
N
N
O
TBDMSO
TBDMSO
OTBDMS
9
8
7
6
5
4
3
2
1
0 ppm

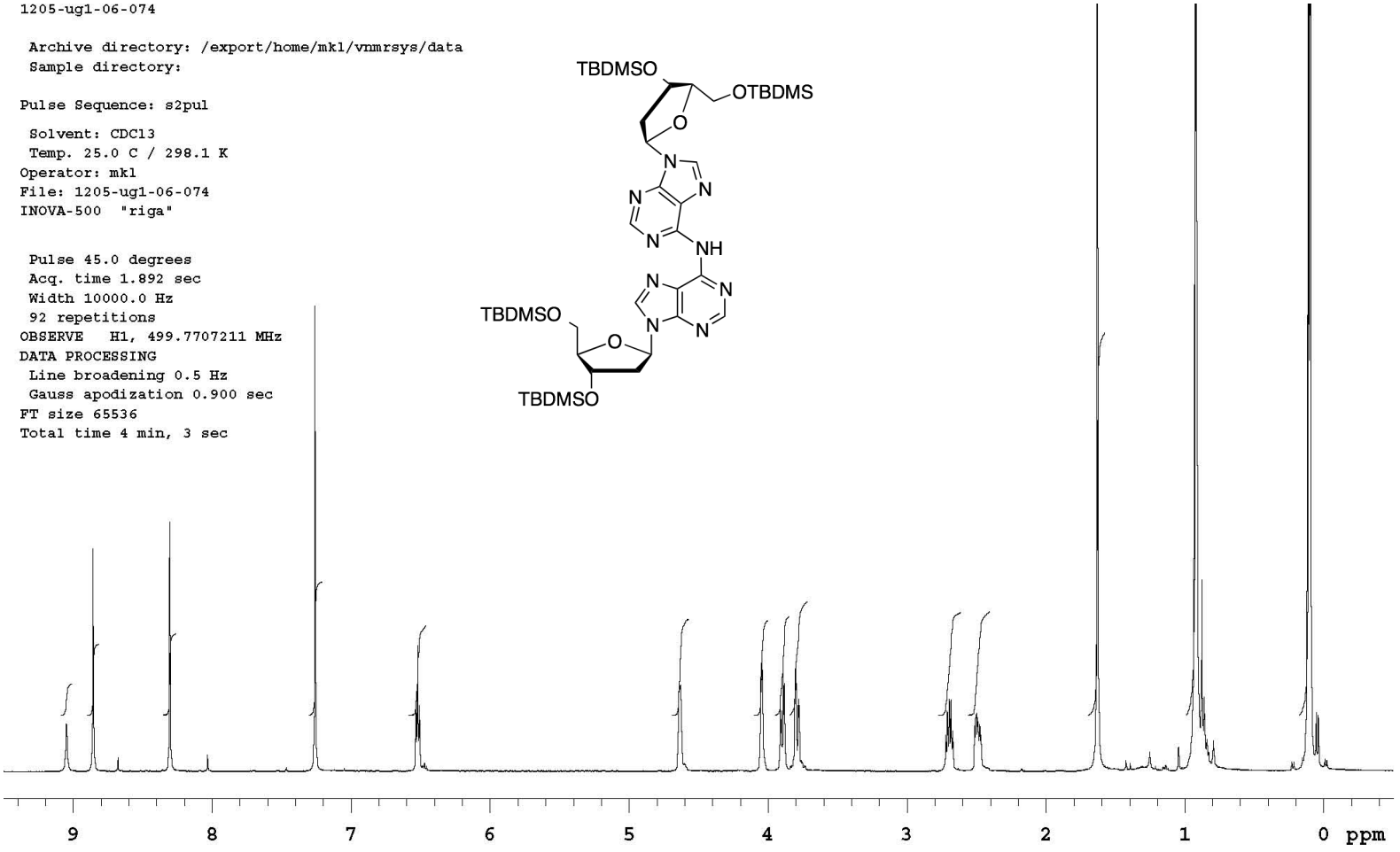
1205-ug1-06-074
Archive directory: /export/home/mkl/vnmrsys/data
Sample directory:
Pulse Sequence: s2pul
Solvent: CDCl3
Temp. 25.0 C / 298.1 K
Operator: mkl
File: 1205-ug1-06-074
INOVA-500 "riga"
Pulse 45.0 degrees
Acq. time 1.892 sec
Width 10000.0 Hz
92 repetitions
OBSERVE H1, 499.7707211 MHz
DATA PROCESSING
Line broadening 0.5 Hz
Gauss apodization 0.900 sec
FT size 65536
Total time 4 min, 3 sec
TBDMSO
OTBDMS
O
N
N
N
N
NH
N
N
N
N
TBDMSO
O
TBDMSO
9
8
7
6
5
4
3
2
1
0 ppm

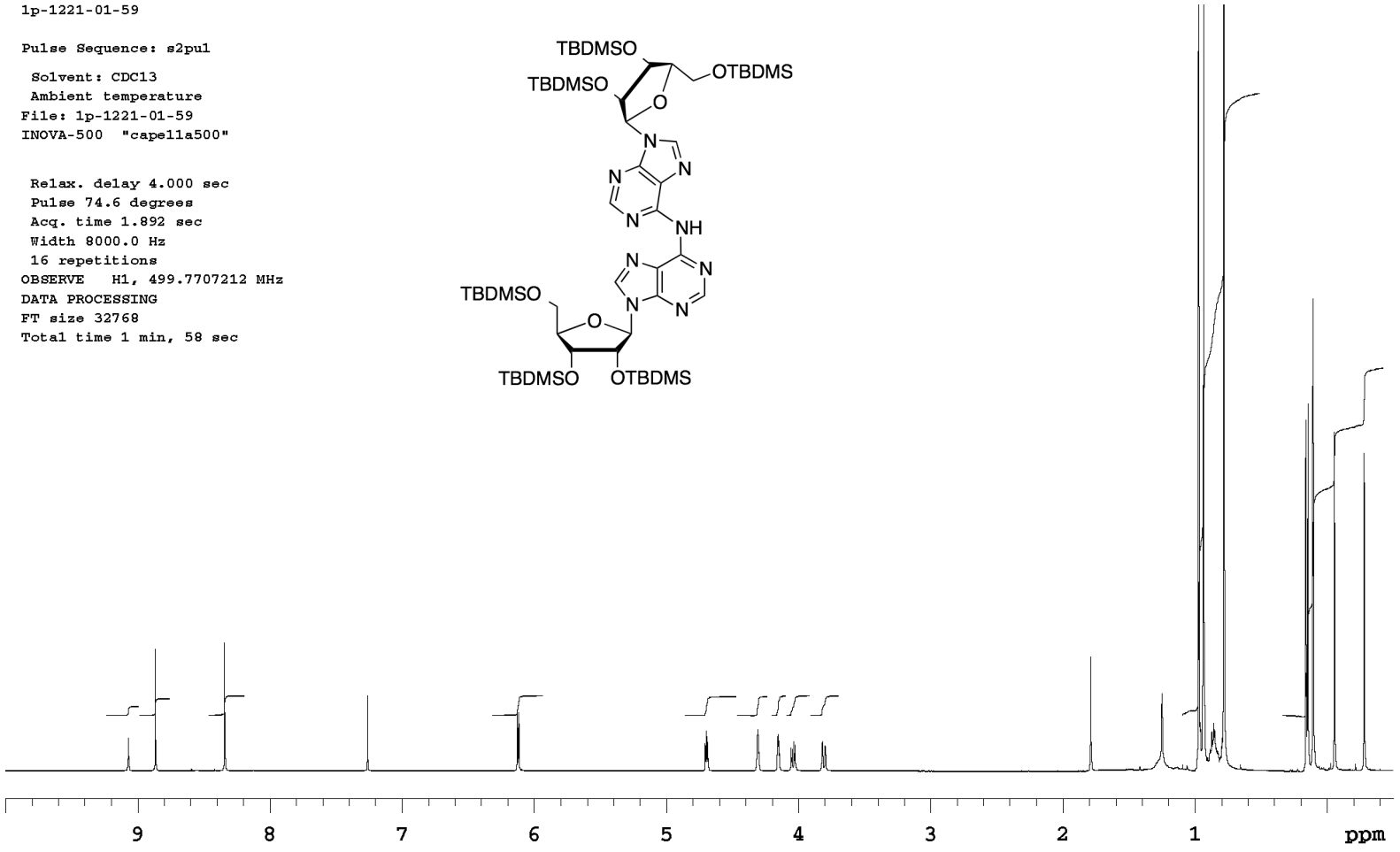
1p-1221-01-59
Pulse Sequence: s2pul
Solvent: CDCl3
Ambient temperature
File: 1p-1221-01-59
INOVA-500 "capella500"
Relax. delay 4.000 sec
Pulse 74.6 degrees
Acq. time 1.892 sec
Width 8000.0 Hz
16 repetitions
OBSERVE H1, 499.7707212 MHz
DATA PROCESSING
FT size 32768
Total time 1 min, 58 sec
TBDMSO
TBDMSO
OTBDMS
O
N
N
N
N
NH
N
N
N
N
TBDMSO
O
TBDMSO
OTBDMS
9
8
7
6
5
4
3
2
1
ppm

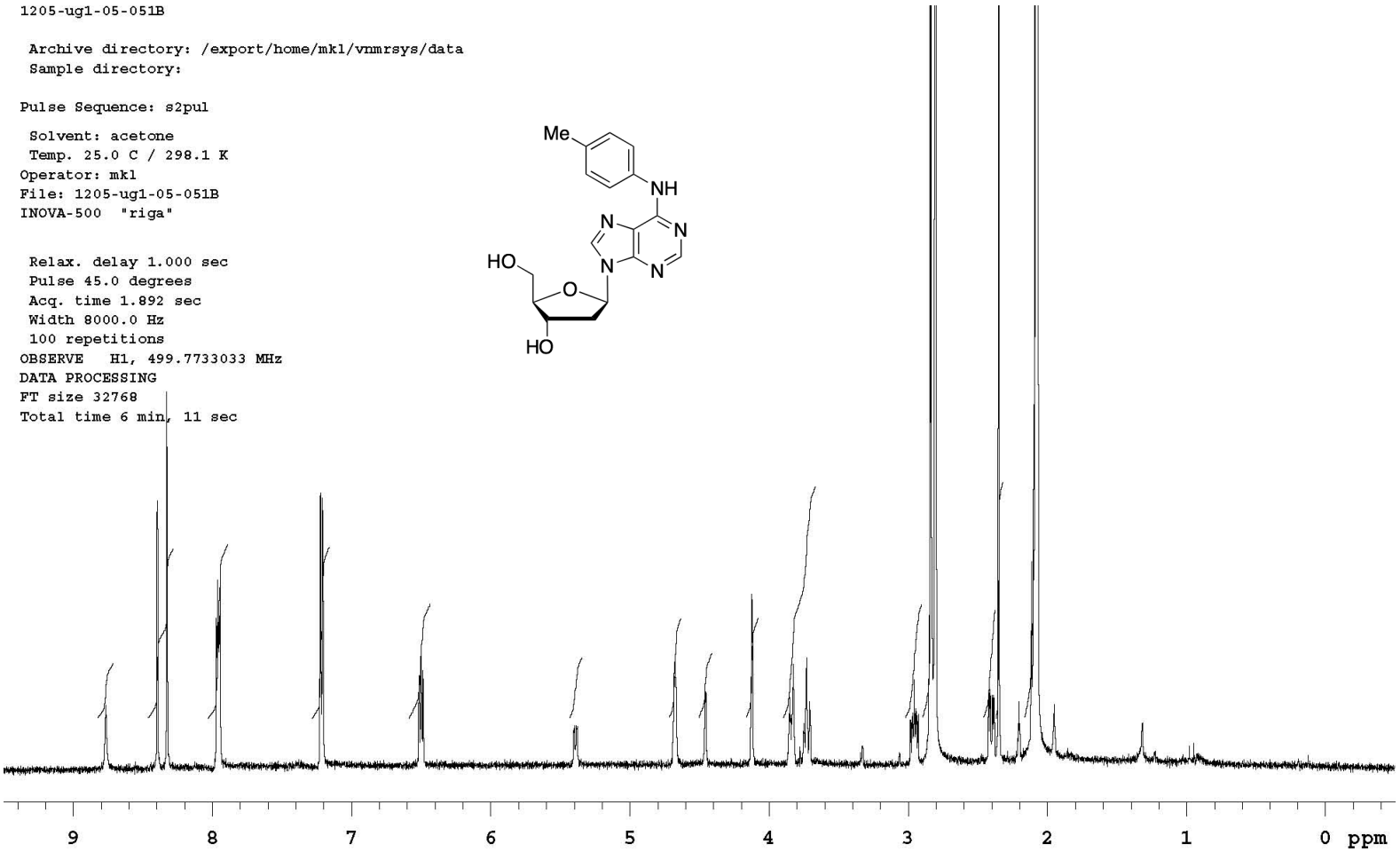
1205-ug1-05-051B
Archive directory: /export/home/mkl/vnmrsys/data
Sample directory:
Pulse Sequence: s2pul
Solvent: acetone
Temp. 25.0 C / 298.1 K
Operator: mkl
File: 1205-ug1-05-051B
INOVA-500 "riga"
Relax. delay 1.000 sec
Pulse 45.0 degrees
Acq. time 1.892 sec
Width 8000.0 Hz
100 repetitions
OBSERVE H1, 499.7733033 MHz
DATA PROCESSING
FT size 32768
Total time 6 min, 11 sec
Me
NH
N
N
N
N
HO
O
HO
9
8
7
6
5
4
3
2
1
0 ppm

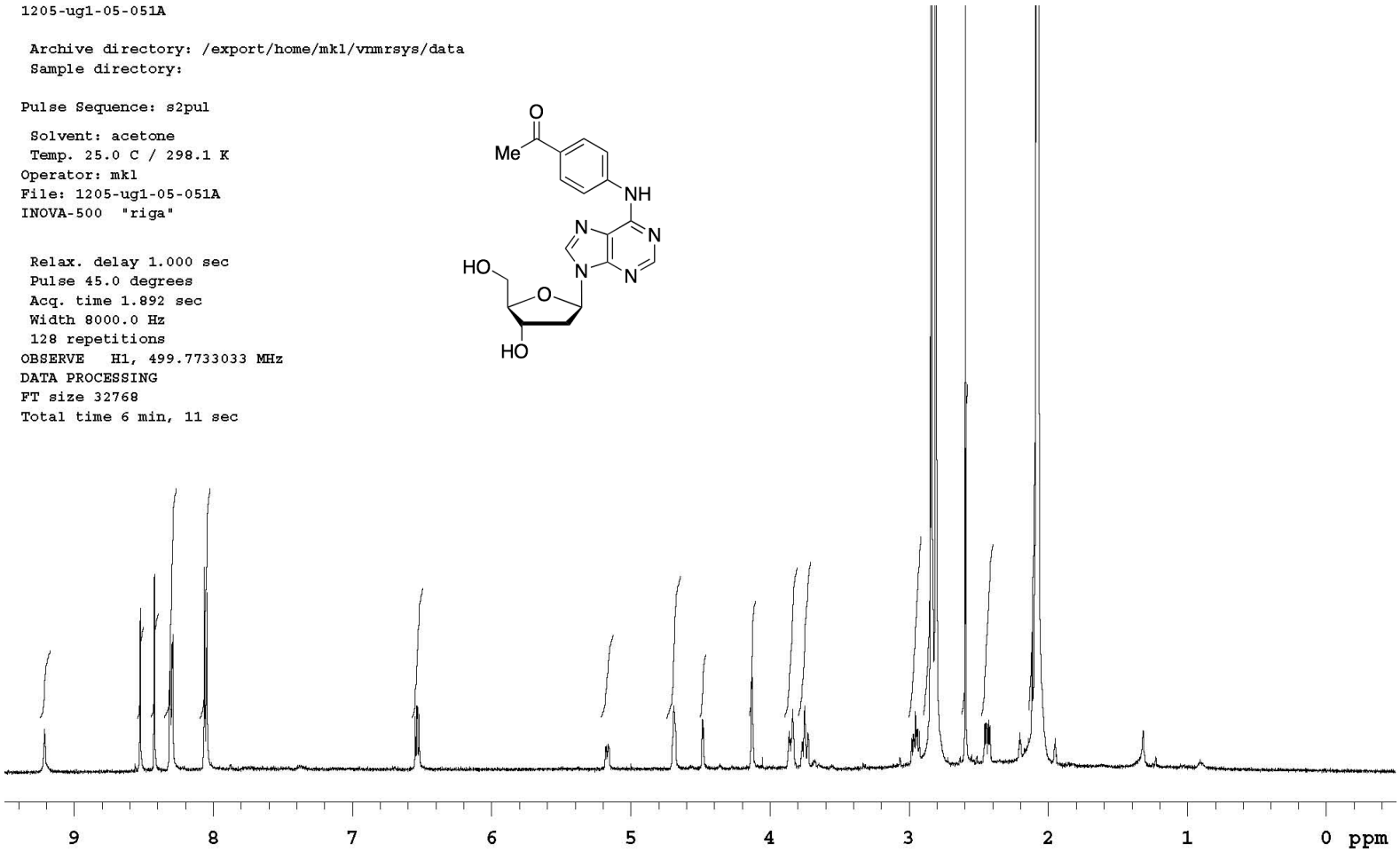
1205-ug1-05-051A
Archive directory: /export/home/mkl/vnmrsys/data
Sample directory:
Pulse Sequence: s2pul
Solvent: acetone
Temp. 25.0 C / 298.1 K
Operator: mkl
File: 1205-ug1-05-051A
INOVA-500 "riga"
Relax. delay 1.000 sec
Pulse 45.0 degrees
Acq. time 1.892 sec
Width 8000.0 Hz
128 repetitions
OBSERVE H1, 499.7733033 MHz
DATA PROCESSING
FT size 32768
Total time 6 min, 11 sec
O
Me
NH
N
N
N
N
HO
O
HO
9
8
7
6
5
4
3
2
1
0 ppm

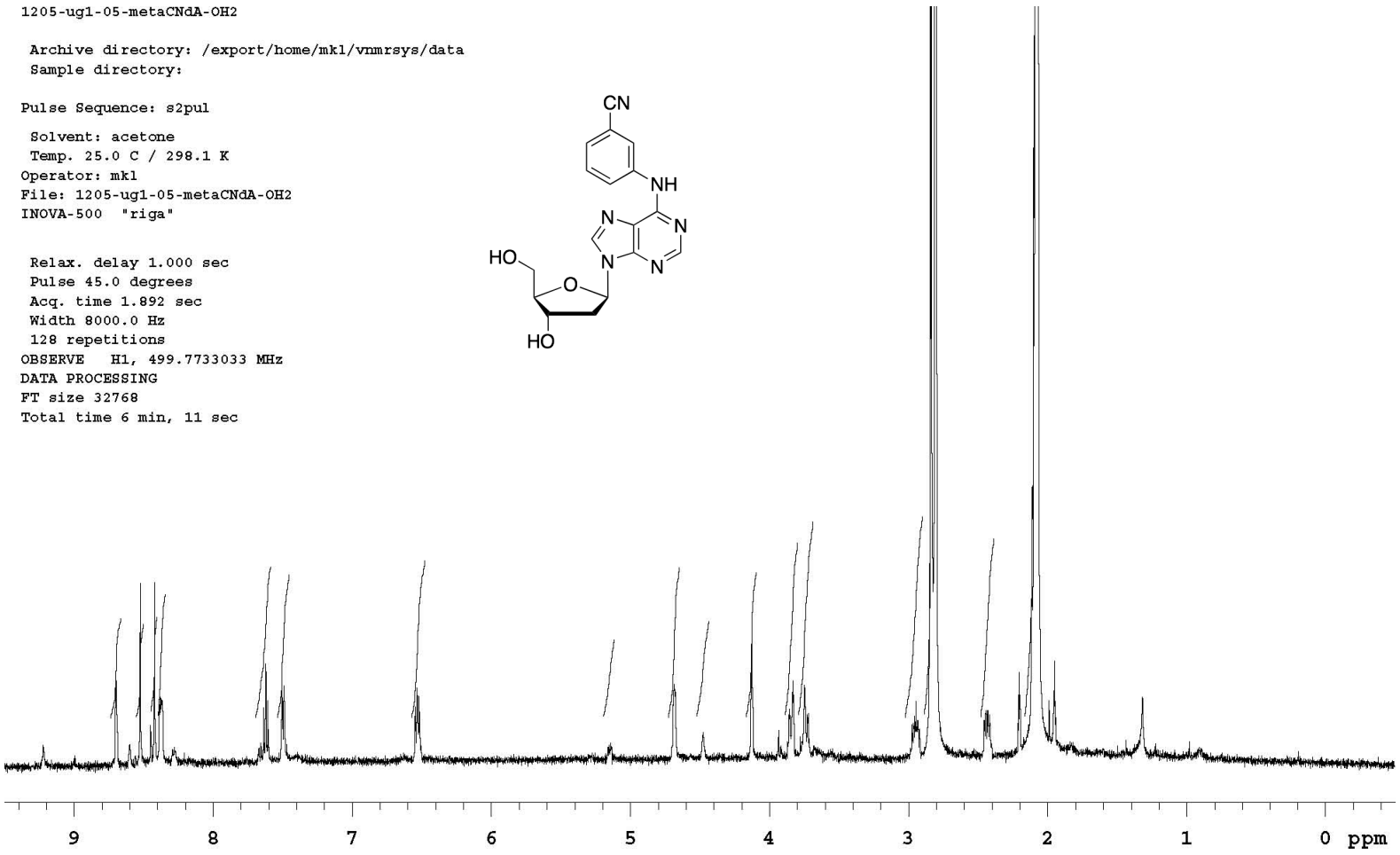
1205-ug1-05-metaCNdA-OH2
Archive directory: /export/home/mkl/vnmrsys/data
Sample directory:
Pulse Sequence: s2pul
Solvent: acetone
Temp. 25.0 C / 298.1 K
Operator: mkl
File: 1205-ug1-05-metaCNdA-OH2
INOVA-500 "riga"
Relax. delay 1.000 sec
Pulse 45.0 degrees
Acq. time 1.892 sec
Width 8000.0 Hz
128 repetitions
OBSERVE H1, 499.7733033 MHz
DATA PROCESSING
FT size 32768
Total time 6 min, 11 sec
CN
NH
N
N
N
N
HO
O
HO
9
8
7
6
5
4
3
2
1
0 ppm

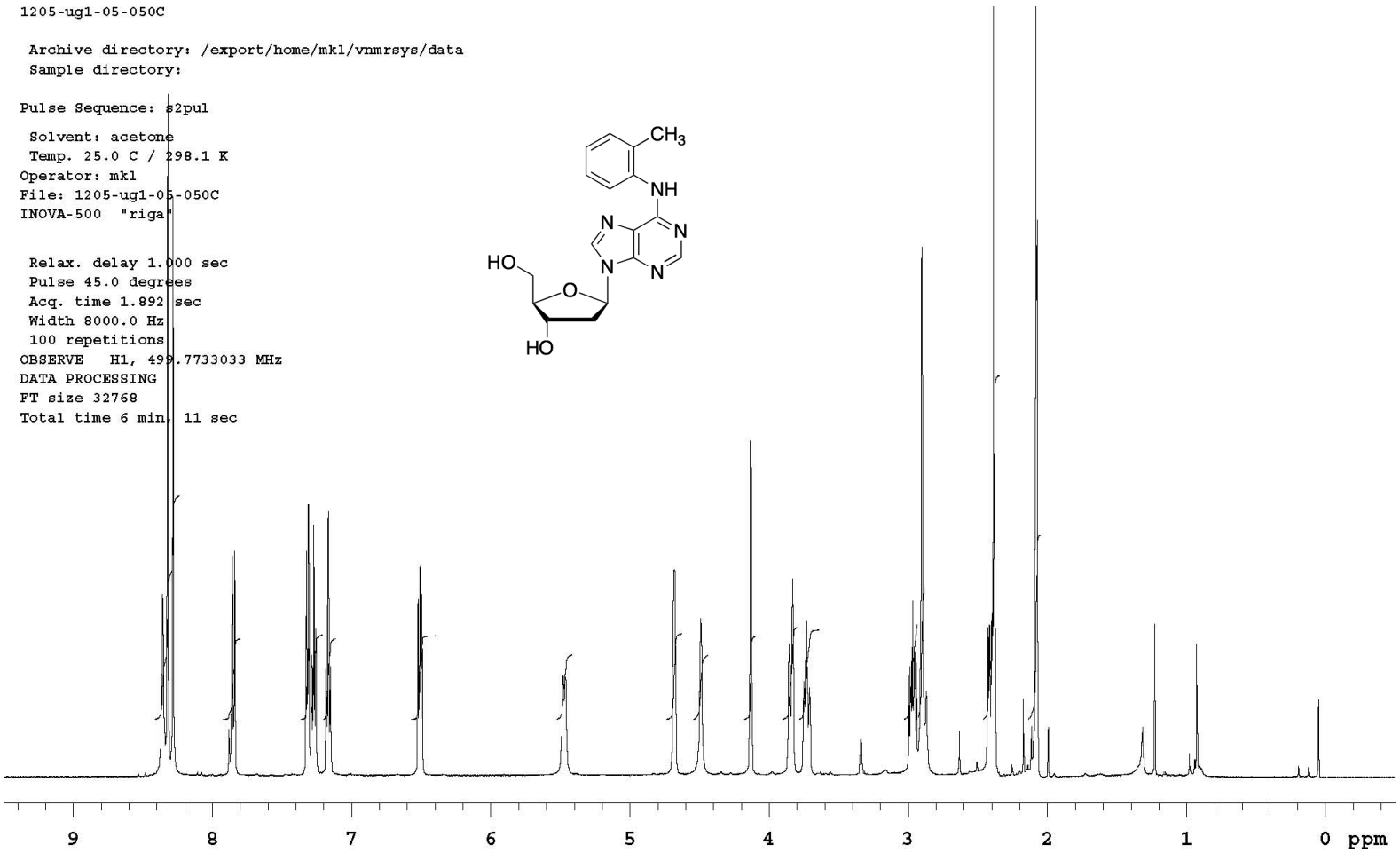
1205-ug1-05-050C
Archive directory: /export/home/mkl/vnmrsys/data
Sample directory:
Pulse Sequence: s2pul
Solvent: acetone
Temp. 25.0 C / 298.1 K
Operator: mkl
File: 1205-ug1-05-050C
INOVA-500 "riga"
Relax. delay 1.000 sec
Pulse 45.0 degrees
Acq. time 1.892 sec
Width 8000.0 Hz
100 repetitions
OBSERVE H1, 499.7733033 MHz
DATA PROCESSING
FT size 32768
Total time 6 min, 11 sec
CH3
NH
N
N
N
N
HO
O
HO
9
8
7
6
5
4
3
2
1
0 ppm

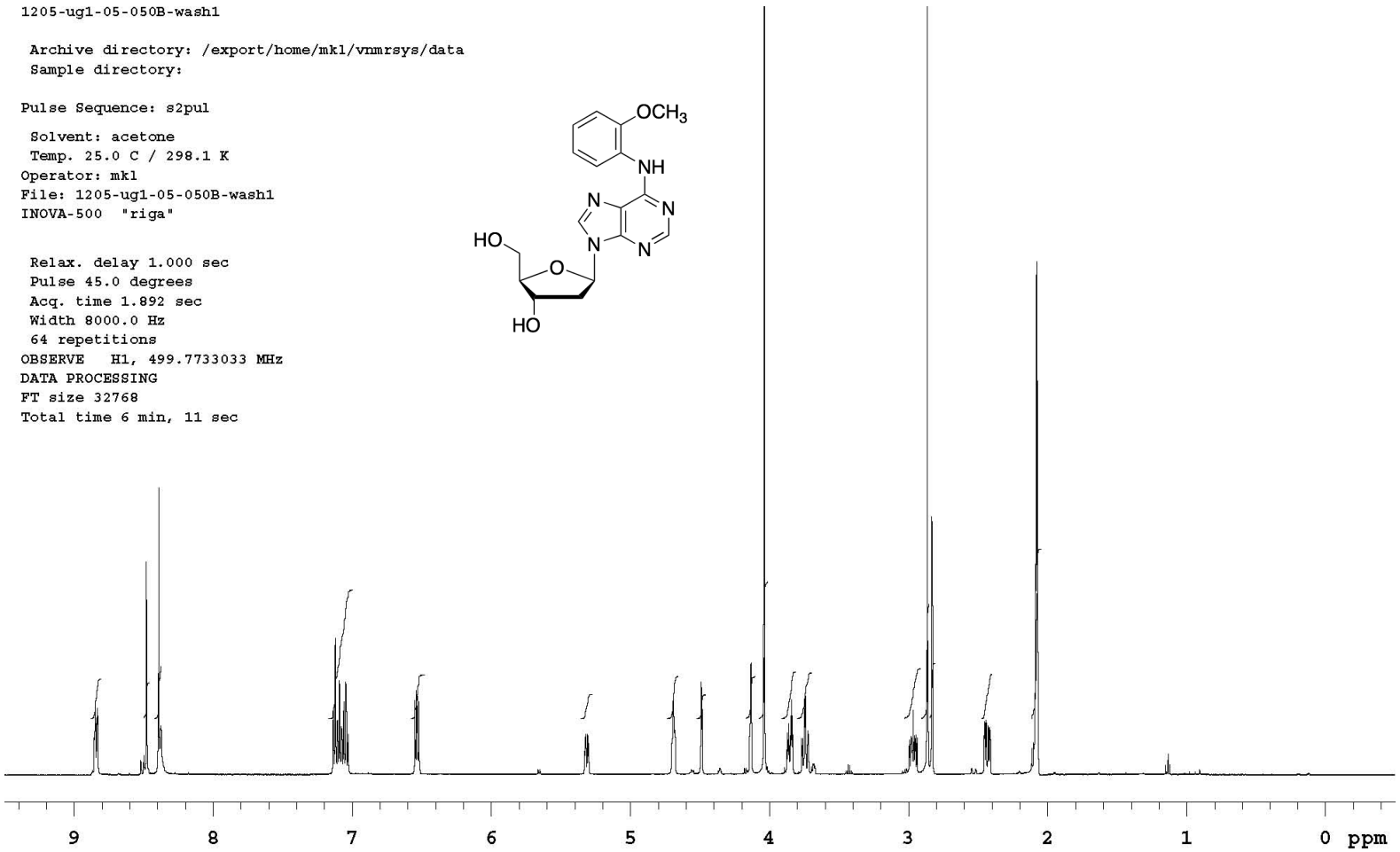
1205-ug1-05-050B-wash1
Archive directory: /export/home/mkl/vnmrsys/data
Sample directory:
Pulse Sequence: s2pul
Solvent: acetone
Temp. 25.0 C / 298.1 K
Operator: mkl
File: 1205-ug1-05-050B-wash1
INOVA-500 "riga"
Relax. delay 1.000 sec
Pulse 45.0 degrees
Acq. time 1.892 sec
Width 8000.0 Hz
64 repetitions
OBSERVE H1, 499.7733033 MHz
DATA PROCESSING
FT size 32768
Total time 6 min, 11 sec
OCH3
NH
N
N
N
N
HO
O
HO
9
8
7
6
5
4
3
2
1
0 ppm

1205-ug1-05-050A-ODwash

Archive directory: /export/home/mkl/vnmrsys/data
Sample directory:

Pulse Sequence: s2pul

Solvent: acetone
Temp. 25.0 C / 298.1 K
Operator: mkl
File: 1205-ug1-05-050A-ODwash
INOVA-500 "riga"

Relax. delay 1.000 sec
Pulse 45.0 degrees
Acq. time 1.892 sec
Width 8000.0 Hz
64 repetitions
OBSERVE H1, 499.7733033 MHz
DATA PROCESSING
FT size 32768
Total time 6 min, 11 sec

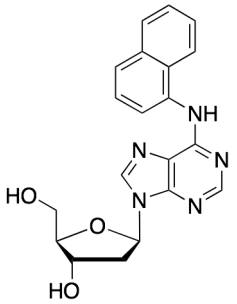

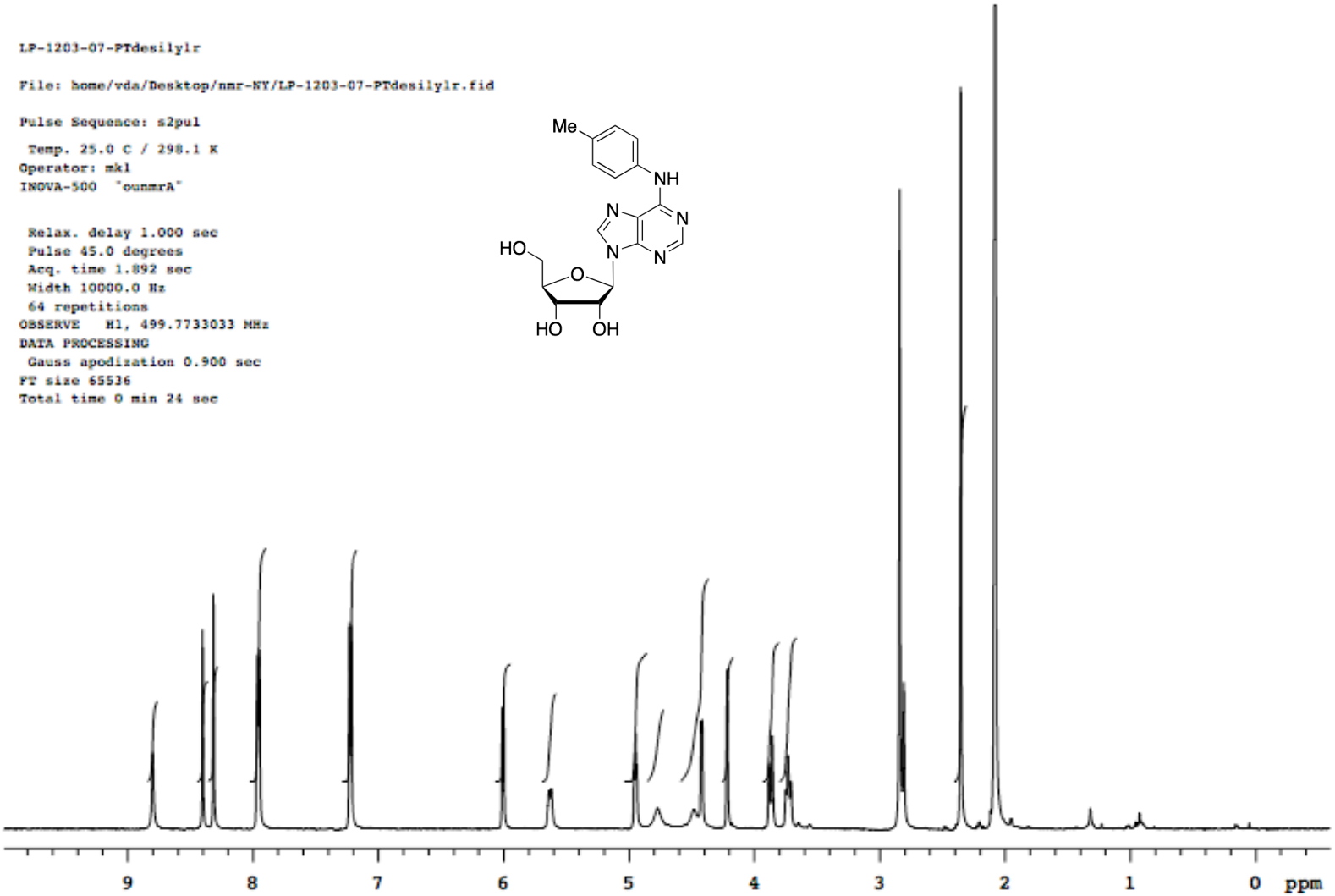
LP-1203-07-PTdesilylr
File: home/vda/Desktop/nmr-NY/LP-1203-07-PTdesilylr.fid
Pulse Sequence: s2pul
Temp. 25.0 C / 298.1 K
Operator: mkl
INOVA-500 "ounmrA"
Relax. delay 1.000 sec
Pulse 45.0 degrees
Acq. time 1.892 sec
Width 10000.0 Hz
64 repetitions
OBSERVE H1, 499.7733033 MHz
DATA PROCESSING
Gauss apodization 0.900 sec
FT size 65536
Total time 0 min 24 sec
Me
NH
N
N
N
N
HO
O
HO
OH
9
8
7
6
5
4
3
2
1
0
ppm

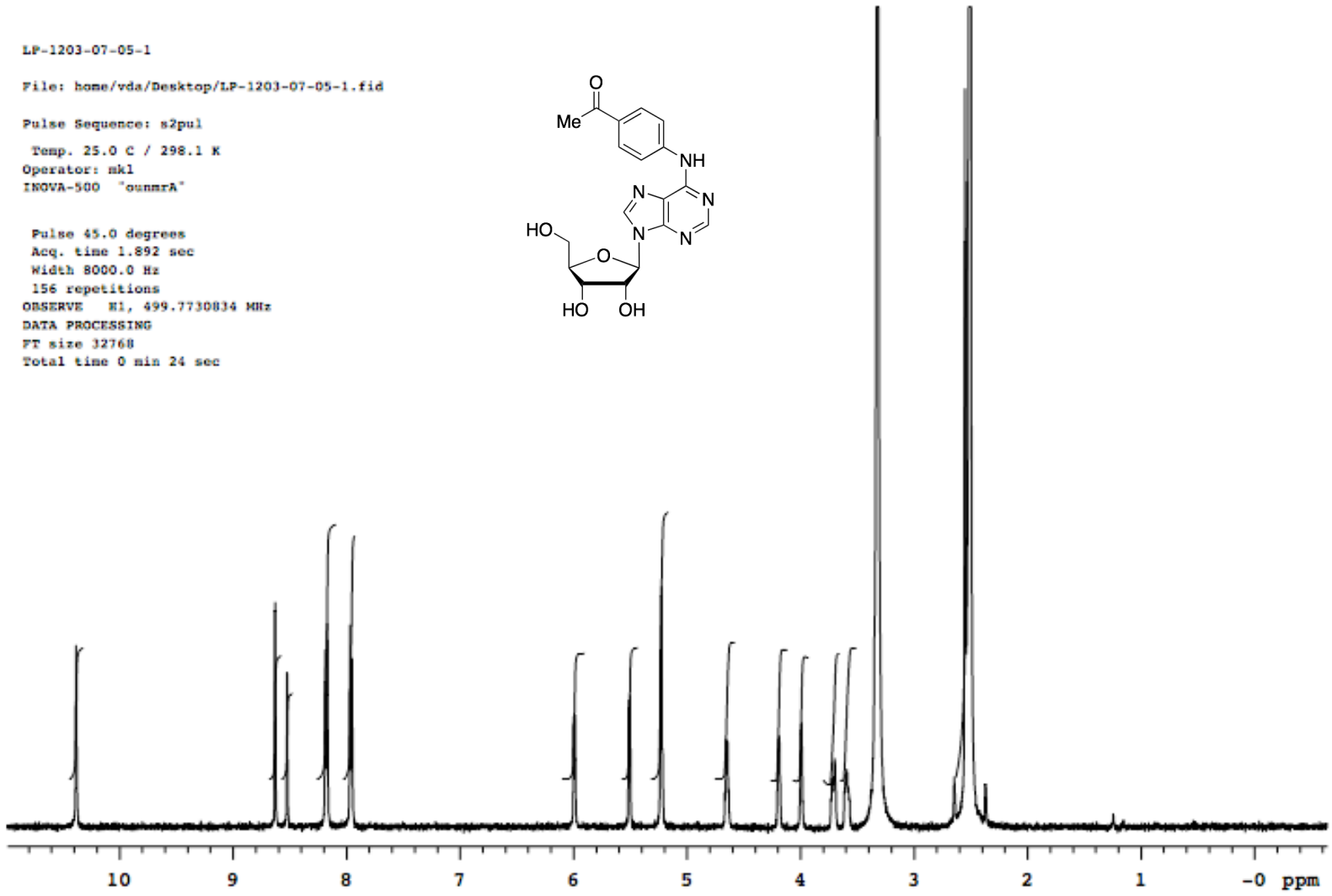
LP-1203-07-05-1
File: home/vda/Desktop/LP-1203-07-05-1.fid
Pulse Sequence: s2pul
Temp. 25.0 C / 298.1 K
Operator: mkl
INOVA-500 "ounmrA"
Pulse 45.0 degrees
Acq. time 1.892 sec
Width 8000.0 Hz
156 repetitions
OBSERVE H1, 499.7730834 MHz
DATA PROCESSING
FT size 32768
Total time 0 min 24 sec
O
Me
NH
N
N
N
N
HO
O
HO
OH
10
9
8
7
6
5
4
3
2
1
-0 ppm

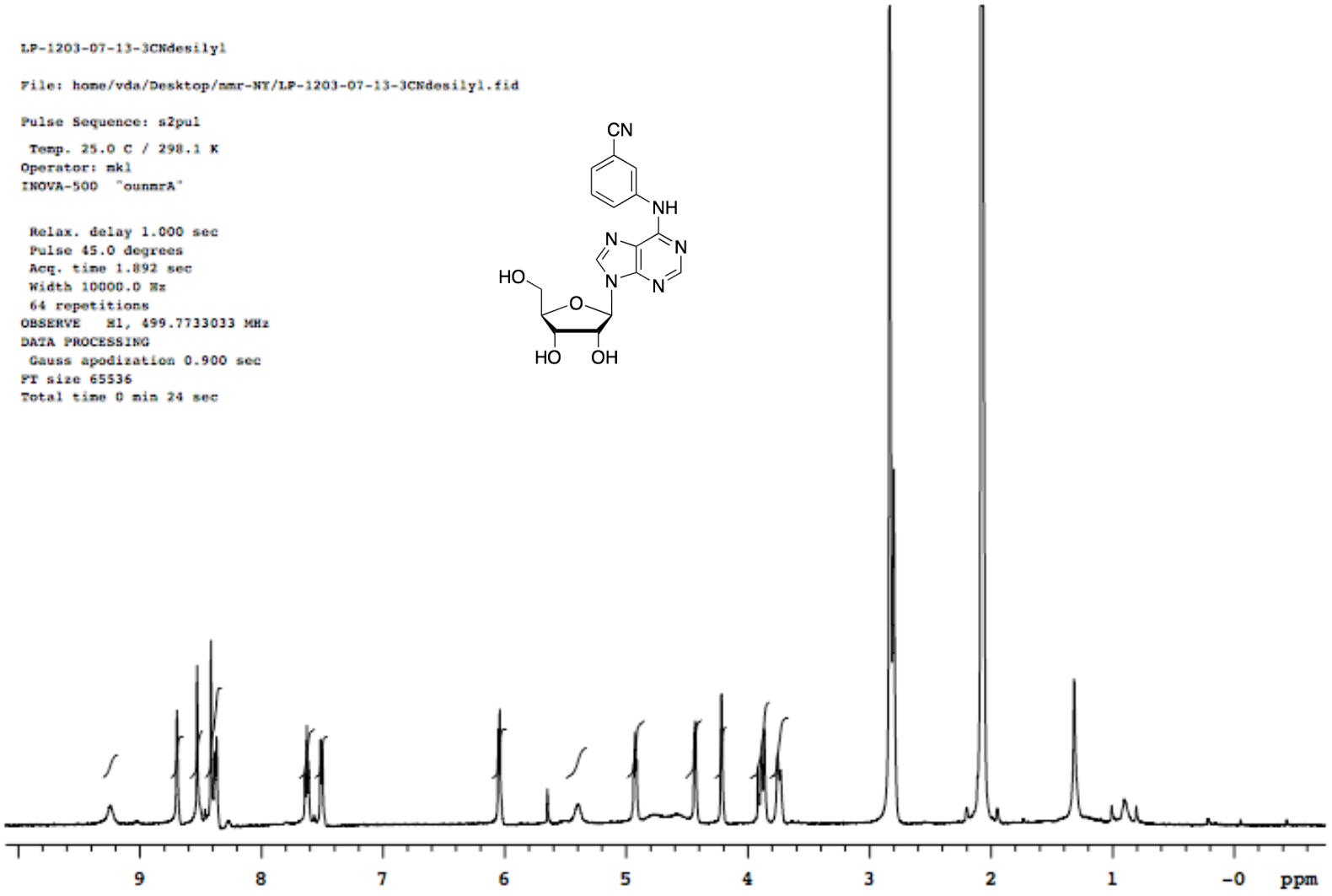
LP-1203-07-13-3CNdesilyl
File: home/vda/Desktop/nmr-NY/LP-1203-07-13-3CNdesilyl.fid
Pulse Sequence: s2pul
Temp. 25.0 C / 298.1 K
Operator: mkl
INOVA-500 "ounmrA"
Relax. delay 1.000 sec
Pulse 45.0 degrees
Acq. time 1.892 sec
Width 10000.0 Hz
64 repetitions
OBSERVE H1, 499.7733033 MHz
DATA PROCESSING
Gauss apodization 0.900 sec
FT size 65536
Total time 0 min 24 sec
CN
NH
N
N
N
N
HO
O
HO
OH
9
8
7
6
5
4
3
2
1
-0
ppm

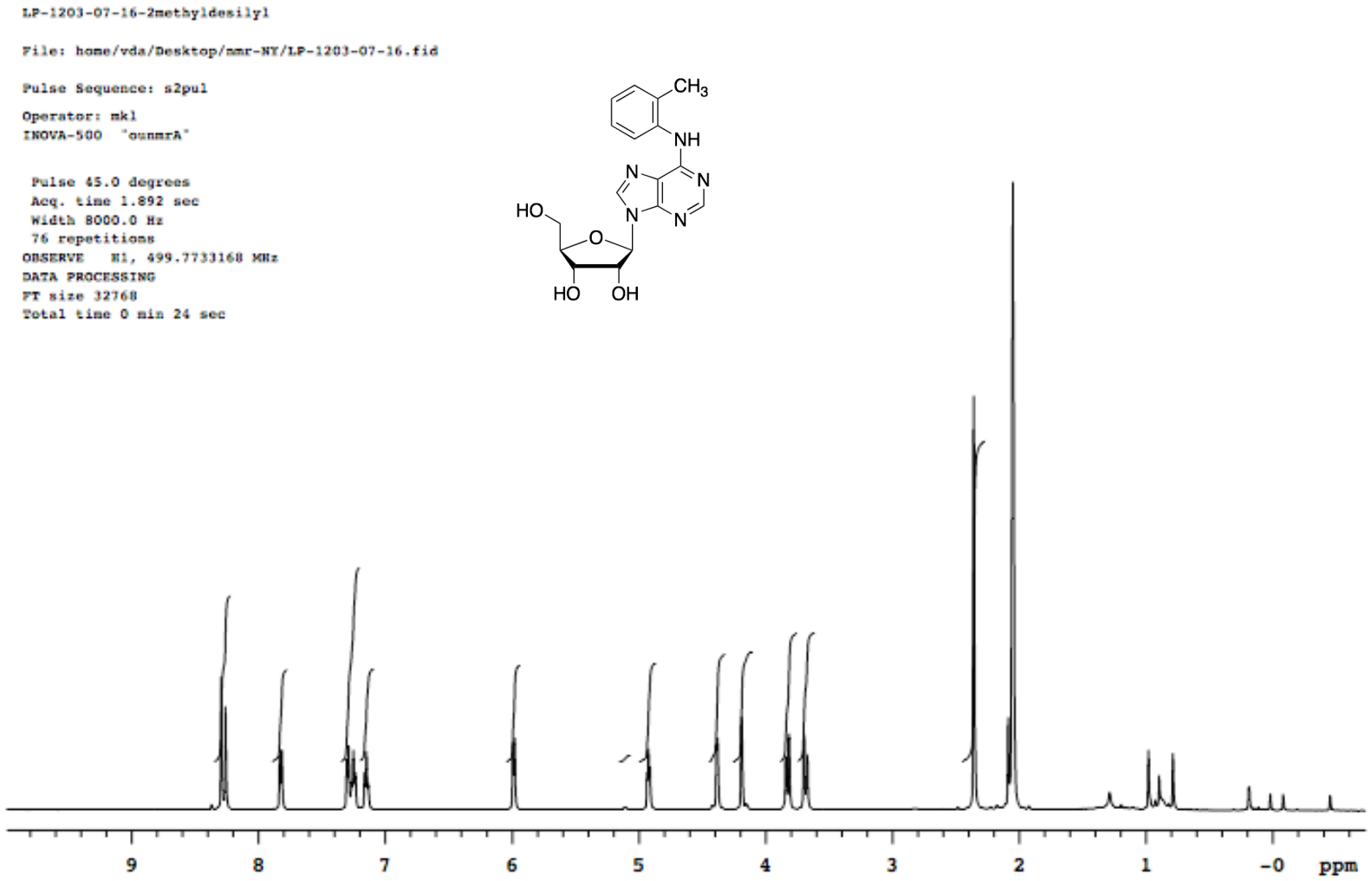
LP-1203-07-16-2methyldesilyl
File: home/vda/Desktop/nmr-NY/LP-1203-07-16.fid
Pulse Sequence: s2pul
Operator: mkl
INOVA-500 "ounmrA"
Pulse 45.0 degrees
Acq. time 1.892 sec
Width 8000.0 Hz
76 repetitions
OBSERVE H1, 499.7733168 MHz
DATA PROCESSING
FT size 32768
Total time 0 min 24 sec
CH3
NH
N
N
N
N
HO
O
HO
OH
9
8
7
6
5
4
3
2
1
-0
ppm

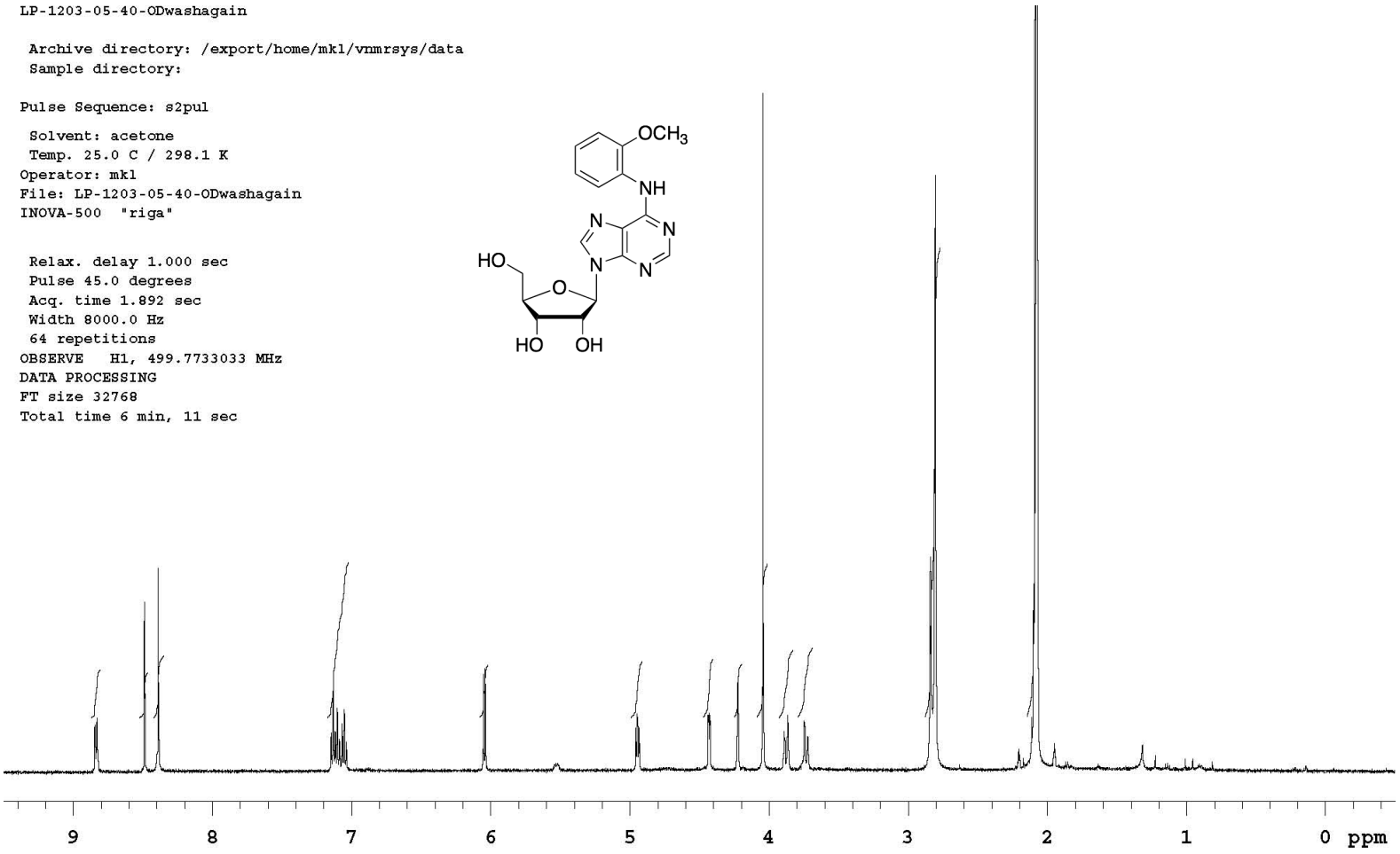
LP-1203-05-40-ODwashagain
Archive directory: /export/home/mkl/vnmrsys/data
Sample directory:
Pulse Sequence: s2pul
Solvent: acetone
Temp. 25.0 C / 298.1 K
Operator: mkl
File: LP-1203-05-40-ODwashagain
INOVA-500 "riga"
Relax. delay 1.000 sec
Pulse 45.0 degrees
Acq. time 1.892 sec
Width 8000.0 Hz
64 repetitions
OBSERVE H1, 499.7733033 MHz
DATA PROCESSING
FT size 32768
Total time 6 min, 11 sec
OCH3
NH
N
N
N
N
HO
O
HO
OH
9
8
7
6
5
4
3
2
1
0
ppm

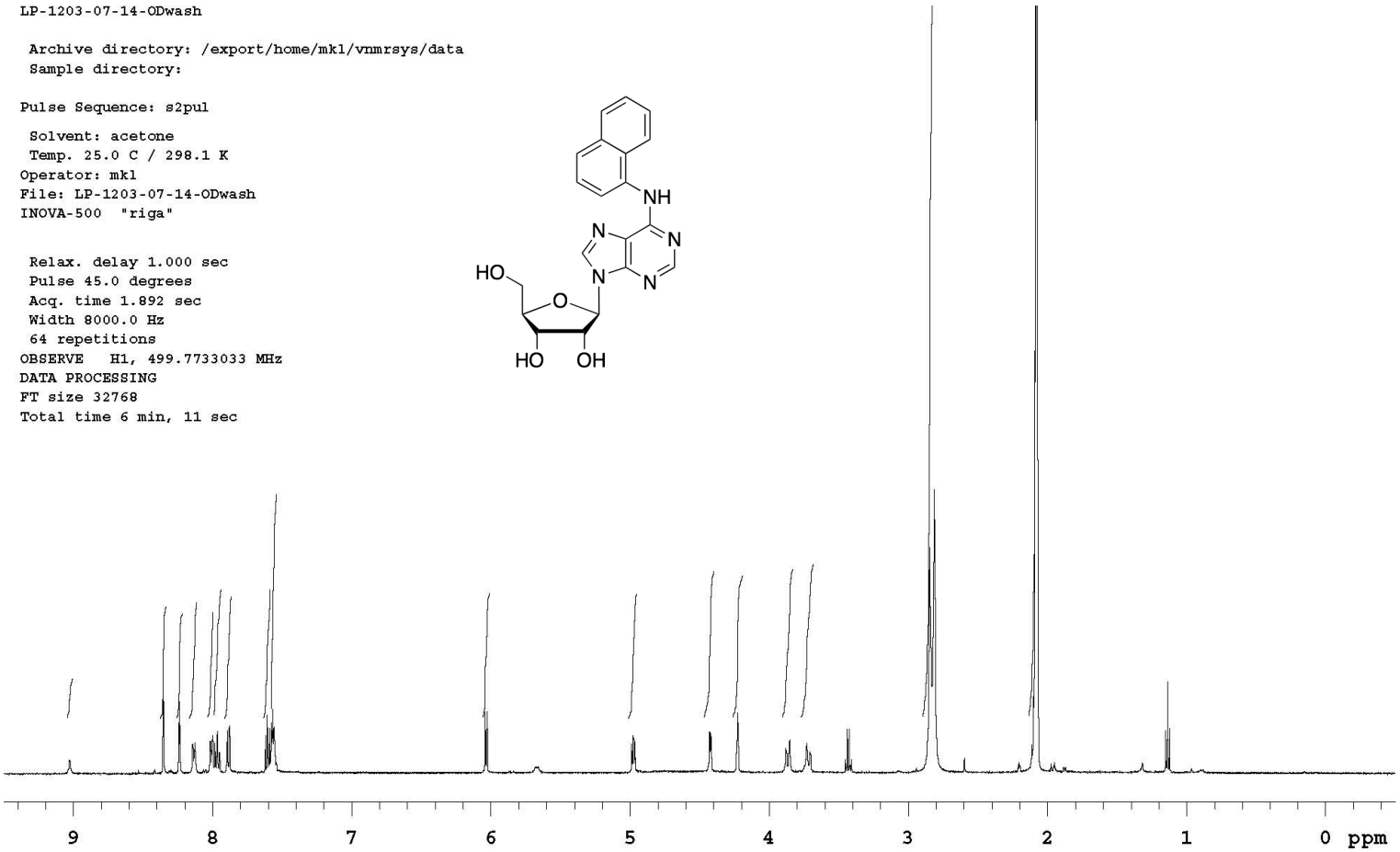
LP-1203-07-14-ODwash
Archive directory: /export/home/mkl/vnmrsys/data
Sample directory:
Pulse Sequence: s2pul
Solvent: acetone
Temp. 25.0 C / 298.1 K
Operator: mkl
File: LP-1203-07-14-ODwash
INOVA-500 "riga"
Relax. delay 1.000 sec
Pulse 45.0 degrees
Acq. time 1.892 sec
Width 8000.0 Hz
64 repetitions
OBSERVE H1, 499.7733033 MHz
DATA PROCESSING
FT size 32768
Total time 6 min, 11 sec
NH
N
N
N
N
HO
O
HO
OH
9
8
7
6
5
4
3
2
1
0 ppm

Chapter 2

2.1 General Introduction to Studies in Chemical Carcinogenesis

Polycyclic aromatic hydrocarbons (PAHs) are fused aromatic systems. Many PAHs result from the incomplete combustion of organic matter and activities in a modern society. A few examples that result in the formation of PAHs include the burning of tobacco products and coals, combustion of oil and tar products, refuse burning, and even the grilling and barbequing of meats.[1] Human exposure to PAHs is constant and unavoidable, via air, soil and water. PAHs and their metabolites are known to damage DNA resulting in mutations, tumorigenesis, and cancer. Thus, PAHs are considered health hazards and warrant study.[1,2] Though there is a vast number of PAHs, Figure 1 shows two examples that contain important structural elements called *bay* and *fjord* regions, which are important for carcinogenic activity of many alternant PAHs.[1] The bay region is formed by the angular arrangement of benzo rings as shown in benzo[*a*]pyrene (B*a*P) (Figure 1). The fjord region arises due to the addition of a benzo ring to a bay region as shown in benzo[*c*]phenanthrene (B*c*Ph). The K region, an area of marked olefinic character, was previously thought to correlate with carcinogenic activity. However, later work showed that DNA reactive intermediates formed via oxidation that are responsible for carcinogenic activity were at the bay and fjord regions of PAHs, and not at the K region.[2a,c]

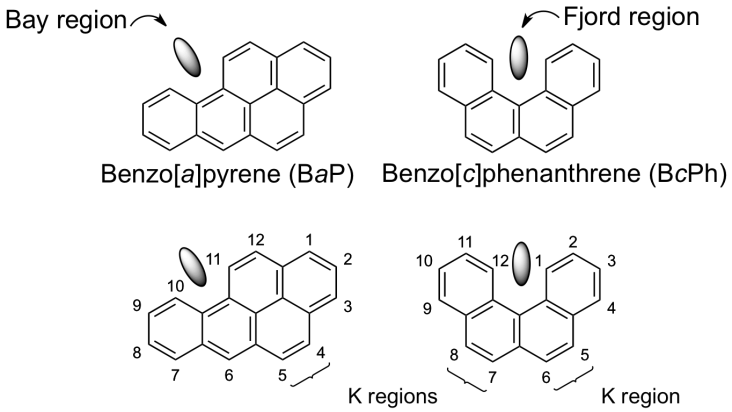

Figure 1. Structures of Two Polycyclic Aromatic Hydrocarbons (PAHs).

The bay and fjord region-containing PAHs are known to undergo metabolic activation to produce electrophilic agents that can result in DNA damage leading to malignant events.[1,2] When foreign compounds (xenobiotics) enter mammalian systems, biotransformation processes occur for the

detoxification and subsequent elimination of the xenobiotic via excretion pathways.[1] PAHs undergo such types of biotransformations that convert them into more hydrophilic (water soluble), and thus excretable, derivatives. This multi-step metabolism results in activated reactive intermediates (electrophilic agents) through oxidation reactions, which covalently bind to cellular components such as proteins and DNA.[1,2]

2.2 Metabolism of PAHs

There are at least three main metabolic pathways for activation of PAHs to electrophilic agents that can lead to DNA damage, which is considered the first step towards tumor formation.

1. Single Electron Oxidation Pathway

A single electron oxidation pathway involves the enzymatic removal of a single electron from the PAH that can result in a radical cation, which is capable of interacting with DNA and leading to subsequent damage (Scheme 1).[3] Using B*a*P as an example, the radical cation species can be formed by the action of enzymes such as peroxidases and cytochrome P450 (CYP450) present in mammalian systems. The ensuing electrophilic radical cation is trapped by the nitrogen atoms of purine bases in DNA, such as the N7 or N3 of adenine and guanine, which results in DNA damage (Scheme 1 and Figure 2).[3,4]

Scheme 1. Single Electron Oxidation Pathway and Resulting Events using B*a*P

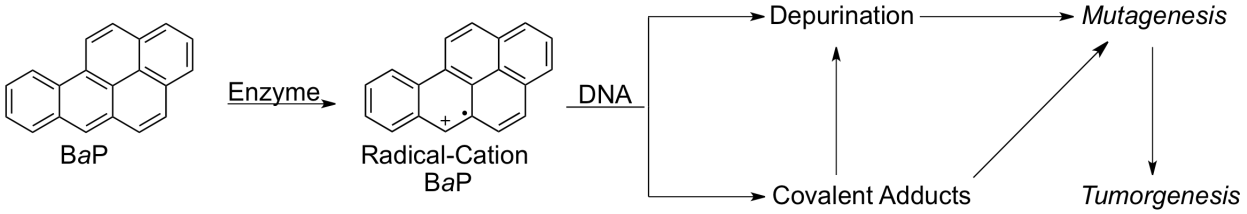

Due to the lability of the N-glycosidic bond in the resulting DNA adducts, depurination (the expulsion of purine bases) can occur yielding apurinic sites within DNA (Figure 2).[4] Reports by Cavalieri et. al. suggest that apurinic sites generated by depurinating PAH-DNA adducts from radial cations may be responsible for the induction of mutations in critical target genes leading to carcinogenesis.[4,5] Additionally, due to the high level of apurinic sites generated by PAH-DNA adduct depurination, the cells is unable to repair itself, thus resulting in mutations that may result in tumorgenesis.[4,6]

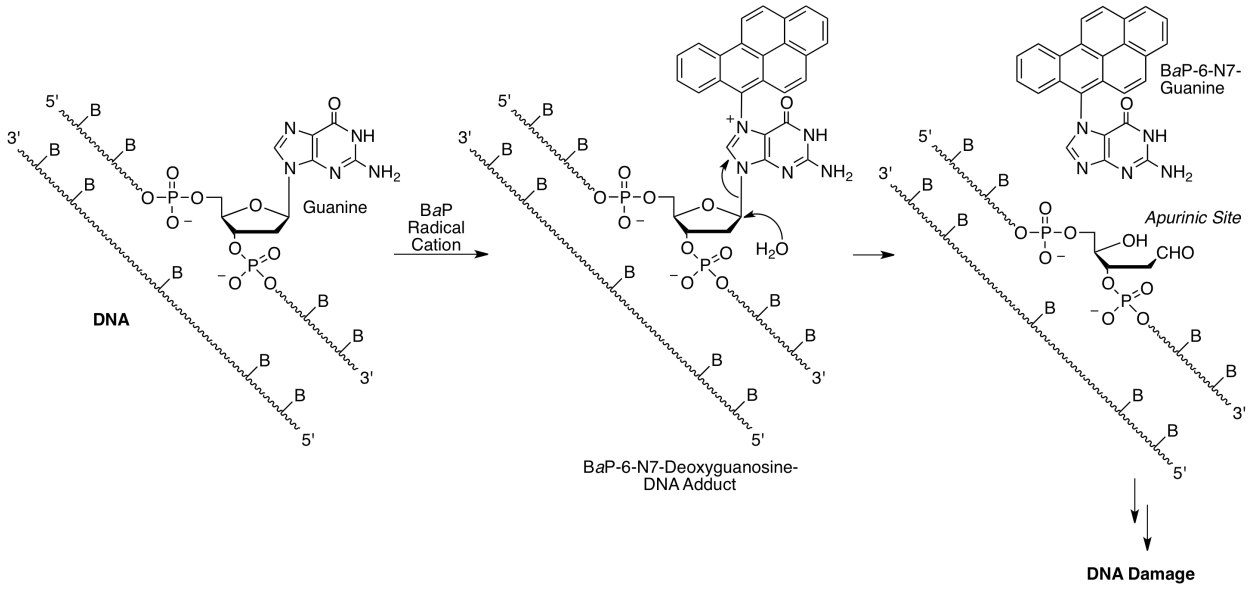

Figure 2. Pathway Showing Formation of an Apurinic Site from B*a*P-6-N7-Deoxyguanosine DNA Adduct.[4]

2. ortho-Quinone and Reactive Oxygen Species Pathway

The second pathway involves cellular oxidation of PAHs to dihydrodiols, which can be further oxidized to quinones that are capable of interacting with DNA, leading to covalent modifications. Alternatively, this pathway can cause DNA damage due to reactive oxygen species liberated as a result of the oxidation.[7] A representation of this cellular oxidation pathway is shown in Scheme 2. The PAH undergoes oxidation by dihydrodiol dehydrogenase that are typically found in mammalian livers (e.g. AKR1C9 in rats, and AKR1C1–1C4 in humans).[7,8] These proteins are members of a superfamily of nicotinamide adenine dinucleotide phosphate-dependent (NADPH-dependent) aldo-keto reductases (AKR), and are found to be active against a wide range of dihydrodiols of carcinogenic PAHs.[7,8] Initially, the NADPH-dependent enzymatic oxidation of the PAH dihydrodiol produces a ketol derivative that spontaneously tautomerizes to a catechol. These catechols are unstable and undergo autoxidation in the presence of oxygen (Scheme 2). This process involves one-electron steps that generate a semiquinone anion radical intermediate, and then the subsequent *ortho*-quinone derivative along with reactive oxygen species (Scheme 2).[7]

Scheme 2. Cellular Oxidation of a PAH Giving *ortho*-Quinone and Reactive Oxygen Species

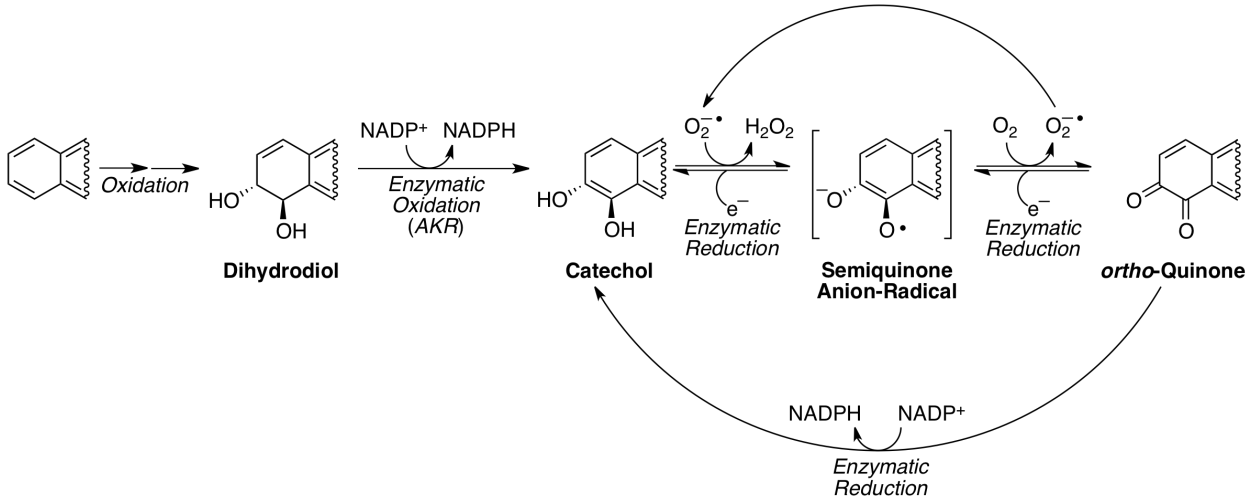

The reactive oxygen species, such as hydrogen peroxide (H_2O_2) and superoxide radical anion ($O_2^{-\bullet}$) are known to cause oxidative DNA to damage.[7a] For example, 8-hydroxy-2'-deoxyguanosine (8-oxoguanine, Figure 3), a product from oxidation at guanine in DNA, undergoes base mispairing with deoxyadenosine (dA) during DNA replication. Reports show that *in vitro*, these legions are mutagenic and account for deoxyguanosine (dG) to deoxythymidine (dT) transversions.[7a,9] The *ortho*-quinones of PAHs are also detrimental due to their chemically reactive α,β-unsaturated carbonyl functionality. For example, *in vitro* studies have shown that they induce stable as well as depurinating DNA adducts, thus leading to DNA damage.[7b]

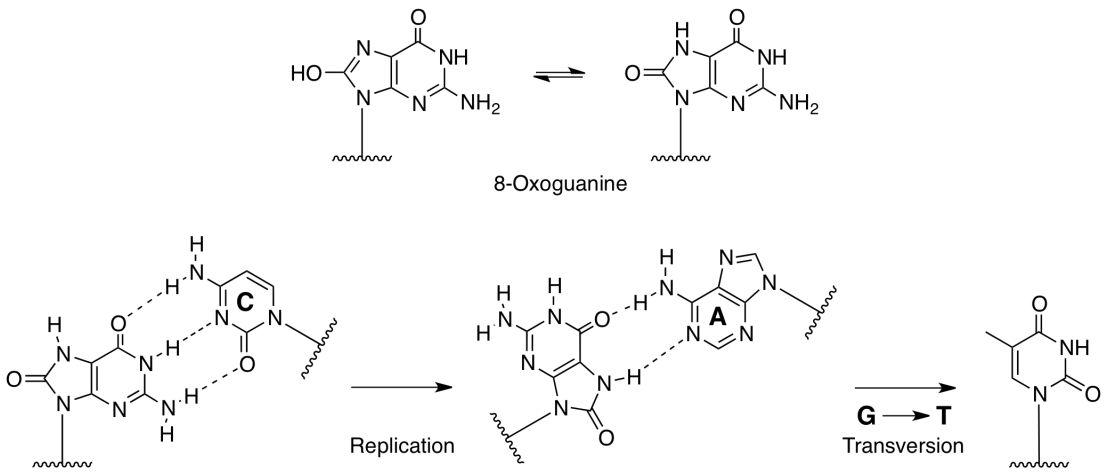

Figure 3. 8-Hydroxy-2'-Deoxyguanosine and Transversion Event.

3. Diol Epoxide Pathway

Over the past two decades however, there has been much focus on the third metabolic sequence, the "*diol epoxide*" pathway (Scheme 3). The formation of diol epoxides in bay and fjord region-containing PAHs is considered the predominant metabolic pathway leading to most mutagenic and carcinogenic events.[1,2] This, as implied by Harvey and Geacintov,[2c] is because the bay and fjord regions seem to provide a pocket of protection for the epoxide ring long enough for it to survive and interact with DNA.[2]

Scheme 3. Example of Diol Epoxide Pathway for PAH Metabolism and Subsequent Events

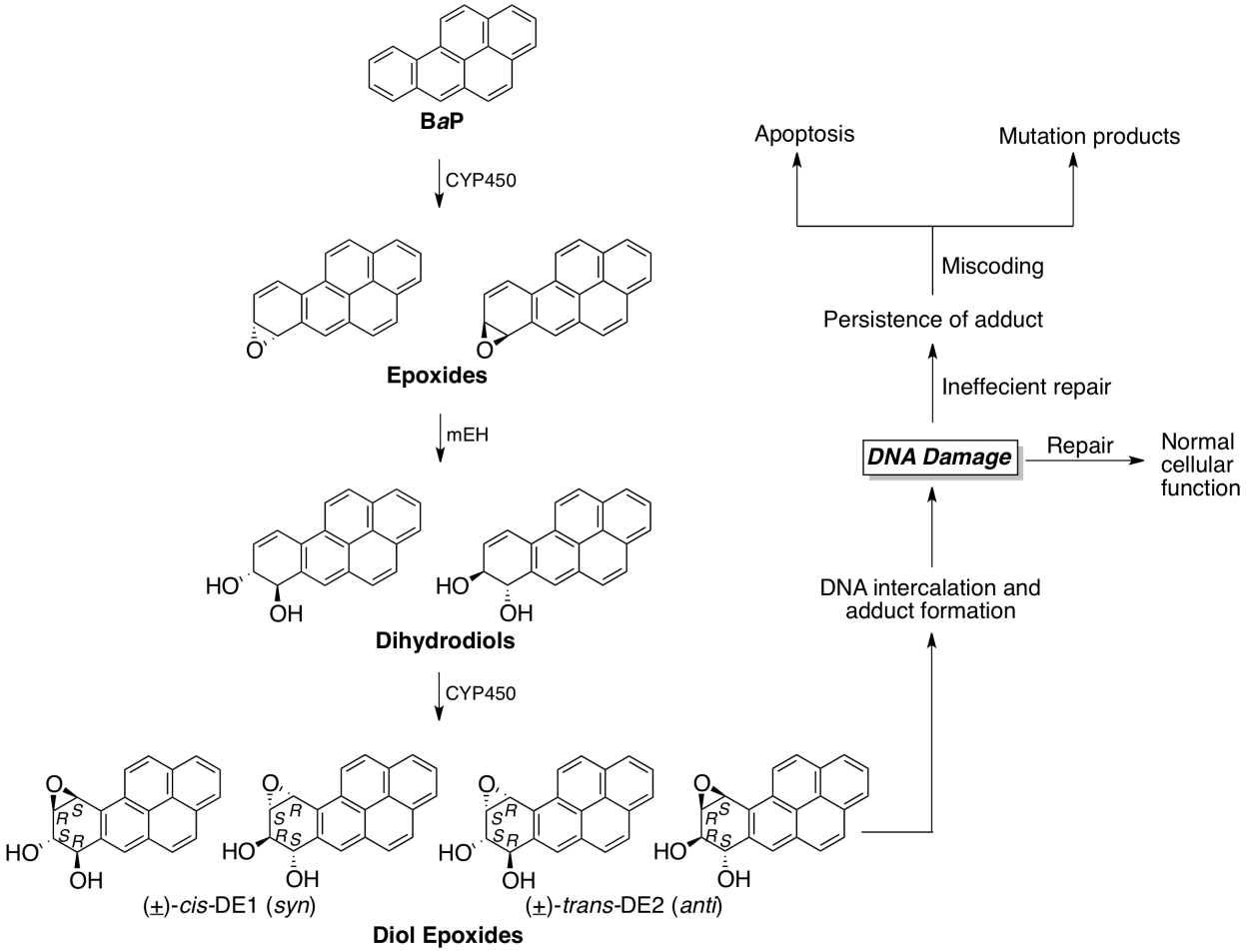

In a mammalian system a PAH undergoes metabolic activation by monooxygenase cytochrome P450 (CYP450)[10] and microsomal epoxide hydrolase (mEH),[11] enzymes typically found in mammalian liver, and specifically the endoplasmic reticulum in the cell.[10,11] Initially, mono-oxidation involving a CYP450, (for example CYP450 1A1, CYP450 1B1 and CYP450 3A4 are predominate in mammals

including humans), results in the formation of arene oxides.[12a] These arene oxides undergo enzymatic hydrolysis to *trans* dihydrodiols catalyzed by mEH (Scheme 3).[11,12b] The dihydrodiols are considered proximate carcinogens since they lead to the formation of diol epoxides, and as described earlier, are themselves involved with producing reactive oxygen species and *ortho*-quinone derivatives.[7] CYP is again responsible for the subsequent epoxidation of the dihydrodiols to yield four isomeric diol epoxides (two enantiomeric pairs of diastereomers). The diol epoxides are considered the ultimate carcinogenic species.[1,2,13]

The series 1 diol epoxides (DE1 or *syn*) have a *cis* arrangement of benzylic hydroxyl group and oxirane. These normally exhibit a quasi-diaxial arrangement of the hydroxyls and lack tumorigenic activity.[13] The series 2 diol epoxides (DE2 or *anti*) have a *trans* arrangement of the benzylic hydroxyl group and oxirane. These normally have quasi-diequatorial hydroxyls and are tumorigenic (Scheme 3).[14] The bay region-containing B*a*P exemplifies the trends shown for these diol epoxides. However, there are exceptions. For example, *both* the series 1 and series 2 diol epoxides of B*c*Ph exhibit quasi-diequatorial hydroxyl groups.[13a] This atypical result conformation observed for DE1 of B*c*Ph may be attributable to steric overcrowding at the fjord region.[13a]

The DE2 (*R*,*S*,*S*,*R*) (as read from the benzylic hydroxyl carbon to the benzylic epoxide carbon) isomers of B*a*P and B*c*Ph have shown to exhibit the highest genotoxicity in mammalian cells and high carcinogenic potency in mouse tumor models compared to the other three isomers.[15-17] Notably, the DE1 (*S*,*R*,*S*,*R*) isomer, typically devoid of any tumorigenic activity, exhibits marked tumorigenic activity in B*c*Ph.[13] This may be attributed to the unusual quasi-diequatorial hydroxyl group arrangement as a result of the steric overcrowding of the fjord region, as previously mentioned.[13] All four diol epoxides however, are potent electrophiles capable of reacting with biological nucleophiles such as adenine or guanine within DNA.

Interestingly, though the parent hydrocarbon B*c*Ph is a weak carcinogen and is poorly metabolized to DNA adducts as observed in mouse skin models, reactions of DNA with the diol epoxides of B*c*Ph demonstrate high levels of DNA alkylation.[16] In contrast, the parent hydrocarbon B*a*P is a strong carcinogen but its resulting diol epoxides exhibit low levels of DNA alkylation.[17] The data in Figure 4 graphically show the relative extents of reaction of the diol epoxides of B*a*P[17a] and B*c*Ph[16a] with calf

thymus DNA in vitro. The extent of reaction is measured as the percentage of the diol epoxide used that is trapped by DNA adduct formation. Clearly, for any diol epoxide isomer, B*c*Ph demonstrates higher levels of DNA alkylation as compared to B*a*P. However, the extent of alkylation does not correlate to high levels of carcinogenicity for B*c*Ph.[16,17]

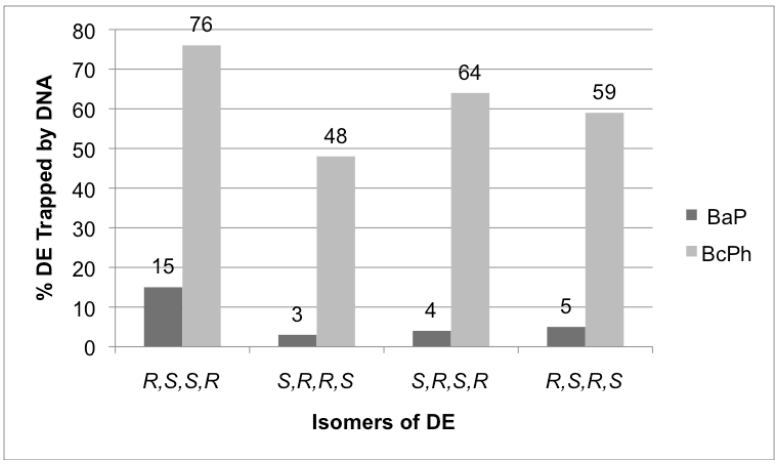

Figure 4. Relative Extents of Reaction of B*a*P and B*c*Ph Diol Epoxides.[18]

This shows that the extent of DNA alkylation by the diol epoxides of different PAHs, whether high or low, does not shed insight on their carcinogenicity.[16,17] Additionally, among different PAHs the extent of metabolic activation varies, and may depend on the molecular structure of that PAH, e.g. B*a*P is planar while B*c*Ph shows 27º non-planarity between its outermost rings.[1,13,14]

Also, DNA alkylation by diol epoxides of B*c*Ph are known to occur to a high extent at the N^6-amino group of 2'-deoxyadenosine residues in the major groove of DNA.[18] On the other hand, diol epoxides of planar PAHs, such as B*a*P, are known to alkylate the N^2-amino group of 2'-deoxyguanosine residues in the minor groove of DNA.[18] The general trends suggest that DNA alkylation by non-planar PAHs exhibit a higher adenine/guanine adduct ratio as compared to planar PAHs.[1c,18]

The mechanism for this interaction between diol epoxides and DNA leading to alkylation is shown in Scheme 4. After rapid intercalation of the diol epoxide, protonation, then ring opening of the oxirane at the benzylic position on the diol epoxide follows, giving rise to a carbocationic intermediate. This carbocationic intermediate is subsequently trapped by the nucleophilic sites in the DNA, predominately the exocyclic amino groups of the purine bases adenine and guanine, giving covalently modified DNA.[1c,2b] Since the mechanism of DNA alkylation is S_N1-like, ring opening of any diol epoxide followed by

nucleophilic capture results in two adducts. Thus, any diol epoxide produces four nucleoside adducts (adenine and guanine) by reaction with DNA. Overall, the metabolism of any PAH and reaction with DNA produces sixteen possible nucleoside adducts (Figure 5).[13-18]

Scheme 4. Mechanism of Diol Epoxide Interacting with Nucleophilic Amino Group from DNA

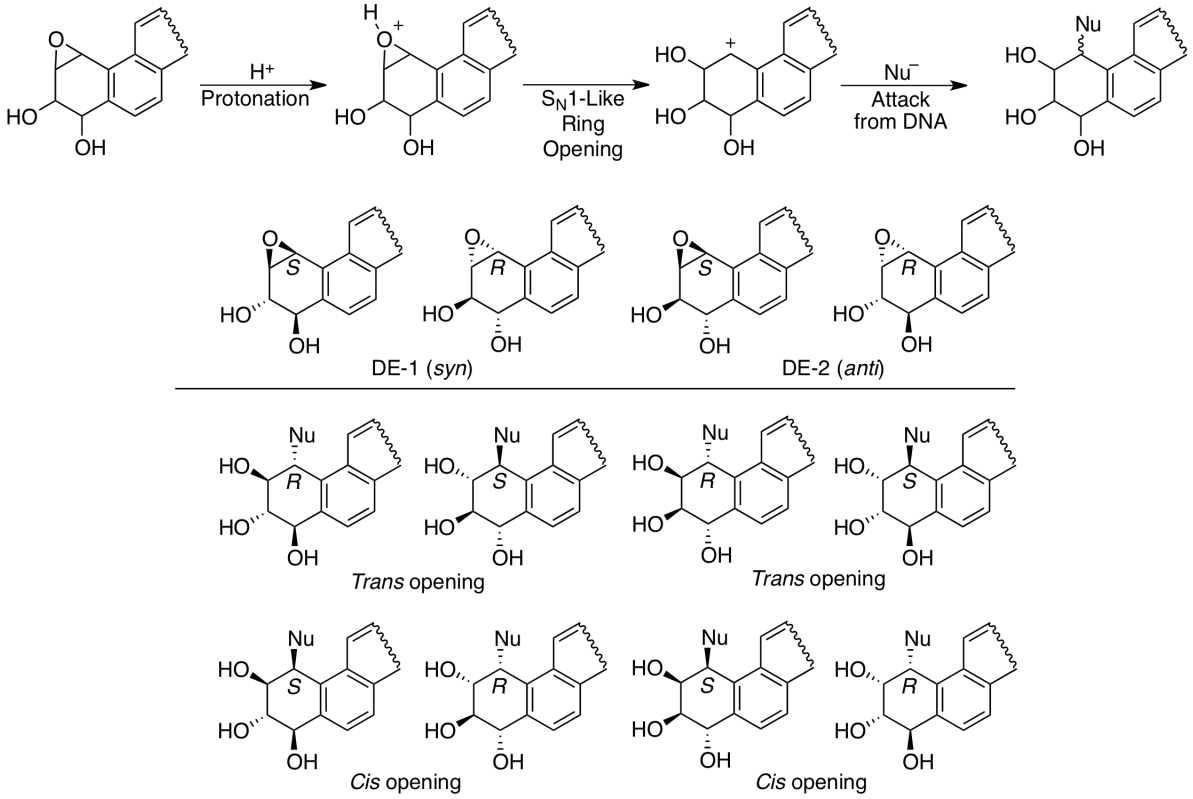

Figure 5. The Sixteen Nucleoside Adducts Formed from the Four Diol Epoxides of Any PAH, (Nu = Exocyclic Amino Group of Adenine or Guanine).

Upon DNA alkylation, covalent adducts perturb local DNA structures, which can then influence replication and/or repair mechanisms. Such events may result in either the introduction of mutations and pathways leading to tumorigenesis (carcinogenic isomers), or to benign results such as error-free replication or efficient repair (inactive isomers).[14,17] In order to gain a better understanding of the interactions of PAH metabolites with DNA and the ensuing cause for adverse or innocuous biological effects, it is necessary to have access to stereospecifically defined nucleoside and DNA adducts.

2.3 Aims

In the context of all the previously mentioned information on PAHs involving the extent of metabolic activation, carcinogenicity, and DNA alkylation, this research centers on two main aims.

1. Evaluate the effect of PAH structure, through use of newly synthesized PAHs, on the metabolic activation.
2. Develop a diastereoselective synthesis of a *cis* ring-opened amino triol from B*a*P DE1 for adduct synthesis. This will help understand the role of B*a*P DE1 DNA adducts and their biological response.

The first aim involves gaining an understanding of PAH non-planarity and its influence on the efficiency of metabolic activation. For this the B*c*Ph skeleton was selected for the following reasons. B*c*Ph is non-planar by 27º and upon metabolic activation it produces strong DNA alkylating diol epoxides.[1,16] The introduction of 1,4-dimethyl-[19a] and 1,4-difluoro-substituents[19b] into B*c*Ph increase molecular distortion (non-planarity) and this appears to decrease metabolic activation (Figure 6).[19]

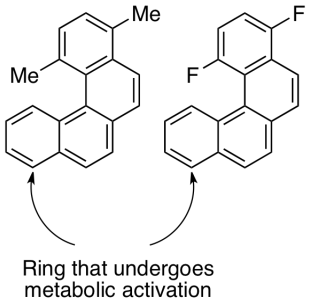

Figure 6. 1,4-Dimethyl- and 1,4-Difluoro B*c*Phs.

The non-planarity of the dimethyl and difluoro B*c*Phs is likely due to the location of the substituents proximal to the angular ring undergoing metabolic activation (Figure 6).[19] In this work we wanted to evaluate if the presence of substituents remote from the ring undergoing metabolism could influence metabolic activation (Figure 7). However, new chemistry needed development for the synthesis of our novel B*c*Phs since the prior protocol was inadequate.[19] Chapter 3 presents the synthesis of two new B*c*Ph derivatives with remote functionalization and an assessment of their influence on molecular structure.

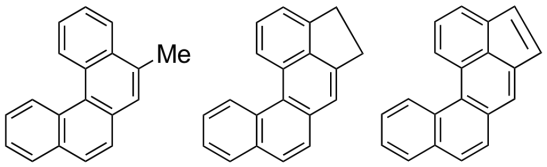

B*c*Ph Derivatives

Figure 7. B*c*Ph Derivatives Required for Study.

The second aim centers on development of a diastereoselective synthesis of a *cis* ring opened aminotriol of B*a*P (Figure 7). Synthesis of this racemic aminotriol intermediate is important as it allows access to four B*a*P DE1-derived nucleoside adducts, namely two from deoxyadenosine and two from deoxyguanosine (Figure 8). In this context, stereoselective synthesis of twelve B*a*P adducts have been accomplished.[20-30] Thus, stereoselective synthesis of these four adducts will help to complete the set of all sixteen adducts of B*a*P.

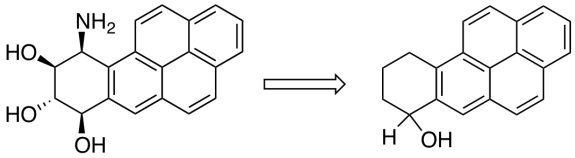

(±)-*cis*-Aminotriol B*a*P

Figure 8. (±)-*cis* B*a*P Aminotriol Derivative Needed for Adduct Synthesis.

In order to synthesize these adducts, the desired *cis* B*a*P DE1 aminotriol is a lynch pin intermediate and Chapter 4 describes approaches towards the diastereoselective synthesis of this compound. The data to be gained based on the site-specific incorporation of these adducts into DNA will help to better the understanding of PAH-DNA adducts and their effects on intracellular processes.

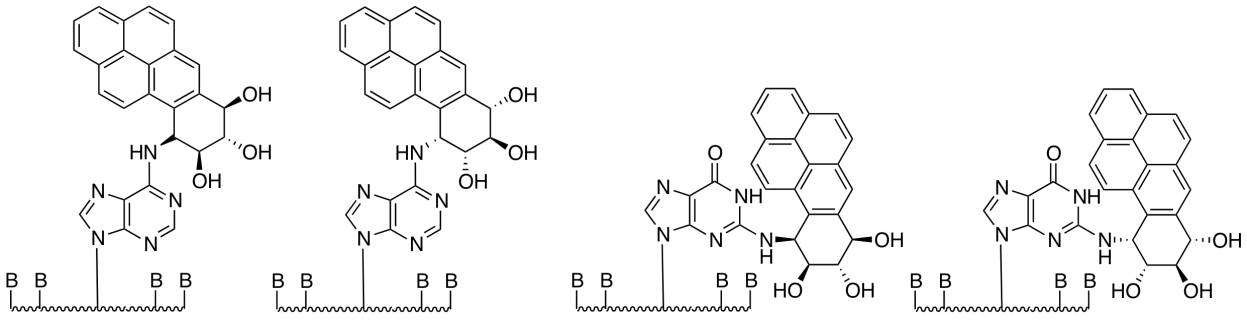

Two Deoxyadenosine Adducts

Two Deoxyguanosine Adducts

Figure 9. Four Stereochemically Defined B*a*P DE1 Adducts of Interest.

Studies in Chemical Carcinogenesis

Chapter 3

A New Approach to Substituted Benzo[*c*]phenanthrenes and their Putative Metabolites via Metal-Mediated Chemistry

3.1 Introduction

Polycyclic aromatic hydrocarbons (PAHs) exert their carcinogenic activity through covalent binding to genomic DNA. The most potent PAHs often have four to six benzo rings and contain structural features such as sterically crowded bay or fjord regions.[1] The bay region is formed by angular condensation of benzo rings as shown using benzo[*a*]pyrene (B*a*P, **2**) in Figure 1. Fjord regions arises from the peri-condensation (angular arrangement) of a benzo ring at the bay region of precursor PAHs.[2] For example, addition of an aromatic ring at the 3,4 positions of phenanthrene and 11,12 position of B*a*P, gives benzo[*c*]phenanthrene (B*c*Ph, **3**) and dibenzo[*a,l*]pyrene (DB[*a,l*]P, **4**), respectively (Figure 1).[1] PAHs that have these bay and fjord regions typically possess carcinogenic activity.[1] This genotoxicity of bay and fjord region-containing PAHs is elicited upon metabolic conversion to electrophilic derivatives, for example, the diol epoxide pathway described in the General Introduction.[1-6] Formation of diol epoxides at bay and fjord regions is considered the major pathway for metabolic activation of the most mutagenic and carcinogenic PAHs.[2]

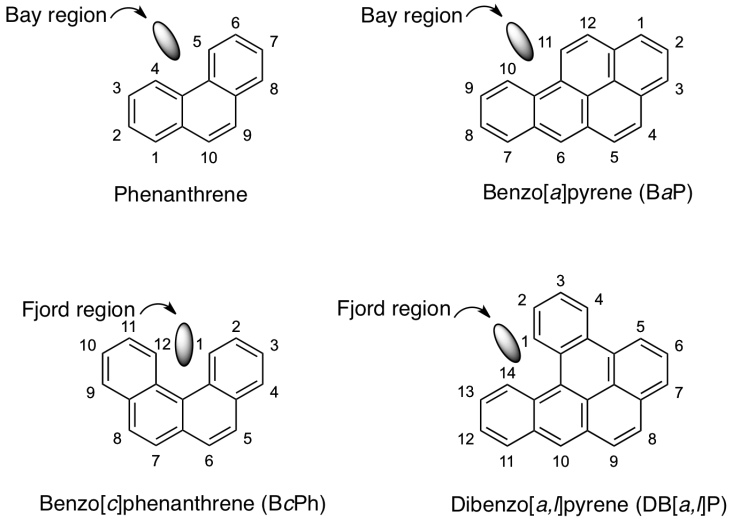

Figure 1. Bay and Fjord Region Containing Polycyclic Aromatic Hydrocarbons.

The angularly fused fjord-region containing compounds **3** and **4** are non-planar as opposed to typical bay-region containing compounds such as **1** and **2**, which are planar. The non-planarity arises due to steric hindrance between the hydrogen atoms at positions 1 and 12 for B*c*Ph **3**, and 1 and 14 for DB[*a,l*]P **4**. This causes such compounds to become non-planar.[1] B*c*Ph is 26.7º out of plane[7a] and DB[*a,l*]P is 27.6º out of planarity.[8a] Though there is only a slight difference in non-planarity, these PAH

are markedly different. DB[*a,l*]P is one of the most carcinogenic PAHs known to date, its diol epoxide metabolites exhibit 100 times the potency than that of B*a*P.[8b,c] B*c*Ph is weakly carcinogenic as compared to B*a*P in mouse skin models,[7b,c] and is poorly metabolized to diol epoxides.[9] All four diol epoxides, however, are strong DNA alkylating agents.[1,10]

Interestingly, though the (*R*,*S*,*S*,*R*) isomer (as read from the benzylic hydroxyl carbon to the benzylic oxirane carbon) of any PAH diol epoxide is generally tumorigenic, the (*S*,*R*,*S*,*R*) and the (*R*,*S*,*S*,*R*) isomers of B*c*Ph diol epoxides (Figure 2) are *both* tumorigenic.[11] Notably, the (*S*,*R*,*S*,*R*) isomer is a series 1 diol epoxide (DE1), and normally this isomer is devoid of tumorigenic activity.[12] B*c*Ph DE1 epoxides however, have quasi-diequatorial hydroxyls, a deviation from other DE1 epoxides that have quasi-diaxial hydroxyls, and may account for the difference observed.[13]

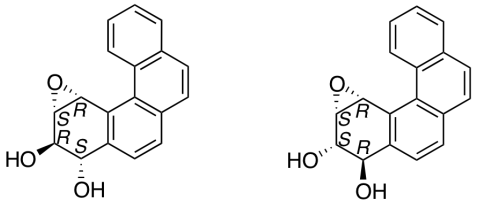

(+)-*cis*-DE1 B*c*Ph (*syn*) (–)-*trans*-DE2 B*c*Ph (*anti*)

Figure 2. The (*S*,*R*,*S*,*R*) and (*R*,*S*,*S*,*R*) Isomers of B*c*Ph Diol Epoxides.

DNA alkylation by diol epoxides of B*c*Ph occur to a significantly higher extent at the N^6-amino group of 2'-deoxyadenosine (N^6-dA) residues in the major groove of DNA.[14] On the other hand, diol epoxides of planar PAHs, such as B*a*P and chrysene, alkylate the N^2-amino group of 2'-deoxyguanosine (N^6-dG) residues in the minor grooves of DNA.[14] The trend suggests that DNA alkylation by non-planar PAHs exhibit a higher adenine/guanine adduct ratio compared to planar PAHs.[1c,14]

In addition, there are differences in the repair efficiencies of DNA adducts resulting from bay and fjord region PAH diol epoxides. Using codon 61 (a mutational hot spot of human H-*ras* and N-*ras* oncogenes), Geacintov and co-workers compared the removal of bay region-containing B*a*P diol epoxide and fjord region-containing B*c*Ph diol epoxide adducts using the human nucleotide excision repair (NER) system.[15] NER is a key mammalian mechanism against promutagenic bulky DNA lesions.[15] Eight different oligonucleotides containing (+)- or (–)-*trans*-B*a*P-DE2-N^6-dA and (+)- or (–)-*trans*-B*c*Ph-DE2-N^6-dA were synthesized, they were annealed and ligated with partially overlapping oligonucleotides to generate DNA duplexes as substrates for the standard NER-proficient HeLa cell extract.[15] The results

showed that the (+)- and (–)-*trans*-B*a*P-DE2-N^6-dA adducts were excised efficiently, where as the (+)- and (–)-*trans*-B*c*Ph-DE2-N^6-dA adducts were recalcitrant to repair.[15] This difference is attributed to the structure of the PAH attached to the nucleoside. Investigations by others[16,17] using NMR and molecular modeling analyses also showed that the (–)-*trans*-B*a*P-DE2-N^6-dA adduct inserts into the DNA double helix in a way that distorts the base pairing at the site of covalent modification.[16] On the other hand, both the (+)- and (–)-*trans*-B*c*Ph-DE2-N^6-dA adducts are intercalated into the helix without disturbing the Watson–Click base pairing at the site of adduction, thus avoiding excision.[17] Apparently, the molecular planarity of different PAHs play a crucial role in DNA repair efficiency.

There are other examples of planar PAHs that exhibit unusual and interesting properties, and which is due to the introduction of substituents. For example, the addition of methyl groups into benz[*a*]anthracene (B*a*A, **5**) to give 7,12-dimethylbenz[*a*]anthracene (DMBA, **6**), results in metabolic activation greater than B*a*A itself (Figure 3).[18] The introduction of methyl substituents into the bay region at position 12 and at position 7 of the planar B*a*A results in the pseudo-fjord region-containing DMBA that is non-planar by 22º.[19a] DMBA is also a more potent carcinogen as compared to B*a*A, with carcinogenic activity so pronounced that it exceeds B*a*P as evident from experiments that show a higher tumor-initiating activity in mouse skin and rat mammary glands.[19b,c]

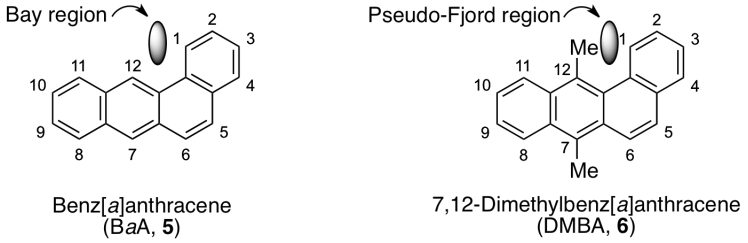

Figure 3. Structures of B*a*A and DMBA Showing Bay and Pseudo-fjord Regions.

The non-planar DMBA also shows similar DNA alkylation trends to B*c*Ph. Though all diol epoxide isomers of DMBA are DNA alkylating, the series 2 (*R*,*S*,*S*,*R*)- and series 1 (*S*,*R*,*S*,*R*)-diol epoxides of DMBA show equally high levels of DNA binding to both the N^6-exocyclic amino group of 2'-deoxyadenosine and N^2-exocyclic amino group of 2'-deoxyguanosine, with deoxyadenosine adducts prevailing.[20] The low level binding of planar bay-region B*a*P series 2 (*R*,*S*,*S*,*R*)-diol epoxide, however, shows exclusivity to the N^2-exocyclic amino group of 2'-deoxyguanosine residues in DNA.[14] Interestingly, in the case of DB[*a,l*]P (Figure 1, **4**), a fjord region containing compound resulting from a benzo ring

substituent added to the bay region of B*a*P, the series 2 (*R*,*S*,*S*,*R*)-diol epoxide predominately targets the N^6-exocyclic amino group of 2'-deoxyadenosine and to a lesser extent the N^2-exocyclic amino group of 2'-deoxyguanosine residues in DNA.[21] On the basis of the foregoing, the non-planarity of DMBA (22º), DB[*a,l*]P (27.6º) and B*c*Ph (26.7º), and their preferences for adenosine residues in DNA, supports the notion that non-planar PAHs demonstrate a higher adenine/guanine adduct ratio.[1,14]

Though the presence of substituents in or near a bay or fjord region of PAHs can influence molecular structure and metabolism, there are examples where substitution at non-bay or -fjord regions can cause a change in carcinogenic activity compared to the parent hydrocarbon. Substitution at the peri-positions, as in 6-methyl B*a*P[22a] and 7-methyl B*a*A,[22b] showed increased carcinogenic activity as compared to their respective parent hydrocarbons. 7-Methyl B*a*A is even considered most active among all mono-methylated derivatives of B*a*A (Figure 4).[1d,22b] All these observations involving the introduction of substituents into angularly fused PAHs that can ultimately alter metabolic activation and DNA binding trends, are reasons for interest in the studies of substituent effects and PAH structure.

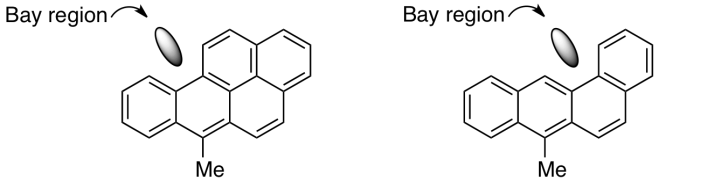

6-Methylbenzo[*a*]pyrene (6-Methyl B*a*P, **7**)

7-Methylbenz[*a*]anthracene (7-Methyl B*a*A, **8**)

Figure 4. Structures of 6-Methylbenzo[*a*]pyrene and 7-Methylbenz[*a*]anthracene.

In this regard, Lakshman and co-workers have been seeking correlation between the non-planarity of PAHs and its influence on metabolic activation and DNA binding of the metabolites, using substituted, angularly-fused B*c*Ph derivatives and their metabolites.[23] This involves the use of X-ray crystallography to evaluate molecular structures, combined with metabolic activation and DNA binding experiments using human breast cancer MCF7 cells. Human breast cancer cells exhibit a high level of CYP450 1B1, a key cytochrome involved in oxidative metabolic activation of PAHs leading to tumor formation, hence the experimental data could disclose the level of metabolic activation and DNA alkylation for PAHs.[24,25] The first report described the synthesis of the dimethylated analogue of B*c*Ph, 1,4-dimethybenzo[*c*]phenanthrene, (1,4-DMB*c*Ph, **9**), its (±)-*trans*-9,10-dihydrodiol [(±)-*trans*-9,10-

dihydroxy-9,10-dihydro-1,4-dimethylbenzo[*c*]phenanthrene, (**10**)], and the (±)-DE2 diol epoxide [(±)-11α,12α-epoxy-9β,10α-dihydroxy-9,10-dihydro-1,4-dimethylbenzo[*c*]phenanthrene, (**11**)], shown in Figure 5.[23a]

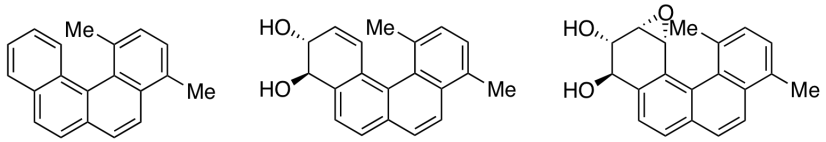

1,4-DMB*c*Ph, **9** (±)-*trans*-dihydrodiol-1,4-DMB*c*Ph, **10** (±)-*cis*-DE2-1,4-DMB*c*Ph, **11**

Figure 5. Dimethylated Analogue of B*c*Ph as well as its Putative Dihydrodiol and Diol Epoxide Metabolites.[23a]

The dimethylated B*c*Ph was investigated for a few reasons. The unique structure of B*c*Ph along with its metabolic activation profile and DNA binding trends are well documented. These offer a good starting point for further work. Since B*c*Ph has an overall molecular distortion of 26.7°,[7a] the presence of added methyl groups is likely to increase the degree of non-planarity due to the steric crowding in the fjord region. Also, synthesis of 1,4-DMB*c*Ph and its metabolites seemed accessible using known photochemical methodology.[26]

Indeed, syntheses of 1,4-DMBcPh as well as the metabolites, was achieved using photochemical ring-closure methodology (Scheme 1).[26] Commercially available 2,5-dimethylbenzyl chloride, was converted to 2,5-dimethylbenzyltriphenylphosphonium chloride salt **14** by reaction with PPh_3 in toluene. Wittig condensation of **14** with 2-naphthaldehyde (**12)** provided a mixture of *cis*/*trans* alkenes **15**.[27] These alkenes were irradiated with a 450-W medium pressure Hg lamp and a catalytic amount of iodine under an air-sparge in benzene that successfully gave the ring closed product 1,4-DMB*c*Ph **9**, in 55% yield.[23a,27] The isomeric benz[*a*]anthracene derivative by closure of **15** at the other *ortho*-position in the naphthalene was not observed.[28]

Scheme 1. Synthesis of 1,4-DMB*c*Ph and its Metabolites[a]

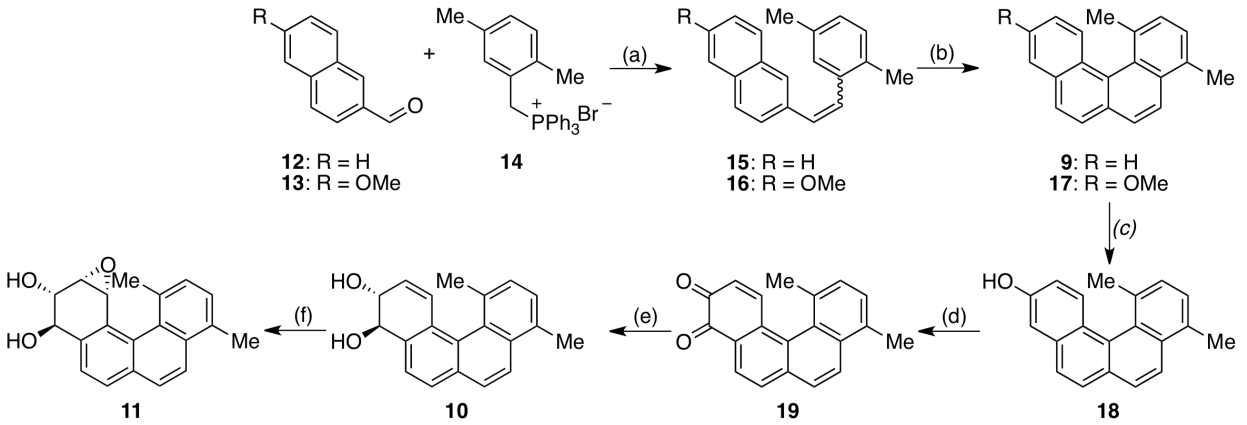

[a] Reagents and conditions: (a) NaOMe, MeOH, rt; (b) PhH, I_2, air, $h\upsilon$ or PhH, I_2, PPO; (c) BBr_3, CH_2Cl_2, -78 °C to rt; (d) $(PhSeO)_2O$, THF, reflux; (e) $NaBH_4$, EtOH, O_2, rt; (f) *m*-CPBA, THF, $NaHCO_3$, rt.

Correspondingly, Wittig reaction of phosphonium salt **14** with 6-methoxy-2-napthaldehyde (**13**) gave a *cis*/*trans* alkene mixture **16**. Irradiation of **16** gave 10-methoxy-1,4-dimethylbenzo[*c*]phenanthrene (**17**), in a low yield of 38%. Katz modification of this photochemical method using stoichiometric iodine and propylene oxide,[29] provided a higher 58% yield of **17**. The methoxy group in **17** was then cleaved using boron tribromide (BBr_3) in CH_2Cl_2 to give phenol **18**, which was then oxidized to the *o*-quinone **19** using benzeneseleninic anhydride in refluxing THF.[23a] Reduction of the *o*-quinone using sodium borohydride in ethanol under an oxygen atmosphere[30] gave the corresponding (±)-*trans*-9,10-dihydroxy-9,10-dihydro-1,4-dimethylbenzo[*c*]phenanthrene (**10**), in a yield of 60%. By NMR this dihydrodiol was found to be a 3:1 mixture of diastereomeric isomers (see below).[23a] Finally, epoxidation of the dihydrodiols with *m*-CPBA afforded the same 3:1 mixture of diastereomeric series 2 diol epoxide **11** isomers in a yield of 78%. This face-selective epoxidation with *m*-CPBA was achieved with **10** since the dihydrodiol possesses quasi-equatorial hydroxyl groups. Dihydrodiols with such an arrangement of hydroxyls normally undergo epoxidation with *m*-CPBA from the same side as the allylic hydroxyl group.[31a]

X-ray crystallographic analysis of 1,4-DMB*c*Ph revealed about a 10º increase in out-of-plane distortion as compared to B*c*Ph. The addition of methyl groups led to an angle of 36.6º between the outer most rings for 1,4-DMB*c*Ph.[23a] This distortion also resulted in the display of helical properties of the compound. 1,4-DMB*c*Ph was found to exist as an enantiomeric pair of *P* and *M* atropisomers (Figure 6). It is this helical phenomenon that resulted in the 3:1 mixture of diastereomers observed for the dihydrodiol

and diol epoxide metabolites during the synthesis.[23a,30] In addition, the high steric hindrance in the fjord region allowed for a slow *P* to *M* interconversion on the NMR time scale, and the dihydrodiol diastereomers showed individual NMR resonances.[23a]

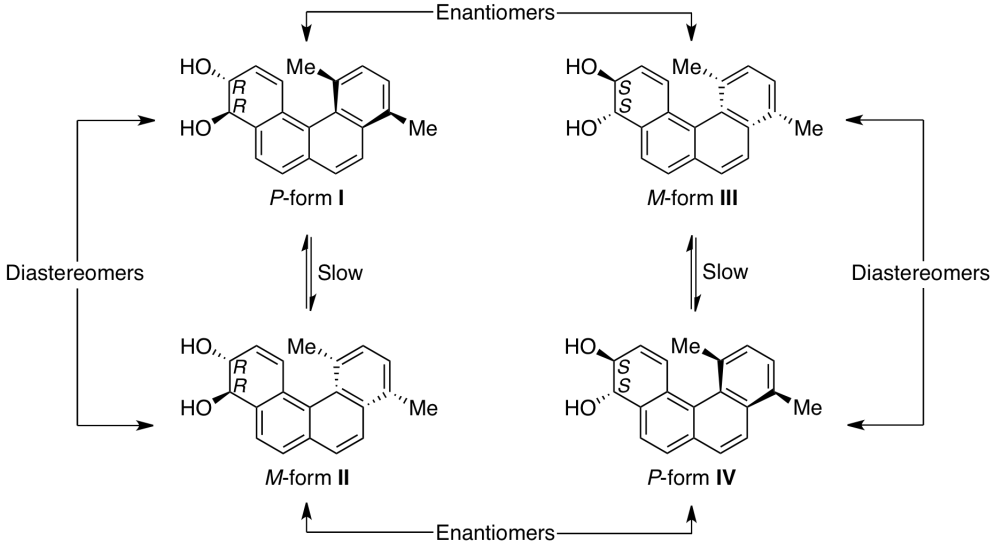

Figure 6. Structures of the Four Dihydrodiols of 1,4-DMB*c*Ph and their Relationship to each other.

The metabolic activation of the 1,4-DMB*c*Ph was studied using MCF-7 cells. These human mammary carcinoma cells express high levels of CYP450 1B1 enzymes that have the ability to activate PAHs to DNA binding intermediates via oxidation pathways.[24,25] Cells were treated with 1,4-DMB*c*Ph, B*a*P, and B*c*Ph, as well as the dihydrodiol metabolites of 1,4-DMB*c*Ph and B*c*Ph, for 24 hours. The DNA was isolated and analyzed by ^{33}P postlabeling and HPLC.[23a] In comparison to B*a*P, both B*c*Ph derivatives were overall poor converters to DNA damaging intermediates.[23a] A 3-fold lower level of DNA adduct levels was observed with 1,4-DMB*c*Ph as compared to B*c*Ph.[23a] This observation was the first indication that an increase in non-planarity of PAHs can influence metabolic activation. The experiments with the dihydrodiol derivatives revealed a 11-fold decreased conversion of the 1,4-DMB*c*Ph dihydrodiol to DNA alkylating agents, as compared to the B*c*Ph dihydrodiol. This supported the idea that non-planarity at the site of final P450 oxidation may decrease the metabolic activation leading to diol epoxides. Though B*c*Ph is poorly metabolized compared to planar B*a*P, its non-planarity may be a contributor to lowered metabolic activation. However, these non-planar metabolites, once produced, can still potently alkylate DNA.[23a]

Lakshman and co-workers then became interested in evaluating the influence of fluorine substituents on the B*c*Ph system.[23b] Fluorine atom is highly electronegative but is smaller than a methyl group. Fluorine substituent is also known to influence the tumorigenic properties of PAHs. For example, the 1-fluorobenzo[*c*]phenanthrene (1-FB*c*Ph) exhibits a marginal increase in tumorigenic activity compared to parent B*c*Ph at comparable doses in mouse skin models (Figure 7 and Table 1).[7b] Tumor-initiating activity is also notably higher in 3-, 4-, and 6-FB*c*Ph derivatives. 2-FB*c*Ph, however, has a much lower level of tumorigenic activity (Table 1).[7b]

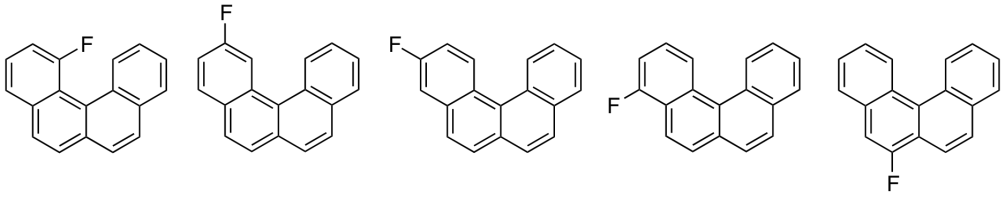

1-FB*c*Ph, **20** 2-FB*c*Ph, **21** 3-FB*c*Ph, **22** 4-FB*c*Ph, **23** 6-FB*c*Ph, **24**

Figure 7. Mono-fluorinated B*c*Phs that Exhibit Tumorigenic Activity.

Table 1. Tumor-initiating Activity of Fluorobenzo[*c*]phenanthrenes

Compound	B*c*Ph, **1**	1-FB*c*Ph, **20**	2-FB*c*Ph, **21**	3-FB*c*Ph, **22**	4-FB*c*Ph, **23**	6-FB*c*Ph, **24**
Dose, μmol	0.4	0.4	0.4	0.4	0.4	0.4
% of Mice with Tumors	29	33	17	48	69	64

In the light of the tumorigenicity data for the 1- and 4-FB*c*Ph derivatives, 1,4-difluorobenzo[*c*]phenanthrene (1,4-DFB*c*Ph) was of interest in the context of seeking correlation with B*c*Ph and 1,4-DMB*c*Ph. Also, the data gained should help in understanding how molecular distortion of B*c*Ph derivatives influences metabolic activation and DNA binding of the metabolites.[23b]

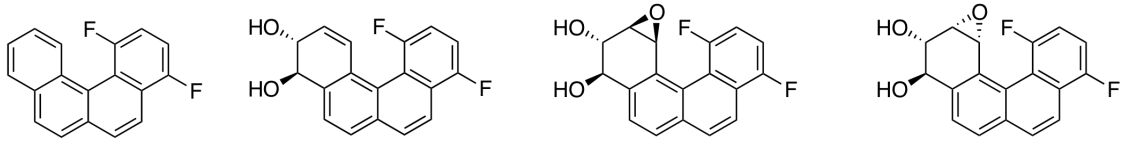

1,4-DFMB*c*Ph, **25** (±)-*trans*-dihydrodiol-1,4-DFMB*c*Ph, **26** (±)-*cis*-diol epoxide-1,4-DFMB*c*Ph, **27** [Series 1 (*syn*)] (±)-*trans*-diol epoxide-1,4-DFMB*c*Ph, **28** [Series 2 (*anti*)]

Figure 8. Difluorinated B*c*Ph Analogues of Interest for the Second Set of Studies.[23b]

Synthesis for 1,4-DFB*c*Ph, **25**, and its putative metabolites, **26**, **27** and **28** (Figure 8), was again achieved, via photochemical ring closure using starting materials that are commercially available.[23b] 2,5-Difluorobenzyl bromide was converted to its phosphonium salt **31**. A Wittig reaction between **31** and 2-naphthaldehyde (**29)** gave a ~1:2 mixture of *cis*/*trans* alkenes **32**.[27] Photochemical ring closure of the alkenes with a 450-W medium pressure Hg lamp and catalytic iodine with air sparging gave a 64% yield of 1,4-DFB*c*Ph **25** (Scheme 2).[23b,27]

For synthesis of the putative metabolites, Wittig reaction of **31** with commercially available 6-methoxy-2-naphthaldehyde (**30**) gave a 1:3 mixture of *cis*/*trans* alkenes **33**. Photochemical ring closure gave 1,4-difluoro-10-methoxy B*c*Ph **34**, in a yield of 58%.[23b,27] The methoxyl group in **34** was cleaved using BBr_3 in CH_2Cl_2. Phenol **35** was then oxidized to the *o*-quinone **36** using benzeneseleninic anhydride in THF. Reduction of **36** with sodium borohydride in ethanol under an oxygen atmosphere led to the (±)-*trans*-9,10-dihydroxy-9,10-dihydro-1,4-difluorobenzo[*c*]phenanthrene (**26**) in a yield of 79%.[23b,30] ^{1}H NMR showed that (±)-**26** exhibits a diequatorial arrangement of the hydroxyls groups with no unusual conformational changes due to the presence of fluorine atoms.[23b]

Scheme 2. Synthesis of 1,4-DFB*c*Ph and its Dihydrodiol[a]

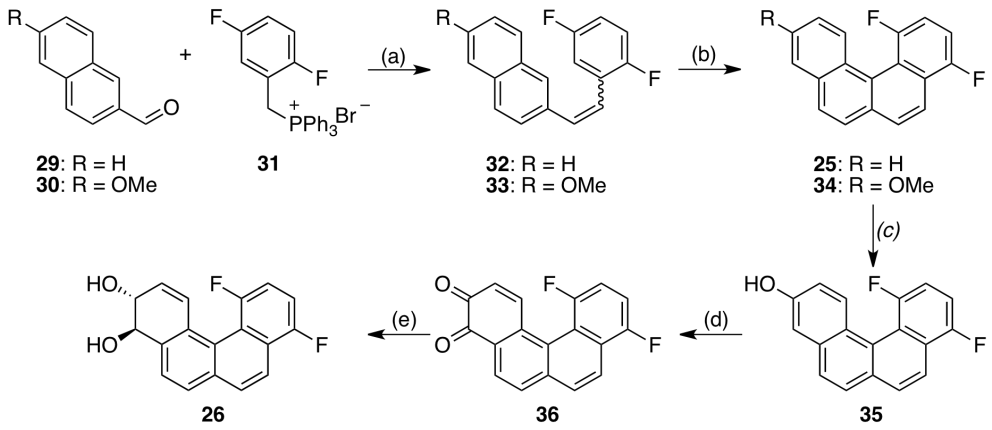

[a] Reagents and conditions: (a) NaOMe, MeOH, rt; (b) PhH, I_2, air, $h\upsilon$; (c) BBr_3, CH_2Cl_2, -78 °C to rt; (d) $(PhSeO)_2O$, THF, reflux; (e) $NaBH_4$, EtOH, O_2, rt.

Racemic dihydrodiol **26** was then readily converted to the series 1 and series 2 diol epoxides via known procedures.[31] For access to the series 1 diol epoxide, **26** was converted to the bromo triol **29** using *N*-bromoacetamide with THF-H_2O. The bromo triol **37** was cyclized using IRA-400 Amberite HO^- in anhydrous THF to give (±)-11β,12β-epoxy-1,4-difluoro-9β,10α-dihydroxy-9,10,11,12-

tetrahydrobenzo[*c*]phenanthrene (**27**) in a yield of 68% over two steps (Scheme 3).[23b,31] Epoxidation reaction of **26** with *m*-CBPA in THF afforded (±)-11α,12α-epoxy-1,4-difluoro-9β,10α-dihydroxy-9,10,11,12-tetrahydrobenzo[*c*]phenanthrene (**28**) in a yield of 92% (Scheme 3).[23b,31]

Scheme 3. Synthesis of 1,4-DFB*c*Ph Series 1 (*Syn*) and Series 2 (*Anti*) Diol Epoxides[a]

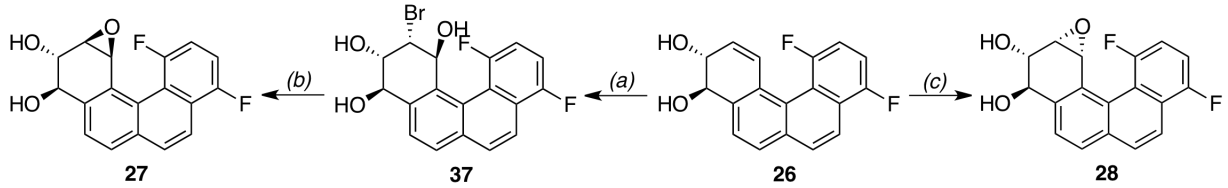

[a] Reagents and conditions: (a) *N*-bromoacetamide, THF-H_2O, rt; (b) Amberlite HO^-, THF, rt; (c) *m*-CPBA, THF, $NaHCO_3$.

Interestingly, unlike 1,4-DMB*c*Ph and its derivatives, no *P* and *M* helicity was observed for 1,4-DFB*c*Ph and its dihydrodiol and diol epoxide metabolites. However, ^1H and ^{19}F NMR analysis showed differences in the series 1 and series 2 diol epoxides. Most notably, DE1 and DE2 derivatives of B*c*Ph exhibit quasi-diequatorial hydroxyl groups, but in the case of 1,4-DFB*c*Ph, the DE1 derivative has quasi-diaxial hydroxyls, just as the DE1 of bay-region PAHs. The DE2 of 1,4-DFB*c*Ph demonstrates quasi-diequatorial hydroxyl groups, as anticipated.[13] This difference was attributed to the influence of the fluorine atom in the fjord region of the B*c*Ph derivative and/or the overall molecular distortion that may have caused the conformational change.[23b] A through-space, fjord region H–F coupling was also observed for 1,4-DFB*c*Ph and its metabolite derivatives, possibly because of the spatial proximity.[23b]

Data from X-ray crystallographic analysis revealed that 1,4-DFB*c*Ph was non-planar by a 33.5º.[23b] Comparatively, this placed the difluorinated derivative between B*c*Ph (26.7º)[7a] and 1,4-DMB*c*Ph (36.6º)[23a] in overall molecular distortion (Table 2). Comparative analysis between the dihydrodiol derivatives of B*c*Ph and 1,4-DFB*c*Ph showed a difference of 6º; B*c*Ph dihydrodiol was 16.3º out of plane, while 1,4-DFB*c*Ph was 22.4º (DFT computational analysis of 1,4-DMB*c*Ph gave an overall non-planarity of 29.6º,[32] as no crystals were available for X-ray analysis).[23b]

Table 2. X-Ray Crystallographically Determined Out-of-Plane Distortion for BcPh Derivatives

Angle Between	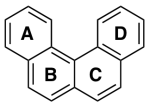	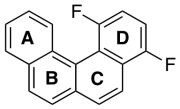	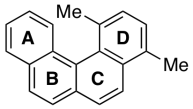	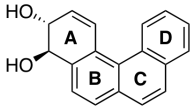	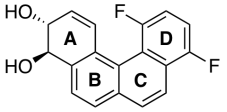
A,**D**	26.7º	33.5º	36.6º	16.3º	22.4º

To understand the influence of molecular distortion on metabolic activation and DNA binding leading to DNA damaging events, 1,4-DFB*c*Ph and its dihydrodiol were subjected to metabolism experiments. The extent of DNA damage was assessed by the amount of DNA binding observed in human breast cancer MCF-7 cells using ^{33}P postlabeling of the DNA and HPLC analysis of the DNA adducts produced.[23] These data were then compared with results from B*c*Ph, 1,4-DMB*c*Ph and their dihydrodiols, with B*a*P (benzo[*a*]pyrene) as a positive control.[23b] The results showed that 1,4-DFB*c*Ph gave poorer metabolic activation, which was consistent with results from the previous report with B*c*Ph and 1,4-DMB*c*Ph exhibiting low levels of activation (by 3-fold) compared to B*c*Ph.[23a] In contrast, 1,4-DFB*c*Ph and B*c*Ph dihydrodiols exhibited notable metabolic activation to DNA binding intermediates, and where 1,4-DFB*c*Ph dihydrodiol gave lower amounts of DNA adducts.[23b]

Conversion of the 1,4-DMB*c*Ph dihydrodiol was found to be 11-fold lower than that of the parent B*c*Ph dihydrodiol. This result supported the idea that an increase in molecular distortion influences metabolic activation pathways, particularly the final CYP450-mediated oxidation step where dihydrodiols are converted to DNA-damaging diol epoxides.[18a] Consistent with this proposal, the 1,4-DFB*c*Ph dihydrodiol showed a 4-fold lower metabolic activation compared to B*c*Ph dihydrodiol. This result offered additional support for the role of non-planarity in relation to metabolic activation especially the final oxidation of dihydrodiols to diol epoxides in the fjord region.[23b] Additionally, the diol epoxides resulting from this metabolic activation were determined to be the ultimate agents leading to DNA damage. Results from HPLC profiles of DNA adducts revealed that the series 2 diol epoxides of B*c*Ph and 1,4-DFB*c*Ph are strong DNA alkylating species.[23b] Overall, these results suggest that an increase in molecular distortion and possibly steric effects caused by substituents in the fjord region may be responsible for the observed lowered metabolic conversion. However, once the metabolites are produced, the potential for DNA binding events (alkylation) is significant.[23]

Based on both prior reports, the data implies that non-planarity does have a role in metabolic activation leading to DNA damaging species. However, it is not exactly clear whether these results are due to the influence of substituents in the fjord region of these B*c*Ph compounds, or if it is primarily based on the overall molecular distortion exhibited by these compounds. To address this question, an investigation using B*c*Ph derivatives that have remote functionalization (i.e. modification with no direct influence by substituents in the fjord regions), and which display varied molecular distortion, are needed. This would help to further establish the relation between the extent of non-planarity and the resulting metabolic activation involving cytochrome P450. Hence, a novel series of alkylated B*c*Ph derivatives (**38**, **42** and **43**) were envisioned for further studies (Figure 9).

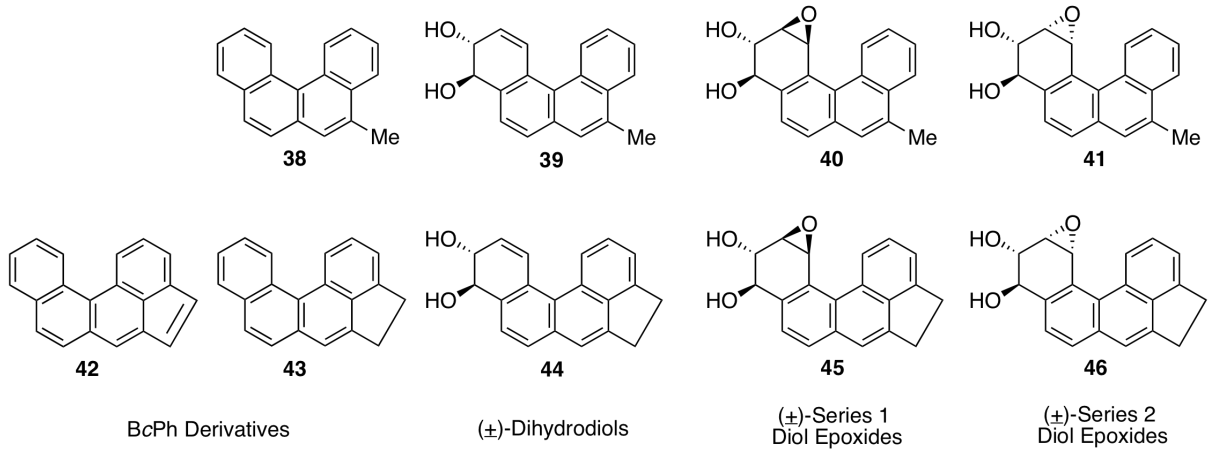

Figure 9. B*c*Ph Derivatives of Interest for the Current Study.

Once successful synthesis is achieved, the new B*c*Ph derivatives (**38**, **42**, and **43**) can be used for X-ray crystallographic analysis, to determine the extent of molecular distortion. The putative metabolites (**39**-**41**, and **44**-**46**) will help establish the relation between non-planarity, metabolic activation, and DNA binding. This study entails the development of *novel chemical syntheses* of unknown B*c*Ph derivatives, which are expected to help an understanding of non-planarity related to metabolic processes.

3.2 Results and Discussion

At present, the most convenient method for synthesis of B*c*Ph derivatives involves a Wittig reaction between naphthaldehydes and aryl phosphonium salts to give naphthylstyrenes. These are photocyclized to form the fused 4-ring systems (Schemes 1 and 2, steps a and b).[23,27] However, for this route, availability of appropriate starting substrates is crucial (Scheme 4, eq. 1). Retrosynthetic analysis for our desired B*c*Phs shows that the required precursors for cyclization are not readily available (Scheme 4, eq. 2 and 3), hence necessitating development of alternative approaches. In addition, the photocyclization methodology is limited to concentrations of 0.01 M of stilbenes.[33] Higher concentrations lead to [2+2] cycloaddition between the stilbene derivatives giving dimeric products. Thus, reaction scale up is often difficult.[33] For these reasons as well, alternative methods need to be considered.

Scheme 4. Retrosynthetic Analysis for Synthesis of B*c*Ph Derivatives

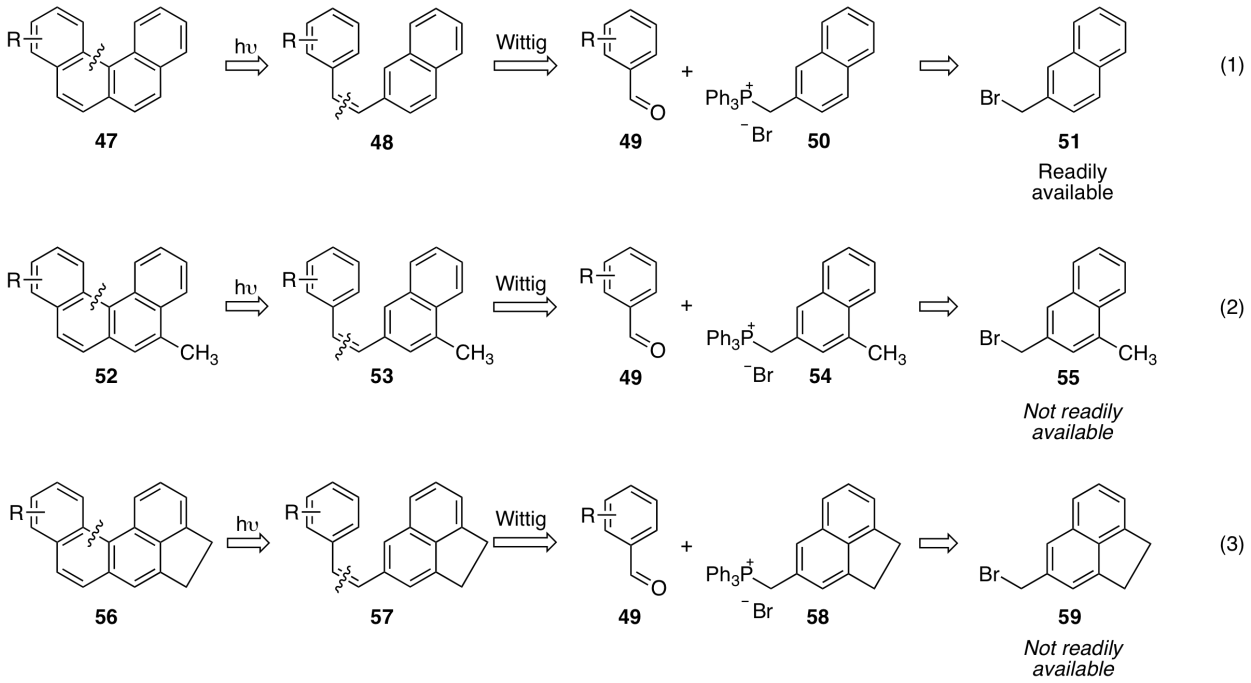

Due to our interest in and experience with metal catalysis chemistry and cross coupling reactions, the following retrosynthetic analysis led to a plausible route to the desired B*c*Ph derivatives (Scheme 5). We envisioned development of a general synthetic strategy that would circumvent the photocyclization, and would allow for rapid, modular assembly of a large variety as well as quantity of PAHs and their derivatives. The retrosynthetic plan shows the use of cross coupling precursors giving access to an

alkyne on a biphenyl system. The alkyne will yield an additional benzene ring via a key step involving a metal-catalyzed cyclization, thereby giving the angularly fused B*c*Ph core (Scheme 5).

Scheme 5. Retro Synthetic Plan for B*c*Ph derivatives

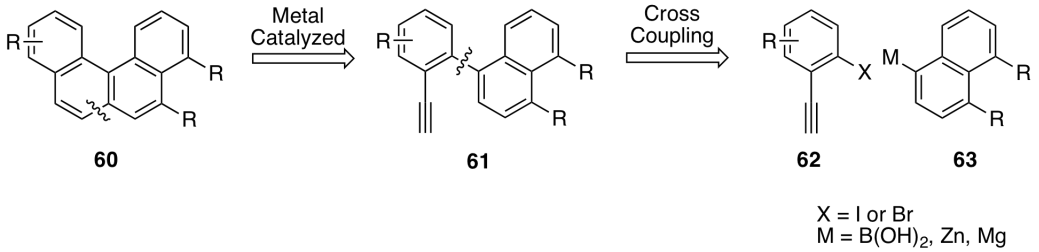

The basis of this proposal was founded in work by Fürstner et al.[34] In that work *ortho*-alkynylated biaryls were cyclized to phenanthrene derivatives using a metal chloride catalyst, particularly platinum chloride ($PtCl_2$) (Scheme 6).[34] Suitable biaryl aldehydes **64** obtained via Suzuki-Miyaura cross-coupling reactions[35] can be converted to the desired alkynes **65** by Corey-Fuchs methodology,[36] or by reaction with lithio trimethylsilyl diazomethane.[37] The addition of an electrophilic metal chloride in toluene at 80 ºC led to an equilibrium between the alkyne **65** and η^2 complex **66**. This complex is then believed to form a C–C bond with the adjacent aromatic ring, which with release of the metal catalyst, gives cyclized product.[34] $PtCl_2$ worked well overall, although, gold chloride ($AuCl_3$) and gallium chloride ($GaCl_3$) also gave good results. The cyclization showed a high preference for the 6-*endo*-*dig*-cyclization giving access to phenanthrenes **67** rather than the 5-*exo*-*dig*-cyclization product **68**.[34] Exceptions occurred if an electron-withdrawing ester group was present on the alkyne or when indium chloride ($InCl_3$) was used instead of $PtCl_2$.[34]

Cyclization of terminal alkynes with a metal catalyst, is thought to proceed through a metal vinylidene complex such as **73** in Scheme 7.[38] However, since the Pt-catalyzed phenanthrene cyclization involves *both* terminal as well as internal biaryl alkynes, another pathway had to account for the internal alkyne cyclization. Although Fürstner et al. suggests that activation of the π-system of the alkyne due to coordination of the metal (Scheme 6, complex **66**) may be responsible for efficient cyclization, no mechanistic pathway was detailed.[34]

Scheme 6. Metal-Catalyzed Cycloisomerization Reaction for Synthesis of Phenanthrenes Derivatives

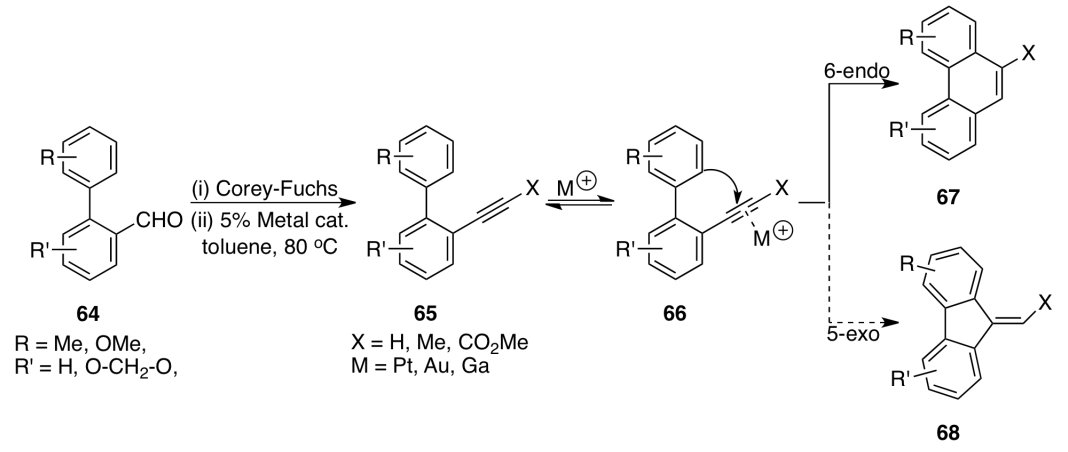

Examples:

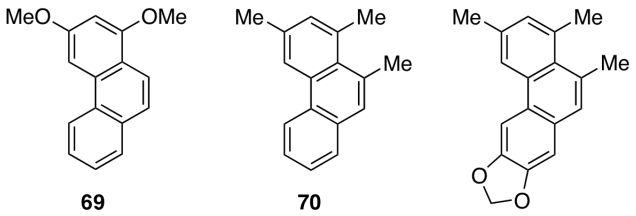

Scheme 7. Typical Cyclization Pathway for Terminal Alkynes

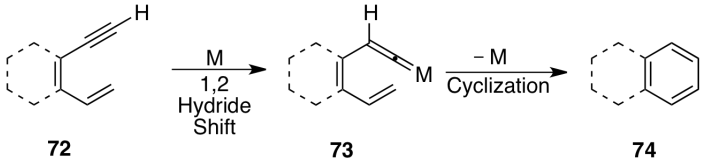

To gain further mechanistic insight, DFT[32a] computational studies by Soriano et al.[39] suggested a mechanism for these intramolecular cyclizations involving biaryl alkynes catalyzed by electrophilic transition metal complexes. The report showed that the computed results generally agreed with prior experimental results for a range of substrates and catalyst systems, and that the reaction is reminiscent of a Friedel–Craft type mechanism using electrophilic carbenes.[39] In addition, both the structural and electronic effects in the substrates undergoing cyclization, as well as the metal complexes formed in the reaction, played crucial roles in the *exo-dig* or *endo-dig* outcome of the cyclization.[39] Therefore, for the Pt-mediated *endo-dig* intramolecular cyclizations, the computational results suggests biaryls with alkyne that are electrophilic and/or electron-rich arenes that make them nucleophilic towards the alkyne, as suitable substrates. Once the metal coordinates to the alkyne, it facilitates the formation of electrophilic

metal-carbenes, which act as Lewis acids, and promote nucleophilic attack by the electron-rich arene.[39] Scheme 8 shows the possible computated intermediates that may be formed in such reactions, and involve a series of metal-cyclopropyl carbenes.[39] Interestingly, the calculated activation energies for reactions involving Pt show intermediate **77** having the lowest energy, and which may be the key reaction intermediate involved in the desired cyclization.[39]

Scheme 8. Reaction Pathway for Metal-Catalyzed Phenanthrene Synthesis from Computational Studies

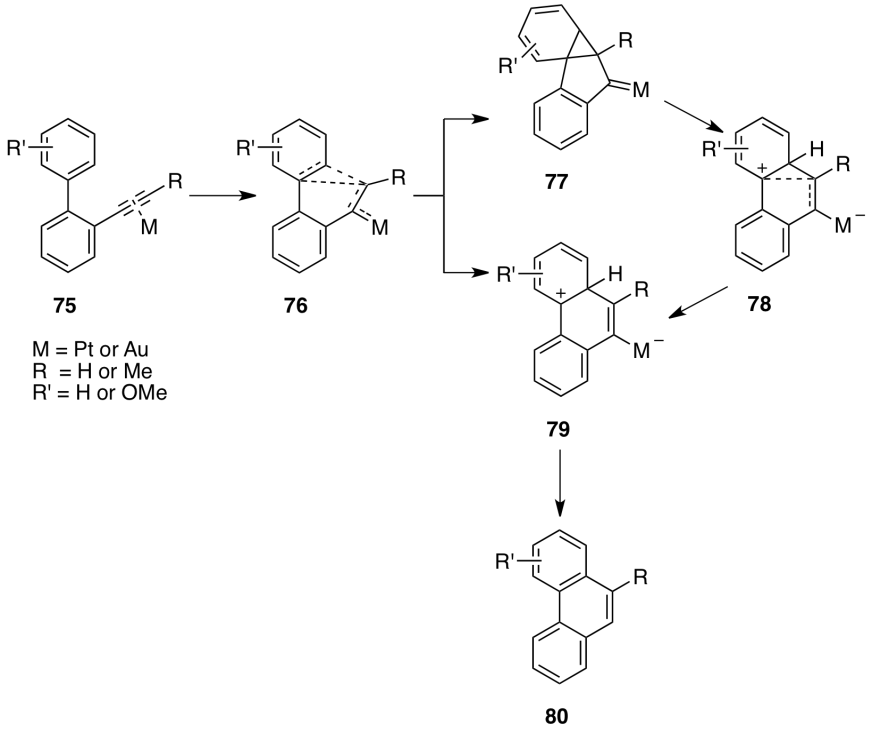

Based on the previous data, we anticipated the application of Pt-mediated cyclization as a viable route to the synthesis of our requisite B*c*Ph derivatives. The retrosynthetic analysis in Scheme 9 depicts a pathway that circumvents need for the photochemical protocol. Through the use of boronic acid derivatives and aryl bromides as starting materials, this route allows ready access to our desired B*c*Ph derivatives, and potentially many others, in a modular fashion.

Scheme 9. Retro Synthetic Analysis for Desired B*c*Ph Derivatives

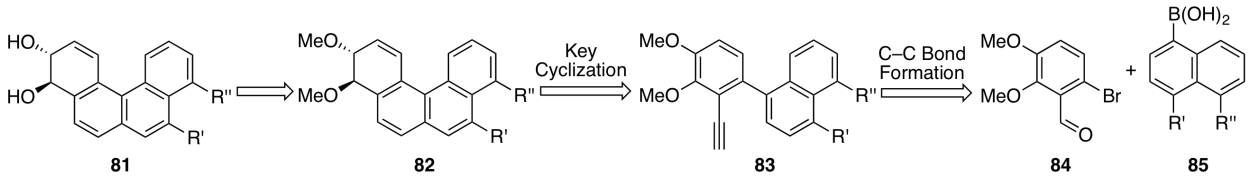

Our approach for the synthesis of the methylated B*c*Ph derivatives and their putative metabolites (Figure 9), from readily available starting materials, involves the following key steps (Scheme 10): (a) synthesis of suitable biaryl aldehydes, (b) alkynylation of that aldehyde, and (c) metal-catalyzed cyclization using $PtCl_2$ or $AuCl_3$. Using this protocol, we anticipated the synthesis of the desired B*c*Ph derivatives and their putative metabolites (dihydrodiol and diol epoxides).

Scheme 10. Planned Modular Synthesis for B*c*Ph derivatives

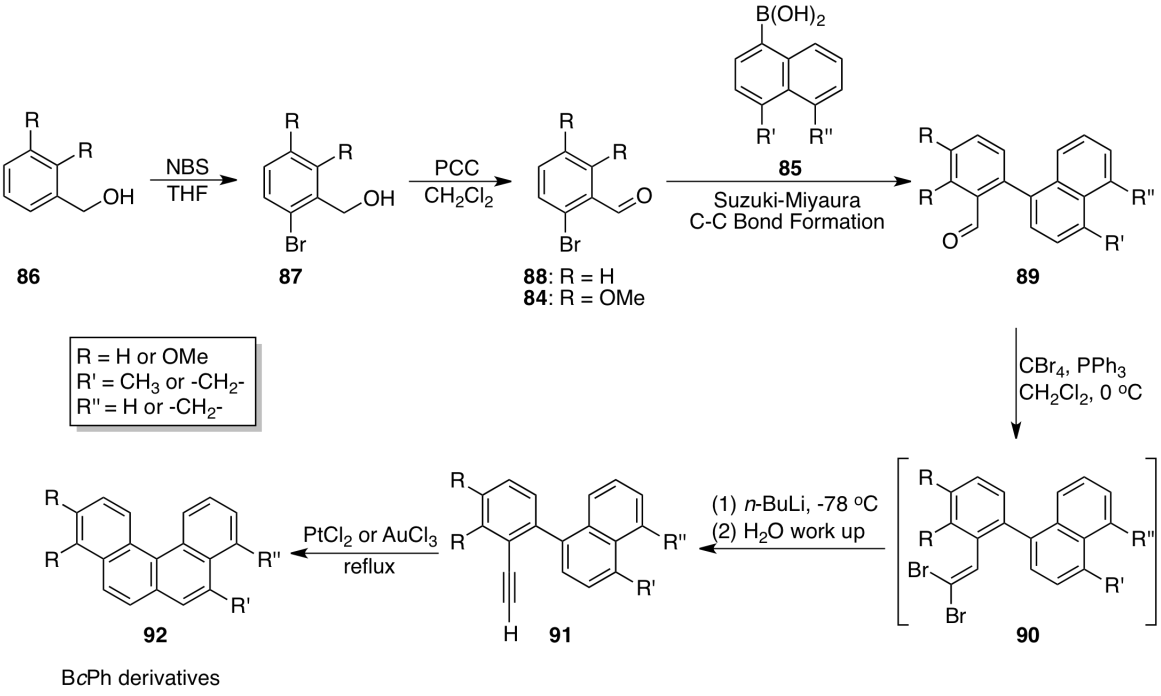

For the unsubstituted (parent) B*c*Ph derivatives, *o*-bromobenzaldehyde (Scheme 10, **88**: R = H) was a suitable precursor. For the dimethoxy B*c*Ph derivatives, needed for access to the putative metabolites, 2,3-dimethoxybenzyl alcohol (Scheme 10, **86**, R = OMe) was utilized. The alcohol was first converted to the bromo alcohol **87** under known bromination conditions[40] using *N*-bromosuccinimide (NBS) in THF. Then, oxidation[41] of **87** with pyridinium chlorochromate (PCC) in CH_2Cl_2 gave the requisite 6-bromo-2,3-dimethoxybenzaldehyde (**84** in Scheme 10).

For synthesis of the biaryl aldehyde derivative **89**, a trial one-pot synthesis developed by Giroux et al.[42] involving an in-situ generated aryl boronate was attempted (Table 3). The results in Table 3 show that after palladium catalyzed generation of the boronate with using bis(pinacolato)diboron in DMF at 80 ºC (step 1), addition of the aryl bromide to the mixture followed (step 2), and gave the desired biaryl

aldehyde. Though the reaction was conducted twice, purification of the aldehyde **96** proved arduous due to multiple impurities in close proximity to the desired material. Later attempts to reverse the roles of the aryl boronate and aryl bromide produced worse results.[43] For these reasons, the one-pot approach was abandoned and C–C bond formation between aryl bromides and boronic acids was used instead.

Table 3. Preliminary Results in a One-Pot Synthesis of Biaryl Aldehydes

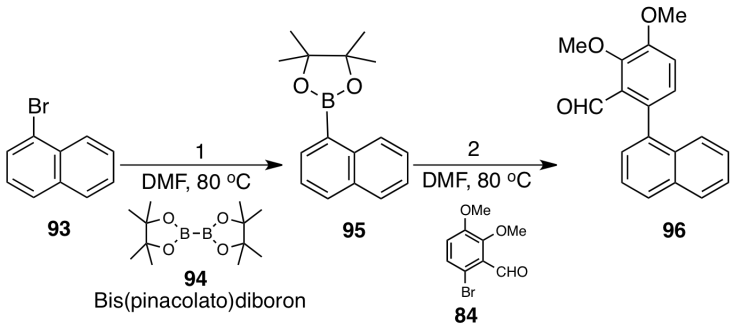

	Step 1					Step 2				
Entry	**93**	**94**	Base	Pd	Results	**95**	**84**	Base	Pd	Results[a]
1	1.0 eq	1.1 eq	KOAc 3 eq	$PdCl_2$(dppf) 0.033 eq	14 h, **93** consumed, multiple spots	1.0 eq	0.5 eq	2M Na_2CO_3 5 eq	$PdCl_2$(dppf) 0.033 eq	21 h, 79% of **96**
2	1.0 eq	1.1 eq	KOAc 3 eq	$PdCl_2$(dppf) 0.033 eq	18 h, **93** consumed, multiple spots	1.0 eq	0.5 eq	2M Na_2CO_3 5 eq	$PdCl_2$(dppf) 0.033 eq	24 h, 86% of **96**

[a] Yield of pure product obtained after several column chromatographies.

Though the boronic acids required for synthesis are commercially available, to save cost (4-methylnaphthalen-1-yl)boronic acid (**98**) and (1,2-dihydroacenaphthylen-5-yl)boronic acid (**100**) were synthesized by known literature procedures (Scheme 11).[44] The respective aryl bromides were subjected to lithiation with *n*-butyllithium (*n*-BuLi) in THF at –78 ºC followed by reaction with trimethyl borate [$B(OMe)_3$]. Workup, followed by trituration gave the boronic acids as off-white solids, in good yields.

Scheme 11. Synthesis of Requisite Boronic Acid Derivatives[a]

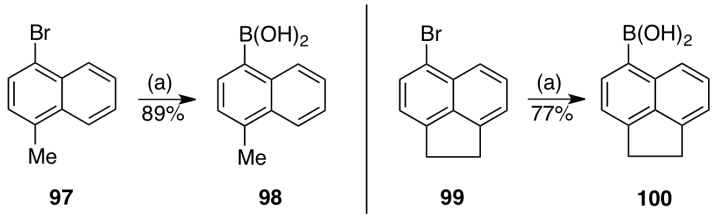

[a] Reagents and conditions (a) (i) *n*-BuLi, $B(OMe)_3$, -78 ºC; (ii) 10% HCl workup.

In the report by Fürstner et. al.,[34] among the synthesis of various phenanthrene derivatives, one example for a four-ring fused aromatic system was reported, namely that of B*c*Ph in a yield of 65% using $PtCl_2$. We initially decided to test this protocol for synthesis of B*c*Ph while evaluating any advantageous modifications (Scheme 12). The Suzuki–Miyaura coupling conditions[35] employing 1-bromobenzaldehyde and 1-naphthylboronic acid with $Pd(PPh_3)$ and CsF in refluxing 1,3-DME afforded the biaryl aldehyde **102** in a high 92% yield. The aldehyde was subjected Corey-Fuchs olefination[36b] using CBr_4 and PPh_3 in CH_2Cl_2, to give a quantitative yield of the dibromo olefin **103**. Modification of the protocol by substituting PPh_3 with hexamethylphosphorous triamide (HMPT), gave an incomplete reaction. Alkynylation of dibromo olefin **103** with *n*-BuLi gave, after aqueous work-up, alkyne **104** in a yield of 66%. Efforts to improve the yield at this step using lithium diisopropyl amide (LDA)[45] gave a low 29% yield of the alkyne. Metal-catalyzed cyclization of the alkyne using 5% $PtCl_2$ gave a 69% yield of B*c*Ph, which was comparable to the literature result.[34] The $AuCl_3$-catalyzed reaction however, gave a much lower 45% yield, and was incomplete even after 24 h.

Scheme 12. Synthesis of Benzo[*c*]phenanthrene (**3**)

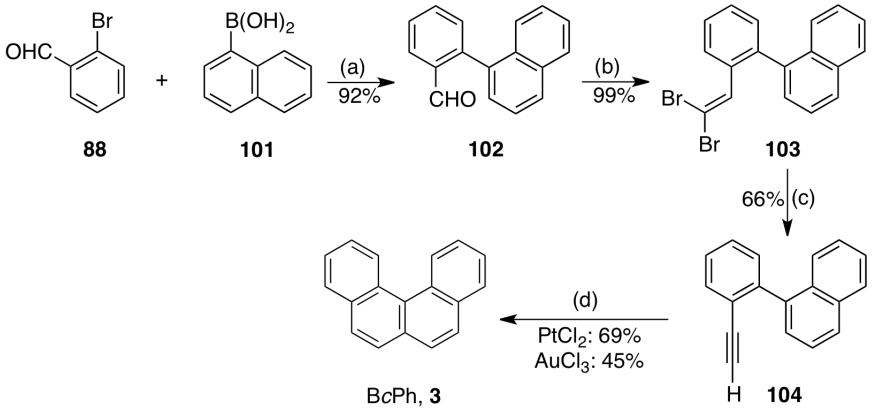

[a] Reagents and Conditions: (a) $Pd(PPh_3)_4$, CsF, DME, reflux 16 h; (b) (i) PPh_3, CH_2Cl_2, 0 °C, then CBr_4, 10 min (ii) **102**, 0 °C, 2 h; (c) (i) **103**, THF, -78 ° C, *n*-BuLi, 5 h, then rt, 2 h (ii) H_2O workup; (d) 5% $PtCl_2$ or 5% $AuCl_3$, toluene, 80 °C, 16 h.

We next utilized the protocol for the other B*c*Ph derivatives, after gaining successful results with parent B*c*Ph. As a means of testing the robustness of the method, the more challenging dimethoxy derivatives were first synthesized. Synthesis of 3,4-dimethoxy-8-methylbenzo[*c*]phenanthrene (**108**), started with the Suzuki-Miyaura coupling between 6-bromo-2,3-dimethoxybenzaldehyde (**84**) and (4-methylnaphthalen-1-yl)boronic acid (**98**) (Scheme 13). This C–C bond-forming reaction resulted in

aldehyde **105** in a good yield of 83%. The Corey-Fuchs olefination followed by alkynylation led to alkyne **107** in a yield of 79% over two steps. The final metal-catalyzed cyclization of the alkyne gave a yield of 75% for the B*c*Ph derivative **108** when $PtCl_2$ was used. An improved yield of 84% for **108** was obtained when $AuCl_3$ was used (Scheme 13). These results showed an overall improvement compared to the previous results with parent B*c*Ph, and demonstrated the efficiency of the protocol for the synthesis of such B*c*Ph derivatives.

Scheme 13. Synthesis of 3,4-Dimethoxy-8-methylbenzo[*c*]phenanthrene (**108**)

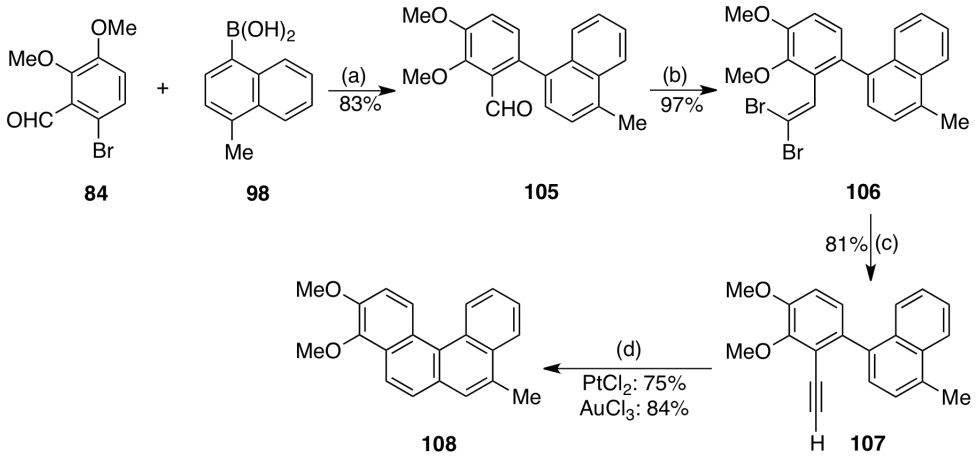

[a] Reagents and Conditions: (a) $Pd(PPh_3)_4$, CsF, DME, reflux 16 h; (b) (i) PPh_3, CH_2Cl_2, 0 °C, then CBr_4, 10 min (ii) **105**, 0 °C, 2 h; (c) (i) **106**, THF, -78 ° C, *n*-BuLi, 5 h, then rt 2 h (ii) H_2O workup; (d) 5% $PtCl_2$ or 5% $AuCl_3$, toluene, 80 °C, 17-24 h.

As an alternative to the two-step Corey-Fuchs protocol, a procedure by Bestmann et al. involving a modified Seyferth-Gilbert phosphonate reagent for a one-step conversion of aliphatic and aromatic aldehydes to the respective alkynes was tried.[46] A typical reaction involves a Horner-Wadsworth-Emmons type reaction with the aldehyde followed by loss of nitrogen and rearrangement of the resulting alkenylidenecarbene to the alkyne.[46]

Initially, dimethyl-1-diazo-2-oxopropylphosphonate (**111**) was generated in situ by addition of dimethyl-2-oxopropylphosphonate (**109**) to K_2CO_3 and *p*-toluenesulphonylazide (*p*-TsN_3, **110**) in acetonitrile. This suspension was allowed to stir for 2 hours at room temperature, after which time phosphonate reagent **111** was produced. The aldehyde **105**, dissolved in methanol, was then added to the reaction mixture and allowed to stir for 8 hours at room temperature to yield the desired alkyne **107**.

The isolated yield of **107** was only 55% via this procedure (Table 4). Since the Corey-Fuchs protocol gave better yields over two steps, it was chosen for the remaining B*c*Ph derivatives.

Table 4. Attempted Bestmann One-Step Alkynylation[42] using Biarylaldehyde **105**

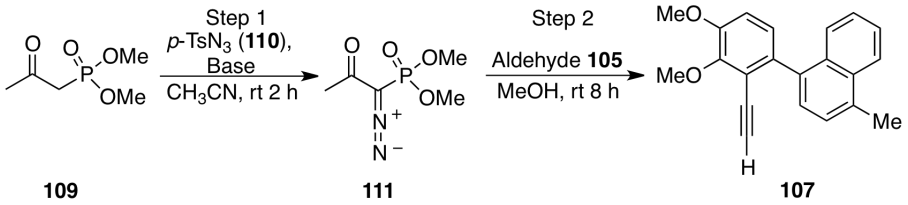

109 **111** **107**

Step 1					Step 2		
Entry	**109**	Base	*p*-TsN_3	**111**	**105**	Yield of **107**	Notes
1	1.2 eq	K_2CO_3, 3.0 eq	1.2 eq	1.2 eq	1.0 eq	55%	Literature conditions
2	2.0 eq	K_2CO_3, 3.0 eq	2.0 eq	2.0 eq	1.0 eq	55%	Modified **109**, **110**, **111**
3	2.0 eq	K_2CO_3, 4.0 eq	2.0 eq	2.0 eq	1.0 eq	53%	Modified base
4	2.0 eq	NaH, 3.0 eq	2.0 eq	2.0 eq	1.0 eq	39%	Modified to NaH base

Synthesis of the dimethoxy cyclopenta-B*c*Ph derivative **115** began with a C–C bond formation between bromoaldehyde **84** and boronic acid **100**, in an excellent yield of 92% of the biaryl aldehyde **112** (Scheme 14). Corey-Fuchs olefination and alkynylation protocol gave a good 78% yield of the alkyne **114,** over two steps. Cyclization of the alkyne using 5% $PtCl_2$ in refluxing toluene afforded **115** in a yield of 73%, after 21 hours. Cyclization of **114** with 5% $AuCl_3$ gave a lower 59% yield of the cyclized product, and was not complete even at 29 hours (a trace of starting alkyne was detectable by TLC).

Scheme 14. Synthesis of 9,10-Dimethoxy-4,5-dihydrobenzo[*l*]acephenanthrylene (**115**)

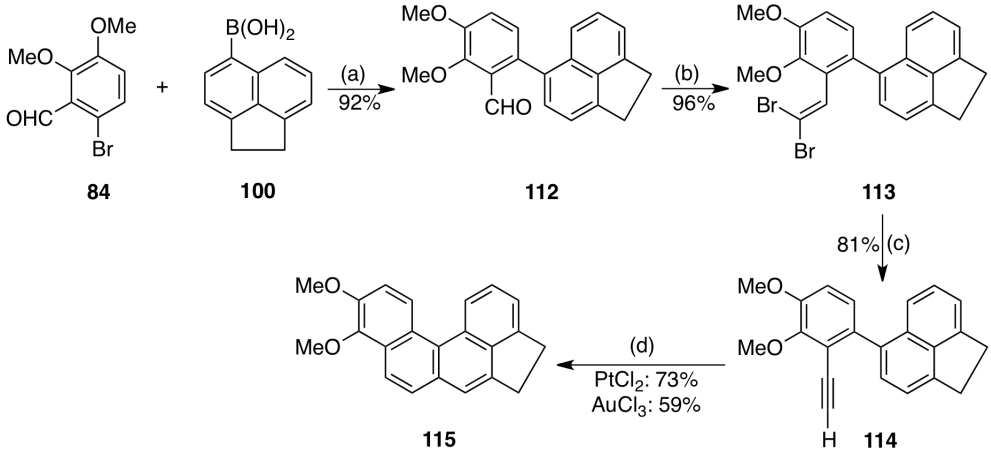

84 **100** **112** **113** **114** **115**

[a] Reagents and Conditions: (a) $Pd(PPh_3)_4$, CsF, DME, reflux 16 h; (b) (i) PPh_3, CH_2Cl_2, 0 °C, then CBr_4, 10 min (ii) **112**, 0 °C, 2 h; (c) (i) **113**, THF, -78 ° C, *n*-BuLi, 5 h, then rt 2 h (ii) H_2O workup; (d) 5% $PtCl_2$ or 5% $AuCl_3$, toluene, 80 °C, 21-29 h.

With synthesis of the dimethoxy B*c*Ph derivatives completed, synthesis of the remaining parent hydrocarbons **38**, **42**, and **43** were addressed (Figure 10). For these syntheses, *o*-bromobenzaldehyde was utilized with respective boronic acids to access the key aldehyde, alkyne, and then the parent-B*c*Ph compounds. These results are shown in Figure 9. For synthesis of parent hydrocarbon **38**, *o*-bromobenzaldehyde was coupled with (4-methylnaphthalen-1-yl)boronic acid (**98**) via Suzuki-Miyaura C–C bond-forming reaction to give the biaryl aldehyde **116** in a good yield of 86%. Corey-Fuchs olefination and alkynylation led to biaryl alkyne **118** in a yield of 61% after two steps. Cyclization of the **118** with 5% $PtCl_2$ led to the desired cyclized product **38** in a good yield of 81% in 24 h. Similarly, for synthesis of compound **43**, Suzuki-Miyaura C–C bond-formation with *o*-bromobenzaldehyde and (1,2-dihydroacenaphthylen-5-yl)boronic acid (**100**) led to biaryl aldehyde **119** in an excellent yield of 94%. Corey–Fuchs olefination and alkynylation gave biaryl alkyne **121** in a yield of 56% after two steps. Cyclization of **121** with 5% $PtCl_2$ gave cyclized product **43** in a good yield of 69% in 24 h (Figure 10). The final cyclization step was done with 5% $PtCl_2$ in both cases since the gold catalyst ($AuCl_3$) seemed to deteriorate over time.

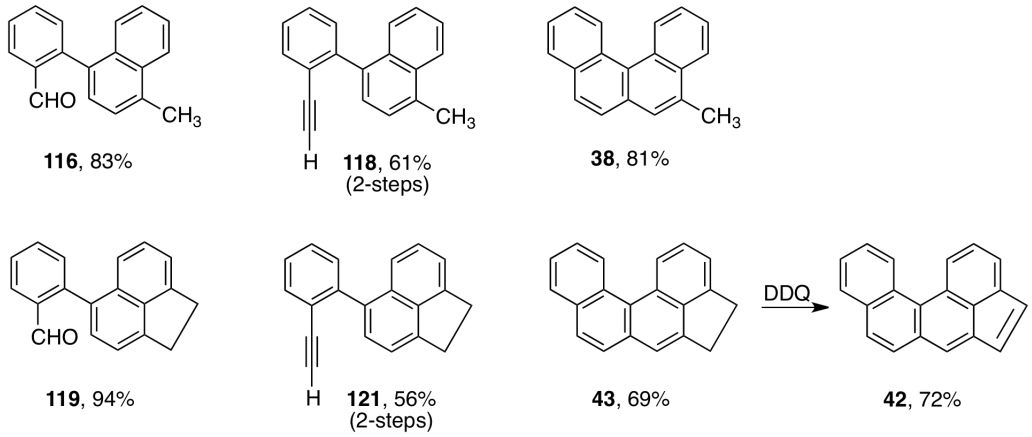

Figure 10. Yields of Unsubstituted B*c*Ph Derivatives.

Olefination of **43** with 2,3-dichloro-5,6-dicyano-1,4-benzoquinone (DDQ) in refluxing toluene for 24 hours gave compound **42** in a yield of 72%. Synthesis of this compound was of interest since it is structurally similar to that of cyclopenta[*c*,*d*]pyrene (Figure 11). Cyclopenta[*c*,*d*]pyrene is a PAH found in carbon black soots and automobile exhaust that does not have a bay or fjord region, but is highly

mutagenic and reported to be carcinogenic in mouse models.[47] Thus, we synthesized **42** for comparisons.

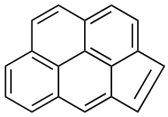

Cyclopenta[*c*,*d*]pyrene, **122**

Figure 11. Structure of Cyclopenta[*c*,*d*]pyrene.

Overall, synthesis of parent biaryl aldehydes gave reasonably consistent yields to that of their dimethoxy biaryl aldehydes. However, the Corey-Fuchs olefination and alkynylation protocol gave lower yields for the parent hydrocarbons compared to the dimethoxy counterparts. In addition, syntheses of the dimethoxy-B*c*Ph derivatives were better yielding than their parent hydrocarbon counterparts. This is consistent with the previous experimental and computation studies that indicated the need for electron-rich arenes for efficient metal-catalyzed cyclization,[34,39] and our results support this observation. In comparison to the photocyclization methodology, which is limited to concentrations of 0.01 M of stilbenes and can cause formation of dimers as a side product at higher concentrations;[33] our metal-catalyzed protocol was found to be successful up to a concentration of 0.23 M of alkyne, but seemly not limited to that concentration.

Synthesis of the putative dihydrodiol metabolites (**39** and **44**) then followed. Using literature protocols[23,30] with some modifications, the respective dihydrodiols were obtained. For synthesis of dihydrodiol **39**, the methoxyl groups in **108** were cleaved using BBr_3 in CH_2Cl_2 to give the catechol **123** in quantitative yield. Without additional manipulations, catechol **123** was oxidized to *o*-quinone **124** using pyridinium dichromate (PDC) in CH_2Cl_2 (modification)**.** Reduction of **124** with sodium borohydride in ethanol under O_2 sparging led to the (±)-*trans*-9,10-dihydroxy-9,10-dihydroB*c*Ph derivative **39** in a yield of 62%, over three steps (Scheme 15, eq. 1). Similarly, synthesis of dihydrodiol **44** began with cleavage of the methoxyl groups in **115** using BBr_3 in CH_2Cl_2 to give catechol **125** in quantitative yield. Oxidation of catechol **125** then followed using PDC in CH_2Cl_2 to give *o*-quinone **126**. This *o*-quinone was readily reduced using $NaBH_4$ in ethanol under O_2 sparing, and led to the desired dihydrodiol **44** in a yield of 61% over three steps (Scheme 15, eq. 2).

Scheme 15. Synthesis of Dihydrodiol Derivatives **39** and **44**

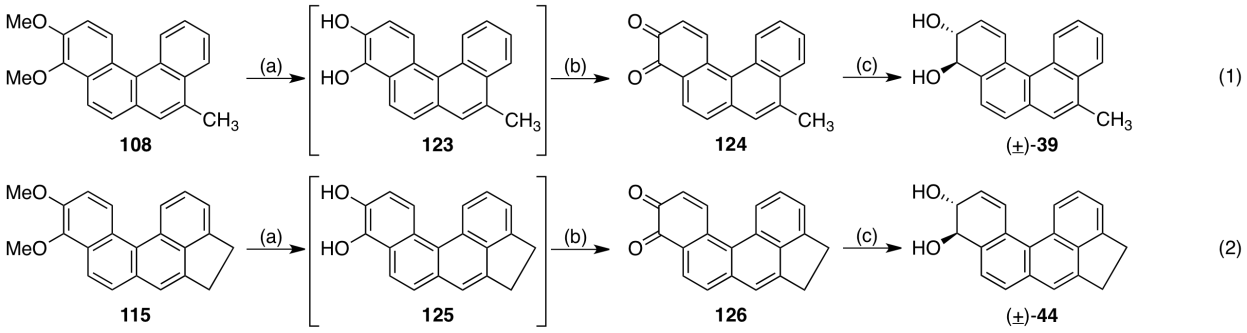

[a] Reagents and conditions: (a) BBr_3, CH_2Cl_2, -78 °C to rt; (b) PDC, CH_2Cl_2, reflux; (c) $NaBH_4$, EtOH, O_2, rt.

^{1}H NMR analyses of the *o*-quinone and dihydrodiol derivatives showed comparable patterns to previously synthesized B*c*Ph derivatives. In *o*-quinones **124** and **126**, the most downfield quinonoid vinyl proton that resides in the fjord-region appears as a doublet with $J_{H,H}$ = 10.5 Hz for both derivatives. This is in good agreement with *o*-quinones of parent B*c*Ph ($J_{H,H}$ = 10.5 Hz),[23b] 1,4-DMB*c*Ph ($J_{H,H}$ = 10.3 Hz)[23a] and 1,4-DFB*c*Ph ($J_{H,H}$ = 10.6 Hz),[23b] although in the fluorinated *o*-quinone this proton appears as a doublet of doublets owing to a unique coupling to the fjord-region fluorine ($J_{H,F}$ = 15.6 Hz). As expected, in racemic dihydrodiols **39** and **44** no *P* and *M* helicity was observed, which was opposite the case with 1,4-DMB*c*Ph dihydrodiol.[23a] The fjord-region vinyl protons in **39** and **44** appear as doublets with $J_{H,H}$ = 10.5 Hz, respectively, for each. These results complement data for the dihydrodiol derivatives of parent B*c*Ph ($J_{H,H}$ = 10.1 Hz),[6c] as well as the major isomer of 1,4-DMB*c*Ph ($J_{Major\ H,H}$ = 10.1 Hz).[23a] The proton for the dihydrodiol of 1,4-DFB*c*Ph appears as a doublet of doublets of doublets because of coupling with the fjord-region fluorine ($J_{H,H}$ = 2.2 and 10.5 Hz, $J_{H,F}$ = 15.6 Hz),[23b] however the coupling constant value of 10.5 Hz is consistent. Dihydrodiols **39** and **44** exhibit quasi-diequatorial arrangement of the hydroxyl groups. This is in complete agreement with all other previously described dihydrodiols of B*c*Ph derivatives.[23]

For synthesis of the series 1 and series 2 diol epoxides, literature methodology was employed with no further modifications (Scheme 16).[23,31] For access to the series 1 diol epoxides, (±)-*trans*-dihydrodiol **39** and **44** were converted to the bromo triols **127** and **128**, respectively, using *N*-

bromoacetamide (NBA) in 33% water in THF. Bromo triols **127** and **128** were then cyclized using IRA-400 Amberite HO^- resin in anhydrous THF. Series 1 diol epoxide (±)-**40** was obtained in a yield of 62% and the corresponding series 1 diol epoxide (±)-**45** was obtained in a yield of 58%, each over two steps (Scheme 16). The epoxidation reactions of **39** and **44** with *m*-CBPA in anhydrous THF afforded the series 2 diol epoxide (±)-**41** in 69% yield, where as series 2 diol epoxide (±)-**46** was obtained in a yield of 80% (Scheme 16).

Scheme 16. Synthesis of Series 1 Diol Epoxides **40** and **45**, and Series 2 Diol Epoxides **41** and **46**

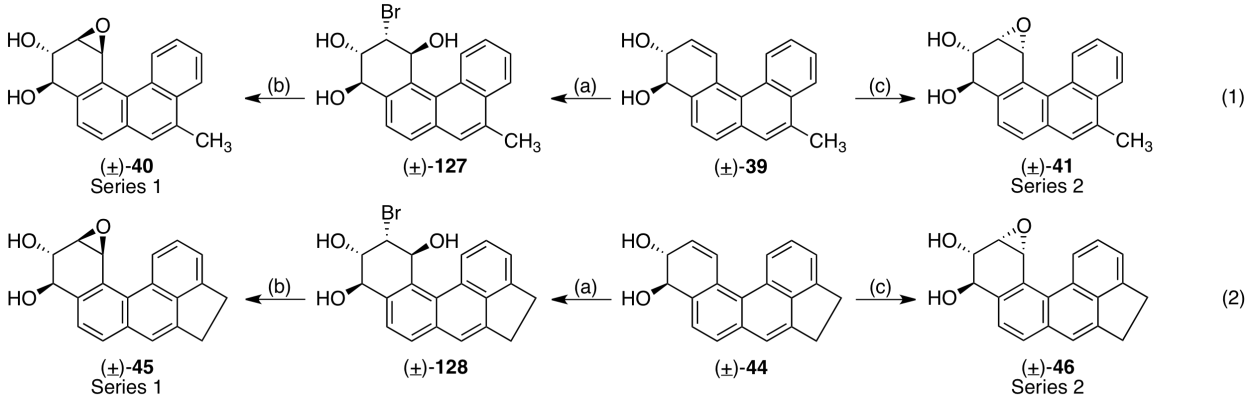

[a] Reagents and conditions: (a) *N*-bromoacetamide, THF-H_2O, rt; (b) Amberlite HO^-, THF, rt; (c) *m*-CPBA, THF.

Analysis of the ^{1}H NMR spectra for both series 1 and series 2 diol epoxides of the new alkylated B*c*Phs gave insight into the conformational preferences of the hydroxyl groups. As shown in Table 5, the series 2 diol epoxides **41** and **46** have comparable quasi-diequatorial arrangement of their hydroxyl groups (entries 8 and 9, respectively), which is in agreement with the series 2 diol epoxide of parent B*c*Ph (entry 5)[6] and the other previously described B*c*Ph diol epoxides (entries 6 and 7).[23] The series 1 diol epoxides **40** and **45** also exhibited quasi-equatorial arrangement of their hydroxyl groups (entries 3 and 4), which is in good agreement with the series 1 diol epoxide of parent B*c*Ph that is known to display this arrangement (entry 1).[6] These results for the series 1 compounds suggest however that the quasi-diaxial arrangement of the hydroxyls for 1,4-DFB*c*Ph (entry 2) is unusual and may be due to the presence of the fluorine in the fjord region. Additionally, this conformational change from the norm for B*c*Ph series 1 diol epoxides observed for 1,4-DFB*c*Ph is likely due to the overall large molecular distortion of the compound.[23b]

Table 5. Conformational Arrangement of Hydroxyls based on Coupling Constants (Hz) of the Carbinol Protons in the Series 1 and Series 2 B*c*Ph Derivatives

Entry	Diol Epoxide	NMR Solvent	Coupling Constant (Hz)	Hydroxyl Arrangement
1[6]	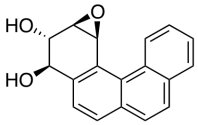	DMSO-d_6	$J_{3,4}$ = 9.0	Quasi-diequatorial
2[23b]	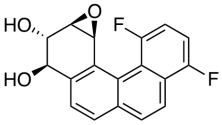	Acetone-d_6	$J_{9,10}$ = 2.1	Quasi-diaxial
3	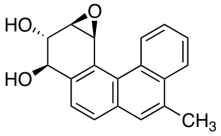	Acetone-d_6	$J_{3,4}$ = 8.8	Quasi-diequatorial
4	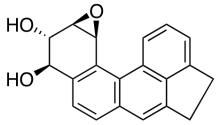	Acetone-d_6	$J_{9,10}$ = 9.5	Quasi-diequatorial
5[6]	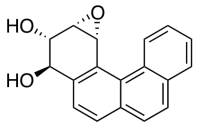	DMSO-d_6	$J_{3,4}$ = 8.3	Quasi-diequatorial
6[23a]	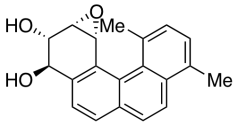	THF-d_8	$J_{9,10}$ = 8.8	Quasi-diequatorial
7[23b]	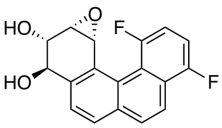	DMSO-d_6	$J_{9,10}$ = 8.5	Quasi-diequatorial
8	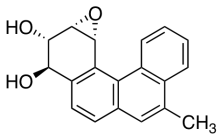	Acetone-d_6	$J_{3,4}$ = 8.5	Quasi-diequatorial
9	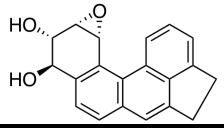	Acetone-d_6	$J_{9,10}$ = 8.0	Quasi-diequatorial

Additionally, the NOESY spectra for the series 1 diol epoxides of **40** and **45** were analyzed to check the relative stereochemistry of the products. The NOESY spectrum for **40** shows a through-space interaction between H-4 and H-2. This indicates that both these protons reside on the same face (Figure

12). Similarly, for **45** the NOESY spectrum shows a through-space interaction between H-11 and H-9 (Figure 13). These data supports the desired relative stereochemistry in the two diol epoxides.

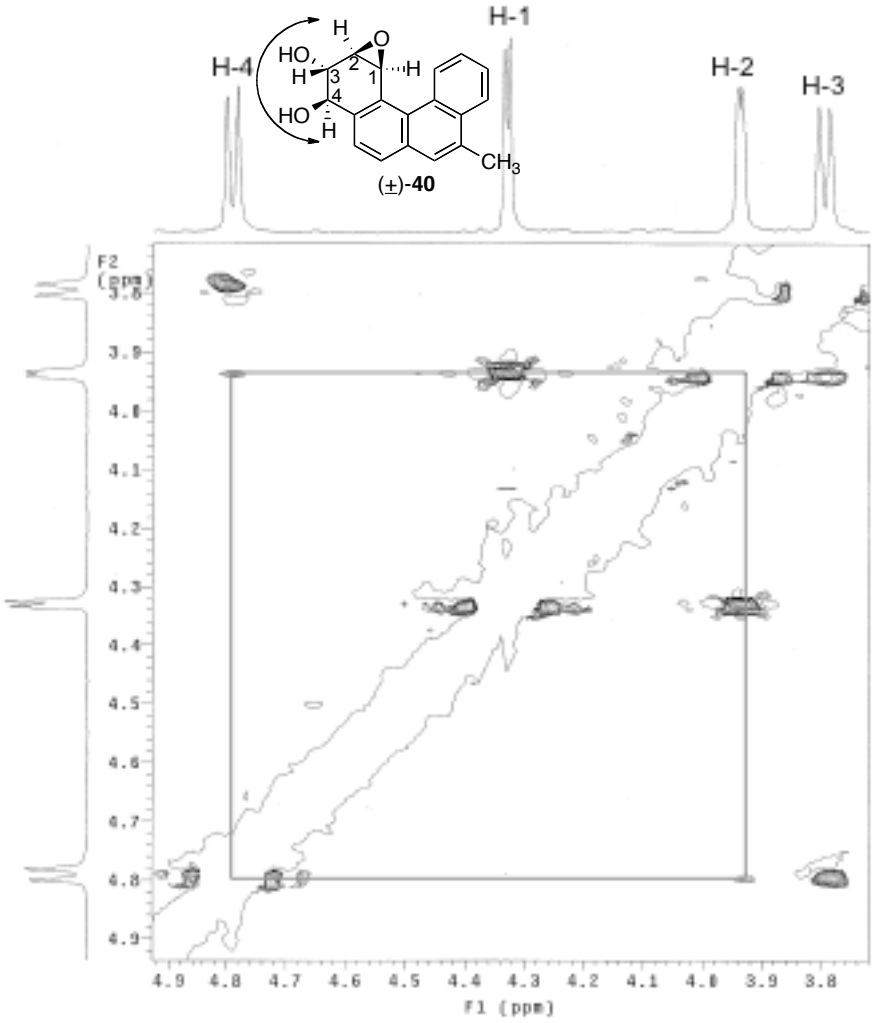

Figure 12. NOESY Spectrum showing Correlation between the α Hydrogens H-4 and H-2 in (±)-**40**.

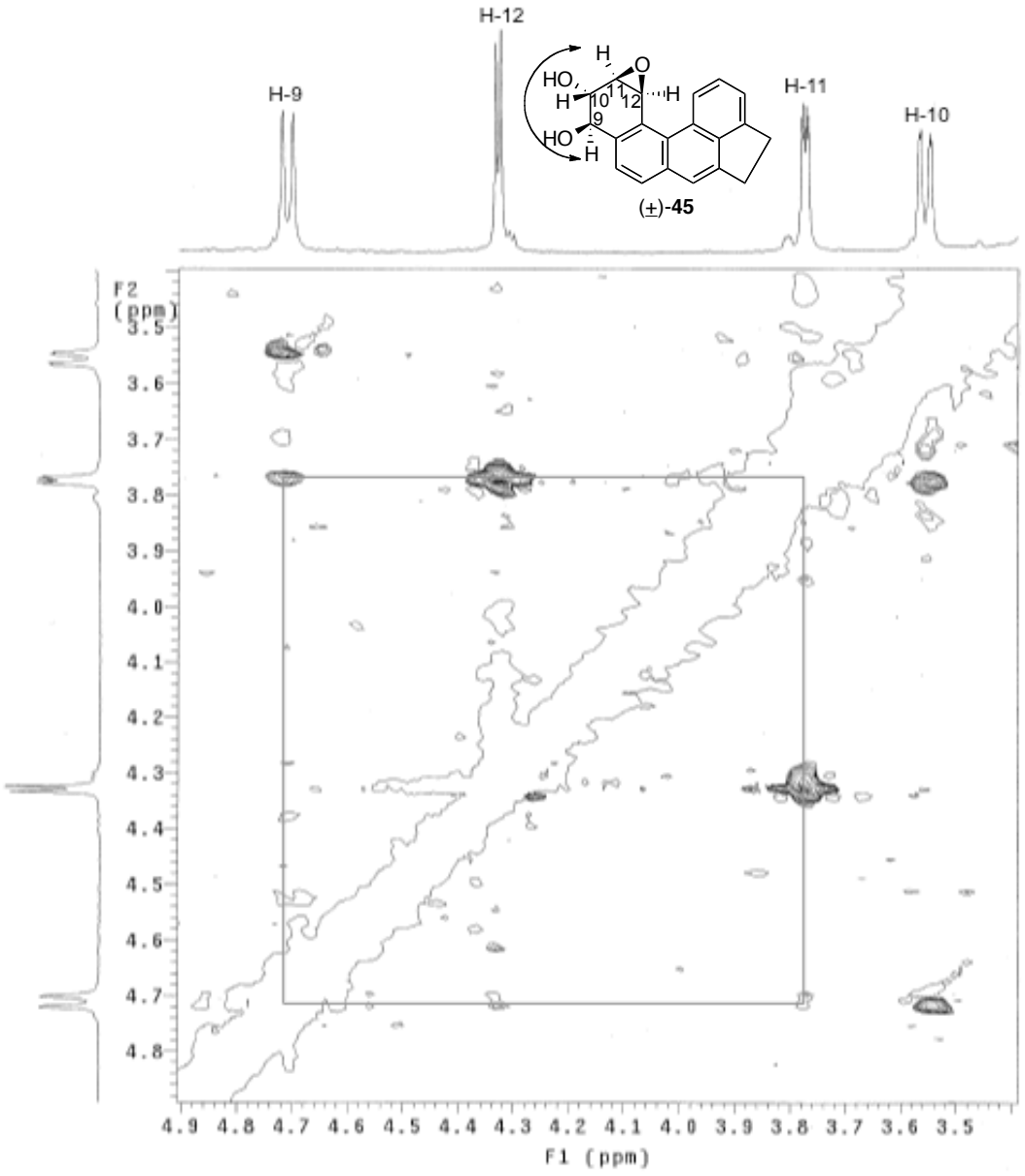

Figure 13. NOESY Spectrum showing Correlation between the α Hydrogens H-9 and H-11 in (±)-**45**.

X-ray crystallographic analysis of the available alkylated B*c*Ph derivatives also gave some interesting data. The results showed that subtle changes in the molecular distortion of these alkylated B*c*Phs could be achieved without the direct influence of substituents in the fjord region. The most obvious feature to support this is seen in the A,D plane angles of the various compounds (Table 6). The presence of the remote methyl group in compound **38** causes an overall molecular distortion of 23.3º. This is a small decrease in non-planarity as compared to parent B*c*Ph (26.7º; with a difference of 3.4º).[7a] However, a more significant decrease (>10º) is observed when comparing with 1,4DFB*c*Ph (33.5º)[23b] and

1,4DMB*c*Ph (36.6º).[23a] This clearly demonstrates the dramatic impact substituents in the fjord region can have on the molecular distortion of the B*c*Ph skeleton.

The overall molecular distortion observed for the cyclopenta compound **43** showed a much lower A,D plane angle of 18.7º. Introduction of an additional unsaturation in **42** showed a pronounced decrease in non-planarity with the A,D plane angle of 2.2º. This result for **42** was anticipated, and we look forward to a comparison with structurally similar cyclopenta[*c*,*d*]pyrene (Figure 11), which does not have a bay or fjord region, but is highly mutagenic and carcinogenic in mouse models.[47] The difference between the out-of-plane angles (overall molecular distortion) for the saturated **43** and unsaturated **42** B*c*Ph derivatives is pronounced and demonstrates that the B*c*Ph framework can be manipulated by remote placement of substituents.

The impact of the remote alkylation on the overall molecular distortion was also observed for the dimethoxy derivatives **108** and **115**, the synthetic precursors used for synthesis of the putative metabolites. These two compounds were also crystallized and analyzed by X-ray crystallography. Compound **108** has an A,D angle of 26.0º, a slight increase by 2.7º from its parent hydrocarbon (**38**), while in compound **115** the A,D angle of 18.3º was comparable to its parent hydrocarbon (**43**).

Table 6. Angles Between Planes of B*c*Ph Derivatives Determined Crystallographically

Angle Between	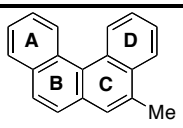	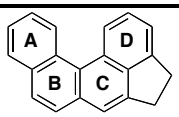	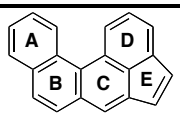	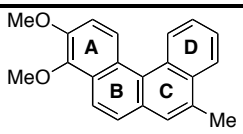	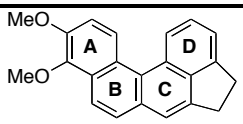
	38	**43**	**42**	**108**	**115**
A,B	9.79º	7.53º	0.60º	9.06º	6.61º
A,C	16.09º	12.70º	1.59º	16.58º	12.18º
A,D	**23.27º**	**18.72º**	**2.20º**	**26.04º**	**18.30º**
B,C	6.30º	5.19º	1.00º	7.52º	5.57º
B,D	13.81º	11.20º	1.62º	17.02º	11.70º
C,D	8.24º	6.13º	0.62º	9.53º	6.15º
C,E	-	-	0.45º	-	-
D,E	-	-	0.25º	-	-

Table 7 shows the X-ray crystal structures of the new compounds. Among these, compound **42** is nearly planar in comparison to the rest (entry 3). The other compounds clearly show an overall molecular distortion that epitomizes non-planarity.

The X-ray crystallographically determined internuclear distances between atoms on either side of the fjord region in the new B*c*Ph derivatives were compared. This distance between the fjord region hydrogen atoms in B*c*Ph is reported to be 1.90(1) Å.[23b] A larger internuclear distance of 2.10(1) Å was reported between a methyl hydrogen atom and the fjord-region hydrogen atom for 1,4-DMB*c*Ph.[23a] Similarly, the distance between the fjord-region fluorine and the hydrogen atoms in 1,4-DFB*c*Ph was reported as 2.20(1) Å.[23b] For compound **38** and **43**, the internuclear distance between fjord-region hydrogen atoms was found to be 1.93(1) Å and 1.86(1) Å, respectively. These values are close to that of the parent B*c*Ph derivative. This distance was found to be even shorter for compound **42** [1.68(1) Å]. Given this information, it would be interesting to compare the metabolism DNA binding abilities, adduct formations, and mutagenicity profiles of these newly synthesized B*c*Phs to parent B*c*Ph, and the previously described B*c*Ph derivatives.

Table 7. B*c*Ph Derivatives as Determined by X-ray Crystallography

Entry	Top View	Side View
1	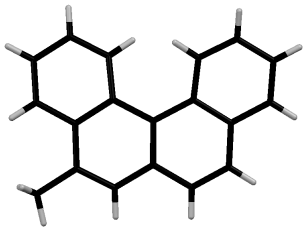	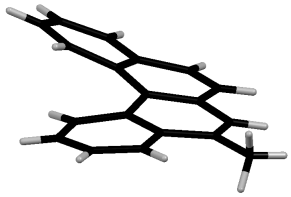
2	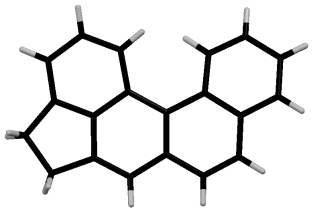	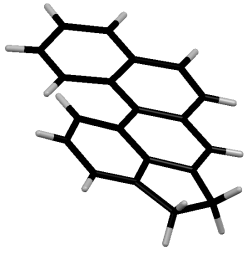

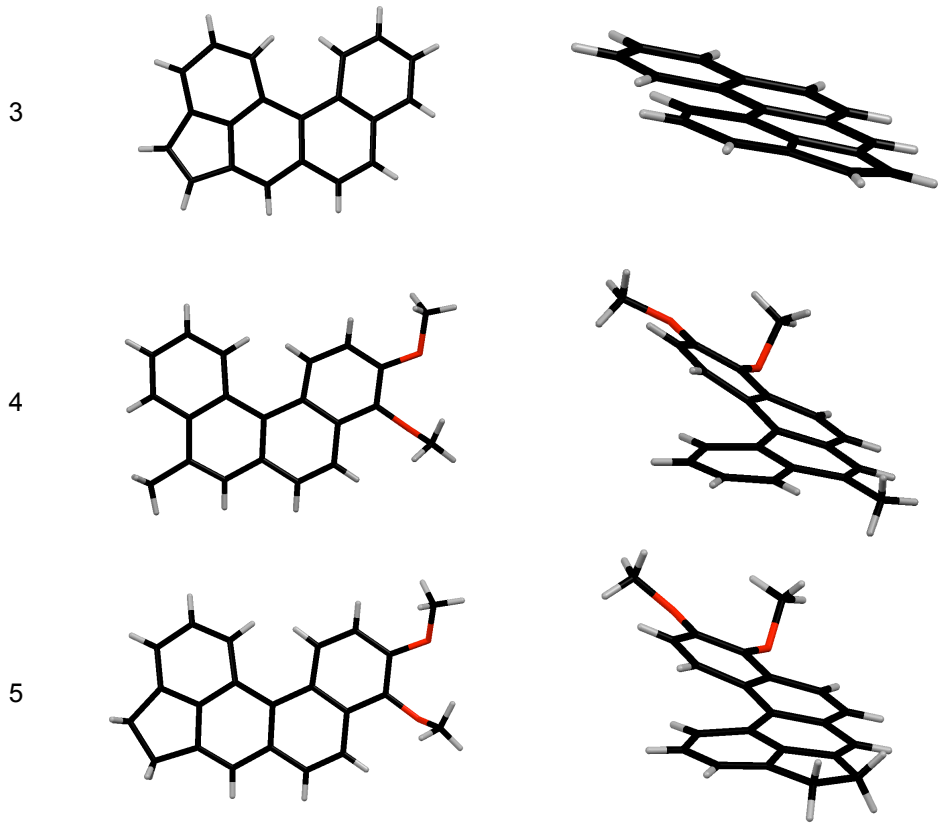

Based on the foregoing, it will be interesting to assess how the new alkylated B*c*Ph derivatives undergo metabolic activation and DNA binding. This information can then be compared to results from B*c*Ph, 1,4-DMB*c*Ph, and 1,4-DFB*c*Ph derivatives in order to fully understand how molecular distortion, and/or substituents near or remote from the fjord region influence the extent of DNA damaging events produced by metabolism and DNA alkylation. The 1,4-DMB*c*Ph with an overall molecular distortion of 36.6º showed ~3-fold lower metabolic activation compared to poorly metabolized B*c*Ph.[23a] Additionally, the sterically congested dihydrodiol derivative of 1,4-DMB*c*Ph was found to show ~11-fold lower metabolic activation to the diol epoxide as compared to the dihydrodiol of B*c*Ph. Similarly, 1,4-DFB*c*Ph with an overall molecular distortion of 33.5º, and its sterically congested dihydrodiol derivative, exhibited ~4-fold lower metabolic activation as compared to dihydrodiol of B*c*Ph. Given this information, we speculate that the metabolic activation profiles of **38** and **43** will at least be comparable to that of parent B*c*Ph. The results from these experiments along with the data gathered here are expected to give

greater insight into the influence of molecular distortion of fjord region B*c*Phs, their influence on metabolic activation, and DNA binding properties.

3.3 Conclusions

We have described a multi-step synthetic approach for the synthesis of a new, remotely alkylated benzo[*c*]phenanthrene derivatives. The synthesis utilizes a key metal-catalyzed cyclization step of suitable alkynes for access to the requisite B*c*Phs.[34] This approach circumvents the conventional photochemical protocol and offers an alternative route that allows access to a wide range of alkylated B*c*Phs, and potentially other substituted B*c*Ph products. This is in part due to the commercial and/or easy availability of the starting materials used, and ease of the synthetic protocol. The route also allows for the increased scalability of any B*c*Ph products.

The current method utilizes Suzuki-Miyaura cross-coupling reaction between aryl bromides and aryl boronic acids for the synthesis of key biaryl aldehydes via a C–C bond formation.[35] Application of the two-step Corey-Fuchs protocol affords biaryl alkynes,[36] which are then subjected to Pt-catalyzed cyclization for synthesis of requisite B*c*Ph derivatives in good yields.[34] The method was also convenient for synthesis of suitable dimethoxy B*c*Ph derivatives that were needed for synthesis of the putative dihydrodiol and diol epoxide metabolites. Interestingly, no *P* and *M* helicity was observed, which was the case for metabolites of 1,4-dimethyl B*c*Ph.[23a] Additionally, the diol epoxides of the new alkylated B*c*Phs exhibited diequatorial arrangement of their hydroxyl groups, which correlates well with diol epoxides of parent B*c*Ph,[6,7,23a] but opposite to the series 1 diol epoxides of 1,4-difluoro B*c*Ph.[23b]

X-ray Crystallographic data helped to gain quantitative data on the overall molecular distortion achieved by remote functionalization of the B*c*Ph skeleton. The data supports the idea that out-of-plane distortion that can be controlled without the direct influence of substituents in the fjord region of the B*c*Ph.[23] The results showed decreases in non-planarity due to the remote alkyl functionalization in comparison to B*c*Ph. This data was in good agreement with that of parent B*c*Ph, but opposite to the pronounced overall molecular distortion angles of 1,4-dimethyl or 1,4-difluro B*c*Phs.[23]

Based on the results, biological testing of these newly synthesized compounds is anticipated. This should help to elucidate and give a better understanding as to how molecular distortion is ultimately linked to and has a direct influence on the metabolic activation of B*c*Phs leading to DNA damaging species. This data should offer much needed insight into the role of PAH structures in relation to their carcinogenic activities.

3.4 Experimental Section – Chapter 3

General Comments. All reactions were carried out in oven-dried flasks and vials, and under nitrogen gas if an inert atmosphere is needed. All commercially available compounds were used without further purification. Air or water sensitive liquids and solutions were transferred via syringe under inert conditions. The following solvents used were purified by distillation over respective drying agents: THF was refluxed over LAH, then collected and distilled over Na, toluene was distilled over Na, CH_2Cl_2 and DME were both distilled over CaH_2, and hexanes and EtOAc were distilled over calcium sulfate. Thin-layer chromatography was performed on 250 μm glass-back silica plates and 200 μm aluminum-back silica plates. Purification of reaction products by column chromatography was performed on 230-400 mesh silica gel. Proton nuclear magnetic spectra (^{1}H NMR) were generally recorded in the solvents indicated on a 500 MHz instrument. Chemical shifts (δ) are given in ppm, and coupling constants (*J*) in Hz. ^{1}H NMR splitting patterns are designated as singlet (s), doublet (d), triplet (t), quartet (q) and quintet (quint) where appropriate. All first-order splitting patterns are assigned on the basis of the appearance of the resonance. Those splitting patterns that could not be easily interpreted, a designation of multiplet (m) or broad (br) is used as appropriate.

6-Bromo-2,3-dimethoxybenzyl alcohol (87)

In an oven-dried 100 mL round-bottom flask equipped with a magnetic stirring bar was placed 2,3-dimethoxybenzyl alcohol **86** (4 g, 23.8 mmol) in dry THF (18 mL). *N*-bromosuccinimide (NBS) (4.66 g, 26.2 mmol) was added, and the suspension was allowed to stir at room temperature for 30 min at which time TLC showed the reaction to be complete. The THF was evaporated and the crude residue was diluted with Et_2O. The insoluble succinimide was removed by filtration and the resulting ethereal layer was washed twice with 2N aqueous NaOH. The organic layer was dried over Na_2SO_4, filtered and concentrated. Recrystallization using 1:1 ethyl-hexane yielded a white, gummy solid that needed purification. Chromatographic purification on a silica gel column packed in hexanes using 20% EtOAc in hexanes as eluent afforded compound **87** as a whitish solid (5.33 g, 90% yield). R_f (20% EtOAc in hexanes): 0.21. ^{1}H NMR (500 MHz, $CDCl_3$): δ 7.27 (d, 1H, Ar-H, *J* = 9.0 Hz), 6.77 (d, 1H, Ar-H, *J* = 9.0

Hz), 4.83 (d, 2H, CH_2, *J* = 7.0 Hz), 3.90 (s, 3H, OCH_3), 3.85 (s, 3H, OCH_3), 2.32 (t, 1H, OH, *J* = 7.0 Hz). ^{13}C NMR (125 MHz, $CDCl_3$): δ 152.3, 148.8, 133.9, 127.9, 114.8, 113.4, 61.7, 60.4, 56.0.

6-Bromo-2,3-dimethoxybenzaldehyde (84)

In an oven-dried 50 mL round-bottom flask equipped with a magnetic stirring bar was placed 6-bromo-2,3-dimethoxybenzyl alcohol **87** (2 g, 8.09 mmol) in dry CH_2Cl_2 (10 mL), and cooled to 0 ºC. Pyridinium chlorochromate (PCC) (3.49 g, 16.2 mmol) was added and the orange suspension was allowed to stir at 0 ºC for 5 minutes and, then at room temperature for 5 h, at which time TLC showed the reaction to be complete. The black suspension was filtered through Celite using CH_2Cl_2. The filtrate obtained was concentrated to give a yellowish solid. The crude product was chromatographed on a silica gel column packed in hexanes using sequential elution with 20% CH_2Cl_2 in hexanes, followed by 50% CH_2Cl_2 in hexanes. Compound **84** was obtained as a whitish-yellow solid (1.43 g, 72% yield). R_f (20% EtOAc in hexanes): 0.32. ^1H NMR (500 MHz, $CDCl_3$): δ 10.37 (s, 1H, CHO), 7.37 (d, 1H, Ar-H, *J* = 9.0 Hz), 6.98 (d, 1H, Ar-H, *J* = 9.0 Hz), 3.96 (s, 3H, OCH_3), 3.91 (s, 3H, OCH_3). ^{13}C NMR (125 MHz, $CDCl_3$): δ 190.6, 152.9, 152.3, 129.5, 128.7, 117.7, 112.9, 62.5, 56.4.

(4-Methylnaphthalen-1-yl)boronic acid (98)[44]

In an oven-dried 100 mL 3-neck round-bottom flask equipped with a magnetic stirring bar was placed 1-bromo-4-methylnaphthalene (**97**) (1.5 g, 6.78 mmol) in dry THF (30 mL), under a nitrogen gas-filled balloon. The mixture was stirred at room temperature for 5 mins and cooled to –78 ºC. 1.6M solution of *n*-BuLi in hexanes (5.10 mL, 8.14 mmol) was added dropwise and the yellow suspension was allowed to stir at –78 ºC for 30 mins. Trimethyl borate [$B(OMe)_3$] (2.12 g, 20.3 mmol) was added rapidly and the suspension became colorless. The mixture was allowed to stir at –78 ºC for 30 mins, and at room temperature for 30 mins, at which time TLC showed the reaction to be complete. The mixture was diluted with Et_2O and washed with 10% aq. HCl (4x). The organic layer was dried over Na_2SO_4 and concentrated to give a yellow-white solid. The crude product was suspended in cold hexanes, sonicated, and filtered to afford compound **98** as a white solid (1.12 g, 89% yield). R_f (CH_2Cl_2): 0.03. ^1H NMR (500

MHz, $CDCl_3$): 9.33 (d, 1H, Ar-H, *J* = 8.5 Hz), 8.58 (d, 1H, Ar-H, *J* = 7.0 Hz), 8.14 (d, 1H, Ar-H, *J* = 8.5 Hz), 7.66 (t, 1H, Ar-H, *J* = 7.3), 7.62 (t, 1H, Ar-H, *J* = 7.5), 7.53 (d, 1H, Ar-H, *J* = 7.0 Hz), 2.82 (s, 3H, CH_3).

(1,2-Dihydroacenaphthylen-5-yl)boronic acid (100)[44]

As described for the synthesis of **98**, **100** was prepared by the reaction of 5-bromo-1,2-dihydroacenaphthylene (**99**) (2 g, 8.58 mmol), 1.6M solution of *n*-BuLi in hexanes (6.43 mL, 10.3 mmol), trimethyl borate [$B(OMe)_3$] (2.67 g, 25.7 mmol) in dry THF (37 mL) at –78 ºC over 1 h, and then at room temperature for 30 mins. After the 10% aq. HCl work up and drying, the crude product was suspended in cold hexanes, sonicated, and filtered. Compound **100** was obtained as an off-white solid (1.33 g, 78% yield). R_f (CH_2Cl_2): 0.06. ^{1}H NMR (500 MHz, $CDCl_3$): Trimer, δ 8.91 (br d, 2H, Ar-H, *J* = 8.5 Hz), 8.66 (br d, 2H, Ar-H, *J* = 7.0 Hz), 8.14 (br d, 1H, Ar-H, *J* = 8.5 Hz), 8.80 (br d, 1H, Ar-H, *J* = 7.0 Hz), 7.63 (br t, 2H, Ar-H, *J* = 8.5 Hz), 7.52-7.46 (m, 3H, Ar-H), 7.39 (br d, 2H, Ar-H, *J* = 6.5 Hz), 7.31 (t, 2H, Ar-H, *J* = 6.5 Hz), 4.76 (br, OH), 3.46 (br s, 7H, CH_2–CH_2), 3.40 (br s, 5H, CH_2–CH_2).

2,3-Dimethoxy-6-napthalen-1-yl-benzaldehyde (96)

4,4,5,5-Tetramethyl-2-(naphthalen-1-yl)-1,3,2-dioxaborolane. In an oven-dried reaction vial equipped with a magnetic stirring bar was placed $PdCl_2$(dppf) (29.5 mg, 0.040 mmol) in dry DMF (4.0 mL). Bis(pinacolato)diboron (**94**) (342 mg, 1.36 mmol), KOAc, (360 mg, 3.67 mmol) and 1-bromonaphthalene (**93**) (254 mg, 1.22 mmol) were added. The vial was flushed with nitrogen gas and allowed to stir at 80 ºC in a sand bath for 14 h at which time TLC showed the consumption of all starting material and the formation of a new spot. R_f (20% EtOAc in hexanes): 0.13. *2,3-Dimethoxy-6-napthalen-1-yl-benzaldehyde*. To the mixture, dimethoxy bromobenzaldehyde **84** (150 mg, 0.612 mmol), 2M aq. Na_2CO_3 (0.51mL, 12.2 mmol), and $PdCl_2$(dppf) (29.5 mg, 0.040 mmol) were added. The vial was flushed with nitrogen gas and allowed to stir at 80 ºC in a sand bath for 21 h at which time TLC showed the reaction to be complete. The crude product was extracted with Et_2O and washed twice with water, and brine. The organic layer was dried over Na_2SO_4 and concentrated to give a black solid. The crude product was chromatographed several times on a silica gel column packed in hexanes using sequential elution with 20% CH_2Cl_2 in hexanes, followed by 20% EtOAc in hexanes. Compound **96** was obtained as a whitish-

yellow solid (141 mg, 79% yield). R_f (20% EtOAc in hexanes): 0.29. ^{1}H NMR (500 MHz, $CDCl_3$): δ 9.94 (s, 1H, Ar-H), 7.88 (t, 2H, Ar-H, *J* = 8.0 Hz), 7.51-7.45 (m, 3H, Ar-H), 7.38 (t, 1H, Ar-H, *J* = 8.0 Hz), 7.32 (d, 1H, Ar-H, *J* = 7.0 Hz), 7.21 (d, 1H, Ar-H, *J* = 8.0 Hz), 7.09 (d, 1H, Ar-H, *J* = 8.0 Hz), 4.02 (s, 3H, OCH_3), 3.98 (s, 3H, OCH_3). ^{13}C NMR (125 MHz, $CDCl_3$): δ 191.2, 152.9, 150.7, 137.1, 135.2, 133.6, 132.8, 129.9, 128.5, 128.2, 127.7, 127.5, 126.5, 126.1, 125.9, 125.3, 116.7, 62.4, 56.4

Synthesis of the biaryl aldehyde derivatives.

2-(Naphthalen-1-yl)benzaldehyde (102)[34]

In an oven-dried 50 mL round-bottom flask equipped with a magnetic stirring bar was placed 2-bromobenzaldehyde (**88**) (1 g, 5.41 mmol) in dry DME (27 mL). 1-Naphthalylboronic acid (**101**) (1.02 g, 5.95 mmol), CsF (2.30 g, 15.1 mmol), and $Pd(PPh_3)_4$ (250 mg, 0.216 mmol) were added. The resulting yellow suspension was allowed to stir at reflux for 16 h under a nitrogen gas-filled balloon, at which time TLC showed the reaction to be complete. The resulting black reaction mixture was diluted with EtOAc and washed with water (2x). The aqueous layer was extracted with EtOAc (2x). The combined organic layers were dried over Na_2SO_4 and concentrated to give an orange residue. The crude product was chromatographed on a silica gel column packed in hexanes using 5% EtOAc in hexanes as eluent. Compound **102** was afforded as a whitish-yellow solid (1.16 g, 92% yield). R_f (CH_2Cl_2): 0.56. ^{1}H NMR (500 MHz, $CDCl_3$): δ 9.63 (s, 1H, CHO), 8.12 (d, 1H, Ar-H, *J* = 8.0 Hz), 7.94 (dd, 2H, Ar-H, *J* = 3.0, 8.0 Hz), 7.71 (t, 1H, Ar-H, *J* = 7.0 Hz), 7.61-7.41 (m, Ar-H, 7H).

2,3-Dimethoxy-6-(4-methyl-napthalen-1-yl)benzaldehyde (105)

As described for the synthesis of **102**, **105** was prepared by a reaction of 6-bromo-2,3-dimethoxybenzaldehyde (**84**) (2 g, 8.16 mmol), (4-methylnaphthalen-1-yl)boronic acid (**98**) (1.67 g, 8.98 mmol), CsF (3.47 g, 22.8 mmol), and $Pd(PPh_3)_4$ (377 mg, 0.326 mmol) in dry DME (40 mL). The mixture was allowed to stir at reflux for 16 h under a nitrogen gas-filled balloon. Chromatographic purification using a silica gel column packed in hexanes using sequential elution with 10% EtOAc in hexanes, followed by 100% CH_2Cl_2 afforded **105** as a yellow-light brown solid (2.08 g, 83% yield). R_f (CH_2Cl_2): 0.44. ^{1}H NMR (500 MHz, $CDCl_3$): 9.91 (s, 1H, CHO), 8.05 (d, 1H, Ar-H, *J* = 8.5 Hz), 7.53-7.50 (m, 2H, Ar-

H), 7.39 (t, 1H, Ar-H, *J* = 8.0 Hz), 7.35 (d, 1H, Ar-H, *J* = 7.0 Hz), 7.22-7.19 (m, 2H, Ar-H), 7.08 (d, 1H, Ar-H, *J* = 8.5 Hz), 4.01 (s, 3H, OCH_3), 3.98 (s, 3H, OCH_3), 2.74 (s, 3H, CH_3). ^{13}C NMR (125 MHz, $CDCl_3$): δ 191.2, 152.2, 150.4, 135.4, 135.1, 134.4, 132.6, 132.5, 129.8, 127.4, 127.2, 126.4, 125.93, 125.91, 125.7, 124.5, 116.5, 62.2, 56.2, 19.6. HRMS (ESI) *m/z* calcd for $C_{20}H_{18}O_3Na$ $[M + Na]^+$: 329.1148, found 329.1141.

6-Acenaphthen-5-yl-2,3-dimethoxybenzaldehyde (112)

As described for the synthesis of **102**, **112** was prepared by a reaction of 6-bromo-2,3-dimethoxybenzaldehyde (**84**) (5 g, 20.4 mmol), (1,2-dihydroacenaphthylen-5-yl)boronic acid (**100**) (4.44 g, 22.4 mmol), CsF (8.68 g, 57.1 mmol) and $Pd(PPh_3)_4$ (943 mg, 0.816 mmol) in dry DME (105 mL). The mixture was allowed to stir with reflux for 24 h under a N_2 balloon. Chromatographic purification using a silica gel column packed in hexanes using sequential elution with 50% CH_2Cl_2 in hexanes, followed by 100% CH_2Cl_2 afforded **112** as a yellow-light brown solid (5.96 g, 92% yield). R_f ($1CH_2Cl_2$): 0.32. ^1H NMR (500 MHz, $CDCl_3$): δ 9.94 (s, 1H, CHO), 7.38 (t, 1H, Ar-H, *J* = 7.0 Hz), 7.31-7.25 (m, 4H, Ar-H), 7.17 ($AB_{quartet}$, 2H, Ar-H, *J* = 8.5 Hz), 4.00 (s, 3H, OCH_3), 3.97 (s, 3H, OCH_3), 3.47-3.41 (m, 4H, CH_2–CH_2). ^{13}C NMR (125 MHz, $CDCl_3$): δ 191.4, 152.6, 150.2, 146.2, 146.1, 139.2, 135.0, 132.0, 130.8, 129.8, 129.5, 128.3, 127.4, 120.6, 119.5, 118.8, 116.6, 62.2, 56.2, 30.6, 30.2. HRMS (ESI) *m/z* calcd for $C_{21}H_{18}O_3Na$ $[M + Na]^+$: 341.1148, found 341.1150.

2-(4-Methylnaphthalen-1-yl)benzaldehyde (116)

As described for the synthesis of **102**, **116** was prepared by a reaction of 2-bromobenzaldehyde (**88**) (1.2 g, 6.49 mmol), (4-methylnaphthalen-1-yl)boronic acid (**98**) (1.33 g, 7.13 mmol), CsF (2.76 g, 18.16 mmol) and $Pd(PPh_3)_4$ (300 mg, 0.259 mmol) in dry DME (33 mL). The mixture was allowed to stir at reflux for 18 h under a nitrogen gas-filled balloon. Chromatographic purification using a silica gel column packed in hexanes using sequential elution with hexanes, followed by 30% CH_2Cl_2 in hexanes afforded **116** as a yellow solid (1.34 g, 83% yield). R_f (10% EtOAc in hexanes): 0.62. ^1H NMR (500 MHz, $CDCl_3$): δ 9.63 (s, 1H, CHO), 8.10 (d, 1H, Ar-H, *J* = 7.0 Hz), 8.09 (d, 1H, Ar-H, *J* = 8.0 Hz), 7.69 (t, 1H, Ar-H, *J* = 7.5 Hz), 7.59-7.54 (m, 2H, Ar-H), 7.51 (d, 1H, Ar-H, *J* = 8.5 Hz), 7.44 (t, 2H, Ar-H, *J* = 6.5 Hz), 7.40 (d, 1H, Ar-H, *J*

= 7.5 Hz), 7.30 (d, 1H, Ar-H, *J* = 7.0 Hz), 2.78 (s, 3H, CH_3). ^{13}C NMR (125 MHz, $CDCl_3$): δ 192.2, 144.6, 135.1, 135.0, 133.7, 133.6, 132.8, 132.5, 131.9, 128.1, 128.0, 127.0, 126.5, 126.4, 126.0, 125.8, 124.5, 19.6. HRMS (ESI) *m/z* calcd for $C_{18}H_{14}ONa$ $[M + Na]^+$: 269.0937, found 296.0940.

2-(1,2-Dihydroacenaphthylen-5-yl)benzaldehyde (119)

As described for the synthesis of **102**, **119** was prepared by a reaction of 2-bromobenzaldehyde (**88**) (4.5 g, 24.32 mmol), (1,2-dihydroacenaphthylen-5-yl)boronic acid (**100**) (5.30 g, 26.75 mmol), CsF (10.34 g, 68.10 mmol), and $Pd(PPh_3)_4$ (1.12 g, 0.973 mmol) in dry DME (123 mL). The mixture was allowed to stir at reflux for 23 h under a nitrogen gas-filled balloon. Chromatographic purification using a silica gel column packed in hexanes using sequential elution with hexanes, followed by 50% CH_2Cl_2 in hexanes afforded **119** as a yellow-orange solid (4.66 g, 74% yield). R_f (100% CH_2Cl_2): 0.51. ^1H NMR (500 MHz, $CDCl_3$): δ 9.72 (s, 1H, CHO), 8.11 (d, 1H, Ar-H, *J* = 8.0 Hz), 7.69 (t, 1H, Ar-H, *J* = 7.5 Hz), 7.56 (t, 1H, Ar-H, *J* = 7.5 Hz), 7.50 (d, 1H, Ar-H, *J* = 8.0 Hz), 7.42 (t, 1H, Ar-H, *J* = 8.0 Hz), 7.36-7.33 (m, 3H, Ar-H), 7.28 (d, 1H, Ar-H, *J* = 8.5 Hz), 3.48 (br s, 4H, CH_2–CH_2). ^{13}C NMR (125 MHz, $CDCl_3$): δ 192.4, 146.8, 146.3, 144.1, 139.2, 134.8, 133.6, 131.8, 131.0, 130.8, 130.2, 128.8, 127.9, 127.2, 120.6, 119.8, 118.8, 30.5, 30.2. HRMS (ESI) *m/z* calcd for $C_{19}H_{14}ONa$ $[M + Na]^+$: 281.0937, found 381.0938.

1,1-Dibromoolefin derivatives.

1-[2-(2,2-Dibromovinyl)-phenyl]-naphthalene (103)[34]

In an oven-dried 50 mL round-bottom flask equipped with a magnetic stirring bar was placed PPh_3 (2.82 g, 10.8 mmol) in dry CH_2Cl_2 (3.0 mL). The mixture was cooled to 0 ºC, CBr_4 (1.78 g, 5.38 mmol) was added and the mixture was stirred for 10 minutes 0 ºC. 2-(Naphthalen-1-yl)benzaldehyde (**102**) (0.5 g, 2.15 mmol) dissolved in dry CH_2Cl_2 (5.0 mL) was added slowly. The mixture was flushed with nitrogen gas and allowed to stir at 0 ºC for 2 h at which time TLC showed the reaction to be complete. The mixture was diluted with CH_2Cl_2 and washed with brine (2x) and H_2O (2x). The aqueous layer was back extracted with CH_2Cl_2 (2x). The combined organic layer was dried over Na_2SO_4 and concentrated to give an orange-red residue. The crude product was chromatographed on a silica gel column packed in CH_2Cl_2 using CH_2Cl_2 as eluent. Compound **103** was obtained as an orange-red solid (0.828 g, 99% yield). (R_f

(CH_2Cl_2): 0.65. ^{1}H NMR (500 MHz, $CDCl_3$): δ 7.92-7.89 (m, 2H, Ar-H), 7.81-7.79 (m, 1H, Ar-H), 7.53 (t, 1H, Ar-H, *J* = 7.5 Hz), 7.51-7.45 (m, 4H, Ar-H), 7.41 (dt, 1H, Ar-H, *J* = 1.5, 6.5 Hz), 7.36-7.35 (m, 1H, Ar-H), 7.33 (dd, 1H, Ar-H, *J* = 1.0, 7.0), 6.93 (s, 1H, CH).

1-[2-(2,2-Dibromo-vinyl)-3,4-methoxyphenyl]-4-methylnaphthalene (106)

As described for the synthesis of **103**, **106** was prepared by a reaction of PPh_3 (7.71 g, 29.4 mmol), CBr_4 (4.87 g, 14.7 mmol), and 2,3-dimethoxy-6-(4-methyl-napthalen-1-yl)-benzaldehyde (**105**) (1.8 g, 5.87 mmol) in dry CH_2Cl_2 (22 mL) at 0 ºC for 2 h. Chromatographic purification using a silica gel column packed in CH_2Cl_2 using CH_2Cl_2 as eluent afforded **106** as a foamy, yellow solid (2.634 g, 97% yield). R_f (20% EtOAc in hexanes): 0.56. ^{1}H NMR (500 MHz, $CDCl_3$): δ 8.04 (d, 1H, Ar-H, *J* = 8.5 Hz), 7.60 (d, 1H, Ar-H, *J* = 8.5 Hz), 7.51 (t, 1H, Ar-H, *J* = 7.0 Hz), 7.39 (t, 1H, Ar-H, *J* = 8.0 Hz), 7.34 (d, 1H, Ar-H, *J* = 7.0 Hz), 7.23 (d, 1H, Ar-H, *J* = 7.0 Hz), 7.07-7.02 (m, 3H, Ar-H, CH), 3.95 (s, 3H, OCH_3), 3.88 (s, 3H, OCH_3), 2.74 (s, 3H, CH_3). ^{13}C NMR (125 MHz, $CDCl_3$): δ 152.1, 146.2, 135.9, 134.0, 133.9, 132.8, 132.7, 131.9, 130.9, 127.2, 126.65, 126.61, 126.0, 125.50, 125.47, 124.4, 112.2, 93.7, 61.1, 55.9, 19.6.

5-[2-(2,2-Dibromovinyl)-3,4-dimethoxyphenyl]acenaphthene (113)

As described for the synthesis of **103**, **113** was prepared by a reaction of PPh_3 (824 mg, 3.14 mmol), CBr_4 (521 mg, 1.57 mmol), and 6-acenaphthen-5-yl-2,3-dimethoxybenzaldehyde (**112**) (200 mg, 0.628 mmol) in dry CH_2Cl_2 (2.3 mL) at 0 ºC for 2 h. Chromatographic purification using a silica gel column packed in hexanes using sequential elution with 50% CH_2Cl_2 in hexanes, followed by 100% CH_2Cl_2 afforded **113** as a foamy, yellow solid (284 mg, 96% yield). R_f (20% EtOAc in hexanes): 0.47. ^{1}H NMR (500 MHz, $CDCl_3$): δ 7.38-7.34 (m, 2H, Ar-H), 7.30-7.28 (m, 3H, Ar-H, superimposed with the $CHCl_3$ resonance), 7.14 (s, 1H, CH), 7.12 (d, 1H, Ar-H, *J* = 8.0 Hz), 7.03 (d, 1H, Ar-H, *J* = 8.0 Hz), 3.95 (s, 3H, OCH_3), 3.87 (s, 3H, OCH_3), 3.48-3.40 (m, 4H, CH_2–CH_2). ^{13}C NMR (125 MHz, $CDCl_3$): δ 152.0, 146.1, 145.6, 139.4, 134.1, 133.0, 132.3, 130.7, 130.2, 129.4, 127.8, 126.6, 120.9, 119.1, 118.7, 112.21, 112.20, 93.6, 61.0, 55.9, 30.5, 30.1.

1-(2-(2,2-Dibromovinyl)phenyl)-4-methylnaphthalene (117)

As described for the synthesis of **103**, **117** was prepared by a reaction of PPh_3 (6.39 g, 24.36 mmol), CBr_4 (4.04 g, 12.18 mmol), and 2-(4-methylnaphthalen-1-yl)benzaldehyde (**116**) (1.2 g, 4.87 mmol) in dry CH_2Cl_2 (18 mL) at 0 ºC for 2 h. Chromatographic purification using a silica gel column packed in hexanes using hexanes as eluent afforded **117** as a yellow solid/oil (1.939 g, 99% yield). R_f (50% CH_2Cl_2 in hexanes): 0.76. ^{1}H NMR (500 MHz, $CDCl_3$): δ 8.07 (d, 1H, Ar-H, *J* = 8.5 Hz), 7.81-7.79 (m, 1H, Ar-H), 7.55-7.33 (m, 7H, Ar-H), 7.22 (d, 1H, Ar-H, *J* = 7.5 Hz), 6.94 (s, 1H, CH), 2.76 (br s, 3H, CH_3). ^{13}C NMR (125 MHz, $CDCl_3$): δ 140.1, 136.9, 136.1, 135.4, 134.5, 132.6, 131.8, 131.1, 128.8, 128.2, 127.3, 127.2, 126.6, 126.0, 125.8, 125.7, 124.4, 90.6, 19.6.

5-(2-(2,2-Dibromovinyl)phenyl)-1,2-dihydroacenaphthylene (120)

As described for the synthesis of **103**, **120** was prepared by a reaction of PPh_3 (12.69 g, 48.39 mmol), CBr_4 (8.02 g, 24.19 mmol), and 2-(1,2-dihydroacenaphthylen-5-yl)benzaldehyde (**119**) (2.5 g, 9.68 mmol) in dry CH_2Cl_2 (35 mL) at 0 ºC for 2 h. Chromatographic purification using a silica gel column packed in hexanes using hexanes as eluent afforded **120** as a yellow solid (3.774 g, 94% yield). R_f (50% CH_2Cl_2 in hexanes): 0.68. ^{1}H NMR (500 MHz, $CDCl_3$): δ 7.81-7.79 (m, 1H, Ar-H), 7.44 (app dd, 2H, Ar-H, J_{app} ~ 3.5, 5.5 Hz), 7.42-7.37 (m, 2H, Ar-H), 7.34-7.27 (m, 4H, Ar-H), 7.01 (s, 1H, CH), 3.49-3.43 (m, 4H, CH_2–CH_2). ^{13}C NMR (125 MHz, $CDCl_3$): δ 146.2, 146.1, 139.5, 139.3, 137.2, 135.1, 133.1, 131.0, 130.1, 129.5, 129.0, 128.3, 128.1, 127.1, 120.9, 119.5, 118.8, 90.4, 30.5, 30.2.

Alkynyl biaryl derivatives.

1-(2-Ethynyl-phenyl)-naphthalene (104)[34]

In an oven-dried 25 mL 3-neck round-bottom flask equipped with a magnetic stirring bar and under a nitrogen-gas filled balloon was placed 1-[2-(2,2-dibromo-vinyl)-phenyl]-naphthalene, **103** (200 mg, 0.515 mmol) in dry THF (1.20 mL). The mixture was cooled to –78 ºC, and 1.6M solution of *n*-BuLi in hexanes (0.80 mL, 1.29 mmol) was added dropwise. The mixture was allowed to stir at –78 ºC for 5 h, and then 1 h at room temperature, at which time TLC showed the reaction to be complete. The mixture was quenched with cold water and the aqueous layer was extracted with Et_2O (3x). The combined organic layer was dried over Na_2SO_4 and concentrated to give an orange-yellow oil/solid. The crude product was

chromatographed on a silica gel column packed in hexanes using hexanes as eluent. Compound **104** was obtained as a yellow solid (77.5 mg, 66% yield).

Use of LDA in place of n-BuLi. As described previously, **104** was prepared by a reaction of 1-[2-(2,2-dibromo-vinyl)-phenyl]naphthalene, **103** (100 mg, 0.258 mmol) and 2.0M solution of LDA in heptane/THF/ethylbenzene (0.32 mL, 0.644 mmol) in dry THF (0.60 mL) at –78 ºC for 5 h, then for 13 h at room temperature. The reaction was incomplete. Chromatographic purification using a silica gel column packed in hexanes using hexanes as eluent afforded **104** as a yellow solid (19.7 mg, 29% yield). R_f (100% hexanes): 0.17. ^{1}H NMR (500 MHz, $CDCl_3$): δ 7.90 (t, 2H, Ar-H, *J* = 7.8 Hz), 7.51 (dd, 1H, Ar-H, *J* = 1.5, 7.8 Hz), 7.59 (d, 1H, Ar-H, *J* = 8.5 Hz), 7.53 (t, 1H, Ar-H, *J* = 7.0 Hz), 7.49-7.44 (m, 3H, Ar-H), 7.42-7.37 (m, 3H, Ar-H), 2.75 (s, 1H, CH).

1-(2-Ethynyl-3,4-dimethoxyphenyl)-4-methylnaphthalene (107)

As described for the synthesis of **104**, **107** was prepared by a reaction of 1-[2-(2,2-dibromo-vinyl)-3,4-methoxyphenyl]-4-methylnaphthalene, (**106**) (200 mg, 0.433 mmol) and 1.6M solution of *n*-BuLi in hexanes (0.68 mL, 1.08 mmol) in dry THF (1.0 mL) at –78 ºC for 5 h, then for 1 h at room temperature. Chromatographic purification using a silica gel column packed in hexanes using 10% EtOAc in hexanes as eluent afforded **107** as a yellowish-white solid (106 mg, 81% yield). R_f (20% EtOAc in hexanes): 0.38. ^{1}H NMR (500 MHz, $CDCl_3$): δ 8.04 (d, 1H, Ar-H, *J* = 8.0 Hz), 7.65 (d, 1H, Ar-H, *J* = 8.0 Hz), 7.51 (t, 1H, Ar-H, *J* = 7.0 Hz), 7.40 (t, 1H, Ar-H, *J* = 7.5 Hz), 7.34 ($AB_{quartet}$, 2H, Ar-H, *J* = 7.5 Hz), 7.03 ($AB_{quartet}$, 2H, Ar-H, *J* = 8.5 Hz), 4.00 (s, 3H, OCH_3), 3.95 (s, 3H, OCH_3), 2.93 (s, 1H, CH), 2.74 (s, 3H, CH_3). ^{13}C NMR (125 MHz, $CDCl_3$): δ 151.8, 151.2, 137.1, 136.4, 134.0, 132.5, 132.2, 127.1, 126.9, 126.4, 125.9, 126.5, 126.4, 124.2, 117.8, 112.7, 84.5, 78.5, 61.1, 56.1, 19.6. HRMS (ESI) *m/z* calcd for $C_{21}H_{18}O_2Na$ $[M + Na]^+$: 325.1199, found 325.1197.

5-(2-Ethynyl-3,4-dimethoxyphenyl)acenaphthene (114)

As described for the synthesis of **104**, **114** was prepared by a reaction of 5-[2-(2,2-dibromovinyl)-3,4-dimethoxyphenyl]acenaphthene (**113**) (1.99 g, 4.19 mmol) and 1.6M solution of *n*-BuLi in hexanes (6.54 mL, 10.5 mmol) in dry THF (10 mL) at –78 ºC for 5 h, then for 1 h at room temperature. Chromatographic

purification using a silica gel column packed in hexanes using 10% EtOAc in hexanes as eluent afforded **114** as a yellow solid (106 mg, 81% yield). R_f (20% EtOAc in hexanes): 0.42. ^{1}H NMR (500 MHz, $CDCl_3$): δ 7.44-7.36 (m, 3H, Ar-H), 7.32 (d, 1H, Ar-H, *J* = 7.0 Hz), 7.27 (d, 1H, Ar-H, *J* = 6.0 Hz), 7.06 ($AB_{quartet}$, 2H, Ar-H, *J* = 8.5 Hz), 4.01 (s, 3H, OCH_3), 3.94 (s, 3H, OCH_3), 3.44 (br s, 4H, CH_2–CH_2), 2.99 (s, 1H, CH). ^{13}C NMR (125 MHz, $CDCl_3$): δ 151.7, 151.4, 145.0, 145.7, 139.3, 136.4, 133.3, 130.4, 129.3, 127.7, 126.3, 121.3, 119.1, 118.7, 117.5, 112.8, 84.5, 78.7, 61.1, 56.1, 30.5, 30.2. HRMS (ESI) *m/z* calcd for $C_{22}H_{18}O_2Na$ $[M + Na]^+$: 337.1199, found 337.1198.

1-(2-Ethynylphenyl)-4-methylnaphthalene (118)

As described for the synthesis of **104**, **118** was prepared by a reaction of 1-(2-(2,2-dibromovinyl)phenyl)-4-methylnaphthalene (**117**) (2.08 g, 5.17 mmol) and 1.6M solurion of *n*-BuLi in hexanes (8.07 mL, 12.92 mmol) in dry THF (12 mL) at –78 ºC for 5 h, then for 1 h at room temperature. Chromatographic purification using a silica gel column packed in hexanes using hexanes as eluent afforded **118** as an orange-yellow solid (773 mg, 62% yield). R_f (20% EtOAc in hexanes): 0.61. ^{1}H NMR (500 MHz, $CDCl_3$): δ 8.06 (d, 1H, Ar-H, *J* = 8.5 Hz), 7.67 (d, 1H, Ar-H, *J* = 7.5 Hz), 7.62 (d, 1H, Ar-H, *J* = 8.5 Hz), 7.51 (t, 1H, Ar-H, *J* = 7.0 Hz), 7.46-7.42 (m, 2H, Ar-H), 7.39 (t, 2H, Ar-H, *J* = 7.5 Hz), 7.35 (t, 2H, Ar-H, *J* = 7.0 Hz), 2.76 (s, 3H, CH_3). ^{13}C NMR (125 MHz, $CDCl_3$): δ 143.7, 136.8, 134.2, 134.2, 133.2, 132.6, 131.9, 131.0, 128.5, 127.2, 126.9, 126.8, 126.0, 125.5, 124.3, 122.6, 82.7, 80.2, 19.9. HRMS (EI/TOF) *m/z* calcd for $C_{19}H_{14}$ [M]: 242.1096, found 242.1094.

5-(2-Ethynylphenyl)-1,2-dihydroacenaphthylene (121)

As described for the synthesis of **104**, **121** was prepared by a reaction of 5-(2-(2,2-dibromovinyl)phenyl)-1,2-dihydroacenaphthylene (**120**) (3.5 g, 8.45 mmol) and 1.6 M *n*-BuLi (13.2 mL, 21.13 mmol) in dry THF (20 mL) at –78 ºC for 5 h, then 1 h at room temperature. Chromatographic purification using silica gel in hexanes with 100% hexanes as an eluent afforded **121** as a whitish-yellow solid (1.282 g, 60% yield). R_f (10% EtOAc in hexanes): 0.53. ^{1}H NMR (500 MHz, $CDCl_3$): δ 7.68 (d, 1H, Ar-H, *J* = 7.5 Hz), 7.45 (t, 2H, Ar-H, *J* = 7.0 Hz), 7.43-7.36 (m, 4H, Ar-H), 7.34 (d, 1H, Ar-H, *J* = 7.5 Hz), 7.29-7.28 (m, 1H, Ar-H), 3.55 (br s, 4H, CH_2–CH_2), 2.81 (s, 1H, CH). ^{13}C NMR (125 MHz, $CDCl_3$): δ 146.1, 146.0, 143.1, 139.3, 133.7,

133.4, 130.9, 130.1, 129.2, 128.5, 127.8, 127.1, 122.2, 121.2, 119.2, 118.7, 83.0, 80.1, 30.6, 30.2. HRMS (ESI) *m/z* calcd for $C_{20}H_{15}$ $[M + H]^+$: 255.1168, found 255.1170.

Synthesis of the B*c*Ph derivatives.

Benzo[*c*]phenanthrene (3)[34]

In an oven-dried reaction vial equipped with a magnetic stirring bar was placed 1-(2-ethynylphenyl)naphthalene (**104**) (30 mg, 0.131 mmol) in dry toluene (0.6 mL). $PtCl_2$ (1.7 mg, 6.39 μmol) was added, the vial was flushed with nitrogen gas and the mixture allowed to stir at 80 ºC in a sand bath for 17 h, at which time TLC showed the reaction to be complete. The dark brownish material was evaporated under a stream of nitrogen gas to give a brownish solid. Chromatographic purification using a silica gel column packed in hexanes using hexanes as eluent afforded **3** as a yellow solid (20.7 mg, 69% yield).

Using $AuCl_3$. As described previously, **3** was prepared by a reaction of 1-(2-ethynylphenyl)naphthalene (**104**) (53.3 mg, 0.233 mmol) and $AuCl_3$ (3.5 mg, 11.5 μmol) in dry toluene (1.0 mL) at 80 ºC over 24 h. This reaction proceeded to completion. Chromatographic purification using a silica gel column packed in hexanes using hexanes as eluent afforded **3** as a yellow solid (23.9 mg, 45% yield). R_f (hexanes): 0.28. ^{1}H NMR (500 MHz, $CDCl_3$): δ 9.14 (d, 2H, Ar-H, *J* = 8.0 Hz), 8.03 (d, 2H, Ar-H, *J* = 8.0 Hz), 7.87 ($AB_{quartet}$, 4H, Ar-H, *J* = 8.5 Hz), 7.70 (t, 2H, Ar-H, *J* = 7.5 Hz), 7.64 (t, 2H, Ar-H, *J* = 7.5 Hz).

5-Methylbenzo[*c*]phenanthrene (38)

As described for the synthesis of **3**, **38** was prepared by a reaction of 1-(2-ethynylphenyl)-4-methylnaphthalene (**118**) (771 mg, 3.183 mmol) and $PtCl_2$ (42.3 mg, 0.159 mmol) in dry toluene (14 mL) at 80 ºC in a sand bath for 24 h. Chromatographic purification using silica gel in hexanes with 100% hexanes as an eluent afforded **38** as a yellow solid (626 mg, 81% yield). R_f (100% hexanes): 0.18. ^{1}H NMR (500 MHz, $CDCl_3$): δ 9.14 (d, 1H, Ar-H, *J* = 8.5 Hz), 9.07 (d, 1H, Ar-H, *J* = 8.5 Hz), 8.20-8.18 (m, 1H, Ar-H), 8.00 (d, 1H, Ar-H, *J* = 8.0 Hz), 7.88 (d, 1H, Ar-H, *J* = 8.5 Hz), 7.77 (d, 1H, Ar-H, *J* = 8.5 Hz), 7.71-7.65 (m, 4H, Ar-H), 7.59 (t, 1H, Ar-H, *J* = 7.6 Hz), 2.82 (s, 3H, CH_3). ^{13}C NMR (125 MHz, $CDCl_3$): δ 133.3,

133.1, 133.1, 130.8, 130.5, 130.2, 128.5, 128.4, 127.9, 127.5, 127.1, 126.5, 126.4, 126.1, 125.8, 125.7, 125.4, 124.4, 19.8. HRMS (ESI) *m/z* calcd for $C_{19}H_{15}$ $[M + H]^+$: 243.1168, found 243.1168.

Benzo[*l*]acephenanthrylene (42)

In an oven-dried reaction vial equipped with a magnetic stirring bar were placed 4,5-dihydrobenzo[*l*]acephenanthrylene (**43**) (25.4 mg, 0.1 mmol) in dry toluene. DDQ (29.5 mg, 0.13 mmol) was added, the vial was flushed with nitrogen gas and the mixture was allowed to stir at 80 ºC over 24 h. TLC showed complete reaction and the mixture was evaporated under a stream of nitrogen gas to give a dark yellow solid. The crude product was chromatographed on ¼ basic alumina–¾ silica gel column packed in hexanes using hexanes as eluent. Compound **42** was obtained as a yellow solid (18.1 mg, 72% yield). R_f (100% hexanes): 0.14. ^{1}H NMR (500 MHz, $CDCl_3$): δ 9.21 (d, 1H, Ar-H, *J* = 8.5 Hz), 8.96-8.93 (m, 1H, Ar-H), 8.09 (s, 1H, Ar-H), 8.03 (d, 1H, Ar-H, *J* = 8.0 Hz), 7.93 ($AB_{quartet}$, 2H, Ar-H, *J* = 8.5 Hz), 7.76-7.72 (m, 3H, Ar-H), 7.65 (dt, 1H, Ar-H, *J* = 1.0, 8.0 Hz), 7.23 (d, 1H, Ar-H, *J* = 5.0 Hz), 7.14 (d, 1H, Ar-H, *J* = 5.0 Hz). ^{13}C NMR (125 MHz, $CDCl_3$): δ 139.9, 138.9, 134.0, 133.3, 131.9, 131.3, 129.3, 129.0, 128.7, 128.4, 128.1, 128.0, 127.3, 126.6, 126.5, 126.4, 126.0, 122.6. HRMS (ESI) *m/z* calcd for $C_{20}H_{13}$ $[M + H]^+$: 253.1012, found 253.1012.

4,5-Dihydrobenzo[*l*]acephenanthrylene (43)

As described for the synthesis of **3**, **38** was prepared by a reaction of 5-(2-ethynylphenyl)-1,2-dihydroacenaphthylene (**121**) (1.07 g, 4.207 mmol) and $PtCl_2$ (55.96 mg, 0.210 mmol) in dry toluene (18 mL) at over 24 h. Chromatographic purification using a silica gel column packed in hexanes using sequential elution with hexanes, followed by 10% CH_2Cl_2 in hexanes afforded **43** as a pale reddish-brown solid (716 mg, 69% yield). R_f (100% hexanes): 0.16. ^{1}H NMR (500 MHz, $CDCl_3$): δ 9.30 (d, 1H, Ar-H, *J* = 8.5 Hz), 8.94 (d, 1H, Ar-H, *J* = 8.5 Hz), 8.02 (d, 1H, Ar-H, *J* = 8.0 Hz), 7.86 ($AB_{quartet}$, 2H, Ar-H, *J* = 8.5 Hz), 7.72-7.68 (m, 2H, Ar-H), 7.65 (s, 1H, Ar-H), 7.60 (t, 1H, Ar-H, *J* = 7.5 Hz), 7.50 (d, 1H, Ar-H, *J* = 7.0 Hz), 3.53-3.48 (m, 4H, CH_2–CH_2). ^{13}C NMR (125 MHz, $CDCl_3$): δ 146.1, 145.1, 139.2, 133.7, 132.8, 131.3, 129.0, 128.6, 128.3, 127.7, 127.3, 127.0, 126.2, 125.3, 124.8, 123.5, 120.6, 120.2, 30.7, 29.4. HRMS (ESI) *m/z* calcd for $C_{20}H_{15}$ $[M + H]^+$: 255.1168, found 255.1170.

3,4-Dimethoxy-8-methylbenzo[*c*]phenanthrene (108)

As described for the synthesis of **3**, **108** was prepared by a reaction of 1-(2-ethynyl-3,4-dimethoxyphenyl)-4-naphthalene (**107**) (40 mg, 0.132 mmol) and $PtCl_2$ (1.8 mg, 6.77 μmol) in dry toluene (0.6 mL) at 80 ºC over 17 h. Chromatographic purification using a silica gel column packed in hexanes using 50% CH_2Cl_2 in hexanes as eluent afforded **108** as a yellow solid (29.8 mg, 75% yield).

Using $AuCl_3$. As described previously, **108** was prepared by a reaction of 1-(2-ethynyl-3,4-dimethoxyphenyl)-4-naphthalene (**107**) (30 mg, 0.100 mmol) and $AuCl_3$ (1.5 mg, 4.94 μmol) in dry toluene (0.43 mL) at 80 ºC over 24 h. Chromatographic purification using a silica gel column packed in hexanes using 50% CH_2Cl_2 in hexanes as eluent afforded **108** as a yellow solid of (25.3 mg, 84% yield). R_f (50% CH_2Cl_2 in hexanes): 0.28. ^{1}H NMR (500 MHz, $CDCl_3$): δ 9.08-9.06 (m, 1H, Ar-H), 8.80 (d, 1H, Ar-H, *J* = 9.3 Hz), 8.23 (d, 1H, Ar-H, *J* = 8.5 Hz), 8.17-8.15 (m, 1H, Ar-H), 7.76 (d, 1H, Ar-H, *J* = 8.5 Hz), 7.67-7.65 (m, 3H, Ar-H), 7.40 (d, 1H, Ar-H, *J* = 9.5 Hz), 4.07 (s, 3H, OCH_3), 4.06 (s, 3H, OCH_3), 2.80 (s, 3H, CH_3). ^{13}C NMR (125 MHz, $CDCl_3$): δ 148.6, 143.3, 133.2, 132.3, 132.3, 130.3, 129.6, 128.9, 128.4, 127.1, 127.0, 126.5, 125.7, 125.5, 124.42, 124.39, 120.7, 113.5, 61.4, 56.6, 19.7. HRMS (ESI) *m/z* calcd for $C_{20}H_{18}O_2Na$ $[M + Na]^+$: 325.1199, found 325.1198.

9,10-Dimethoxy-4,5-dihydrobenzo[*l*]acephenanthrylene (115)

As described for the synthesis of **3**, **115** was prepared by a reaction of 5-(2-ethynyl-3,4-dimethoxyphenyl)acenaphthene (**114**) (30 mg, 0.095 mmol) and $PtCl_2$ (1.27 mg, 4.77 μmol) in dry toluene (0.42 mL) at 80 ºC over 21 h. The mixture was filtered through Celite and the residue was washed with CH_2Cl_2. Chromatographic purification using a silica gel column packed in hexanes using 50% CH_2Cl_2 in hexanes as eluent afforded **115** as a yellow solid (21.7 mg, 72% yield).

Using $AuCl_3$. As described previously, **115** was prepared by a reaction of 5-(2-ethynyl-3,4-dimethoxyphenyl)acenaphthene (**114**) (30 mg, 0.095 mmol) and $AuCl_3$ (1.45 mg, 4.78 μmol) in dry toluene (0.42 mL) at 80 ºC over 29 h. Chromatographic purification using a silica gel column packed in hexanes using 50% CH_2Cl_2 in hexanes as eluent afforded **115** as a yellow solid (17.8 mg, 59%). R_f (20% EtOAc in hexanes): 0.32. ^{1}H NMR (500 MHz, $CDCl_3$): δ 9.01 (d, 1H, Ar-H, *J* = 9.0 Hz), 8.84 (d, 1H, Ar-H,

J = 8.5 Hz), 8.23 (d, 1H, Ar-H, *J* = 8.5 Hz), 7.82 (d, 1H, Ar-H, *J* = 9.0 Hz), 7.66 (t, 1H, Ar-H, *J* = 7.0 Hz), 7.63 (s, 1H, Ar-H), 7.47 (d, 1H, Ar-H, *J* = 7.0 Hz), 7.44 (d, 1H, Ar-H, *J* = 9.0 Hz), 4.07 (d, 3H, OCH_3), 4.06 (d, 3H, OCH_3), 3.52-3.48 (m, 4H, CH_2–CH_2). ^{13}C NMR (125 MHz, $CDCl_3$): δ 148.5, 146.1, 144.4, 139.3, 132.5, 128.8, 128.5, 128.2, 128.1, 126.9, 126.8, 124.9, 123.43, 123.37, 120.5, 120.4, 120.2, 113.6, 61.4, 56.6, 30.7, 29.4. HRMS (ESI) *m/z* calcd for $C_{22}H_{18}O_2Na$ $[M + Na]^+$: 337.1199, found 337.1195.

Synthesis of the Quinone derivatives.

8-Methylbenzo[*c*]phenanthrene-3,4-dione (124)

Demethylation. In an oven-dried 15 mL 2-neck round-bottom flask equipped with a magnetic stiring bar and under a nitrogen gas-filled balloon was placed 3,4-dimethoxy-8-methylbenzo[*c*]phenanthrene (**108**) (30.24 mg, 0.1 mmol) in dry CH_2Cl_2 (1.5 mL). The mixture was cooled to –70 ºC and a 1M solution of BBr_3 in pentane (0.3 mL, 0.3 mmol) was added. The purple-pink suspension was allowed to stir at –70 ºC for 5 mins, then allowed to warm to room temperature and stirred for 2 h. TLC showed completion of the reaction and the mixture was by quenched with ice and cold water. The mixture was diluted with CH_2Cl_2, and washed several times with brine and cold water. The organic layer was dried over Na_2SO_4 and concentrated to give a crude reddish solid of catechol **123**. R_f (CH_2Cl_2): 0.16. *Oxidation.* In an oven-dried 25 mL 3-neck round-bottom flask equipped with a magnetic stirring bar was placed crude catechol **123** (27.43 mg, 0.1 mmol) in dry CH_2Cl_2 (2 mL). The mixture was cooled to 0 ºC and PDC (104.4 mg, 0.3 mmol) was added. The mixture was allowed to stir at room temperature for 4 h, at which time TLC showed the reaction to be complete. The mixture was filtered through Celite and the reddish orange filtrate was obtained was concentrated to give a reddish solid. The crude product was chromatographed on a silica gel column packed in CH_2Cl_2 using sequential elution with CH_2Cl_2, followed by 5% MeOH in CH_2Cl_2. Compound **124** was obtained as a reddish-orange solid (22.3 mg, 82% yield). R_f (5% MeOH in CH_2Cl_2): 0.82. ^1H NMR (500 MHz, CD_3OD): δ 8.53 (d, 1H, H-1, *J* = 10.5 Hz), 8.41 (d, 1H, Ar-H, *J* = 8.0 Hz), 8.21 (t, 2H, Ar-H, *J* = 8.0 Hz), 7.94 (d, 1H, Ar-H, *J* = 8.0 Hz), 7.81 (dt, 1H, Ar-H, *J* = 1.0, 7.0 Hz), 7.74 (dt, 1H, Ar-H, *J* = 1.0, 8.0 Hz), 7.63 (s, 1H, Ar-H), 6.51 (d, 1H, H-2, *J* = 10.5 Hz), 2.79 (s, 3H, CH_3). ^{13}C NMR (125 MHz, DMSO): δ 178.4, 137.3, 136.8, 133.4, 133.1, 132.6, 131.4, 130.9, 129.4, 128.5, 128.0,

126.0, 125.1, 124.23, 124.22, 123.22, 111.2, 57.0, 19.9. HRMS (ESI) *m/z* calcd for $C_{19}H_{12}O_2Na$ [M + Na]$^+$: 295.0730, found 295.0730.

4,5-Dihydrobenzo[*l*]acephenanthrylene-9,10-dione (126)

Demethylation. As described for the synthesis of **124**, **126** was prepared by a reaction of 9,10-dimethoxy-4,5-dihydrobenzo[*l*]acephenanthrylene (**115**) (31.4 mg, 0.1 mmol) and 1M solution of BBr_3 in pentane (0.3 mL, 0.3 mmol) in dry CH_2Cl_2 (1.5 mL) cooled to –70 ºC, then allowed to warm to room temperature and stirred for 2 h. Workup as in the case of **124** gave a reddish-orange solid of crude catechol **125** was obtained. R_f (CH_2Cl_2): 0.07. *Oxidation.* As described for the synthesis of **124**, **126** was prepared by a reaction of crude catechol **125** (28.6 mg, 0.1 mmol) and PDC (112.7 mg, 0.3 mmol) in dry CH_2Cl_2 (2.0 mL) cooled to 0 ºC, then allowed to warm to room temperature and stirred for 4 h. Chromatographic purification using a silica gel column packed in CH_2Cl_2 using CH_2Cl_2 as eluent afforded compound **126** as a dark red solid (22.5 mg, 79% yield). R_f (5% MeOH in CH_2Cl_2): 0.81. ^{1}H NMR (500 MHz, acetone-d_6): δ 8.84 (d, 1H, H-12, *J* = 10.5 Hz), 8.36 (d, 1H, Ar-H, *J* = 8.5 Hz), 8.18 (d, 1H, Ar-H, *J* = 8.0 Hz), 8.06 (d, 1H, Ar-H, *J* = 8.0 Hz), 7.76 (t, 1H, Ar-H, *J* = 7.0 Hz), 7.74 (d, 1H, Ar-H, *J* = 7.0 Hz), 7.65 (s, 1H, Ar-H), 6.58 (d, 1H, H-11, *J* = 10.5 Hz), 3.54-3.48 (m, 4H, CH_2–CH_2). ^{13}C NMR (125 MHz, DMSO): δ 178.0, 149.5, 146.8, 143.7, 139.6, 139.3, 135.9, 133.1, 130.7, 129.3, 127.7, 127.4, 125.9, 125.6, 123.7, 120.3, 119.9, 30.6, 29.4. HRMS (ESI) *m/z* calcd for $C_{20}H_{12}O_2Na$ [M + Na]$^+$: 307.0730, found 307.0732.

Synthesis of the Dihydrodiol derivatives.

(±)-*Trans*-8-methyl-3,4-dihydrobenzo[*c*]phenanthrene-3,4-diol [(±)-39]

In an oven-dried 200 mL round-bottom flask equipped with a magnetic stirring bar was placed quinone **124** (134.8 mg, 0.5 mmol) in dry THF (9 mL), and ethanol (60 mL). The mixture was cooled to 0 ºC, sparged with O_2 for 15 mins, and $NaBH_4$ (187.3 mg, 5.0 mmol) was added portionwise. The yellow mixture was allowed to stir at room temperature with O_2 sparging for 4 h, then allowed to stir under an O_2 balloon overnight for 15 h protected from light. The mixture was again cooled to 0 ºC, sparged with O_2 for 15 mins, and another aliquot of $NaBH_4$ (187.3 mg, 5.0 mmol) was added portionwise. The mixture was allowed to stir at room temperature with O_2 sparging for 5 h, at which time TLC showed the reaction to be

complete. The mixture was concentrated to a third of its volume. Addition of ice and cold water resulted in a creamy yellow suspension. The mixture was transferred to a separatory funnel and was dissolved with EtOAc and washed with H_2O (3x). The organic layer was dried over Na_2SO_4 and concentrated to give a yellow-orange-white solid. The crude product was suspended in cold Et_2O and sonicated to yield (±)-**39** as a whitish solid (104.5 mg, 76% yield). R_f (5% MeOH in CH_2Cl_2): 0.35. ^{1}H NMR (500 MHz, acetone-d_6): δ 8.63 (d, 1H, Ar-H, *J* = 8.0 Hz), 8.13 (d, 1H, Ar-H, *J* = 8.0 Hz), 7.94 (d, 1H, Ar-H, *J* = 8.0 Hz), 7.81 (d, 1H, Ar-H, *J* = 8.0 Hz), 7.71-7.64 (m, 2H, Ar-H), 7.61 (s, 1H, Ar-H), 7.27 (d, 1H, H-1, *J* = 10.5 Hz), 6.31 (dd, 1H, H-2, *J* = 1.5, 10.0 Hz), 4.74-4.68 (m, 2H, H-3, OH-3), 4.64 (br d, 1H, H-4, *J* = 11.0 Hz), 4.42 (br, 1H, OH-4), 2.73 (s, 3H, CH_3). ^{13}C NMR (125 MHz, DMSO): δ 137.9, 133.4, 133.0, 132.21, 132.20, 130.2, 129.0, 128.8, 127.4, 127.1, 126.9, 126.8, 126.4, 125.6, 124.9, 74.9, 71.4, 19.7. HRMS (ESI) *m/z* calcd for $C_{19}H_{16}O_2Na$ $[M + Na]^+$: 299.1043, found 299.1043.

(±)-*Trans*-4,5,9,10-tetrahydrobenzo[*l*]acephenanthrylene-9,10-diol [(±)-44]

As described for the synthesis of (±)-**39**, (±)-**44** was prepared by reaction of quinone **126** (180 mg, 0.633 mmol), $NaBH_4$ (187.3 mg, 5.0 mmol) added portionwise twice, in THF (10.5 mL) and ethanol (72.5 mL), with O_2 sparging at room temperature for 24 h. The crude yellow solid was suspended in cold Et_2O with sonicated to afford (±)-**44** as an off-white solid (144.5 mg, 79% yield). R_f (5% MeOH in CH_2Cl_2): 0.26. ^{1}H NMR (500 MHz, acetone-d_6): δ 8.41 (d, 1H, Ar-H, *J* = 8.0 Hz), 7.89 ($AB_{quartet}$, 2H, Ar-H, *J* = 8.5 Hz), 7.62 (t, 1H, Ar-H, *J* = 8.0 Hz), 7.54 (s, 1H, Ar-H), 7.52-7.47 (m, 2H, Ar-H, H-12), 6.34 (d, 1H, H-11, *J* = 10.5 Hz), 4.75 (d, 1H, H-9, *J* = 11.5 Hz), 4.69-4.66 (br d, 1H, OH-9, *J* = 5.0 Hz), 4.60 (d, 1H, H-10, *J* = 11.5 Hz), 4.42-4.39 (m, 1H, OH-10), 3.48-3.41 (m, 4H, CH_2–CH_2). ^{13}C NMR (125 MHz, DMSO): δ 145.7, 143.9, 139.1, 137.1, 134.7, 133.6, 129.9, 128.7, 128.2, 128.1, 126.4, 124.9, 124.5, 124.4, 121.9, 120.1, 74.9, 71.4, 30.6, 28.9. HRMS (ESI) *m/z* calcd for $C_{20}H_{16}O_2Na$ $[M + Na]^+$: 311.1043, found 311.1043.

Synthesis of Series 1 Diol Epoxides

1*β*,2*β*-Epoxy-3*α*,4*β*-dihydroxy-8-methyl-1,2,3,4-tetrahydrobenzo[*c*]phenanthrene [(±)-40]

Synthesis of (±)-2α-bromo-8-methyl-1β,3α,4β-trihydroxyl-1,2,3,4-tetrahydrobenzo[*c*]phenanthrene, (±)-**127**. In an oven-dried reaction vial equipped with a magnetic stirring bar was placed dihydrodiol (±)-**39**

(20.0 mg, 72.38 μmol) in dry THF (3.0 mL) and H_2O (1.5 mL). *N*-bromoacetamide (29.95 mg, 0.217 mmol) was added and the mixture was allowed to stir at room temperature under subdued light for 25 h, at which time TLC showed the reaction to be complete. The orange mixture was evaporated to half its volume, diluted with Et_2O and washed sequentially with H_2O and brine. The organic layer was dried over Na_2SO_4 and concentrated to give a yellow-white solid. Trituration using cold Et_2O containing a little hexane afforded (±)-**127** as a white solid (26.2 mg, 97% yield). R_f (5% MeOH in CH_2Cl_2): 0.20.

Cyclization to 1β,2β-epoxy-3α,4β-dihydroxy-8-methyl-1,2,3,4-tetrahydrobenzo[*c*]phenanthrene, (±)-**40**. In an oven-dried reaction vial equipped with a magnetic stirring bar was placed bromo triol (±)-**127** (15.3 mg, 40.99 μmol) in dry THF (1.6 mL). IRA-Amberite 400 HO^- (248.5 mg) was added and the mixture was allowed to stir at room temperature under subdued light for 4 h, at which time TLC showed the reaction to be complete. The Amberite was filtered off, and the filtrate obtained was concentrated to give a white solid. Trituration with cold Et_2O afforded (±)-**40** as a white solid (7.7 mg, 64% yield). R_f (5% MeOH in CH_2Cl_2): 0.39. ^{1}H NMR (500 MHz, acetone-d_6): δ 9.19 (d, 1H, Ar-H, *J* = 7.5 Hz), 8.17 (d, 1H, Ar-H, *J* = 8.0 Hz), 7.94 ($AB_{quartet}$, 2H, Ar-H, *J* = 8.0 Hz), 7.76-7.69 (m, 2H, Ar-H), 7.68 (s, 1H, Ar-H), 4.87 (br, 1H, OH-4, D_2O exchangeable), 4.82 (d, 1H, H-4, *J* = 8.5 Hz), 4.66 (d, 1H, OH-3, *J* = 6.5 Hz, D_2O exchangeable), 4.36 (d, 1H, H-1, *J* = 4.0 Hz), 3.95 (dd, 1H, H-2, *J* = 2.0, 4.5 Hz), 3.84 (dd, 1H, H-3, *J* = 1.5, 9.0 Hz), 2.74 (s, 3H, CH_3). The following signals were observed to sharpen upon exchange with D_2O: 4.82 (d, 1H, H-4, *J* = 9.0 Hz), 4.36 (d, 1H, H-1, *J* = 4.5 Hz), 3.95 (dd, 1H, H-2, *J* = 2.0, 4.5 Hz), 3.84 (dd, 1H, H-3, *J* = 2.0, 9.0 Hz). ^{13}C NMR (125 MHz, acetone-d_6): δ 136.4, 133.4, 132.5, 132.40, 132.37, 130.2, 129.2, 127.8, 127.1, 126.7, 125.8, 124.8, 124.6, 113.9, 72.4, 72.1, 62.4, 50.9, 19.0. HRMS (ESI) *m/z* calcd for $C_{19}H_{16}O_3Na$ $[M + Na]^+$: 315.0992, found 315.0992.

11β,12β-Epoxy-4,5,9,10,11,12-hexahydrobenzo[*l*]acephenanthrylene-9β,10α-diol [(±)-45]

Synthesis of 11α-bromo-4,5,9,10,11,12-hexahydrobenzo[*l*]acephenanthrylene-9β,10α,12β-triol, (±)-**128**. In an oven-dried reaction vial equipped with a magnetic stirring bar was placed dihydrodiol (±)-**44** (30.0 mg, 0.104 mmol) in dry THF (4.4 mL) and H_2O (2.2 mL). *N*-bromoacetamide (17.2 mg, 0.124 mmol) was added and the mixture was allowed to stir at room temperature under subdued light for 19 h, at which time TLC showed the reaction to be complete. The orange mixture was evaporated to half its volume,

diluted with Et_2O and washed sequentially with H_2O and brine. The organic layer was dried over Na_2SO_4 and concentrated to give a reddish-white solid. Trituration using cold Et_2O containing a little hexane afforded (±)-**128** as a pale reddish-white solid (39.1 mg, 95% yield). R_f (5% MeOH in CH_2Cl_2): 0.16.

Cyclization to 11β,12β-epoxy-4,5,9,10,11,12-hexahydrobenzo[*l*]acephenanthrylene-9β,10α-diol, (±)-**45**. In an oven-dried reaction vial equipped with a magnetic stirring bar was placed bromo triol (±)-**128** (39.1 mg, 0.101 mmol) in dry THF (4.0 mL). IRA-Amberite 400 HO^- (615.1 mg) was added and the mixture was allowed to stir at room temperature under subdued light for 4 h, at which time TLC showed the reaction to be complete. The Amberite was filtered off, and the filtrate obtained was concentrated to give a yellow-white solid. Trituration with cold Et_2O afforded (±)-**45** as a pale yellow-white solid (18.7 mg, 60.5% yield). R_f (5% MeOH in CH_2Cl_2): 0.32. ^{1}H NMR (500 MHz, acetone-d_6, 1 drop DMSO): δ 8.80 (d, 1H, Ar-H, J = 8.5 Hz), 7.95 ($AB_{quartet}$, 2H, Ar-H, J = 8.5 Hz), 7.65 (t, 1H, Ar-H, J = 7.8 Hz), 7.59 (s, 1H, Ar-H), 7.50 (d, 1H, Ar-H, J = 7.0 Hz), 5.19 (br, 2H, OH-9, OH-10), 4.83 (d, 1H, H-9, J = 9.5), 4.45 (d, 1H, H-12, J = 4.0 Hz), 3.90 (dd, 1H, H-11, J = 2.0, 4.0 Hz), 3.68 (dd, 1H, H-10, J = 2.0, 9.5 Hz), 3.48-3.39 (m, 4H, CH_2–CH_2). ^{13}C NMR (125 MHz, acetone-d_6, 1 drop DMSO): δ 156.5, 146.2, 145.6, 144.2, 139.2, 138.9, 129.7, 128.5, 128.0, 127.6, 124.2, 123.5, 121.7, 119.8, 73.1, 71.9, 61.9, 50.2, 30.2, (resonance embedded in acetone-d_6 peak). HRMS (ESI) *m/z* calcd for $C_{20}H_{16}O_3Na$ $[M + Na]^+$: 327.0992, found 327.0997.

Synthesis of Series 2 Diol Epoxides

1*α*,2*α*-Epoxy-3*α*,4*β*-dihydroxy-8-methyl-1,2,3,4-tetrahydrobenzo[*c*]phenanthrene [(±)-41]

In an oven-dried 10 mL round-bottom flask equipped with a magnetic stirring bar was placed dihydrodiol (±)-**39** (20.0 mg, 72.38 μmol) in THF (4 mL). The mixture was cooled to –78 ºC and purified *m*CPBA (125.8 mg, 0.724 mmol) was added. The mixture was allowed to warm to room temperature and stirred for 2 h, at which time TLC showed the reaction to be complete. The mixture was evaporated to a third of its volume and diluted with EtOAc. The mixture was washed with cold 1M NaOH (2x), with H_2O (2x) and with brine (2x). The organic layer was dried over Na_2SO_4 and concentrated to give a yellow-white solid. Trituration with cold Et_2O afforded (±)-**41** as a pale yellow-white solid (14.6 mg, 69% yield). R_f (5% MeOH in CH_2Cl_2): 0.37. ^{1}H NMR (500 MHz, acetone-d_6): δ 8.79 (d, 1H, Ar-H, J = 8.0 Hz), 8.18 (d, 1H, Ar-H, J = 8.0 Hz), 7.99 (d, 1H, Ar-H, J = 8.5 Hz), 7.88 (d, 1H, Ar-H, J = 8.0 Hz), 7.75 (dt, 1H, Ar-H, J = 1.5, 8.5 Hz),

7.72 (dt, 1H, Ar-H, *J* = 1.5, 8.5 Hz), 7.65 (s, 1H, Ar-H), 4.88 (br d, 2H, H-4, OH-4, *J* = 9.0 Hz, D_2O exchangeable for 1H), 4.80 (d, 1H, H-1, *J* = 4.5 Hz), 4.64 (br, 1H, OH-3, D_2O exchangeable), 3.96 (br d, 1H, H-3, *J* = 8.0 Hz), 3.81 (dd, 1H, H-2, *J* = 1.8, 4.5 Hz), 2.75 (s, 3H, CH_3). The following signals were observed to sharpen upon exchange with D_2O: 4.84 (d, 1H, H-4, *J* = 8.5 Hz), 4.78 (d, 1H, H-1, *J* = 4.0 Hz), 3.96 (dd, 1H, H-3, *J* = 2.0, 8.5 Hz), 3.81 (dd, 1H, H-2, *J* = 2.0, 4.5 Hz). ^{13}C NMR (125 MHz, acetone-d_6): δ 139.8, 133.4, 133.3, 132.2, 132.1, 130.5, 128.2, 127.6, 126.8, 126.6, 125.2, 124.5, 123.4, 72.3, 70.6, 57.2, 54.7, 54.1, 18.8. HRMS (ESI) *m/z* calcd for $C_{19}H_{16}O_3Na$ $[M + Na]^+$: 315.0992, found 315.0995.

11α,12α-Epoxy-4,5,9,10,11,12-hexahydrobenzo[*l*]acephenanthrylene-9β,10α-diol [(±)-46]

In an oven-dried 10 mL round-bottom flask equipped with a magnetic stirring bar was placed dihydrodiol (±)-**39** (30.0 mg, 0.104 mmol) in THF (6 mL). The mixture was cooled to –78 ºC and purified *m*CPBA (179.5 mg, 1.04 mmol) was added. The mixture was allowed to warm to room temperature and stirred for 2 h, at which time TLC showed the reaction to be complete. The mixture was evaporated to a third of its volume and diluted with EtOAc. The mixture was washed with cold 1M NaOH (2x), with H_2O (2x), and with brine (2x). The organic layer was dried over Na_2SO_4 and concentrated to give a yellow-white solid. Trituration with cold Et_2O afforded (±)-**46** as a pale yellow-white solid (25.5 mg, 80% yield). R_f (5% MeOH in CH_2Cl_2): 0.11. ^{1}H NMR (500 MHz, acetone-d_6, 1 drop DMSO): δ 8.50 (d, 1H, Ar-H, *J* = 8.5 Hz), 7.91 ($AB_{quartet}$, 2H, Ar-H, *J* = 8.3 Hz), 7.63 (t, 1H, Ar-H, *J* = 7.8 Hz), 7.55-7.52 (m, 2H, Ar-H), 4.97 (d, 1H, H-12, *J* = 4.5 Hz), 4.88-4.86 (m, 1H, OH-9), 4.77 (d, 1H, H-9, *J* = 8.0 Hz), 3.95 (dd, 1H, H-10, *J* = 2.0, 8.0 Hz), 3.79 (dd, 1H, H-11, *J* = 2.0, 4.5 Hz), 3.53-3.52 (m, 1H, OH-10), 3.47-3.39 (m, 4H, CH_2–CH_2). ^{13}C NMR (125 MHz, acetone-d_6, 1 drop DMSO): δ 159.5, 145.7, 135.0, 134.6, 129.3, 128.5, 127.9, 127.6, 123.7, 123.6, 121.8, 119.5, 72.1, 70.6, 56.7, 53.8, 30.3, 29.6. HRMS (ESI) *m/z* calcd for $C_{20}H_{16}O_3Na$ $[M + Na]^+$: 327.0992, found 327.0992.

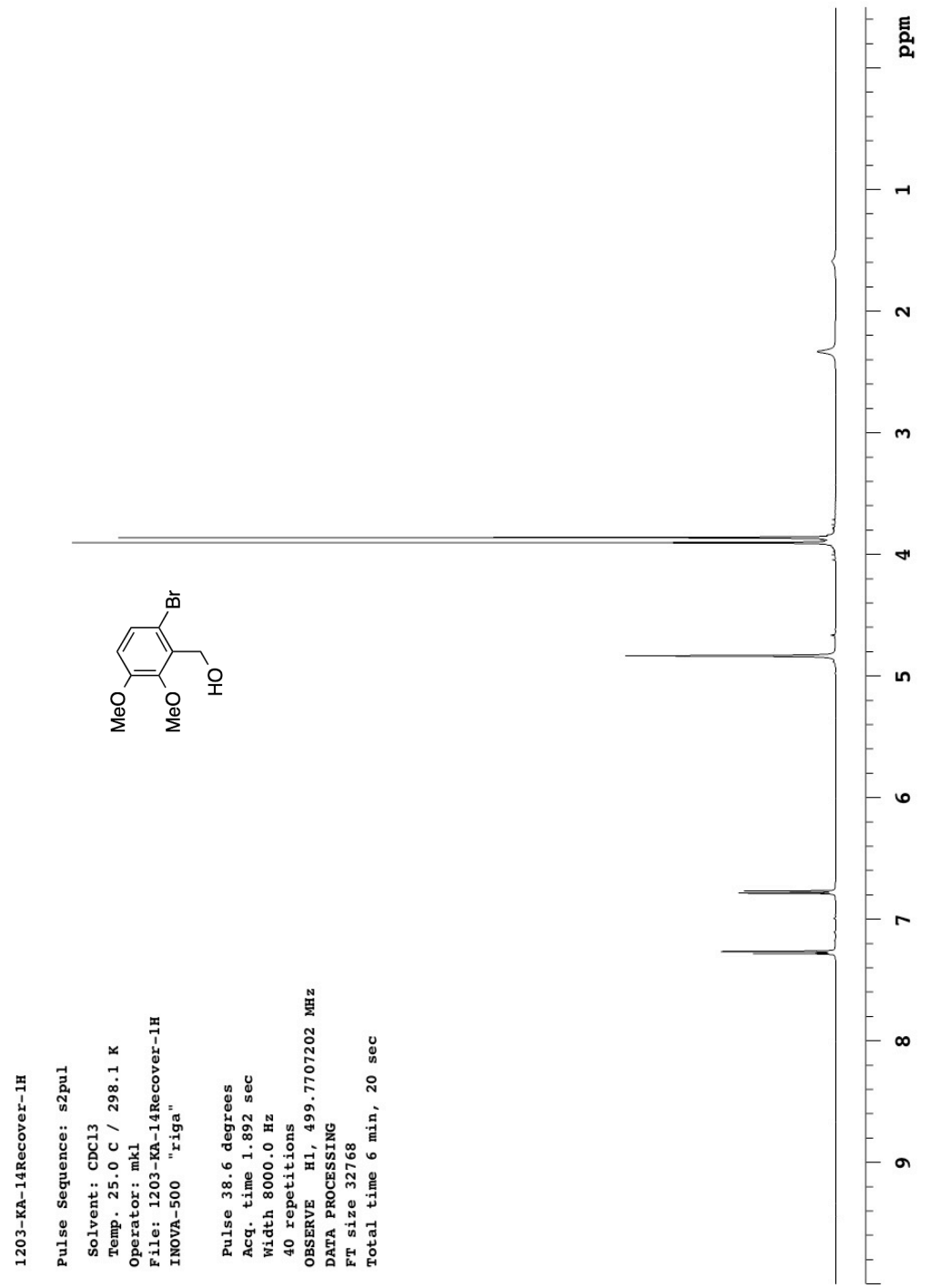
1203-KA-14Recover-1H
Pulse Sequence: s2pul
Solvent: CDCl3
Temp. 25.0 C / 298.1 K
Operator: mkl
File: 1203-KA-14Recover-1H
INOVA-500 "riga"
Pulse 38.6 degrees
Acq. time 1.892 sec
Width 8000.0 Hz
40 repetitions
OBSERVE H1, 499.7707202 MHz
DATA PROCESSING
FT size 32768
Total time 6 min, 20 sec
MeO
MeO
Br
HO
9
8
7
6
5
4
3
2
1
ppm

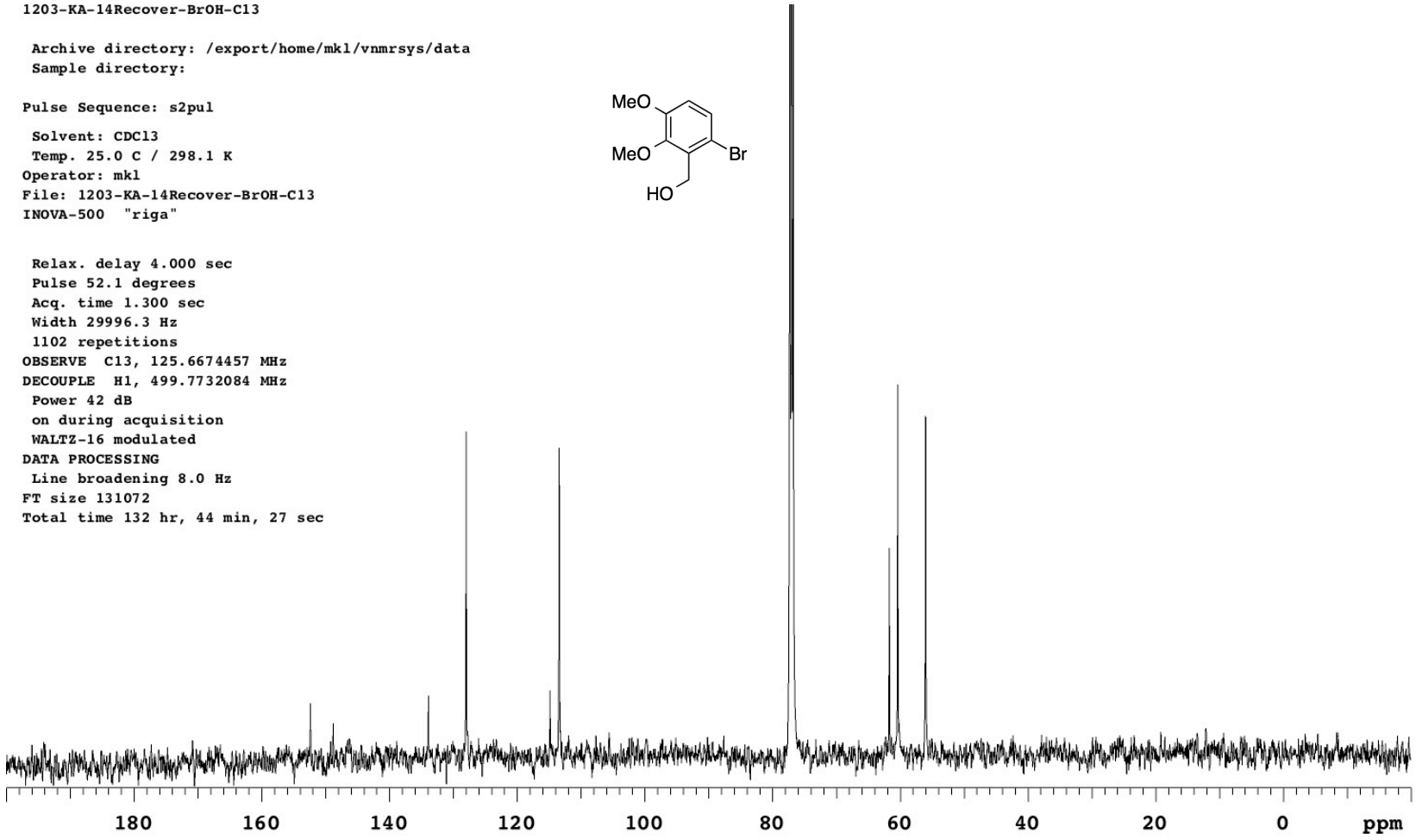
1203-KA-14Recover-BrOH-C13
Archive directory: /export/home/mkl/vnmrsys/data
Sample directory:
Pulse Sequence: s2pul
Solvent: CDCl3
Temp. 25.0 C / 298.1 K
Operator: mkl
File: 1203-KA-14Recover-BrOH-C13
INOVA-500 "riga"
Relax. delay 4.000 sec
Pulse 52.1 degrees
Acq. time 1.300 sec
Width 29996.3 Hz
1102 repetitions
OBSERVE C13, 125.6674457 MHz
DECOUPLE H1, 499.7732084 MHz
Power 42 dB
on during acquisition
WALTZ-16 modulated
DATA PROCESSING
Line broadening 8.0 Hz
FT size 131072
Total time 132 hr, 44 min, 27 sec
MeO
MeO
Br
HO
180
160
140
120
100
80
60
40
20
0
ppm

1205-ug1-04-20

Pulse Sequence: s2pul

Solvent: CDCl3
Temp. 25.0 C / 298.1 K
Operator: mkl
File: 1205-ug1-04-20
INOVA-500 "riga"

Pulse 38.6 degrees
Acq. time 1.892 sec
Width 8000.0 Hz
89 repetitions
OBSERVE H1, 499.7707095 MHz
DATA PROCESSING
FT size 32768
Total time 6 min, 20 sec

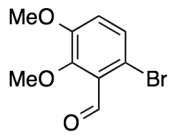

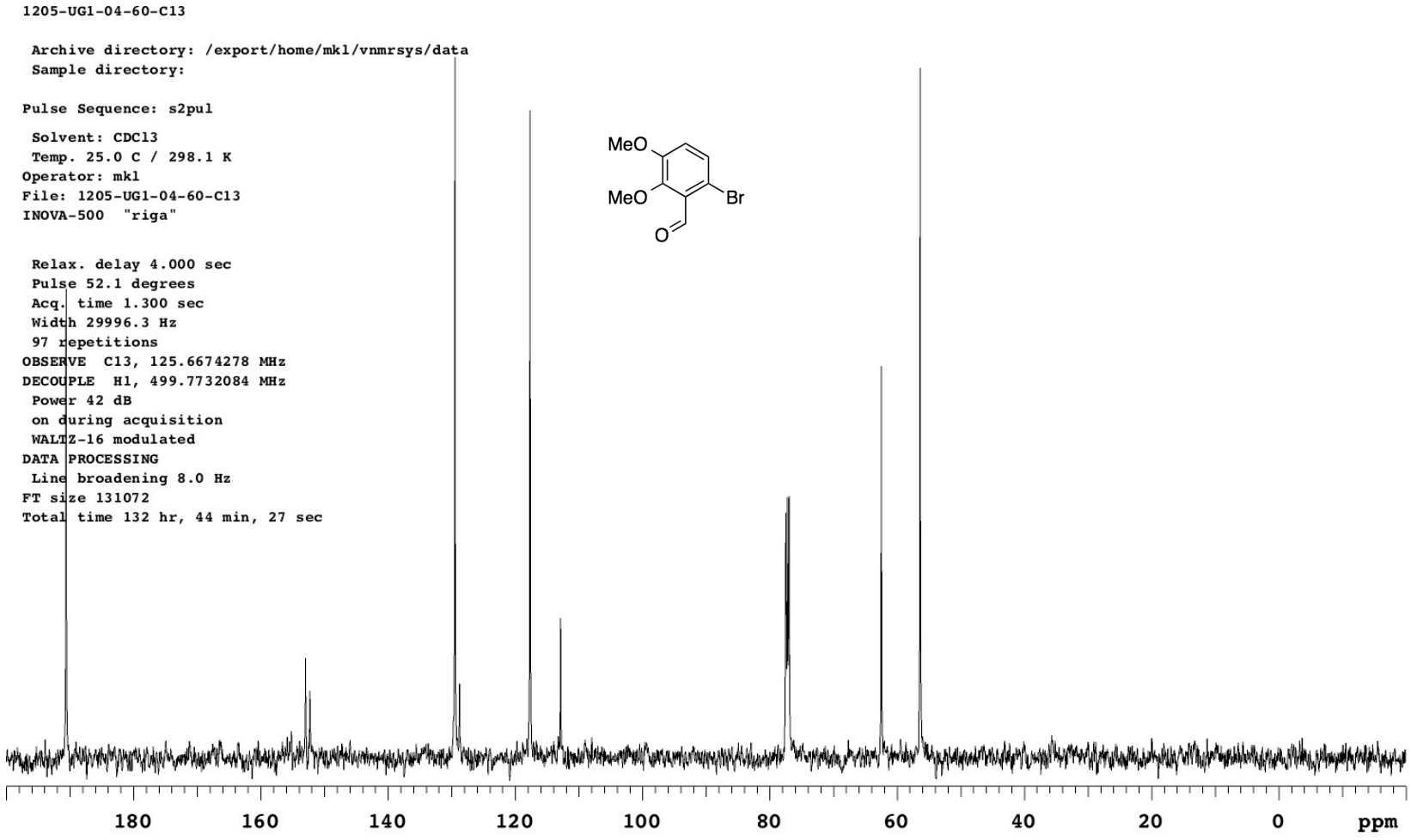
1205-UG1-04-60-C13
Archive directory: /export/home/mkl/vnmrsys/data
Sample directory:
Pulse Sequence: s2pul
Solvent: CDCl3
Temp. 25.0 C / 298.1 K
Operator: mkl
File: 1205-UG1-04-60-C13
INOVA-500 "riga"
Relax. delay 4.000 sec
Pulse 52.1 degrees
Acq. time 1.300 sec
Width 29996.3 Hz
97 repetitions
OBSERVE C13, 125.6674278 MHz
DECOUPLE H1, 499.7732084 MHz
Power 42 dB
on during acquisition
WALTZ-16 modulated
DATA PROCESSING
Line broadening 8.0 Hz
FT size 131072
Total time 132 hr, 44 min, 27 sec
MeO
MeO
Br
O
180
160
140
120
100
80
60
40
20
0
ppm

1205-ug1-04-048

Pulse Sequence: s2pul

Solvent: CDCl3
Ambient temperature
Operator: mkl
File: 1205-ug1-04-048
INOVA-500 "riga"

Pulse 45.0 degrees
Acq. time 1.892 sec
Width 8000.0 Hz
64 repetitions
OBSERVE H1, 499.7707222 MHz
DATA PROCESSING
FT size 32768
Total time 2 min, 1 sec

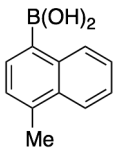

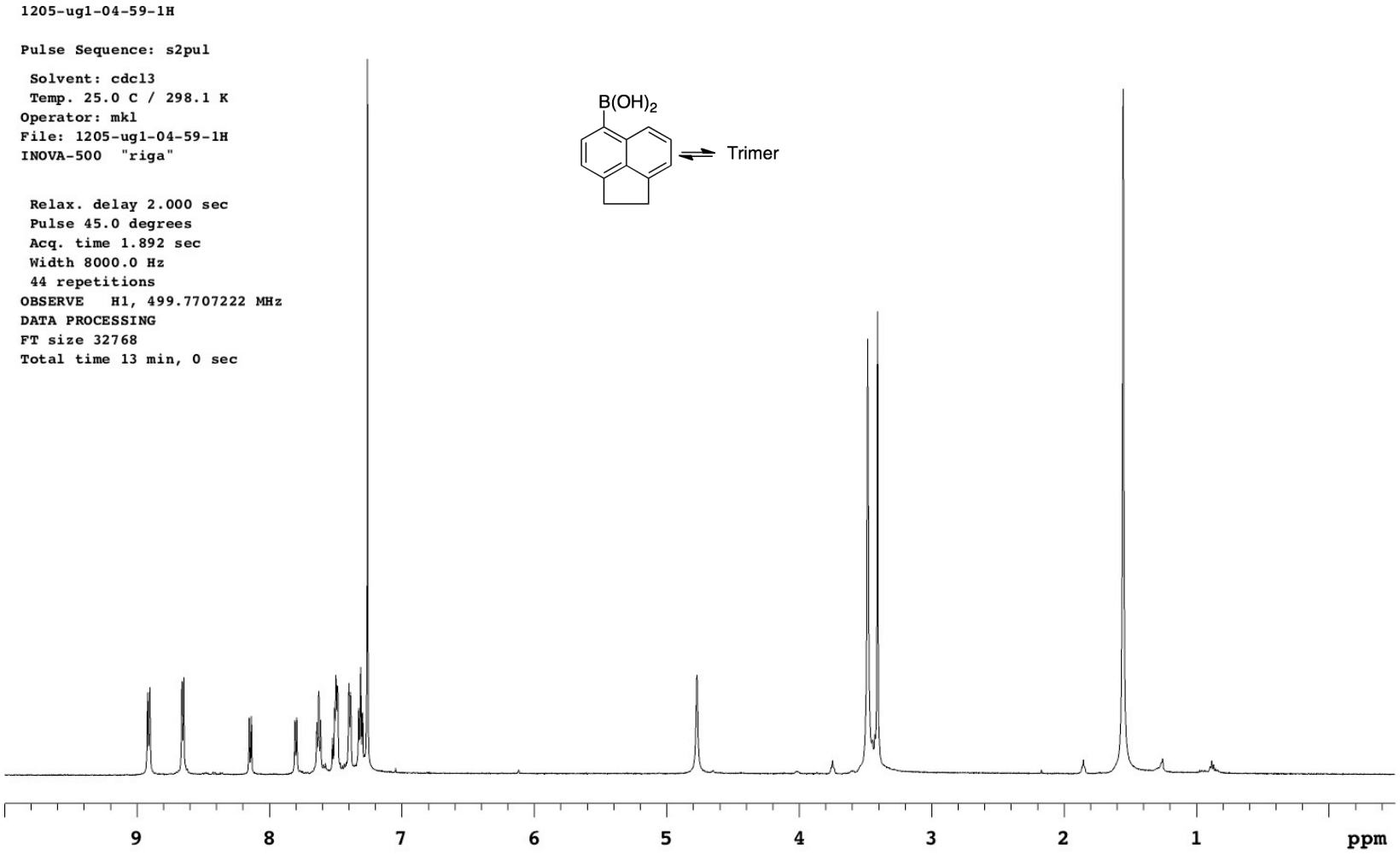
1205-ug1-04-59-1H
Pulse Sequence: s2pul
Solvent: cdcl3
Temp. 25.0 C / 298.1 K
Operator: mkl
File: 1205-ug1-04-59-1H
INOVA-500 "riga"
Relax. delay 2.000 sec
Pulse 45.0 degrees
Acq. time 1.892 sec
Width 8000.0 Hz
44 repetitions
OBSERVE H1, 499.7707222 MHz
DATA PROCESSING
FT size 32768
Total time 13 min, 0 sec
B(OH)2
Trimer
9
8
7
6
5
4
3
2
1
ppm

1205-ug1-04-30

Pulse Sequence: s2pul

Solvent: cdcl3
Temp. 25.0 C / 298.1 K
Operator: mkl
File: 1205-ug1-04-30
INOVA-500 "riga"

Relax. delay 2.000 sec
Pulse 45.0 degrees
Acq. time 1.892 sec
Width 8000.0 Hz
20 repetitions
OBSERVE H1, 499.7707222 MHz
DATA PROCESSING
FT size 32768
Total time 13 min, 0 sec

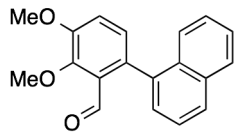

1205-UG1-04-30-C13

Archive directory: /export/home/mkl/vnmrsys/data
Sample directory:

Pulse Sequence: s2pul

Solvent: CDCl3
Temp. 25.0 C / 298.1 K
Operator: mkl
File: 1205-UG1-04-30-C13
INOVA-500 "riga"

Relax. delay 4.000 sec
Pulse 52.1 degrees
Acq. time 1.300 sec
Width 29996.3 Hz
128 repetitions
OBSERVE C13, 125.6674228 MHz
DECOUPLE H1, 499.7732084 MHz
Power 42 dB
on during acquisition
WALTZ-16 modulated
DATA PROCESSING
Line broadening 8.0 Hz
FT size 131072
Total time 132 hr, 44 min, 27 sec

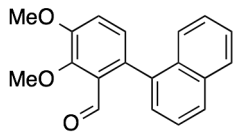

1205-ug1-04-038

Pulse Sequence: s2pul

Solvent: CDCl3
Temp. 25.0 C / 298.1 K
Operator: mkl
File: 1205-ug1-04-038
INOVA-500 "riga"

Pulse 45.0 degrees
Acq. time 1.892 sec
Width 8000.0 Hz
80 repetitions
OBSERVE H1, 499.7707212 MHz
DATA PROCESSING
FT size 32768
Total time 1 hr, 4 min, 52 sec

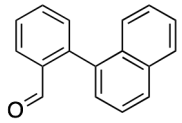

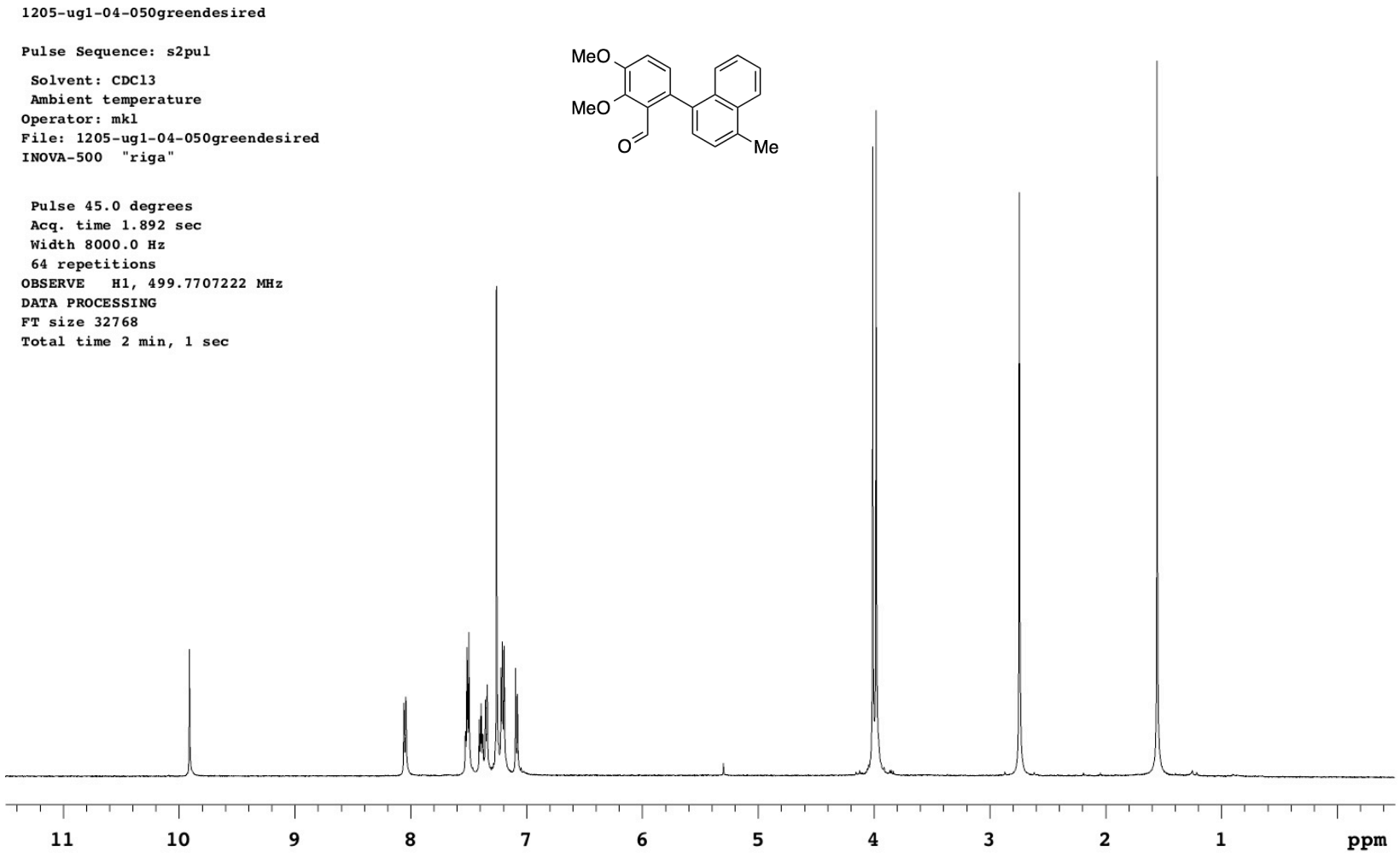
1205-ug1-04-050greendesired
Pulse Sequence: s2pul
Solvent: CDCl3
Ambient temperature
Operator: mkl
File: 1205-ug1-04-050greendesired
INOVA-500 "riga"
Pulse 45.0 degrees
Acq. time 1.892 sec
Width 8000.0 Hz
64 repetitions
OBSERVE H1, 499.7707222 MHz
DATA PROCESSING
FT size 32768
Total time 2 min, 1 sec
MeO
MeO
O
Me
11
10
9
8
7
6
5
4
3
2
1
ppm

1205-ug1-04-50-C13

Archive directory: /export/home/mkl/vnmrsys/data
Sample directory:

Pulse Sequence: s2pul

Solvent: CDCl3
Temp. 25.0 C / 298.1 K
Operator: mkl
File: 1205-ug1-04-50-C13
INOVA-500 "riga"

Relax. delay 4.000 sec
Pulse 52.1 degrees
Acq. time 1.300 sec
Width 29996.3 Hz
1684 repetitions
OBSERVE C13, 125.6674457 MHz
DECOUPLE H1, 499.7732084 MHz
Power 42 dB
on during acquisition
WALTZ-16 modulated
DATA PROCESSING
Line broadening 8.0 Hz
FT size 131072
Total time 132 hr, 44 min, 27 sec

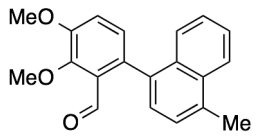

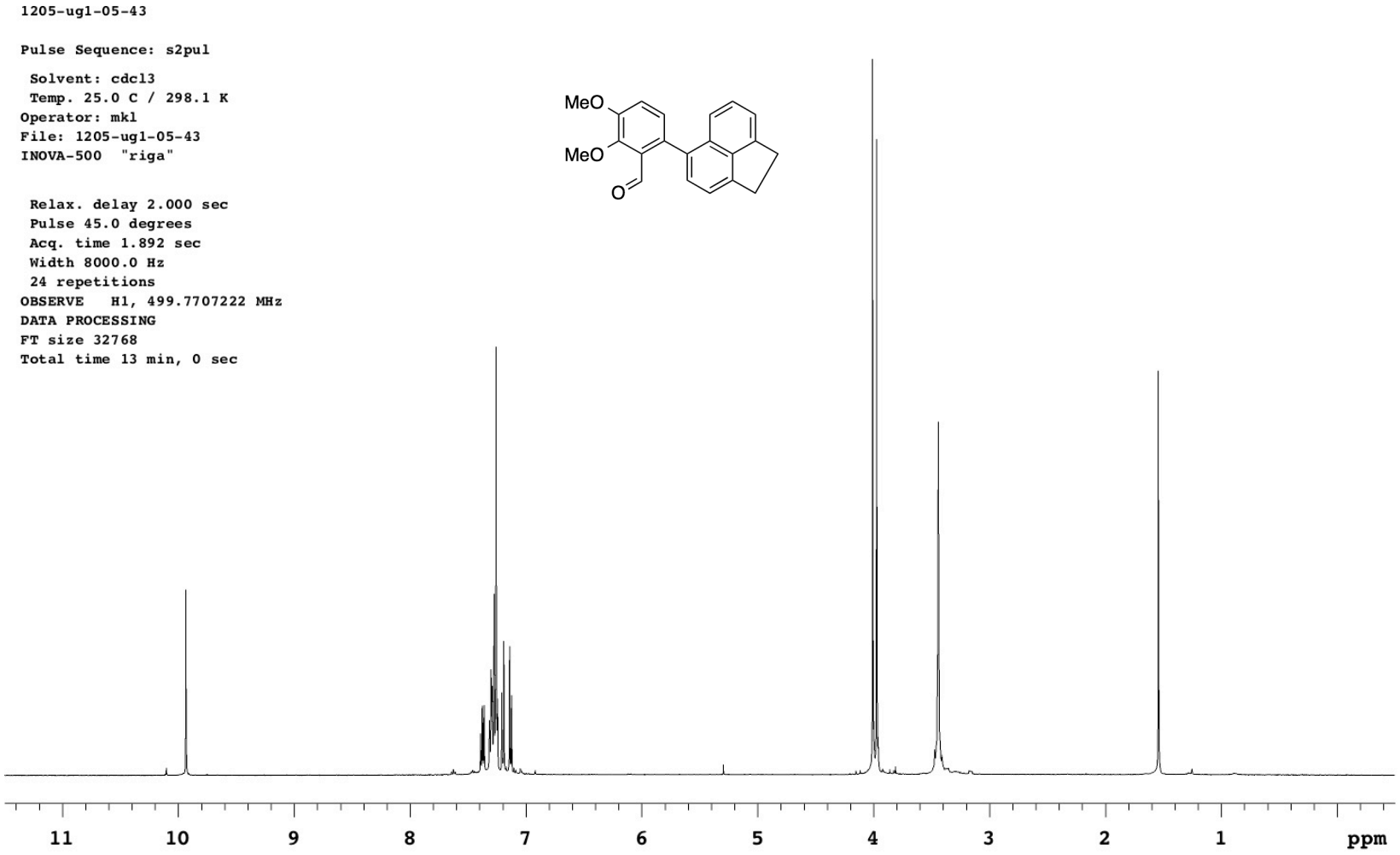
1205-ug1-05-43
Pulse Sequence: s2pul
Solvent: cdcl3
Temp. 25.0 C / 298.1 K
Operator: mkl
File: 1205-ug1-05-43
INOVA-500 "riga"
Relax. delay 2.000 sec
Pulse 45.0 degrees
Acq. time 1.892 sec
Width 8000.0 Hz
24 repetitions
OBSERVE H1, 499.7707222 MHz
DATA PROCESSING
FT size 32768
Total time 13 min, 0 sec
MeO
MeO
O
11
10
9
8
7
6
5
4
3
2
1
ppm

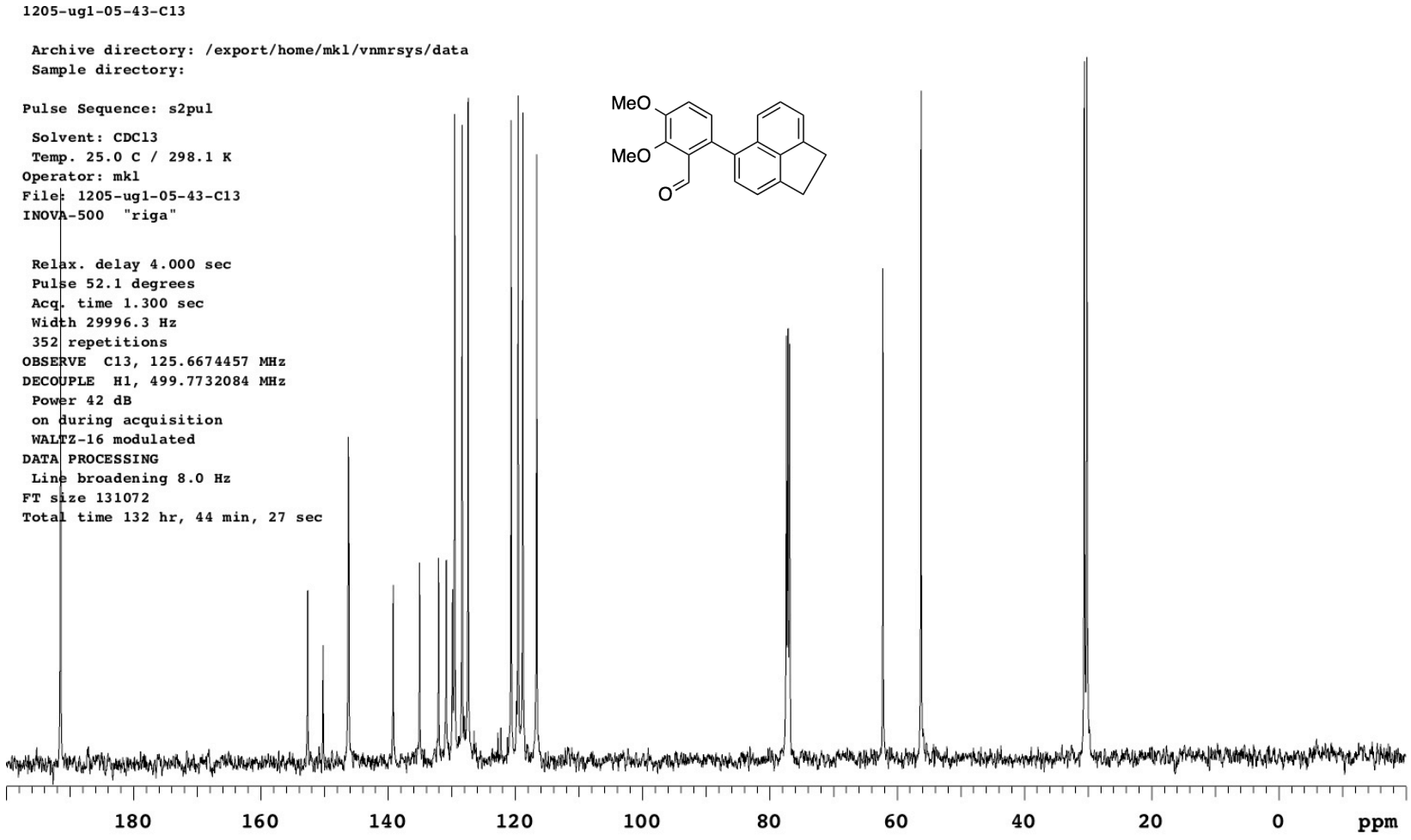
1205-ug1-05-43-C13
Archive directory: /export/home/mkl/vnmrsys/data
Sample directory:
Pulse Sequence: s2pul
Solvent: CDCl3
Temp. 25.0 C / 298.1 K
Operator: mkl
File: 1205-ug1-05-43-C13
INOVA-500 "riga"
Relax. delay 4.000 sec
Pulse 52.1 degrees
Acq. time 1.300 sec
Width 29996.3 Hz
352 repetitions
OBSERVE C13, 125.6674457 MHz
DECOUPLE H1, 499.7732084 MHz
Power 42 dB
on during acquisition
WALTZ-16 modulated
DATA PROCESSING
Line broadening 8.0 Hz
FT size 131072
Total time 132 hr, 44 min, 27 sec
MeO
MeO
O
180
160
140
120
100
80
60
40
20
0
ppm

1205-ug1-05-24

Pulse Sequence: s2pul

Solvent: cdcl3
Temp. 25.0 C / 298.1 K
Operator: mkl
File: 1205-ug1-05-24
INOVA-500 "riga"

Relax. delay 2.000 sec
Pulse 45.0 degrees
Acq. time 1.892 sec
Width 8000.0 Hz
16 repetitions
OBSERVE H1, 499.7707222 MHz
DATA PROCESSING
FT size 32768
Total time 13 min, 0 sec

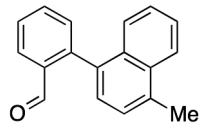

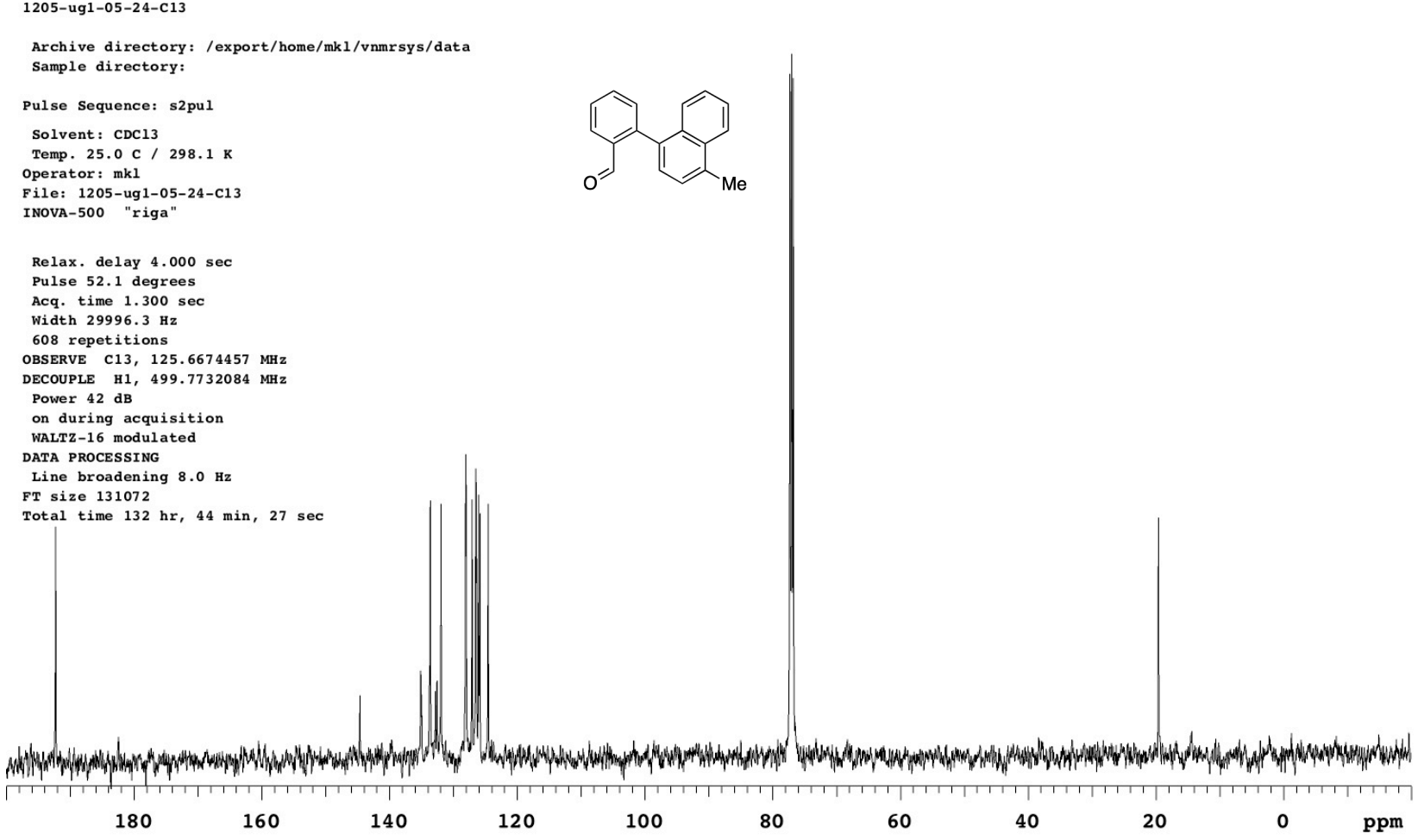
1205-ug1-05-24-C13
Archive directory: /export/home/mkl/vnmrsys/data
Sample directory:
Pulse Sequence: s2pul
Solvent: CDCl3
Temp. 25.0 C / 298.1 K
Operator: mkl
File: 1205-ug1-05-24-C13
INOVA-500 "riga"
Relax. delay 4.000 sec
Pulse 52.1 degrees
Acq. time 1.300 sec
Width 29996.3 Hz
608 repetitions
OBSERVE C13, 125.6674457 MHz
DECOUPLE H1, 499.7732084 MHz
Power 42 dB
on during acquisition
WALTZ-16 modulated
DATA PROCESSING
Line broadening 8.0 Hz
FT size 131072
Total time 132 hr, 44 min, 27 sec
O
Me
180
160
140
120
100
80
60
40
20
0
ppm

1205-ug1-05-047

Pulse Sequence: s2pul

Solvent: CDCl3
Ambient temperature
Operator: mkl
File: 1205-ug1-05-047
INOVA-500 "riga"

Pulse 45.0 degrees
Acq. time 1.892 sec
Width 8000.0 Hz
64 repetitions
OBSERVE H1, 499.7707222 MHz
DATA PROCESSING
FT size 32768
Total time 2 min, 1 sec

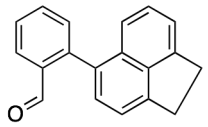

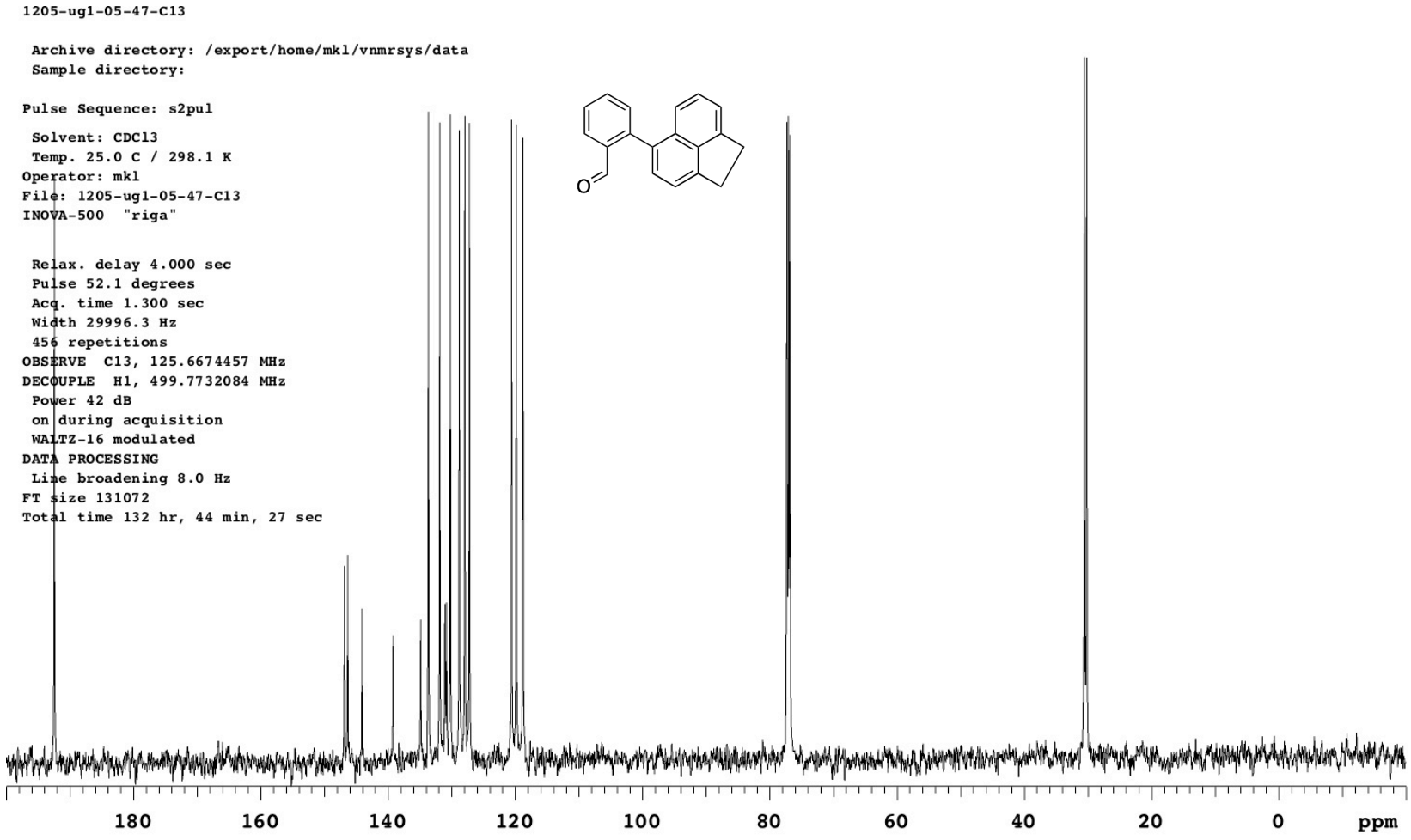
1205-ug1-05-47-C13
Archive directory: /export/home/mkl/vnmrsys/data
Sample directory:
Pulse Sequence: s2pul
Solvent: CDCl3
Temp. 25.0 C / 298.1 K
Operator: mkl
File: 1205-ug1-05-47-C13
INOVA-500 "riga"
Relax. delay 4.000 sec
Pulse 52.1 degrees
Acq. time 1.300 sec
Width 29996.3 Hz
456 repetitions
OBSERVE C13, 125.6674457 MHz
DECOUPLE H1, 499.7732084 MHz
Power 42 dB
on during acquisition
WALTZ-16 modulated
DATA PROCESSING
Line broadening 8.0 Hz
FT size 131072
Total time 132 hr, 44 min, 27 sec
O
180
160
140
120
100
80
60
40
20
0
ppm

1205-ug1-04-43

Pulse Sequence: s2pul

Solvent: cdcl3
Temp. 25.0 C / 298.1 K
Operator: mkl
File: 1205-ug1-04-43
INOVA-500 "riga"

Relax. delay 2.000 sec
Pulse 45.0 degrees
Acq. time 1.892 sec
Width 8000.0 Hz
24 repetitions
OBSERVE H1, 499.7707222 MHz
DATA PROCESSING
FT size 32768
Total time 13 min, 0 sec

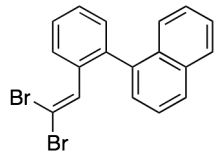

1205-ug1-05-68-1H

Pulse Sequence: s2pul

Solvent: cdcl3
Temp. 25.0 C / 298.1 K
Operator: mkl
File: 1205-ug1-05-68-1H
INOVA-500 "riga"

Relax. delay 2.000 sec
Pulse 45.0 degrees
Acq. time 1.892 sec
Width 8000.0 Hz
28 repetitions
OBSERVE H1, 499.7707207 MHz
DATA PROCESSING
FT size 32768
Total time 13 min, 0 sec

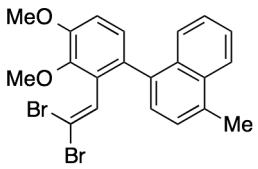

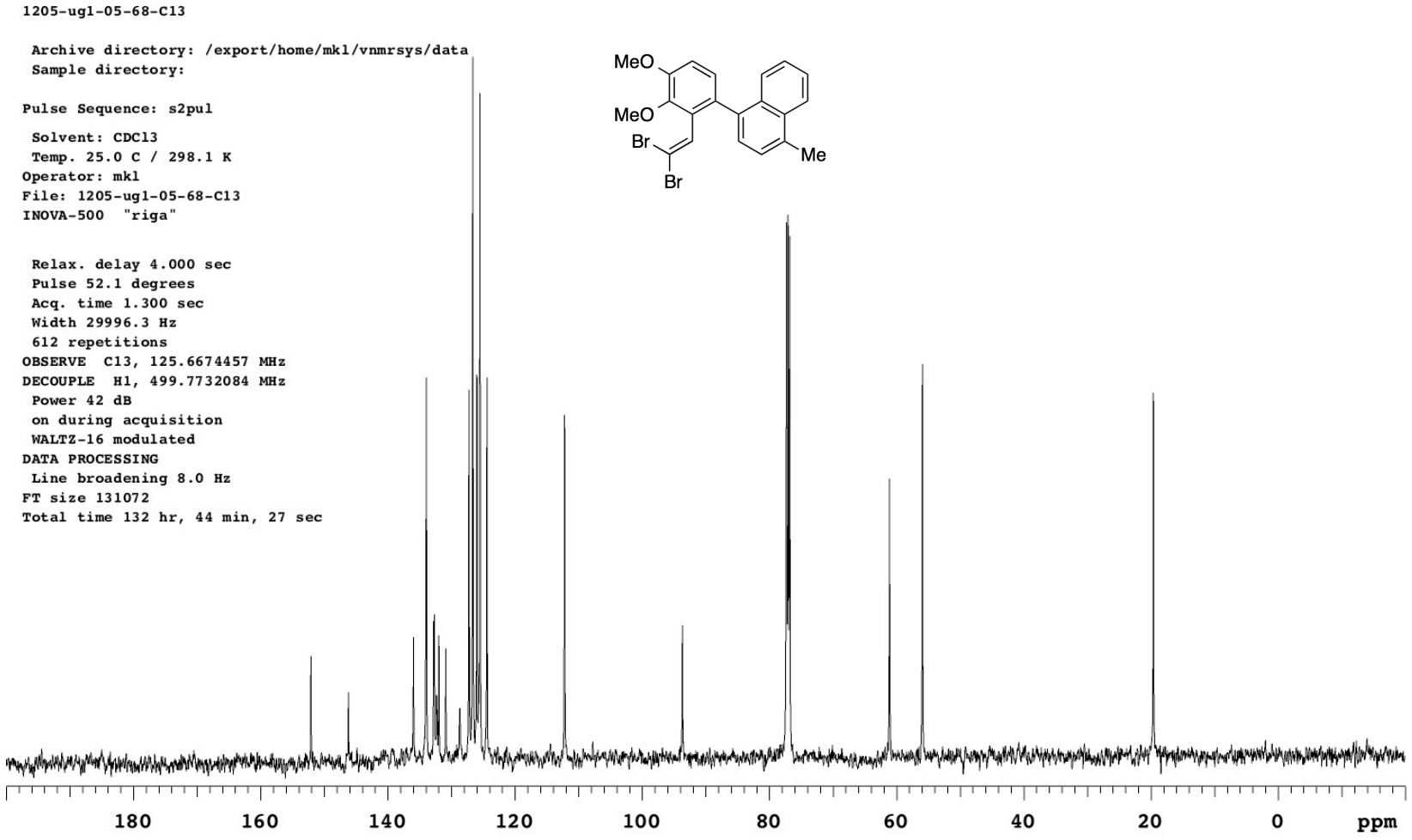
1205-ug1-05-68-C13
Archive directory: /export/home/mkl/vnmrsys/data
Sample directory:
Pulse Sequence: s2pul
Solvent: CDCl3
Temp. 25.0 C / 298.1 K
Operator: mkl
File: 1205-ug1-05-68-C13
INOVA-500 "riga"
Relax. delay 4.000 sec
Pulse 52.1 degrees
Acq. time 1.300 sec
Width 29996.3 Hz
612 repetitions
OBSERVE C13, 125.6674457 MHz
DECOUPLE H1, 499.7732084 MHz
Power 42 dB
on during acquisition
WALTZ-16 modulated
DATA PROCESSING
Line broadening 8.0 Hz
FT size 131072
Total time 132 hr, 44 min, 27 sec
MeO
MeO
Br
Br
Me
180
160
140
120
100
80
60
40
20
0
ppm

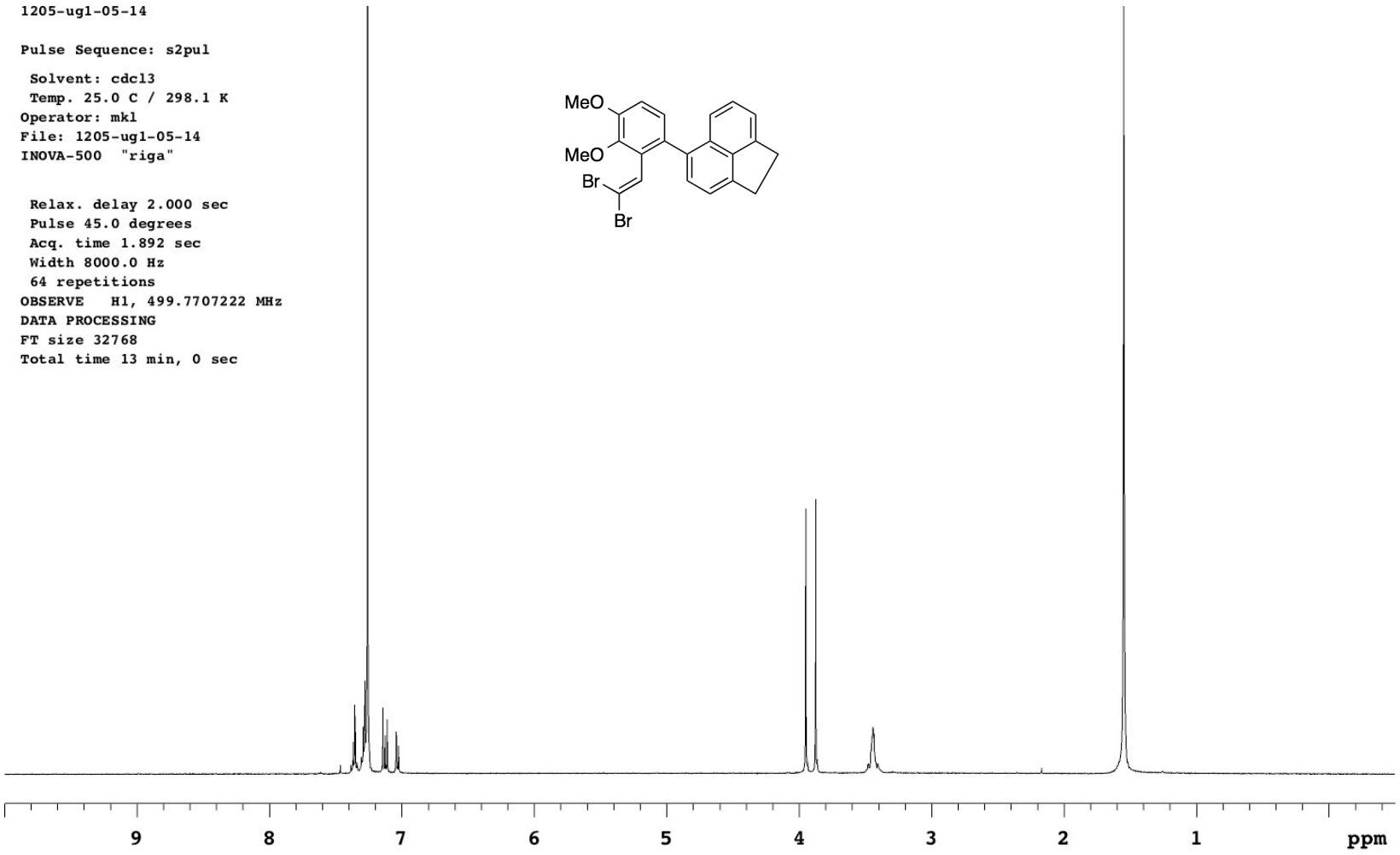
1205-ug1-05-14
Pulse Sequence: s2pul
Solvent: cdcl3
Temp. 25.0 C / 298.1 K
Operator: mkl
File: 1205-ug1-05-14
INOVA-500 "riga"
Relax. delay 2.000 sec
Pulse 45.0 degrees
Acq. time 1.892 sec
Width 8000.0 Hz
64 repetitions
OBSERVE H1, 499.7707222 MHz
DATA PROCESSING
FT size 32768
Total time 13 min, 0 sec
MeO
MeO
Br
Br
9
8
7
6
5
4
3
2
1
ppm

1205-ug1-05-14-C13

Archive directory: /export/home/mkl/vnmrsys/data
Sample directory:

Pulse Sequence: s2pul

Solvent: CDCl3
Temp. 25.0 C / 298.1 K
Operator: mkl
File: 1205-ug1-05-14-C13
INOVA-500 "riga"

Relax. delay 4.000 sec
Pulse 52.1 degrees
Acq. time 1.300 sec
Width 29996.3 Hz
800 repetitions
OBSERVE C13, 125.6674457 MHz
DECOUPLE H1, 499.7732084 MHz
Power 42 dB
on during acquisition
WALTZ-16 modulated
DATA PROCESSING
Line broadening 8.0 Hz
FT size 131072
Total time 132 hr, 44 min, 27 sec

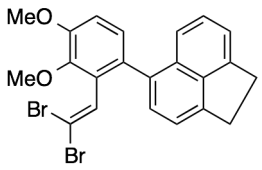

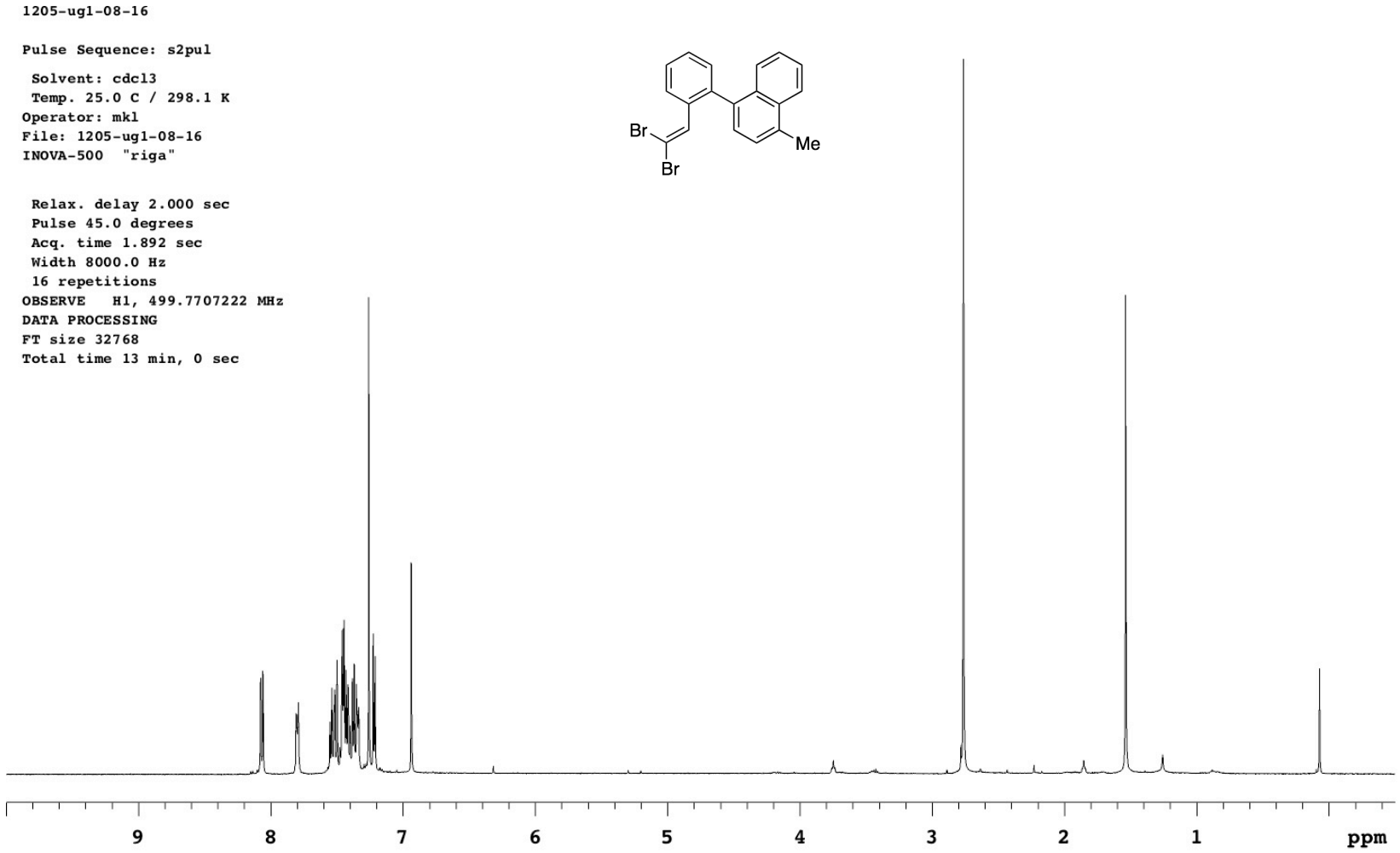
1205-ug1-08-16
Pulse Sequence: s2pul
Solvent: cdcl3
Temp. 25.0 C / 298.1 K
Operator: mkl
File: 1205-ug1-08-16
INOVA-500 "riga"
Relax. delay 2.000 sec
Pulse 45.0 degrees
Acq. time 1.892 sec
Width 8000.0 Hz
16 repetitions
OBSERVE H1, 499.7707222 MHz
DATA PROCESSING
FT size 32768
Total time 13 min, 0 sec
Br
Br
Me
9
8
7
6
5
4
3
2
1
ppm

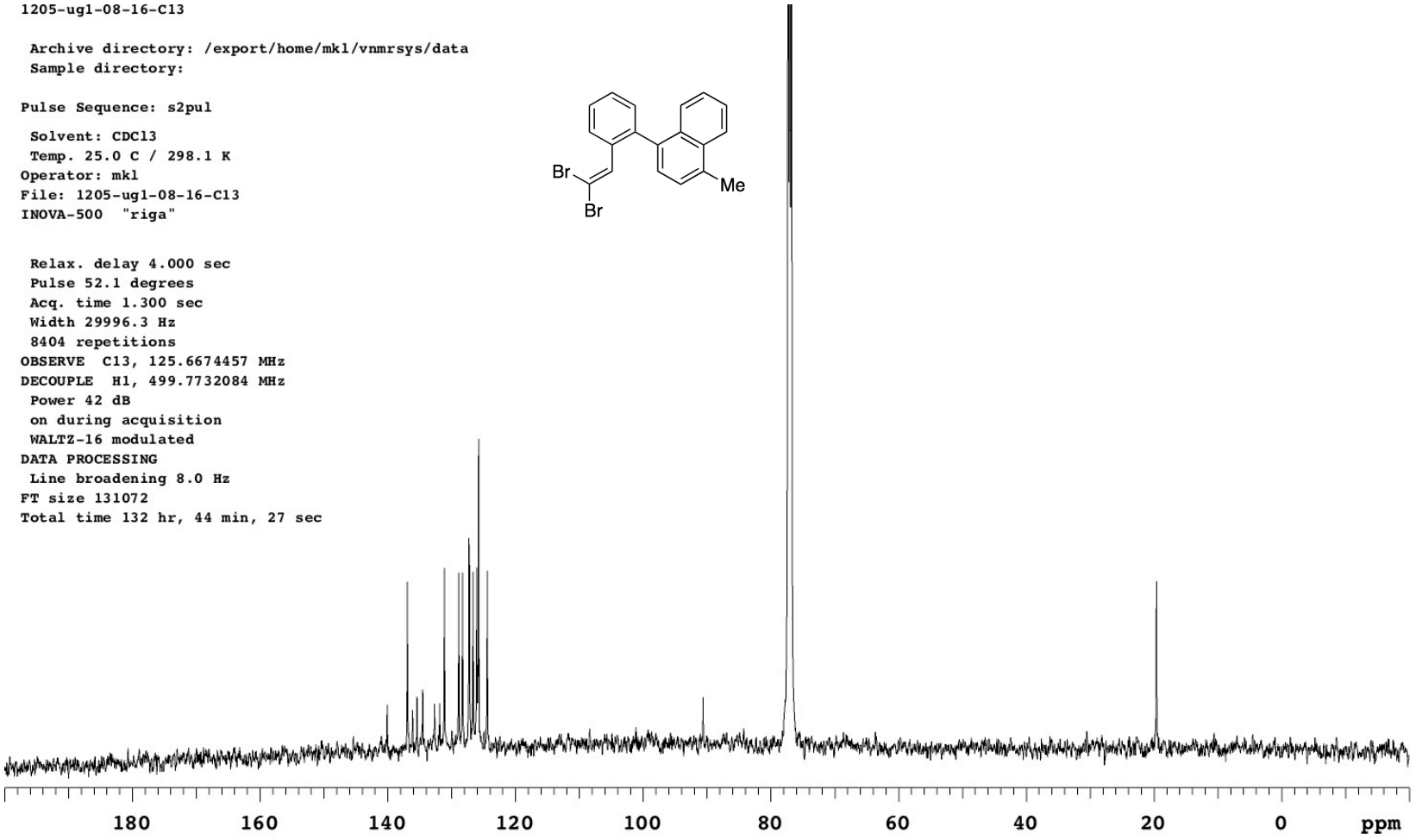
1205-ug1-08-16-C13
Archive directory: /export/home/mkl/vnmrsys/data
Sample directory:
Pulse Sequence: s2pul
Solvent: CDCl3
Temp. 25.0 C / 298.1 K
Operator: mkl
File: 1205-ug1-08-16-C13
INOVA-500 "riga"
Relax. delay 4.000 sec
Pulse 52.1 degrees
Acq. time 1.300 sec
Width 29996.3 Hz
8404 repetitions
OBSERVE C13, 125.6674457 MHz
DECOUPLE H1, 499.7732084 MHz
Power 42 dB
on during acquisition
WALTZ-16 modulated
DATA PROCESSING
Line broadening 8.0 Hz
FT size 131072
Total time 132 hr, 44 min, 27 sec
Br
Br
Me
180
160
140
120
100
80
60
40
20
0
ppm

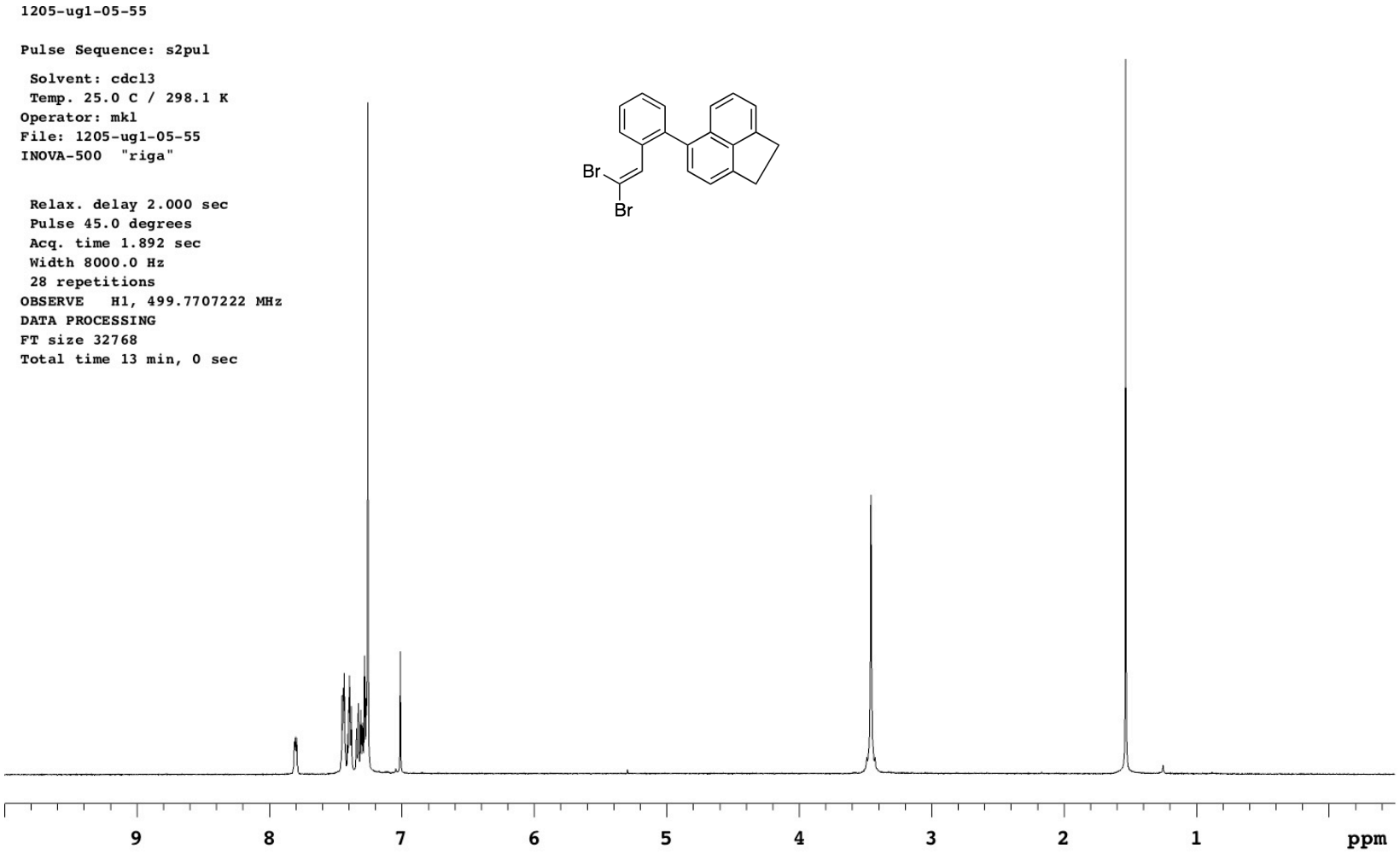
1205-ug1-05-55
Pulse Sequence: s2pul
Solvent: cdcl3
Temp. 25.0 C / 298.1 K
Operator: mkl
File: 1205-ug1-05-55
INOVA-500 "riga"
Relax. delay 2.000 sec
Pulse 45.0 degrees
Acq. time 1.892 sec
Width 8000.0 Hz
28 repetitions
OBSERVE H1, 499.7707222 MHz
DATA PROCESSING
FT size 32768
Total time 13 min, 0 sec
Br
Br
9
8
7
6
5
4
3
2
1
ppm

1205-ug1-05-55-C13

Archive directory: /export/home/mkl/vnmrsys/data
Sample directory:

Pulse Sequence: s2pul

Solvent: CDCl3
Temp. 25.0 C / 298.1 K
Operator: mkl
File: 1205-ug1-05-55-C13
INOVA-500 "riga"

Relax. delay 4.000 sec
Pulse 52.1 degrees
Acq. time 1.300 sec
Width 29996.3 Hz
508 repetitions
OBSERVE C13, 125.6674457 MHz
DECOUPLE H1, 499.7732084 MHz
Power 42 dB
on during acquisition
WALTZ-16 modulated
DATA PROCESSING
Line broadening 8.0 Hz
FT size 131072
Total time 132 hr, 44 min, 27 sec

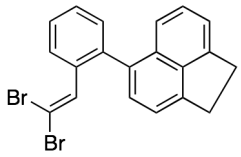

1205-ug1-04-44

Pulse Sequence: s2pul

Solvent: cdcl3
Temp. 25.0 C / 298.1 K
Operator: mkl
File: 1205-ug1-04-44
INOVA-500 "riga"

Relax. delay 2.000 sec
Pulse 45.0 degrees
Acq. time 1.892 sec
Width 8000.0 Hz
28 repetitions
OBSERVE H1, 499.7707222 MHz
DATA PROCESSING
FT size 32768
Total time 13 min, 0 sec

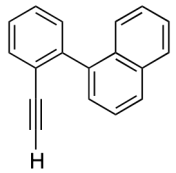

1205-ug1-04-054

Pulse Sequence: s2pul

Solvent: CDCl3
Ambient temperature
Operator: mkl
File: 1205-ug1-04-054
INOVA-500 "riga"

Pulse 45.0 degrees
Acq. time 1.892 sec
Width 8000.0 Hz
64 repetitions
OBSERVE H1, 499.7707222 MHz
DATA PROCESSING
FT size 32768
Total time 2 min, 1 sec

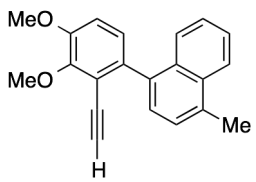

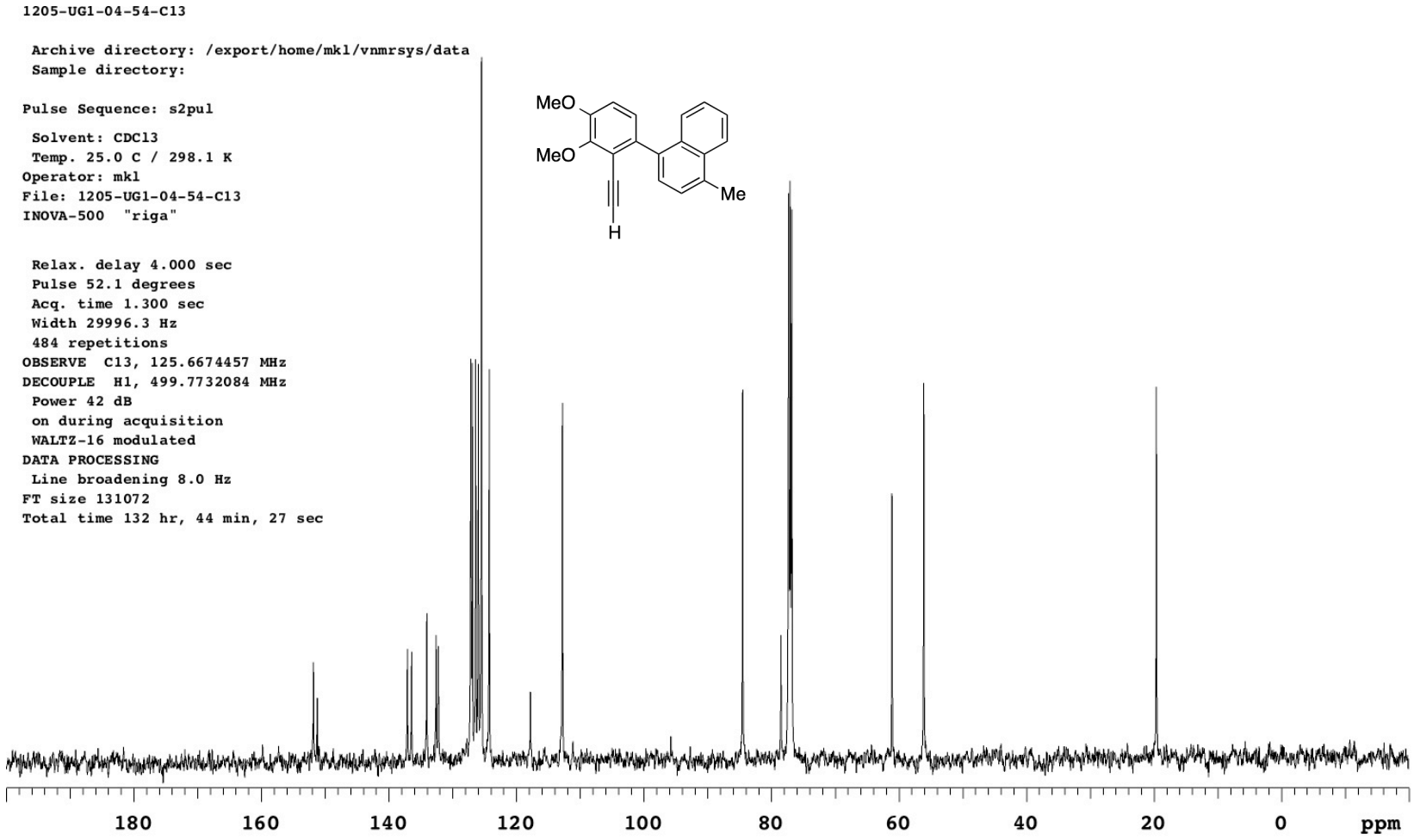
1205-UG1-04-54-C13
Archive directory: /export/home/mkl/vnmrsys/data
Sample directory:
Pulse Sequence: s2pul
Solvent: CDCl3
Temp. 25.0 C / 298.1 K
Operator: mkl
File: 1205-UG1-04-54-C13
INOVA-500 "riga"
Relax. delay 4.000 sec
Pulse 52.1 degrees
Acq. time 1.300 sec
Width 29996.3 Hz
484 repetitions
OBSERVE C13, 125.6674457 MHz
DECOUPLE H1, 499.7732084 MHz
Power 42 dB
on during acquisition
WALTZ-16 modulated
DATA PROCESSING
Line broadening 8.0 Hz
FT size 131072
Total time 132 hr, 44 min, 27 sec
MeO
MeO
Me
H
180
160
140
120
100
80
60
40
20
0
ppm

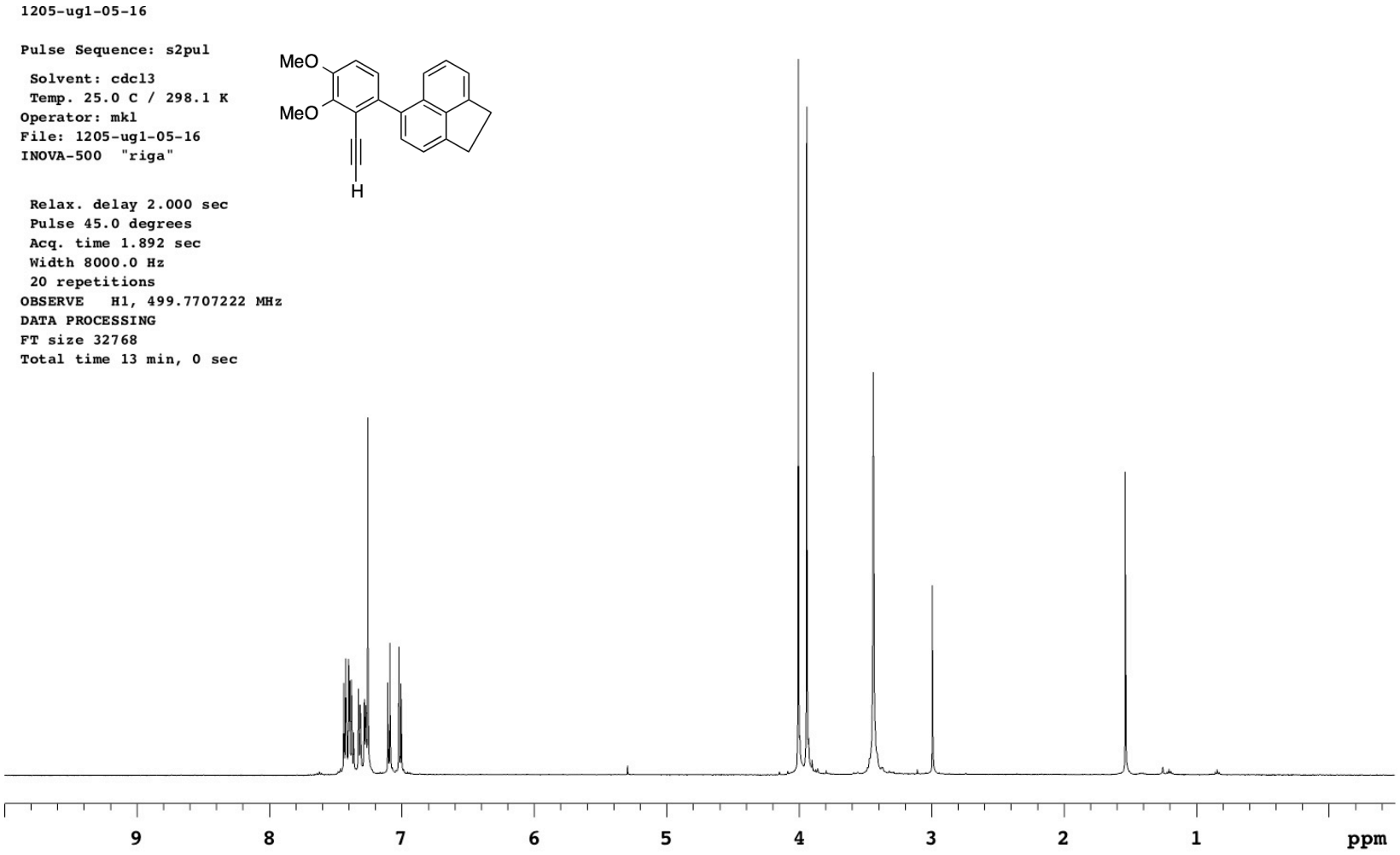
1205-ug1-05-16
Pulse Sequence: s2pul
Solvent: cdcl3
Temp. 25.0 C / 298.1 K
Operator: mkl
File: 1205-ug1-05-16
INOVA-500 "riga"
Relax. delay 2.000 sec
Pulse 45.0 degrees
Acq. time 1.892 sec
Width 8000.0 Hz
20 repetitions
OBSERVE H1, 499.7707222 MHz
DATA PROCESSING
FT size 32768
Total time 13 min, 0 sec
MeO
MeO
H
9
8
7
6
5
4
3
2
1
ppm

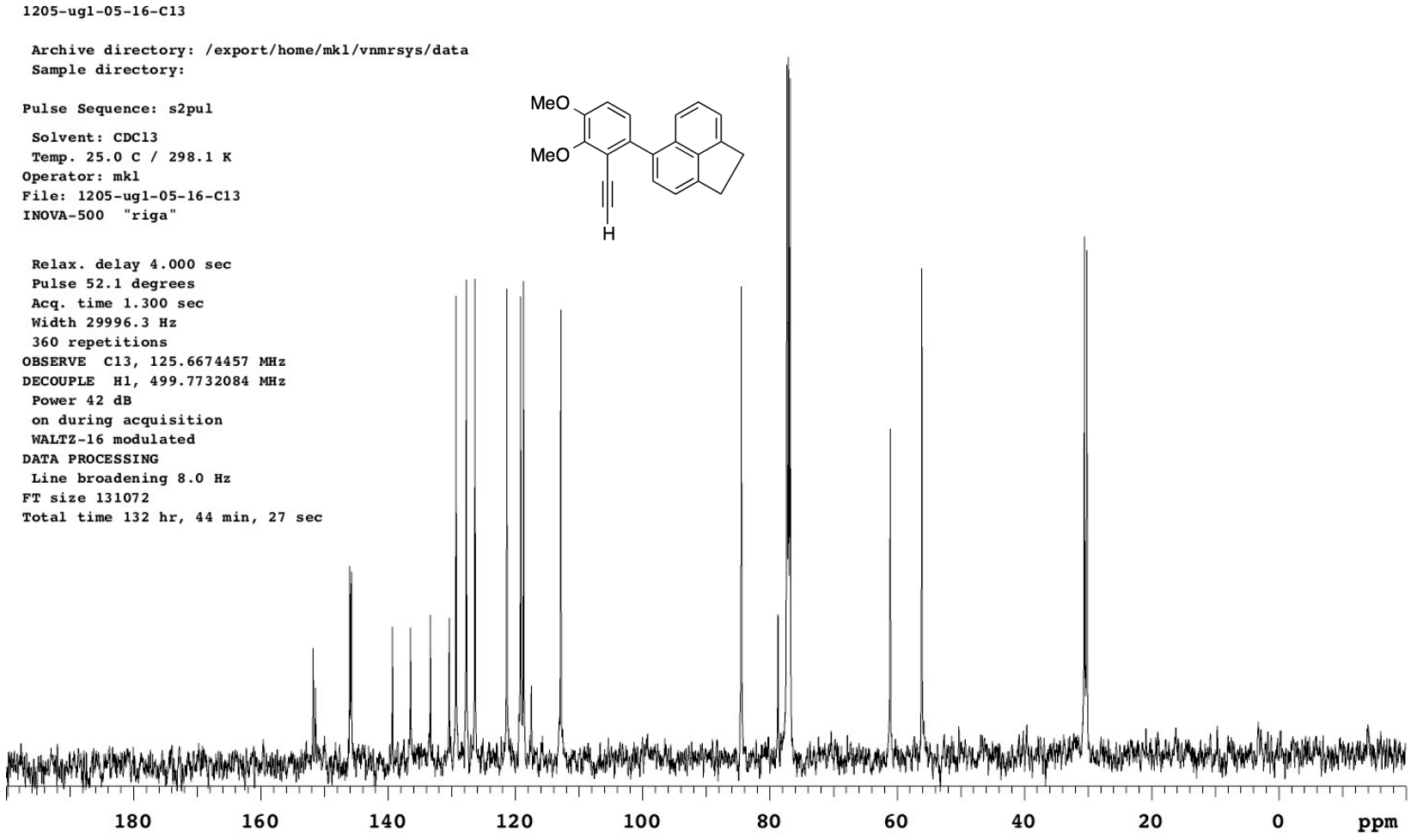
1205-ug1-05-16-C13
Archive directory: /export/home/mkl/vnmrsys/data
Sample directory:
Pulse Sequence: s2pul
Solvent: CDCl3
Temp. 25.0 C / 298.1 K
Operator: mkl
File: 1205-ug1-05-16-C13
INOVA-500 "riga"
Relax. delay 4.000 sec
Pulse 52.1 degrees
Acq. time 1.300 sec
Width 29996.3 Hz
360 repetitions
OBSERVE C13, 125.6674457 MHz
DECOUPLE H1, 499.7732084 MHz
Power 42 dB
on during acquisition
WALTZ-16 modulated
DATA PROCESSING
Line broadening 8.0 Hz
FT size 131072
Total time 132 hr, 44 min, 27 sec
MeO
MeO
H
180
160
140
120
100
80
60
40
20
0
ppm

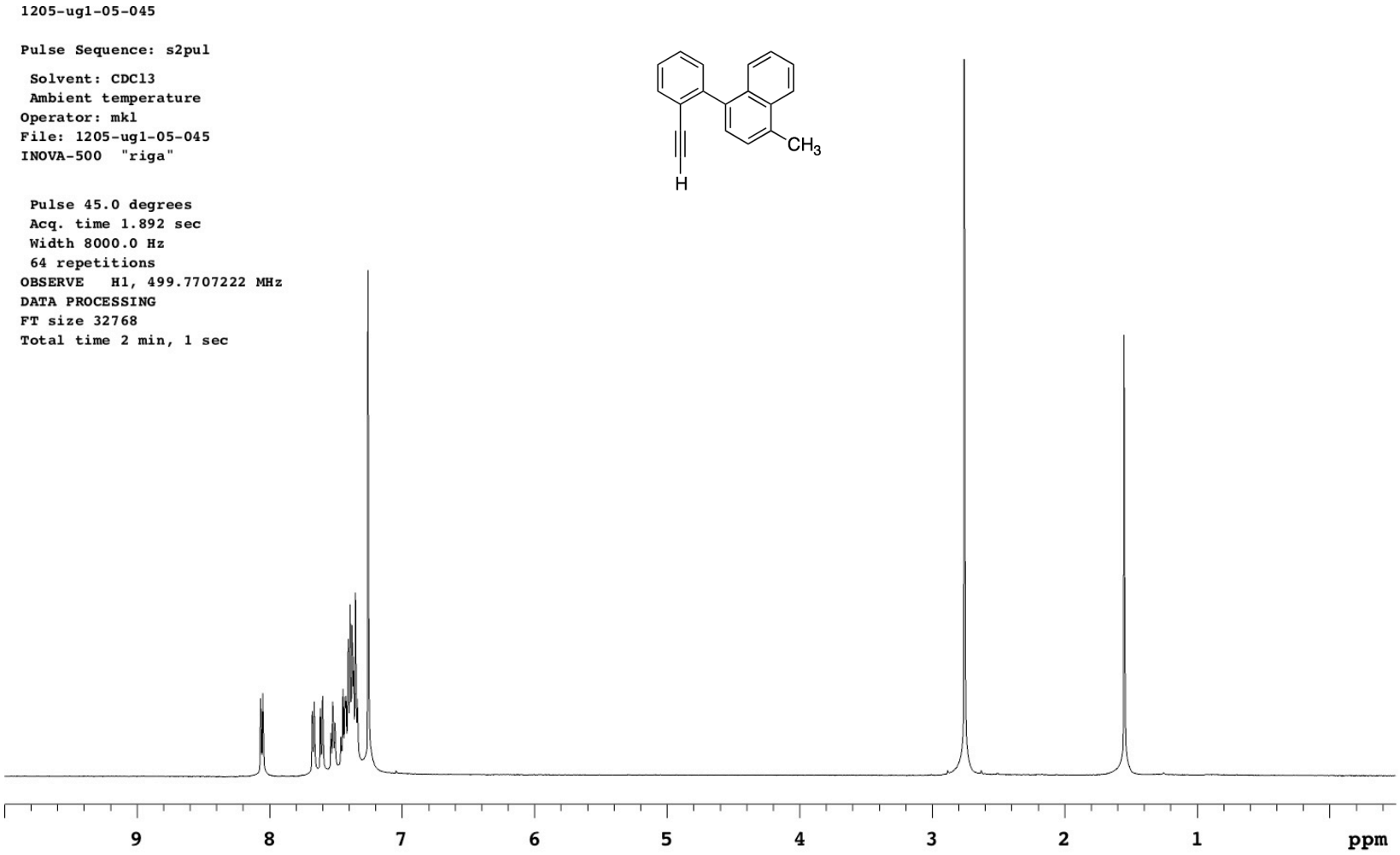
1205-ug1-05-045
Pulse Sequence: s2pul
Solvent: CDCl3
Ambient temperature
Operator: mkl
File: 1205-ug1-05-045
INOVA-500 "riga"
Pulse 45.0 degrees
Acq. time 1.892 sec
Width 8000.0 Hz
64 repetitions
OBSERVE H1, 499.7707222 MHz
DATA PROCESSING
FT size 32768
Total time 2 min, 1 sec
CH3
H
9
8
7
6
5
4
3
2
1
ppm

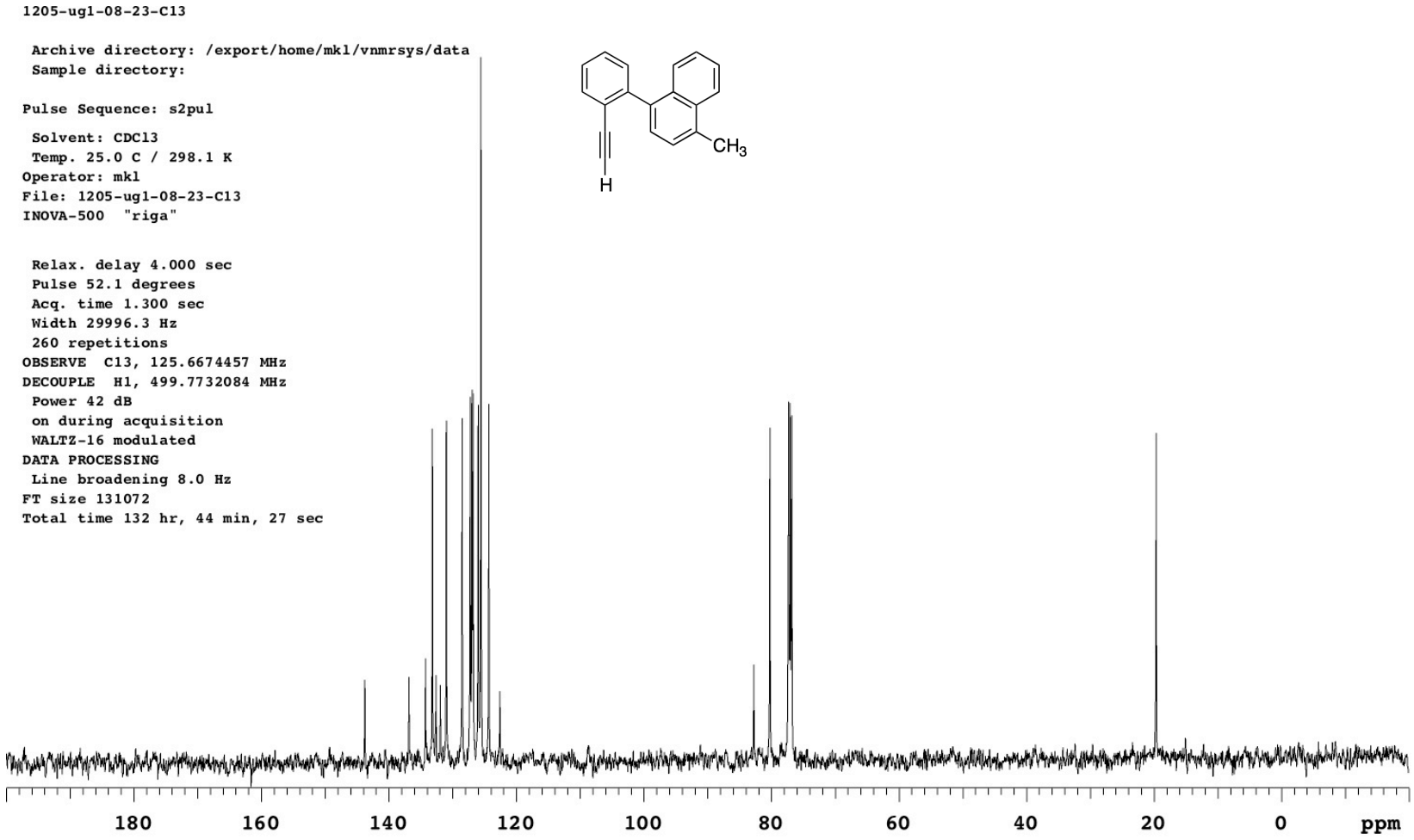
1205-ug1-08-23-C13
Archive directory: /export/home/mkl/vnmrsys/data
Sample directory:
Pulse Sequence: s2pul
Solvent: CDCl3
Temp. 25.0 C / 298.1 K
Operator: mkl
File: 1205-ug1-08-23-C13
INOVA-500 "riga"
Relax. delay 4.000 sec
Pulse 52.1 degrees
Acq. time 1.300 sec
Width 29996.3 Hz
260 repetitions
OBSERVE C13, 125.6674457 MHz
DECOUPLE H1, 499.7732084 MHz
Power 42 dB
on during acquisition
WALTZ-16 modulated
DATA PROCESSING
Line broadening 8.0 Hz
FT size 131072
Total time 132 hr, 44 min, 27 sec
CH3
H
180
160
140
120
100
80
60
40
20
0
ppm

1205-ug1-05-57-1H

Pulse Sequence: s2pul

Solvent: cdcl3
Temp. 25.0 C / 298.1 K
Operator: mkl
File: 1205-ug1-05-57-1H
INOVA-500 "riga"

Relax. delay 2.000 sec
Pulse 45.0 degrees
Acq. time 1.892 sec
Width 8000.0 Hz
32 repetitions
OBSERVE H1, 499.7707207 MHz
DATA PROCESSING
FT size 32768
Total time 13 min, 0 sec

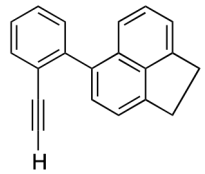

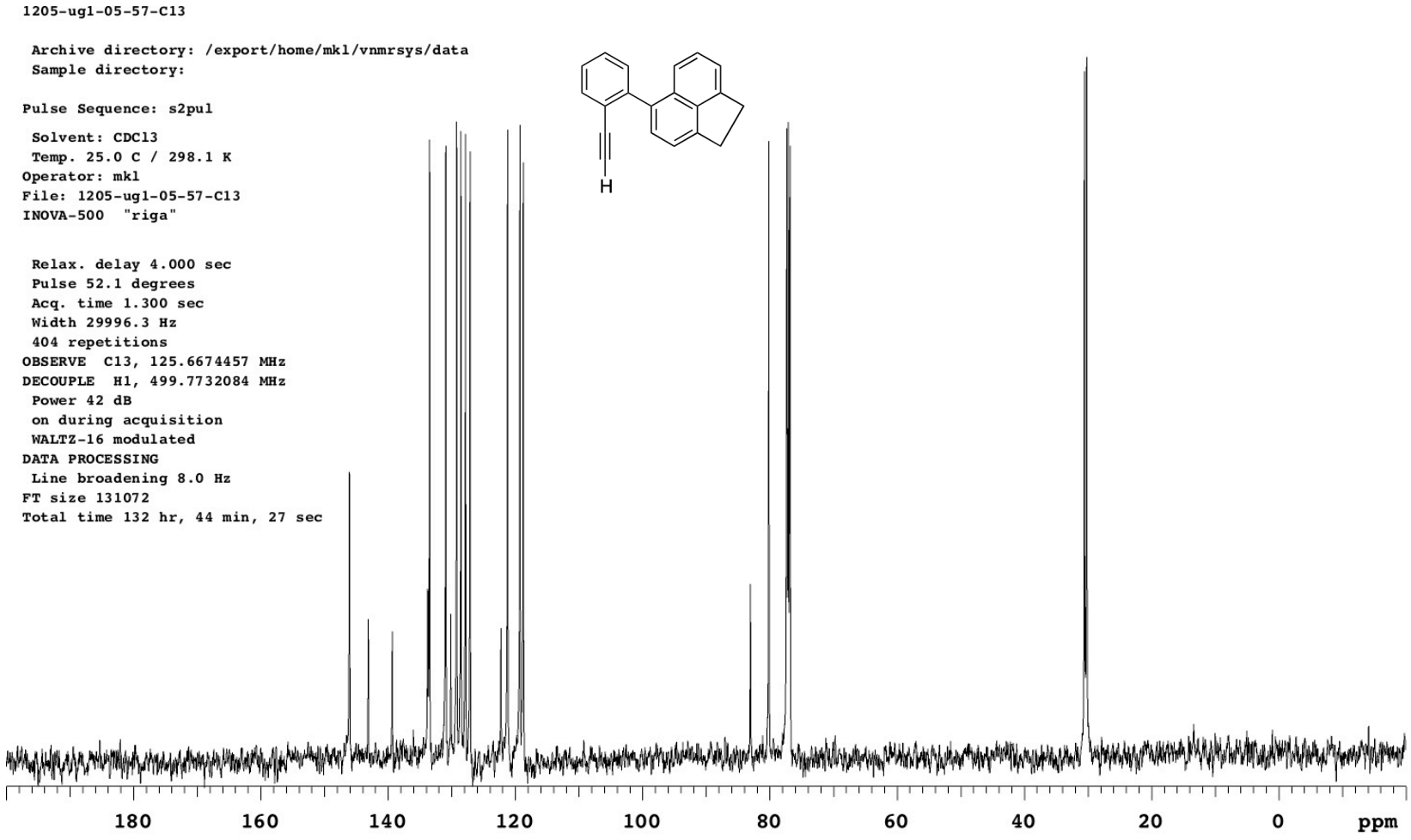
1205-ug1-05-57-C13
Archive directory: /export/home/mkl/vnmrsys/data
Sample directory:
Pulse Sequence: s2pul
Solvent: CDCl3
Temp. 25.0 C / 298.1 K
Operator: mkl
File: 1205-ug1-05-57-C13
INOVA-500 "riga"
Relax. delay 4.000 sec
Pulse 52.1 degrees
Acq. time 1.300 sec
Width 29996.3 Hz
404 repetitions
OBSERVE C13, 125.6674457 MHz
DECOUPLE H1, 499.7732084 MHz
Power 42 dB
on during acquisition
WALTZ-16 modulated
DATA PROCESSING
Line broadening 8.0 Hz
FT size 131072
Total time 132 hr, 44 min, 27 sec
H
180
160
140
120
100
80
60
40
20
0
ppm

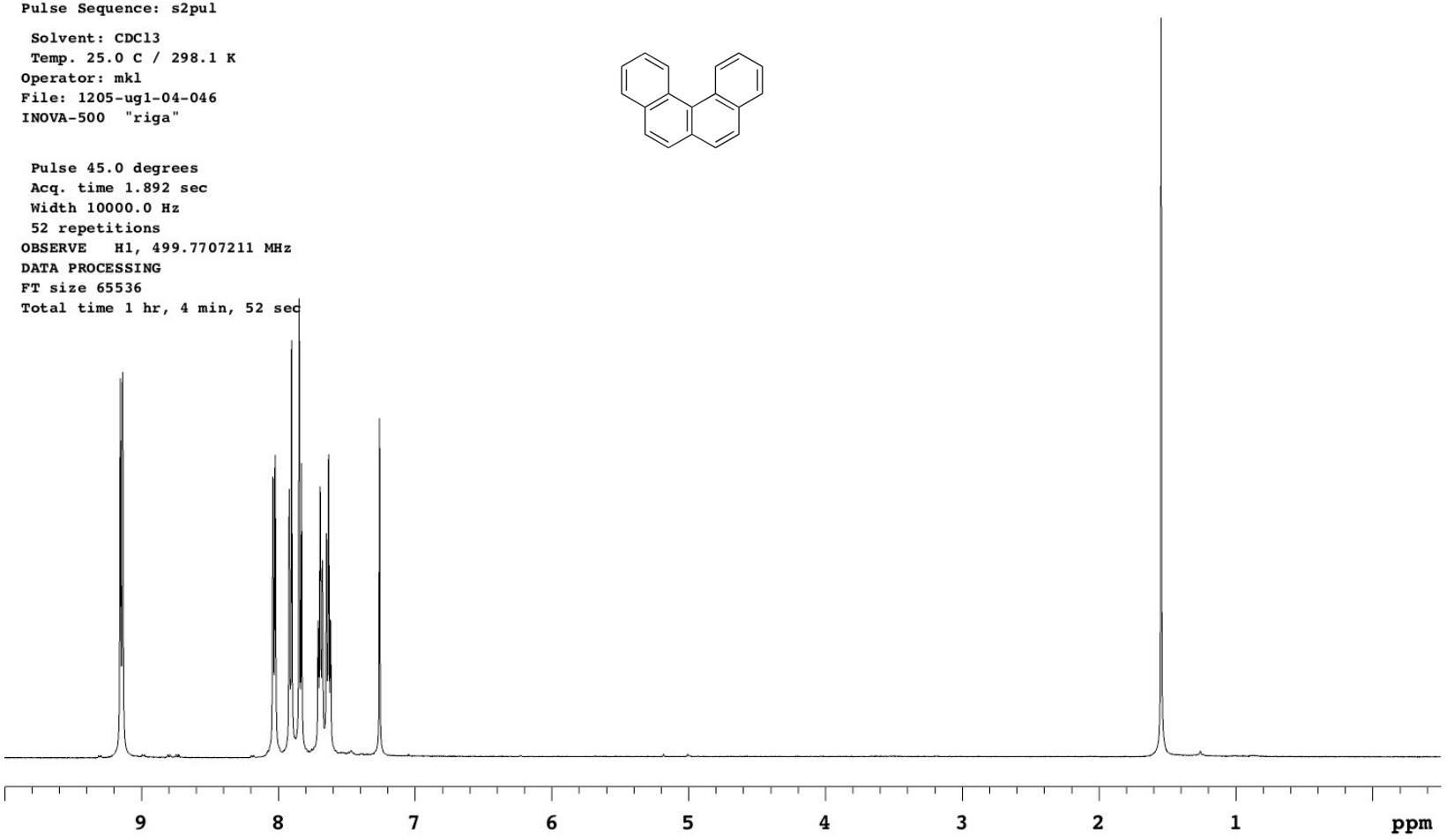
1205-ug1-04-046
Pulse Sequence: s2pul
Solvent: CDCl3
Temp. 25.0 C / 298.1 K
Operator: mkl
File: 1205-ug1-04-046
INOVA-500 "riga"
Pulse 45.0 degrees
Acq. time 1.892 sec
Width 10000.0 Hz
52 repetitions
OBSERVE H1, 499.7707211 MHz
DATA PROCESSING
FT size 65536
Total time 1 hr, 4 min, 52 sec
9
8
7
6
5
4
3
2
1
ppm

1205-ug1-05-42-1H

Pulse Sequence: s2pul

Solvent: cdcl3
Temp. 25.0 C / 298.1 K
Operator: mkl
File: 1205-ug1-05-42-1H
INOVA-500 "riga"

Relax. delay 2.000 sec
Pulse 45.0 degrees
Acq. time 1.892 sec
Width 8000.0 Hz
32 repetitions
OBSERVE H1, 499.7707222 MHz
DATA PROCESSING
FT size 32768
Total time 13 min, 0 sec

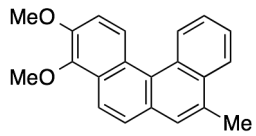

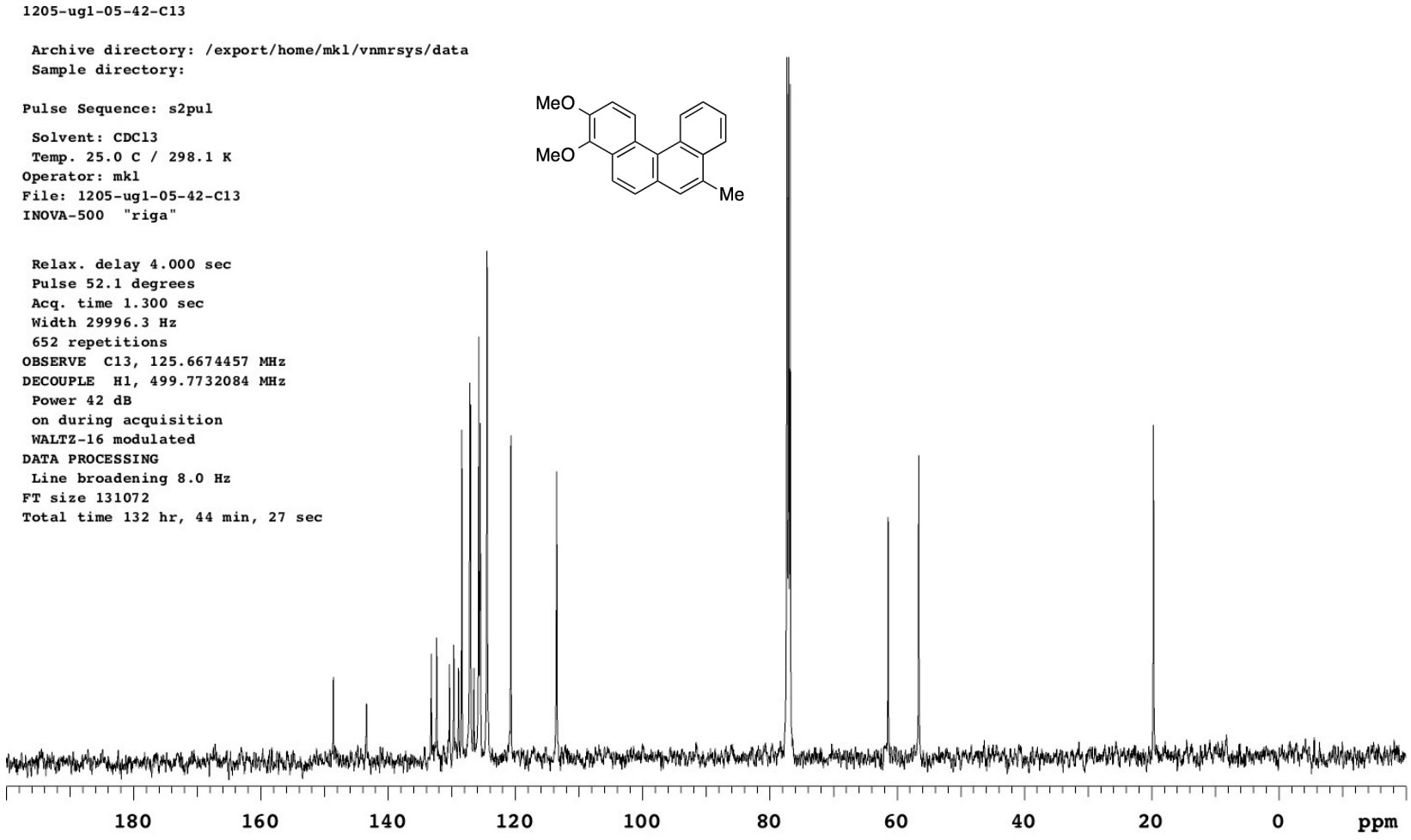
1205-ug1-05-42-C13
Archive directory: /export/home/mkl/vnmrsys/data
Sample directory:
Pulse Sequence: s2pul
Solvent: CDCl3
Temp. 25.0 C / 298.1 K
Operator: mkl
File: 1205-ug1-05-42-C13
INOVA-500 "riga"
Relax. delay 4.000 sec
Pulse 52.1 degrees
Acq. time 1.300 sec
Width 29996.3 Hz
652 repetitions
OBSERVE C13, 125.6674457 MHz
DECOUPLE H1, 499.7732084 MHz
Power 42 dB
on during acquisition
WALTZ-16 modulated
DATA PROCESSING
Line broadening 8.0 Hz
FT size 131072
Total time 132 hr, 44 min, 27 sec
MeO
MeO
Me
180
160
140
120
100
80
60
40
20
0
ppm

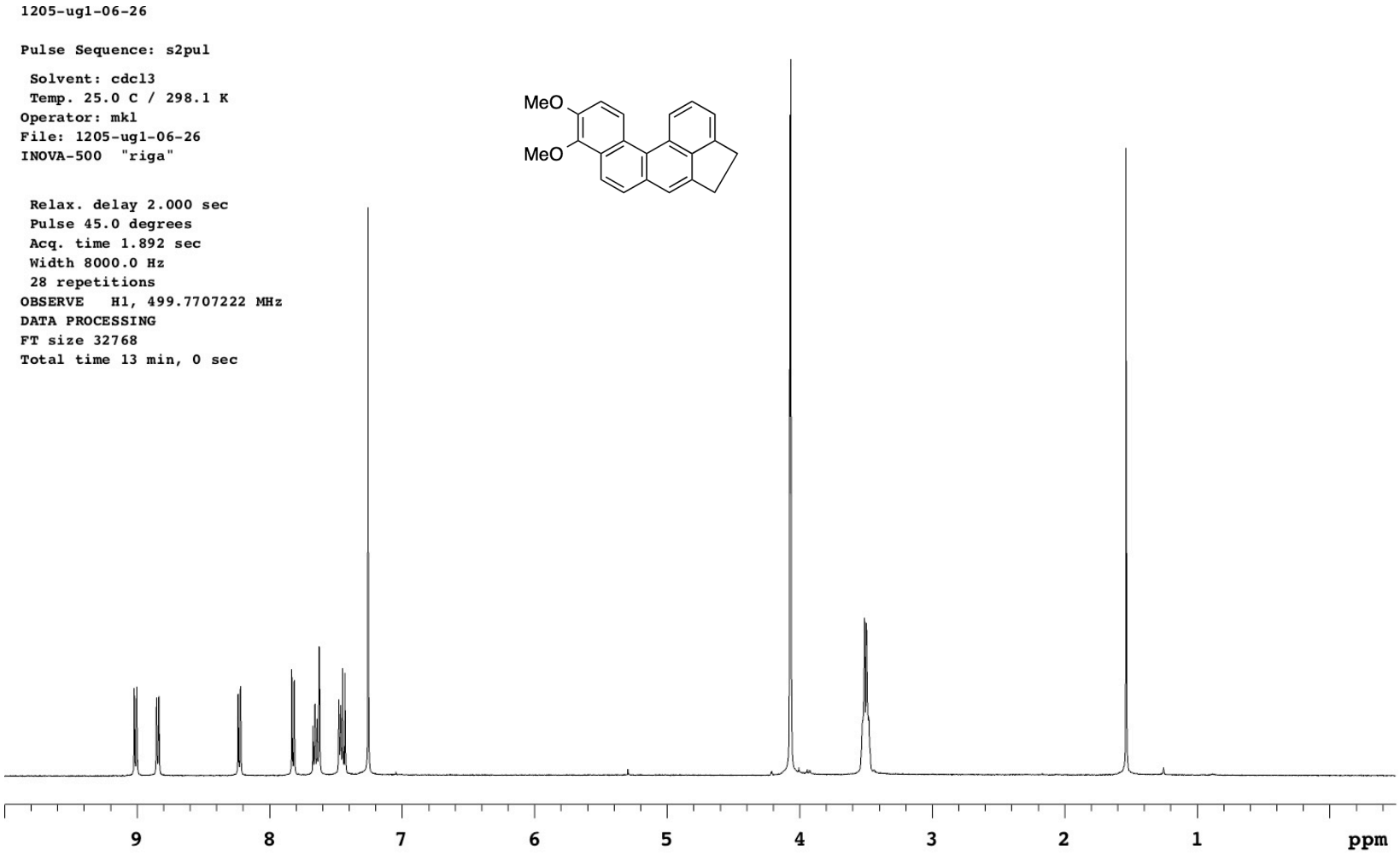
1205-ug1-06-26
Pulse Sequence: s2pul
Solvent: cdcl3
Temp. 25.0 C / 298.1 K
Operator: mkl
File: 1205-ug1-06-26
INOVA-500 "riga"
Relax. delay 2.000 sec
Pulse 45.0 degrees
Acq. time 1.892 sec
Width 8000.0 Hz
28 repetitions
OBSERVE H1, 499.7707222 MHz
DATA PROCESSING
FT size 32768
Total time 13 min, 0 sec
MeO
MeO
9
8
7
6
5
4
3
2
1
ppm

1205-ug1-06-26-C13

Archive directory: /export/home/mkl/vnmrsys/data
Sample directory:

Pulse Sequence: s2pul

Solvent: CDCl3
Temp. 25.0 C / 298.1 K
Operator: mkl
File: 1205-ug1-06-26-C13
INOVA-500 "riga"

Relax. delay 4.000 sec
Pulse 52.1 degrees
Acq. time 1.300 sec
Width 29996.3 Hz
644 repetitions
OBSERVE C13, 125.6674457 MHz
DECOUPLE H1, 499.7732084 MHz
Power 42 dB
on during acquisition
WALTZ-16 modulated
DATA PROCESSING
Line broadening 8.0 Hz
FT size 131072
Total time 132 hr, 44 min, 27 sec

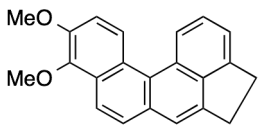

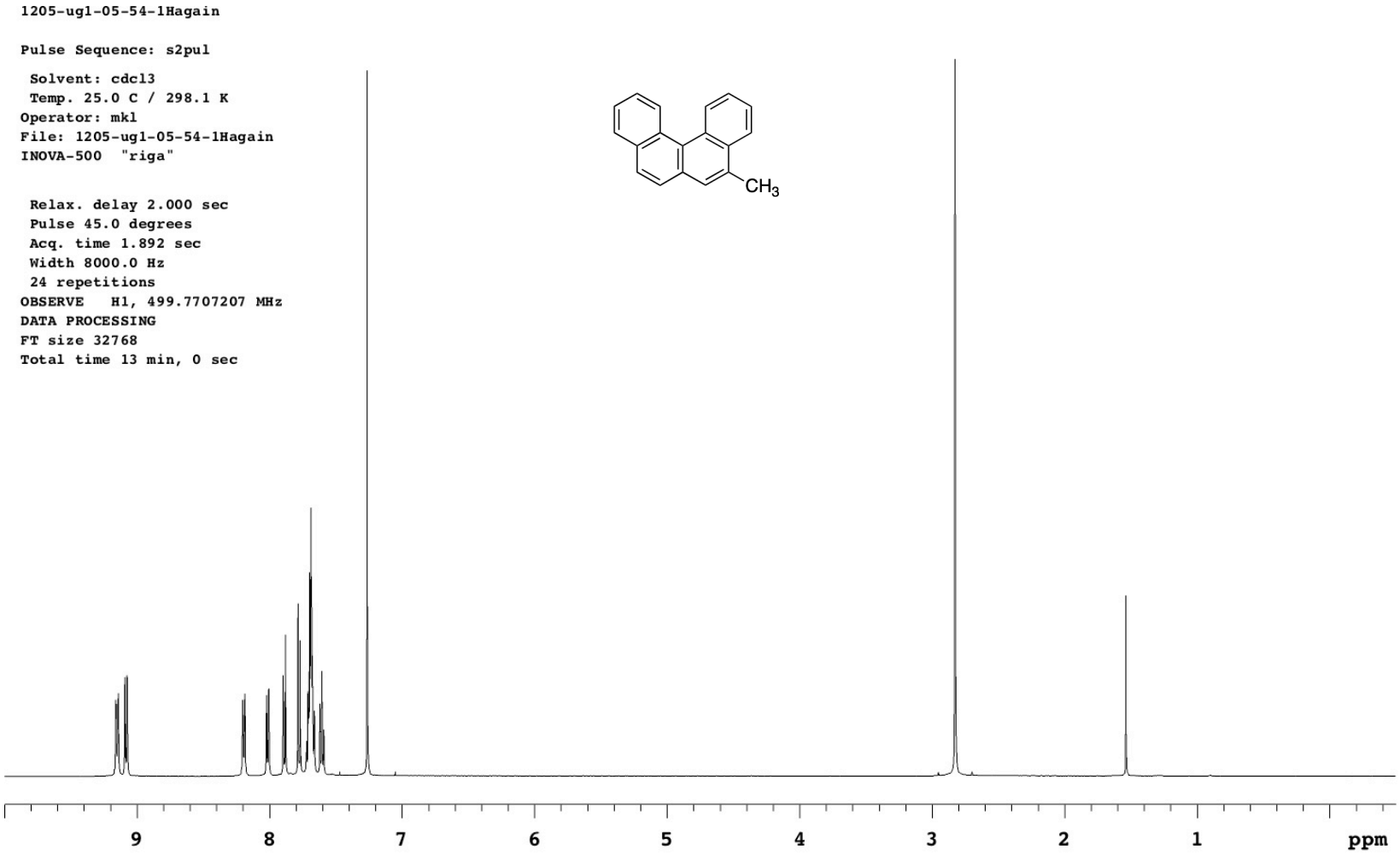
1205-ug1-05-54-1Hagain
Pulse Sequence: s2pul
Solvent: cdcl3
Temp. 25.0 C / 298.1 K
Operator: mkl
File: 1205-ug1-05-54-1Hagain
INOVA-500 "riga"
Relax. delay 2.000 sec
Pulse 45.0 degrees
Acq. time 1.892 sec
Width 8000.0 Hz
24 repetitions
OBSERVE H1, 499.7707207 MHz
DATA PROCESSING
FT size 32768
Total time 13 min, 0 sec
CH3
9
8
7
6
5
4
3
2
1
ppm

1205-ug1-05-54-C13

Archive directory: /export/home/mkl/vnmrsys/data
Sample directory:

Pulse Sequence: s2pul

Solvent: CDCl3
Temp. 25.0 C / 298.1 K
Operator: mkl
File: 1205-ug1-05-54-C13
INOVA-500 "riga"

Relax. delay 4.000 sec
Pulse 52.1 degrees
Acq. time 1.300 sec
Width 29996.3 Hz
480 repetitions
OBSERVE C13, 125.6674457 MHz
DECOUPLE H1, 499.7732084 MHz
Power 42 dB
on during acquisition
WALTZ-16 modulated
DATA PROCESSING
Line broadening 8.0 Hz
FT size 131072
Total time 132 hr, 44 min, 27 sec

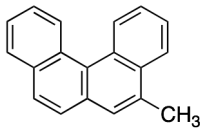

1205-ug1-05-058

Archive directory: /export/home/mkl/vnmrsys/data
Sample directory:

Pulse Sequence: s2pul

Solvent: CDCl3
Temp. 25.0 C / 298.1 K
Operator: mkl
File: 1205-ug1-05-058
INOVA-500 "riga"

Pulse 45.0 degrees
Acq. time 1.892 sec
Width 10000.0 Hz
72 repetitions
OBSERVE H1, 499.7707211 MHz
DATA PROCESSING
Line broadening 0.5 Hz
Gauss apodization 0.900 sec
FT size 65536
Total time 4 min, 3 sec

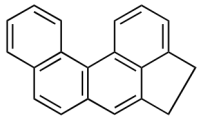

1205-ug1-05-058-13C

Archive directory: /export/home/mkl/vnmrsys/data
Sample directory:

Pulse Sequence: s2pul

Solvent: CDCl3
Temp. 25.0 C / 298.1 K
Operator: mkl
File: 1205-ug1-05-058-13C
INOVA-500 "riga"

Relax. delay 4.000 sec
Pulse 52.1 degrees
Acq. time 1.300 sec
Width 29996.3 Hz
608 repetitions
OBSERVE C13, 125.6674457 MHz
DECOUPLE H1, 499.7732084 MHz
Power 42 dB
on during acquisition
WALTZ-16 modulated
DATA PROCESSING
Line broadening 8.0 Hz
FT size 131072
Total time 132 hr, 44 min, 27 sec

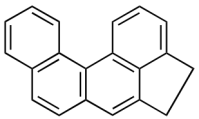

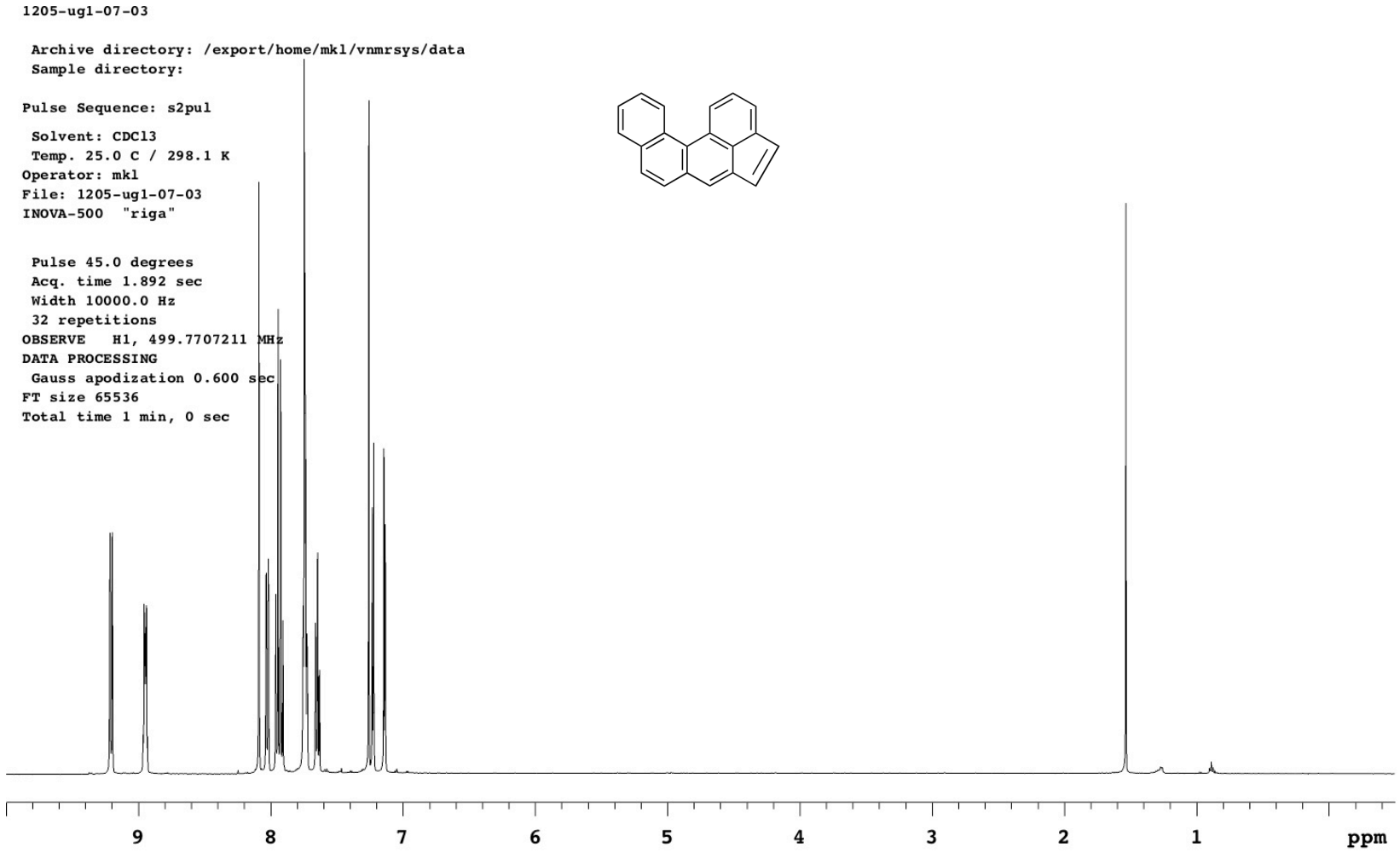
1205-ug1-07-03
Archive directory: /export/home/mkl/vnmrsys/data
Sample directory:
Pulse Sequence: s2pul
Solvent: CDCl3
Temp. 25.0 C / 298.1 K
Operator: mkl
File: 1205-ug1-07-03
INOVA-500 "riga"
Pulse 45.0 degrees
Acq. time 1.892 sec
Width 10000.0 Hz
32 repetitions
OBSERVE H1, 499.7707211 MHz
DATA PROCESSING
Gauss apodization 0.600 sec
FT size 65536
Total time 1 min, 0 sec
9
8
7
6
5
4
3
2
1
ppm

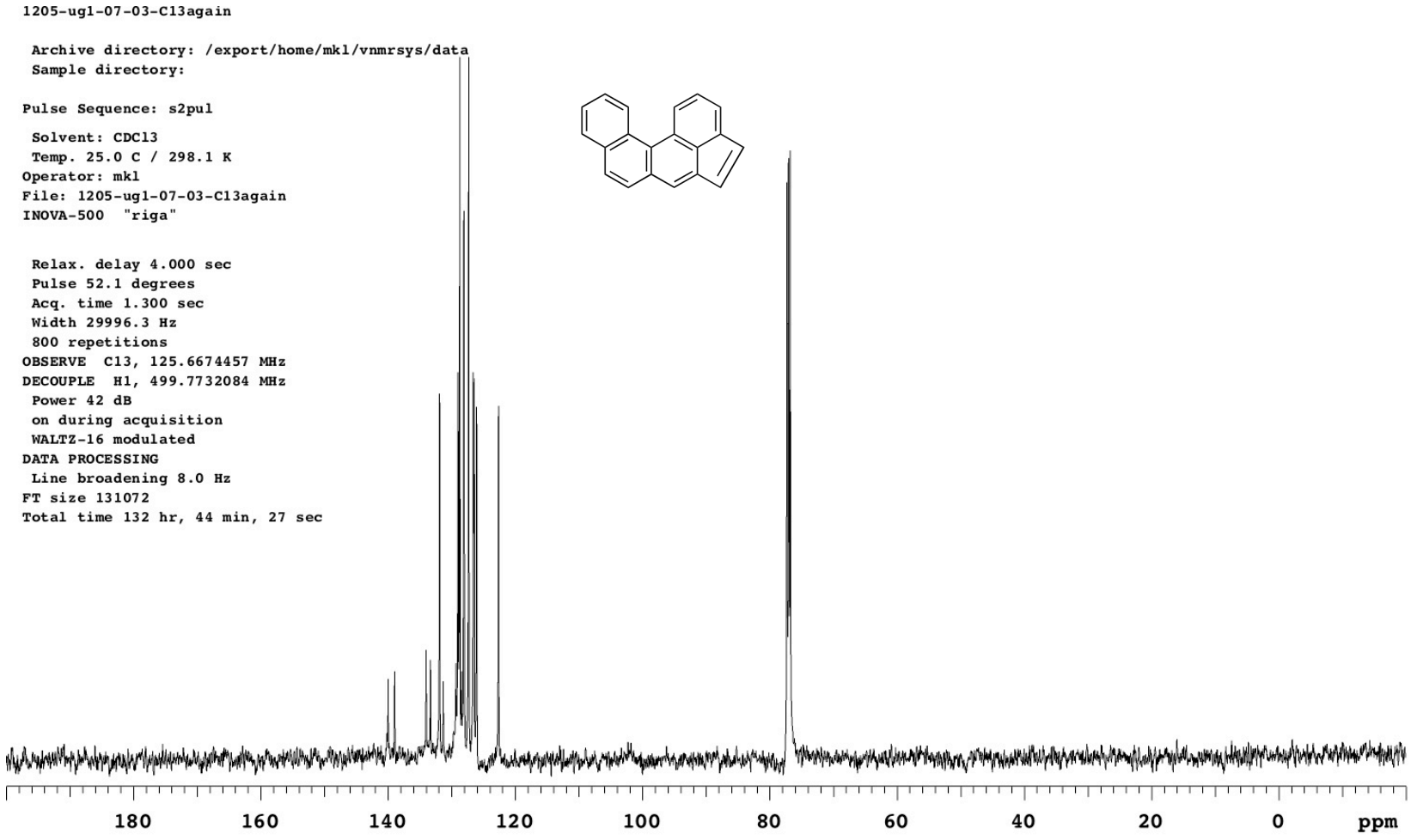
1205-ug1-07-03-C13again
Archive directory: /export/home/mkl/vnmrsys/data
Sample directory:
Pulse Sequence: s2pul
Solvent: CDCl3
Temp. 25.0 C / 298.1 K
Operator: mkl
File: 1205-ug1-07-03-C13again
INOVA-500 "riga"
Relax. delay 4.000 sec
Pulse 52.1 degrees
Acq. time 1.300 sec
Width 29996.3 Hz
800 repetitions
OBSERVE C13, 125.6674457 MHz
DECOUPLE H1, 499.7732084 MHz
Power 42 dB
on during acquisition
WALTZ-16 modulated
DATA PROCESSING
Line broadening 8.0 Hz
FT size 131072
Total time 132 hr, 44 min, 27 sec
180
160
140
120
100
80
60
40
20
0
ppm

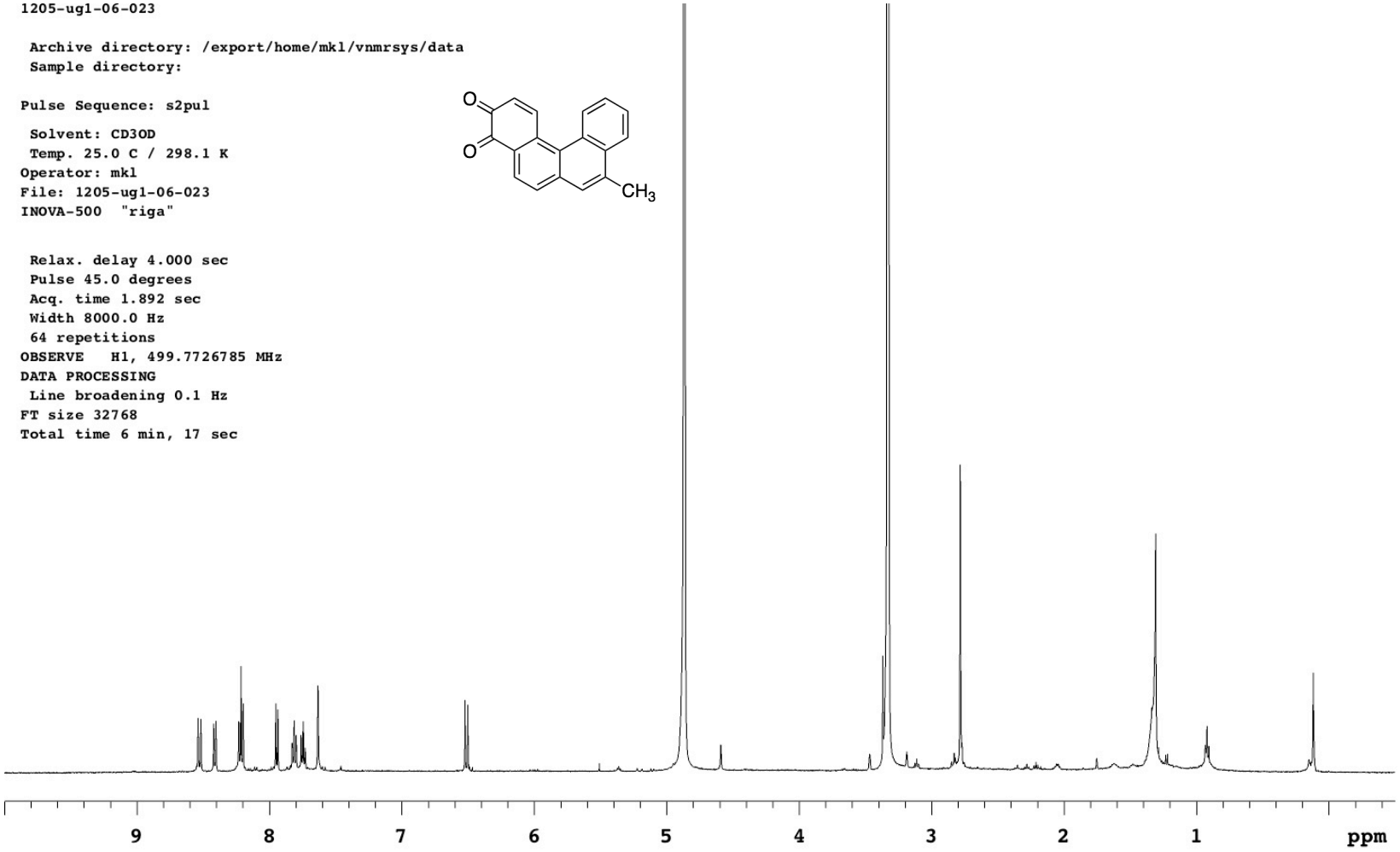
1205-ug1-06-023
Archive directory: /export/home/mkl/vnmrsys/data
Sample directory:
Pulse Sequence: s2pul
Solvent: CD3OD
Temp. 25.0 C / 298.1 K
Operator: mkl
File: 1205-ug1-06-023
INOVA-500 "riga"
Relax. delay 4.000 sec
Pulse 45.0 degrees
Acq. time 1.892 sec
Width 8000.0 Hz
64 repetitions
OBSERVE H1, 499.7726785 MHz
DATA PROCESSING
Line broadening 0.1 Hz
FT size 32768
Total time 6 min, 17 sec
O
O
CH3
9
8
7
6
5
4
3
2
1
ppm

1205-ug1-06-11-dmso-C13

Archive directory: /export/home/mkl/vnmrsys/data
Sample directory:

Pulse Sequence: s2pul

Solvent: dmso
Temp. 25.0 C / 298.1 K
Operator: mkl
File: 1205-ug1-06-11-dmso-C13
INOVA-500 "riga"

Relax. delay 4.000 sec
Pulse 52.1 degrees
Acq. time 1.300 sec
Width 29996.3 Hz
1632 repetitions
OBSERVE C13, 125.6680426 MHz
DECOUPLE H1, 499.7755824 MHz
Power 42 dB
on during acquisition
WALTZ-16 modulated
DATA PROCESSING
Line broadening 2.0 Hz
FT size 131072
Total time 132 hr, 44 min, 27 sec

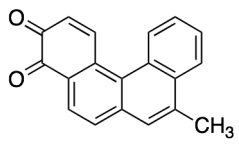

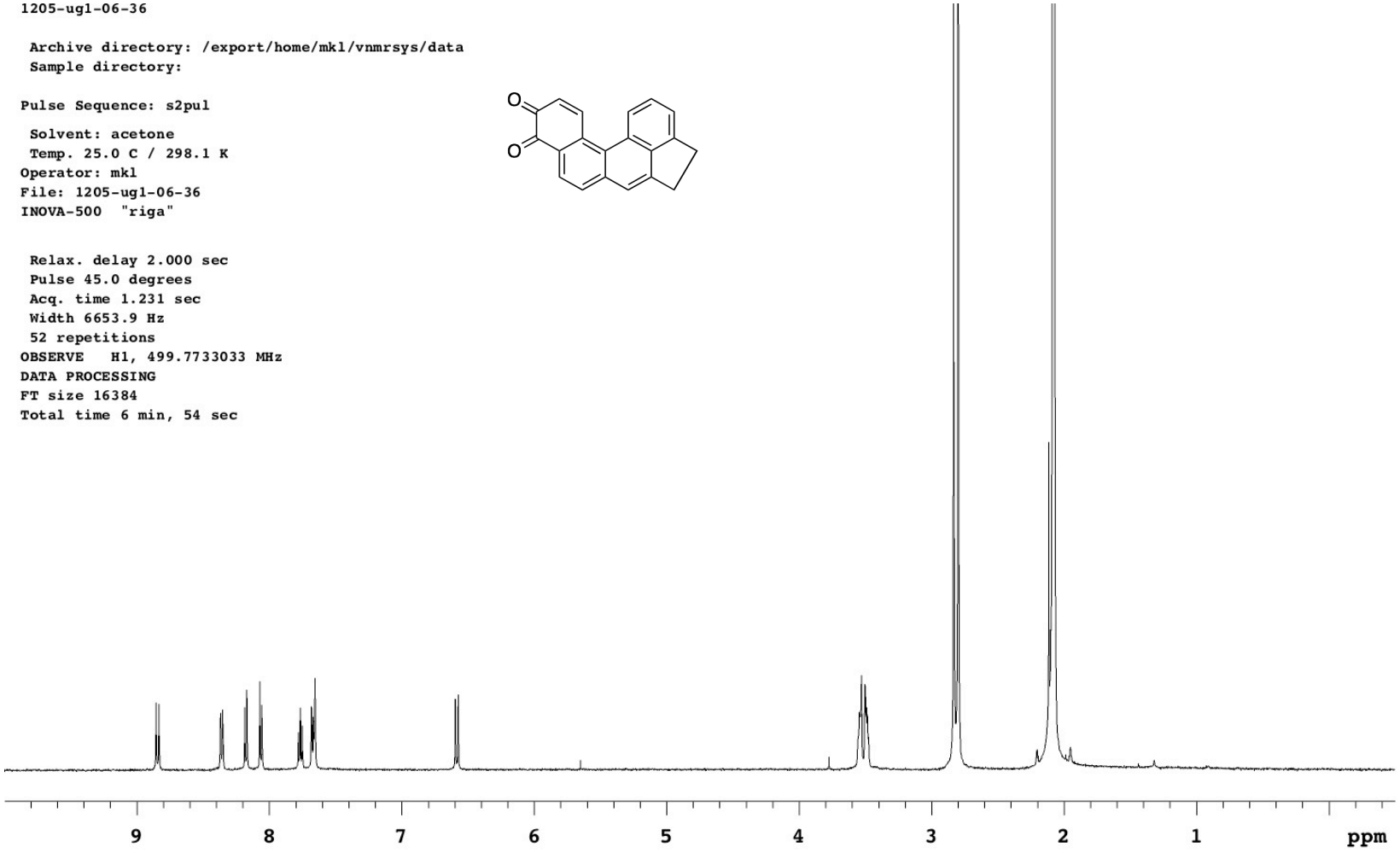
1205-ug1-06-36
Archive directory: /export/home/mkl/vnmrsys/data
Sample directory:
Pulse Sequence: s2pul
Solvent: acetone
Temp. 25.0 C / 298.1 K
Operator: mkl
File: 1205-ug1-06-36
INOVA-500 "riga"
Relax. delay 2.000 sec
Pulse 45.0 degrees
Acq. time 1.231 sec
Width 6653.9 Hz
52 repetitions
OBSERVE H1, 499.7733033 MHz
DATA PROCESSING
FT size 16384
Total time 6 min, 54 sec
O
O
9
8
7
6
5
4
3
2
1
ppm

1205-ug1-06-36-C13-dmso

Archive directory: /export/home/mkl/vnmrsys/data
Sample directory:

Pulse Sequence: s2pul

Solvent: dmso
Temp. 25.0 C / 298.1 K
Operator: mkl
File: 1205-ug1-06-36-C13-dmso
INOVA-500 "riga"

Relax. delay 4.000 sec
Pulse 52.1 degrees
Acq. time 1.300 sec
Width 29996.3 Hz
2040 repetitions
OBSERVE C13, 125.6680426 MHz
DECOUPLE H1, 499.7755824 MHz
Power 42 dB
on during acquisition
WALTZ-16 modulated
DATA PROCESSING
Line broadening 2.0 Hz
FT size 131072
Total time 132 hr, 44 min, 27 sec

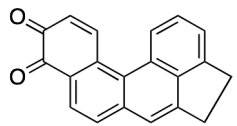

1205-ug1-06-08again

Archive directory: /export/home/mkl/vnmrsys/data
Sample directory:

Pulse Sequence: s2pul

Solvent: acetone
Temp. 25.0 C / 298.1 K
Operator: mkl
File: 1205-ug1-06-08again
INOVA-500 "riga"

Relax. delay 2.000 sec
Pulse 45.0 degrees
Acq. time 1.231 sec
Width 6653.9 Hz
28 repetitions
OBSERVE H1, 499.7733033 MHz
DATA PROCESSING
FT size 16384
Total time 1 min, 43 sec

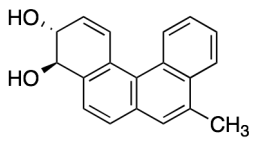

1205-ug1-06-8-dmso-C13

Archive directory: /export/home/mkl/vnmrsys/data
Sample directory:

Pulse Sequence: s2pul

Solvent: dmso
Temp. 25.0 C / 298.1 K
Operator: mkl
File: 1205-ug1-06-8-dmso-C13
INOVA-500 "riga"

Relax. delay 4.000 sec
Pulse 52.1 degrees
Acq. time 1.300 sec
Width 29996.3 Hz
1120 repetitions
OBSERVE C13, 125.6680426 MHz
DECOUPLE H1, 499.7755824 MHz
Power 42 dB
on during acquisition
WALTZ-16 modulated
DATA PROCESSING
Line broadening 2.0 Hz
FT size 131072
Total time 132 hr, 44 min, 27 sec

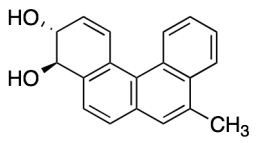

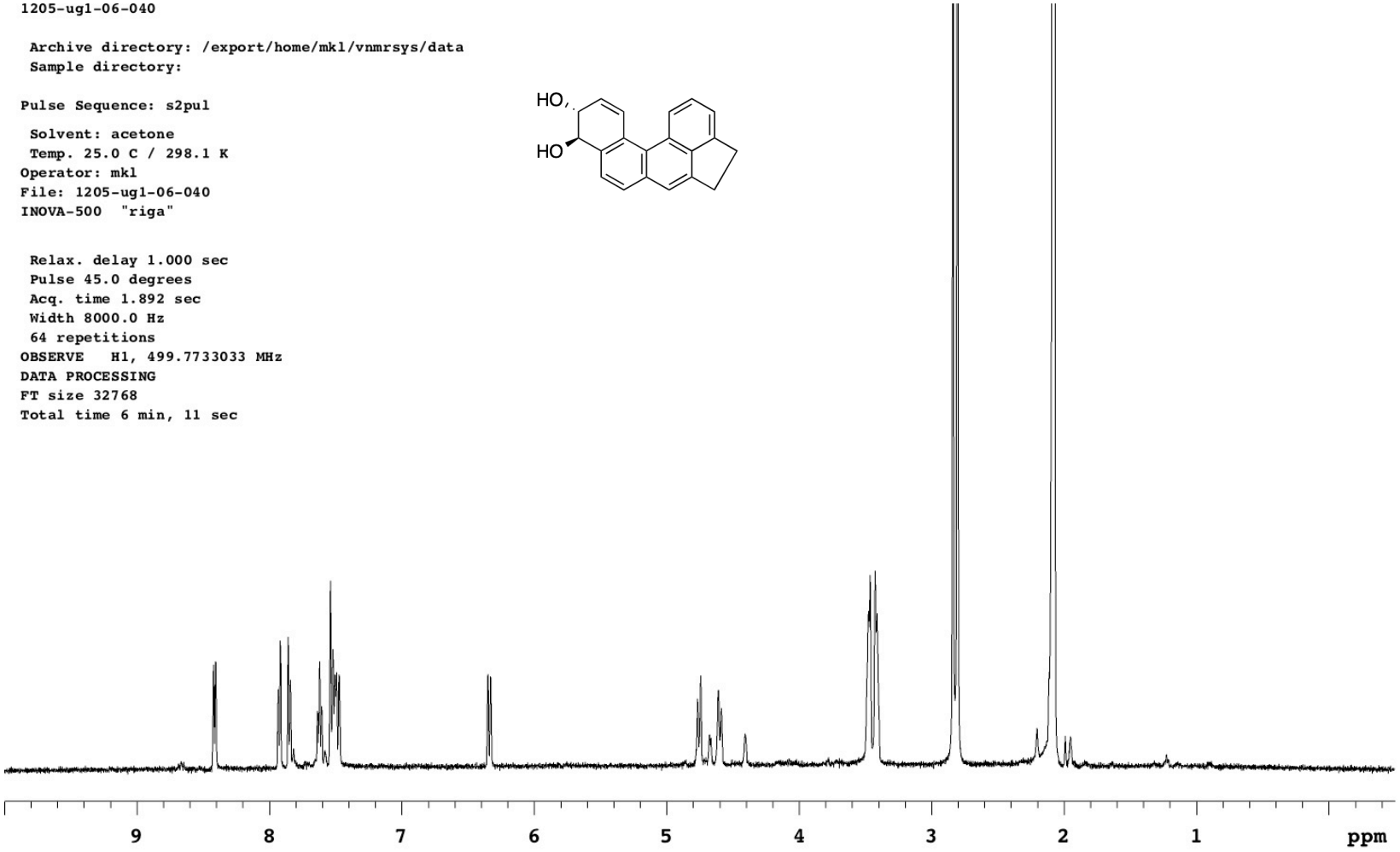
1205-ug1-06-040
Archive directory: /export/home/mkl/vnmrsys/data
Sample directory:
Pulse Sequence: s2pul
Solvent: acetone
Temp. 25.0 C / 298.1 K
Operator: mkl
File: 1205-ug1-06-040
INOVA-500 "riga"
Relax. delay 1.000 sec
Pulse 45.0 degrees
Acq. time 1.892 sec
Width 8000.0 Hz
64 repetitions
OBSERVE H1, 499.7733033 MHz
DATA PROCESSING
FT size 32768
Total time 6 min, 11 sec
HO
HO
9
8
7
6
5
4
3
2
1
ppm

1205-ug1-06-40-C13-dmso

Archive directory: /export/home/mkl/vnmrsys/data
Sample directory:

Pulse Sequence: s2pul

Solvent: dmso
Temp. 25.0 C / 298.1 K
Operator: mkl
File: 1205-ug1-06-40-C13-dmso
INOVA-500 "riga"

Relax. delay 4.000 sec
Pulse 52.1 degrees
Acq. time 1.300 sec
Width 29996.3 Hz
520 repetitions
OBSERVE C13, 125.6680426 MHz
DECOUPLE H1, 499.7755824 MHz
Power 42 dB
on during acquisition
WALTZ-16 modulated
DATA PROCESSING
Line broadening 2.0 Hz
FT size 131072
Total time 132 hr, 44 min, 27 sec

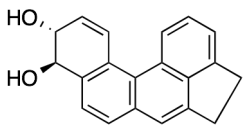

1205-ug1-06-033

Archive directory: /export/home/mkl/vnmrsys/data
Sample directory:

Pulse Sequence: s2pul

Solvent: acetone
Temp. 25.0 C / 298.1 K
Operator: mkl
File: 1205-ug1-06-033
INOVA-500 "riga"

Relax. delay 1.000 sec
Pulse 45.0 degrees
Acq. time 1.892 sec
Width 8000.0 Hz
88 repetitions
OBSERVE H1, 499.7733033 MHz
DATA PROCESSING
FT size 32768
Total time 6 min, 11 sec

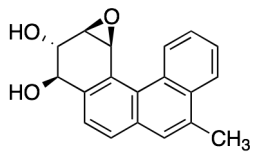

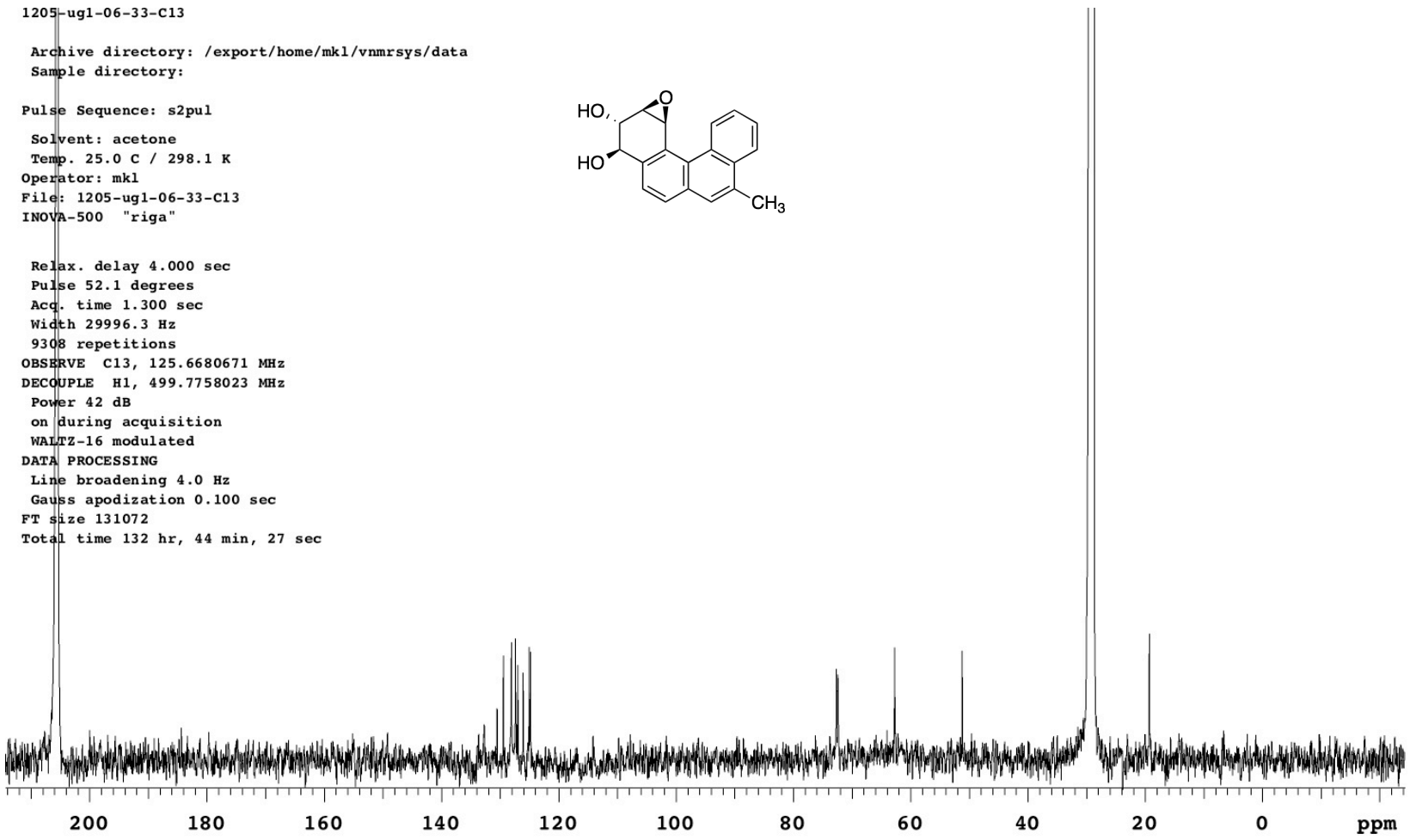
1205-ug1-06-33-C13
Archive directory: /export/home/mkl/vnmrsys/data
Sample directory:
Pulse Sequence: s2pul
Solvent: acetone
Temp. 25.0 C / 298.1 K
Operator: mkl
File: 1205-ug1-06-33-C13
INOVA-500 "riga"
Relax. delay 4.000 sec
Pulse 52.1 degrees
Acq. time 1.300 sec
Width 29996.3 Hz
9308 repetitions
OBSERVE C13, 125.6680671 MHz
DECOUPLE H1, 499.7758023 MHz
Power 42 dB
on during acquisition
WALTZ-16 modulated
DATA PROCESSING
Line broadening 4.0 Hz
Gauss apodization 0.100 sec
FT size 131072
Total time 132 hr, 44 min, 27 sec
HO
HO
O
CH3
200
180
160
140
120
100
80
60
40
20
0
ppm

1205-ug1-09-28-a1d-1H

Archive directory: /export/home/mkl/vnmrsys/data
Sample directory:

Pulse Sequence: s2pul

Solvent: acetone
Temp. 25.0 C / 298.1 K
Operator: mkl
File: 1205-ug1-09-28-a1d-1H
INOVA-500 "riga"

Relax. delay 1.000 sec
Pulse 45.0 degrees
Acq. time 1.892 sec
Width 8000.0 Hz
32 repetitions
OBSERVE H1, 499.7733033 MHz
DATA PROCESSING
Line broadening 0.5 Hz
FT size 32768
Total time 1 min, 32 sec

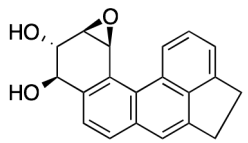

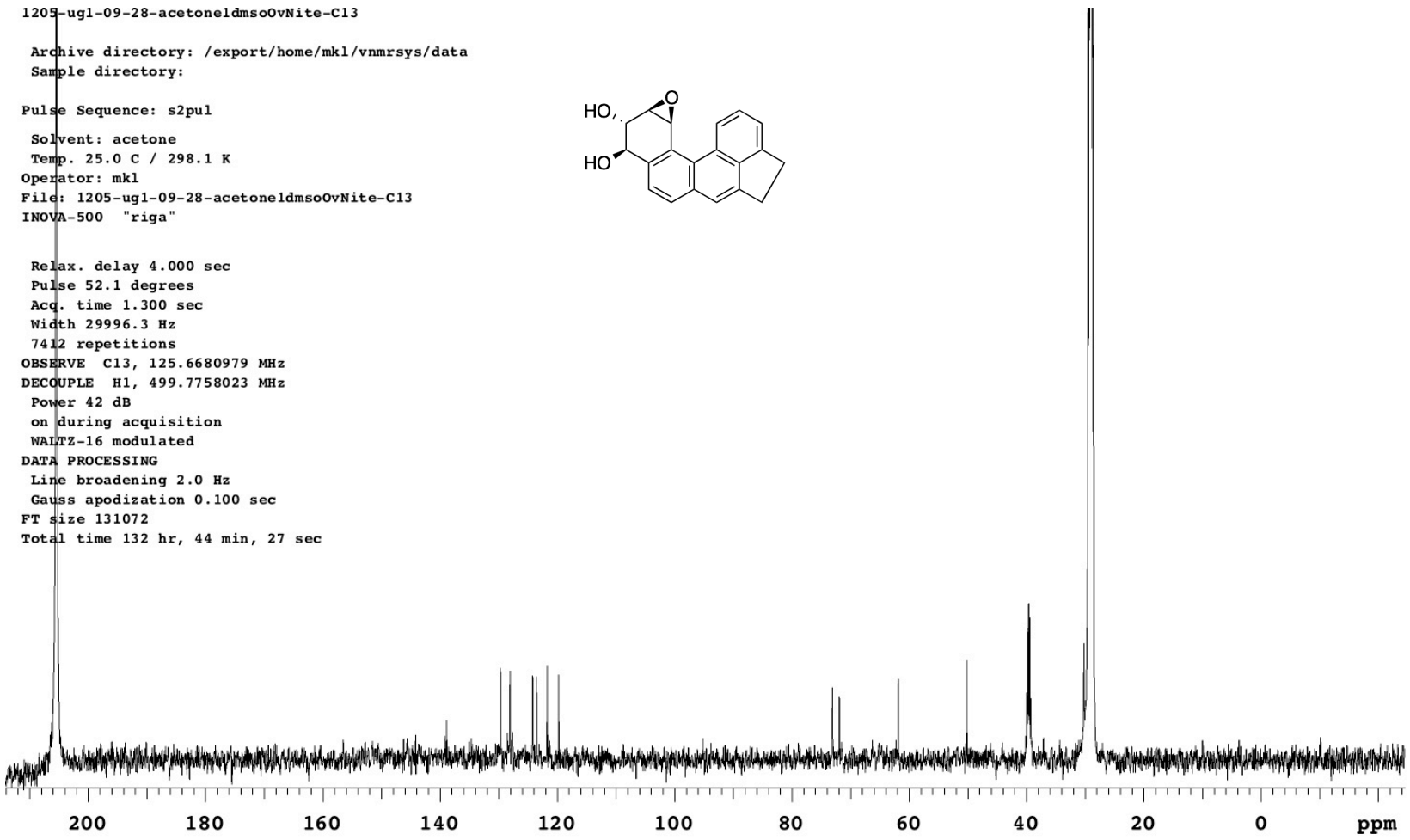
1205-ug1-09-28-acetone1dmsoOvNite-C13
Archive directory: /export/home/mkl/vnmrsys/data
Sample directory:
Pulse Sequence: s2pul
Solvent: acetone
Temp. 25.0 C / 298.1 K
Operator: mkl
File: 1205-ug1-09-28-acetone1dmsoOvNite-C13
INOVA-500 "riga"
Relax. delay 4.000 sec
Pulse 52.1 degrees
Acq. time 1.300 sec
Width 29996.3 Hz
7412 repetitions
OBSERVE C13, 125.6680979 MHz
DECOUPLE H1, 499.7758023 MHz
Power 42 dB
on during acquisition
WALTZ-16 modulated
DATA PROCESSING
Line broadening 2.0 Hz
Gauss apodization 0.100 sec
FT size 131072
Total time 132 hr, 44 min, 27 sec
HO
HO
O
200
180
160
140
120
100
80
60
40
20
0
ppm

1205-ug1-06-034

Archive directory: /export/home/mkl/vnmrsys/data
Sample directory: auto_13Dec2004

Pulse Sequence: s2pul

Solvent: Acetone
Temp. 25.0 C / 298.1 K
Operator: barbara
File: 1205-ug1-06-034
INOVA-500 "riga"

Relax. delay 1.000 sec
Pulse 45.0 degrees
Acq. time 1.892 sec
Width 10000.0 Hz
16 repetitions
OBSERVE H1, 499.7733033 MHz
DATA PROCESSING
Line broadening 0.5 Hz
FT size 65536
Total time 0 min, 46 sec

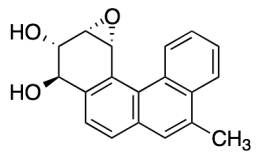

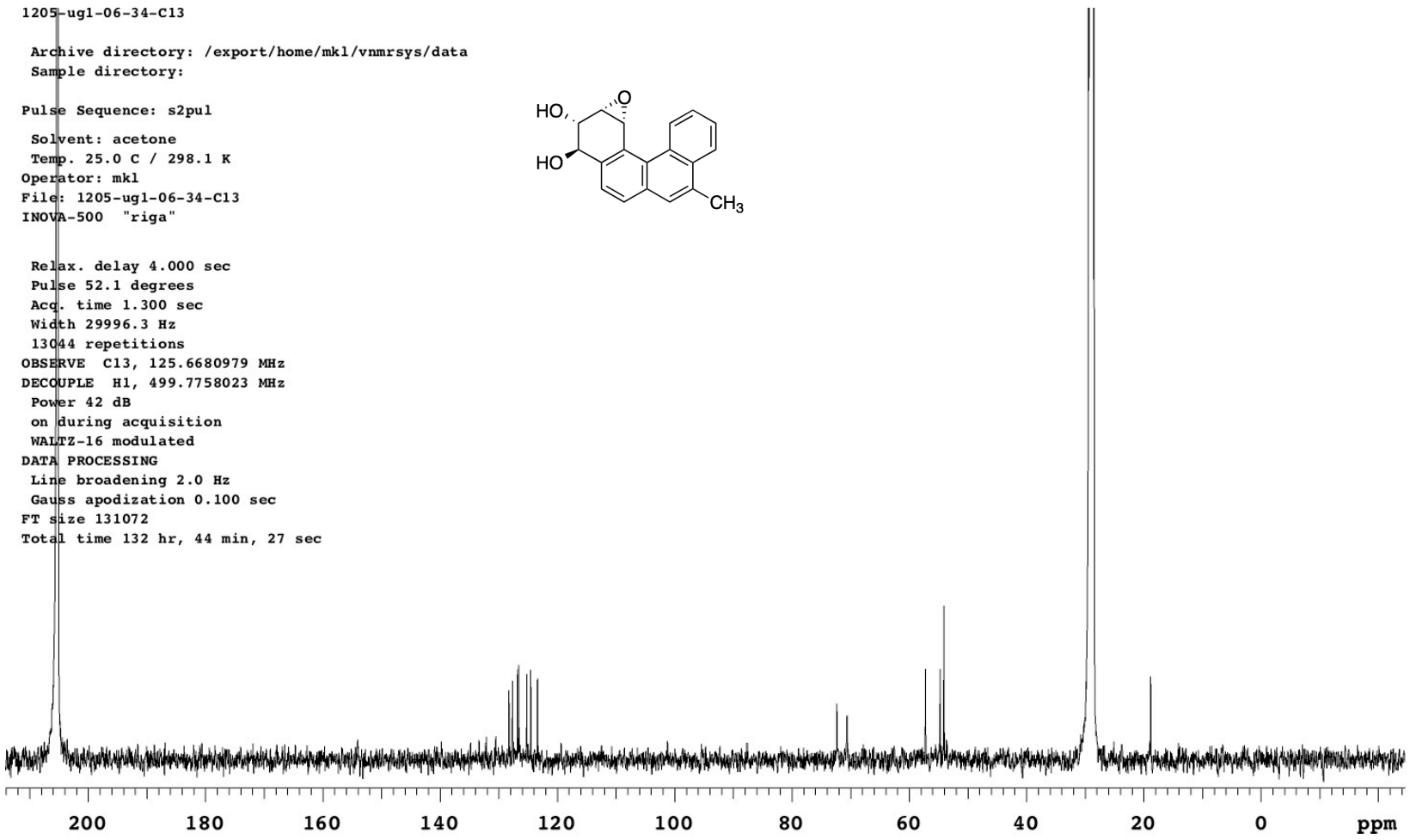
1205-ug1-06-34-C13
Archive directory: /export/home/mkl/vnmrsys/data
Sample directory:
Pulse Sequence: s2pul
Solvent: acetone
Temp. 25.0 C / 298.1 K
Operator: mkl
File: 1205-ug1-06-34-C13
INOVA-500 "riga"
Relax. delay 4.000 sec
Pulse 52.1 degrees
Acq. time 1.300 sec
Width 29996.3 Hz
13044 repetitions
OBSERVE C13, 125.6680979 MHz
DECOUPLE H1, 499.7758023 MHz
Power 42 dB
on during acquisition
WALTZ-16 modulated
DATA PROCESSING
Line broadening 2.0 Hz
Gauss apodization 0.100 sec
FT size 131072
Total time 132 hr, 44 min, 27 sec
HO
HO
O
CH3
200
180
160
140
120
100
80
60
40
20
0
ppm

1205-ug1-06-44-ace1dmso

Archive directory: /export/home/mkl/vnmrsys/data
Sample directory:

Pulse Sequence: s2pul

Solvent: acetone
Temp. 25.0 C / 298.1 K
Operator: mkl
File: 1205-ug1-06-44-ace1dmso
INOVA-500 "riga"

Relax. delay 2.000 sec
Pulse 45.0 degrees
Acq. time 1.231 sec
Width 6653.9 Hz
36 repetitions
OBSERVE H1, 499.7733154 MHz
DATA PROCESSING
FT size 16384
Total time 6 min, 54 sec

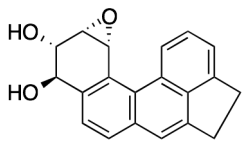

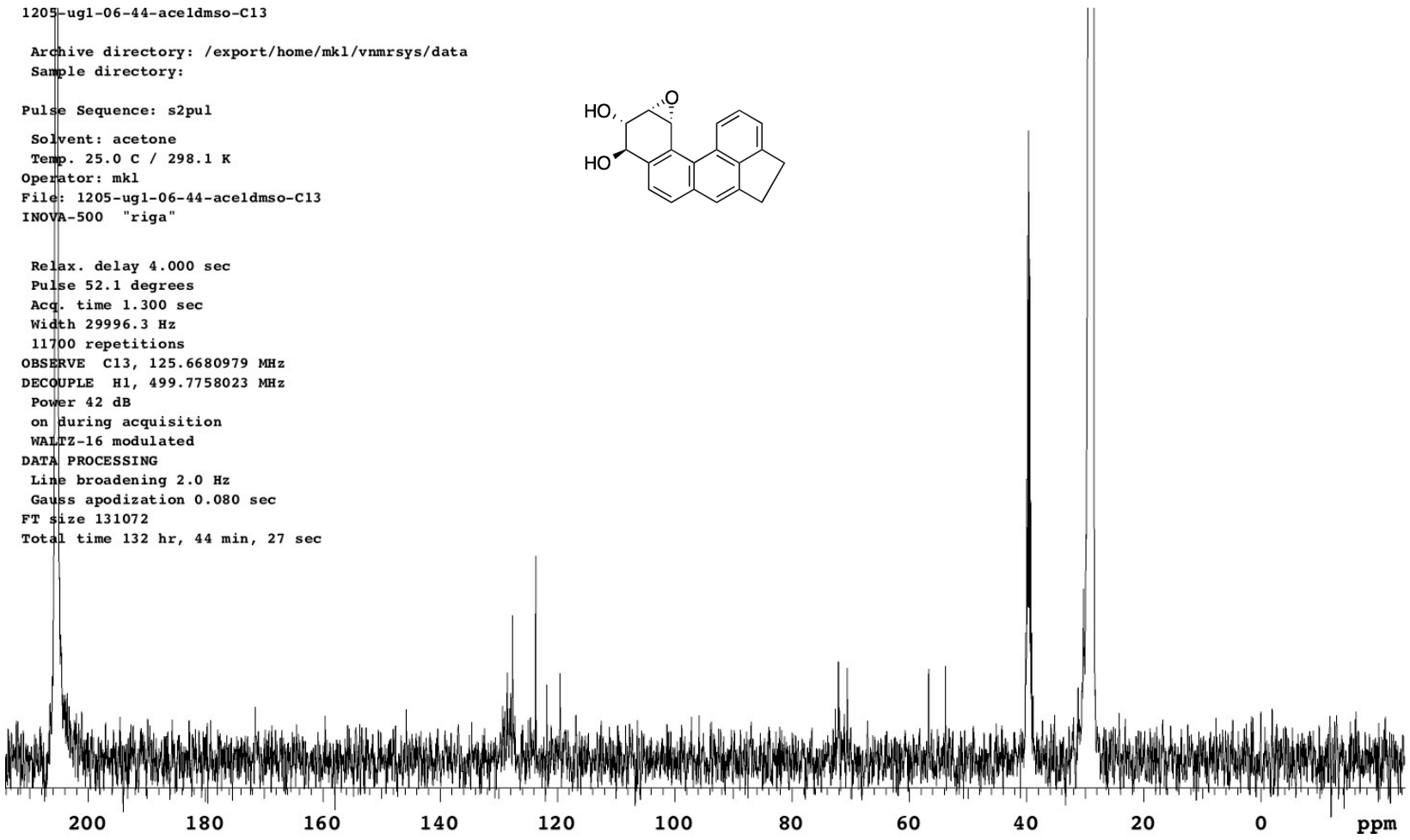
1205-ug1-06-44-acetdmso-C13
Archive directory: /export/home/mkl/vnmrsys/data
Sample directory:
Pulse Sequence: s2pul
Solvent: acetone
Temp. 25.0 C / 298.1 K
Operator: mkl
File: 1205-ug1-06-44-acetdmso-C13
INOVA-500 "riga"
Relax. delay 4.000 sec
Pulse 52.1 degrees
Acq. time 1.300 sec
Width 29996.3 Hz
11700 repetitions
OBSERVE C13, 125.6680979 MHz
DECOUPLE H1, 499.7758023 MHz
Power 42 dB
on during acquisition
WALTZ-16 modulated
DATA PROCESSING
Line broadening 2.0 Hz
Gauss apodization 0.080 sec
FT size 131072
Total time 132 hr, 44 min, 27 sec
HO
HO
O
200
180
160
140
120
100
80
60
40
20
0
ppm

Studies in Chemical Carcinogenesis

Chapter 4

Diastereoselective Synthesis of a Benzo[*a*]pyrene Amino Triol Derivative Required for Site-Specific DNA Modification

4.1 Introduction

As stated in the General Introduction and in Chapter 3, the PAH, benzo[*a*]pyrene (B*a*P), is a ubiquitous environmental pollutant that is a known carcinogen.[1] This planar, bay region-containing PAH is usually formed by the incomplete combustion of organic matter, and is commonly found in coal tar, automobile exhaust, tobacco smoke, and even in barbequed meats.[1] For example, B*a*P found in tobacco smoke was shown to cause genetic damage upon metabolic activation in human lung cells, and is considered to be one of the components leading to lung cancer.[2] Also, over-grilled charcoaled beef has been shown to contain 62.6 mg of B*a*P per kg,[3a] while fried chicken was found to contain 5.5 mg of B*a*P per kg.[3b]

In mammalian systems B*a*P undergoes metabolic activation by cytochrome P450 (CYP450)[4] and microsomal epoxide hydrolase (mEH),[5] to form 4 isomeric diol epoxides that can alkylate with DNA (Figure 1).[1,6] These diol epoxides are divided into two sets, series 1 diol epoxide isomers (also called DE1 or *syn*), which typically are devoid of tumorigenicity, whereas series 2 diol epoxide isomers (also called DE2 or *anti*) show potent tumorigenicity.[7] Between the two series 2 enantiomers of all PAHs, the (*R*,*S*,*S*,*R*)-DE2 isomer is the most tumorigenic and the (*S*,*R*,*R*,*S*) enantiomer typically shows modest tumorigenic activity.[7] Interestingly, though B*a*P is a strong carcinogen, the extent of DNA alkylation by its diol epoxides occurs at low levels.[8] In contrast, B*c*Ph is a weak carcinogen, but its diol epoxides alkylate DNA at astoundingly high levels (see the General Introduction).[9] Hence, the extent of DNA alkylation by diol epoxides of different PAHs bears no relation to the carcinogenicity of any specific PAH.[10] All the diol epoxide isomers, however, are good electrophile and are DNA alkylating agents.[1]

DNA alkylation occurs via a S_N1-type of mechanism.[1,11] After a rapid DNA intercalation step, the diol epoxides undergo protonation of the oxirane and ring opening, to form stabilized benzylic carbocations. Then, the exocyclic amino groups of adenine or guanine in DNA act as nucleophiles and trap these cations. This results in covalent bonding to give PAH-DNA adducts (see General Introduction).[1,11]

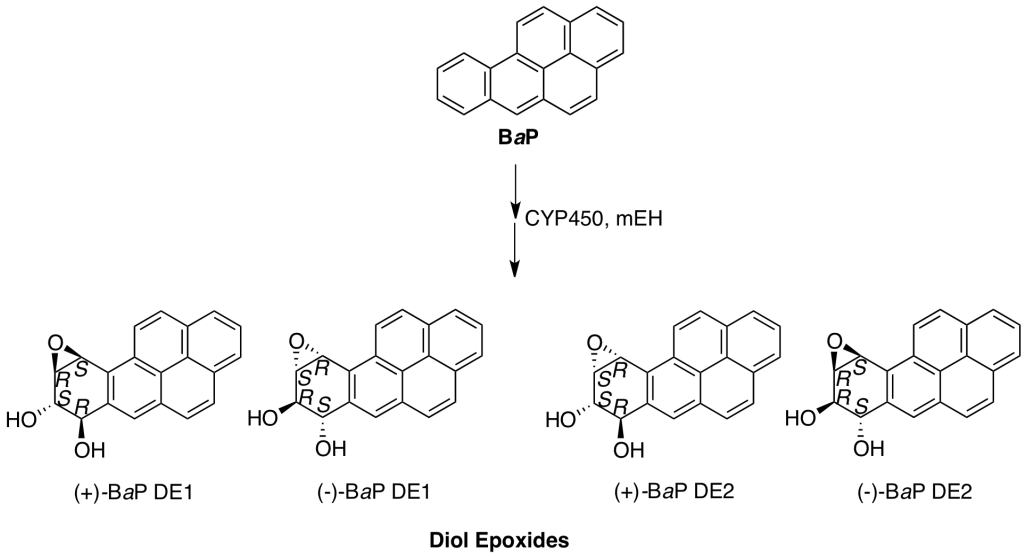

Figure 1. Series 1 and Series 2 Diol Epoxide Isomers of B*a*P.

For each diol epoxide there are four adducts that can be produced in reactions with DNA, via *cis* and *trans* ring opening by 2'-deoxyadenosine (dA) and 2'-deoxyguanosine (dG) (Figure 2, below). Thus, the total adducts resulting from metabolism of any PAH and DNA binding of the four isomeric diol epoxides are sixteen altogether.[1,11] Interestingly, diol epoxides of planar PAHs, such as B*a*P, tend to alkylate the N^2-amino group of 2'-deoxyguanosine residues in the minor groove of DNA.[10,12] DNA alkylation by diol epoxides of non-planar PAHs, such as B*c*Ph, occurs predominately at the N^6-amino group of 2'-deoxyadenosine residues in the major groove of DNA.[10,12] This suggests that DNA alkylation is directly influenced by the shape of the PAHs involved and that various PAH diol epoxide isomers show different 2'-deoxyadenosine/2'-deoxyguanosine adduct ratios.

These isomeric, covalently-bonded PAH-DNA adducts potentially perturb local DNA structures and thereby influence biological processes.[1] For example, they can affect replication and/or repair mechanisms leading to either the introduction of mutations and hence pathways to tumorigenesis (e.g. carcinogenic DE2 isomers), or they can lead to innocuous results such as error-free replication or efficient repair (e.g. inactive DE1 isomers).[1c]

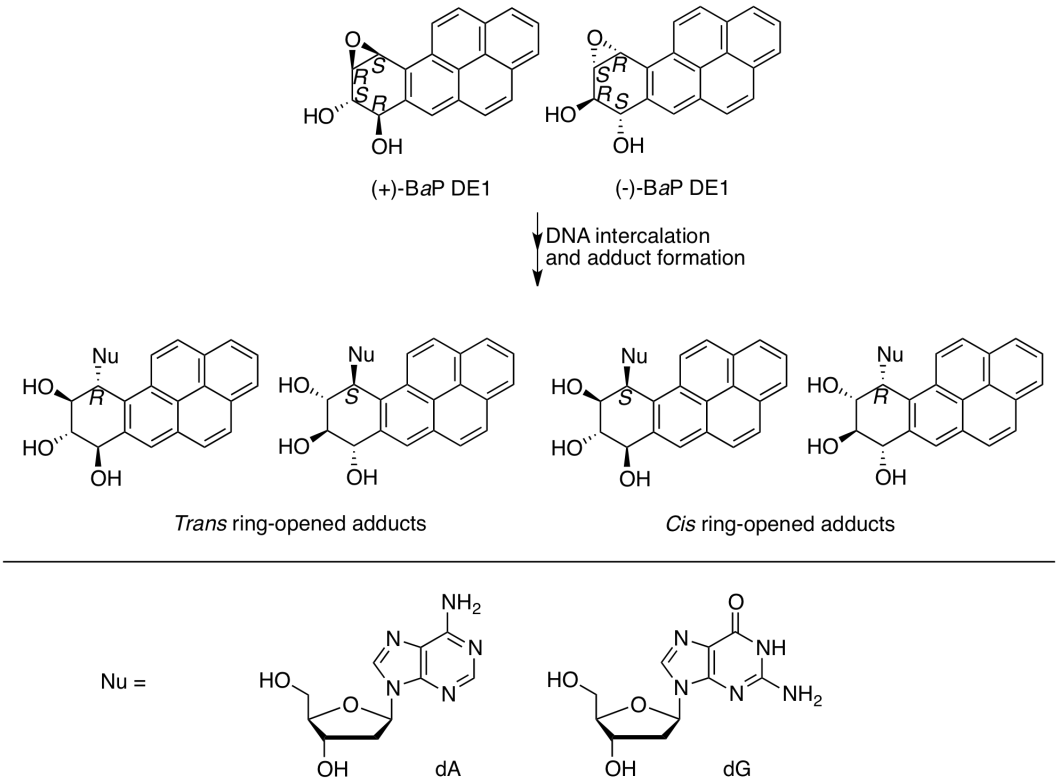

Figure 2. B*a*P DE1 adducts with dA and dG.

As an example, tumorigenic diol epoxides are known to induce DNA damage and mutations in growth-controlling genes, such as tumor suppressor genes (*p*53)[13] and in oncogenes (H-*ras*)[14] during DNA replication. The (*R*,*S*,*S*,*R*)-DE2 of B*a*P (Figure 3), a bay region containing PAH that predominately reacts with the N^2-amino group of 2'-deoxyguanosine, shows G → T transversion mutations within codon 12 of the H-*ras* in mouse skin upon exposure.[15] Similarly, treatment with (*R*,*S*,*S*,*R*)-DE2 of dibenzo[*a,l*]pyrenes (DB[*a,l*]P, Figure 3), a fjord region containing PAH that predominately reacts with the N^6-exocyclic amino group of 2'-deoxyadenosine, shows A → T transversions within codon 61 of the H-*ras* in mouse skin.[16]

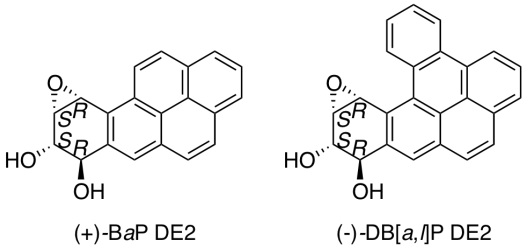

Figure 3. (*R*,*S*,*S*,*R*) Diol Epoxides of B*a*P and DB[*a*,*l*]P.

Based on the forgoing discussion, the following understanding about PAH diol epoxides has emerged: (1) the relative chemical reactivity rates of various diol epoxides, (2) the extent to which various diol epoxides bind to DNA, and (3) the preference for alkylation to adenine or guanine in DNA by the various diol epoxides. However, these have not led to a clear understanding of the molecular basis for chemical carcinogenesis.

Since specific isomers of PAH diol epoxides show different mutagenic and carcinogenic activities, it becomes important to synthesize stereochemically defined diol epoxide nucleoside adduct isomers for site-specific modification of DNA. Such an approach will assist in developing strategies for evaluating the influence of specific DNA adducts on biochemical and biological processes. In this way, a better understanding of specific structural perturbations of DNA induced by various PAH diol epoxides and their influence on intracellular processes can be attained.

There are three general approaches to the site-specific modification of DNA. Scheme 1 summarizes these approaches.

Scheme 1. Three General Approaches to Site-Specific DNA Modification

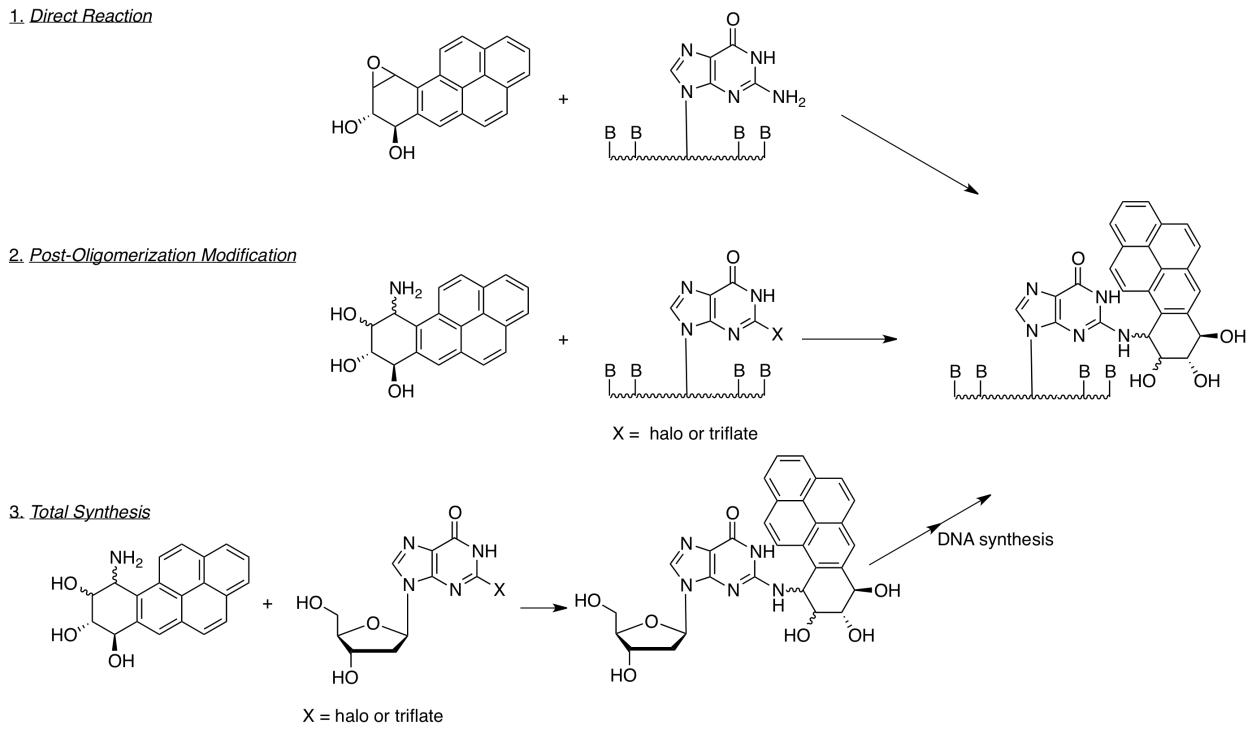

1. *Direct reaction of a diol epoxide and DNA*. This approach, utilized by Loechler et al.[17] and Geacintov et al.,[18] involves the use of specific PAH diol epoxides that are allowed to react directly with short oligonucleotides to be studied. A prime limitation to this method is that the types of adducts as well as quantity of products obtained are determined by the reactivity properties of the PAH diol epoxide used. For example, the B*a*P DE2 preferentially reacts to the N^2-amino group of 2'-deoxyguanosine, while the deoxyadenosine adducts are minor.[15] Alternatively, the DB[*a,l*]P DE2 diol epoxide preferentially binds to the N^6-amino group of 2'-deoxyadenosine, while the deoxyguanosine adducts are minor.[16] Access to minor products however are necessary, as they may play a vital role in biochemical processes leading to mutagenesis and carcinogenesis. Another limitation is that direct reactions of diol epoxides with DNA are low yielding.[15,17,18] This is primarily because of competing hydrolysis. Also, the presence of multiple purines in a DNA sequence increases the likelihood for reactions at multiple sites, giving multiple products. In addition, the extent of reaction of DNA is inherently low due to the poor nucleophilicity of the exocyclic amino group of nucleobases. [15,17,18]
2. *Post-oligomerization modification*. This approach, developed by Harris et al.[19] involves the use of stereochemically defined PAH amino triol derivatives, which are reacted with a matrix-bound oligonucleotide which has a halide- or triflate-containing nucleoside. The stereochemically defined amino triol derivatives correspond to either *cis* or *trans* ring opening of diol epoxides and are synthesized by diastereoselective approaches. The main difference of this approach compared to the previous one is that key *nucleophilic* PAH intermediates are synthesized for reaction with *electrophilic* nucleosides that are within a preassembled DNA oligomer. Hence, in the post-oligomerization approach the nucleophile/electrophile roles are reversed to that of the direct reaction approach. However, problems involving low yields as well as DNA sequence dependence, still remain as limitations to this approach.[19,20]
3. *Total synthesis*. This approach, developed primarily by Lakshman,[21] Zajc,[22] and others,[23] involves synthesis of stereochemically defined nucleophilic amino triol PAH intermediates. These upon reaction with electrophilic (halo[24-27] or triflate[28]) nucleoside derivatives give defined PAH-nucleoside adducts. The adducts are then incorporated into oligonucleotides via solid-phase

DNA synthesis techniques.[21-23,29] Although this approach may be labor intensive because of the synthetic effort required, it enables the development of general methodologies applicable to a broad range of PAHs, as well as their adducts. In addition, this approach offers amelioration of most problems in the direct reaction and post-oligomerization approaches. For example, total synthesis can allow access to *all* possible stereochemically defined PAH-nucleoside adducts. Hence, the minor adduct isomers become accessible. Also, since gram quantities of PAH intermediates are achievable, larger quantities of PAH-DNA adducts that can be generated, and used for studies.[21] For example, DNA sequence variation with any adduct is easily accomplishable. This total synthesis approach therefore is very appealing, and is our preferred route to stereochemically defined B*a*P diol epoxide-nucleoside adducts.

Once PAH-DNA adducts are obtained, studies using site-specifically modified DNAs become possible. There are currently two investigational avenues for studying the structure and function of modified DNAs. These include structural studies and biological studies, and the two approaches are described below:

1. *Solution NMR studies*. This involves structure determination of site-specifically modified DNA using NMR techniques,[30] and to a lesser extent, X-ray diffraction.[31] For the latter, crystal structures of B*a*P diol epoxide-dA or -dG adducts have been extremely elusive. A report by Jerina et al.[31] however shows an example. The absolute configuration and conformation of a *trans* ring-opened B*a*P DE2-N^2-deoxyguanosine adduct was determined through X-ray diffraction. These results were also found to be in good agreement with NMR and CD solution studies.[31] In regards to the NMR studies, a number of solution structures of duplexes containing *cis* and *trans* ring-opened PAH-nucleoside adducts have been evaluated.[30,32-45] The structural trends involving the dG and dA adducts of B*a*P diol epoxides in DNA duplexes are briefly described below and are summarized in Table 1.

   NMR studies of deoxyguanosine adducts have predominately focused on the B*a*P DE2 isomer.[32-36] This is because B*a*P DE2 shows a high preference for dG alkylation.[15] The oligomers were generally prepared by direct reactions of the (±)-diol epoxide with DNA, and **G** represents the adducted deoxyguanosine in that DNA.[17,18] Here, adducts with 10*R* or 10*S* configurations are

defined on the basis of the absolute configuration at the point of attachment of the PAH to the nucleobase.

For adducts with 10*S* configuration, the PAH is oriented towards the 5' end of the modified strand, not intercalated, and resides in the minor groove of the DNA (Table 1, entries 1,4,5).[32,35,36] However, minor conformers are apparent. For example the *cis* ring-opened 10*S* adduct of (*S*,*R*,*R*,*S*) DE2 has the **G** in the minor groove but the complementary C displaced in the major groove, while the PAH is intercalated (Table 1, entry 4).[35]

In adducts with 10*R* configuration, the PAH is oriented towards the 3' end of the modified strand, may or may not be intercalated, and is in the minor groove. Where as the *trans* ring-opened 10*R* adduct of (*S*,*R*,*R*,*S*) DE2 is an apparent single conformer, the *cis* ring-opened 10*R* adduct from (*R*,*S*,*S*,*R*) DE2 has major and minor conformers. The minor conformer is present to an extent of about 15% (Table 1, entry 3). To date, there is no solution structure data on the deoxyguanosine adducts of *cis* ring-opened DE1 B*a*P isomer.

For NMR studies involving deoxyadenosine adducts, both B*a*P DE2 and DE1 isomers have been used, and the adducted oligomers were synthesized by the previously described methods.[16-18] The adducted deoxyadenosine is represented as **A**. Adducts with 10*R* or 10*S* configurations are defined on the basis of absolute configuration at the point of attachment of the PAH to the nucleobase.

In adducts with 10*S* configuration, the PAH is oriented towards the 3' end of the modified strand, is situated in the major groove, and the PAH is intercalated (Table 1, entries 7 and 10).[38,41] The glycosidic bond of the modified dA is *syn* for the major conformer, while for the minor conformer, the glycosidic bond is *anti*. This is evident in both the *trans* ring-opened 10*S* adduct from (*R*,*S*,*S*,*R*) DE2 as well as the *trans* ring-opened 10*S* adduct from (*S*,*R*,*S*,*R*) DE1, and both show multiple conformers (entries 7 and 10).[38,41] Earlier work by Lakshman and Chaturvedi had indicated from thermal denaturation studies that the *trans* ring-opened 10*S* adduct from DE1 exist as a single conformer (along with the trans ring-opened 10R adduct from DE1 and 10R adduct from DE2).[46] The *trans* ring-opened 10*S* adduct from (R,S,S,R) DE2 however seems to indicate multiple conformers and less potential for intercalation.[46] Also, for the 10*S* adduct from (*R*,*S*,*S*,*R*)

DE2, the **A** is mismatched with G (entry 7),[38] whereas for the 10*S* adduct of (*S*,*R*,*S*,*R*) DE1, the **A** has the normal complement with T (entry 10).[41]

In adducts with 10*R* configuration, the PAH is typically oriented towards the 5' end of the modified strand, situated in the major groove, and intercalated. In most studies, the **A** has a complementary T,[39-40,42-45] however in one example the *trans* ring-opened 10*R* adduct from (*R*,*S*,*S*,*R*) DE2 has a mismatched G (Table 1, entry 6).[37] Single and multiple conformers are apparent whether the adducts are derived from DE1 or DE2, and these conformers may or may not disrupt Watson-Crick base pairing. The glycosidic bond for the adducted **A** is usually *anti* for the major conformer, and *syn* for the minor conformer.[39-40,42-45] A descriptive summary of all the features for both dG and dA adducts of BaP diol epoxides are shown in Table 1.

Table 1. Summary of NMR Structure Studies of B*a*P Diol Epoxide Adducted DNA Duplexes

Entry	DNA sequence	Adduct configuration (DE series and configuration)	Ring opening	Features
NMR studies on deoxyguanosine adducts				
1[32]	5'-CCATC**G**CTACC-3' 3'-GGTAGCGAGG-5'	10*S* adduct [DE2 (7*R*,8*S*,9*S*,10*R*)]	*trans*	PAH is oriented towards the 5'-end, not intercalated is in the minor groove. Apparently single conformer.
2[33]	5'-CCATC**G**CTACC-3' 3'-GGTAGCGAGG-5'	10*R* adduct [DE2 (7*S*,8*R*,9*R*,10*S*)]	*trans*	PAH is oriented towards the 3'-end, not intercalated is in the minor groove. Apparently single conformer.
3[34]	5'-CCATC**G**CTACC-3' 3'-GGTAGCGAGG-5'	10*R* adduct [DE2 (7*R*,8*S*,9*S*,10*R*)]	*cis*	Adducted G is displaced into the minor groove, complementary C is displaced into the major groove, PAH resides intercalatively in the pocket created by base displacement. Minor conformer (15%): G:C paired, PAH not intercalated.
4[35]	5'-CCATC**G**CTACC-3' 3'-GGTAGCGAGG-5'	10*S* adduct [DE2 (7*S*,8*R*,9*R*,10*S*)]	*cis*	Adducted G is displaced into the major groove, complementary C is displaced into the major groove, PAH resides intercalatively in the pocket created by base displacement. Minor conformer: conformers in slow equilibrium (could not determine the structure).
5[36]	5'-CCTATGT**G**CAC-3' 3'-GGATACACGTG-5'	10*S* adduct [DE2 (7*R*,8*S*,9*S*,10*R*)]	*trans*	PAH is oriented towards the 5'-end, not intercalated is in the minor groove. Minor conformer: conformers in equilibrium (cannot accurately determine the structure) possibly has the PAH inserted into the duplex with duplex disruption.
NMR studies on deoxyadenosine adducts				
6[37]	5'-GGTC**A**CGAG-3' 3'-CCAGGGCTC-3'	10*R* adduct [DE2 (7*S*,8*R*,9*R*,10*S*)]	*trans*	PAH is intercalated, situated in the major groove and towards the 5'-end, complementary G is displaced into the

				major groove. Minor conformer (20%): in slow equilibrium with major conformer.
7[38]	5'-GGTC**A**CGAG-3' 3'-CCAGGGCTC-3'	10*S* adduct DE2 (7*R*,8*S*,9*S*,10*R*)	*trans*	PAH is intercalated, situated in the major groove and towards the 3'-end, modified A and complementary G remain hydrogen-bonded, but modified A has a *syn* glycosidic bond. Minor conformer (17%): The modified A has an *anti* glycosidic bond, partial unwinding occurs to accommodate the intercalated PAH and to maintain the A:G H-bonds, C-7 O of the PAH hydrogen bonds to the NH of the 3'-C adjacent to the modified A.
8[39]	5'-CGGTC**A**CGAGG-3' 3'-GCCAGTGCTCC-3'	10*R* adduct [DE1 (7*R*,8*S*,9*R*,10*S*)]	*trans*	PAH is intercalated and towards the 5'-end, modified A and complementary T are base-paired.
9[40]	5'-CTCTC**A**CTTCC-3' 3'-GAGAGTGAAGG-5'	10*R* adduct [DE2 (7*R*,8*S*,9*S*,10*R*)]	*cis*	PAH is oriented towards the 5'-end of the modified strand and is intercalated without disruption of the modified base pair.
10[41]	5'-CGGTC**A**CGAGG-3' 3'-GCCAGTGCTCC-5'	10*S* adduct [DE1 (7*S*,8*R*,9*S*,10*R*)]	*trans*	PAH is intercalated and towards the 3'-end of the modified strand, glycosidic bond of modified dA is *syn* in major conformer. Minor conformer: glycosidic bond of modified dA is *anti*. Speculation: H-bonding between 7-OH and N-7 of G in complementary strand perhaps slows rate of interconversion.
11[42]	5'-CGGTC**A**CGAGG-3' 3'-GCCAGTGCTCC-5'	10*R* adduct [Tetrahydro epoxide (9*S*,10*R*)]	*cis*	PAH is oriented towards the 5'-end of modified base. Adducted dA is *anti* with no disruption of Watson-Crick base pairing. Lack of C-7 and C-8 hydroxyls: deeper and more effective stacking of the PAH.
12[43]	5'-CGGAC**A**AGAAG-3' 3'-GCCTGTTCTTC-5'	10*R* adduct DE-2 (7*S*,8*R*,9*R*,10*S*)	*trans*	PAH is intercalated from the major groove and is towards the 5'-end, modified A to complementary T H-bonding disrupted, single conformer. Normal glycosidic torsion angle for the modified nucleoside.
13[44]	5'-CGGACA**A**GAAG-3' 3'-GCCTGTTCTTC-5'	10*R* adduct [DE2 (7*S*,8*R*,9*R*,10*S*)]	*trans*	Two distinct conformations in rapid equilibrium, the PAH is intercalated and pointed towards the 5'-end of the modified A in each case.
14[45]	5'-TAGTCA**A**GGGCA-3' 3'-ATCAGTTCCCGT-5'	10*R* adduct [DE2 (7*S*,8*R*,9*R*,10*S*)]	*trans*	PAH is intercalated and towards the 5'-end of modified strand. Dynamic behavior, predominant *anti* glycosidic torsion of the modified dA, minor is *syn* (less pronounced than in the 10*S* adduct).

2. *Biochemical and biological experiments*. The use of shuttle vectors such as pZ189,[47] M13mp7L2[48] and *E. Coli*[49] have been utilized to study the mutational consequences of DNA

modified with PAH diol epoxides. Studies on the types of mutation, DNA replication and repair induced by specific modified adducts have been carried out.[7,50-57] For example, the UvrABC repair system that recognizes lesions in DNA is greatly influenced by subtle differences in adduct conformation, which affects the excision repair process.[56,57] In this regard a study by Van Houten, Basu and Geocintov et al.[56] examined the rates of UvrABC incision. Here, UvrA recognizes conformational changes induced by structurally different lesions, and where the binding affinities of UvrA and UvrB are correlated with the rates of incision. Incisions can occur between 4 to 8 phosphates from the modified dG adduct and varies with the diol epoxide present. Also, for damaged site with mismatched bases, the size of the bubble formed around that region appears to influence the incision rates.[56] In another study, Zou, Basu and Geocintov et al.[57] compared the efficiencies of UvrABC incision for different types of DNA adducts. For example, the C8-guanine adducts of 2-aminofluorene showed the best incision efficiency in a bubble of three mismatched nucleotides; whereas, the larger N^2-guanine adduct of a *cis* ring-opened B*a*P DE2 showed the best incision efficiency in a bubble of six mismatch nucleotides. This indicates that depending on the size of the aromatic system presiding on the adduct, the extent and number of bases associated with the opened strand region undergoing catalysis by UvrABC, may affected. In addition, the incision efficiency can be affected by the neighboring DNA sequence context, which in turn, is due to differential binding of UvrA to the substrates.[57] Further, studies have proposed that intercalated adducts with minimal duplex distortion are less likely to be repaired compared to groove-bound ones.[58]

Studies involving the different roles of DNA polymerases are also of interest. The recently discovered Y family DNA polymerases has shown interesting activities with B*a*P diol epoxide adducts.[59-62] For example, DNA polymerase ζ has been observed to bypass B*a*P DE-dG adducts in yeast cells.[59] DNA polymerase κ, on the other hand, protects mammalian cells against the mutagenic effects of B*a*P by successfully cleaving the undesired lesions.[62b]

Adducts are also known to influence topisomerases. For example, B*a*P DE2 adducts have been found to be potent suppressors of normal Topisomerase I, and in turn promote new cleavage complexes 3-6 bases away from the lesion site.[63-66]

From the foregoing, it becomes evident that in order to have a better understanding of the differences in biological activities elicited by different PAH-DNA adducts, which may or may not produce mutational events and tumorigenesis, a combined effort involving synthetic strategies, structural studies, biochemical and biological experiments are needed. The overall goal is to establish structure-biology relationships that will provide adequate insight into the nature of DNA damage and the ensuing biological output. In this regard, this work, and those of others, [23,67b,69,70-73] have been heavily involved in synthetic studies that offer *facile* and *general* routes to PAH metabolites, stereochemically defined PAH-nucleoside adducts, and PAH-DNA adducts. The information that follows describes various syntheses of series 1 and series 2 B*a*P diol epoxides, and their respective adducts. The data also provides the necessary background for the current work.

The total synthesis approach to PAH-DNA adducts is appealing since it allows for the scalable diastereoselective synthesis of all possible isomers.[21-23] In this approach, reaction between electrophilic nucleosides and nucleophilic amino PAH derivatives yield PAH-nucleoside adducts. These adducts are then appropriately functionalized and incorporated into DNA oligomers using solid-phase synthesis procedures.[29]

The electrophilic nucleosides typically needed for PAH-nucleoside adduct synthesis are fluorinated purine nucleosides.[24] The high reactivity of these nucleosides are necessary for the S_NAr displacement reactions with poorly-nucleophilic, sterically-hindered amino PAH derivatives.[21-23,67] For dA adducts, 6-fluoro-9-(2-deoxy-β-D-*erythro*-pentofuranosylpurine (6-FP) is used, while for dG adducts, 2-fluoro-2'-deoxyinosine (2-FdI) is utilized (Figure 4).[21-24] A C-2-triflate derivative of 2'-deoxyxanthosine (2-TdX) has also been employed in such displacement reactions, for example O^2-trifluoromethanesulfonyl-O^6-(*p*-nitrophenethyl) 2′-deoxyxanthosine.[28] More recently, Pd catalyzed C–N bond formation of bromo and chloro purine nucleosides and tribenzoyl protected amino triols have also been utilized for PAH-nucleoside adduct synthesis.[25-27] This now allows for the use of the more easily available halopurine nucleosides that are otherwise not reactive enough for this purpose.

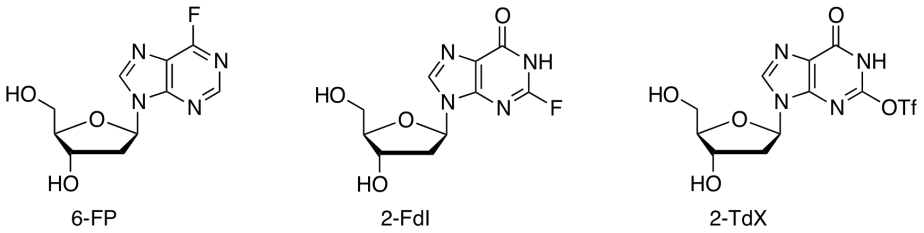

Figure 4. Structures of Nucleoside Derivatives Utilized in PAH-Nucleoside Adduct Synthesis.

For diastereoselective access to nucleophilic PAH intermediates that correspond to *trans* or *cis* ring-opened DE1 or DE2 isomers, several synthetic strategies have been developed. Diol epoxides can be directly converted to amino triols via aminolysis,[21a,46] or converted to azido triols via reaction with azide anion.[68,69] These azido triols are typically converted to azido tribenzoates via benzoyl protection, catalytically hydrogenated to give amino tribenzoates.[27,46,68,69] The amino derivatives are then reacted with electrophilic nucleosides to yield PAH diol epoxide-nucleoside adducts. In this context, Lakshman, Zajc and coworkers[21,22,27,46,67a,68] and others,[23,67b,69] have utilized this approach to synthesize amines arising from a *trans* ring opening of both (±)-B*a*P DE1 and DE2 isomers as a means for synthesis of DNA adducts (Scheme 2).

Scheme 2. General *Trans* Ring Opening of Series 1 and Series 2 B*a*P Diol Epoxide Isomers Using Aminolysis or by Azide Anion

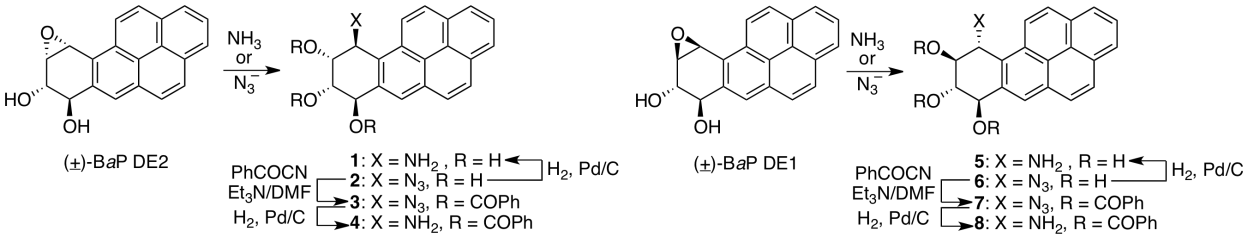

Generally, *trans* ring opening of B*a*P diol epoxides by direct aminolysis or by azide anion is quite facile and trouble-free. Thus, most NMR studies of DNA adducts obtained by total synthesis have focused on those derived from the *trans* ring opening of diol epoxides. On the other hand, the synthesis of *cis* ring-opened B*a*P amino triol derivatives is non-trivial, and they are less readily obtained.

In this context, Meehan and Jhingan[70] reported a highly diastereoselective *cis* ring opening of a B*a*P DE2 derivative. In this procedure, reaction of the 7,8-bistrimethylsilyl ether derivative of (±)-B*a*P DE2 (**9**) with trimethylsilyl azide (TMS-N_3), and titanium isopropoxide [$Ti(OiPr)_4$], in THF gave an azido B*a*P derivative [(±)-**10**]. This azido derivative was reported as a single isomer and was obtained in a yield of

90% (Scheme 3).[70] Desilylation, followed by catalytic hydrogenation then led to the desired *cis* ring-opened amino triol (±)-**11**. Notably, no rationale for the high selectivity observed in this procedure is currently available.

Scheme 3. *Cis* Ring Opening of (±)-B*a*P DE2 with TMS-N_3 and $Ti(OiPr)_4$ Giving (±)-**11**

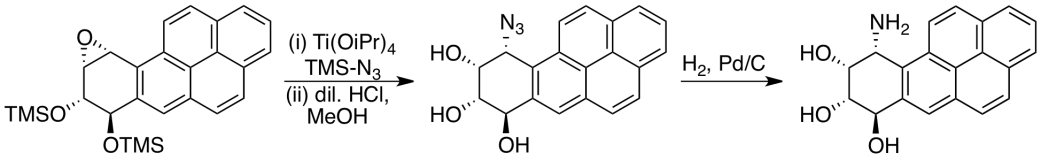

(±)-**9** (±)-**10** (±)-**11**

As an alternative, there is a strategy that circumvents the need for amino triol derivates as key intermediates in the synthesis of *cis* ring-opened B*a*P DE2-2'-deoxyadenosine adducts.[71b] The procedure utilizes an amino hydroxylation protocol[71a] by reaction of the exocyclic amino group of a silyl protected dA with (±)-*trans*-7,8-dihydroxy-7,8-dihydro B*a*P to give the corresponding *cis* opened DE2 adduct.[75b] Thus, reaction of **12** with (±)-**13**, in the presence of *tert*-butyl hypochlorite, catalytic $(DHQD)_2PHAL$, and $K_2OsO_2(OH)_4$ in *n*-propanol, gave a 1:1 mixture of the diastereomeric adduct pair **14a** and **14b**, in a yield of 85% (Scheme 4).[71b] Although this method worked well for synthesis of *cis* dA adducts of (±)-B*a*P DE2, the method could not be applied to the synthesis of dG adducts.[71b]

For *cis* ring-opened dG adducts of (±)-B*a*P DE2, the direct ring opening of the racemic diol epoxide with a protected dG has been reported.[72,73] These generally result in low diastereoselectivity, giving mixtures of *cis* and *trans* dG adducts in low yields (5-54%). This can be problematic for separation.[72,73] Hence, for diastereoselective access to *cis* ring-opened B*a*P DE2 adducts of dG (and dA), Lakshman and co-workers have developed a novel approach.[74]

Scheme 4. Synthesis of *Cis* Ring-opened (±)-BaP DE2 dA Adducts using Silyl Protected dA and (±)-*trans*-7,8-dihydroxy-7,8-dihydro B*a*P

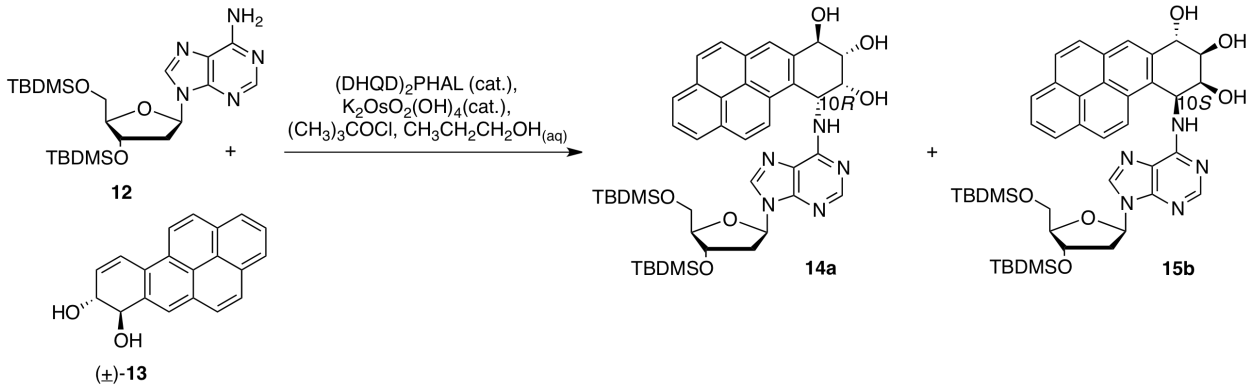

The synthesis reported by Lakshman and co-workers not only provides a highly diastereoselective access to the *cis* ring-opened amino triol but also demonstrates the first synthesis of *cis* dG, and both *cis* dA and dG adducts of B*a*P DE2 are obtained from a common intermediate.[74] Synthesis of (±)-10*α*-amino-7*β*,8*α*,9*α*-trihydroxy-7,8,9,10-tetrahydro B*a*P [(±)-**11**)], began from a 7,8-bis-benzoyloxy-7,8-dihydro B*a*P derivative (±)-**16**, which is also a key intermediate for the present work (Scheme 5).

Scheme 5. Diastereoselective Synthesis of *Cis* Ring-opened B*a*P Amino Triol (±)-**11**

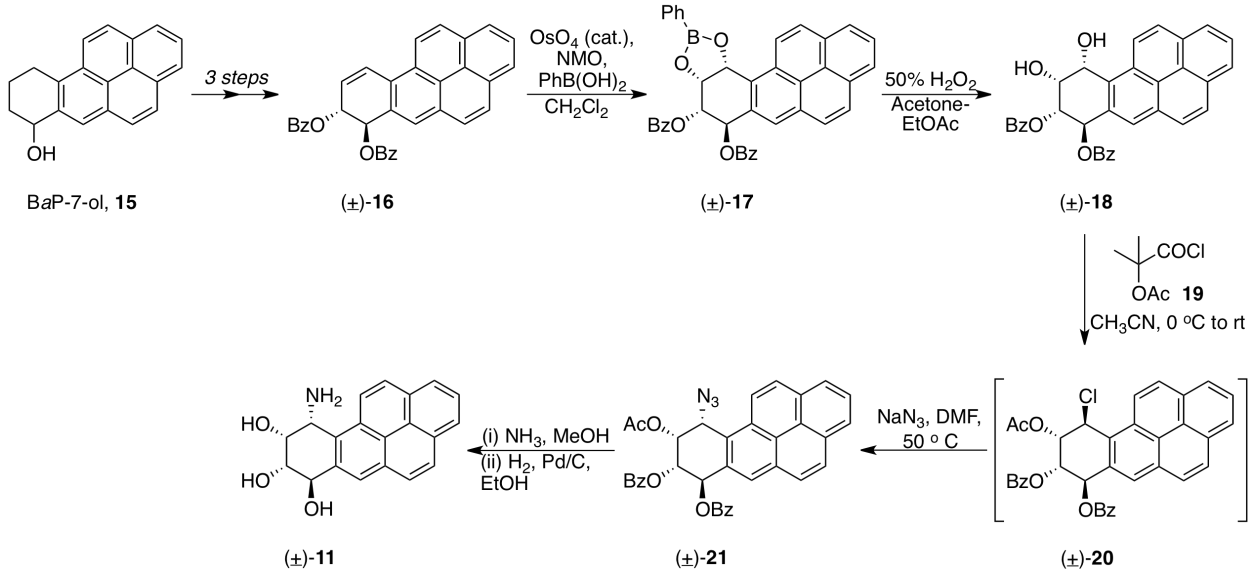

This dihydrodibenzoate derivative (±)-**16** can be obtained in three steps from commercially available 7,8,9,10-tetrahydrobenzo[*a*]pyren-7-ol (B*a*P-7-ol, **15**).[75] Dihydrodibenzoate (±)-**16** undergoes a

highly diastereoselective dihydroylation with catalytic OsO_4 and NMO in CH_2Cl_2. Here, phenylboronic acid is used as a water surrogate.[76] The resulting boronate ester (±)-**17** was obtained as a single isomer and was then oxidized using 50% H_2O_2 in EtOAc-acetone to give the tetraol dibenzoate (±)-**18**.[74]

Next, the chemistry for (±)-**18** → (±)-**21**, relied on previously described work by Lakshman and Zajc.[77] In that work, aryl substituted *cis* aminoalcohols were obtained from aryl substituted *cis* diols. Reaction of *cis* diols with 1-chlorocarbonyl-1-methylethyl acetate (**19**), in acetonitrile, results in the formation of *trans* monochloro acetates where the chloride is benzylic (Scheme 6, **23**). Displacement of the chloride using azide anion, followed by deprotection of the acetate, and reduction of the azide, gave the requisite *cis* aminoalcohols **25** (Scheme 6), where the amino groups is benzylic.[77]

Scheme 6. Synthesis of Aryl Substituted *Cis* Aminoalcohols from Aryl Substituted *Cis* Diols

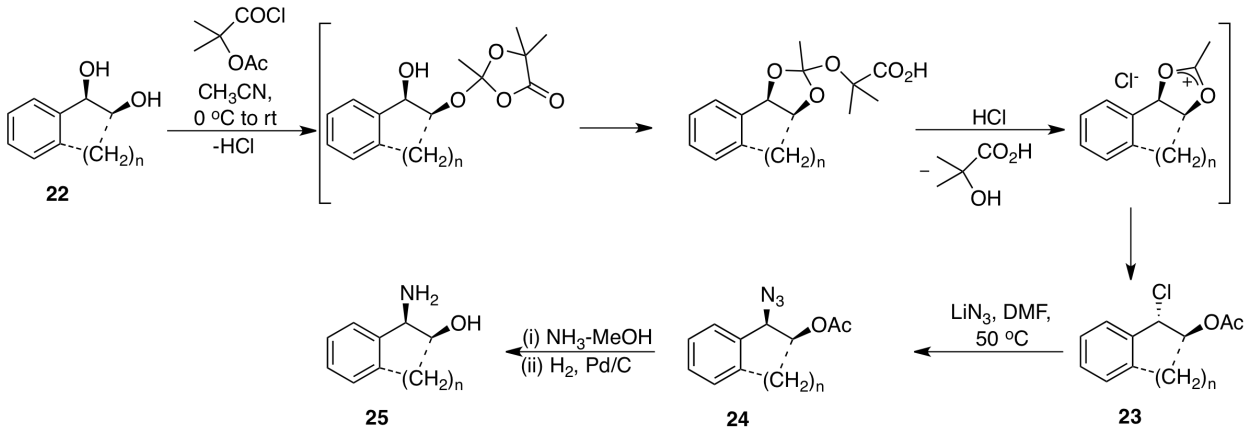

Using similar chemistry, reaction of (±)-**18** with 1-chlorocarbonyl-1-methylethyl acetate (**19**) in acetonitrile gave a *trans* chloro monoacetate intermediate (±)-**20** (Scheme 5).[74] Displacement of chloride from intermediate (±)-**20** by NaN_3 in DMF at 50 ºC gave the *cis* azido triol (±)-**21**, in a yield of 61% over 2 steps. After assignment of relative stereochemistry by NMR, which indicated the desired outcome, hydrolysis followed by catalytic reduction of the azide gave the *cis* amino triol (±)-**11** (Scheme 5).[74] Reaction of amino triol (±)-**11** with silyl protected 2-FdI and 6-FP derivatives led to diastereomeric pairs (10*R* and 10*S*) *cis* ring-opened B*a*P DE2 dG adducts and dA adducts.[74] The respective adducts were then separated and characterized.

To help understand the diastereoselectivity observed in the key dihydroxylation step in this synthesis [Scheme 5, (±)-**16** → (±)-**17**)], the relative energies of formation for the boronate diastereomers and the diol diastereomers were evaluated.[74] The energies showed that the boronate ester **17** and diol

18 (*cis* α isomers) were more energetically favorable than their *cis* β counterparts. A prediction of plausible transition state structures that may account for the observed facial selectivity was also proposed. Osmium (Os) may add to the dihydrodibenzoate (±)-**16**, via a more favorable TS1 (Figure 5).[74] This is because the all-staggered conformation is likely to avoid torsion strain, as opposed to TS2, where eclipsing interactions are possible (Figure 5).[74] Hence, torsion controlled addition by the Os to the dihydrodibenzoate was likely an important factor that influenced the stereochemical outcome. This resulted in the desired *cis* boronate and *cis* diol required for the remaining synthesis.[74] A similar result was also obtained with a bis-TBDMS analog of (±)-**16**.[74]

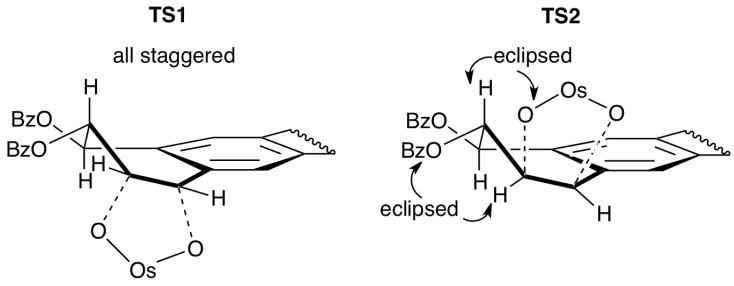

Figure 5. Two Plausible Transition State Structures for the Addition of the OsO_4 to Dihydrodibenzoate (±)-**16**.

Diastereoselective *cis* ring opening of (±)-B*a*P DE1 has been considerably more difficult. In this regard, some work has been done by Jerina and co-workers.[71b] Using the procedure developed by Meehan and Jhingan that produced a single diastereomeric *cis* ring-opened amino triol B*a*P from DE2 (Scheme 3, (±)-**11**),[70] Jerina and coworkers attempted a *cis* ring opening of B*a*P DE1 (Scheme 7, below).[71b] Here, the 7,8-bistrimethylsilyl ether derivative of (±)-B*a*P DE1 (**26**) was stirred with TMS-N_3 and $Ti(OiPr)_4$ in THF, at room temperature. After completion of this reaction and desilylation, the desired *cis* [(±)-**27**, 58%] and undesired *trans* [(±)-**28**, 31%] azido triols were obtained in a 1.5:1 ratio.[71b] Thus, this method did not result in a single isomer. However, the route did allow access to the requisite *cis* ring-opened azido triol diastereomer. The azido triol **27** was separated by HPLC and then catalytically reduced to give the *cis* ring-opened amino triol of B*a*P DE1, (±)-**29**. Amino triol (±)-**29** was then used to displacement fluoride from silyl protected 6-FP (**30**), to give a diastereomeric pair of 10*R* and 10*S* B*a*P DE1 dA adducts **31a** and **31b** respectively.[71b] Since this methodology gave a mixture of *cis* azido triol (±)-

27, along with the *trans* isomer [(±)-**28**] en route to the desired amino triol (±)-**27,** there is still the need for a highly diastereoselective route to (±)-**29**.

Scheme 7. *Cis* Ring Opening of B*a*P DE1 Amino Triol (±)-**29** and Synthesis of the dA Adducts

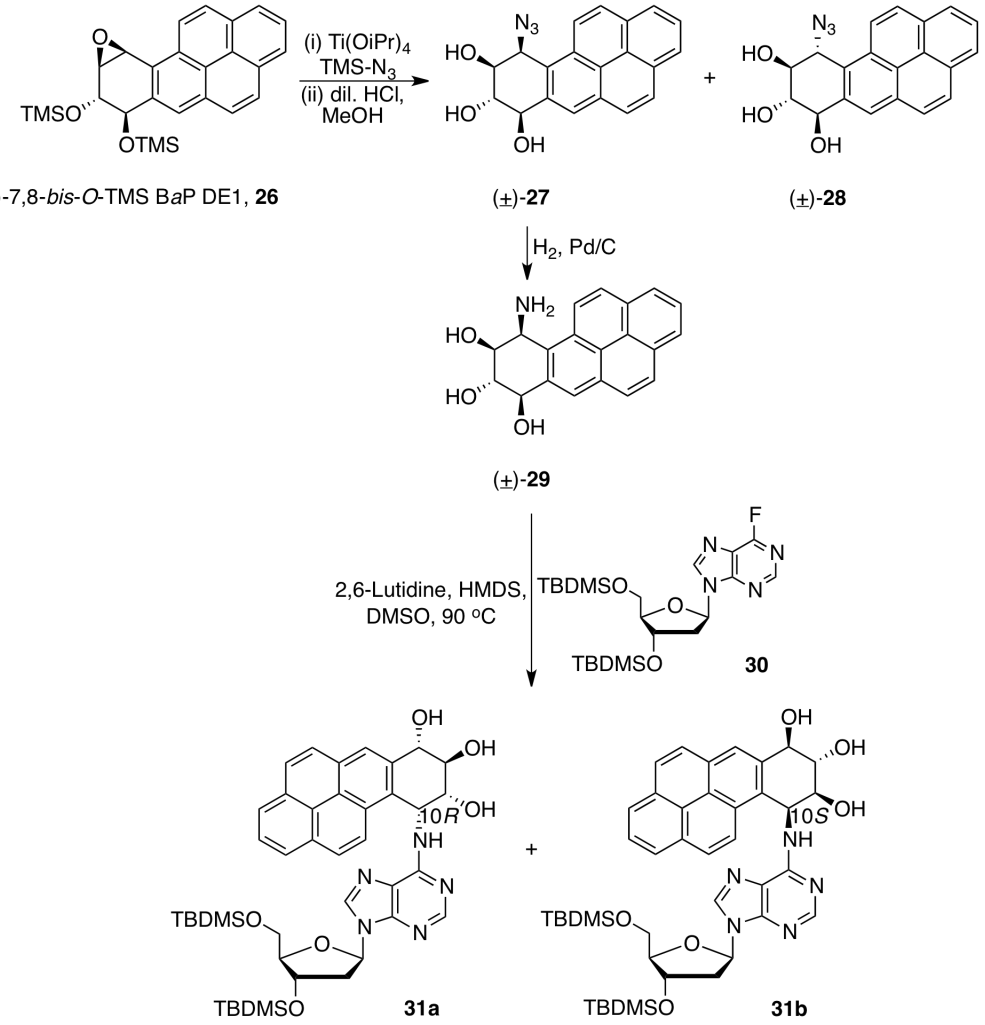

On the basis of previous work, and our interest in developing general strategies for diastereoselective syntheses of PAH amino triols, we aimed to develop a diastereoselective route to the synthesis of 10*β*-amino-7*β*,8*α*,9*β*-trihydroxy benzo[*a*]pyrene derivative (**29**). This PAH derivative is required in order to complete the total synthesis of all sixteen nucleoside adducts from the B*a*P diol epoxides. Using this amino triol, we anticipate completing the synthesis of the 2 *cis* ring-opened BaP DE1 dA adducts and 2 *cis* ring-opened BaP DE1 dG adducts, the latter of which has not been synthesized (Scheme 8, below).

The synthesis of these stereochemically defined diol epoxide-nucleoside adducts are important for studies involving site-specific modification of DNA. The knowledge to be obtained will help towards having a better understanding of how specific DNA adducts perturb DNA, and how these structures influence biochemical and biological processes. The present work describes the stereoselective synthesis of the B*a*P amino triol **29**. This is a lynch pin intermediate in the *cis* ring-opened B*a*P DE1 adducts of synthesis of the 2'-deoxyadenosine and 2'-deoxyguanosine.

Scheme 8. Anticipated dA and dG Adducts from the *Cis* Ring-opened B*a*P Amino Triol (±)-**29**

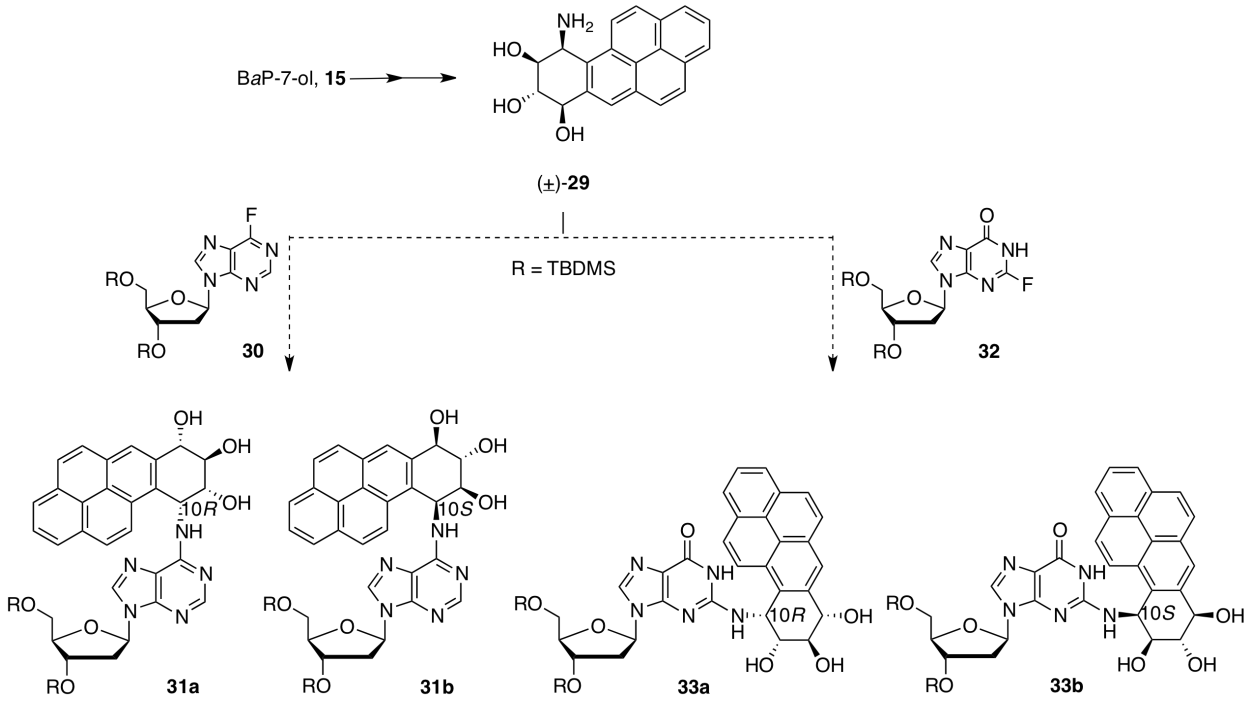

4.2 Results and Discussion

Initial development for the stereoselective synthesis of the *cis* ring-opened B*a*P DE1 amino triol (±)-**29** was based on the synthetic strategy and rationale that was utilized for synthesis of the *cis* ring-opened BaP DE2 derivative (±)-**11**.[74] As previously discussed, the addition of the OsO_4 to the dihydrodibenzoate (±)-**16** occurred in a face-selective fashion (Figure 5). Thus, dihydroxylation occurred from the same face as the allylic benzoate in (±)-**16,** resulting in the single diastereomer (±)-**18** (Scheme 5).[74] Reaction of **18** with 1-chlorocarbonyl-1-methylethyl acetate (**19**) and then azide anion, led to the azido triol derivative (±)-**21**. Hydrolysis and catalytic reduction, gave the desired amino triol (±)-**11** (Scheme 5).[74]

With this understanding, we reasoned that the requisite B*a*P amino triol (±)-**29** could also be readily obtained by suitable diastereoselective addition reactions using the dihydrodibenzoate (±)-**16**. To this end, we proposed three synthetic routes based on the known addition reactions from the literature: (1) $Zn(OTf)_2$/NBS/TMS-N_3,[78] (2) I-Cl/NaN_3,[79] or (3) I_2/AgNCO.[80] Reaction of an electrophile with (±)-**16**, was expected to proceed via TS3 in Figure 6. This resulting intermediate could undergo ring opening by azide or isocyanate to give (±)-**34**, (±)-**36**, or (±)-**37** respectively (Scheme 9). Inversion of chirality can be achieved by displacement of the halide with a suitable nucleophilic acetate, such as CsOAc.[81] This should give the requisite *cis* ring-opened derivative (±)-**35** and (±)-**38**. Reduction of (±)-**35** or hydrolysis of (±)-**38,** should then result in the desired *cis* amino triol (±)-**29** (Scheme 9).

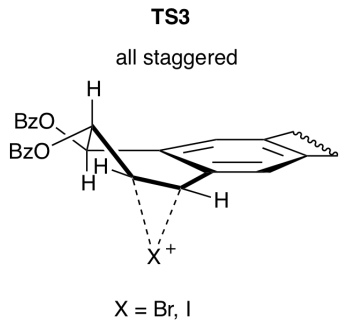

Figure 6. Plausible Transition State Involving Addition of X^+ to Dihydrodibenzoate (±)-**16**.

Scheme 9. Planned Synthetic Routes to the *Cis* Ring-opened Amino Triol from B*a*P DE1 (±)-**16**

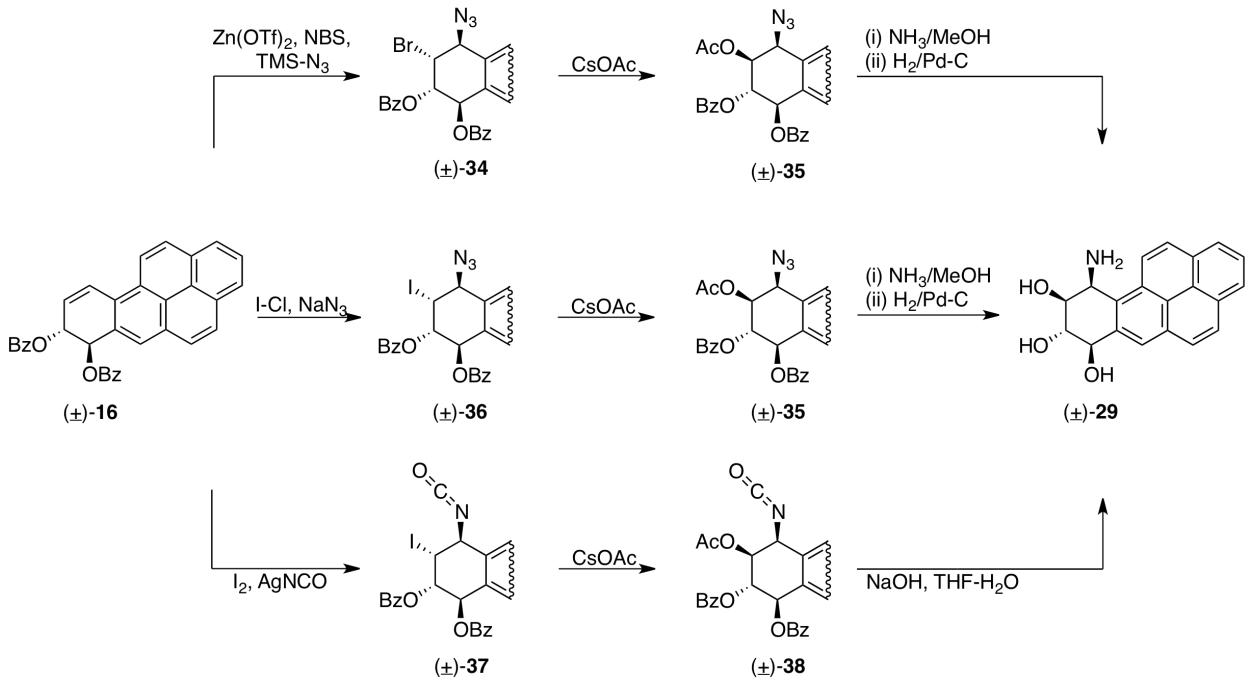

We anticipated these reactions to proceed in a regio- and stereo-controlled manner based on the chemistry with the DE2 isomer.[74] Further, the types of transformation chemistry shown in Scheme 7 have been reported for simpler aryl-substituted olefinic systems.[78-80] In the context of PAH reactions, the expected formation of the iodonium or bromonium intermediate (Figure 6) is consistent with the known reaction of (±)-**16** with *N*-bromoacetamide/H_2O (Scheme 10, (±)-**39**).[82] Here, a face-selective formation of the bromonium ion occurs from the same side as the allylic benzoate and attack of water occurs at the benzylic carbon from the opposite side, leading to bromohydrin (±)-**40**.[82] In fact, synthesis of this bromohydrin has been accomplished in consistently good yields of 70-88% by us.

Scheme 10. Synthesis of (±)-7β,8α-Bisbenzoyloxy-9α-bromo-10β-hydroxy-7,8,9,10-tetrahydrobenzo[*a*]pyrene, (±)-**40**

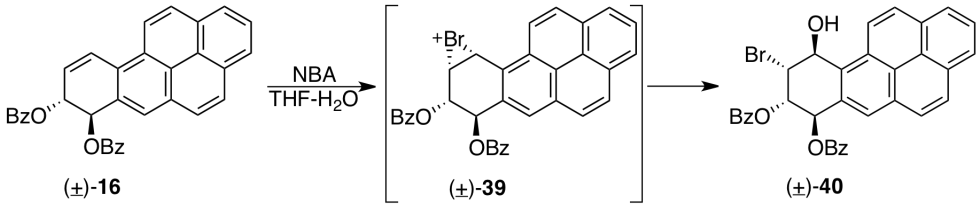

Synthesis of B*a*P dihydrodibenzoate (±)-**16** was needed for this work. This was achieved in three steps from commercially available B*a*P-7-ol **15** (Scheme 11).[75] First, B*a*P-7-ol **15** was dehydrated using

p-toluenesulphonic acid (*p*-TsOH) in refluxing benzene (or toluene) for 25 mins. This gave 7,8-dihydro B*a*P derivative **41** in a yield of 96%. Alkene **41** was then subjected to the Prévost reaction using iodine and silver benzoate in refluxing benzene (or toluene) for 16 h to give the *trans* dibenzoate (±)-**42** in a yield of 83%. Dehydrogenation of (±)-**42** using 2,3-dichloro-5,6-dicyano-1,4-benzoquinone (DDQ) in refluxing benzene (or toluene) for 17 h led to the desired 7,8-*bis*-benzoyloxy-7,8-dihydro B*a*P derivative (±)-**16** in a 70% yield (Scheme 11).

Scheme 11. Synthesis of 7,8-*bis*-Benzoyloxy-7,8-dihydro B*a*P derivative (±)-**16** from Commercially Available 7,8,9,10-Tetrahydrobenzo[*a*]pyren-7-ol (B*a*P-7-ol, **15**)

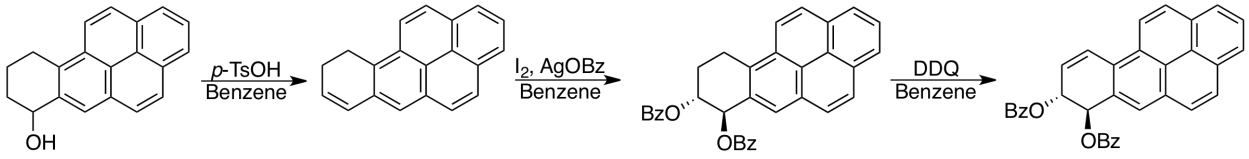

15 **41** (±)-**42** (±)-**16**

Synthesis of bromo azide derivative (±)-**34** shown in Scheme 9 was attempted from (±)-**16**.[78] Using $Zn(OTf)_2$ as a catalyst in CH_2Cl_2, the bromo azidation of (±)-**16** using NBS and TMS-N_3 was achieved in 1 h at 0 ºC, and gave a 59% yield of (±)-**34**. Next, displacement of the C-9 bromide in (±)-**34** was attempted (Scheme 9), using of CsOAc in DMF at 80 ºC.[81] However, after 24 hour of stirring the reaction was practically incomplete with 95% recovered starting material. Modifications to this method, some of which included, drying of all reagents, use of an inert N_2 or Ar atmosphere, increasing the molar equivalence of CsOAc, and addition of 18-crown-6 to increase the nucleophilicity of the acetate, all led to incomplete reactions and/or undesired results.

We then envisioned synthesis of the B*a*P iodo azide (±)-**36** (Scheme 9) as an alternative.[79] In initial model experiments, we utilized the synthetically less valuable **41** to test feasibility (Scheme 12). Reaction of **41** with ICl and NaN_3 in CH_3CN at 0 ºC, gave 70% of the iodo azide derivative (±)-**43** after 3 h. Displacement of the iodide in (±)-**43** was then attempted. Unfortunately, several attempted reactions involving 18-crown-6 and CsOAc in DMF, led to incomplete reactions and undesired non-productive results.

Scheme 12. Model Reaction towards Synthesis of *Cis* Ring Opened B*a*P Azido Acetate Derivative (±)-**44**

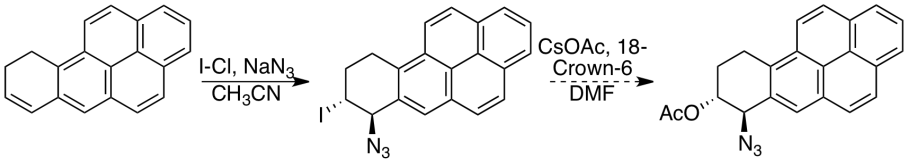

41 (±)-**43** (±)-**44**

Since displacement of the halide at the C-9 position by acetate anion was difficult to achieve, we envisioned intramolecular halide displacement from suitable halo-amidated products instead (Scheme 13).[83,84] Here, once the halo-amide is synthesized, deprotonation and formation of an oxazoline, followed by hydrolysis, should provide the requisite amino triol (±)-**29** (Scheme 13). Again, as a test case, compound **41** was subjected to haloamidation using 10% $InBr_3$ and NBS in CH_3CN at room temperature,[83] in an attempt to obtain compound (±)-**45** (Scheme 13, eq. 1). After two attempts however, undesired products were obtained by this procedure.

In the second case we utilized dihydrodibenzoate (±)-**16**, which was subjected to stereoselective bromo amidation under Ritter-type conditions reported by Corey et al.[84] (Scheme 13, eq. 2). Unfortunately, use of NBA with boron trifluoride etherate in CH_3CN, and water, led to the formation the bromohydrin derivative (±)-**40** shown in Scheme 8, instead of the expected bromo amide (±)-**48**.

Scheme 13. Synthesis of Potential Bromo Amide B*a*P Derivatives

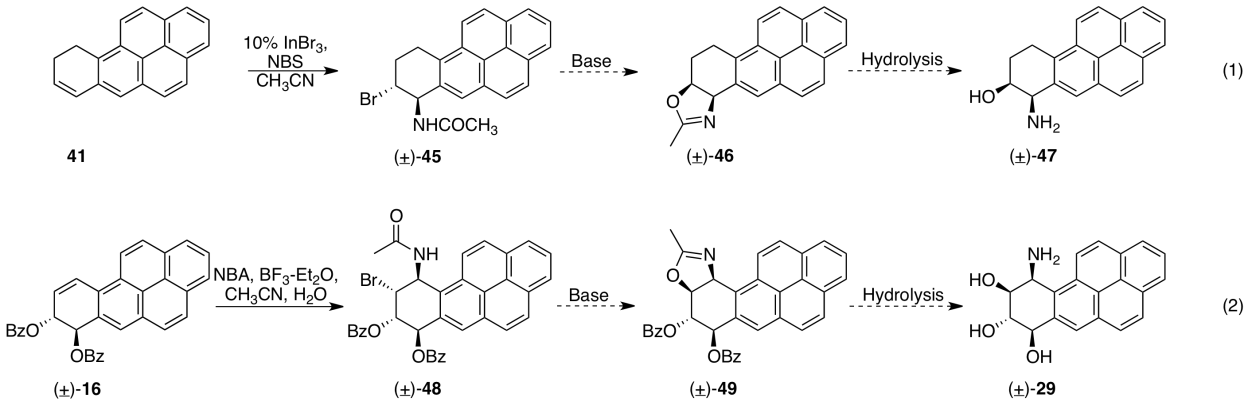

41 (±)-**45** (±)-**46** (±)-**47**

(±)-**16** (±)-**48** (±)-**49** (±)-**29**

Due to the inefficiency of the methods proposed earlier, we considered other approaches. Bromohydrin (±)-**40** is a precursor to BaP DE1 dibenzoate (±)-**50** (Scheme 14). Synthesis of (±)-**50** can be accomplished from bromohydrin (±)-**40** with NaH in THF at 0 ºC in 1 h,[27] and in our hands this gave

appreciably good yields (79-84%). Alternatively, (±)-**50** can be obtained from (±)-**40** using Amberlite IRA-400 (hydroxide form) resin in THF over 3 days (92% yield).[82]

Scheme 14. Synthesis of the Series 1 Diol Epoxide Dibenzoate Derivative of BaP, (±)-**50**

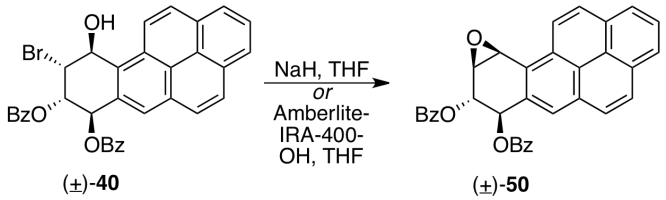

(±)-**40** (±)-**50**

We envisioned a route to the *cis* ring-opened amino triol (±)-**29** involving use of the dibenzoate derivative (±)-**50**. The epoxide could undergo a facially selective ring opening by a nucleophile, which in turn can be displaced by azide anion, at the more reactive benzylic carbon (Scheme 15). Support for this idea stems from the previously described work by Lakshman and Zajc (Scheme 6)[77] and Lakshman et al. (Scheme 5)[74] involving displacement of chlorides from *trans* chlorohydrin intermediates using azide yielding a *cis* stereochemistry. Further support for this idea can be found in work described by Meehan et. al.[85] Here, *tran* chlorohydrin intermediates were made from (*R*,*S*,*S*,*R*) B*a*P DE2 using NaCl. These *trans* chlorohydrins then undergo S_N2 inversion of configuration by direct reaction with the exocyclic amino group of dA to give preferentially *cis* adducts.[85] For example, in the presence of 175 mM NaCl salt concentration, reaction of B*a*P DE2 with dA gives *cis* adducts in a yield of 68%. The yield of the adducts were determined as a function of chloride concentration. In the absence of salt however, the *trans* adduct is preferred giving a 69% yield, and only 31% of *cis* adduct was observed.[85] These results showed that ring opening of a B*a*P epoxide can be accomplished using chloride ions, and that *trans* chlorohydrin intermediates can undergo nucleophilic displacement of the chloride at the C-10 position by dA to preferentially gives *cis* isomers.

Scheme 15. Synthetic Approach using the B*a*P DE1 Dibenzoate (±)-**50**

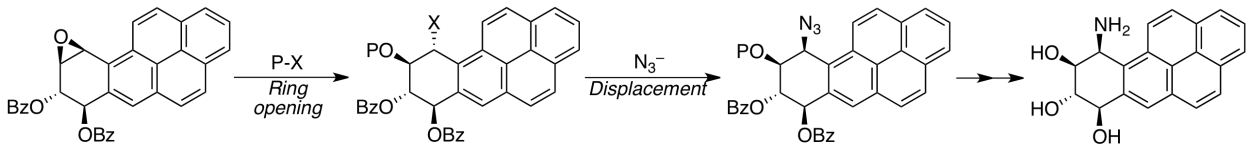

(±)-**50** (±)-**51** (±)-**52** (±)-**29**

P = H or protecting group
X = Halide or leaving group

With this insight, DE1 derivative (±)-**50** was tested using potential ring opening procedures, with a focus on chloride as the first nucleophile. These reactions were monitored for the complete consumption of the epoxide and the results are summarized in Table 2. For entries 1 and 2, we envisioned that (±)-**50** could be ring opened by chloride giving the *trans* chlorohydrin B*a*P derivative required for further steps. Use of LiCl in DMF at room temperature gave an incomplete reaction after 24 h (entry 1). Using $Zn(OTf)_2$ as a catalyst and benzyltriethyl ammonium chloride (BTEAC) as the chloride source, in CH_2Cl_2, gave an incomplete reaction after 21 h at room temperature (entry 2). However, by NMR we detected that a possible diol B*a*P derivative was being formed rather than a *trans* chlorohydrin BaP derivative [(±)-**51**, P = H, X = OH]. Since halohydrins undergo ring closure to give epoxides,[27,82] and solvolysis of the benzylic halide could result in completing side reactions,[86] we reconsidered the reaction procedures. To prevent reclosure of the chlorohydrin, (±)-**50** was stirred with TMS-Cl in THF as a way to accomplishing ring opening, and protection of the resulting alkoxide. After 21 h however, the reaction was incomplete with multiple spots detected by TLC (entry 4).

As an alternative to the chloride ring opening approach, we attempted ring opening of the epoxide with an oxygen nucleophile.[87] We envisioned the deprotonation of allyl alcohol with NaH to produce an allyl oxide that could react with epoxide (±)-**50** to give a *trans* ring-opened B*a*P ether derivative [(±)-**51**, P = H, X = OC_3H_5]. After protection of the non-benzylic hydroxyl, the allyl ether could then be cleaved and converted to an appropriate leaving group. Displacement of the leaving group by an azide ion would then give the desired *cis* azido B*a*P derivative. Hence for entry 4, allyl alcohol and NaH were stirred at 0 ºC in THF, followed by addition of (±)-**50**. The mixture was allowed to warm to room temperature and appeared to be complete after 2 h. Unfortunately, the presence of multiple impurities impeded the isolation of pure product.

Lastly, we reconsidered another nucleophilic chloride approach. We envisioned that after ring opening of epoxide (±)-**50** by chloride, the trapping of the resulting alkoxide under acetylating conditions may ameliorate the problem. To this end, use of LiCl under acetylating conditions in DMF led to a complete reaction of (±)-**50** after 21 h at room temperature (entry 5). Under these conditions, the chlorohydrin produced by the ring opening was directly acetylated, thus preventing ring closure and any halide solvolysis. Alternatively, acetic anhydride may have helped the benzylic ring opening by

interaction with the epoxide oxygen.[88] Also, by NMR one can readily detect presence of the acetyl group at ~ 2.0 ppm. Fortunately, LiCl/Ac_2O worked in our favor as analysis of the NMR of the crude product showed complete consumption of the starting material, and presence of a single new acetylated B*a*P product.

Table 2. Preliminary Ring Opening Systems for B*a*P DE1 Dibenzoate (±)-**50**

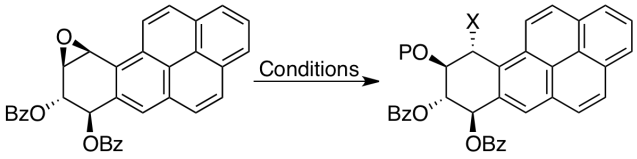

(±)-**50** (±)-**51**

Entry	DE1 BaP	Conditions	P	X	Notes
1	(±)-**50**	LiCl, DMF, r.t.	H	Cl	24 h, incomplete
2	(±)-**50**	$Zn(OTf)_2$, BTEAC, CH_2Cl_2, r.t.	H	Cl	21 h, possible diol (P and X = OH)
3	(±)-**50**	TMS-Cl, THF, r.t.	TMS	Cl	24 h, incomplete
4	(±)-**50**	Allyl alcohol, NaH, THF, 0 ºC to r.t.	H	OC_3H_5	2 h, impurities
5	(±)-**50**	LiCl, Ac_2O, DMAP, DMF	Ac	Cl	21 h, complete

With the favorable result from entry 5 in Table 2, we decided to utilize these conditions for synthesis of the desired amino triol derivative (±)-**29**. The synthesis is shown below in Scheme 16. To B*a*P DE1 dibenzoate (±)-**50** in anhydrous DMF, dried LiCl, Ac_2O, and a catalytic amount of DMAP were added, and the mixture was stirred for 21 h at room temperature. After complete consumption of (±)-**50**, the crude material was rapidly worked-up, dried, then re-dissolved in anhydrous DMF. NaN_3 was added, and the mixture was stirred at 50 ºC for 20 h. The reaction was complete and gave a 53% yield of (±)-**35** after purification (successive tries gave 51% and 52% yield).

NMR analysis of (±)-**35** focused on the chemical shifts and coupling constants of H-7, H-8, H-9 and H-10. These along with NOESY data helped establish the stereochemistry of (±)-**35**. The data showed that H-7 (7.14 ppm), H-8 (5.85 ppm), H-9 (5.91 ppm) and H-10 (5.79 ppm) gave the following coupling constants, $J_{7,8}$ = 6.8 Hz, $J_{8,9}$ = 6.0 Hz, and $J_{9,10}$ = 4.0 Hz. Analysis of the NOESY spectrum showed a key through-space interaction between H-9 and H-10. This is an indication that both of these

protons reside on the same face. In addition, a small correlation was also observed between H-9 and H-7, which also supports their presences on the same face (Figure 7).

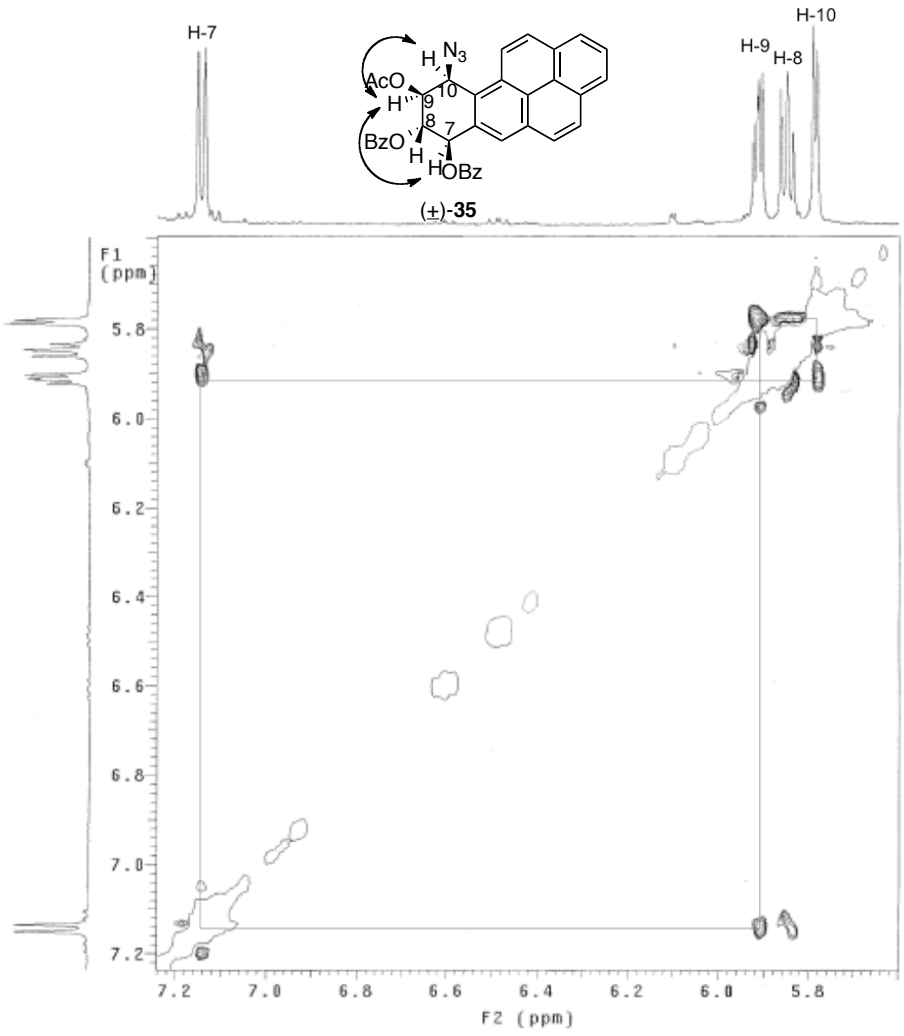

Figure 7. NOESY Spectrum showing Correlation between the α Hydrogens H-7, H-9 and H-10 in (±)-**35**.

Next, (±)-**35** was subjected to hydrolysis of all ester linkages using NH_3-MeOH at 50 ºC, to gave the azido triol (±)-**27** in 91% yield. The azido triol was then subjected to catalytic reduction using 10% Pd/C in EtOH. However, this reaction was incomplete with only 40% of amino triol (±)-**29** that was obtained after purification. Reduction of (±)-**27** with Lindlar catalyst in EtOH gave the desired amino triol (±)-**29** in a better yield of 75% after purification. Additionally, (±)-**53** and (±)-**54** were synthesized for comparison of key chemical shifts and coupling constants with other comparable B*a*P derivatives (Scheme 16).

Scheme 16. Diastereoselective Synthesis of *Cis* Ring-opened B*a*P DE1 Amino Triol (±)-**29**

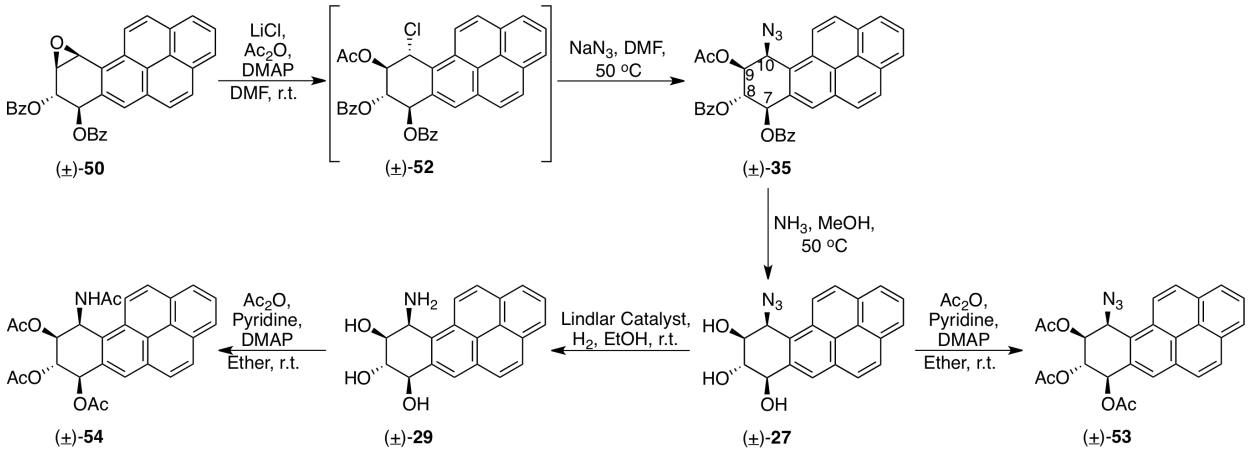

NMR analysis of the synthesized azido triol (±)-**27** and its comparison to that reported by Jerina and co-workers[71b] were in good agreement (Table 3, entry 1, below). Analysis of key chemical shifts and coupling constants showed the chemical shifts H-7 (5.06 ppm), H-8 (3.82 ppm), H-9 (4.35 ppm), H-10 (5.54 ppm), and coupling constants $J_{7,8}$ = 8.0, $J_{8,9}$ = 8.0, $J_{9,10}$ = 5.5 recorded at 500 MHz, correlate well with the reported chemical shifts H-7 (5.03 ppm), H-8 (3.79 ppm), H-9 (4.33 ppm), H-10 (5.52 ppm), and coupling constants $J_{7,8}$ = 8.2, $J_{8,9}$ = 8.2, $J_{9,10}$ = 5.4 recorded at 300 MHz by Jerina et al.[71b] The reported chemical shifts and coupling constants for the *trans* azido triol (±)-**28** is quite different.[71b] The key chemical shifts in the *trans* derivative are H-7 (4.85 ppm), H-8 (4.13 ppm), H-9 (4.07 ppm), H-10 (5.78 ppm), and coupling constants are $J_{7,8}$ = 8.3, $J_{8,9}$ = 10.7, $J_{9,10}$ = 4.2 (recorded at 500 MHz).[71b] Interestingly, both the *cis* and *trans* azido triol DE1 derivatives have a similar $J_{7,8}$ value ~ 8 Hz. This is indicative that the hydroxyls at those positions are oriented diequatorially.

NOESY data of the synthesized azido triol (±)-**27** was also evaluated (Figure 8). Single proton resonance was observed at 5.54 ppm (H-10) and 5.06 ppm (H-7), followed by a resonance at 5.00 ppm for 2 hydroxyl protons, a single hydroxyl proton resonance at ~4.85 ppm, then single proton resonances at 4.35 ppm (H-9) and 3.82 ppm (H-8) are again both single protons. The NOESY spectrum indicates a through-space interaction between H-10 and H-9, but more importantly, a clear through-space interaction can be observed for H-9 and H-7. In protected azido derivative (±)-**35** only a small correlation was observed between H-9 and H-7 (Figure 7). The unprotected azido triol (±)-**27** showing such a clear

correlation between the H-9 and H-7 indicates that both of these protons reside on the same face. Thus, this supports the desired stereochemistry.

Table 3. Key Chemical Shifts and Coupling Constants of Tetrahydro Ring Protons in B*a*P Derivatives

Entry	Compound	H-7	H-8	H-9	H-10
		d 5.06 (d 5.03)[71b]	t 3.82 (t 3.79)[71b]	dd 4.35 (dd 4.33)[71b]	d 5.54 (d 5.52)[71b]
1	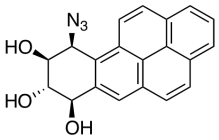	500 MHz (acetone-d_6): $J_{7,8}$ = 8.0; $J_{8,9}$ = 8.0; $J_{9,10}$ = 5.5 [300 MHz ($CDCl_3$-CD_3OD): $J_{7,8}$ = 8.0; $J_{8,9}$ = 8.0; $J_{9,10}$ = 5.5][71b]			
		d 7.14	app t 5.85	dd 5.91	d 5.79
2	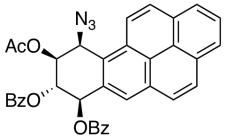	500 MHz ($CDCl_3$): $J_{7,8}$ = 6.8; $J_{8,9}$ = 6.0; $J_{9,10}$ = 4.0			
		d 6.68	t 5.48	dd 5.62	d 5.59
3	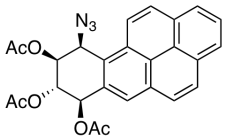	500 MHz ($CDCl_3$): $J_{7,8}$ = 5.8; $J_{8,9}$ = 5.0; $J_{9,10}$ = 3.3			
		d 6.62	t 5.63	dd 5.52	dd 6.34
4	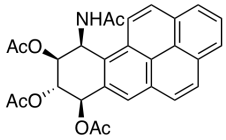	500 MHz ($CDCl_3$): $J_{7,8}$ = 5.0; $J_{8,9}$ = 5.3; $J_{9,10}$ = 3.5; $J_{10,NH}$ = 9.5			
		d 6.64	t 6.02	dd 5.55	d 7.34
5[82]	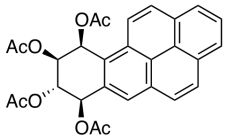	220 MHz ($CDCl_3$): $J_{7,8}$ = 8.0; $J_{8,9}$ = 11.5; $J_{9,10}$ = 3.5			
		m 5.33	m 4.24	m 4.65	d 5.52
6[74]	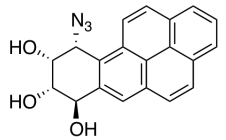	500 MHz (acetone-d_6): $J_{7,8}$ = m; $J_{8,9}$ = m; $J_{9,10}$ = 4.9			
		d 7.08	dd 6.05	dd 6.22	d 6.00
7[74]	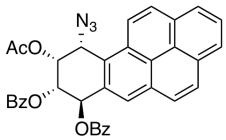	500 MHz ($CDCl_3$): $J_{7,8}$ = 4.0; $J_{8,9}$ = 2.4; $J_{9,10}$ = 5.0			
		d 6.64	dd 5.71	dd 5.90	d 5.74

8[74]	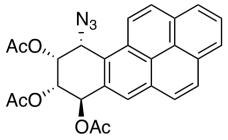	300 MHz ($CDCl_3$): $J_{7,8}$ = 3.6; $J_{8,9}$ = 2.4; $J_{9,10}$ = 5.4			
		d 6.57	br m 5.64	dd 5.80	d 6.53
9[74]	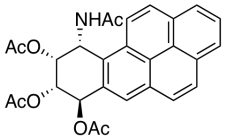	500 MHz (Acetone-d_6): $J_{7,8}$ = 3.4; $J_{8,9}$ = 2.4; $J_{9,10}$ = 5.0; $J_{10,NH}$ = 9.8			
		d 6.67	app t 5.68	dd 5.99	d 7.36
10[74]	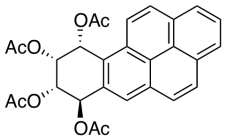	500 MHz ($CDCl_3$): $J_{7,8}$ = 3.5; $J_{8,9}$ = 2.5; $J_{9,10}$ = 4.7			

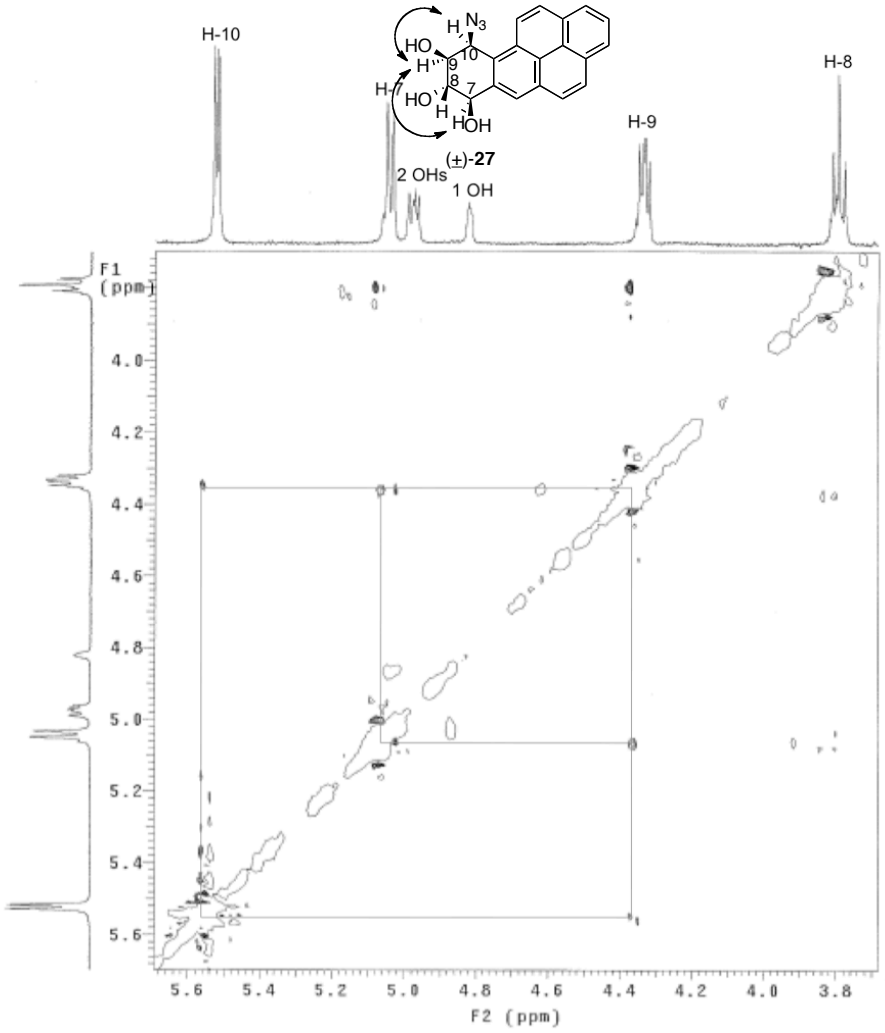

Figure 8. NOESY Spectrum showing Correlation between the α Hydrogens H-7, H-9 and H-10 in (±)-**27**.

The disparity observed in the $J_{7,8}$ and $J_{8,9}$ coupling constants of the unprotected azido triol (**27**) with the protected azido derivatives **35** and **53** is notable (compare entry 1 to entries 2 and 3 in Table 3). The $J_{7,8}$ = 8.0 Hz and $J_{8,9}$ = 8.0 Hz in the unprotected azido triol **27** indicates that the compound adopts a more diequatorial arrangement of the hydroxyls (and more axially disposed protons). The azido triaceyl compounds **35** ($J_{7,8}$ = 6.8 Hz, $J_{8,9}$ = 6.0 Hz), and azido **53** ($J_{7,8}$ = 5.8 Hz, $J_{8,9}$ = 5.0 Hz), the arrangement of the substituents is more diaxial, on the basis of the observed coupling constants. This difference can be rationalized as follows. In azido triol **27**, the N_3 is linear and can be accomadated in an axial orientation. The hydroxyls on the other hand can be equatorial and this would that allows allow for hydrogen-bonded interactions between them, thus resulting in the carbinol hydrogens that are in an axial arrangement. This may possibly account for the large coupling values observed for the azido triol **27**. Upon acylation (acetyl or benzoyl substituents), these coupling constants become smaller. Not only is the possibility of hydrogen bonding between adjacent hydroxyl groups removed upon acylation but the compounds could adopt a conformation that places the substituents more axially, to reduce either steric strain or adverse dipole-dipole interactions. It is interesting to note that the tetraacetylated *cis* ring-opened DE1 tetraol (entry 5) has large $J_{7,8}$ and $J_{8,9}$ coupling constants as well. These values can be accounted for by a conformation wherein the C-7, C-8, and C-9 substituents are all equatorially disposed.

In order to compare our *cis* ring-opened DE1 amino triol (±)-**29** with the other diastereoselectively synthesized *cis* ring-opened DE2 amino triol (±)-**11**,[74] as well as other B*a*P derivatives,[74,82] the protected derivatives were evaluated. Table 3 shows the chemical shifts and coupling constants for the tetrahydro ring protons in these various B*a*P derivatives of interest. A clear difference can be observed with the $J_{7,8}$ coupling values between the DE2 and DE1 derivatives. Those arising by a *cis* ring opening of the DE2 epoxide have a $J_{7,8}$ value between 3.4–4.0 Hz (entries 7-10). This is indicative of a predominantly diaxial orientation of the substituents. In contrast, a $J_{7,8}$ value 8.0–9.3 Hz typifies a predominantly diequatorial orientation of substituents usually found in *trans* ring-opened B*a*P derivatives.[74] Our synthesized B*a*P derivatives that arose from *cis* ring opening of the DE1 epoxide generally showed a $J_{7,8}$ value between 5.0–6.8 Hz (entries 2-4). This, as previously mentioned, seems to indicate an intermediate diaxial/diequatorial orientation of the substituents for this series of B*a*P derivatives. The exception being the tetraacetylated B*a*P derivative with a $J_{7,8}$ value of 8.0 Hz (entry 5). Generality can be found however,

when the key chemical shift values for the azido and amino derivatives for both DE2 and DE1 are compared. Additionally, the $J_{8,9}$, $J_{9,10}$ and $J_{10,NH}$ values are comparable for both DE2 and DE1 derivatives (entries 7-9 vs 2-4).

With assignment of the relative stereochemistry of *cis* ring-opened DE1 amino triol complete, we anticipate synthesis of the dA and dG adducts, the latter of which has not been accomplished. These four remaining adducts will complete the total synthesis of the set of all sixteen nucleoside adducts for the B*a*P series. Additionally, with the combination of structural and biochemical studies, the data to be gathered will help to further understand the influence of adducted DNA structures on subsequent cellular events.

4.3 Conclusions

The present work demonstrated a strategy for the diastereoselective synthesis of 10*β*-amino-7*β*,8*α*,9*β*-trihydroxy benzo[*a*]pyrene (**29**). Thus, this synthesis afforded the *cis* ring-opened DE1 B*a*P derivative that is required in order to complete the total synthesis of all sixteen B*a*P diol epoxide-nucleoside adducts. The protocol involves use of 7,8-bis-benzoyloxy-7,8-dihydro B*a*P derivative (**16**) as a key intermediate, which is common to the synthesis of the *cis* DE2 derivative (**11**).[74] Such a modular approach increases the availability of various diol epoxides for adduct synthesis and biological experiments. For example, minor adducts that were previously unstudied, and which could play a vital role in understanding mutagenesis and other cellular processes.

For access to the desired amino triol **29**, dihydrodibenzoate **16** was appropriately epoxidized.[27,82] This epoxide underwent ring opening with LiCl and acetic anhydride to give a *trans* acetyl chlorohydrin intermediate containing a benzylic chloride. The chloride was readily displaced with an azide anion at the benzylic C-10 position, and the desired *cis* facial selectivity was obtained. [74,77,85] Deprotection of the acyl and benzoyl groups, followed by reduction of the azide afforded the requisite amino triol **29**. Using this amino triol, we anticipate the synthesis of the two *cis* ring-opened B*a*P DE1 dA adducts and 2 *cis* ring-opened B*a*P DE1 dG adducts, the latter of which has not been synthesized. The synthesis of these diol epoxide-nucleoside adducts are important for studies involving site-specific modification of DNA, since to date, there is no solution structure data on the deoxyguanosine adducts of B*a*P DE1.[32-36] The knowledge to be obtained will provide a greater understanding how specific DNA adducts perturb DNA structures, influence biochemical processes, as well as their biological outcomes. The present work described the stereoselective synthesis of the B*a*P amino triol **29**, a lynch pin intermediate towards the synthesis of the 2'-deoxyadenosine and 2'-deoxyguanosine adducts that are needed.

General Comments. All reactions were carried out in oven-dried flasks and vials, and under nitrogen gas or Argon gas if an inert atmosphere is needed. All commercially available compounds were used without further purification. Air or water sensitive liquids and solutions were transferred via syringe under inert conditions. The solvents used were purified by distillation over respective drying agents. LiCl was dried under vacuum with heat overnight before use. Thin-layer chromatography was performed on 250 μm glass-back silica plates and 200 μm aluminum-back silica plates. Purification of reaction products by column chromatography was performed on 230-400 mesh silica gel, or trituration with appropriate solvent. Proton nuclear magnetic spectra (^{1}H NMR) were generally recorded in the solvents indicated on a 500 MHz instrument. Chemical shifts (δ) are given in ppm, and coupling constants (J) in Hz. ^{1}H NMR splitting patterns are designated as singlet (s), doublet (d), triplet (t), quartet (q) and quintet (quint) where appropriate. All first-order splitting patterns are assigned on the basis of the appearance of the resonance. Those splitting patterns that could not be easily interpreted, a designation of multiplet (m) or broad (br) is used as appropriate.

9,10-dihydrobenzo[*a*]pyrene (41)[75]

In an oven-dried 500 mL round-bottom flask equipped with a magnetic stirring bar was placed commercially available B*a*P-7-ol, **15** (6 g, 22.0 mmol) in dry toluene (228 mL). *p*-Toluenesulfonic acid (0.419 g, 0.220 mmol) was added and the mixture was stirred and heated at reflux for 25 mins, at which time TLC showed the reaction to be complete. The mixture was evaporated to half its volume and washed with saturated $NaHCO_3$. The organic layer was dried over Na_2SO_4 and concentrated. The crude product was chromatographed on a silica gel column packed in hexanes column using sequential elution with hexanes, followed by 20% CH_2Cl_2 in hexanes. Compound **41** was obtained as a pale-yellow solid (5.41 g, 96% yield). R_f (20% CH_2Cl_2 in hexanes): 0.46. ^{1}H NMR (500 MHz, $CDCl_3$): δ 8.27 (d, 1H, Ar-H, J = 9.5 Hz), 8.12 (d, 2H, Ar-H, J = 7.5 Hz), 8.07 (d, 1H, Ar-H, J = 9.5 Hz), 7.99 (app s, 2H, Ar-H), 7.94 (t, 1H, Ar-H, J = 7.5 Hz), 7.86 (s, 1H, Ar-H), 6.87 (d, 1H, Ar-H, J = 9.5 Hz), 6.27 (dt, 1H, Ar-H, J = 4.5, 9.5 Hz), 3.51 (t, 2H, CH_2, J = 8.5 Hz), 2.61-2.57 (m, 2H, CH_2).

(±)-7β,8α-Disbenzoyloxy-7,8,9,10-tetrahydrobenzo[*a*]pyrene [(±)-42][75]

In an oven-dried 500 mL round-bottom flask equipped with a magnetic stirring bar was placed AgOBz (7.92 g, 34.6 mmol) in dry toluene (288 mL). To this suspension I_2 (4.48 g, 17.3 mmol) and 9,10-dihydro B*a*P (±)-**41** (4 g, 15.7 mmol) were added. The mixture was allowed to stir at room temperature under a nitrogen gas atmosphere for 2.5 h, at which time TLC showed consumption of all the starting material and a bright yellow suspension was observed. This resulting mixture was then heated at reflux under a nitrogen gas atmosphere for 19 h, at which time TLC showed the reaction to be complete. The reaction mixture was filtered hot through Celite using hot toluene to wash the residue. A greenish residue remained on the Celite bed and a reddish-brown filtrate was obtained. Evaporation of the solvent gave a reddish-brown solid. The crude product was suspended in acetone and sonicated, then set in an ice-bath for 30 mins, and filtered. Compound (±)-**42** was obtained as a light-brown, powdery solid (6.46 g, 83% yield). R_f (50% CH_2Cl_2 in hexanes): 0.07. ^{1}H NMR (500 MHz, $CDCl_3$): δ 8.32 (d, 1H, Ar-H, *J* = 9.0 Hz), 8.22-8.16 (m, 4H, Ar-H), 8.11 (br d, 2H, Ar-H, *J* = 7.5 Hz), 8.03-7.94 (m, 5H, Ar-H), 7.55 (t, 1H, Ar-H, *J* = 7.5 Hz), 7.49 (t, 1H, Ar-H, *J* = 7.5 Hz), 7.42 (t, 2H, Ar-H, *J* = 7.5 Hz), 7.34 (t, 2H, Ar-H, *J* = 8.0 Hz), 6.98 (d, 1H, H-7, *J* = 6.0 Hz), 5.79 (ddd, 1H, H-8, *J* = 3.0, 6.0, 8.5 Hz), 3.80-3.71 (m, 2H, H-9, H-9'), 2.77-2.71 (m, 1H, H-10), 2.58-2.51 (m, 1H, H-10').

(±)-7β,8α-Dibenzoyloxy-7,8-dihydrobenzo[*a*]pyrene [(±)-16][75]

In an oven-dried 100 mL round-bottom flask equipped with a magnetic stirring bar was placed compound (±)-**42** (1 g, 2.01 mmol) in dry toluene (40 mL). DDQ (594 mg, 2.62 mmol) was added and the dark reddish-brown mixture was allowed to stir at reflux under a nitrogen atmosphere for 17 h. At that time TLC showed the reaction to be complete. The dark green suspension was filtered hot through Celite using dry toluene. A dark greenish residue remained on the Celite bed and a green filtrate was obtained. Evaporation of the solvent gave a greenish solid. The crude product was suspended in acetone, sonicated, and filtered to afford (±)-**16** as a fluffy light greenish solid (701 mg, 70% yield). R_f (CH_2Cl_2): 0.54. ^{1}H NMR (500 MHz, $CDCl_3$): δ 8.42 (d, 1H, Ar-H, *J* = 9.5 Hz), 8.21-8.15 (m, 4H, Ar-H), 8.13-8.11 (m, 2H, Ar-H), 8.07 (d, 1H, Ar-H, *J* = 9.0 Hz), 8.03-7.98 (m, 4H, Ar-H), 7.79 (br d, 1H, H-10, *J* = 10.5 Hz), 7.56 (t, 1H, Ar-H, *J* = 7.5 Hz), 7.50 (t, 1H, Ar-H, *J* = 7.5 Hz), 7.43 (t, 2H, Ar-H, *J* = 8.0 Hz), 7.36 (t, 2H, Ar-H, *J* =

7.5 Hz), 7.06 (d, 1H, H-7, *J* = 7.5 Hz), 6.47 (dd, 1H, H-9, *J* = 3.5, 10.0 Hz), 6.21 (dddd, 1H, H-8, *J* = 1.0, 3.5, 7.5 Hz).

(±)-10β-Azido-9α-bromo-7β,8α-dibenzoyloxy-7,8,9,10-tetrahydrobenzo[*a*]pyrene [(±)-34]

In an oven-dried reaction vial equipped with a magnetic stirring bar was placed the B*a*P dihydrodibenzoate (±)-**16** (100 mg, 0.202 mmol) in dry CH_2Cl_2 (1.0 mL). Molecular sieves (4Å, 40.4 mg) and $Zn(OTf)_2$ (3.7 mg, 0.010 mmol) were added, and the vial was flushed with nitrogen gas. The greenish suspension was cooled to 0 ºC, then NBS (43.2 mg, 0.243 mmol) and $TMSN_3$ (34.9 mg, 0.303 mmol) were added. The vial was again flushed with nitrogen gas and allowed to stir at 0 ºC for 1 h, at which time TLC showed the reaction to be complete. The mixture was quenched with sat. $NaHCO_3$ and extracted with CH_2Cl_2 (3x). The organic layer was dried over Na_2SO_4 and concentrated to give a dark reddish brown solid. The crude product was chromatographed on a silica gel column packed in hexanes using 1:1 CH_2Cl_2-hexanes as eluent. Compound (±)-**34** was obtained as a yellowish-brown solid (73.3 mg, 59%). R_f (50% CH_2Cl_2 in hexanes): 0.34. ^{1}H NMR (500 MHz, $CDCl_3$): δ 8.34 ($AB_{quartet}$, 1H, Ar-H, *J* = 9.5 Hz), 8.30 (d, 1H, Ar-H, *J* = 8.0 Hz), 8.24 (d, 1H, Ar-H, *J* = 7.5 Hz), 8.15 (br d, 3H, Ar-H, *J* = 5.5 Hz), 8.12-8.07 (m, 4H, Ar-H), 8.00 (d, 1H, Ar-H, *J* = 9.0 Hz), 7.60-7.55 (m, 2H, Ar-H), 7.44 (ddd, 4H, Ar-H, *J* = 4.0, 8.0, 15.5 Hz), 7.34 (d, 1H, H-7, *J* = 8.5 Hz), 6.08 (dd, 1H, H-8, *J* = 3.0, 8.5 Hz), 6.04 (d, 1H, H-10, *J* = 3.0 Hz), 5.19 (t, 1H, H-9, *J* = 3.0 Hz). ^{13}C NMR (125 MHz, $CDCl_3$): δ 171.0, 166.6, 165.8, 133.61, 133.56, 132.4, 131.4, 131.2, 130.6, 130.2, 130.1, 130.0, 129.7, 129.4, 129.01, 129.0, 128.6, 128.5, 127.2, 126.7, 126.4, 126.2, 124.9, 124.2, 123.9, 122.1, 71.8, 70.9, 62.2, 50.0.

(±)-7β-Azido-8α-iodo-7,8,9,10-tetrahydrobenzo[*a*]pyrene [(±)-43]

In an oven-dried reaction vial equipped with a magnetic stirring bar was placed NaN_3 (28.7 mg, 0.441 mmol) in dry CH_3CN (0.2 mL) under a nitrogen gas atmosphere, and the mixture was cooled to –10 ºC. To this suspension ICl (35.8 mg, 0.221 mmol) in CH_3CN (0.4 mL) was added. After 10 mins, 9,10-dihydro B*a*P **41** (510 mg, 0.200 mmol) in CH_3CN (0.6 mL) was added at –10 ºC (0.4 mL of CH_2Cl_2 was also added since the alkene was only partially soluble in CH_3CN). The mixture was allowed to stir at 0–4 ºC under a nitrogen gas atmosphere for 3 h, at which time TLC showed the reaction to be complete. The

mixture was quenched with cold water, transferred to a separatory funnel and dissolved with CH_2Cl_2. The mixture was then washed with water (2x) and with brine (2x). The organic layer was dried over Na_2SO_4 and concentrated to give an orangish-yellow solid. The crude product was chromatographed on a silica gel column packed in hexanes using sequential elution with hexanes, followed by 20% CH_2Cl_2 in hexanes. Compound (±)-**43** was obtained as a whitish-yellow solid (59.0 mg, 70% yield). R_f (20% CH_2Cl_2 in hexanes): 0.27. ^{1}H NMR (500 MHz, $CDCl_3$): δ 8.29 (d, 1H, Ar-H, *J* = 9.0 Hz), 8.23-8.18 (m, 3H, Ar-H), 8.10 (s, 1H, Ar-H), 8.05-8.01 (m, 3H, Ar-H), 5.29 (d, 1H, H-7, *J* = 3.5 Hz), 4.84-4.81 (m, 1H, H-8), 3.71-3.65 (m,1H, H-10), 3.57 (ddd,1H, H-9, *J* = 6.5, 9.5, 17.4 Hz), 2.57-2.46 (m, 2H, H-9', H-10'). ^{13}C NMR (125 MHz, $CDCl_3$): δ 131.4, 130.9, 130.0, 129.1, 128.9, 128.3, 128.1, 127.4, 127.3, 126.3, 126.1, 125.5, 125.4, 125.0, 124.5, 122.7, 67.1, 28.3, 28.2, 25.1.

(±)-9α-Bromo-7β,8α-dibenzoyloxy-10β-hydroxy-7,8,9,10-tetrahydrobenzo[*a*]pyrene [(±)-40][82]

In an oven-dried 500 mL round-bottom flask equipped with a magnetic stirring bar was placed dihydro dibenzoate (±)-**16** (580 mg, 1.17 mmol) in THF-H_2O (145 mL/58 mL). Recrystallized NBS (271 mg, 1.52 mmol) and NaOAc (289 mg, 3.52 mmol) were added. The pale green mixture was allowed to stir under a nitrogen gas atmosphere at room temperature subdued light for 18 h, at which time TLC showed the reaction to be complete. The reaction mixture was evaporated to a third of its volume, then diluted in CH_2Cl_2 and washed with water (2x) and with brine (2x). The organic layer was dried over Na_2SO_4 and concentrated to give a yellowish solid. The crude product was chromatographed on a silica gel column packed in CH_2Cl_2 using CH_2Cl_2 as eluent. The product was then washed twice with 1:1 Et_2O-hexane to afford (±)-**40** as an off-white powder (611 mg, 88% yield). R_f (100% CH_2Cl_2): 0.27. ^{1}H NMR (500 MHz, $CDCl_3$): δ 8.51 (d, 1H, Ar-H, *J* = 9.5 Hz), 8.29 (d, 1H, Ar-H, *J* = 9.0 Hz), 8.27 (d, 1H, Ar-H, *J* = 7.0 Hz), 8.22 (d, 1H, Ar-H, *J* = 7.5 Hz), 8.13-8.05 (m, 7H, Ar-H), 7.98 (d, 1H, Ar-H, *J* = 9.0 Hz), 7.59-7.55 (m, 2H, Ar-H), 7.43 (t, 4H, Ar-H, *J* = 7.5 Hz), 7.24 (d, 1H, H-7, *J* = 8.5 Hz), 6.33 (dd, 1H, H-8, *J* = 3.0, 8.5 Hz), 6.23 (br t, 1H, H-10, *J* = 4.5 Hz), 5.17 (t, 1H, H-9, *J* = 3.0 Hz), 2.97 (d, 1H, OH, *J* = 5.5 Hz).

(±)-7β,8α-Disbenzoyloxy-9β,10β-epoxy-7,8,9,10-tetrahydrobenzo[*a*]pyrene [(±)-50][82]

Using NaH. In an oven-dried 100 mL round-bottom flask equipped with a magnetic stirring bar was

placed NaH (122 mg, 5.07 mmol) in dry THF (25 mL) under a nitrogen gas atmosphere, and the mixture was cooled to 0 ºC. B*a*P bromotriol dibenzoate (±)-**40** (1.50 g, 2.54 mmol) was then added. The brownish suspension was allowed to stir under a nitrogen gas atmosphere at 0 ºC for 1 h, and at room temperature for 0.5 h. TLC showed the reaction to be complete. The reddish brown mixture was quenched with ice, diluted with 1:1 EtOAc-Et_2O, and washed with water (2x). The organic layer was dried over Na_2SO_4, and concentrated. The crude product was suspended in 1:1 Et_2O-hexanes, sonicated, and filtered to afford (±)-**50** as a pinkish-red powdery solid (1.09 g, 84% yield).

Using Amberlite. In an oven-dried 200 mL round-bottom flask equipped with a magnetic stirring bar was placed Amberlite IRA 400 ($^-$OH) (9 g) in dry THF (75 mL) under an argon gas atmosphere. B*a*P bromotriol dibenzoate B*a*P (±)-**40** (300 mg, 0.507 mmol) was added. The suspension was protected from light and allowed to stir at room temperature under an argon balloon for 3 days, at which time TLC showed the reaction to be complete. The suspension was filtered and the resin was washed with dry THF. The filtrate was concentrated to give a yellowish-white solid. The crude product was suspended in Et_2O, sonicated and filtered to afford (±)-**50** as a white solid (0.239 g, 92% yield). R_f (20% EtOAc in CH_2Cl_2): 0.46. ^{1}H NMR (500 MHz, $CDCl_3$): δ 8.62 (d, 1H, Ar-H, *J* = 9.0 Hz), 8.33 (s, 1H, Ar-H), 8.27-8.23 (m, 3H, Ar-H), 8.13 (br d, 3H, Ar-H, *J* = 9.0 Hz), 8.08-8.05 (m, 2H, Ar-H), 7.92 (br d, 2H, Ar-H, *J* = 8.5 Hz), 7.54 (t, 1H, Ar-H, *J* = 7.5 Hz), 7.51 (t, 1H, Ar-H, *J* = 7.5 Hz), 7.42 (t, 2H, Ar-H, *J* = 8.0 Hz), 7.34 (t, 2H, Ar-H, *J* = 7.5 Hz), 6.96 (d, 1H, H-7, *J* = 4.5 Hz), 6.02 (dd, 1H, H-9, *J* = 2.0, 4.0 Hz), 5.12 (d, 1H, H-10, *J* = 4.0 Hz), 4.24 (m, 1H, H-8).

(±)-9β-Acetoxy-10β-azido-7β,8α-dibenzoyloxy-7,8,9,10-tetrahydrobenzo[*a*]pyrene [(±)-35]

In an oven-dried reaction vial equipped with a magnetic stirring bar was placed B*a*P diol epoxide derivative (±)-**50** (150 mg, 0.294 mmol) in dry DMF (3.0 mL) with a few crystals of DMAP. The vial was then transferred to a glove bag maintained under a nitrogen gas atmosphere. Dry LiCl (187 mg, 4.41 mmol) and Ac_2O (600 mg, 5.88 mmol) were added. The reaction vial was then capped, removed from the glove bag, and the mixture was allowed to stir at room temperature for 18 h. TLC analysis showed consumption of starting material and the emergence of a new product spot. R_f (20% EtOAc in CH_2Cl_2): 0.93. The reaction mixture was diluted with EtOAc and rapidly washed with H_2O (3x). The organic layer

was dried over Na_2SO_4 and concentrated to give an orange oil. To this crude (±)-**52**, dry DMF (3 mL) and NaN_3 (191 mg, 2.94 mmol) were added. The vial was flushed with nitrogen gas and allowed to stir at 50 ºC in a sand bath for 16 h, at which time TLC showed the reaction to be complete. The mixture was diluted with EtOAc, and washed with H_2O (2x) and with brine (2x). The organic layer was dried over Na_2SO_4 and concentrated to give an orange oil. The crude product was chromatographed on a silica gel column packed in CH_2Cl_2 using CH_2Cl_2 as eluent. The resulting product was suspended in 1:1 Et_2O-hexane, sonicated, and filtered to afford (±)-**35** as a pale orange-white solid (91.4 mg, 53% yield). R_f (CH_2Cl_2): 0.60. ^{1}H NMR (500 MHz, $CDCl_3$): δ 8.42 (d, 1H, Ar-H, *J* = 9.5 Hz), 8.29 (d, 2H, Ar-H, *J* = 9.0 Hz), 8.26 (d, 1H, Ar-H, *J* = 7.5 Hz), 8.18-8.02 (m, 8H, Ar-H), 7.59 (t, 1H, Ar-H, *J* = 7.5 Hz), 7.54 (t, 1H, Ar-H, *J* = 7.5 Hz), 7.46 (t, 2H, Ar-H, *J* = 7.5 Hz), 7.41 (t, 2H, Ar-H, *J* = 7.5 Hz), 7.14 (d, 1H, H-7, *J* = 7.5 Hz), 5.91 (dd, 1H, H-9, *J* = 4.0, 6.0 Hz), 5.85 (br t, 1H, H-8, *J* = 6.0 Hz), 5.79 (d, 1H, H-10, *J* = 4.0 Hz), 2.03 (s, 3H, $OCOCH_3$). ^{13}C NMR (125 MHz, $CDCl_3$): δ 169.7, 166.0, 165.6, 133.6, 133.5, 132.2, 131.2, 130.6, 130.1, 130.0, 129.9, 129.5, 129.3, 128.9, 128.6, 128.5, 127.3, 126.7, 126.3, 126.1, 124.8, 124.3, 123.0, 122.6, 122.2, 72.7, 72.6, 70.9, 59.4, 20.8. HRMS (ESI) *m/z* calcd for $C_{36}H_{25}N_3O_6Na$ $[M + Na]^+$: 618.1636, found 618.1649.

(±)-10β-Azido-7β,8α,9β-trihydroxy-7,8,9,10-tetrahydrobenzo[*a*]pyrene [(±)-27]

In an oven-dried reaction vial equipped with a magnetic stirring bar was placed azido acetoxy dibenzoate (±)-**35** (30 mg, 0.050 mmol) and NH_3/MeOH (1 mL). The vial was sealed and allowed to stir at 50 ºC in a sand bath for 24 h. The vial was cooled to room temperature and checked by TLC, which showed the reaction to be complete. The mixture was diluted with EtOAc, and washed with water (3x) and with brine (3x). The organic layer was dried over Na_2SO_4 and concentrated to give a brown oil. The crude product was dried under vacuum and then washed using 1:1 Et_2O-hexanes using sonication. Filtration gave compound (±)-**27** as a beige solid (15.8 mg, 91% yield). R_f (EtOAc): 0.17. ^{1}H NMR (500 MHz, acetone-d_6): δ 8.58 (s, 1H, Ar-H), 8.56 (d, 2H, Ar-H, *J* = 9.0 Hz), 8.37-8.33 (m, 3H, Ar-H), 8.21 (br s, 2H, Ar-H), 8.11 (t, 1H, Ar-H, *J* = 7.5 Hz), 5.54 (d, 1H, H-10, *J* = 5.5 Hz), 5.06 (d, 1H, H-7, *J* = 8.0 Hz), 5.00 (dd, 2H, OH-7, OH-8, *J* = 5.5, 7.8 Hz), 4.85-4.84 (m, 1H, OH-9), 4.35 (dd, 1H, H-9, *J* = 5.5, 8.0 Hz), 3.82 (t, 1H, H-8, *J* = 8.0 Hz). ^{13}C NMR (125 MHz, acetone-d_6): δ 137.8, 131.6, 131.2, 130.6, 129.4, 128.1, 128.0, 127.5,

126.3, 125.64, 125.60, 124.3, 124.2, 123.62, 123.57, 123.3, 75.6, 75.3, 72.0, 64.4. HRMS (ESI) *m/z* calcd for $C_{20}H_{15}N_3O_3Na$ $[M + Na]^+$: 368.1006, found 368.1000.

(±)-10β-Amino-7β,8α,9β-trihydroxy-7,8,9,10-tetrahydrobenzo[*a*]pyrene [(±)-29]

In an oven-dried reaction vial equipped with a magnetic stirring bar was placed azido triol (±)-**27** (30 mg, 0.087 mmol) in EtOH (6.5 mL). Lindlar catayst (Lancaster Synthesis, 5% Pd on $CaCO_3$, Pb poisoned) (150 mg) was added, the mixture was evacuated, filled with hydrogen gas and allowed to stir under a hydrogen gas-filled balloon for 2.5 h, at which time TLC showed the reaction to be complete. The mixture was filtered through Celite using MeOH and concentrated to a yellow solid. The crude product was suspended in Et_2O, sonicated and filtered to obtain compound (±)-**29** as a yellow solid (26.6 mg, 96% yield). R_f (10% MeOH in CH_2Cl_2): 0.05. ^{1}H NMR (500 MHz, $CDCl_3$): δ 8.51 (br s, 1H, Ar-H), 8.24-8.22 (m, 2H, Ar-H), 8.16-8.10 (m, 3H, Ar-H), 8.03-7.78 (m, 2H, Ar-H), 5.77 (d, 1H, H-10, *J* = 4.0 Hz), 5.12 (d, 1H, H-7, *J* = 6.5 Hz), 4.05 (dd, 1H, H-9 *J* = 4.5, 6.5 Hz), 3.94 (t, 1H, H-8, *J* = 6.5 Hz), 3.14-2.78 (m, 5H, 3OH/NH_2). ^{13}C NMR (125 MHz, acetone-d_6): δ 136.5, 131.3, 130.62, 130.61, 130.1, 129.5, 127.5, 127.3, 127.1, 125.9, 125.1, 125.0, 124.9, 124.6, 124.4, 123.6, 75.1, 74.7, 72.7, 63.3. HRMS (ESI) *m/z* calcd for $C_{20}H_{17}N_3O_3Na$ $[M + Na]^+$: 342.1101, found 342.1110.

(±)-10β-Azido-7β,8α,9β-triacetoxy-7,8,9,10-tetrahydrobenzo[*a*]pyrene [(±)-53]

In an oven-dried reaction vial equipped with a magnetic stirring bar was placed azido acetoxy dibenzoate (±)-**35** (10.0 mg, 0.017 mmol) in NH_3/MeOH (1 mL). The reaction vial was sealed and allowed to stir at 50 ºC in a sand bath. After 24 h, the vial was cooled to room temperature and TLC analysis showed the reaction to be complete. The solvent was carefully evaporated and the resulting product was dried under vacuum for 2 h. To the crude azido triol (±)-**27** (5.80 mg, 0.017 mmol) in Et_2O (0.16 mL) were added DMAP (2 crystals), Ac_2O (34.3 mg, 0.336 mmol), and pyridine (26.6 mg, 0.336 mmol). The mixture was flushed with nitrogen gas and allowed to stir at room temperature for 24 h, at which time TLC showed the reaction to be complete. The mixture was diluted with CH_2Cl_2, washed with 1N HCl (1x), saturated $NaHCO_3$ (3x), and finally with H_2O (1x). The organic layer was dried over Na_2SO_4 and concentrated to give a yellow oil. The crude product was chromatographed on a silica gel column packed in CH_2Cl_2 using

sequential elution with CH_2Cl_2, followed by 10% EtOAc in CH_2Cl_2. Compound (±)-**53** was obtained as a pale yellow solid (7.84 mg, 99%). R_f (100% CH_2Cl_2): 0.21. ^{1}H NMR (500 MHz, $CDCl_3$): δ 8.37 (d, 1H, Ar-H, *J* = 9.0 Hz), 8.27 (dt, 3H, Ar-H, *J* = 3.0, 9.0 Hz), 8.16-8.13 (m, 2H, Ar-H), 8.10-8.06 (m, 2H, Ar-H), 6.68 (d, 1H, H-7, *J* = 6.0 Hz), 5.62 (dd, 1H, H-9, *J* = 3.5, 4.5 Hz), 5.59 (d, 1H, H-10, *J* = 3.0 Hz), 5.48 (t, 1H, H-8, *J* = 5.5 Hz), 2.26 (s, 3H, $OCOCH_3$), 2.16 (s, 3H, $OCOCH_3$), 2.02 (s, 3H, $OCOCH_3$). ^{13}C NMR (125 MHz, $CDCl_3$): δ 170.1, 169.6, 132.2, 131.2, 130.6, 129.8, 129.5, 128.9, 127.2, 126.7, 126.3, 126.1, 125.7, 124.9, 124.6, 124.3, 123.4, 122.6, 122.1, 121.6, 71.7, 70.9, 69.7, 58.1, 21.1, 20.8. HRMS (ESI) *m/z* calcd for $C_{26}H_{21}N_3O_6Na$ $[M + Na]^+$: 494.1323, found 494.1342.

(±)-10β-Acetylamino-7β,8α,9β-triacetoxy-7,8,9,10-tetrahydrobenzo[*a*]pyrene [(±)-54]

In an oven-dried reaction vial equipped with a magnetic stirring bar was placed azido triol (±)-**27** (4.50 mg, 0.031 mmol) in dry DMF (0.31 mL). DMAP (2 crystals), Ac_2O (63.9 mg, 0.626 mmol), and pyridine (49.5 mg, 0.626 mmol) were added. The reaction mixture was flushed with nitrogen gas and allowed to stir at room temperature for 24 h, at which time TLC showed the reaction to be complete. The mixture was diluted with CH_2Cl_2, washed with 1N HCl (1x), saturated $NaHCO_3$ (3x), and finally with H_2O (1x). The organic layer was dried over Na_2SO_4 and concentrated to give a yellow oil. The crude product was chromatographed on a silica gel column packed in CH_2Cl_2 using 1:1 EtOAc-CH_2Cl_2 as eluent. Compound (±)-**54** was afforded as a pale yellow solid (11.8 mg, 77%). R_f (50% EtOAc in CH_2Cl_2): 0.44. ^{1}H NMR (500 MHz, $CDCl_3$): δ 8.26-8.21 (m, 4H, Ar-H), 8.11-8.01 (m, 4H, Ar-H), 6.62 (d, 1H, H-7, *J* = 5.0 Hz), 6.34 (dd, 1H, H-10, *J* = 3.5, 9.5 Hz), 5.86 (d, 1H, NH, *J* = 9.5 Hz), 5.63 (t, 1H, H-8, *J* = 5.0), 5.52 (dd, 1H, H-9, *J* = 3.5, 5.5 Hz), 2.21 (s, 3H, $NHCOCH_3$), 2.11 (s, 3H, $OCOCH_3$), 2.06 (s, 3H, $OCOCH_3$), 2.00 (s, 3H, $OCOCH_3$). ^{13}C NMR (125 MHz, $CDCl_3$): δ 170.3, 169.8, 168.8, 168.7, 131.7, 131.1, 130.6, 130.0, 129.5, 129.1, 128.5, 127.0, 126.5, 125.93, 125.87, 125.76, 125.0, 124.11, 124.09, 122.8, 71.2, 69.7, 69.4, 48.1, 23.1, 21.08, 20.84, 20.81. HRMS (ESI) *m/z* calcd for $C_{28}H_{25}NO_7Na$ $[M + Na]^+$: 510.1523, found 510.1551.

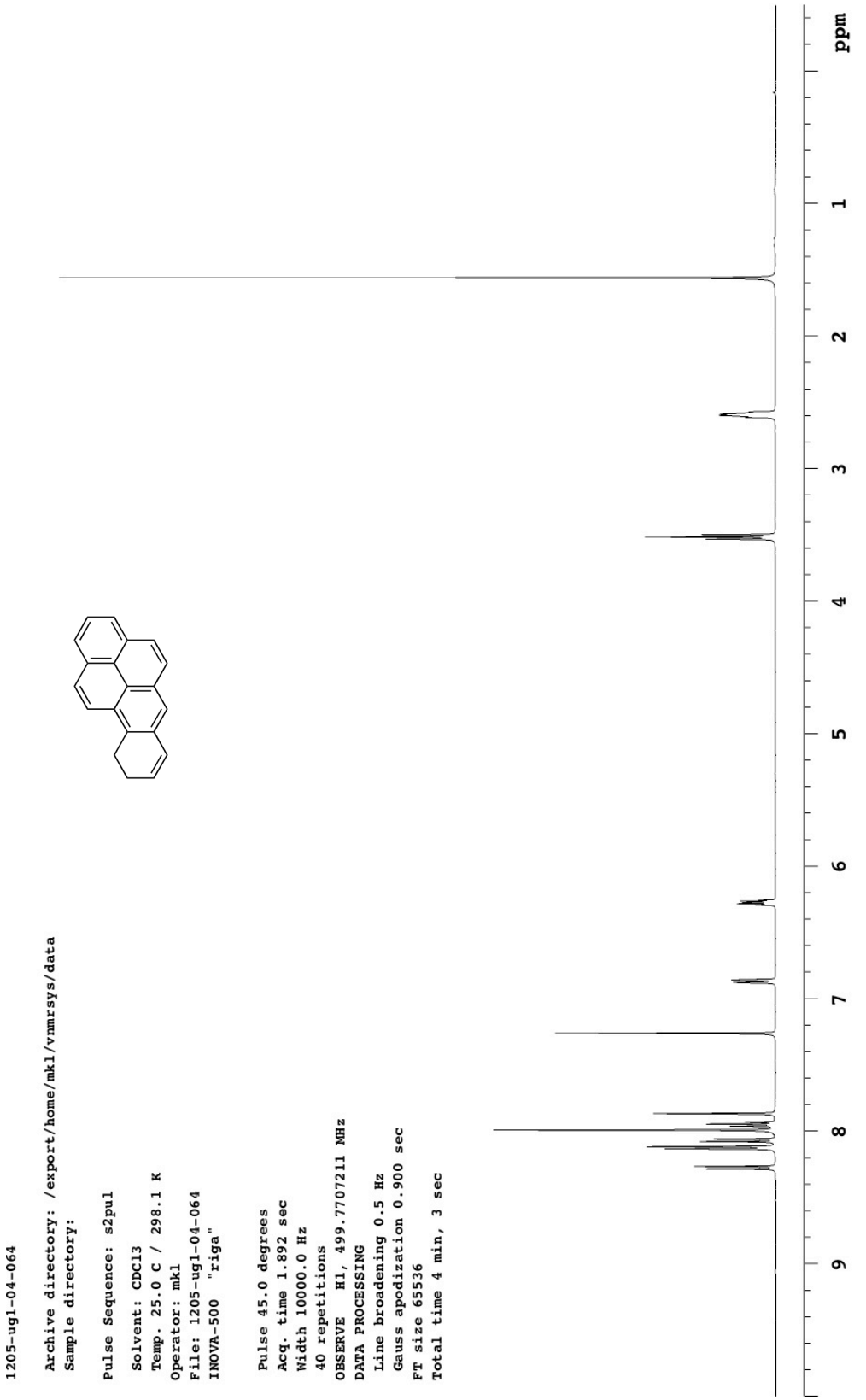
1205-ug1-04-064
Archive directory: /export/home/mk1/vnmrsys/data
Sample directory:
Pulse Sequence: s2pul
Solvent: CDCl3
Temp. 25.0 C / 298.1 K
Operator: mk1
File: 1205-ug1-04-064
INOVA-500 "riga"
Pulse 45.0 degrees
Acq. time 1.892 sec
Width 10000.0 Hz
40 repetitions
OBSERVE H1, 499.7707211 MHz
DATA PROCESSING
Line broadening 0.5 Hz
Gauss apodization 0.900 sec
FT size 65536
Total time 4 min, 3 sec
9
8
7
6
5
4
3
2
1
ppm

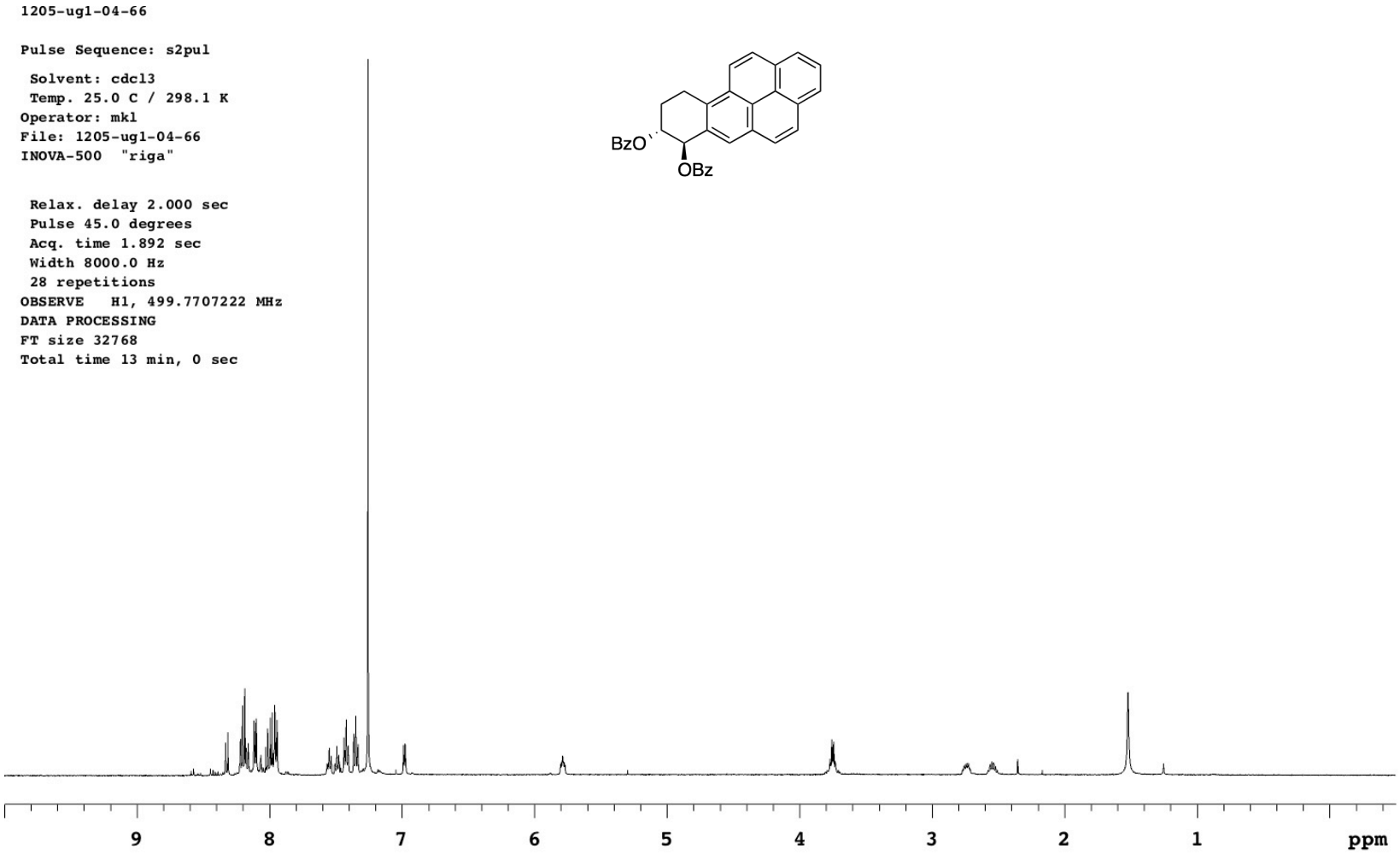
1205-ug1-04-66
Pulse Sequence: s2pul
Solvent: cdcl3
Temp. 25.0 C / 298.1 K
Operator: mkl
File: 1205-ug1-04-66
INOVA-500 "riga"
Relax. delay 2.000 sec
Pulse 45.0 degrees
Acq. time 1.892 sec
Width 8000.0 Hz
28 repetitions
OBSERVE H1, 499.7707222 MHz
DATA PROCESSING
FT size 32768
Total time 13 min, 0 sec
BzO
OBz
9
8
7
6
5
4
3
2
1
ppm

1205-ug1-08-62

Pulse Sequence: s2pul

Solvent: cdcl3
Temp. 25.0 C / 298.1 K
Operator: mkl
File: 1205-ug1-08-62
INOVA-500 "riga"

Relax. delay 2.000 sec
Pulse 45.0 degrees
Acq. time 1.892 sec
Width 8000.0 Hz
36 repetitions
OBSERVE H1, 499.7707222 MHz
DATA PROCESSING
FT size 32768
Total time 13 min, 0 sec

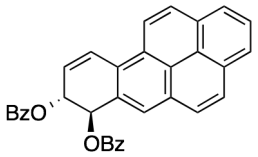

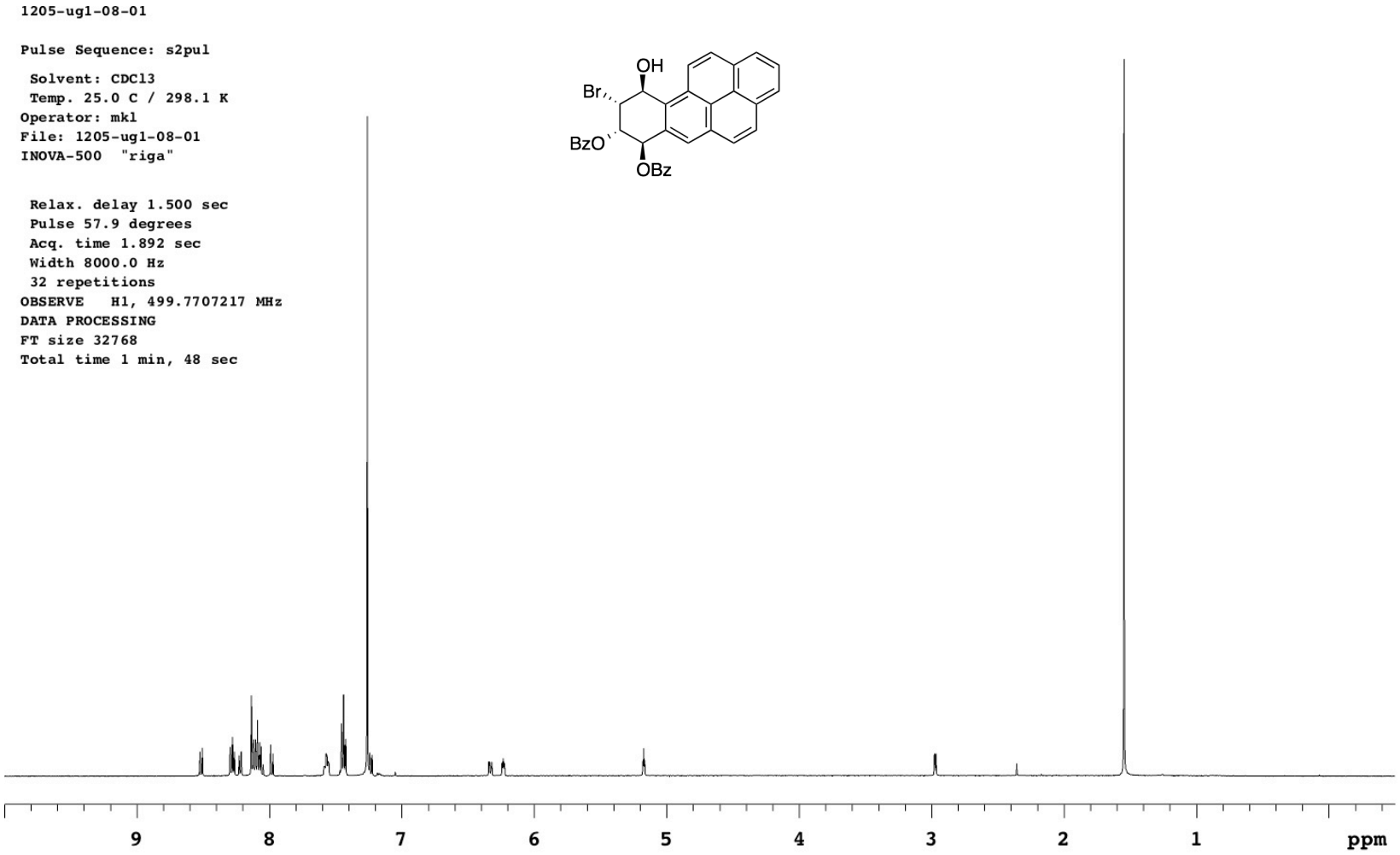
1205-ug1-08-01
Pulse Sequence: s2pul
Solvent: CDCl3
Temp. 25.0 C / 298.1 K
Operator: mkl
File: 1205-ug1-08-01
INOVA-500 "riga"
Relax. delay 1.500 sec
Pulse 57.9 degrees
Acq. time 1.892 sec
Width 8000.0 Hz
32 repetitions
OBSERVE H1, 499.7707217 MHz
DATA PROCESSING
FT size 32768
Total time 1 min, 48 sec
OH
Br
BzO
OBz
9
8
7
6
5
4
3
2
1
ppm

1205-ug1-05-08again

Pulse Sequence: s2pul

Solvent: cdcl3
Temp. 25.0 C / 298.1 K
Operator: mkl
File: 1205-ug1-05-08again
INOVA-500 "riga"

Relax. delay 2.000 sec
Pulse 45.0 degrees
Acq. time 1.892 sec
Width 8000.0 Hz
28 repetitions
OBSERVE H1, 499.7707207 MHz
DATA PROCESSING
FT size 32768
Total time 13 min, 0 sec

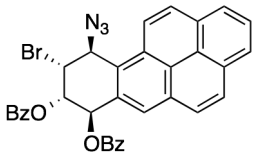

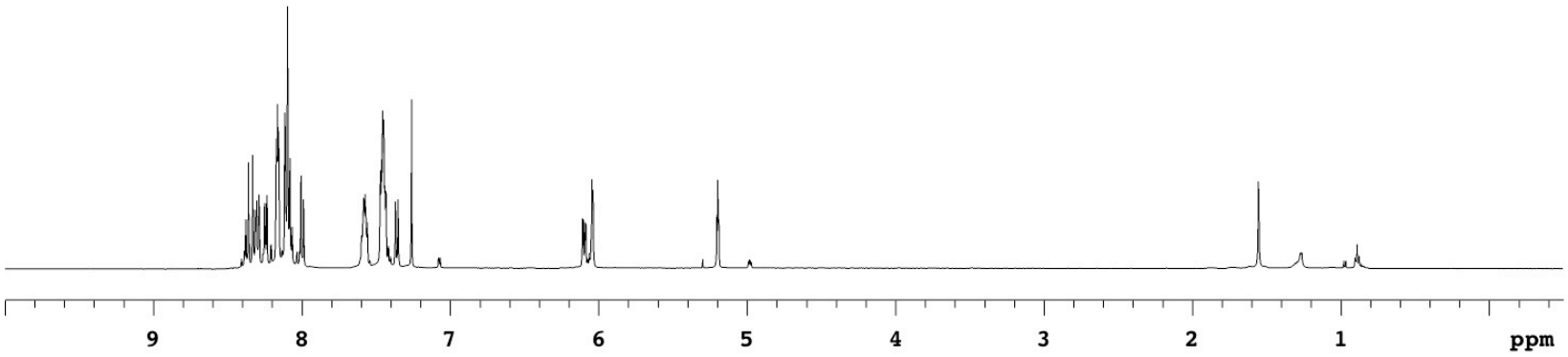

1205-ug1-05-08again-C13

Archive directory: /export/home/mkl/vnmrsys/data
Sample directory:

Pulse Sequence: s2pul

Solvent: CDCl3
Temp. 25.0 C / 298.1 K
Operator: mkl
File: 1205-ug1-05-08again-C13
INOVA-500 "riga"

Relax. delay 4.000 sec
Pulse 52.1 degrees
Acq. time 1.300 sec
Width 29996.3 Hz
1052 repetitions
OBSERVE C13, 125.6674457 MHz
DECOUPLE H1, 499.7732084 MHz
Power 42 dB
on during acquisition
WALTZ-16 modulated
DATA PROCESSING
Line broadening 8.0 Hz
FT size 131072
Total time 132 hr, 44 min, 27 sec

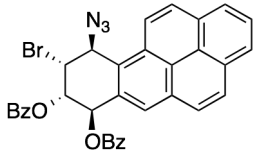

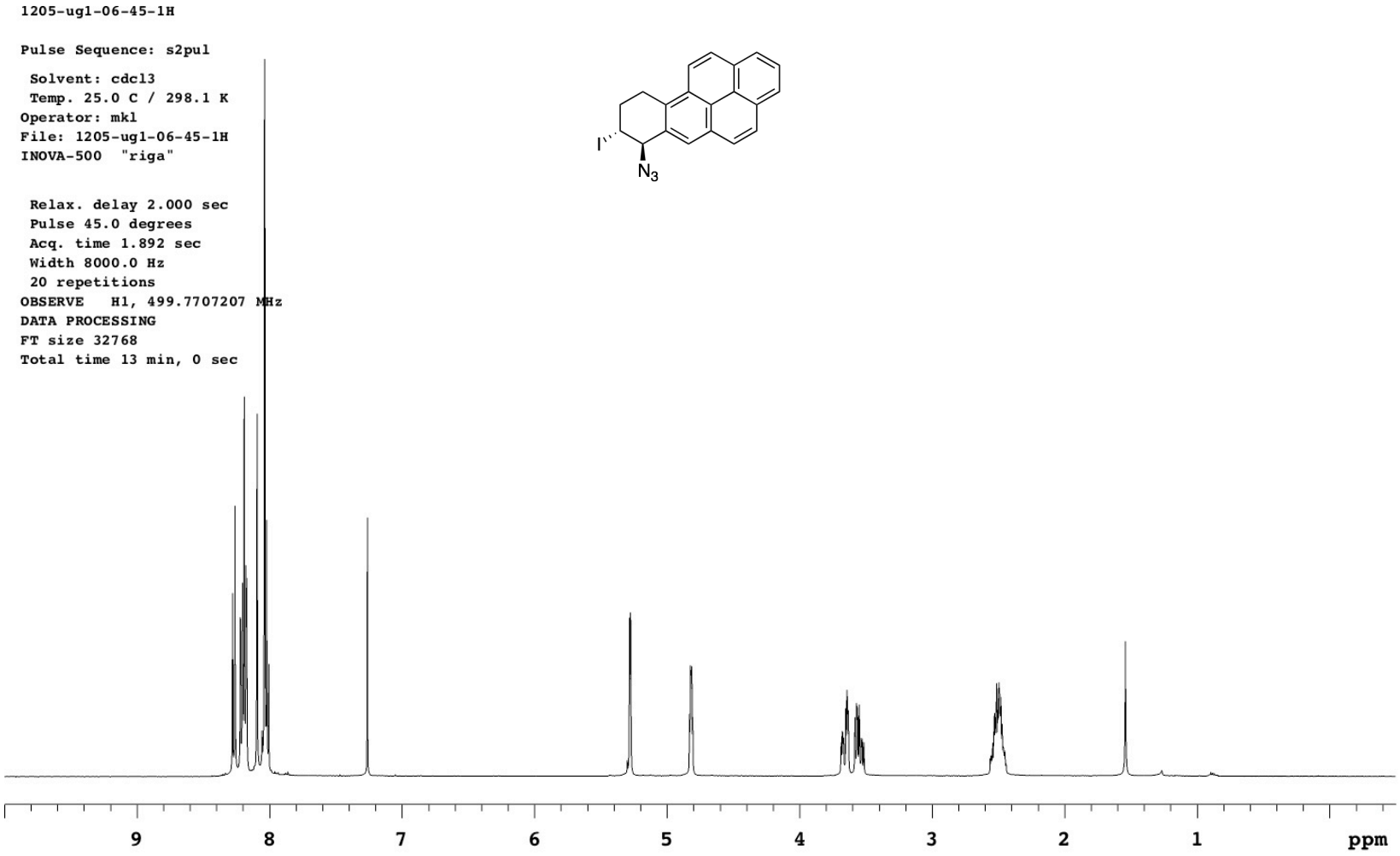
1205-ug1-06-45-1H
Pulse Sequence: s2pul
Solvent: cdcl3
Temp. 25.0 C / 298.1 K
Operator: mkl
File: 1205-ug1-06-45-1H
INOVA-500 "riga"
Relax. delay 2.000 sec
Pulse 45.0 degrees
Acq. time 1.892 sec
Width 8000.0 Hz
20 repetitions
OBSERVE H1, 499.7707207 MHz
DATA PROCESSING
FT size 32768
Total time 13 min, 0 sec
I
N3
9
8
7
6
5
4
3
2
1
ppm

1205-ug1-06-45-C13

Archive directory: /export/home/mkl/vnmrsys/data
Sample directory:

Pulse Sequence: s2pul

Solvent: CDCl3
Temp. 25.0 C / 298.1 K
Operator: mkl
File: 1205-ug1-06-45-C13
INOVA-500 "riga"

Relax. delay 4.000 sec
Pulse 52.1 degrees
Acq. time 1.300 sec
Width 29996.3 Hz
640 repetitions
OBSERVE C13, 125.6674457 MHz
DECOUPLE H1, 499.7732084 MHz
Power 42 dB
on during acquisition
WALTZ-16 modulated
DATA PROCESSING
Line broadening 2.0 Hz
FT size 131072
Total time 132 hr, 44 min, 27 sec

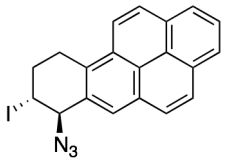

1205-ug1-08-025

Archive directory: /export/home/mkl/vnmrsys/data
Sample directory:

Pulse Sequence: s2pul

Solvent: CDCl3
Temp. 25.0 C / 298.1 K
Operator: mkl
File: 1205-ug1-08-025
INOVA-500 "riga"

Pulse 45.0 degrees
Acq. time 1.892 sec
Width 10000.0 Hz
44 repetitions
OBSERVE H1, 499.7707211 MHz
DATA PROCESSING
Gauss apodization 0.600 sec
FT size 65536
Total time 6 min, 20 sec

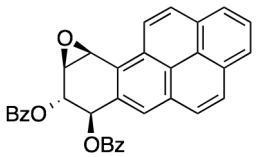

1205-ug1-08-031N3_1H

Archive directory: /export/home/mkl/vnmrsys/data
Sample directory:

Pulse Sequence: s2pul

Solvent: CDCl3
Temp. 25.0 C / 298.1 K
Operator: mkl
File: 1205-ug1-08-031N3_1H
INOVA-500 "riga"

Relax. delay 3.000 sec
Pulse 45.0 degrees
Acq. time 1.892 sec
Width 6662.2 Hz
32 repetitions
OBSERVE H1, 499.7707211 MHz
DATA PROCESSING
Resol. enhancement 0.5 Hz
Gauss apodization 0.600 sec
FT size 32768
Total time 2 min, 36 sec

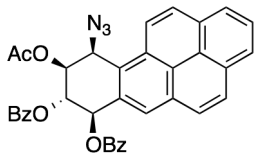

1205-ug1-09-7-C13

Archive directory: /export/home/mkl/vnmrsys/data
Sample directory:

Pulse Sequence: s2pul

Solvent: CDCl3
Temp. 25.0 C / 298.1 K
Operator: mkl
File: 1205-ug1-09-7-C13
INOVA-500 "riga"

Relax. delay 4.000 sec
Pulse 52.1 degrees
Acq. time 1.300 sec
Width 29996.3 Hz
1116 repetitions
OBSERVE C13, 125.6674457 MHz
DECOUPLE H1, 499.7732084 MHz
Power 42 dB
on during acquisition
WALTZ-16 modulated
DATA PROCESSING
Line broadening 2.0 Hz
FT size 131072
Total time 132 hr, 44 min, 27 sec

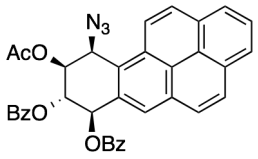

1205-ug1-09-8-1Hagain

Archive directory: /export/home/mkl/vnmrsys/data
Sample directory:

Pulse Sequence: s2pul

Solvent: acetone
Temp. 25.0 C / 298.1 K
Operator: mkl
File: 1205-ug1-09-8-1Hagain
INOVA-500 "riga"

Relax. delay 1.000 sec
Pulse 45.0 degrees
Acq. time 1.892 sec
Width 8000.0 Hz
12 repetitions
OBSERVE H1, 499.7733163 MHz
DATA PROCESSING
FT size 32768
Total time 6 min, 11 sec

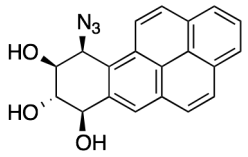

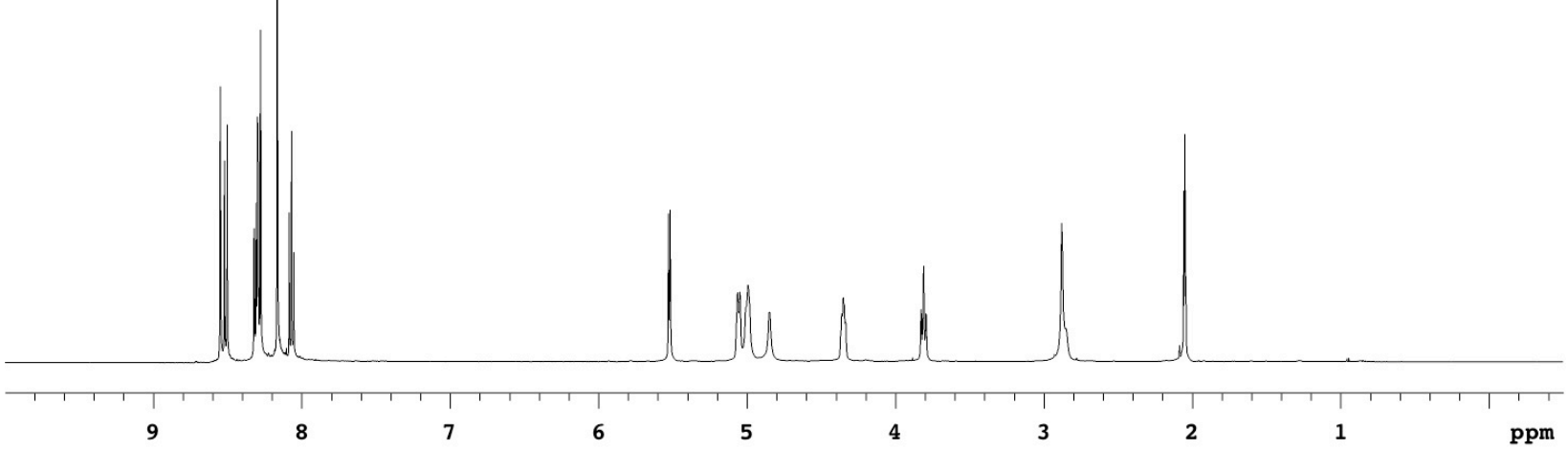

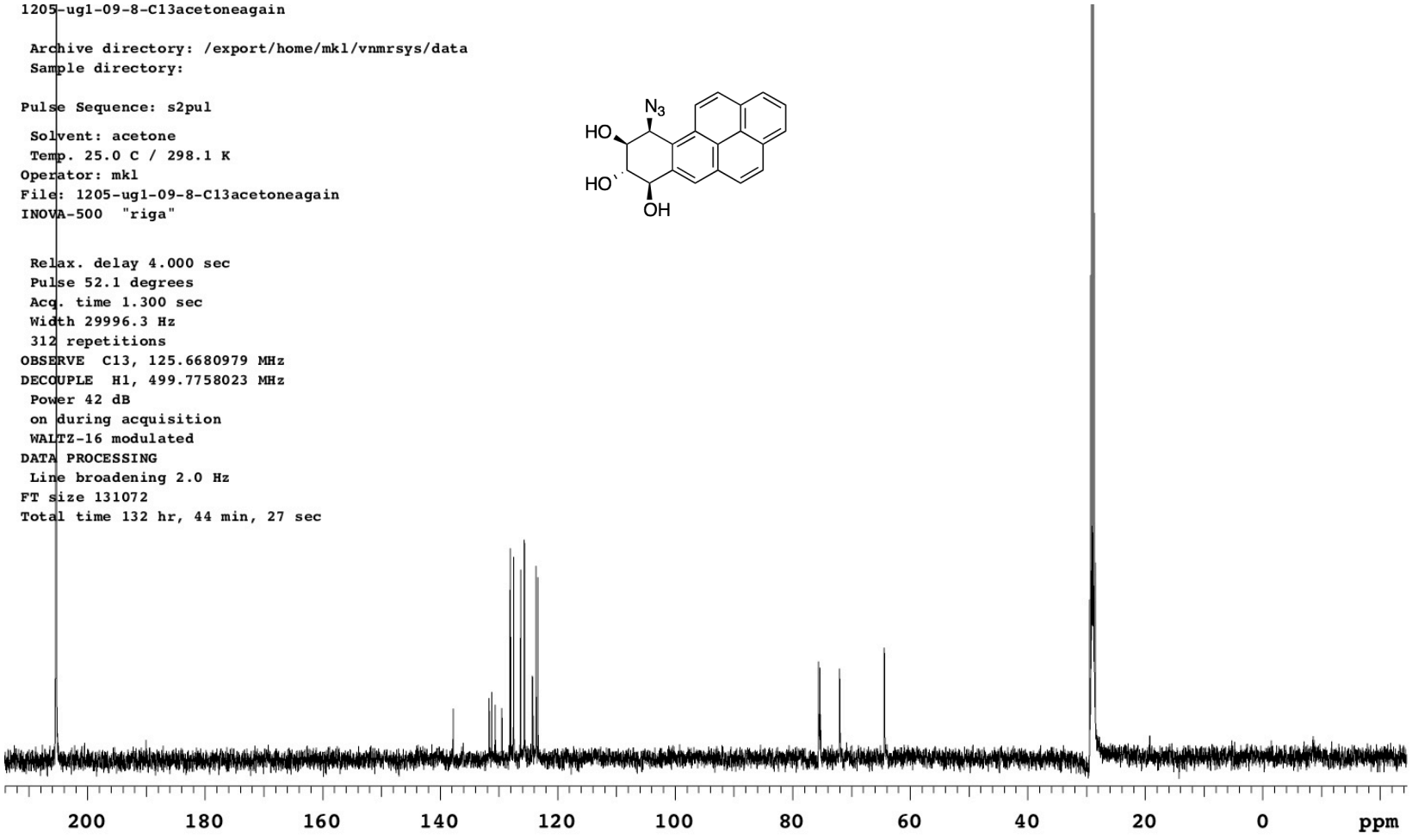
1205-ug1-09-8-C13acetoneagain
Archive directory: /export/home/mkl/vnmrsys/data
Sample directory:
Pulse Sequence: s2pul
Solvent: acetone
Temp. 25.0 C / 298.1 K
Operator: mkl
File: 1205-ug1-09-8-C13acetoneagain
INOVA-500 "riga"
Relax. delay 4.000 sec
Pulse 52.1 degrees
Acq. time 1.300 sec
Width 29996.3 Hz
312 repetitions
OBSERVE C13, 125.6680979 MHz
DECOUPLE H1, 499.7758023 MHz
Power 42 dB
on during acquisition
WALTZ-16 modulated
DATA PROCESSING
Line broadening 2.0 Hz
FT size 131072
Total time 132 hr, 44 min, 27 sec
N3
HO
HO
OH
200
180
160
140
120
100
80
60
40
20
0
ppm

1205-ug1-09-25-1Hagain

Archive directory: /export/home/mkl/vnmrsys/data
Sample directory:

Pulse Sequence: s2pul

Solvent: acetone
Temp. 25.0 C / 298.1 K
Operator: mkl
File: 1205-ug1-09-25-1Hagain
INOVA-500 "riga"

Relax. delay 2.000 sec
Pulse 45.0 degrees
Acq. time 1.231 sec
Width 6653.9 Hz
24 repetitions
OBSERVE H1, 499.7733162 MHz
DATA PROCESSING
FT size 16384
Total time 6 min, 54 sec

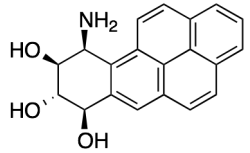

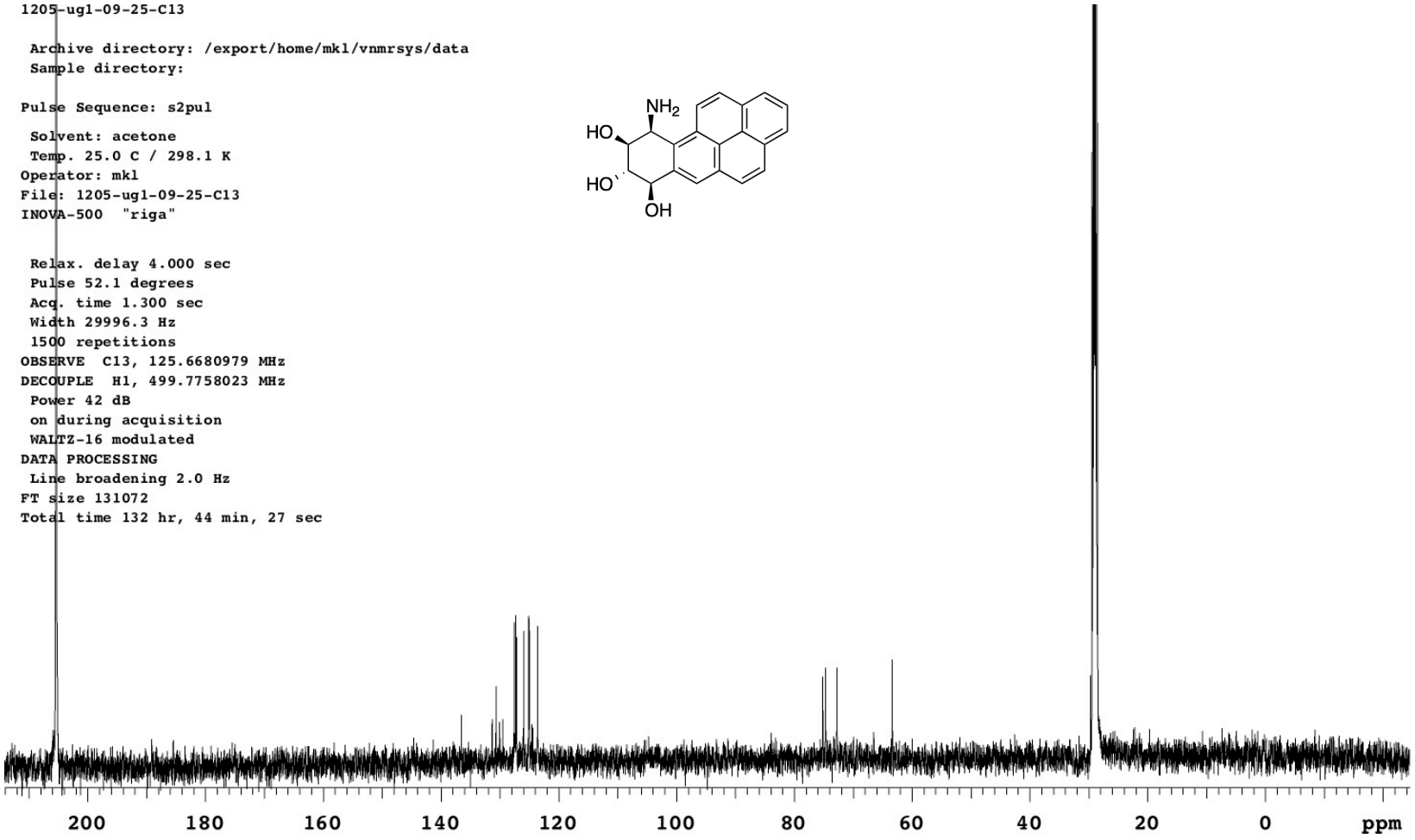
1205-ug1-09-25-C13
Archive directory: /export/home/mkl/vnmrsys/data
Sample directory:
Pulse Sequence: s2pul
Solvent: acetone
Temp. 25.0 C / 298.1 K
Operator: mkl
File: 1205-ug1-09-25-C13
INOVA-500 "riga"
Relax. delay 4.000 sec
Pulse 52.1 degrees
Acq. time 1.300 sec
Width 29996.3 Hz
1500 repetitions
OBSERVE C13, 125.6680979 MHz
DECOUPLE H1, 499.7758023 MHz
Power 42 dB
on during acquisition
WALTZ-16 modulated
DATA PROCESSING
Line broadening 2.0 Hz
FT size 131072
Total time 132 hr, 44 min, 27 sec
NH2
HO
HO
OH
200
180
160
140
120
100
80
60
40
20
0
ppm

1205-ug1-08-74B-1H

Pulse Sequence: s2pul

Solvent: cdcl3
Temp. 25.0 C / 298.1 K
Operator: mkl
File: 1205-ug1-08-74B-1H
INOVA-500 "riga"

Relax. delay 2.000 sec
Pulse 45.0 degrees
Acq. time 1.892 sec
Width 8000.0 Hz
16 repetitions
OBSERVE H1, 499.7707222 MHz
DATA PROCESSING
FT size 32768
Total time 13 min, 0 sec

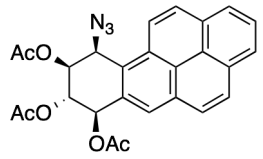

1205-ug1-08-74B-C13

Archive directory: /export/home/mkl/vnmrsys/data
Sample directory:

Pulse Sequence: s2pul

Solvent: CDCl3
Temp. 25.0 C / 298.1 K
Operator: mkl
File: 1205-ug1-08-74B-C13
INOVA-500 "riga"

Relax. delay 4.000 sec
Pulse 52.1 degrees
Acq. time 1.300 sec
Width 29996.3 Hz
820 repetitions
OBSERVE C13, 125.6674457 MHz
DECOUPLE H1, 499.7732084 MHz
Power 42 dB
on during acquisition
WALTZ-16 modulated
DATA PROCESSING
Line broadening 2.0 Hz
FT size 131072
Total time 132 hr, 44 min, 27 sec

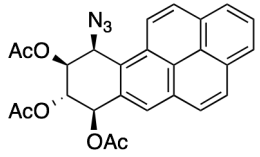

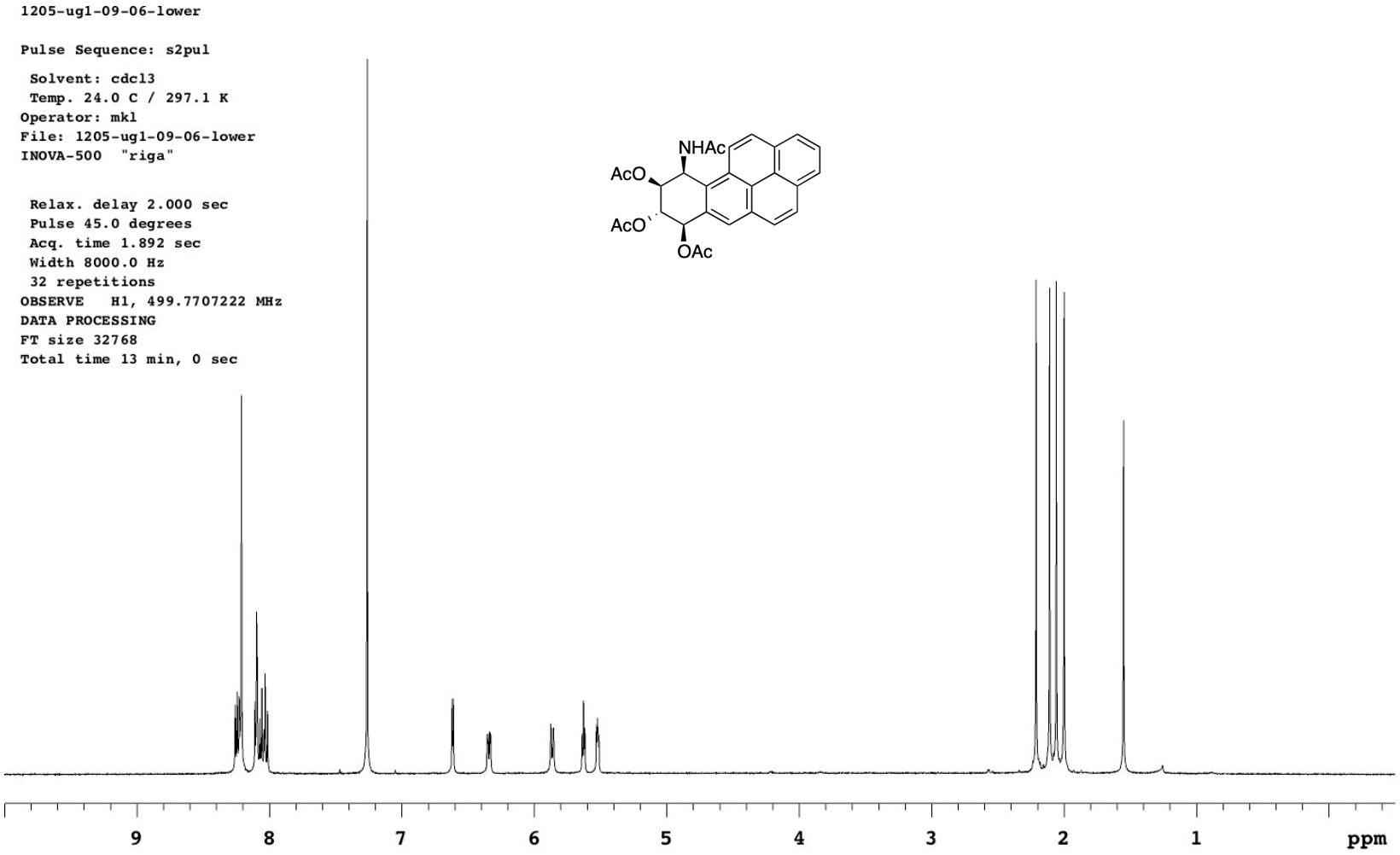
1205-ug1-09-06-lower
Pulse Sequence: s2pul
Solvent: cdcl3
Temp. 24.0 C / 297.1 K
Operator: mkl
File: 1205-ug1-09-06-lower
INOVA-500 "riga"
Relax. delay 2.000 sec
Pulse 45.0 degrees
Acq. time 1.892 sec
Width 8000.0 Hz
32 repetitions
OBSERVE H1, 499.7707222 MHz
DATA PROCESSING
FT size 32768
Total time 13 min, 0 sec
NHAc
AcO
AcO
OAc
9
8
7
6
5
4
3
2
1
ppm

1205-ug1-09-29-C13

Archive directory: /export/home/mkl/vnmrsys/data
Sample directory:

Pulse Sequence: s2pul

Solvent: CDCl3
Temp. 25.0 C / 298.1 K
Operator: mkl
File: 1205-ug1-09-29-C13
INOVA-500 "riga"

Relax. delay 4.000 sec
Pulse 52.1 degrees
Acq. time 1.300 sec
Width 29996.3 Hz
1840 repetitions
OBSERVE C13, 125.6674457 MHz
DECOUPLE H1, 499.7732084 MHz
Power 42 dB
on during acquisition
WALTZ-16 modulated
DATA PROCESSING
Line broadening 2.0 Hz
FT size 131072
Total time 132 hr, 44 min, 27 sec

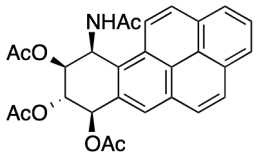

Bibliography

Chapter 1

1. (a) Yang, B. H.; Buchwald, S. L. *J. Organomet. Chem.* **1999**, *576*, 125-146.

   (b) Hartwig J. F. in *Modern Amination Methods* (Ed.: A. Ricci), Wiley-VCH, Weinheim, **2000**, pp. 195-262.

   (c) Muci, A. R.; Buchwald S. L. in *Topics in Current Chemistry, Vol. 219* (Ed.: N. Miyaura), Springer-Verlag, Berlin, Germany, **2002**, pp 131-209.

   (d) Schlummer, B.; Scholz, U. *Adv. Synth. Catal.* **2004**, *346*, 1599-1626.

   (e) Hartwig J. F. in *Modern Arene Chemistry* (Ed.: D. Astruc), Wiley-VCH, Weinheim, **2004**, pp. 107-168.

   (f) Surrey, D. S.; Buchwald, S. L. *Angew. Chem. Int. Ed.* **2008**, *47*, 6338-6361.

2. (a) Wurtz, A. *Ann. Chim. Phys.* **1855**, *44*, 275-312.

   (b) Ullmann, F.; Bielecki, J. *Chem. Ber.* **1901**, *34,* 2174–2185.

   (c) Goldberg, I. *Chem. Ber.* **1906**, *39,* 1691-1692.

   (d) Taylor, B. L. H.; Jarvo, E. R. *J. Org. Chem.* **2011**, *76*, 7573-7576.

3. Lindley, J. *Tetrahedron*, **1984**, *40*, 1433-1456.

4. Kosugi, M.; Kameyama, M.; Migita, T. *Chem. Lett.* **1983**, 927-928.

5. Paul, F.; Patt, J.; Hartwig, J. F. *J. Am. Chem. Soc.* **1994**, *116*, 5969-5970.

6. Guram, A.; Buchwald, S. *J. Am. Chem. Soc.* **1994**, *116*, 7901-7902.

7. Guram, A. S.; Rennels, R. A.; Buchwald, S. L. *Angew. Chem. Int. Ed. Engl.* **1995**, 34, 1348-1350.

8. Louie, J.; Hartwig, J. F. *Tetrahedron Lett.* **1995**, *36*, 3609-3612.

9. Wolfe, J.; Wagaw, S.; Buchwald, S. *J. Am. Chem. Soc.* **1996**, *118*, 7215-7216.

10. (a) Driver, M. S.; Hartwig, J. F. *J. Am. Chem. Soc.* **1996**, 118, 7217-7218.

    (b) Driver, M.; Hartwig, J. *J. Am. Chem. Soc*. **1997**, *119*, 8232-8233.

11. (a) Mann, G.; Hartwig, J.; Driver, M. S.; Fernández-Rivas, C. *J. Am. Chem. Soc.* **1998**, *120*, 827-828.

(b) Yin, J.; Buckwald, S. *J. Am. Chem. Soc.* **2002**, *124*, 6043-6044.

12. Louie, J.; Driver, M. S.; Hamann, B. C.; Hartwig, J. F. *J. Org. Chem*. **1997**, *62*, 1268-1273.

13. Old, D. W.; Wolfe, J.; Buchwald, S. *J. Am. Chem. Soc.* **1998**, *120*, 9722-9722.

14. (a) Alcazar-Roman, L. M.; Hartwig, J. F.; Rheingold, A. L.; Liable-Sands, L. M.; Guzei, I. A. *J. Am. Chem. Soc.* **2000**, *122*, 4618-4630.

(b) Singh, U. K.; Strieter, E. R.; Blackmond, D. G.; Buchwald, S. L. *J. Am. Chem. Soc.* **2002**, *124*, 14104-14114.

(c) Shekhar, S.; Ryberg, P.; Hartwig, J. F.; Mathew, J. S.; Blackmond, D. G.; Strieter, E. R.; Buckwald, S. L. *J. Am. Chem. Soc.* **2006**, *128*, 3584-3591.

15. Wagaw, S.; Buchwald, S. L. *J. Org. Chem.* **1996**, *61*, 7240-7241.

16. Lakshman, M. K.; Keeler, J. C.; Hilmer, J. H.; Martin, J. Q. *J. Am. Chem. Soc.* **1999**, *121*, 6090-6091.

17. Panzica, R. J.; Rousseau, R. J.; Robins, R. J.; Townsend, L. B. *J. Am. Chem. Soc.* **1972***, 94*, 4708-4714.

18. (a) Suhadolnik, R. J. *Nucleosides as Biological Probes*, Wiley, New York, **1979**.

(b) Simons, C. *Nucleoside Mimetics: Their Chemistry and Biological Properties*, Gordon and Breach, Amsterdam, **2001**.

(c) *Perspectives in Nucleoside and Nucleic Acid Chemistry* (Eds.: Kisakürek, M. V.; Rosemeyer, H.), Verlag Helvetica Chimica Acta, Zurich and Wiley-VCH, Weinheim, **2000**.

(d) *Nucleic Acids in Chemistry and Biology*, 3rd edn. (Eds.: Blackburn, G. M.; Gait, M. J.; Loakes, D.; Williams, D. M.), RSC Publishing, Cambridge, UK, **2006**.

(e) *Modified Nucleosides in Biochemistry, Biotechnology and Medicine*, (Ed. P. Herdewijn), Wiley-VCH, Weinheim, **2008**.

19. (a) Daly, J. W. *J. Med. Chem.* **1982**, *25*, 197-207.

(b) van der Wenden, E. M.; von Freijtag Drabbe Künzel, J. K.; Mathôt, R. A. A.; Danhof, M.; IJzerman A. P.; Soudijn, W. *J. Med. Chem.* **1995**, *38*, 4000-4006.

20. Wright, G. E.; Dudycz, L. W. *J. Med. Chem.* **1984**, *27*, 175-181.

21. (a) Golisade, A.; Wiesner, J.; Herforth, C.; Jomaa, H.; Link, A. *Bioorg. Med. Chem.* **2002**, *10*, 769-777.

(b) Zohrabi-Kalantari, V.; Heider, P.; Kaiser, M.; Brun, R.; Kamper, C.; Link, A. *Mol. Divers.* **2009**, *14*, 307-320.

22. For a review see: Lakshman, M. K. *Curr. Org. Synth.* **2005**, *2*, 83-112.

23. Harwood, E. A.; Sigurdsson, S. T.; Edfeldt, N. F.; Reid, B. R.; Hopkins, P. B. *J. Am. Chem. Soc.* **1999**, *121*, 5081-5082.

24. Shapiro, R.; Dubelman, S.; Feinberg, A. M.; Crain, P. F.; McCloskey, J. A. *J. Am. Chem. Soc.* **1977**, *99*, 302-303.

25. De Riccardis, F.; Johnson, F. *Org. Lett.* **2000**, *2*, 293-295.

26. Lakshman, M. K.; Hilmer, J. H.; Martin, J. Q.; Keeler, J. C.; Dinh, Y. Q. V.; Ngassa, F. N.; Russon, L. M. *J. Am. Chem. Soc*. **2001**, *123*, 7779-7787.

27. De Riccardis, F.; Bonala, R. R.; Johnson, F. *J. Am. Chem. Soc.* **1999**, *121*, 10453-10460.

28. Harwood, E. A.; Hopkins, P. B.; Sigurdsson, S. T. *J. Org. Chem.* **2000**, *65*, 2959-2964.

29. Bonala, R. R.; Shishkina, I. G.; Johnson, F. *Tetrahedron Lett.* **2000**, *41*, 7281-7284.

30. Wang, Z.; Rizzo, C. J. *Org. Lett.* **2001**, *3*, 565-568.

31. Meier, C.; Gräsl, S. *Synlett* **2002**, 802-804.

32. Schoffers, E.; Olsen, P. D.; Means, J. C. *Org. Lett.* **2001**, *3*, 4221-4223.

33. Shabad, L. M. *J. Natl. Cancer Inst.* **1980**, *64*, 405-410.

34. (a) Buening, M. K.; Wislocki, P. G.; Levin, W.; Yagi, H.; Thakker, D. R.; Akagi, H.; Koreeda, M.; Jerina, D. M.; Conney, A. H. *Proc. Natl. Acad. Sci. USA* **1978**, *75*, 5358-5361.

(b) Cosman, M.; Ibanez, V.; Geacintov, N. E.; Harvey, R. G. *Carcinogenesis* **1990**, *11*, 1667-1672.

(c) Szeliga, J.; Dipple, A. *Chem. Res. Toxicol.* **1998**, *11*, 1-11.

35. Lakshman, M. K.; Ngassa, F. N.; Bae, S.; Buchanan, D. G.; Hahn, H.-G.; Mah, H. *J. Org. Chem.* **2003**, *68*, 6020-6030.

36. Johnson, F.; Bonala, R.; Tawde, D.; Torres, M. C.; Iden, C. R. *Chem. Res. Toxicol.* **2002**, *12*, 1489-1494.

37. Champeil, E.; Pradhan, P.; Lakshman, M. K. *J. Org. Chem*. **2007**, *72*, 5035-5045.

38. (a) Bunnet, J. F.; Zahler, R. E. *Chem. Re*v. **1951**, *49*, 273-412.

(b) Liu, J.; Robins, M. J. *J. Am. Chem. Soc.* **2007**, *129*, 5926-5968.

39. Véliz, E. A.; Beal, P. A. *J. Org. Chem.* **2001**, *66*, 8592-8598.

40. Lakshman, M. K.; Gunda, P. *Org. Lett.* **2003**, *5*, 39-42.

41. Lagisetty, P.; Russon, L. M.; Lakshman, M. K. *Angew. Chem. Int. Ed.* **2006**, *118*, 3742-3745.

42. Barends, J. van der Linden, J. B. van Delft, F. L. Koomen, G.-J. *Nucleosides Nucleotides* **1999**, *18*, 2121-2126.

43. (a) Lakshman, M. K. *J. Organomet. Chem.* **2002**, *653*, 234-251.

(b) Hocek, M. *Eur. J. Org. Chem.* **2003**, 245-254.

(c) Agrofoglio, L. A.; Gillaizeau, I.; Saito, Y. *Chem. Rev.* **2003**, *103*, 1875-1916.

44. Nair, V.; Richardson, S. G. *J. Org. Chem.* **1980**, *45*, 3969-3974.

45. Maruenda, H.; Chenna, A.; Liem, L.-K.; Singer, B. *J. Org. Chem.* **1998**, *63*, 4385-4389.

46. Robins, M. J.; Basom, G. L. *Can. J. Chem.* **1973**, *51*, 3161-3169.

47. Bergstrom, D. E.; Reddy, P. A.; *Tetrahedron Lett.* **1982**, *23*, 4191-4194.

48. (a) Gerster, J. F.; Jones, J. W.; Robins, R. K. *J. Org. Chem.* **1963**, *28*, 945-948.

(b) Véliz, E. A.; Beal, P. A. *Tetrahedron Lett.* **2000**, *41*, 1695-1697.

49. (a) Böge, N.; Gräsl, S.; Meier, C. *J. Org. Chem.* **2006**, *71*, 9728-9738.

(b) Böge, N.; Jacobsen, M. I.; Szombati, Z.; Baerns, S.; Di Pasquale, F.; Marx, A.; Meier, C. *Chem. Eur. J.* **2008**, *14*, 11194-11208.

50. (a) Takamura-Enya, T.; Ishikawa, S.; Mochizuki, M.; Wakabayashi, K. *Tetrahedron Lett.* **2003**, *44*, 5969-5973.

(b) Takamura-Enya, T.; Enomoto, S.; Wakabayashi, K. *J. Org. Chem.* **2006**, *71*, 5599-5606.

51. (a) Wang, Z.; Rizzo, C. J. *Org. Lett.* **2001**, *3*, 565-568.

(b) Stover, J. S.; Rizzo, C. J. *Org. Lett.* **2004**, *6*, 4985-4988.

(c) Elmquist, C. E.; Stover, J.; Wang, S. Z.; Rizzo, C. J. *J. Am. Chem. Soc.* **2004**, *126*, 11189-11201.

52. Chakraborti, D.; Colis, L.; Schneider, R.; Basu, A. K. *Org. Lett.* **2003**, *5*, 2861-2864.

53. Gillet, L. C. J.; Schärer, O. D. *Org. Lett.* **2002**, *4*, 4205-4208.

54. Gunda, P.; Russon, L. M.; Lakshman, M. K. *Angew. Chem. Int. Ed.* **2004**, *43*, 6372-6377 (also see corrigendum: Gunda, P.; Russon, L. M.; Lakshman, M. K. *Angew. Chem. Int. Ed.* **2005**, *44*, 1154).

55. Ngassa, F. N.; DeKorver, K. A.; Melistas, T. S.; Yeh, E. A.-H.; Lakshman, M. K. *Org. Lett.* **2006**, *8*, 4613-4616.

56. (a) Havelková, M.; Hocek, M.; Cesnek, M.; Dvorák, D. *Synlett* **1999**, 1145-1147.

(b) Hocek, M.; Holý, A.; Votruba, I.; Dvoráková, H. *J. Med. Chem.* **2000**, *43*, 1817-1825.

57. Myers, A. G.; Harrington, P. M.; Kuo, E. Y. *J. Am. Chem. Soc.* **1991**, *113*, 694-695.

58. Noyori, R.; Nishida, I.; Sakata, J.; Nishizawa, M. *J. Am. Chem. Soc.* **1980**, *102*, 1223-1225.

59. Assays conducted by Drs. Jan Balzarini and Erik De Clercq, and their co-workers, at the Rega Institute for Medical Research, Minderbroedersstraat 10, B-3000, Leuven, Belgium.

Chapter 2

1. The initial studies on PAH and carcinogenesis has been reviewed in:

(a) *Polycyclic Aromatic Hydrocarbon Carcinogenesis: Structure-Activity Relationships* Yang, S. K.; Silverman, B. D., Eds.; CRC Press: Boca Raton, FL, 1988 (Volumes I and II).

(b) *Polycyclic Aromatic Hydrocarbons: Chemistry and Carcinogenicity* Harvey, R. G., Ed.; Cambridge Unviersity Press: Cambridge, 1991. *Polycyclic Hydrocarbons and Carcinogenesis* Harvey, R. G., Ed.; ACS Symposium Series 283: Washington, DC, 1985.

(c) Dipple, A.: Reactions of polycyclic aromatic hydrocarbons with DNA. In *DNA Adducts: Identification and Biological Significance*; Hemminki, K.; Dipple, A.; Shuker, D. E. G.; Kadlubar, F. F.; Sagerbäck, D.; Bartsch, H., Eds.; Scientific Publication No. 125, International Agency for Research on Cancer: Lyon, 1994; pp. 107-129.

(d) For a detailed survey of the chemistry of polycyclic aromatic hydrocarbons, please see: *Polycyclic Aromatic Hydrocarbons* Harvey, R. G.; Wiley-VCH, NY, 1997.

2. (a) Sims, P.; Grover, P. L. *Adv. Cancer Res.* **1974**, *20*, 165-174.

(b) Shabad, L. M. *J. Natl. Cancer Inst.* **1980**, *64*, 405-410.

(c) Harvey, R. G.; Geacintov, N. E. *Acc. Chem. Res.* **1988**, *21*, 66-73.

(d) Garner, C. R. *Mutat. Res.* **1998**, *402*, 67-75.

3. Chen, L.; Devanesan, P. D.; Higginbotham, S.; Ariese, F.;Jankowiak, R.; Small, G. J.; Rogan, E. G.; Cavalieri, E. L. *Chem. Res. Toxicol.* **1996**, *9*, 897-903.

4. Cavalieri, E. L.; Rogan, E. G. *Xenobiotica* **1995**, *25*, 677-688.

5. Cavalieri, E. L.; Rogan, E. G. *Ann. N.Y. Acad. Sci.* **2002**, *959*, 341-354.

6. Cavalieri, E. L.; Rogan, E. G. *Polycycl. Aromat. Compds.* **1996**, *10*, 251-258.

7. (a) Penning, T. M.; Burczynski, M. E.; Hung, C.-F.; McCoull, K. D.; Palackal, N. T.; Tsuruda, L. S. *Chem. Res. Toxicol.* **1999**, *12*, 1-18.

(b) Bolton, J. L.; Trush, M. A.; Penning, T. M.; Dryurst, G.; Monks, T. J. *Chem. Res. Toxicol.*

2000, *13*, 135-160.

8. Smithgall, T. E.; Harvey, R. G.; Penning, T. M. *J. Biol. Chem.* **1988**, *263*, 1814-1820.

9. Cheng, K. C.; Cahill, D. S.; Kasai, H.; Nishimura, S.; Loeb, L. A. *J. Biol. Chem.* **1992**, *267*, 166-172.

10. Guengerich, F. P.; Shimada, T. *Chem. Res. Toxicol.* **1991**, *4*, 391-407.

11. (a) Oesch, F. *Xenobiotica* **1973**, *3*, 305-340.

(b) Conney, A. H. *Cancer Res.* **1982**, *42*, 4875-4917.

12. (a) Jerina, D. M.; Daly, J. W. *Science* **1974**, *185*, 573-582.

(b) Lacourciere, G. M.; Armstrong, R. N. *J. Am. Chem. Soc.* **1993**, 115, 10466-10467.

13. (a) Sayer, J. M.; Yagi, H.; Croisy-Delcey, M.; Jerina, D. M. *J. Am. Chem. Soc.* **1981**, *103*, 4970-4972.

(b) Yang, S. K. *Biochem. Pharmacol.* **1988**, *37*, 61-70.

14. For studies on the influence of PAH diol epoxide chirality on biological output:

(a) Wei, S.-J.C.; Chang, R. L.; Hennig, E.; Cui, E. E.; Merkler, K. A.; Wong, C.-Q.; Yagi, H.; Jerina, D. M.; Conney, A. H. *Carcinogenesis* **1994**, *15*, 1729-1735.

(b) Jelinsky, S. A.; Liu, T.; Geacintov, N. E.; Loechler, E. L. *Biochemistry* **1995**, *34*, 13545-13553.

(c) Zou, Y.; Liu, T.-M.; Geacintov, N. E.; Van Houten, B. *Biochemistry* **1995**, *34*, 13582-13593.

(d) Chary, P.; Lloyd, R. S. *Chem. Res. Toxicol.* **1996**, *9*, 409-417.

(e) Hanrahan, C. J.; Bacolod, M. D.; Vyas, R. R.; Liu, T.; Geacintov, N. E.; Loechler, E. L.; Basu, A. K. *Chem. Res. Toxicol.* **1997**, *10*, 369-377.

(f) Shukla, R.; Liu, T.; Geacintov, N. E.; Loechler, E. L. *Biochemistry* **1997**, *36*, 10256-10261.

(g) Fernandes, A.; Liu, T.; Amin, S.; Geacintov, N. E.; Grollman, A. P.; Moriya, M. *Biochemistry* **1998**, *37*, 10164-10172.

15. Levin, W.; Chang, R. L.; Wood, A. W.; Thakker, D. R.; Yagi, H.; Jerina, D. M.; Conney, A. H. *Cancer Res.* **1986**, *46*, 2257-2261.

16. (a) Agarwal, S. K.; Sayer, J. M.; Yeh, H. J. C.; Pannell, L. K.; Hilton, B. D.; Pigott, M. A.; Dipple, A.; Yagi, H.; Jerina, D. M. *J. Am. Chem. Soc.* **1987**, *109*, 2497-2504.

(b) Einholf, H. J.; Amin, S.; Yagi, H.; Jerina, D. M.; Baird, W. M. *Carcinogenesis* **1996**, *17*, 2237-

2244.

17. (a) Sayer, J. M.; Chadha, A., Agarwal, S. K.; Yeh, H. J. C.; Yagi, H.; Jerina, D. M. *J. Org. Chem.* **1991**, *56* 20-29.

(b) Jerina, D. M.; Chadha, A.; Cheh, A. M.; Schurdak, M. E.; Wood, A. W.; Sayer, J. M. *Biological Reactive Intermediates IV*, Witmer, C. M.; Snyder, R.; Jollow, D. J.; Kalf, G. F.; Kocsis, J. J.; Sipes, I. G., Eds.; Plenum Press: New York, 1991; pp. 533-553.

18. Szeliga, J.; Dipple, A. *Chem. Res. Toxicol.* **1998**, *11*, 1-11.

19. (a) Lakshman, M. K.; Kole, P. L.; Chaturvedi, S.; Saugier, J. H.; Yeh, H. J. C.; Glusker, J. P.; Carrell, H. L.; Katz, A. K.; Afshar, C. E.; Dashwood, W. –M.; Kenniston, G. J.; Baird, W. M. *J. Am. Chem. Soc.*, **2000**, *122*, 12629-12636.

(b) Lakshman, M. K.; Ngassa, F. N.; Bae, S.; Buchanan, D. G.; Hahn, H.-G.; Mah, H. *J. Org. Chem.* **2003**, *68*, 6020-6030.

20. (a) Lakshman, M. K.; Sayer, J. M.; Jerina, D. M. *J. Am. Chem. Soc.* **1991**, *113*, 6589-6594.

(b) Lakshman, M. K.; Sayer, J. M.; Jerina, D. M. *J. Org. Chem.* **1992**, *57*, 3438-3443.

(c) Lakshman, M. K.; Sayer, J. M.; Yagi, H.; Jerina, D. M. *J. Org. Chem.* **1992**, *57*, 4585-4590.

(d) Chaturvedi, S.; Lakshman, M. K. *Carcinogenesis* **1996**, *17*, 2747-2752.

21. (a) Lakshman, M.; Lehr, R. E. *Tetrahedron Lett.* **1990**, *31*, 1547-1550.

(b) Kim, S. J.; Harris, C. M.; Jung, K.-Y.; Koreeda, M.; Harris, T. M. *Tetrahedron Lett.* **1991**, *32*, 6073-6076.

22. (a) Lakshman, M.; Nadkarni, D. V.; Lehr, R. E. *J. Org. Chem.* **1990**, *55*, 4892-4897.

(b) Lakshman, M. K.; Chaturvedi, S.; Lehr, R. E. *Synth. Commun.* **1994**, *24*, 2983-2988.

23. Champeil, E.; Pradhan, P.; Lakshman, M. K. *J. Org. Chem.* **2007**, *72*, 5035-5045.

24. (a) Zajc, B.; Lakshman, M. K.; Sayer, J. M.; Jerina, D. M. *Tetrahedron Lett.* **1992**, *33*, 3409-3412.

(b) Custer, L.; Zajc, B.; Sayer, J. M.; Cullinane, C.; Phillips, D. R.; Cheh, A. M.; Jerina, D. M.; Bohr, V. A.; Mazur, S. J. *Biochemistry* **1999**, *38*, 569-581.

25. (a) Steinbrecher, T.; Becker, A.; Stezowski, J. J.; Oesch, F.; Seidel, A. *Tetrahedron Lett.* **1993**, *34*, 1773-1774.

(b) Lee, H.; Luna, E.; Hinz, M.; Stezowski, J. J.; Kiselyov, A. S.; Harvey, R. G. *J. Org. Chem.*

1995, *60*, 5604-5613.

26. Jhingan, A. K.; Meehan, T. *J. Chem. Res. (S*) **1991**, 122-123.

27. Pilcher, A. S.; Yagi, H.; Jerina, D. M. *J. Am. Chem. Soc.* **1998**, *120*, 3520-3521.

28. Kroth, H.; Yagi, H.; Seidel, A.; Jerina, D. M. *J. Org. Chem.* **2000**, *65*, 5558-5564.

29. (a) Ramesha, A. R.; Kroth, H.; Jerina, D. M. *Org. Lett.* **2001**, *3*, 531-533.

(b) Ramesha, A. R.; Kroth, H.; Jerina, D. M. *Tetrahedron Lett.* **2001**, *42*, 1003-1005.

30. Lakshman, M. K.; Keeler, J. C.; Ngassa, F. N.; Hilmer, J. H.; Pradhan, P.; Zajc, B.; Thomasson, K. A. *J. Am. Chem.* Soc. **2007**, *129*, 68-76.

Chapter 3

1. The initial studies on PAH and carcinogenesis has been reviewed in:

(a) *Polycyclic Aromatic Hydrocarbon Carcinogenesis: Structure-Activity Relationships* Yang, S. K.; Silverman, B. D., Eds.; CRC Press: Boca Raton, FL, 1988 (Volumes I and II).

(b) *Polycyclic Aromatic Hydrocarbons: Chemistry and Carcinogenicity* Harvey, R. G., Ed.; Cambridge Unviersity Press: Cambridge, 1991. *Polycyclic Hydrocarbons and Carcinogenesis* Harvey, R. G., ed.; ACS Symposium Series 283: Washington, DC, 1985.

(c) Dipple, A.: Reactions of polycyclic aromatic hydrocarbons with DNA. In *DNA Adducts: Identification and Biological Significance*; Hemminki, K.; Dipple, A.; Shuker, D. E. G.; Kadlubar, F. F.; Sagerbäck, D.; Bartsch, H., Eds.; Scientific Publication No. 125, International Agency for Research on Cancer: Lyon, 1994; pp. 107-129.

(d) For a detailed survey of the chemistry of polycyclic aromatic hydrocarbons, please see: *Polycyclic Aromatic Hydrocarbons* Harvey, R. G.; Wiley-VCH, NY, 1997.

2. (a) Sims, P.; Grover, P. L. *Adv. Cancer Res.* **1974**, *20*, 165-174.

(b) Shabad, L. M. *J. Natl. Cancer Inst.* **1980**, *64*, 405-410.

(c) Harvey, R. G.; Geacintov, N. E. *Acc. Chem. Res.* **1988**, *21*, 66-73.

(d) Garner, C. R. *Mutat. Res.* **1998**, *402*, 67-75.

3. Guengerich, F. P.; Shimada, T. *Chem. Res. Toxicol.* **1991**, *4*, 391-407.

4. (a) Oesch, F. *Xenobiotica* **1973**, *3*, 305-340.

(b) Conney, A. H. *Cancer Res.* **1982**, *42*, 4875-4917.

5. (a) Jerina, D. M.; Daly, J. W. *Science* **1974**, *185*, 573-582.

(b) Lacourciere, G. M.; Armstrong, R. N. *J. Am. Chem. Soc.* **1993**, *115*, 10466-10467.

6. (a) Sayer, J. M.; Yagi, H.; Croisy-Delcey, M.; Jerina, D. M. *J. Am. Chem. Soc.* **1981**, *103*, 4970-4972.

(b) Yang, S. K. *Biochem. Pharmacol.* **1988**, *37*, 61-70.

(c) Croisy-Delcey, M.; Ittah, Y,; Jerina, D. M. *Tetrahedron Lett.* **1979**, *31*, 2849-2852.

7. (a) Hirshfeld, F. L.; Sandler, S.; Schmidt, G. M. J. *J. Am. Chem. Soc. Abstr*, **1963**, 2108-2125.

(b) Jerina, D. M.; Sayer, J. M.; Yagi, H.; Croisy-Delcey, M.; Ittah, Y.; Thakker, D. R.; Wood, A. W; Chang, R. L.; Levin, W.; Conney, A. H. In *Biological Reactive Intermediates II Part A*; Snyder, R., Parke, D. V., Kocsis, J. J., Jollow, D. J., Gibson, C. G., Witmer, C. M., Eds.; Plenum Press: New York, 1982; pp 501-523.

(c) Levin, W.; Wood, A. W.; Chang, R. L.; Newman, M. S.; Thakker, D. R.; Conney, A. H.; Jerina, D. M. *Cancer Lett.* **1983**, *20*, 139-146.

8. (a) Kaufman-Katz, A; Carrell, H. L.; Glusker, J. P. *Carcinogenesis* **1998**, *19*, 1641-1648.

(b) Luch A.: On the impact of the molecule structure in chemical carcinogenesis. In *Molecular, Clinical and Environmental Toxicology Volume 1: Molecular Toxicology*. Luch, A., Ed.; Birkhäuser: Basel, Switzerland, 2009; 99, pp. 151-179.

(c) Bailey, G. S.; Reddy, A. P.; Pereira, C. B.; Harttig, U.; Baird, W.; Spitsbergen, J. M.; Hendricks, J. D.; Orner, G. A.; Williams, D. E.; Swenberg, J. A. *Chem. Res. Toxicol.* **2009**, *22*, 1264–1276.

9. (a) Ittah, Y.; Thakker, D. R.; Levin, W.; Croisy-Delcey, M.; Ryan, D. E.; Thomas, P. E.; Conney, A. H.; Jerina, D. M. *Chem.-Biol. Interact.* **1983**, *45*, 15-28.

(b) Thakker, D. R.; Levin, W.; Yagi, H.; Yeh, H. J. C.; Ryan, D. E.; Thomas, P. E.; Conney, A. H.; Jerina, D. M. *J. Biol. Chem.* **1986**, *261*, 5404-5413.

10. Agarwal, S. K.; Sayer, J. M.; Yeh, H. J. C.; Pannell, L. K.; Hilton, B. D.; Pigott, M. A.; Dipple, A.; Yagi, H.; Jerina, D. M. *J. Am. Chem. Soc.* **1987**, *109*, 2497-2504.

11. Jerina, D. M.; Chadha, A.; Cheh, A. M.; Schurdak, M. E.; Wood, A. W.; Sayer, J. M. *Biological Reactive Intermediates IV*, Witmer, C. M.; Snyder, R.; Jollow, D. J.; Kalf, G. F.; Kocsis, J. J.; Sipes, I. G., Eds.; Plenum Press: New York, 1991; pp. 533-553.

12. Levin, W.; Chang, R. L.; Wood, A. W.; Thakker, D. R.; Yagi, H.; Jerina, D. M.; Conney, A. H. *Cancer Res.* **1986**, *46*, 2257-2261.

13. Sayer, J. M.; Yagi, H.; Croisy-Delcey, M.; Jerina, D. M. *J. Am. Chem. Soc.* **1981**, *103*, 4970-4972.

14. (a) Dipple, A.; Pigott, M. A.; Agarwal, S. K.; Yagi, H.; Sayer, J. M.; Jerina, D. M. *Nature* **1987**, *327*, 535-536.

(b) Szeliga, J.; Dipple, A. *Chem. Res. Toxicol.* **1998**, *11*, 1-11.

15. Buterin, T.; Hess, M. T.; Luneva, N.; Geacintov, N. E.; Amin, S.; Kroth, H.; Seidel A.; Naegeli, H. *Cancer Res.* **2000**, *60*, 1849-1856.

16. Zegar, I. S.; Kim, S. J.; Johansen, T. N.; Horton, P. J.; Harris, C. M.; Harris, T. M.; Stone, M. P. *Biochemistry* **1996**, *35*, 6212-6224.

17 (a) Cosman, M.; Fiala, R.; Hingerty, B. E.; Laryea, A.; Lee, H.; Harvey, R. G.; Amin, S.; Geacintov, N. E.; Broyde, S.; Patel, D. J. *Biochemistry* **1993,** *32*, 12488-12497.

(b) Cosman, M.; Laryea, A.; Fiala, R.; Hingerty, B. E,; Amin, S.; Geacintov, N. E.; Broyde, S.; Patel, D. J. *Biochemistry* **1995**, *34*, 1295-1307.

18. (a) Levin, W.; Wood, A. W. Chang, R. L.; Newman, M. S.; Thakker, D. R.; Conney, A. H.; Jerina, D. M. *Cancer Lett.* **1983**, *20*, 139-146.

(b) Harvey, R. G.; Cortez, T.; Sugiyama, T.; Ito, Y.; Sawyer, T. W.; DiGiovanni, J. *J. Med. Chem.* **1988**, *31*, 154-159.

19. (a) Klein, C. L.; Stevens, E. D.; Zacharias, D. E.; Glusker, J. P. *Carcinogenesis* **1987**, *8*, 5-18.

(b) Cavalieri, E. L.; Higginbotham, S.; RamaKrishna, N. V. S.; Devanesan, P. D.; Todorovic, R.; Rogan, E. G.; Salmasi, S. *Carcinogenesis* **1991**, *12*, 1939-1944.

(c) Higginbotham, S.; RamaKrishna, N. V. S.; Johansson, S. L.; Rogan, E. G.; Cavalieri, E. L. *Carcinogenesis* **1993**, *14*, 875-878.

20. (a) Sawicki, J. T.; Moschel, R. C.; Dipple, A. *Cancer Res.* **1983**, *43*, 3212-3218.

(b) Cheng, S. C.; Prakash, A. S.; Pigott, M. A.; Hilton, B. D.; Roman, J. M.; Lee, H.; Harvey, R.

G.; Dipple, A. *Chem. Res. Toxicol.* **1988**, *1*, 216-221.

21. (a) Ralston, S. L.; Lau, H. H. S.; Seidel, A.; Luch, A.; Piatt, K. L.; Baird, W. M. *Cancer Res.* **1994**, *54*, 887-890.

(b) Ralston, S. L.; Seidel, A.; Luch, A.; Piatt, K. L.; Baird, W. M. *Carcinogenesis* **1995**,*16*, 2899-2907.

22. (a) Flesher, J. W.; Sydnor, K. L. *Int. J. Cancer* **1973**, *11*, 433-437.

(b) Dipple, A.; Tomaszewski, J. E.; Moschel, R. C.; Bigger, C. A.; Nebzydoski, J. A.; Egan, M. *Cancer Res.* **1979**, *39*, 1154-1158.

23. (a) Lakshman, M. K.; Kole, P. L.; Chaturvedi, S.; Saugier, J. H.; Yeh, H. J. C.; Glusker, J. P.; Carrell, H. L.; Katz, A. K.; Afshar, C. E.; Dashwood, W. M.; Kenniston, G. J.; Baird, W. M. *J. Am. Chem. Soc.*, **2000**, *122*, 12629-12636.

(b) Lakshman, M. K.; Ngassa, F. N.; Bae, S.; Buchanan, D. G.; Hahn, H.-G.; Mah, H. *J. Org. Chem.* **2003**, *68*, 6020-6030.

24. (a) Oesch, F. *Xenobiotica* **1973**, *3*, 305-340.

(b) Conney, A. H. *Cancer Res.* **1982**, *42*, 4875-4917.

25. (a) Jerina, D. M.; Daly, J. W. *Science* **1974**, *185*, 573-582.

(b) Lacourciere, G. M.; Armstrong, R. N. *J. Am. Chem. Soc.* **1993**, *115*, 10466-10467.

26. (a) Carruthers, W. *J. Chem. Soc.* **1967**, 1525-1527.

(b) Mallory, F. B.; Rudolph, M. J.; Oh, S. M. *J. Org. Chem.* **1989**, *54*, 4619-4626.

27. (a) Plater, J. M. *Tetrahedron Lett.* **1994**, *35*, 6147-6150.

(b) Plater, J. M. *J. Chem. Soc., Perkin Trans. 1* **1997**, 2903-2909.

28. Mallory, F. B.; Mallory, C. W.; Loeb, S. E. S. *Tetrahedron Lett.* **1985**, *25*, 3773-3776.

29. Liu, L.; Yang, B.; Katz, T. J.; Poindexter, M. K. *J. Org. Chem.* **1991**, *56*, 3769-3775.

30. Platt, K. L.; Oesch, F. *J. Org. Chem.* **1983**, *48*, 265-268.

31. (a) Henbest, H. B.; Wilson, R. A. L. *J. Chem. Soc.* **1957**, 1958-1965.

(b) Yagi, H.; Thakker, D. R.; Hernandez, O.; Koreeda, M.; Jerina, D. M. *J. Am. Chem. Soc.* **1977**, *99*, 1604-1611.

(c) Zajc, B. *J. Org. Chem.* **1999**, *64*, 1902-1907.

32. (a) Lee, C.; Yang, W.; Parr, R. *Phys. Rev. B* **1988**, *37*, 785-789

(b) The B3LYP/6-31G(d) medium-sized basis set, (a hybrid density functional theory {DFT} model consisting of Becke's three-parameter and Lee-Yang-Parr correlation function) was used to compute calculations for this compound.

33. Mallory, F.B.; Wood, C.S. *J. Org. Chem.* **1964**, *29*, 3374-3377.

34. (a) Fürstner, A.; Mamane, V. *J. Org. Chem.* **2002**, *67*, 6264-6267.

(b) Mamane, V.; Hannen, P.; Fürstner, A. *Chem. Eur. J.* **2004**, *10*, 4556-4575.

35. (a) Miyaura, N.; Suzuki, A. *Chem. Rev*. **1995**, *95*, 2457-2483.

(b) Suzuki, A. *J. Organomet. Chem*. **1999**, *576*, 147-168.

36. (a) Ramirez, F.; Desai, N. B.; McKelvie, N, *J. Am. Chem. Soc.* **1962**, *84*, 1745-1747.

(b) Corey, E. J.; Fuchs, P. L. *Tetrahedron Lett*. **1972**, 3769-3772.

37. Miwa, K.; Aoyama, T.; Shioiri, T. *Synlett* **1994**, 107-108.

38. (a) Bruneau, C.; Dixneuf, P. H. *Acc. Chem. Res*. **1999**, *32*, 311-323.

(b) McDonald, F. E. *Chem. Eur. J*. **1999**, *5*, 3103-3106.

39. Soriano, E.; Marco-Contelles, J. *Organometallics*, **2006**, *25*, 4542-4553.

40. Qandil, A. M.; Ghosh, D.; Nichols, D. E. *J. Org. Chem.* **1999**, *64*, 1407-1409.

41. Corey, E. J.; Suggs, J. W. *Tetrahedron Lett.* **1975**, *16*, 2647-2650.

42. Giroux, A.; Han, Y.; Prasit, P. *Tetrahedron Lett*. **1997**, *38*, 3841-3844.

43. Jones, S. B.; He, L.; Castle, S. L. *Org. Lett*. **2006**, *8*, 3757-3760.

44. Pathak, R.; Nhlapo, J. M.; Govender, S.; Michael, J. P.; Van Otterlo, W. A. L.; De Koning, C. B. *Tetrahedron* **2006**, *62*, 2820-2830.

45. Fabian, K. H. H.; Elwahy, A. H. M.; Hafner, K. *Tetrahedron Lett.* **2000**, *41*, 2855-2858.

46. Roth, G. J., Liepold, B., Muller, S. G., Bestmann, H. J. *Synthesis* **2004**, *1*, 59-62.

47. Eisenstadt, E.; Gold, A. *Biochemistry* **1978**, *75*, 1667-1669.

Chapter 4

1. The initial studies on PAH and carcinogenesis has been reviewed in:

(a) *Polycyclic Aromatic Hydrocarbon Carcinogenesis: Structure-Activity Relationships* Yang, S. K.; Silverman, B. D., Eds.; CRC Press: Boca Raton, FL, 1988 (Volumes I and II).

(b) *Polycyclic Aromatic Hydrocarbons: Chemistry and Carcinogenicity* Harvey, R. G., Ed.; Cambridge Unviersity Press: Cambridge, 1991. *Polycyclic Hydrocarbons and Carcinogenesis* Harvey, R. G., Ed.; ACS Symposium Series 283: Washington, DC, 1985.

(c) Dipple, A.: Reactions of polycyclic aromatic hydrocarbons with DNA. In *DNA Adducts: Identification and Biological Significance*; Hemminki, K.; Dipple, A.; Shuker, D. E. G.; Kadlubar, F. F.; Sagerbäck, D.; Bartsch, H., Eds.; Scientific Publication No. 125, International Agency for Research on Cancer: Lyon, 1994; pp. 107-129.

(d) For a detailed survey of the chemistry of polycyclic aromatic hydrocarbons, please see: *Polycyclic Aromatic Hydrocarbons* Harvey, R. G.; Wiley-VCH, NY, 1997.

2. Denissenko, M. F.; Pao, A.; Tang, M.; Pfeifer, G. P. *Science* **1996**, *274*, 430-432.

3. (a) Aygün, S. F.; Kabadayi, F. *Int. J. Food Sci. Nutr*. **2005**, *56*, 581-585.

(b) Lee, B. M.; Shim, G. A.; *J. Toxicol. Environ. Health A*. **2007**, *70*, 1391-1394.

4. Guengerich, F. P.; Shimada, T. *Chem. Res. Toxicol.* **1991**, *4*, 391-407.

5. (a) Oesch, F. *Xenobiotica* **1973**, *3*, 305-340.

(b) Conney, A. H. *Cancer Res.* **1982**, *42*, 4875-4917.

6. (a) Sayer, J. M.; Yagi, H.; Croisy-Delcey, M.; Jerina, D. M. *J. Am. Chem. Soc.* **1981**, *103*, 4970-4972.

(b) Yang, S. K. *Biochem. Pharmacol.* **1988**, *37*, 61-70.

7. (a) Wei, S.-J.C.; Chang, R. L.; Hennig, E.; Cui, E. E.; Merkler, K. A.; Wong, C.-Q.; Yagi, H.; Jerina, D. M.; Conney, A. H. *Carcinogenesis* **1994**, *15*, 1729-1735.

(b) Jelinsky, S. A.; Liu, T.; Geacintov, N. E.; Loechler, E. L. *Biochemistry* **1995**, *34*, 13545-13553.

(c) Zou, Y.; Liu, T.-M.; Geacintov, N. E.; Van Houten, B. *Biochemistry* **1995**, *34*, 13582-13593.

(d) Chary, P.; Lloyd, R. S. *Chem. Res. Toxicol.* **1996**, *9*, 409-417.

(e) Hanrahan, C. J.; Bacolod, M. D.; Vyas, R. R.; Liu, T.; Geacintov, N. E.; Loechler, E. L.; Basu, A. K. *Chem. Res. Toxicol.* **1997**, *10*, 369-377.

(f) Shukla, R.; Liu, T.; Geacintov, N. E.; Loechler, E. L. *Biochemistry* **1997**, *36*, 10256-10261.

(g) Fernandes, A.; Liu, T.; Amin, S.; Geacintov, N. E.; Grollman, A. P.; Moriya, M. *Biochemistry* **1998**, *37*, 10164-10172.

8. (a) Sayer, J. M.; Chadha, A., Agarwal, S. K.; Yeh, H. J. C.; Yagi, H.; Jerina, D. M. *J. Org. Chem.* **1991**, *56* 20-29.

(b) Jerina, D. M.; Chadha, A.; Cheh, A. M.; Schurdak, M. E.; Wood, A. W.; Sayer, J. M. *Biological Reactive Intermediates IV*, Witmer, C. M.; Snyder, R.; Jollow, D. J.; Kalf, G. F.; Kocsis, J. J.; Sipes, I. G., Eds.; Plenum Press: New York, 1991; pp. 533-553.

9. (a) Agarwal, S. K.; Sayer, J. M.; Yeh, H. J. C.; Pannell, L. K.; Hilton, B. D.; Pigott, M. A.; Dipple, A.; Yagi, H.; Jerina, D. M. *J. Am. Chem. Soc.* **1987**, *109*, 2497-2504.

(b) Einholf, H. J.; Amin, S.; Yagi, H.; Jerina, D. M.; Baird, W. M. *Carcinogenesis* **1996**, *17*, 2237-2244.

10. Szeliga, J.; Dipple, A. *Chem. Res. Toxicol.* **1998**, *11*, 1-11.

11. (a) Sims, P.; Grover, P. L. *Adv. Cancer Res.* **1974**, *20*, 165-174.

(b) Shabad, L. M. *J. Natl. Cancer Inst.* **1980**, *64*, 405-410.

(c) Harvey, R. G.; Geacintov, N. E. *Acc. Chem. Res.* **1988**, *21*, 66-73.

(d) Garner, R. C. *Mutat. Res.* **1998**, *402*, 67-75.

12. Dipple, A.; Pigott, M. A.; Agarwal, S. K.; Yagi, H.; Sayer, J. M.; Jerina, D. M. *Nature* **1987**, *327*, 535-536.

13. (a) Denissenko, M. F.; Pao, A.; Tang, M. S.; Pfeifer, G. P. *Science* **1996**, *214*, 430-432.

(b) Pfeifer, G. P.; Denissenko, M. F. *Environ. Mol. Mutagen.* **1998**, *31*, 197-205.

14. (a) Nesnow, S.; Ross, J. A.; Mass, M. J.; Stoner, G. D. *Exp. Lung Res.* **1998**, *24*, 395-305.

(b) Ross, J. A.; Nesnow, S. *Mutat. Res.* **1999**, *424*, 155-166.

15. (a) Reardon, D. B.; Bigger, C. A. H.; Strandberg, J.; Yagi, H.; Jerina, D. M.; Dipple, A. *Chem. Res. Toxicol.* **1989**, *2*, 12-14.

(b) Colapietro, A. M.; Goodell, A. L.; Smart ,R. C. *Carcinogenesis* **1993**,*14*, 2289-2295.

16. Chakravarti, D. Mailander, P.; Franzen, J.; Higginbotham, S.; Cavalieri, E. L.; Rogan, E. G. *Oncogene* **1998**, *16*, 3203-3210.

17. Benasutti, M.; Ezzedine, Z. D.; Loechler, E. L. *Chem. Res. Toxicol.* **1988**, *1*, 160-168.

18. (a) Cosman, M.; Ibanez, V.; Geacintov, N. E.; Harvey, R. G. *Carcinogenesis* **1990**, *11*, 1667-1672.

(b) Mao, B.; Xu, J.; Li, B.; Margulis, L. A.; Smirnov, S.; Ya, N. Q.; Coutney, S.; Geacintov, N. E. *Carcinogenesis* **1995**, *16*, 357-365.

19. (a) Harris, C. M.; Zhou, L.; Strand, E. A.; Harris, T. M. *J. Am. Chem. Soc.* **1991**, *113*, 4328-4329.

(b) Kim, S. J.; Stone, M. P.; Harris, C. M.; Harris, T. M. *J. Am. Chem. Soc.* **1992**, *114*, 5480-5481.

(c) Cooper, M. D.; Hodge, R. P.; Tamura, P. J.; Wilkinson, A. S.; Harris, C. M.; Harris, T. M. *Tetrahedron Lett.* **2000**, *41*, 3555-3558.

20. (a) Page, J. E.; Zajc, B.; Oh-hara, T.; Lakshman, M. K.; Sayer, J. M.; Jerina, D. M.; Dipple, A. *Biochemistry* **1998**, *37*, 9127-9137.

(b) Lakshman, M. K. unpublished work suggests that for the post-oligomerization approach, the yields are dependent on the particular sequence that is used.

21. (a) Lakshman, M. K.; Sayer, J. M.; Jerina, D. M. *J. Am. Chem. Soc.* **1991**, *113*, 6589-6594.

(b) Lakshman, M. K.; Sayer, J. M.; Jerina, D. M. *J. Org. Chem.* **1992**, *57*, 3438-3443.

(c) Lakshman, M. K.; Sayer, J. M.; Yagi, H.; Jerina, D. M. *J. Org. Chem.* **1992**, *57*, 4585-4590.

22. (a) Zajc, B.; Lakshman, M. K.; Sayer, J. M.; Jerina, D. M. *Tetrahedron Lett.* **1992**, *33*, 3409-3412.

(b) Custer, L.; Zajc, B.; Sayer, J. M.; Cullinane, C.; Phillips, D. R.; Cheh, A. M.; Jerina, D. M.; Bohr, V. A.; Mazur, S. J. *Biochemistry* **1999**, *38*, 569-581.

23. (a) Steinbrecher, T.; Becker, A.; Stezowski, J. J.; Oesch, F.; Seidel, A. *Tetrahedron Lett.* **1993**, *34*, 1773-1774.

(b) Lee, H.; Luna, E.; Hinz, M.; Stezowski, J. J.; Kiselyov, A. S.; Harvey, R. G. *J. Org. Chem.* **1995**, *60*, 5604-5613.

24. Robins, M. J.; Basom, G. L. *Can. J. Chem.* **1973**, *51*, 3161-3169.

25. Lakshman, M. K.; Gunda, P. *Org. Lett.* **2003**, *5*, 39-42.

26. Johnson, F.; Bonala, R.; Tawde, D.; Torres, M. C.; Iden, C. R. *Chem. Res. Toxicol.* **2002**, *12*, 1489-1494.

27. Champeil, E.; Pradhan, P.; Lakshman, M. K. *J. Org. Chem.* **2007**, *72*, 5035-5045.

28. Cooper, M. D.; Hodge, R. P.; Tamura, P. J.; Wilkinson, A. S.; Harris, C. M.; Harris, T. M. *Tetrahedron Lett.* **2000**, *41*, 3555-3558.

29. Caruthers, M. H. *Acc. Chem. Res.* **1991**, *24*, 278-284.

30. Geacintov, N. E.; Cosman, M.; Hingerty, B. E.; Amin, S.; Broyde, S.; Patel, D. J. *Chem. Res. Toxicol.* **1997**, *10*, 111-146.

31. Karle, I. L; Yagi, H.; Sayer, J. M.; Jerina, D. M. *Proc. Natl. Acad. Sci. USA*, **2004**, *101*, 1433-1438.

32. Cosman, M.; de los Santos, C.; Fiala, R.; Hingerty, B. E.; Singh, S. B.; Ibanez, V.; Margulis, L. A.; Live, D.; Geacintov, N. E.; Broyde, S.; Patel, D. J. *Proc. Natl. Acad. Sci. USA,* **1992**, *89*, 1914-1918.

33. de los Santos, C.; Cosman, M.; Hingerty, B. E.; Ibanez, V.; Margulis, L. A.; Geacintov, N. E.; Broyde, S.; Patel, D. J. *Biochemistry* **1992,** *31,* 5245-5252.

34. Cosman, M.; de los Santos, C.; Fiala, R.; Hingerty, B. E.; Ibanez, V.; Luna, E.; Harvey, R.; Geacintov, N. E.; Broyde, S.; Patel, D. J. *Biochemistry* **1993,** *32,* 4145-4155.

35. Cosman, M.; Hingerty, B. E.; Luneva, N.; Amin, S.; Geacintov, N. E.; Broyde, S.; Patel, D. J. *Biochemistry* **1996,** *35,* 9850-9863.

36. Fountain, M. A.; Krugh, T. R. *Biochemistry* **1995,** *34,* 3152-3161.

37. Schurter, E. J.; Yeh, H. J. C.; Sayer, J. M.; Lakshman, M. K.; Yagi, H.; Jerina, D. M.; Gorenstein, D. G. *Biochemistry* **1995**, *34*, 1364-1375.

38. (a) Yeh, H. J. C.; Sayer, J. M.; Liu, X.; Altieri, A. S.; Byrd, R. A.; Lakshman, M. K.; Yagi, H.; Schurter, E. J.; Gorenstein, D. G.; Jerina, D. M. *Biochemistry* **1995**, *34*, 13570-13581.

(b) Schwartz, J. L.; Rice, J. S.; Luxon, B. A.; Sayer, J. M.; Xie, G.; Yeh, H. J. C.; Liu, X.; Jerina, D. M. Gorenstein, D. G. *Biochemistry*, **1997**, *36*, 11069-11076.

39. Schurter, E. J.; Sayer, J. M.; Oh-hara, T.; Yeh, H. J. C.; Yagi, H.; Luxon, B. A.; Jerina, D. M.; Gorenstein, D. G. *Biochemistry* **1995**, *34*, 9009-9020.

40. Mao, B.; Gu, Z.; Gorin, A.; Chen, J.; Hingerty, B. E.; Amin, S.; Broyde, S.; Geacintov, N. E.; Patel, D. J. *Biochemistry* **1999**, *38*, 10831-10842.

41. Pradhan, P.; Tirumala, S.; Liu, X.; Sayer, J. M.; Jerina, D. M.; Yeh, H. J. C. *Biochemistry* **2001**, *40*, 5870-5881.

42. Volk, D. E.; Thiviyanathan, V.; Rice, J. S.; Luxon, B. A.; Shah, J. H.; Yagi, H.; Sayer, J. M.; Yeh, H. J. C.; Jerina, D. M.; Gorenstein, D. G. *Biochemistry* **2003**, *42,* 1410-1420.

43. Zegar, I. S.; Kim, S. J.; Johansen, T. N.; Horton, P. J.; Harris, C. M.; Harris, T. M.; Stone, M. P. *Biochemistry* **1996,** *35,* 6212-6224.

44. Zegar, I. S.; Chary, P.; Jabil, R. J.; Tamura, P. J.; Johansen, T. N.; Lloyd, R. S.; Harris, C. M.; Harris, T. M.; Stone, M. P. *Biochemistry* **1998**, *37*, 16516-16528.

45. Volk, D. E.; Rice, J. S.; Luxon, B. A.; Yeh, H. J. C.; Liang, C.; Xie, G.; Sayer, J. M.; Jerina, D. M.; Gorenstein, D. G. *Biochemistry* **2000**, *39*, 14040-14053.

46. Chaturvedi, S.; Lakshman, M. K. *Carcinogenesis* **1996**, *17*, 2747-2752.

47. Yang, J.-L.; Maher, V. M.; McCormick, J. J. *Proc. Natl. Acad. Sci.* **1987**, *84*, 3787-3791.

48. (a) Page, J. E.; Pilcher, A. S.; Yagi, H.; Sayer, J. M.; Jerina, D. M.; Dipple, A. *Chem. Res. Toxicol.* **1999**, *12*, 258-263.

(b) Pontén, I.; Sayer, J. M.; Pilcher, A. S.; Yagi, H.; Kumar, S.; Jerina, D. M.; Dipple, A. *Biochemistry* **1999**, *38*, 1144-1152.

(c) Pontén, I.; Sayer, J. M.; Pilcher, A. S.; Yagi, H.; Kumar, S.; Jerina, D. M.; Dipple, A. *Biochemistry* **2000**, *39*, 4136-4144.

(d) Pontén, I.; Kroth, H.; Sayer, J. M.; Dipple, A.; Jerina, D. M. *Chem. Res. Toxicol.* **2001**, *14*, 720-726.

49. Benasutti, M.; Ezzedine, Z. D.; Loechler, E. L. *Chem. Res. Toxicol.* **1988**, *1*, 160-168.

50. Christner, D. F.; Lakshman, M. K.; Sayer, J. M.; Jerina, D. M.; Dipple, A. *Biochemistry* **1994**, *33*, 14297-14305.

51. Shukla, R.; Jelinsky, S.; Liu, T.; Geacintov, N. E.; Loechler, E. L. *Biochemistry* **1997**, *36*, 13263-13269.

52. Zou, Y.; Luo, C.; Geacintov, N. E. *Biochemistry* **2001**, *40*, 2923-2931.

53. Roth, R. B.; Amin, S.; Geacintov, N. E.; Scicchitano, D. A. *Biochemistry* **2001**, *40*, 5200-5207.

54. Zhuang, P.; Kolbanovskiy, A.; Amin, S.; Geacintov, N. E. *Biochemistry* **2001**, *40*, 6660-6669.

55. Kramata, P.; Zajc, B.; Sayer, J. M.; Jerina, D. M.; Wei, C. S.-J. *J. Biol. Chem.* **2003**, *278*, 14940-14948.

56. Hoare, S.; Zou, Y.; Purohit, V.; Krishnasamy, R.; Skorvaga, M.; Van Houten, B.; Geacintov, N. E.; Basu, A. K. *Biochemistry* **2000**, *39*, 12252-12261.

57. Zhu, Y.; Shell, S. M.; Utzat, C. D.; Luo, C.; Yang, Z.; Geacintov, N. E.; Basu, A. K. *Biochemistry* **2003**, *42*, 12654-12661.

58. Buterin, T.; Hess, M. T.; Luneva, N.; Geacintov, N. E.; Amin, S.; Kroth, H.; Seidel, A.; Naegeli, H. *Cancer Res.* **2000**, *60*, 1849-1856.

59. Simhadri, S.; Kramata, P.; Zajc, B.; Sayer, J. M.; Jerina, D. M.; Hinkle, D. C.; Wei, C. S.-J. *Mutation Research* **2002**, *508*, 137-145.

60. Xie, M.; Braithwaite, E.; Guo, D.; Zhao, B.; Geacintov, N. E.; Wang, Z. *Biochemistry* **2003**, *42*, 11253-11262.

61. Chiapperino, D.; Kroth, H.; Kramarczuk, I. H.; Sayer, J. M.; Masutani, C.; Hanaoka, F.; Jerina, D. M.; Cheh, A. M. *J. Biol. Chem.* **2002**, *277*, 11765-11771.

62. (a) Suzuki, N.; Ohashi, E.; Kolbanovskiy, A.; Geacintov, N. E.; Grollman, A. P.; Ohmori, H.; Shibutani, S. *Biochemistry* **2002**, *41*, 6100-6106.

(b) Ogi, T.; Shinkai, Y.; Tanaka, K.; Ohmori, H. *Proc. Natl. Acad. Sci. USA,* **2002**, *99*, 15548-15553.

63. Pommier, Y.; Kohlhagen, G.; Pourquier, P.; Sayer, J. M.; Kroth, H.; Jerina, D. M. *Proc. Natl. Acad. Sci. USA*, **2000**, *97*, 2040-2045.

64. Pommier, Y.; Laco, G. S.; Kohlhagen, G.; Sayer, J. M.; Kroth, H.; Jerina, D. M. *Proc. Natl. Acad. Sci. USA*, **2000**, *97*, 10739-10744.

65. Pommier, Y.; Kohlhagen, G.; Laco, G. S.; Kroth, H.; Sayer, J. M.; Jerina, D. M. *J. Biol. Chem.* **2002**, *277*, 13666-13672.

66. Khan, Q. A.; Kohlhagen, G.; Marshall, R.; Austin, C. A.; Kalena, G. P.; Kroth, H.; Sayer, J. M.; Jerina, D. M.; Pommier, Y. *Proc. Natl. Acad. Sci. USA*, **2003**, *100*, 12498-12503.

67. (a) Lakshman, M.; Lehr, R. E. *Tetrahedron Lett.* **1990**, *31*, 1547-1550.

(b) Kim, S. J.; Harris, C. M.; Jung, K.-Y.; Koreeda, M.; Harris, T. M. *Tetrahedron Lett.* **1991**, *32*, 6073-6076.

68. (a) Lakshman, M.; Nadkarni, D. V.; Lehr, R. E. *J. Org. Chem.* **1990**, *55*, 4892-4897.

(b) Lakshman, M. K.; Chaturvedi, S.; Lehr, R. E. *Synth. Commun.* **1994**, *24*, 2983-2988.

69. Steinbrecher, T.; Wameling, C.; Oesch, F.; Seidel, A. *Angew. Chem., Int. Ed. Engl.* **1993**, *32*, 404-406.

70. Jhingan, A. K.; Meehan, T. *J. Chem. Res. (S*) **1991**, 122-123.

71. (a) Li, G.; Angert, H. H.; Sharpless, K. B. *Angew. Chem., Int. Ed. Engl.* **1996**, *35*, 2813-2817.

(b) Pilcher, A. S.; Yagi, H.; Jerina, D. M. *J. Am. Chem. Soc.* **1998**, *120*, 3520-3521.

72. Kroth, H.; Yagi, H.; Seidel, A.; Jerina, D. M. *J. Org. Chem.* **2000**, *65*, 5558-5564.

73. (a) Ramesha, A. R.; Kroth, H.; Jerina, D. M. *Org. Lett.* **2001**, *3*, 531-533.

(b) Ramesha, A. R.; Kroth, H.; Jerina, D. M. *Tetrahedron Lett.* **2001**, *42*, 1003-1005.

74. Lakshman, M. K.; Keeler, J. C.; Ngassa, F. N.; Hilmer, J. H.; Pradhan, P.; Zajc, B.; Thomasson, K. A. *J. Am. Chem.* Soc. **2007**, *129*, 68-76.

75. McCaustland, D. J.; Engel, J. F. *Tetrahedron Lett.* **1975**, *30*, 2549-2552.

76. (a) Iwasawa, N.; Kato, T.; Narasaka, K. *Chem. Lett.* **1988**, 1721-1724.

(b) Sakurai, H.; Iwasawa, N.; Narasaka, K. *Bull. Chem. Soc. Jpn.* **1996**, *69*, 2585-2594.

(c) Gypser, A.; Michel, D.; Nirschl, D. S.; Sharpless, K. B. *J. Org. Chem.* **1998**, *63*, 7322-7327.

77. (a) Lakshman, M. K.; Zajc, B. *Tetrahedron Lett.* **1996**, *37*, 2529-2532.

(b) Lakshman, M. K.; Chaturvedi, S.; Zajc, B.; Gibson, D. T.; Resnick, S. M. *Synthesis* **1998**, 1352-1356.

78. Haija, S.; Sinha, D.; Bhowmick, M. *Tetrahedron Lett.* **2006**, *47*, 7017-7019.

79. (a) Fowler, F. W.; Hassner, A.; Levy, L. A. *J. Am. Chem. Soc.* **1967**, *89*, 2077-2082.

(b) Kirschning, A.; Hashem, M. A.; Monenschein, H.; Rose, L.; Schöning, K.-U. *J. Org. Chem.* **1999,** *64***,** 6522-6526.

(c) Kirschning, A.; Monenschein, H.; Schmeck, C. *Angew. Chem. Int. Ed.* **1999,** *38*, 2594-2596.

80. Hassner, A.; Lorber, M. E.; Heathcock, C. H. *J. Org. Chem.* **1967**, *32*, 540-549.

81. Kiselyov, A. S.; Steinbrecher, T.; Harvey, R. G. *J. Org. Chem*. **1995**, *60*, 6129-6134.

82. Yagi, H.; Thakker, D. R.; Hernandez, O.; Koreeda, M.; Jerina, D. M. *J. Am. Chem. Soc.* **1977**, *99*, 1604-1611.

83. Yadav, J. S.; Subba Reddy, B. V.; Narasimha Chary, D.; Chandrakanth, D. *Tetrahedron Lett.* **2009**, *50*, 1136-1138.

84. Yeung, Y.-Y.; Gao, X.; Corey, E. J. *J. Am. Chem. Soc.* **2006**, *128*, 9644-9655.

85. Meehan, T; Wolfe, A. R.; Negrete, G. R.; Song, Q *Proc. Natl. Acad. Sci.* **1997**, *94*, 1947-1754.

86. Doan, L.; Yagi, H,; Jerina, D. M.; Whalen, D. L. *J. Org. Chem.* **2004**, *69*, 8012-8017.

87. Lakshman, M. K.; Ngassa, F. N.; Keeler, J. C.; Dinh, Y. Q. V.; Hilmer, J. H.; Russon, L. M. *Org. Lett.* **2000**, *2*, 927-930.

88. Hudlicky, T.; Nugent, T.; Griffith, W. *J. Org. Chem.* **1994**, *59*, 7944-7946.